Hydrological Studies: An Eco-Environmental Significance of an Important Eastern River Basin in India

Thesis Submitted by

SWETASREE NAG

Doctor of Philosophy (Science)

School of Water Resources Engineering
Faculty of Interdisciplinary Studies, Law and Management, Jadavpur University, Kolkata, India

2023

JADAVPUR UNIVERSITY
KOLKATA- 700032, INDIA

Index No. D-7/ISLM/80/18

Title of Thesis

Hydrological Studies: An Eco-Environmental Significance of an Important Eastern River Basin in India

Name, Designation & Institution of the Supervisor

1. Prof. (Dr.) Pankaj Kumar Roy

Director & Professor,

School of Water Resources Engineering, Jadavpur University

Former Dean,

Faculty of Interdisciplinary Studies Law & Management,

&

Chairman and Convener of the Research Committee

Jadavpur University

Kolkata- 700032

2. Dr. Malabika Biswas Roy

Associate Professor and Head,

Department of Geography,

Women's College, Calcutta

University of Calcutta

Kolkata- 700003

DEDICATION

To my beloved husband,

who taught me how to conquer life's battles with grace and unwavering strength. Thank you for being my source of inspiration and my guiding star through the darkest nights.

LISTS OF RESEARCH PUBLICATIONS

Sl. No	Type of publication	ISSN/ISBN No/ DOI No	Name of Journal/ Book	International /National	Title of the paper	Year of publication
1	Journal	ISSN: 0253-7141	Indian Journal of Environmental Protection	National	Study of Ganga River Health Condition Based on Water Quality Indicators with Environmental Aspects and Adaptation Strategies Thereof	2018
2	Conference Paper	--	Conference: International Conference of Energy and Sustainable Development 2020 (ICESD 2020) At: Jadavpur University, Kolkata, India	International	Surface water source estimation for sustainable management using Remote Sensing and GIS	2020
3	Journal	DOI: 10.1007/s40808-020-00768-z	Modeling Earth Systems and Environment	International	Optimum Prioritisation of Sub-watersheds based on Erosion Susceptible Zones through Modelling and GIS Techniques	2020
4	Book Chapter	ISBN No-978-81-941009-4-2	Water Resources: Current and Future Challenges and Research Direction	National	A Changing Nature of Surface Water Resources Scenario (1984-2018)	2020
5	Book Chapter	DOI: 10.1016/B978-0-12-823895-0.00027-0	Land Reclamation and Restoration Strategies for Sustainable Development	International	Land reclamation and reuse of waste water on the backdrop of urban sprawl of Kolkata metropolitan: a case study of East Kolkata, Wetland, India	2021
6	Book Chapter	DOI: 10.1007/978-981-33-6412-7_4	Advances in Water Resources Management for Sustainable Use (Part of the Lecture Note in Civil Engineering book series, LNCE, Volume 131)	International	Tri-Decadal Visualization Analysis on River Health Studies: A Global Perspective	2021

7	Book Chapter	DOI: 10.1007/978-981-33-6412-7_4	Advances in Water Resources Management for Sustainable Use (Part of the Lecture Note in Civil Engineering book series, LNCE, Volume 131)	International	Assessment of Drought Using Multi-parameter Indices	2021
8	Book Chapter	DOI: 10.1007/978-981-33-6412-7_4	Advances in Water Resources Management for Sustainable Use (Part of the Lecture Note in Civil Engineering book series, LNCE, Volume 131)	International	Assessment of Topographic Complexity Zone of a Drainage Basin Using Geographic Information System	2021
9	Book Chapter	DOI: 10.1007/978-981-16-6966-8_16	Climate, Environment and Disaster in Developing Countries, Springer	International	An Analytical Study on Interplay Between Physiographic Condition and Land Use Land Cover Dynamicity	2022
10	Journal	DOI: 10.1186/s42269-022-00740-0	Bulletin of the National Research Centre	International	Assessment of wetland potential and bibliometric review: a critical analysis of the Ramsar sites of India	2022
11	Journal	DOI: 10.1007/s12040-022-01872-7	Journal of Earth System Science	International	Study on the functionality of land use land cover over the evaluation of groundwater potential zone: A fuzzy AHP based approach	2022
12	Preprint	DOI: 10.21203/rs.3.rs-2409387/v1	Research Square	International	A Combined use of Hydraulic and Hydrological Model to Characterise Channel Hydro-Geomorphology of a Tropical River Basin of West Bengal, India	2022

LISTS OF PAPER/POSTER PRESENTATIONS IN NATIONAL/INTERNATIONAL.CONFERENCES/WORKSHOPS

Name of the Seminar/ Conference	Topic of presentation	Held at	Year
30th IGI Conference, 2018	"Study on Interplay between Physiographic Condition and Land Use land Cover Dynamicity through an Analytical Approach"	New Delhi	2018
National Seminar on Environmental issues, 2018	"Land Use Land Cover Reconfiguration: A Case Study of Mayurakshi River Basin, West Bengal"	Kolkata	2018
5th International Conference on Water Resource and Environment (WRE 2019)	" Prioritisation of Sub-watersheds based on Morphometric Characteristics using TOPSIS Model and Geographical Information System-A Study of Mayurakshi River Basin, West Bengal, India.	Macao, China	2019
1st international conference on Sustainable Water Management organised by BBMB under the aegis of National Hydrology Project, Ministry of Water Resources, River Development & Ganga Rejuvenation	Non Parametric Trend Analysis of Groundwater Scenario in Mayurakshi River Basin, West Bengal	Chandigarh, India	2018
2nd International Conference On Sustainable Water Management Hosted by: Water Resources Department, Govt. of Maharashtra	Watershed Erodibility Prioritization Based On Morphometric Analysis A TOPSIS Based Approach	Pune, India	2019

PARTICIPATION IN NATIONAL/INTERNATIONAL.CONFERENCES/WORKSHOPS

- Participating in the two-day Technical Knowledge Exchange Workshop for Bangladesh and India, on Vulnerability of Sundarban in Changing Climate, at Kolkata, India organized by The World Bank Group, 2017
- Completed 3 days training course on "Local Ground Water Management Issues" held at Central Ground Water Board (Eastern Region), in collaboration with Govt. of India, Ministry of Water Resources, River Development & Ganga Rejuvenation, under the aegis of Rajiv Gandhi National Water Training & Research Institute, Raipur, 2018.
- Participated in 1day workshop on Qualitative and Quantitative Research Methods in Geographical Studies organized by Department of Geography, Vivekananda College, Thakurpukur, Kolkata, India, 2018.
- Participated in the conference on "Water, Sanitation and Sustainability Issues under Rural Indian Conditions" under TEQIP III held at IIEST Shibpur, Howrah, India, 2018.
- Participated on 1 day workshop on " Environmental Challenges at Present Issues of Concern" organized by the Department of Civil Engineering in collaboration with Institute of Engineers and Centre for Environment Education, 2018.
- Participated in ESRI India User Conference 2019 held at Kolkata, India.
- Participated in the webinar series on "Remote Sensing application for Earth and Atmospheric Monitoring" hosted by Centre for Remote sensing and Geo-informatics Sathyabama Institute of Science and Technology, Chennai from 11-05-2020 to 13-05-2020.
- Participated in the webinar on "3D Terrain Mapping from Satellite Imagery and Topographical Maps using Mobile Application", organized by Department of Geography, East Calcutta Girls College, Kolkata- 700089
- Participated in the two days international webinar on "INNOVATION IN DISASTER RISK REDUCTION: AIMING TOWARDS A RESILIENT SOCIETY", Organized by Department of Geography, Diamond Harbour Women's University in association with Commission on Hazard and Risk, International Geographical Union (IGU), 10-11 September 2020.
- Participated in One-Day National Webinar entitled "River Basin and its Influence on Surrounding Inhabitants " organised by Department of Geography in collaboration with IQAC, Ranaghat College on Tuesday 11th August, 2020.
- Participated in the online workshop on "WORKING WITH PYTHON PROGRAMMING" Organized by Department of Computer Science and IQAC East Calcutta Girls' College in Collaboration With Department of Computer Science West Bengal State University, 15th MAY 2020 to 21st MAY 2020
- Participated in the International Webinar on "Challenges of Climate Change and Sustainable Development Goals" organized by the Department of Geography, School of Basic and Applied Sciences, Adamas University on 29th June 2020.
- Participated in the Webinar on Distinct Landforms of West Bengal: Alluvial Fans and Badlands held on 31st July ,2020 organized by Department of Geography, Vivekananda College for Women, Barisha
- Participated in the Webinar on Evolution of Geomorphological Thoughts and Ideas held on 4th September,2020, organized by Department of Geography, Vivekananda College for Women, Barisha

- Participated in the webinar series on "Remote Sensing application for Earth and Atmospheric Monitoring"hosted by Centre for Remote sensing and Geoinformatics Sathyabama Institute of Science and Technology, Chennai from 11-05-2020 to 13-05-2020.
- Participated in Two Days Lecture Series organized by Department of Geography, Surendranath College for Women from September 26-27th, 2020
- Participated in online lecture on 3D Terrain Mapping from Satellite Imagery and Topographical Maps using Mobile Application organized by Department of Geography, East Calcutta Girls College, on 24th August, 2020
- Participated in the national webinar on "Impact of Covid-19 pandemic on our Water Resources" held on 3rd July 2021, jointly organised by Dept. of Physics, Kabi Nazrul Mahavidyalaya, Sonamura & Dept. of Physics, Ambedkar College, Fatikroy, Tripura, India.
- Participated in the webinar on GCMS and LCMSMS organized by PerkinElmer on 13th October, 2020
- Participated in IGU India International Conference (virtual) 2020 on "Global to Local Sustainability and Future Earth" organized by Department of Geography, MLSU, Udaipur India, on 18-20th December, 2020
- Participated in the Webinar on Innovation in Disaster Risk Reduction: Aiming Towards a Resilient Society, organized by the Department of Geography, Diamond Harbour Women's University, West Bengal, India during 10-11 September 2020.
- Participated in One-Day National Webinar entitled "River Basin and its Influence on Surrounding Inhabitants " organised by Department of Geography in collaboration with IQAC, Ranaghat College on Tuesday 11th August, 2020.
- Participated in the online workshop on "WORKING WITH PYTHON PROGRAMMING" Organized by Department of Computer Science and IQAC East Calcutta Girls' College in Collaboration with Department of Computer Science West Bengal State University held on 15th -21st May 2020
- Participating in the two-day Technical Knowledge Exchange Workshop for Bangladesh and India, on Vulnerability of Sundarban in Changing Climate, at Kolkata, India organized by The World Bank group, 2017
- Participated in the International Webinar on "Challenges of Climate Change and Sustainable Development Goals" organized by the Department of Geography, School of Basic and Applied Sciences, Adamas University on 29th June 2020.
- Participated in the Webinar on Distinct Landforms of West Bengal: Alluvial Fans and Badlands organized by Department of Geography & IQAC Vivekananda College for Women,Barisha held on 31st July ,2020
- Participated in the Webinar on Evolution on Geomorphological Thoughts and Ideas organized by Department of Geography & IQAC Vivekananda College for Women, Barisha held on 4th September ,2020
- Paricipated in the 2nd Intensive Training Programme for the Young Geomorphologists organized by IGI Young Geomorphologists Forum, during 1-2nd November, 2021.

Training Programme attended

- Successfully completed the MIKE powered by DHI training course on "Introduction to River and Channel Modelling" using the software MIKE HYDRO River, from 9-11th June 2021.
- Successfully completed the 3 days national level workshop on "Fundamental Concept of SPSS" organized by Integrated Institute for Advanced Research and Information from 17th February, 2021 to 19th February, 2021.
- Successfully completed Two Weeks short term training programme through ICT Mode on Environmental Pollution: Laboratory and Testing organized by National institute of technical teachers' Training and research (NITTTR), Kolkata from 17/01/2022 to 28/01/2022

STATEMENT OF ORIGINALITY

I, **Swetasree Nag**, Index No: **D-7/ISLM/80/18** registered on the academic session 2018-2023 do hereby declare that this thesis entitled **"Hydrological Studies: An Eco-Environmental Significance of an Important Eastern River Basin in India"** contains literature survey and original research work done by the undersigned candidate as part of Doctoral studies.

All information in this thesis have been acquired and provided with existing academic rules and ethical conduct. I declare that, as required by these rules and conduct, I have fully cited and referred all materials and results that are not original to this work.

I also declare that I have checked this thesis as per the "Policy on Anti-Plagiarism, Jadavpur University, 2019" and the **level of similarity as checked by iThenticate Software is 7%**

Name of the candidate: SWETASREE NAG

Signature: Swetasree Nag

Date: 07.09.2023

Certified by Supervisor:

07/09/23

Prof. (Dr.) Pankaj Kumar Roy
Director & Professor
School of Water Resources Engineering
Jadavpur University

Prof. (Dr.) Pankaj Kumar Roy
Professor
School of Water Resources Engineering
Jadavpur University

Malabika Biswas Roy
07/09/2023

Dr. Malabika Biswas Roy
Associate Professor
Department of Geography
Women's College, Calcutta

Dr. Malabika Biswas Roy
Associate Professor & Head
Department of Geography
Women's College, Calcutta

CERTIFICATE FROM SUPERVISORS

This is to certify that the thesis entitled **"Hydrological Studies: An Eco-Environmental Significance of an Important Eastern River Basin in India"** submitted by **Mrs. Swetasree Nag**, who got her name registered on the academic session **2018-2023** for the award of the Ph.D. (Science) degree of Jadavpur University is absolutely based on her own work under the supervision of Prof. (Dr.) Pankaj Kumar Roy and Dr. Malabika Biswas Roy and that neither her thesis nor any part of her thesis has been submitted for any degree/diploma or any other academic award anywhere before.

07/09/23

Prof. (Dr.) Pankaj Kumar Roy
Director & Professor
School of Water Resources Engineering
Jadavpur University

Prof. (Dr.) Pankaj Kumar Roy
Professor
School of Water Resources Engineering
Jadavpur University

Malabika Biswas Roy
7/09/2023

Dr. Malabika Biswas Roy
Associate Professor
Department of Geography
Women's College, Calcutta

Dr. Malabika Biswas Roy
Associate Professor & Head
Department of Geography
Women's College, Calcutta

ACKNOWLEDGEMENT

I would like to express my deep gratitude and sincere appreciation to all those who have supported me throughout this remarkable journey of pursuing my Ph.D.

First and foremost, I am profoundly grateful for the invaluable guidance, mentorship, and a continuous support provided by my esteemed supervisors Professor (Dr.) Pankaj Kumar Roy, Director of School of Water Resources Engineering, Jadavpur University and Dr. Malabika Biswas Roy, Associate Professor and Head of department of Geography, Women's College, Calcutta, for their invaluable guidance, support, and scholarly insights. Their dedication to mentoring me has been instrumental in shaping the direction and quality of my research. Their expertise and thoughtful feedback have consistently pushed me to strive for excellence. I am grateful for their unwavering belief in my abilities and their consistent support in times of academic challenges.

I extend my appreciation to my fellow researchers, whose stimulating discussions and camaraderie made this academic endeavour both enriching and enjoyable. I would like to express my sincere thankfulness to Dr. Gourab Banerjee, Dr. Nil Sadhan Mondal, Dr. Arnab Ghosh, Dr. Debanjana Chatterjee, Dr. Sritama Chatterjee, Dr. Minakshi Ghosh, Sudipa Halder, Saurabh Kumar Basak, Bishal Ghosh, Priyabrata Mondal, Debdas Chowdhury, Poulami Ray, Shilpa Saha and also some of my juniors namely Sayak Karmakar, Pratik Maiti, Souvik Mondal, Shuvosri Bhattacharayay for their enormous help during the field survey of my thesis work.

I am grateful to the laboratory of School of Water Resources Engineering, Jadavpur University for providing the necessary resources, research facilities, and a conducive academic environment that enabled me to embark on this intellectual journey. I also owe my sincere gratitude to the Irrigation and Waterways, Government of West Bengal and Central Water Commission, Government of India for providing necessary data for my thesis work. I am also thankful to the officials and staff members of the Suri irrigation guest house for their immense coordination during my field visit in Birbhum, West Bengal. I also thank Mr. Soumyajyoti Mandal, Application Engineer of AllTerra Solution LLP, for his continuous guidance throughout the study of DGPS survey. Lastly, I am immensely grateful to Dr. Ratnadeep Ray, Assistant Professor of JIS University, for his endless support and guidance in the field of Remote Sensing and Geographical

Information System that has truly benefitted me towards the completion of my research work.

I owe a debt of gratitude to my family for their unwavering support, patience, and encouragement throughout my academic pursuits. This work would not have been possible without the collective contributions of these remarkable individuals. My parents, my sister, my brother-in-law, my uncle and also my father-in-law and mother-in-law, who are the major driving force towards this long journey. Their belief in me has been a driving force in reaching this significant milestone.

Lastly, my deepest appreciation goes to my loving husband, Mr. Anirban Dutta whose encouragement, positivity and shear inspiration that enabled me to continue with the research work and has made me focussed on my research towards its completion. In your embrace, I have found the courage to overcome, and the strength to rise. Thank you for being my guiding light and my source of inspiration.

Thank you all for being an integral part of this accomplishment.

With sincere gratitude,

Swetasree Nag

07.09.2023

Swetasree Nag

ABSTRACT

River is considered as one of the important source of fresh water. Since from the time of civilisation, the river water has been used in various purposes like agricultural activity, daily domestic needs and with further advancement of the society it also cater the need of industrial sector. It also plays a vital role in global hydrological cycle marinating the environmental balance. But this complex riverine ecosystem is getting damaged by the effect of population growth and unprecedented changes in global climatic scenario in the world (Khorooshi et al. 2015). According to the International Panel on Climate Change, 2008, about 1–5 degree centigrade temperature increase over 20–80 years, while precipitation is predicted to decrease by 5–20% in around the world. These undetermined conditions, along with uncertainty about the trend in summer rainfall create an effect on available water resources both in terms of its quality and quantity. This situation has also accelerated the imbalance between demand and supply of water resources. Since the time of World War II fresh water consumption has been increased significantly which will expect to expand another 25% in the next 25 to 30 years (Statistical Yearbook for Asia and the Pacific 2007). India has about 20 river basins of which only 4% of world renewable water resources are distributed. As the country experiences tropical monsoon climate, it receives about 4000 billion cubic metres (BCM) of average annual precipitation which is the primary source of fresh water in India (Annual flood report, 2016). However, a significant variation in rainfall has been observed both in spatially and temporarily manner. Some region like in western Rajasthan receives less than 100 mm rainfall whereas Meghalaya in North East India receives more than 1100mm rainfall in a monsoonal time. Because of such rainfall anomaly condition, major numbers of river are being now in a stressed condition. In addition to that, increasing demand from the growing population coupled with various agricultural and other economic activities generates more pressure on the existed water resources. In a large river, ecological processes are controlled by their flow variability. But in recent years, the health condition of a river faces several ecological and environmental problems in terms of its flow pattern, water quality, water availability etc. Various water footprints such as green water, blue water availability continues to be declined. As the effect of climate change, high seasonal variability and extreme weather events was occurred and degrade the natural drainage system, which create an imbalance between ecological and environmental flow of a river. In such juncture, the study on eco-environmental protection and high-quality development of a watershed has emerged as an increasingly popular subject and has drawn more academic attention, as it directly or indirectly influences the region's total economic prosperity.

Therefore, the novel approach of the current research places special emphasis on the development of comprehensive strategies through the combination of multifaceted indicators (physical, ecological, and social) which holds considerable potentiality for discovering the challenges causing overall river ecosystem deterioration and come up with a few possible conclusions that could help in restoring the ecological and social equilibrium of the river basin area.

CONTENT

Page No.

Chapter 1: Introduction 1-28

1. Introduction 1

1.1. The Concept of River Science 2

1.2. Tri-Decadal Visualization Analysis on River Health Studies: A Global Perspective 3

1.2.1. Methodology 6

1.2.2. Year-wise Publication Output 7

1.2.3. Citation Analysis 9

1.2.4. Keyword Analysis 12

1.2.5. Most Productive Countries 13

1.2.6. Research Trend Analysis 15

1.2.7. Conclusion 17

1.3. Major Drivers and Challenges in Indian River System 18

1.4. Overview of Surface Water Resources in West Bengal 21

References 26

Chapter 2: Literature Review 29-63

2. Introduction 29

2.1. Review to Literatures Based on Different Issues Related to the Mayurakshi River 29

2.2. Review of Literatures Relevant to the Research 35

2.2.1. Channel Morphological Evaluation and the Flow Variability 35

2.2.2. Impact of Land Use and Land Cover Alterations 41

2.2.3. Significance of Environmental Flow and the Riverine Ecology 46

2.2.4. Impact of Surface and Ground Water Quality 51

References 56

Chapter 3: Research Design 64-75

3. Significance of Eco-environmental Hydrological Studies 64

3.1. Need for Research in this Area 65

3.2. Research Gap 69

3.3. Research Hypothesis 70

3.4. Research Objectives 71

3.4.1. Scope of Research 71

3.5. Novelty of Research 72

References 74

Chapter 4: Methodological Framework 76-79

4. Introduction 76

4.1. Pre-field Work 76

4.2. Field Work 77

4.3. Post-field work 78

References 79

Chapter 5: Description of the Study Area 80-97

5. Introduction 80

5.1. Locational Description 80

5.2. Physical Set-up of Study Area 82

5.2.1. The Physiography 82

5.2.2. Slope 84

5.2.3. Geology 86

5.2.4. Geomorphology 87

5.2.5. Soil 87

5.2.6. Land Use Land Cover 89

5.3. Climatological Condition of the Study Area 90

5.3.1. Temperature 91

5.3.2. Rainfall 92

5.4. Hydrological Condition of the Study Area 93

5.4.1. Watershed and Sub-Watersheds 93

5.4.2. Flow Direction & Accumulation 94

References 97

Chapter 6: Assessment of the Physical Indicators of the Study Area 98-259

6. Introduction 98

6.1. Spatio-temporal Trend Analysis of Annual Air Temperature and Precipitation of Mayurakshi River Basin Area 98

6.1.1. Data Source 100

6.1.2. Methodology 100

- Mann Kendall (MK) Test 100
- Sen's Slope Estimator 101
- Innovative Trend Analysis (ITA) Test 102

6.1.3. Result and Discussion 104

- Variability and Trends in Air Temperature 104
- Variability and Trends in Rainfall 109

6.1.4. Conclusion 116
6.2. Construction of Intensity-Duration-Frequency (IDF) Curve 117
6.2.1 Data Source 118
6.2.2. Methodology 119
- Generation of the IDF curves 119
- Gumbel Frequency Distribution 119
- Log Pearson Type (LPT) III Frequency Distribution 120
- Derivation of IDF Equation 120
- Goodness of Fit Test 121
6.2.3. Results and Discussion 121
6.2.4. Conclusion 127
6.3. Morphological Character of the Channel 128
6.3.1. Database & Methodology 128
6.3.2. Results and Discussions of Morphometric Analysis 130
- Analysis of Linear Parameters 130
- Analysis of Areal Parameters 133
- Analysis of Relief Parameters 134
6.3.3. Hypsometric Analysis 135
- Results of Hypsometric analysis 136
6.4. Identification of Erosion Susceptible Zones using Morphometric Analysis 138
6.4.1. Methodology 139
- TOPSIS Model 140
6.4.2. Calculation of Rainfall Erosivity Index (R factor) to Validate the Model's Output 140
6.4.3. Prioritisation of Sub Watersheds using TOPSIS model 141
6.4.4. Validation of Model's Output 144
6.4.5. Conclusions 148
6.5. Application of Hydraulic and Hydrological Model to Study the Hydro-Geomorphological Behaviour of the Channel 149
6.5.1. Study Area 151
6.5.2. Materials and Methods 153
- Application of Manning's equation for Discharge Estimation 155
- Application of Kinematic Wave Parameter (KWP) for Discharge Estimation 158
- Evaluation of Model Performance 159
6.5.3. Results 160

- Channel Hydro-geomorphological Properties 160
- Application of Hydraulic and Hydrological Model for Discharge Estimation 165
- Model Performance Evaluation 168

6.5.4. Discussions 172

6.5.5. Conclusion 173

6.6. Assessment of Available Surface Water Resources 174

6.6.1. Data Used 175

6.6.2. Methods 175

- Normalized Difference Water Index (NDWI) 176
- Modified Normalized Difference Water Index (MNDWI) 176
- Normalized Difference Moisture Index (NDMI) 176
- Water Ratio Index (WRI) 176
- Automated Water Extraction Index (AWEI) 177
- Accuracy Assessment 177

6.6.3. Results and Discussion 177

6.6.4. Conclusion 180

6.7. Assessment of Groundwater Recharge Potential Zone 182

6.7.1. Study Area 185

6.7.2. Methodology 186

- Data Source and Preparation of the Thematic Layers 189
- Land Use Land Cover Classification 190
- Accuracy Assessment 190
- Application of Fuzzy AHP Method to Delineate Groundwater Potential Zones 191
- Validation 193

6.7.3. Results and Discussions 193

- Areal Changes in Land Use Land Cover Map from 2000 to 2018 193
- Conditioning Factors to Delineate Groundwater Potential Zones 195
- Relief (R) 195
- Slope (S) 195
- Geology (G) 196
- Lineament Density (LD) 196
- Lineament Intersection (LI) 197
- Geomorphology (GM) 197
- Hydrological Soil Group (HSG) 197

- Topographic Wetness Index (TWI) 198
- Drainage Density (D_d) 198
- Rainfall Variability (Rv) 199
- Groundwater Table Fluctuation (GWF) 199
- Land use land cover (LULC) 200
- Surface Retention (S_r) 200
- Evaluation of Groundwater Potential Zone and Its Spatio-Temporal Variations for the Year 2000 & 2018 204
- Validation of Groundwater Potential Zonation Map 207

6.7.4. Study the Functionality of Land Use Land Cover over the Shifting of Groundwater Potential Zone 210

6.7.5. Conclusion 212

6.8. Estimation of Surface Runoff 214

6.8.1. Data Used and Methodology 215

- Estimation of Curve Number (CN) 216

6.8.2. Result and Discussion 216

- Land Use Land Cover (From 1989 to 2021) 217
- Hydrological Soil Group (HSG) and Estimation of Curve Number (CN) 218

6.8.3. Conclusion 223

6.9. Land use land Cover Analysis 224

6.9.1. Data and Methodology 225

- Pre-processing and Image Classification 226
- Accuracy Assessment 226

6.9.2. Results and Discussions 227

- Analysis of LULC Image Classification and Accuracy Assessment 227
- Areal Change Detection of Land Use Land Cover Analysis 230
- Land Use Land Cover Change Matrix 233

6.10. Future Prediction of Land Use and Land Cover (LULC) using CA-Markov Chain Model (CA-MCM) 235

6.10.1. Data Used 236

6.10.2. Methodology 236

- Future Scenario Predictions Using CA-Markov Chain Model 236
- Accuracy Assessment 240

6.10.3. Result and Discussions 240

- ESRI LULC Change Analysis 240
- Prediction and Validation of LULC for 2021 242

- Projected Land Use Pattern for the Year 2031, 2041 And 2051 243

6.10.4. Conclusion 246

References 247

Chapter 7: Assessment of the Ecological Indicators of the Study Area..... 260-386

7. Introduction 260

7.1. Application of SWAT Hydrological Model on Mayurakshi River Basin.....260

7.1.1. Input Data 262

- Meteorological Data 262
- Digital Elevation Model (DEM), Land Use Land Cover (LULC), Slope and Soil data 263
- Hydrological Data 267

7.1.2. Methodology 267

- SWAT Model Set-Up..... 270
- Model Calibration and Uncertainty Analysis 270
- Model Validation 272

7.1.3. Results & Discussion 272

- Evaluation of SWAT Hydrological Model for Mayurakshi River Basin Area 272
- Sensitivity Analysis 276
- Water Balance Analysis..... 279
- Assessment of Water Availability Indicators 283

7.2.4. Conclusion 286

7.2. Assessment of Riparian Vegetation Health Quality of Mayurakshi River Basin Area …….287

7.2.1. Delineation of Riparian Zone of the Study Site..... 288

7.2.2 Material and Methods 290

- Riparian Strip Quality Index (RSQI) 291
- Land Use Land Cover Classification 291
- Qualitat del Bosc de Ribera (QBR) Index..... 292
- Normalized Difference Vegetation Index (NDVI) 293

7.2.3. Results & Discussion 294

- Riparian Strip Quality Assessment 294
- Assessment of Riparian Vegetation Quality 295
- Assessment of Normalised Difference Vegetation Index 300
- Overall Riparian Health Quality Assessment 300

7.2.4. Conclusion 304

7.3. Variations in Ecosystem Service Value in Response to the Changes in Land use Land Cover in Mayurakshi River Basin Area 305
7.3.1. Materials 306
7.3.2. Methodology 308
- Land Use Land Cover Classification and Accuracy Assessment 308
- Estimation of Ecosystem Service Value (ESV) 309

7.3.3. Result and Discussions 310
- Land Use Land Cover Dynamics 310
- Estimation of Ecosystem Service Value (ESV) 312
- Rate of Change in Total ESV 316
- Estimation of Ecosystem Service Function (ESV_f) 318

7.3.4. Conclusion 318
7.4. An Assessment of Surface Water Quality Using a Combination of Water Quality and Pollution Indices in Mayurakshi River Basin area 319
7.4.1. Location of the Study 320
7.4.2. Materials & Methodology 322
- Sample Collection and Analysis 322
- Water Quality Index (WQI) 326

7.4.3. Methodologies for Pollution Indices 327
- Comprehensive Pollution Index (CPI) 327
- Organic Pollution Index (OPI) 328
- Eutrophication Index (EI) 328

7.4.4. Results & Discussion 330
- Physico-Chemical Properties of Water Quality 330
- Pearson's Correlation of Water Quality Parameters 339
- Analysis of Pollution Indices 342
- Comprehensive Pollution Index (CPI) 342
- Organic Pollution Index (OPI) 342
- Eutrophication Index (EI) 342
- Analysis of Water Quality Index 344

7.4.5. Conclusion 349
7.5. Assessment of Groundwater Quality over the Mayurakshi River Basin Area 350
7.5.1. Methodology 351
- Integrated Water Quality Index (IWQI) 354

7.5.2. Result and Discussion 356
- Analysis of Groundwater Quality Parameters 356

- Analysis of Integrated Water Quality Index 360

7.5.3. Conclusion 362

7.6. An Assessment of Environmental Flows (EFs) Requirements of Mayurakshi River Basin Area 363

7.6.1. Conventional Methodologies for Environmental Flows Assessment (EFA). 364

7.6.2. Regulative Nature of Flow in Mayurakshi River Basin (MRB) 365

7.6.3. Hydrological Approaches Applied to Evaluate EFs 368

- Tennant Method 368
- Flow Duration Curve Method 374

7.6.4. Conclusion 376

References 377

Chapter 8: Assessment of the Social Indicators of the Study Area 387-400

8. People's Perception on Mayurakshi River and its Surroundings 387

8.1. Data Collection and Procedure 388

- Sample Size and Technique 390

8.2. People's Perceptions about the Mayurakshi River and its Surroundings 390

8.3. People's Perceptions on Riparian Health Quality of Mayurakshi River 395

8.4. Conclusion 397

References 399

Chapter 9: Final Conclusion 400-405

9. Overall Conclusion 400

Chapter 10: Recommendations 406-411

10. Recommendations 406

10.1 Limitations of the Work 410

10.2 Future Scope of Research 410

Annexure I 412-435

Annexure II 436-440

Annexure III 441-474

Annexure IV 475-481

LIST OF FIGURES

Page No.

Figure 1.1 Multidisciplinary Interaction and Feedback System of River Science (Sinha et al. 2012) 3

Figure 1.2 Surface and Ground Water Interaction 5

Figure 1.3 Year wise Variation in Total Publication Output 8

Figure 1.4 The Journal Citation Network Analyses on River Health Related Publications (1990-2020) 9

Figure 1.5 The Author's Citation Network Analyses on River Health Related Publications (1990-2020) 11

Figure 1.6 The Co-authorship Network Analyses on River Health Related Publications (1990-2020) 11

Figure 1.7 The Keyword Co-occurrence Network Analyses on River Health Related Publications (1990-2020) 12

Figure 1.8 The Country Citation Network Analyses on River Health Related Publications (1990-2020) 13

Figure 1.9 Scientific Productivity Analysis of the Top 10 Productive Countries on River Health Studies (1990-2020) 15

Figure 1.10 Mann-Kendall Trend Analysis on Research Trend of River Health Studies during 30 Years 16

Figure 1.11 Year Wise Contribution of Publications on Different Research Areas of River Health (1990-2020) 17

Figure 1.12 Maximum Water Extent of West Bengal, 2018 21

Figure 1.13 Water Occurrence Scenario in Brahmaputra River (1984-2018) 23

Figure 1.14 Water Occurrence Scenario in Eastward Flowing Rivers in West Bengal (1984-2018) 23

Figure 1.15 Water Seasonality Scenario of Sundarban (2018) 24

Figure 1.16 Water Occurrence Change Intensity in a Part of Bhagirathi River (1984-1999 & 2000-2018) 25

Figure 4.1 Methodological Framework used in this Research 76

Figure 5.1 Location Map of the Study Area 81

Figure 5.2 Google Earth View of Massanjore Dam and Tilpara barrage 82

Figure 5.3 Physiographic Division of the Mayurakshi River Basin Area 83

Figure 5.4 Long Profile of the Mayurakshi River 83

Figure 5.5 Relative Relief Map of the Mayurakshi River Basin Area 84

Figure 5.6 Slope Map of the Mayurakshi River Basin Area 85
Figure 5.7 Contour Map of the Mayurakshi River Basin Area 85
Figure 5.8 Geological Map of the Mayurakshi River Basin Area 86
Figure 5.9 Geomorphological Map of the Mayurakshi River Basin Area 88
Figure 5.10 Soil Texture Map of the Mayurakshi River Basin Area 88
Figure 5.11 Land Use Land Cover Map for 2000 and 2018 89
Figure 5.12 Mean Annual Temperature of Mayurakshi River Basin Area for the Period of 1980-2021 91
Figure 5.13 Mean Annual Rainfall of Mayurakshi River Basin Area for the Period of 1980-2021 92
Figure 5.14 Decadal Rainfall Distribution Map of Mayurakshi River Basin Area 93
Figure 5.15 Drainage Map of the Mayurakshi River Basin Area 94
Figure 5.16 Coding used for Flow Direction Raster 95
Figure 5.17 Flow Direction Map of the Mayurakshi River Basin Area 95
Figure 5.18 Flow Accumulation Map of the Mayurakshi River Basin Area 96
Figure 6.1 Location of the Meteorological Stations along with the Digital Elevation Model of Mayurakshi River Basin Area 100
Figure 6.2 Surface Layer of 40 Years of Annual Temperature (a) Distribution Map (b) Co-efficient of Variance map (c) Innovative Trend Analysis Slope Map (d) Sen's Slope Map 104
Figure 6.3 Station Wise Plots of Innovative Trend Analysis of Annual Temperature for the period of 1980-2000 (First half) and 2001-2021 (Second half) 106
Figure 6.4 Surface Layer of 40 Years of Annual Rainfall (a) Distribution Map (b) Co-efficient of Variance map (c) Innovative Trend Analysis Slope Map (d) Sen's Slope Map 110
Figure 6.5 Station Wise Plots of Innovative Trend Analysis of Annual Rainfall for the period of 1980-2000 (First half) and 2001-2021 (Second half) 113
Figure 6.6 Methodological Chart of Intensity Duration Frequency Curve 118
Figure 6.7 IDF curves by Gumbel Method for Different Gauge Stations of Mayurakshi River Basin Area 122
Figure 6.8 IDF curves by LPT III method for Different Gauge Stations of Mayurakshi River Basin Area 124
Figure 6.9 Morphometric parameters (a) Digital elevation model (b) Stream order (c) Drainage density (d) Relative relief (e) Slope (f) Length of overland flow (g) Ruggedness index (h) Dissection index 132

Figure 6.10 Hypsometric Curve with Hypsometric Integral Values of the Sub-watersheds of Mayurakshi River Basin 137
Figure 6.11 Flow Chart Showing the Methodology for the Assessment of Erosion Susceptible Zone in Mayurakshi River Basin Area.....139
Figure 6.12 TOPSIS Model Output (a) Ranking of Sub-watersheds (b) Prioritisation of Sub-watersheds based on Erosion Susceptibility of Mayurakshi River Basin Area.....144
Figure 6.13 Rainfall Erosivity Index of Mayurakshi River Basin of 2018 147
Figure 6.14 Location of the Study Area (a) Study Area (b) Location of the Cross-section Sites Over the Mayurakshi River Basin.....152
Figure 6.15 Google Earth View of the Cross-section Sites with Some Field Photographs over the Mayurakshi River.....155
Figure 6.16 (a) Trapezoidal Cross-section of Mayurakshi River (b) A Schematic Representation of an Open Cross-section Channel.....156
Figure 6.17 Variation in Channel Depth from Upstream to Downstream of Mayurakshi River during Post-monsoon Season 161
Figure 6.18 Channel Configuration of 14 different cross-sectional sites of the Mayurakshi River Basin (a) Amarpur right branch (CS 1), (b) Amarpur left branch (CS 2), (c) Asanjor (CS 3), (d) Maharo (CS 4), (e) Dudhani (CS 5), (f) Poljori (CS 6), (g) Banskuli (CS 7) 162
Figure 6.19 Comparison between the Applied Models with Respect to the Field Observed Discharge Data in the Mayurakshi River.....168
Figure 6.20 Visualisation of Surface Water Bodies of Massanjore Dam Area (a) Landsat 8 OLI image (b)NDWI (c) MNDWI (d) NDMI (e) WRI (f) AWEI results 178
Figure 6.21 Extracted Surface Water Bodies of Mayurakshi River Basin Area (a) 2000 year (b) 2018 year.....179
Figure 6.22 Extracted Surface Water Bodies from Principal Component Analysis of the Mayurakshi River Basin Area.....179
Figure 6.23 Pond Density of Mayurakshi River Basin Area (a) Year 2000 (b) Year 2018 180
Figure 6.24 Location Map of the Study Area with Observation Wells.....185
Figure 6.25 Methodological Flow Chart of the Study.....187
Figure 6.26 Influential factors for the generation of groundwater potential zonation map of the Mayurakshi River Basin: (a) Relief, (b) Average slope, (c) Geology, (d) Lineament Density, (e) Lineament Intersection, (f) Geomorphology, (g)

Hydrological Soil Group, (h) Topographic Wetness Index, (i) Drainage Density, (j) Rainfall Variability, (k) Groundwater Fluctuation, (l) Land Use Land Cover, (m) Surface Retention 201
Figure 6.27 Groundwater Potential Zones of Mayurakshi River Basin for the Period of 2000 205
Figure 6.28 Groundwater Potential Zone map of Mayurakshi River Basin for the Period of 2018..... 206
Figure 6.29 Areal Changes in Groundwater Potential Zone from the year 2000 to 2018. 207
Figure 6.30 Land Use Land Cover reconfiguration map from the year 2000 to 2018 211
Figure 6.31 Percentage Share of Land Use Land Cover Area of Mayurakshi River Basin for the Year 1989 & 2021 217
Figure 6.32 Soil Texture Map of the Mayurakshi River Basin Area 218
Figure 6.33 Hydrological Soil Group Map of the Mayurakshi River Basin Area 219
Figure 6.34 SCS Curve Number Generated Runoff Map of the Mayurakshi River Basin Area..... 220
Figure 6.35 Correlation between Rainfall and Runoff of the Mayurakshi River Basin Area for the period of 1989, 2000, 2010, 2018 and 2021..... 221
Figure 6.36 Classified Land Use Land Cover Maps of Mayurakshi River Basin Area 228
Figure 6.37 Percentage of Areal Coverage of Land Use Land Cover Classes of Mayurakshi River Basin Area..... 230
Figure 6.38 Areal Changes in 32 years Land Use Land Cover of Mayurakshi River Basin Area..... 231
Figure 6.39 Land Use Land Cover Reconfiguration Map from the year 1989 to 2021 232
Figure 6.40 Detailed Methodology Used in CA-Markov Chain Model..... 237
Figure 6.41 CA-Markov Model Transition Potential Maps (a) Digital Elevation Model (b) Slope Map (c) Euclidean Distance Map from River (d) Euclidean Distance Map from Road (e) Euclidean Distance Map from Urban Areas (f) Spatial trend of Change Map from Natural Vegetation to Agricultural Land (g) Spatial trend of Change Map from Natural Vegetation to Pasture Land (h) Spatial trend of Change Map from Pasture Land to Agricultural Land (i) Spatial trend of Change Map from Agricultural Land to Settlement (j) Spatial trend of Change Map from Agricultural Land to Pasture Land..... 238
Figure 6.42 ESRI Produced Land Use Land Cover Map of the Mayurakshi River Basin Area for the period of 2017 & 2019 241

Figure 6.43 Areal Coverage in Individual Land Use Classes for the Period of 2017, 2019 and 2021 241
Figure 6.44 (a) Observed and (b) Projected LULC map of Mayurakshi River basin area for the year 2021 242
Figure 6.45 Areal Changes of Observed and Predicted land use Land Cover Classes for the Year of 2021 243
Figure 6.46 Predicted Land Use Land Cover Map of Mayurakshi River basin area (a) Year 2031 (b) Year 2041 (c) Year 2051 244
Figure 6.47 Comparative Analysis of Areal Changes in Observed and Projected Land Use Land Cover Classes in Mayurakshi River Basin Area 244
Figure 7.1 Location Map of the Study Area Used in SWAT Model 263
Figure 7.2 Digital Elevation Model of Mayurakshi River Basin Area 264
Figure 7.3 ESRI Generated Land Use Land Cover Map (2021) of the Mayurakshi River Basin Area 265
Figure 7.4 CA-Markov Model Produced Land use Land Cover Map (2031) of the Mayurakshi River Basin Area 265
Figure 7.5 FAO Soil Map of the Mayurakshi River Basin Area 266
Figure 7.6 Flow Structure of SWAT Model Setup, Calibration and Validation of Stream Flow in Mayurakshi River Basin 269
Figure 7.7 Observed and Modelled Monthly Hydrographs of (a) Massanjore Dam for the Calibration Period (1983-2007) and Validation Period (2008-2017); (b) Tilpara Barrage for the Calibration Period (1992-2008) and Validation Period (2009-2019) 273
Figure 7.8 Scatter plots of Calibrated and Validated Models of Massanjore Dam 275
Figure 7.9 Scatter plots of Calibrated and Validated Models of Tilpara Barrage 275
Figure 7.10 Global Sensitivity Analysis (a) Massanjore Dam (b) Tilpara Barrage 277
Figure 7.11 Water Balance Ratios for Observed (2021) and Projected (2031) Period of Study 279
Figure 7.12 Water Budget Analysis for the Observed Period (1983-2021) of Study 280
Figure 7.13 Monthly Water Budget Analysis for the for the Observed Period (1983-2021) of Study 281
Figure 7.14 Water Budget Analysis for the Projected Period (2020-2050) of Study 282
Figure 7.15 Monthly Water Budget Analysis for the for the Projected Period (2020-2050) of Study 282

Figure 7.16 Schematic Diagram Showing Important Water Availability Indicators (Yuan et al. 2019) 283
Figure 7.17 Surface layers of Water Availability Indicators along with the Annual Coefficient of Variation calculated Using Calibrated SWAT Model (1983-2021) of the Mayurakshi River Basin Area 284
Figure 7.18 Demarcation of Riparian Zone (Munne et al. 2003) 289
Figure 7.19 Location of the Survey Sites along the Mayurakshi River 290
Figure 7.20 Methodological Chart of the Riparian Study 290
Figure 7.21 Land Use Land Cover Map of the Mayurakshi River's Riparian Zone (a) 1989 (b) 2021 292
Figure 7.22 Riparian Strip Quality Index of the Mayurakshi River's Riparian Zone (a) 1989 (b) 2021 294
Figure 7.23 Overall QBR Scores of the studied sites of the Mayurakshi River's Riparian Zone 298
Figure 7.24 NDVI Scores of the Mayurakshi River's Riparian Zone (a) 1989 (b) 2021 ..300
Figure 7.25 Overall Riparian Health Quality Class of the Mayurakshi River's Riparian Zone 301
Figure 7.26 Spatio-temporal Variations of the ESV based on Costanza et al. (1997) 313
Figure 7.27 Spatio-temporal Variations of the ESV based on Costanza et al. (2014) 315
Figure 7.28 Net change rates of ecosystem services for each LULC classes based on (a) Costanza et al. (1997) and (b) Costanza et al. (2014) 316
Figure 7.29 Temporal Variation in the Contribution of Ecosystem Services in the Study Area 318
Figure 7.30 Location of the Sample Sites of Surface water Quality Analysis of Mayurakshi River basin Area 322
Figure 7.31 Seasonal Variation in Selected Physico-chemical Properties of Surface Water of the Sample Sites of Mayurakshi River 335
Figure 7.32 Pearson's Correlation Matrix of Water Quality Parameters for both Dry and Wet season 340
Figure 7.33 Seasonal Variation in Different Water Pollution Indices in Mayurakshi River Basin Area (a) Comprehensive Pollution Index (b) Organic Pollution Index (c) Eutrophication Index 343
Figure 7.34 Spatial Variation in Water Quality Index for Dry Season of the Study 344
Figure 7.35 Spatial Variation in Water Quality Index for Wet Season of the Study 345

Figure 7.36 Dendrogram Results of Cluster Analysis in 17 Locations Based On Water Quality and Water Pollution Indices for the Period of Dry Season 347
Figure 7.37 Dendrogram Results of Cluster Analysis in 17 Locations Based On Water Quality and Water Pollution Indices for the Period of Wet Season 348
Figure 7.38 Location of the Sample Sites of Groundwater Quality Analysis within the Mayurakshi River Basin Area.....352
Figure 7.39 Spatial Distribution of Groundwater Quality Parameters (a) pH (b) EC (c) TDS (d) Turbidity (e) TSS (f) Alkalinity (g) Total Hardness (h) Iron (i) Chloride (j) Nitrate (k) Phosphate (l) Manganese (m) Sulphate (n) Fluoride 358
Figure 7.40 Spatial Distribution of Integrated water Quality Index in Mayurakshi River Basin Area.....361
Figure 7.41 Location of Important Civil Structures of Mayurakshi River.....366
Figure 7.42 FDC at Massanjore Dam (1983-2017).....375
Figure 7.43 FDC at Tilpara Barrage (1992-2019).....375
Figure 8.1 Population Density of the Mayurakshi River Basin Area as per Census 2011 391

LIST OF TABLES

Page No.

Table 1.1 Highly Cited Publications Output (1990-2020) 8

Table 1.2 Top 20 Highly Cited Journals on River Health Studies (1990-2020) 10

Table 1.3 Top 10 Keywords of Highly Cited Publications (1990-2020) 12

Table 1.4 Top 10 Most Productive Countries on River Health Studies in Around the World (1990-2020) 14

Table 1.5 Mann-Kendall Trend Analysis Result of River Health Studies during 30 Years 16

Table 5.1 Areal Statistics of Land Use Land Cover Classes from 2000 to 2018 90

Table 6.1 Descriptive Statistics of 40 years Air Temperature of Mayurakshi River Basin Area 103

Table.6.2 Detailed Output of Annual Temperature Trend Analysis of Mayurakshi River Basin Area 105

Table 6.3 Descriptive Statistics of 40 years Annual Rainfall of Mayurakshi River Basin Area 111

Table 6.4 Detailed Output of Annual Rainfall Trend Analysis of Mayurakshi River Basin Area 112

Table 6.5 The Values of the Parameters that are used in the Development of IDF Curve Formulas in 3 Different Provinces of Mayurakshi River Basin 126

Table 6.6 Summary of the Root Mean Square Error (RMSE) for Different Rain Gauge Stations of Mayurakshi River Basin Area 127

Table 6.7 Details of the Used Datasets 128

Table 6.8 Morphometric Parameters with Formulae 129

Table 6.9 Extraction of Linear, Areal and Relief Parameters of Mayurakshi River Basin Area 133

Table 6.10 Calculated Weighted Normalised Decision Matrix for Morphometric Parameters of Mayurakshi River Basin Area 143

Table 6.11 Extraction of Ideal Positive Solution (Vj+) and Ideal Negative Solution (Vj-) . 146

Table 6.12 Prioritisation of Sub-watersheds of Mayurakshi River Basin Area 146

Table 6.13 Result of Prioritisation Carried out for Each Sub-watersheds of Mayurakshi River Basin Area 146

Table 6.14 Variation in Mean Annual Rainfall Data in Mayurakshi River Basin Area 147

Table 6.15 Computed Data Showing the Analysis of Mean Particle Size Diameter (D50), Equivalent Sand Roughness (Ks) And Manning's Roughness Co-efficient (N) of Each Cross-section Sites of Mayurakshi River 158
Table 6.16 Important Geometrical Character of Cross-Sectional Sites of the Mayurakshi River Basin during Post-Monsoon Season 164
Table 6.17 Lean Period Velocity Measurement Using Current Meter at Different Cross-Sections of the Mayurakshi River 167
Table 6.18 Lean Period Discharge Estimation of Different Cross Section Sites of the Mayurakshi River Using Manning's Equation 169
Table 6.19 Lean Period Discharge Estimation of Different Cross Section Sites of the Mayurakshi River Using Kinematic Wave Parameter (KWP) 170
Table 6.20 Result of Model Performance Analysis 170
Table 6.21 Past Literature on Groundwater Potential Zone Analysis 184
Table 6.22 Details of the Used Dataset 188
Table 6.23 Linguistic Variables for Constructing Pairwise Comparison Matrix 192
Table 6.24 Pairwise Comparison Matrix and Derived Normalized Weight of the Selected 13 Parameters 194
Table 6.25 Areal Changes in Land Use Land Cover Classes in the Study Area from 2000 to 2018 195
Table 6.26 Relationship between Hydrological Soil Groups and Groundwater Potentiality 198
Table 6.27 Validation of GWPZ map of 2000 with CGWB Retrieved Groundwater Level Data of Mayurakshi River Basin 208
Table 6.28 Validation of GWPZ Map of 2018 with Field Observed Groundwater Level Data of Mayurakshi River 209
Table 6.29 Details of the Satellite Data used in this Study 225
Table 6.30 Areal Statistics of Land Use Land Cover Classes of Mayurakshi River Basin Area 229
Table 6.31 Areal Changes of Land Use Land Cover Classes of Mayurakshi River Basin Area 229
Table 6.32 32 Years (1989-2021) Land Use Land Cover Transformation of the Mayurakshi River Basin Area 234
Table 6.33 Details of the Land Use Categories used in this Study 236
Table 6.34 Markov Transitional Probability Matrix of LULC 2051 Used For Simulation of This Study 245

Table 6.35 Areal statistics of Land Use Land Cover Analysis of the Projected Years of 2031, 2041 and 2051 245
Table 7.1 Summary of Data Used In Model Development, Calibration and Validation in Mayurakshi River Basin 262
Table 7.2 Areal Statistics of Land Use Land Cover Classes for the Year 2021 and 2031 .266
Table 7.3 Detailed Characteristics of FAO Soil Classes of Mayurakshi River Basin Area 267
Table 7.4 Summary of statistics for the Model Evaluation 276
Table 7.5 SWAT Input Parameters Used For the Calibration of Stream Flow of Mayurakshi River Basin 278
Table 7.6 Mean Annual Water Balance Components 279
Table 7.7 Classes of habitat quality and associated scores for the QBR index (Munne et al. 2003).....293
Table 7.8 Details of the Riparian Quality of the Studied Sites of Mayurakshi River Based on QBR Values.....296
Table 7.9 Summary of Site Wise Riparian Quality Assessment of the Mayurakshi River 302
Table 7.10 Details of the Satellite Data Used in this Study 307
Table 7.11 Details of the LULC Classes along with Description of Ecosystem Service Coefficient as per Costanza et al. (1997, 2014) 307
Table 7.12 Areal Extent and the Rate of Change of the Classified LULC Types in the Study Landscape (1989–2021) 311
Table 7.13 Areal Extent and the Rate of Change of the Simulated LULC Types in the Study Landscape (2031–2051) 311
Table 7.14 Total Estimated Ecosystem Service Values (ESVs) for Classified LULC Types (1989-2021) Based on Co-efficient of Costanza et al. (1997 & 2014) 312
Table 7.15 Total Estimated Ecosystem Service Values (ESVs) for Simulated LULC Types (2031-2051) Based on Co-efficient of Costanza et al. (1997 & 2014) 314
Table 7.16 Rate of Change in Total ESV in the Study Landscape.....317
Table 7.17 Ecosystem Service Classification (Costanza et al. 1997).....317
Table 7.18 Description of the Sampling Locations for Surface Water Quality Analysis in Mayurakshi River Basin Area 321
Table 7.19 Classification of water quality based on Weighted Arithmetic WQI method (Brown et al. 1972).....327
Table 7.20 Analysed Surface Water Quality Parameters in 17 Different Locations of Mayurakshi River with Their Permissible Limits 329

Table 7.21 Surface Water Quality Parameters with Range, Average Values and Standard Deviation in 17 Different Locations of Mayurakshi River during Dry and Wet Season.....332
Table 7.22 Summary of Water Pollution Indices for both Dry and Wet Season 346
Table 7.23 Detailed Output of Cluster Analysis for both Dry and Wet Season.....348
Table 7.24 Drinking Water Quality Standards and Calculated Range Value (BIS 2012) ...354
Table 7.25 Classification criterion of IWQI. 355
Table 7.26 Descriptive Statistics of Groundwater Samples (n=228) 358
Table 7.27 Structural Details of Massanjore Dam and Tilpara Barrage 367
Table 7.28 Recommended Flow Conditions as per Tennant Method 369
Table 7.29 36 years Mean Monthly Flow (cumec) of Massanjore Dam and Tilpara Barrage 370
Table 7.30 Comparison of Recommended EFs in cumec for Massanjore Dam and Tilprara Barrage assessed through Tennant Method.....372
Table 7.31 Year Satisfying the Different Environmental Flow Conditions for Massanjore Dam and Tilpara Barrage 373
Table 8.1 Site Description for the Study of People's Perception.....391
Table 8.2 General Information of the Surveyed Respondents 392
Table 8.3 People's Perceptions about the Mayurakshi River and its Surroundings Environment 394
Table 8.4 Public Opinion on Riparian Health Quality of Mayurakshi River.....396

LIST OF PLATES

Page No.

Plate No. 3.1 Field Observations Regarding Mayurakshi River and Riparian Health Degradation (a) In stream channel sedimentation (b) Loss of riparian cover due to bridge constructions (c) Sand mining activity on the river bed (d) Channel bed deformation (e) Excessive Use of Groundwater by Submersible Shallow Pump (f) Crop Land Converted into Seasonal Fallow Land due to Lack of Water for Irrigational Purposes 68

Plate No. 4.1 Field Work (a) DGPS Survey (b) Channel Thalweg Measurement (c) VES Survey (d) Soil Infiltration Test.....79

Plate No. 6.1 Mayurakshi River Bed Condition due to Excessive Sand Mining in 2019 ...138

Plate No. 6.2 Upstream Condition of Mayurakshi River during Post Monsoon Season, 2021 163

Plate No. 6.3 Human intervention on the Mayurakshi River (a) No flow condition of river during dry season (b) Fragmented flow pattern in the downstream of Tilpara Barrage during dry season (c) Unscientific sand extraction from the river bed (d) Construction of temporary recharge pools/nullahs for river lift irrigation (e)Disturbed channel flow due to bridge construction, near Sainthia, Birbhum (f) Channel shape and size deformation due to active human interventions (g) Human induced temporary bridges are hampered the natural flow velocity of the channel, near Sainthia, Birbhum. 171

Plate No. 6.4 (a) Excessive Use of Groundwater by Submersible Shallow Pump, (b) Crop Land Converted into Seasonal Fallow Land due to Lack of Water for Irrigational Purposes 186

Plate No. 6.5 Water level measurement from a dug well using Temperature, Water Level and Conductivity Meter (TLC).....209

Plate No. 7.1 Riparian Condition near Upstream of the Mayurakshi River 299

Plate No. 7.2 Status of Riparian Corridor of the Mayurakshi River.....299

Plate No. 7.3 Degraded Riparian Quality near Mayurakshi River due to Construction of Bridges 302

Plate No. 7.4 (a)Dense riparian cover with a good flow condition (Location: Saraiya, Group A) and (b)Healthy vegetation growth with the presence of annual grasses and helophytes (Location: Sibnagar, Group A) (c) Fragmented vegetation over on the left bank and agricultural activity on the other side of the bank (Location: Bile, Group B) (d) Moderate vegetation cover with an active agricultural activity on the riparian zone (Location: Aharinagar, Group B) (e) Most degraded riparian cover due to huge settlement growth and dumping of wastes directly on the active channel (Location: Sainthia, Group C) (f)Very poor condition of the riparian zone with active human interference, large scale sand mining activity on the river bed (Location: Kultore, Group C) 303

Plate No. 7.5 Photographs showing Surface Water Collection from the Sampling Sites near Mayurakshi River.....323

Plate No. 7.6 (a) Spectrophotometer (b) Hach pH, TDS and DO probe 324

Plate No. 7.7 Photographs showing Different Phases of Groundwater Quality Analysis ...353

Plate No. 7.8 Massanjore/Canada Dam, Build in 1954 366

Plate No. 7.9 Tilpara Barrage, Build in 1976 367

Plate No. 8.1 Loss of Riparian Cover after the Construction of Bakreswar Dam 395

Plate No. 8.2 Photographs during Field Study.....397

Plate No. 10.1 Photographs Showing Field Observations 407

CHAPTER 1

INTRODUCTION

1. Introduction

Rivers constitute complex components of the Earth's ecology that represent one of the most fundamental life-sustaining processes that have preserved civilizations and are expected to be a crucial determinant of human civilizations for future sustenance. In a world where the human population is expected to nearly double by the middle of the century, and where the world is likely to be impacted by an unprecedented rate of global change, one of the main sustainability agendas will be the implementation of innovative approaches for the management of natural water resources. Civilizations have thrived in the South Asian region for more than 5,000 years, creating a population hotspot of nearly a sixth of the world's population. As a result, considerable human interventions and impacts on the region's freshwater systems have occurred. Therefore, a holistic approach must be taken to comprehend the interrelationships between land, water, and people in order to ensure water security in this area of the world.

River is considered as one of the important source of fresh water. Since from the time of civilisation, the river water has been used in various purposes like agricultural activity, daily domestic needs and with further advancement of the society it also cater the need of industrial sector. It also plays a vital role in global hydrological cycle marinating the environmental balance. But this complex riverine ecosystem is getting damaged by the effect of population growth and unprecedented changes in global climatic scenario in the world (Khorooshi et al. 2015). According to the International Panel on Climate Change (Bates, Kundzewicz, Wu, & Palutikof, 2008), about 1–5 degree centigrade temperature increase over 20–80 years, while precipitation is predicted to decrease by 5–20% in around the world. These undetermined conditions, along with uncertainty about the trend in summer rainfall create an effect on available water resources both in terms of its quality and quantity. This situation has also accelerated the imbalance between demand and supply of water resources. Since the time of World War II fresh water consumption has been increased significantly which will expect to expand another 25% in the next 25 to 30 years (Statistical Yearbook for Asia and the Pacific 2007). India has about 20 river basins of which only 4% of world renewable water resources are distributed. As the country experiences tropical monsoon climate, it receives about 4000 billion cubic metres (BCM) of average annual precipitation which is the primary source of fresh water in India (Annual flood report, 2016). However, a significant variation in rainfall has been observed both in spatially and temporarily manner. Some region like in western Rajasthan receives less than 100 mm rainfall whereas Meghalaya in North East India receives more than 1100mm rainfall in a monsoonal time. Because of such rainfall anomaly condition,

major numbers of river are being now in a stressed condition. In addition to that, increasing demand from the growing population coupled with various agricultural and other economic activities generates more pressure on the existed water resources. In such juncture, the study on eco-environmental protection and high-quality development of a watershed has emerged as an increasingly popular subject and has drawn more academic attention, as it directly or indirectly influences the region's total economic prosperity.

1.1. The Concept of River Science

Understanding the intricacies of river systems and how they interact with the environment is the goal of the interdisciplinary and dynamic discipline of river science. Researchers support the management, conservation, and sustainable use of these crucial natural resources by studying rivers from a variety of scientific viewpoints. River science is the study of many processes that have an impact on river systems. The explicit integration of two or more fields of knowledge into a unified conceptual-empirical structure is necessary because this is a really interdisciplinary science (Pickett et al. 1995). The study of how hydrological, geological, chemical, and ecological processes interact to affect the form and dynamics of riverine systems and how riverine ecosystems in turn influence these processes at different spatial and temporal scales is an all-inclusive definition outlined in a recent report published by the National Academy of Science (NAS 2007). Three topical areas in river science—environmental flows and river restoration, sediment transport and geomorphology, and groundwater-surface water interactions—have been identified in the NAS (2007) study and may require further attention on a worldwide scale. Additionally, Sinha et al. (2013) said that the river needs its "own space" in order to carry out operations like flooding and floodplain development. Therefore, technological interventions should be carried out using a comprehensive strategy that takes into account all facets of river systems. The interactions between the many disciplines and the feedback from the riverine ecology are depicted in figure 1.1, which also exemplifies the idea of River Science. Integration of the available knowledge across the various scales will be necessary for a thorough understanding of river processes and morphology.

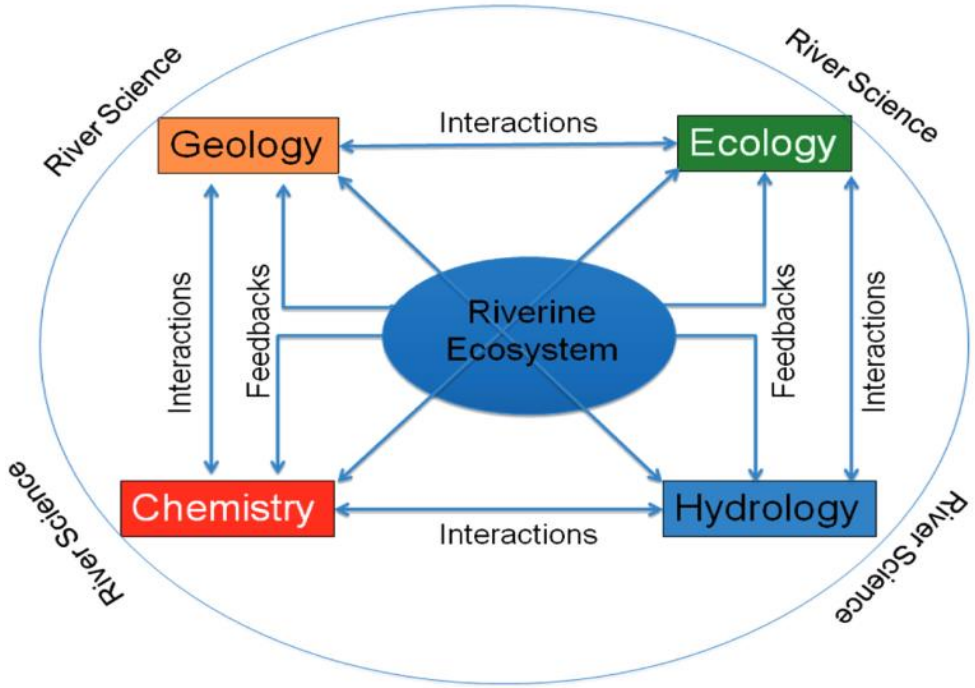

Figure 1.1 *Multidisciplinary Interaction and Feedback System of River Science (Sinha et al. 2012)*

1.2. Tri-Decadal Visualization Analysis on River Health Studies: A Global Perspective

Management of water resources scenario both for surface and ground water resources have been a global concern in a recent decade. The impact of global climate change poses a serious threat to the water resources of the world. Both the ground and surface water hydrology alteration has turned to be an immediate challenge to humankind. Such kinds of alterations in water resources may result in environmental degradation in terms of quality, quantity, flow pattern, water availability, and other environmental aspects. Furthermore, overexploitation and unscientific use of water resources may lead to almost no flow condition in a river during the dry season period (Vörösmarty et al. 2010). Keeping this detrimental issue in mind, the survival of rivers has turned to be an immediate challenge to the humankind (Kumar 2018). To sustain a river basin for a long run, priority wise assessment of the critical areas has been regarded as an important approach to maintain its physical environment and overall health status of the area (Nag et al. 2020).

Rivers are the lifeline of human society. From the period of human civilization, river water plays a vital role in controlling its ecological, social, and economic value for the environment. But excessive human interruptions are deteriorating the fitness of rivers in terms of its physical, chemical, and biological health. At such juncture, the concept of river health has arrived which

focused on the maintenance of the inherent character of the river system and also the management and restoration into an undisturbed environment (Clean Water Act, 1972). To protect the dynamic nature of the river system Nandi et al., (2016) proposed a comprehensive model on River Health Assessment (RHA) which encompasses with numerous influential aspects of river system management like Catchment Health (CH), Floodplain Health (FPH), River Channel Health (RCH), Flow Health (FH), River Water Quality Health (QH) and Biotic Health (BH). Humans are the prime users of river water. Various point and non-point sources of contamination are responsible for the degeneration of the river health condition. Figure 1.2 shows the major contributing sources of waste materials coming from industries, agricultural fields, and domestic sectors which pollutes the river water quality and hampers the ecology. This impure surface water is percolating into the deeper layer of the aquifer and contaminating the groundwater sources which are again used by the inhabitants for their daily uses. Through such kind of surface and groundwater interaction, pollutants are degrading both surface and groundwater hydrology. Not only that, construction of dams and reservoirs, channel diversion, river bed modification are also detrimental for maintaining the catchment health as well as the biotic health causing a no-flow condition of the river system. Several researchers are focusing on the assessment of ecological and environmental flow to sustain the health of the river in the long run. Yang et al. (2009) conducted a study to determine the minimum required flow levels to maintain the different ecological functions and sustain the river for a long period. Minjian et al. (2012) carried out a study on the Liao basin in China to calculate the minimum flow that will sustain the low flow channel and also sustain the aquatic ecosystem. Verma et al. (2015) also conducted a study on environmental flow variability using three different hydrological methods in the sub watershed of the Damodar River basin. However, the development of holistic methodologies by a combination of multidisciplinary information has great potential to quantify the environmental flow requirements (Hao et al. 2016). Karimi and Eslamian, (2012) conduct a study by applying a newly developed hydrological method i.e. Flow Duration Curve (FDC) shifting to investigate potential environmental flows in a river reach of Shahr Chai River in Iran. The results were also compared with the other methods to validate the minimum flow to maintain the basic functions of the river ecosystem. But the direct consequences of human activities affect the river channels through the flow variability and water consumption pattern (Gregory 2006). Apart from this Liu et al. (2017) considered the climatological extremities which affect water scarcity observed over the Euro-Mediterranean region. To understand the behavior of total stream flow for changing climatic scenarios, the use of a daily snowmelt runoff model has also been analyzed for the enhancement of the health

of a river basin (Sarkar 2015). Other than that, Makokha et al. (2016) addressed various indices to minimize the effect of climatological harshness like rainfall, snow, and glacier melt (RSC) standardized anomaly index. Other than the climatic hazards, various anthropogenic activities are also responsible to modify the natural flow of water and degrade its overall health status (Zhang et al. 2018). Various structural constructions such as a dam, barrages impound the natural flow of a river and increase the bed load materials within the channel, which ultimately promotes the formation of bars and increase the channel sinuosity (Evans et al. 2007). Pal et al. (2012) stated that the asymmetric pattern of channel width and depth, riverbank instability, huge siltation are the major outcome of the strong human interference on the channel flow. Such river impounded structures also affect the natural flow rate of the river and may hamper its discharge capacity (Ghosh and Pal 2015).

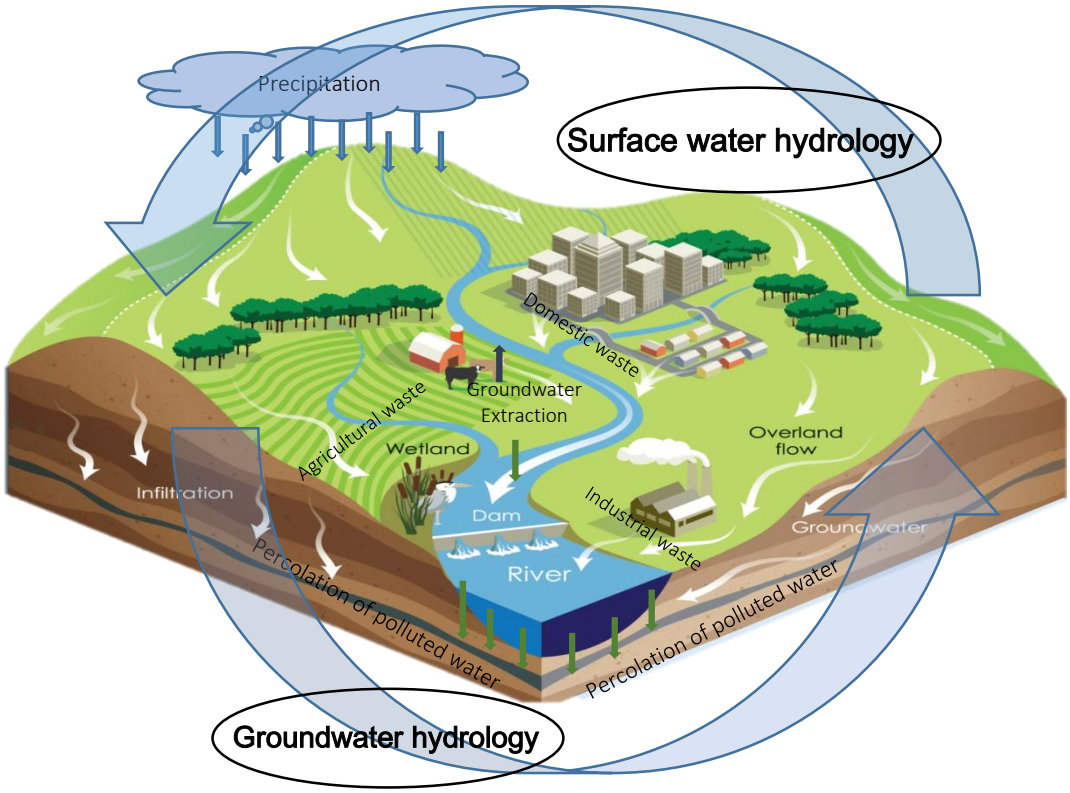

Figure 1.2 *Surface and Ground Water Interaction*

So, focusing on these above-mentioned problems related to water resource management or maintaining the health of riverine hydrological condition, there have been relatively growing research interest has been observed in this field. Therefore to observe the research trend of those studies bibliometric research can be implemented. To assess the global research trend on a specific discipline or to observe the publication material qualitative and quantitatively and also to predict the future research trend, a bibliometric study can be regarded as an important

tool to fulfill such kind of research goal (Cherng et al. 2015). Bibliographic studies have been done through various aspects like publication classification, citations, co-authorship details, important keywords, productive countries, etc. (Ahmi and Mohamad, 2019). Zhai and Ho (2018) made a bibliometric study on controlled publications. Zhang et al. (2018) studied bibliometric analyses on ecosystem services to visualize the global trend and researchers' network on that particular topic. Liao et al. (2018) have done a study focusing on the development and trend of research on medical big data through bibliometric analyses. Not only that, for the assessment of the most influential document in a specific study or the frame the structure of the field of research Aibar et al. (2019) executed bibliometric analyses on socially responsible funds. All these studies reveal a panoramic view of the overall research growth in any kind of scientific discipline which may also provide the future research trend as well.

In this present work, the study focuses on a bibliometric analysis of the global research trends in the field of river health assessment based on highly cited articles for the last three decades (1990-2020). However, there are various dichotomies regarding the definition of highly cited articles. Here, a citation threshold value of more than 100 times has been taken to refer to the highly cited articles (Barbosa and Schneck 2015; Fu and Ho 2016; Khan and Ho 2012). This kind of study will provide a systematic and conceptual review that will encourage future researches to conduct various studies scientifically.

1.2.1. Methodology

The data used in this study has been downloaded from Scopus online databases, one of the largest databases from Elsevier having extensive coverage of research publications and information related to all the cited authors in the reference section more accurately (Zupic and Cater 2015). However, to avoid the impact of other sources on the output of the analysis, Web of Science; Google Scholar has not been considered in this particular study. The authors have accessed the Scopus database on 17th May 2020 to gather research publications on river health for the last 30 years. All the publications related to river health studies have been derived using the term “river health” in the title section. The document types have been defined to all types, which show a total of 3726 documents. By adopting the threshold value of more than 100 times citation (Barbosa and Schneck 2015; Fu and Ho 2016; Khan and Ho 2012), 147 publications have been retrieved, which shows 3.95% to the total publications. The list of various types of retrieved documents is shown in table 1.1.

Major information like authors name, affiliations, subject, publication year, journal name, citations, and countries have been subsequently extracted for fulfilling the objective of this paper. Various indices like Total Citation since Publication to the end of 2020 (TC2020), Citation per Publication (CPP), Number of Author per Publication (AU/TP) has been calculated as well (Zhai and Ho 2018). Finally, a set of network analysis has been performed here using VOSviewer software (www.vosviewer.com). This software has been developed by Van Eck and Waltman in the year of 2010 and recognized as a powerful tool to analyse and visualize different kinds of bibliometric information (Liao et al, 2018; Zhang et al, 2018; Aibar et al, 2019). The following network analysis has been employed using this advanced software system - Co-authorship network analysis, Co-occurrence of all keywords, Citation analysis of source, authors, and countries accordingly. Finally, to understand the year wise research growth or the emergence of river health studies, a non-parametric Mann-Kendall statistical technique (Mann 1945) has been executed on the number publication within the period of 1990 to 2019. Due to the incompletion of the year 2020, the data of this current year has been excluded from the trend analysis. This method assumes two types of hypothesis conditions- null hypothesis (no trend) and the alternative hypothesis (increasing/ decreasing trend). Applying the significance level at 0.05, the Mann-Kendall S statistics have been computed using the following equation 1.1.

$$S = \sum_{i=1}^{n=1} \sum_{j=i+1}^{n} sig(X_j - X_i) \quad (1.1)$$

Where X_j and X_i are the independent variables and n is the period of the dataset.

Also to find out the magnitude and intensity of the trend, Sen's slope (Sen 1968) has been estimated to apply the following equation 1.2.

$$T_i = \frac{X_i + X_k}{j-k} \quad (1.2)$$

Where X_i and X_k represented as variables of the dataset.

1.2.2. Year-wise Publication Output

Figure 1.3 shows a year-wise publication related to river health studies around the world. About 3729 documents have been identified from the Scopus database from 1990 to 2020. It has been observed that the annual number of documents gradually increases with the expansion of the period (Fig. 1.3). In addition to that, due to the combined effect of rapid publication throughout the period, the citation per publication (CPP) has also varied in each year (Fig. 1.3). In this 21st

century, river health-related works have been growing progressively, accelerated by the development of modern methods and techniques of research work.

Among 3726 documents, highly cited publications were sorted out by applying a threshold of more than 100 times cited documents as mentioned earlier. In doing so about 147 publications have been retrieved from the mentioned database. The types of highly cited publications with their percentage of publication, Total Citation of 2020, Number of Authors, and Number of Author per Publication have been tabulated in table 1.1. Table 1.1 shows, among the 147 extracted documents, articles were the mostly dominated document type with the number of 124 and 84% of total publications, followed by conference paper (8.84%), review (4.76%), etc. Based on the number of the authors, per publication variation in authors number has also been calculated for each document type shown in table 1.1.

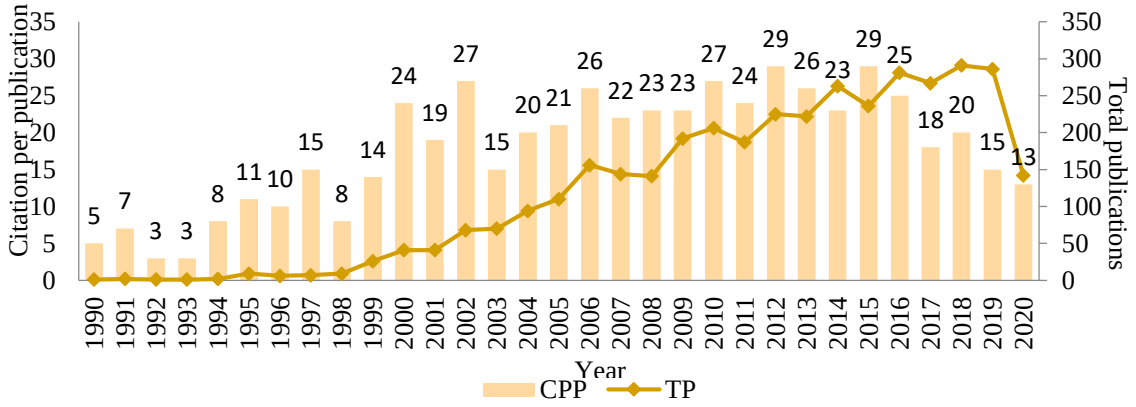

Figure 1.3 *Year wise Variation in Total Publication Output*

Table 1.1 *Highly Cited Publications Output (1990-2020)*

Document Type	***TP**	**TP%**	**TC 2020**	**AU**	**AU/TP**
Article	124	84	28773	476	3.84
Conference Paper	13	8.84	34	23	0.57
Review	7	4.76	10	8	1.14
Book Chapter	2	1.36	4	6	3.00
Book	1	0.68	5	5	5
Total	147	100	-	-	-

*TP: Total number of publications; TP%: Total number of publication in %; TC2020: Total citation since publication to the end of 2020; AU: Number of authors; AU/TP: Number of author per publication

1.2.3. Citation Analysis

Citation analysis has been considered as one of the significant methodology adopted in bibliometric research. This kind of analysis can help to visualize the most influential documents in any field of research following which some advanced research trends or some innovative management approach can be established (Aibar et al, 2019). Using VOSviewer software the following types of analysis have been done.

In this work, more than 100 times cited publications on river health studies have been selected for qualitative analysis. Table 1.2 shows the top 20 journals on river health having a high citation index where freshwater biology journals ranked 1st both in terms of document publication and citation score. All the journals listed in the following table having maximum citation scores indicate more productive journals for publications on river health research. Most of the journals identified with high document publications and citation value are focuses on interdisciplinary studies in connection with the environment, ecology, and aquatic environment which ultimately promotes the priority areas of river health studies on which the researchers and scientists are working. Figure 1.4 shows a network analysis of most cited sources of river health studies where the size of the bubble indicates the number of citations received. Different colours represent different clusters of sources which mainly formed based on their similarity of occurrence. As per the size of the bubble, the journal freshwater biology has the dominant one which received a maximum citation from the others and also has the highest link strength (183) with 35 documents followed by the journal of the North American Benthological Society having link strength of 51 with 8 documents and Hydrobiologia having link strength of 42 with 7 documents.

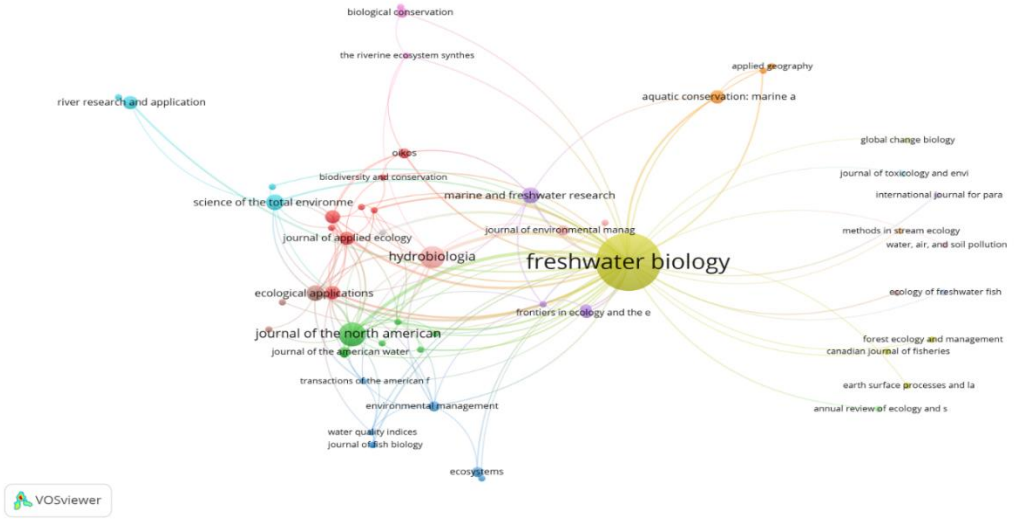

Figure 1.4 *The Journal Citation Network Analyses on River Health Related Publications (1990-2020)*

Table 1.2 *Top 20 Highly Cited Journals on River Health Studies (1990-2020)*

Sl. No	Journal Name	No. of Documents	Citation
1	Freshwater Biology	35	983
2	Hydrobiologia	7	632
3	Journal of The North American Benthological Society	8	594
4	Ecology	2	387
5	Canadian Journal of Fisheries And Aquatic Sciences	1	285
6	Ecological Applications	4	221
7	Bioscience	1	208
8	Environmental Management	2	191
9	Science of The Total Environment	4	179
10	Limnology and Oceanography	1	159
11	Transactions of the American Fisheries Society	1	145
12	Freshw. Biol.	1	133
13	Geomorphology	1	123
14	River Research and Applications	3	123
15	Water Resources Research	1	123
16	Regulated Rivers: Research and Management	1	116
17	Nature	1	113
18	Oikos	2	111
19	Archiv fur Hydrobiologie	1	108
20	Marine and Freshwater Research	4	90

Author co-citation analysis has also been done on highly cited publications related to river health studies which can provide a scenario of the intellectual structure of any scientific publication (White and Griffith, 1981). A total of 480 authors have been identified in the 147 highly cited publications on river health. The VOSviewer software creates 15 clusters of all 480 authors which are signified by individual colours (Fig. 1.5). The size of the orange cluster shows the author ‘allan j.d’ has got the maximum citation (3179) from all the 147 highly cited publications having total link strength of 104. Such kind of link strength represents a strong co-citation relationship with other connected 85 authors. Similarly, the author named as ‘bunn s.e’ and ‘arthington a.h’ have got the following positions based on their citation score.

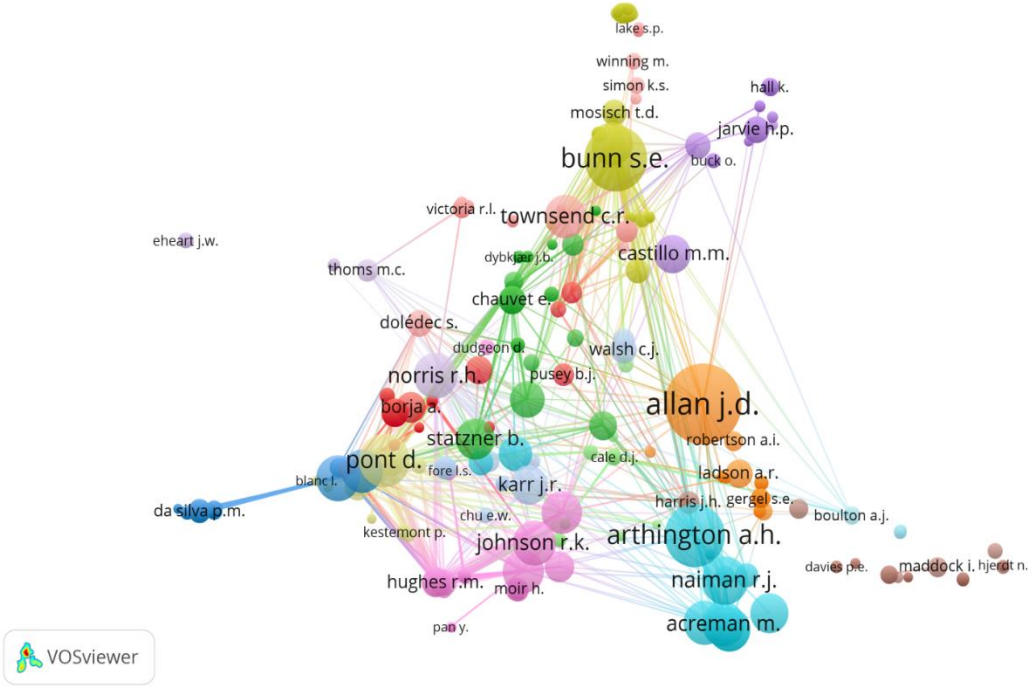

Figure 1.5 *The Author's Citation Network Analyses on River Health Related Publications (1990-2020)*

To interpret the interconnection between all authors or the co-authorship network in detail, another analysis has been performed in VOSviewer software. Among all 480 authors identified from the highly cited publications on river health, 78 authors have a minimum of 2 documents published together (Fig. 1.6). The clusters show among these 78 authors, 59 are well connected. The size of the red cluster indicates that the author named as 'bunn s.e' have the highest link strength (25) with the 16 authors followed by the blue cluster surrounded by the author named as 'pont d' having a link strength of 18 with other 11 authors from violet, blue and yellow clusters.

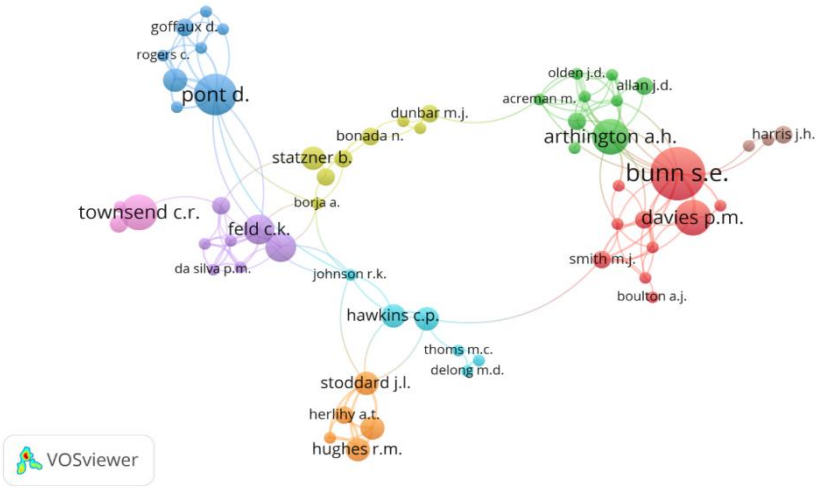

Figure 1.6 *The Co-authorship Network Analyses on River Health Related Publications (1990-2020)*

1.2.4. Keyword Analysis

To visualize the core research terminology used in river health studies authors have done another network analysis map based on co-occurrence of all keywords obtained from the highly cited publications. Such a kind of analysis can help to visualize the research trend in different disciplines around the world (Li et al. 2016).

Table 1.3 *Top 10 Keywords of Highly Cited Publications (1990-2020)*

Keywords	Frequency of occurrences	Total link strength
Invertebrata	26	129
Environmental monitoring	21	145
Fish	20	118
River	19	93
Rivers	19	117
Water quality	19	122
Biodiversity	17	97
Ecosystem health	17	91
Stream	15	75
Ecology	14	93

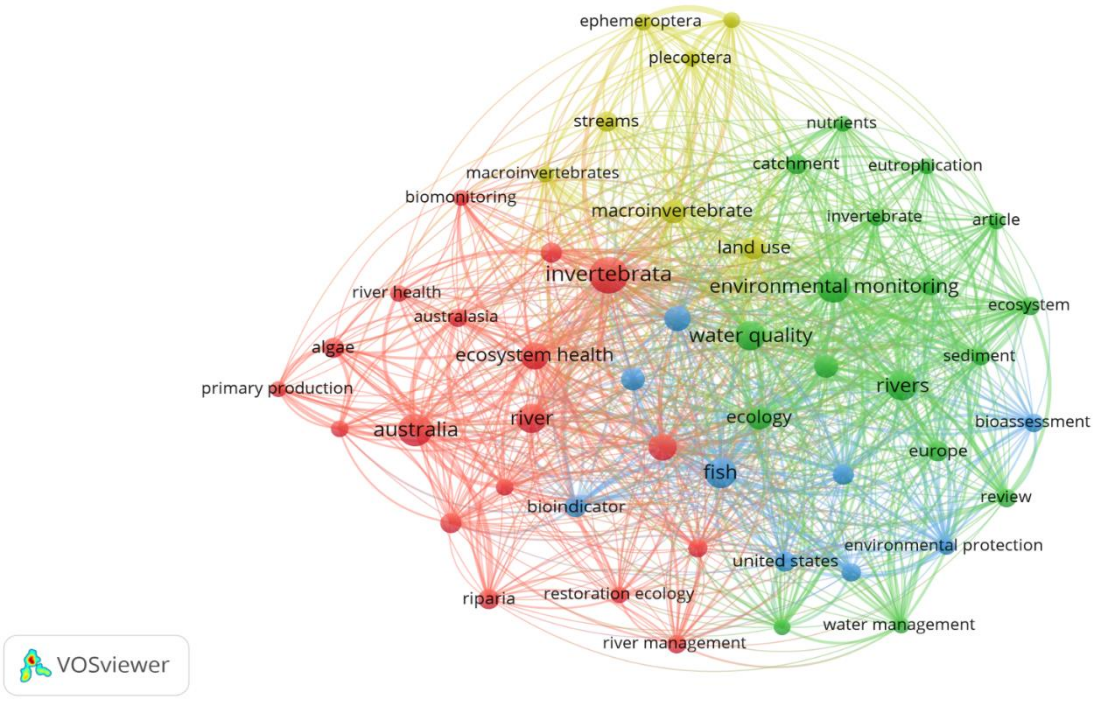

Figure 1.7 *The Keyword Co-occurrence Network Analyses on River Health Related Publications (1990-2020)*

In this study, the co-occurrence of all keywords of river health research has been produced by VOSviewer software shown in figure 1.7 from which four types of clusters have been noticed in the form of red, yellow, green, blue colors. The size of the bubble and words denotes the weights of the words whereas the lines between all keywords represent the frequency of occurrence. The thick line between two keywords indicates more frequently used keywords than the other ones. A keyword used for more than 5 times has been visualized from the figure 5 where the word 'invertebrata'(26) has the highest frequency of co-occurrence followed by 'environmental monitoring' (21), 'fish; (20), 'rivers' (19), 'water quality' (19), etc. However, table 1.3 shows the link strength of 'environmental monitoring' (145) has higher than the word 'invertebrata' (129) representing the cluster as denoted by green color have more frequency of co-occurrence with the remaining 3 clusters.

1.2.5. Most Productive Countries

Based on the number of publications, the top 10 most productive countries have been sorted out and ranked them from 1 to 10. Table 1.4 shows there ranking and % of total publications, single-author articles, corresponding author articles, and internationally collaborative articles. The United States ranked 1st in the publication of documents on river health research with 53 publications, followed by Australia (39), France (20), United Kingdom (10), etc (Figure 1.8 and Table 1.4). The United States published 36.05% of total publication with the highest citation (13674) since publication to the end of 2020. In the other category like CPR %, RPR%, SPR%, the United States stands in the top position which indicates the highest number of publications through various modern methodologies.

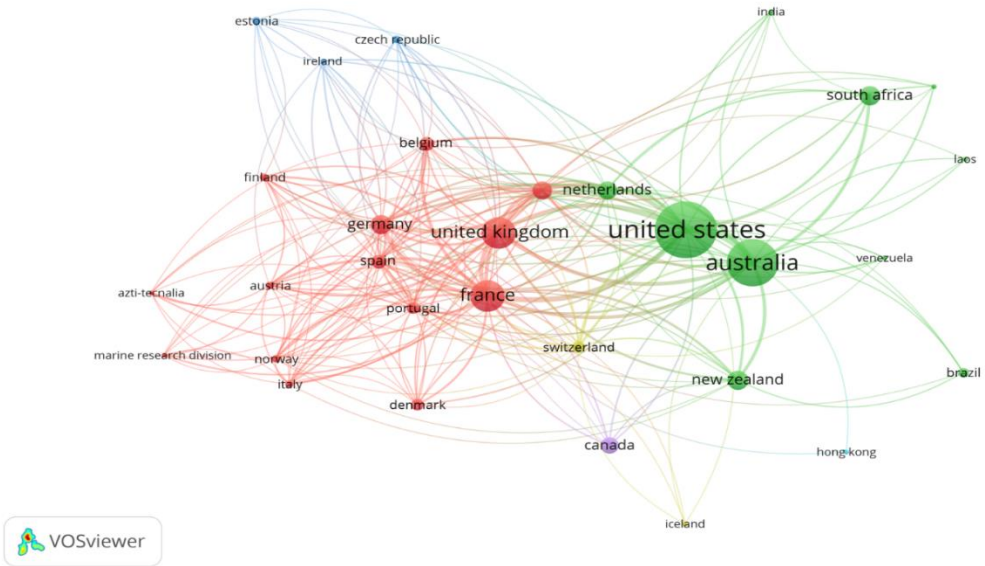

Figure 1.8 *The Country Citation Network Analyses on River Health Related Publications (1990-2020)*

Table 1.4 *Top 10 Most Productive Countries on River Health Studies in Around the World (1990-2020)*

Country	***TP**	**TP %**	**TC 2020**	**TPR %**	**CPR %**	**RPR %**	**SPR %**	**CPP**
United States	53	36.05	13674	1 (36.05)	1 (31.25)	1 (27.3)	1(23.8)	258
Australia	39	26.53	8337	2 (26.53)	3 (18.8)	2(16.5)	3(9.5)	213.77
France	20	13.61	4412	3 (13.61)	4 (18.8)	3(14.2)	4(9.5)	220.60
United Kingdom	10	6.80	5002	4 (6.80)	2 (28.6)	4(8.5)	2(21.9)	500.20
Germany	9	6.12	1937	5 (6.12)	6 (6.25)	5(6.8)	5(9.5)	215.23
New Zealand	4	2.72	1468	6 (2.72)	5 (12.5)	6(6.8)	6(4.8)	367
South Africa	4	2.72	2148	7 (2.72)	7 (3.1)	7(4.5)	7(4.8)	537
Netherlands	3	2.04	2149	8 (2.04)	8 (3.1)	8(2.3)	8(0)	716.33
Sweden	3	2.04	2476	9 (2.04)	9 (0)	9(2.3)	9(0)	825.33
Canada	2	1.36	1487	10 (1.36)	10 (0)	10(1.1)	10(0)	743.50

*TP: Total number of publications; TP%: Total number of publication in %; TC2020: Total citation since publication to the end of 2020; TPR%: rank and the percentage of total publications; CPR%: rank and the percentage of internationally collaborative articles; RPR%: rank and the percentage of the corresponding author articles; SPR%: rank and the percentage of the single author articles; CPP: citations per publication (CPP = TC2020/TP).

To visualize the degree of communication between the countries, a country citation map has been developed by VOSviewer software (Fig. 1.9). The size of the bubble and highest link strength proves that the United States (272) have more research interest on river health studies among the researchers and scientist resultant highest collaborative work with the remaining countries. Furthermore, the authors have also tried to perform an analysis considering the number of researchers working in this field per country. The figure 1.9 shows Australia (53) which has got 2nd ranking in the case of several highly cited publications, have the highest number of researchers involved in river health-related studies. Whereas the United States (49) has acquired the 2nd position followed by France (26), United Kingdom (19) and so on depicting the strength of countries' scientific productivity.

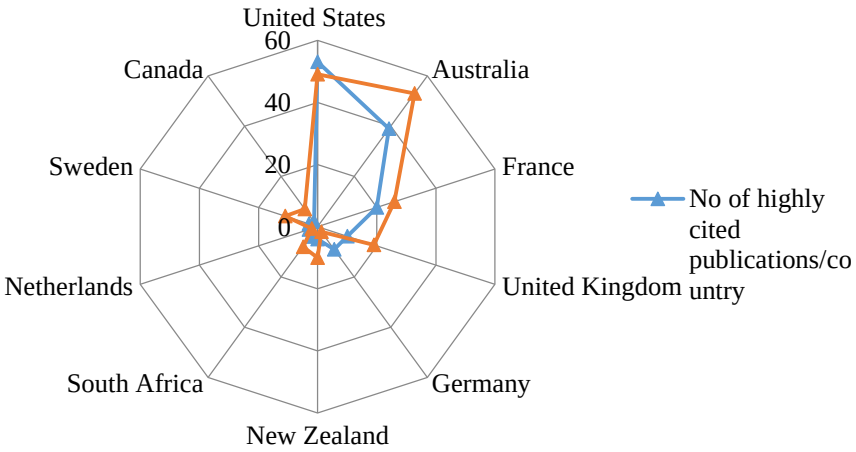

Figure 1.9 *Scientific Productivity Analysis of the Top 10 Productive Countries on River Health Studies (1990-2020)*

1.2.6. Research Trend Analysis

Finally, to detect the statistically significant research trend on river health studies, a rank-based non-parametric Mann-Kendall method has been applied from 1990 to 2019. The year 2020 has been excluded from this analysis because of the incompletion of the year. This method is very common in handling environmental time-series data and one of the major usefulness is it does not require a normally distributed dataset. Mann-Kendall (Mann, 1945) formulated such a statistical trend analysis method where the outliers within the dataset do not affect the output. Here, two hypotheses have been taken into consideration, one is the null hypothesis (H_0) indicating no trend and another is an alternative hypothesis (H_1) depicting an increasing or decreasing trend within the dataset. In this study, the hypothesis has been tested at a significant level of 0.05 for the dataset and the output of the analysis has presented in the following figure 1.10 and table 1.5. The result of the Mann-Kendall test suggests that the two-tailed p-value (<0.0001) is lower than the significance level (alpha= 0.05), hence the null hypothesis (H_0) has been rejected. On accepting the alternative hypothesis (H_1), a statistically significant positive trend has been observed in the research trend on river health studies. With the advancement of time, the number of publications on river health studies has increased showing a perfect correlation with both variables (Kendall's tau= 0.931).

In the early decades, the studies related to river health assessment has been dominated by various ecological aspects, where the value of biotic integrity (Harris and Silveira, 1999), benthic metabolism (Fellows et al. 2006), fish-based index (Harrison and Whitfield, 2004)

played a major role to maintain the riverine ecosystem health. Afterward, researchers were shifted towards the studies related to different aspects of physical factor like the effect of temperature variation in the aquatic environment (Buisson et al. 2008), various landscape approaches to study the health of the aquatic ecosystem, the impact of river discharge and sediment clogging (Li et al. 2011), the impact of climate change, etc. Such progression in river health studies may capture more interest of the scientists and researchers and is rapidly recognized as an emerging field of multidisciplinary research with its conceptual development.

Furthermore, a statistically significant non-parametric trend line approach has been executed using the Mann-Kendall test which shows a positive trend line exhibited in the year wise total publication on river health studies. At a significance level of 0.05, the null hypothesis of no trend has been rejected to prove the growth of rapid research interest in this emerging field. However, there are some research gaps have been observed. With the progression of research published during the last 30 years, the community developmental aspect to manage the river health status is missing. People are using the river water to cater to their daily needs and degrade the quality of water as well. The monitoring of such unscientific activities is needed to be addressed in future studies.

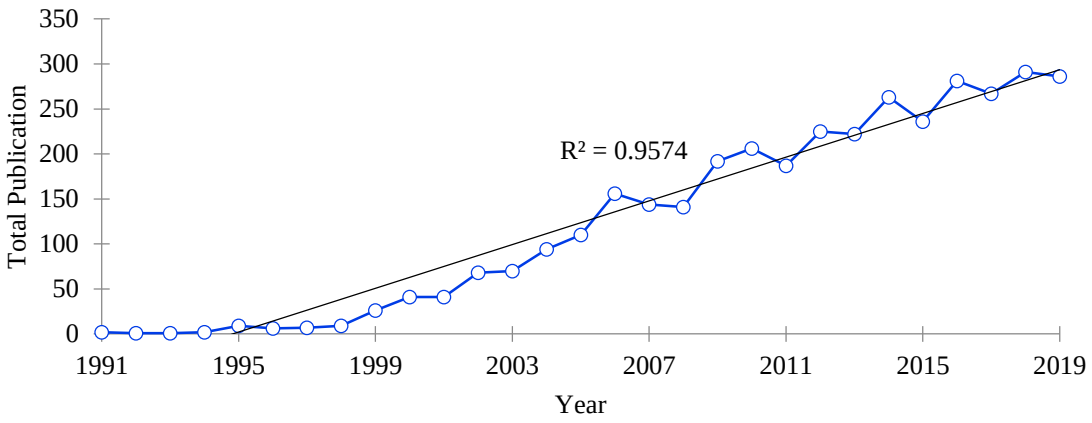

Figure 1.10 *Mann-Kendall Trend Analysis on Research Trend of River Health Studies during 30 Years*

Table 1.5 *Mann-Kendall Trend Analysis Result of River Health Studies during 30 Years*

Kendall's tau	0.931
S	376.00
Sen's slope	12.50
p-value (Two-tailed)	< 0.0001
alpha	0.05

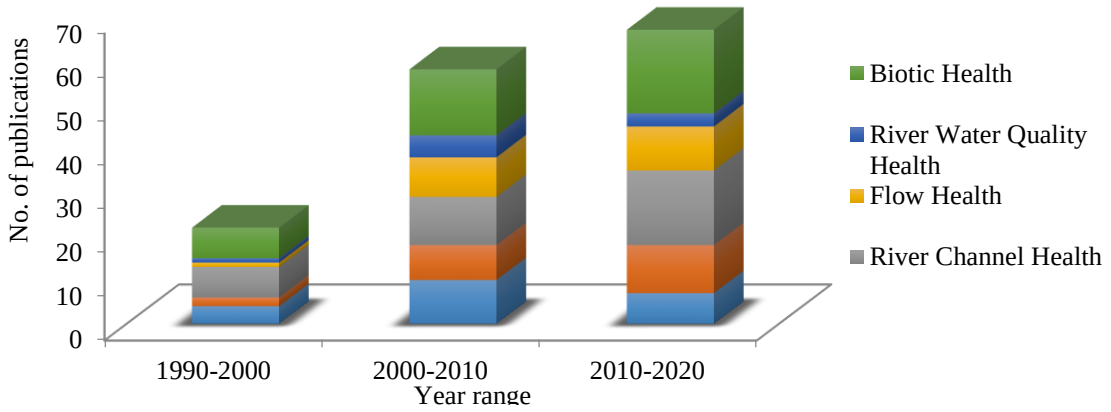

Figure 1.11 *Year Wise Contribution of Publications on Different Research Areas of River Health (1990-2020)*

Also to observe the temporal changes in the research area in river health studies, all the highly cited publications have been grouped into six thematic classes of river health assessment (RHA) which are Catchment Health (CH), Flood plain Health (FPH), River channel Health (RCH), Flow Health (FH), River Water Quality Health (QH) and Biotic Health (BH) (Nandi et al. 2016) shown in Fig. 1.11. The graph shows a considerable increase in research interest on river channel health and biotic health among the researchers whereas the studies focussing on river water quality has been rundown within the studied period.

Despite such applicability of environmental and ecological perspective, the community development approach needs to be considered in the field of river health assessment. In this era, people are facing challenges to restore the stream water quality because of the growing dependency of river water for fulfilling their domestic as well as agricultural and industrial needs. The generated waste from those sectors has dumped their untreated material into the river and degrades the water quality resulting in the decaying of the channel (Kozaki et al. 2017). Despite dumping their untreated materials, recycling of that grey water can be made possible by utilizing in pisciculture, landscape developmental activities, etc. Therefore, it is needless to say that the restoration of river health status in terms of the societal development approach should be maintained and managed in the near future.

1.2.7. Conclusion

A bibliometric investigation has been made on highly cited paper related to river health condition during the period of 1990 to 2020. The database has been extracted from online

Scopus databases. Using the term “river health” about 3726 documents have been found where 147 publications are identified as highly cited papers. These highly cited papers are categorized by applying the threshold value of more than 100 times cited documents. Among all the document types article has been the most dominant one. Various pre-defined indexes were executed here for both quantitative and qualitative evaluation of the publications like CPP, TP, AU, AU/TP, etc. Various knowledge mapping techniques have been applied here using VOSviewer software for better visualization of bibliometric information of Scopus indexed highly cited publications. A gradual increase in the annual trend of the total publications on river health studies shows growing popularity in this research topic across the world. Country-wise citation analysis provides the top 10 most productive countries, among them the United States has been considered as a leading country in terms of total publication and citation in the field of river health condition. Not only in publication rate, in the case of internationally collaborative and corresponding author articles the United States remains in the 1st position followed by Australia, France, and other countries. However, Australia acquired the 1st position in case of the total strength of researchers working in this field. Apart from these, analyses of most frequently used keywords, identification of highly cited journals, assessment of authorship links can provide a picture of worldwide research trends on river health studies. Besides that, a lack of field-based applications has been observed significantly. The use of modern statistical techniques, application of remote sensing and GIS, and various models were highly dominant out of all publications rather than the real-time field study. In that case, to study the dynamicity of river health status at a micro level around the world, some online monitoring system can be implemented in a field-level so that researchers can obtain some continuous data for better output and applications in future studies.

Despite these interesting outcomes of this study, some of the limitations need to be mentioned. Scopus online database has only been used for the collection of initial data where other sources like Web of Science, Google Scholar have been ignored which may have an impact on the output of this study.

1.3. Major Drivers and Challenges in Indian River System

Given the significance of rivers as a significant source of fresh water and the increasing need for the same, there has been an unprecedented global deterioration of river systems, along with substantial concerns about biodiversity and water security. Ironically, environmental processes and biodiversity are negatively impacted by the very infrastructure initiatives intended to "develop" water supplies. Therefore, an effective water management policy must strike a

balance between "human water use" and "ecosystem protection." In these conditions, some of the key forces and difficulties in river study are need to be prioritise including from ecological restoration to water allocation and other climatic variability (NAS 2007).

There is clear distinction between the total available annual flow and utilizable flow of a river. Utilizable water resources are the amount of water that can be consumed from their natural habitat, and they typically depend on physiographic circumstances as well as on the socio-political climatological environment. A major portion of utilizable flow has been comes from the Himalayan River system which further demonstrate the region poses great significance in terms of freshwater supply (Sinha et al. 2012). However, due to an ever-increasing population and the increased need for irrigation, industry, and domestic consumption, the amount of usable water in India has been steadily declining. According to Verma and Phansalkar's 2007 predictions, the global freshwater demand will be 843 km3/year in 2025 and 1,180 km3/year in 2050. About 70% demand is anticipated for the irrigation industry. It is obvious that, by the year 2050, India would have nearly reached its capacity to supply the demand. Water stress, however, could happen much early in some locations due to an exceedingly uneven distribution of freshwater, both spatially and temporally.

The impact of climate change accompanying with the growing population and economic development has been drastically altered the flow pattern of Indian River system. Regarding its flow pattern, water quality, availability of water, etc., a river's health faces a number of ecological and environmental issues. Various water footprints such as green water, blue water availability continues to be declined. As the effect of climate change, high seasonal variability and extreme weather events was occurred and degrade the natural drainage system, which create an imbalance between ecological and environmental flow of a river. Several researches are focusing on the assessment of ecological and environmental flow or management of river flows to minimize the impact of hydrologic alteration has emerged in the last two decades. Yang. Z. F. et al. (2008) conducted a study to determine the ecologically require flow levels considering different ecological functions for sustainable water resources allocation plan and management strategy. Unreasonable development of water resources leads to the dying of channels, declines of ground water level, dying of aquatic habitat etc. Minjian. C et al. (2012) carried out a study on Liao basin in China to calculate the minimum river flow that will sustain the low flow channel and also sustain the aquatic ecosystem. Verma. R.K. et al. (2015) conducted an assessment of environmental flow variability using three different hydrological methods in the sub watershed of Damodar River basin. The result shows that there is a need of

better methodologies to assess environmental flow for all types of watersheds. However the developments of holistic methodologies by combination of multidisciplinary information have a great potential to quantify the environmental flow requirements (Hao. C.F. et al. 2016). Karimi. S.S. and Eslamian. S. (2012) conduct a study by applying a newly developed hydrological method i.e. Flow Duration Curve shifting to investigate potential environmental flows in a river reach of Shahr Chai River in Iran. The results were also compared with the other methods to validate the minimum flow to maintain the basic functions of the river ecosystem. But the direct consequences of human activities affect the river channels through the flow variability and water consumption pattern (Gregor. K. J. 2006). The rapid urbanization, growing population and the current economic structure show a paradigm shift in the consumption pattern of water. The demand supply situation of water resources depicts a continuous deficit in future. The per capita availability of water in India, as a whole, decreased to 1869m^3 from 4000m^3 in last two decades (UNEP, 2008). Various sectors such as domestic, agriculture and industries are now became more energy centric. As West Bengal has an agriculture based economy, the demand of water in agriculture and the energy sector will consume largest share of state water resource. The demand for water in west Bengal is projected to be 10.98 mm in 2025 from 7.71 mm in 2000 leading to a deficit of 59% from 38% (Bhuin, 2014). Several studies have been made on water demand and surface water potentiality in different parts of the world. Liu et al. (2012) carried out a preliminary water resources security evaluation on Yellow river basin. They analyse available water resource, supply demand water resource for the basin in 2009. The result shows that current deficit of water which has been created by over exploiting groundwater, squeezing ecological water and ultimately may not be able to meet future normal demands for living, production and ecological maintenance. Increasing water demand was also observed in urban areas where urban centres are growing while rural regions are dependent on irrigation sector. The City Balance model was developed in this study which shows current demand supply deficit on Hyderabad (George. et at. 2009). Another study has been implemented on Haryana district, to examine the household's daily water consumption, sources, quality, water supply sources, its duration etc. The result shows lacks of awareness do not satisfy the water consumption pattern. In this study Singh. O and Turkiya. S. (2013) also stated that population growth is one of the major factor for declining per capita water availability. Beside the population growth, climate changes is the another factor which affect the water availability of any region (Parish. E. S. et al. 2012). Pal. S and Akoma. O. (2009) conducted a study on a wetland area within Kandi block of West Bengal to assess the water scarcity, where the human intervention is the main inducing factor. Changes

in land use practices ensuing threats of ground water fall and massive negative transformation of the hydrological scenario.

1.4. Overview of Surface Water Resources in West Bengal

It has been worth mentioning that the major constraint for the development of water resources scenario in India is lack of rainfall. The monsoonal rainfall in India occurs only for four months (June to September). In addition to that, utilisation of water in agricultural and industrial field, effect of global climate change adding more stress into it and reduces the water availability for future generation significantly. Interestingly, this country experiences both flood and drought condition periodically. Because of the uneven distribution of water and a prominent effect of the global warming, some of the rivers in India have been considered as a deficit basin whereas some river basin has been denoted as a surplus river basin. So for sustainable enrichment of water availability and its proper distribution, basin by basin analysis and some micro level water linkages project are needed at the earliest concern. The river system of West Bengal has been grouped into several sub river system which are North Bengal river system, Ganga-Padma river system, Bhagirathi- Jalangi-Churni river system, western tributaries to Bhagirathi river system and other tidal creeks of Sundarban. Bandopadhyay et al. (2014) stated that major river system in West Bengal has been governed by various tectonic activities associated with Himalayan and Deccan plateau region. Despite of the north Bengal river system, monsoonal

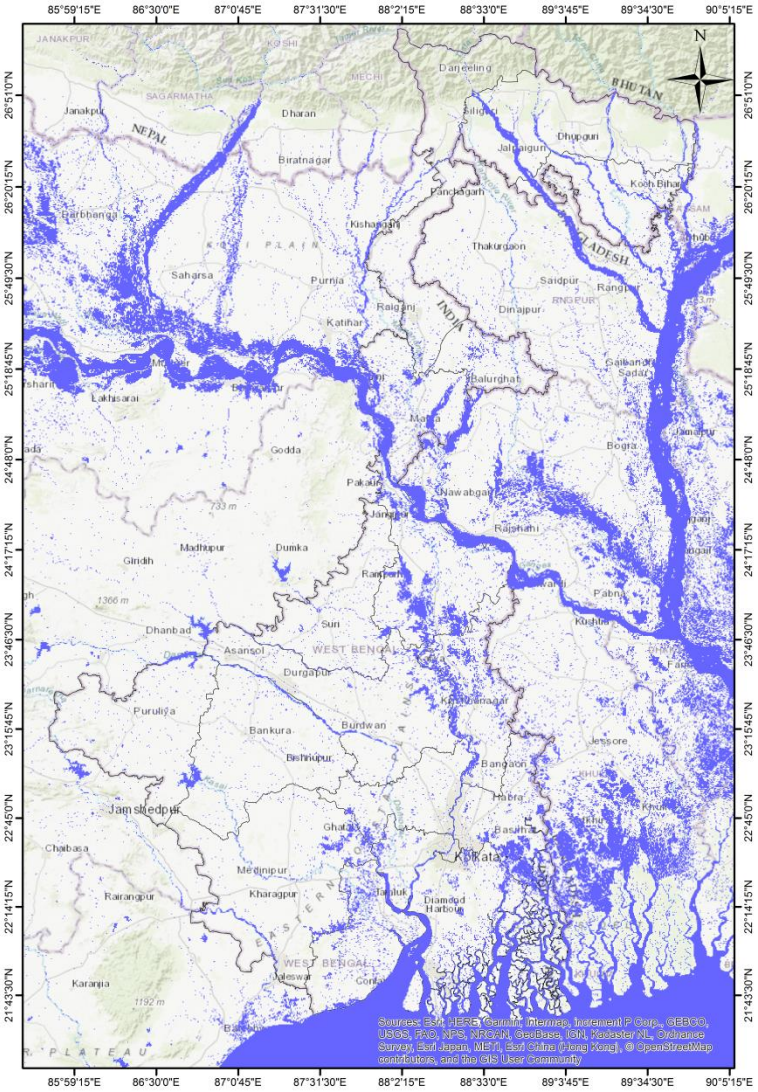

Figure 1.12 *Maximum Water Extent of West Bengal, 2018*

rainfall is the main lifeline of the rivers in West Bengal. While the rivers receive plenty of water during the monsoonal time, the flow and discharge capacity exceeds in some of the area, resultant flood occurs. On the other hand, during the lean period of rainfall, the river loses its flow drastically so that many of the rivers in West Bengal have gone dry and disappeared from the surface. Finally acute drought condition prevails during the summer seasons. Despite of this, decaying of the main channel, river degeneration, channel shifting, urban waterlogging, river pollution, groundwater depletion are the prime issues associated with the river system of West Bengal.

Some of these issues related to river degeneration or reduction in flow of the rivers can easily be interpreted using high resolution satellite imageries, through which the long term changes in the water surface and its quantification can easily analysed. Following the methodology adopted by Pekel et al. (2016) some of the glimpses of water resources scenario in West Bengal have been discussed here. The European Commission's Joint Research Centre developed this water dataset free for everyone, so that researchers and government can take initiatives to manage and plan the water resources issues accordingly. The figure 1.12 shows the maximum water extent scenarios of West Bengal. This map provides information about the presence of water surface over 35 years (1984-2018). The surface detected as water has been shown here in a blue colour. To visualise temporal and seasonal changes in water occurrence or its intensity even how the rivers are getting degenerated through time Pekel et al. (2016) highlighted some of the issues that can be easily interpreted using high resolution satellite imageries. Some of them are discussed as follows-

Water occurrence is an important approach as per as water dynamics is concern. It provides the information about both the intra and inter-annual variability and changes of water surface which has been detected within 1984 to 2018 time period. Two comparative water occurrence scenarios have been shown in figure 1.13 & 1.14, to observe the changes in the occurrences in water surface. The blue colour indicates 100% presence of water during the 35 years and the purple to pale pink colour denotes moderately to less frequently presence of water surfaces.

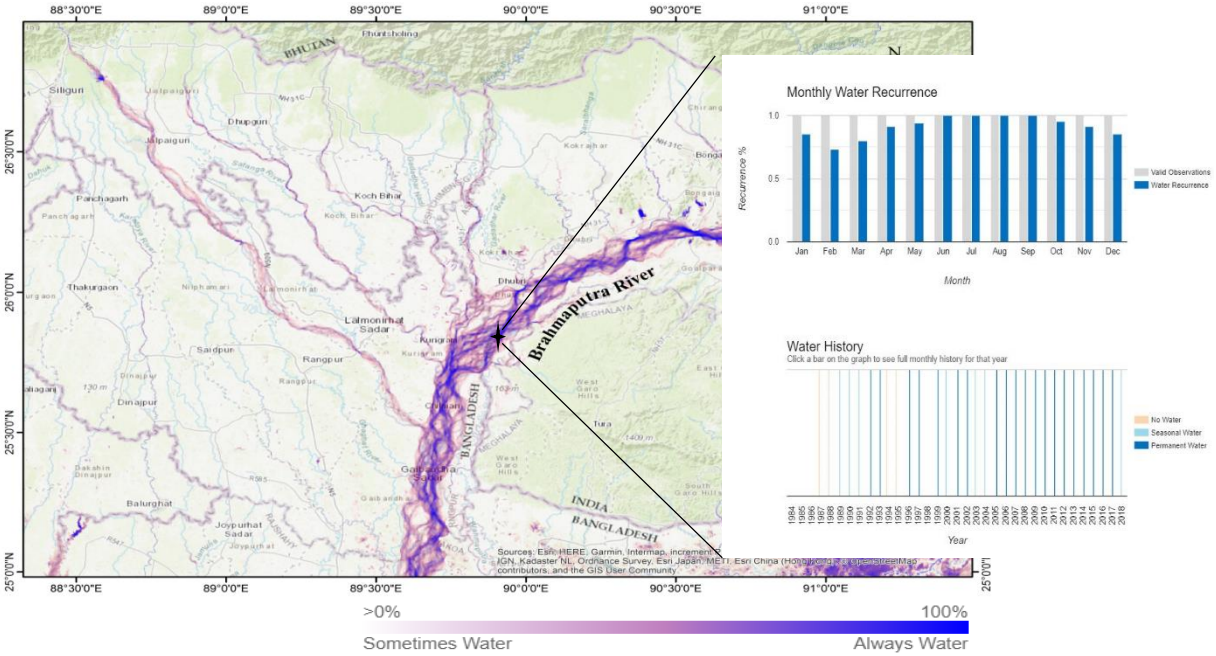

Figure 1.13 *Water Occurrence Scenario in Brahmaputra River (1984-2018)*

Figure 1.13 shows a part of Brahmaputra River, which is primarily fed by snow melt water. For that reason the frequency in the presence of water surfaces is higher over the 35 years' time period. Furthermore the pixel based statistical information about the historical water dynamics shows the presence of water throughout the month.

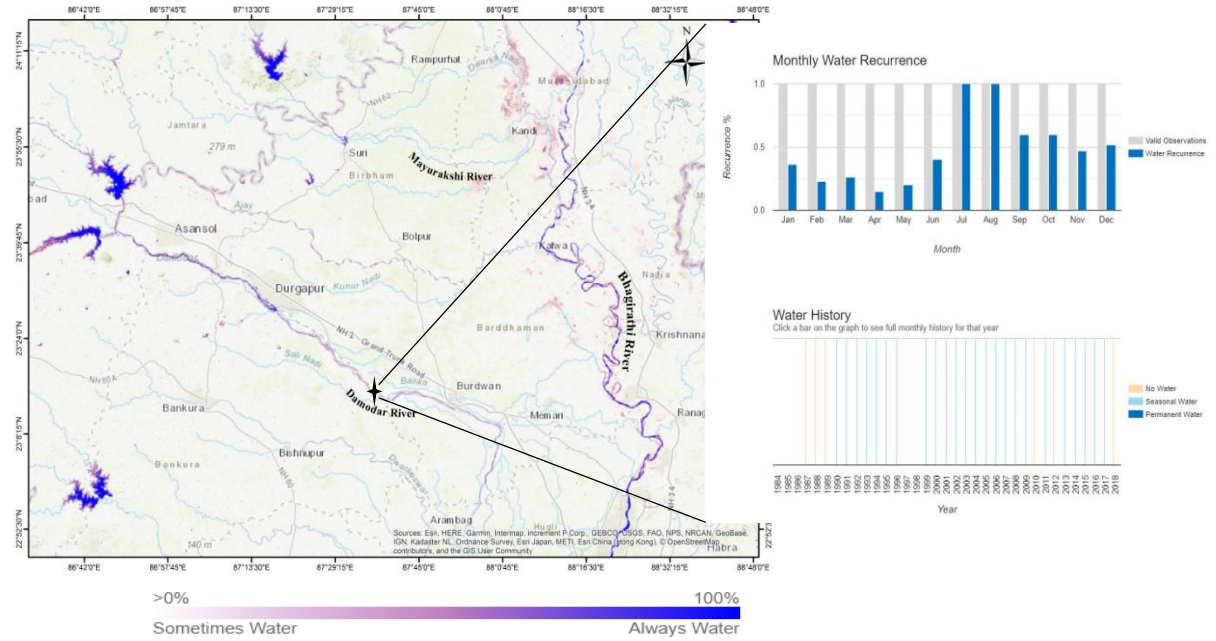

Figure 1.14 *Water Occurrence Scenario in Eastward Flowing Rivers in West Bengal (1984-2018)*

Another contrasting scenario has been observed from the rivers of South Bengal. Fig 1.14 shows the eastward flowing rivers of West Bengal like Bhagirathi, Mayurakshi, Ajoy and Damodar are mainly fed by monsoonal rainfall, which only occurs only for 4 months (June to September) in a year. The Fig. 1.14 shows that the dominance of pale pink colour within the channel depicts that less presence of water throughout the year. Similarly the location specific statistical bar graph shows the maximum dominance of water has been observed between July to August of a year. In spite of that, based on the graph depicting annual water history shows the year 2018 has been categorised under the no water class indicating that the very low distribution of water throughout the year within that particular location.

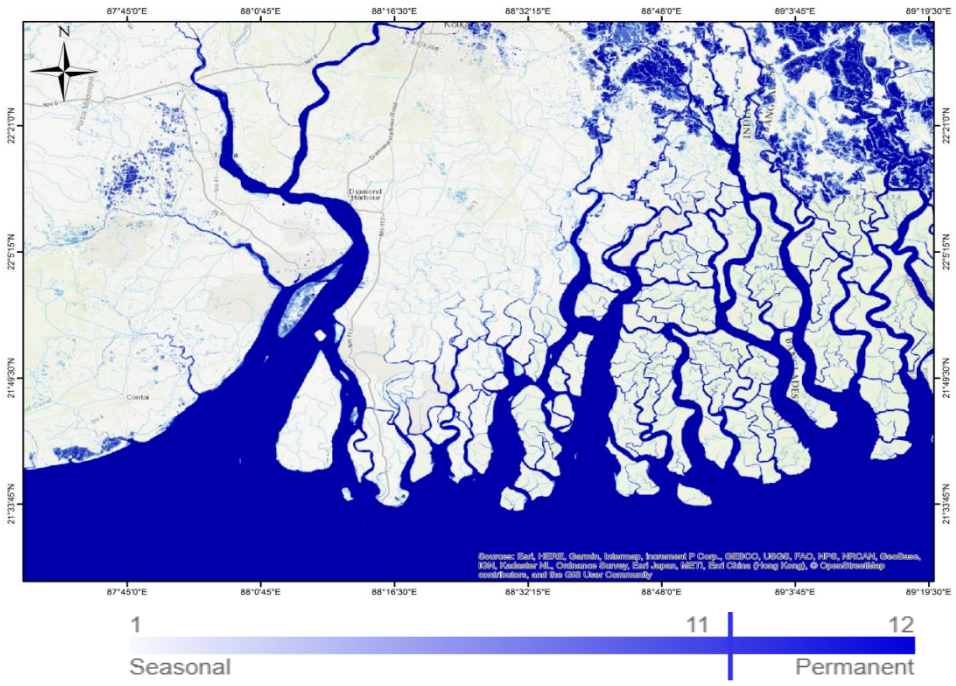

Figure 1.15 *Water Seasonality Scenario of Sundarban (2018)*

In contrast to the rain fed and snow fed rivers of West Bengal, the tidal creeks of Indian Sundarban region show the dominance of permanent water surface. Figure 1.15 provides information about the seasonal presence of water surface in a single year (2018) where the dark blue colour indicate permanently presence of water while the light blue represents seasonal presence of water surface. In the Sundarban region, because of the dominance of active tidal creeks, the channel remains underwater throughout the year. Apart from that, a remarkable change in the land use practices has also been observed within this region. Over last 30 years, many of fields have been converted into fishponds for which saline water concentration increased into that area. With regards to the variation in the presence of water, seasonal and temporal changes in the occurrence, another problem has also been associated with the river

system of West Bengal. That is the channel degeneration, changes in the extent of water occurrence and its intensity as well. The Fig. 1.16 shows a part of Bhagirathi Hoogly River, which has been highly characterised by channel meandering activity. Major shift of channels, its flow path, formation of ox bow lakes and cut offs are very much observable within the channel. To visualize the same, changes in the occurrence of water surface which increased, decreased or remained same from 1984 to 1999 and 2000 to 2018 has been produce in the following figure. The fig. 1.16 shows more presence of dark green and dark red colour indicates that increase and decrease of water occurrence throughout the two epochs representing continuous channel migration and changes in the water surfaces. The areas denoted as a dark red represents no significant changes in the water occurrence within the studied time period.

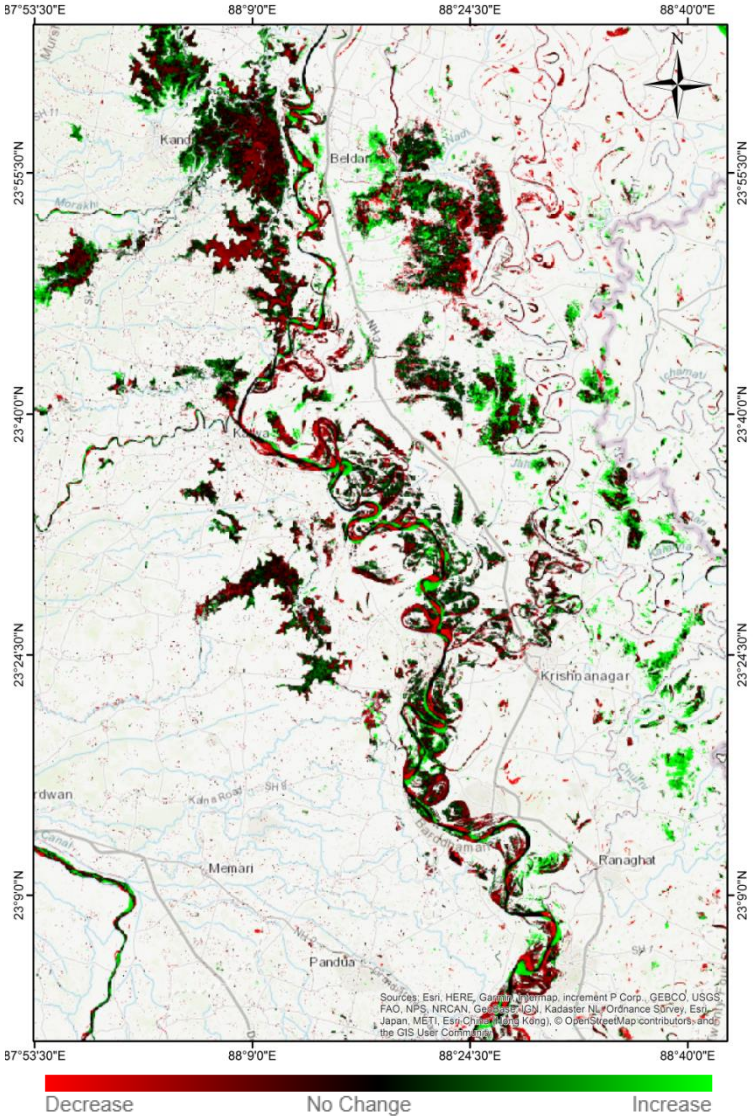

Figure 1.16 *Water Occurrence Change Intensity in a Part of Bhagirathi River (1984-1999 & 2000-2018)*

Such kind of visual interpretation of the water resources scenario using high resolution satellite imageries can help the researchers as well as the policy makers to formulate more suitable water distribution plan for the overall development of the water resources along with maintaining the river health status accordingly.

References

- Act, C. W. (1972). Clean water act. *Texas Tech Law Review*, *47*, 585.
- Aidi Ahmi, R. M. (2019). Bibliometric analysis of global scientific literature on web accessibility. *Nternational Journal of Recent Technology and Engineering (IJRTE)*, *7*(6), 250-258.
- Annual flood report, Irrigation and Waterways Directorate, Government of West Bengal, May 2016.
- Bandyopadhyay, S., Kar, N. S., Das, S., & Sen, J. (2014). River systems and water resources of West Bengal: a review. *Geological Society of India Special Publication*, *3*(2014), 63-84.
- Barbosa, F. G., & Schneck, F. (2015). Characteristics of the top-cited papers in species distribution predictive models. *Ecological Modelling*, *313*, 77-83.
- Bates, B. C., Kundzewicz, Z. W., Wu, S., & Palutikof, J. P. (2008). Climate change and water technical paper of the intergovernmental panel on climate change (Geneva: IPCC Secretariat). *Climate Change*, *95*(96).
- Bhuin, P. K. (2014). Sustainable water resource management in West Bengal: A review. *Bhatter College Journal of Multidisciplinary Studies*, *4*, 94-104.
- Buisson, L., Blanc, L., & Grenouillet, G. (2008). Modelling stream fish species distribution in a river network: the relative effects of temperature versus physical factors. *Ecology of Freshwater Fish*, *17*(2), 244-257.
- Cherng, L. Y., Malim, N. H. A. H., & Singh, M. M. (2015). Trend Analysis in Ageing and ICT Research. *J. Teknol*, *76*(1), 313-327.
- Evans, J. E., Huxley, J. M., & Vincent, R. K. (2007). Upstream channel changes following dam construction and removal using a GIS/remote sensing approach 1. *JAWRA Journal of the American Water Resources Association*, *43*(3), 683-697.
- Fabregat-Aibar, L., Barberà-Mariné, M. G., Terceño, A., & Pié, L. (2019). A bibliometric and visualization analysis of socially responsible funds. *Sustainability*, *11*(9), 2526.
- Fellows, C. S., Clapcott, J. E., Udy, J. W., Bunn, S. E., Harch, B. D., Smith, M. J., & Davies, P. M. (2006). Benthic metabolism as an indicator of stream ecosystem health. *Hydrobiologia*, *572*, 71-87.
- Fu, H. Z., & Ho, Y. S. (2016). Highly cited Antarctic articles using Science Citation Index Expanded: a bibliometric analysis. *Scientometrics*, *109*, 337-357.
- George, B. A., Malano, H. M., Khan, A. R., Gaur, A., & Davidson, B. (2009). Urban water supply strategies for Hyderabad, India–Future scenarios. *Environmental Modeling & Assessment*, *14*, 691-704.
- Ghosh, K. G., & Pal, S. (2015). Impact of dam and barrage on flood trend of lower catchment of Mayurakshi river basin, eastern India. *European Water*, *50*, 3-23.
- Gregory, K. J. (2006). The human role in changing river channels. *Geomorphology*, *79*(3-4), 172-191.
- Hao, C. F., He, L. M., Niu, C. W., & Jia, Y. W. (2016, August). A review of environmental flow assessment: methodologies and application in the Qianhe River. In *IOP Conference Series: Earth and Environmental Science* (Vol. 39, No. 1, p. 012067). IOP Publishing.
- Harris, J. H., & Silveira, R. J. F. B. (1999). Large-scale assessments of river health using an Index of Biotic Integrity with low-diversity fish communities. *Freshwater Biology*, *41*(2), 235-252.

- Harrison, T. D., & Whitfield, A. K. (2004). A multi-metric fish index to assess the environmental condition of estuaries. *Journal of Fish Biology*, *65*(3), 683-710.
- Khan, M. A., & Ho, Y. S. (2012). Top-cited articles in environmental sciences: Merits and demerits of citation analysis. *Science of the Total Environment*, *431*, 122-127.
- Khorooshi, R., Mørch, M. T., Holm, T. H., Berg, C. T., Dieu, R. T., Dræby, D., ... & Owens, T. (2015). Induction of endogenous Type I interferon within the central nervous system plays a protective role in experimental autoimmune encephalomyelitis. *Acta neuropathologica*, *130*, 107-118.
- Kozaki, D., Harun, N. I. B., Rahim, M. H. B. A., Mori, M., Nakatani, N., & Tanaka, K. (2017). Determination of water quality degradation due to industrial and household wastewater in the Galing River in Kuantan, Malaysia using ion chromatograph and water quality data. *Environments*, *4*(2), 35.
- Kumar, C. P. (2018). Water security–Challenges and needs. *Int. Educ. Sci. Res. J*, *4*(1), 26-29.
- Li, H., An, H., Wang, Y., Huang, J., & Gao, X. (2016). Evolutionary features of academic articles co-keyword network and keywords co-occurrence network: Based on two-mode affiliation network. *Physica A: Statistical Mechanics and its Applications*, *450*, 657-669.
- Liao, H., Tang, M., Luo, L., Li, C., Chiclana, F., & Zeng, X. J. (2018). A bibliometric analysis and visualization of medical big data research. *Sustainability*, *10*(1), 166.
- Liu, J., Yang, H., Gosling, S. N., Kummu, M., Flörke, M., Pfister, S., ... & Oki, T. (2017). Water scarcity assessments in the past, present, and future. *Earth's future*, *5*(6), 545-559.
- Liu, K. K., Li, C. H., Yang, X. L., Hu, J., & Xia, X. H. (2012). Water resources supply-consumption (demand) balance analyses in the Yellow River Basin in 2009. *Procedia Environmental Sciences*, *13*, 1956-1965.
- Makokha, G. O., Wang, L., Zhou, J., Li, X., Wang, A., Wang, G., & Kuria, D. (2016). Quantitative drought monitoring in a typical cold river basin over Tibetan Plateau: An integration of meteorological, agricultural and hydrological droughts. *Journal of Hydrology*, *543*, 782-795.
- Makokha, G. O., Wang, L., Zhou, J., Li, X., Wang, A., Wang, G., & Kuria, D. (2016). Quantitative drought monitoring in a typical cold river basin over Tibetan Plateau: An integration of meteorological, agricultural and hydrological droughts. *Journal of Hydrology*, *543*, 782-795.
- Mann, H. B. (1945). Nonparametric tests against trend. *Econometrica: Journal of the econometric society*, 245-259.
- Minjian, C., Gaoxu, W., Huali, F., & Liqun, W. (2012). The calculation of river ecological flow for the Liao Basin in China. *Procedia Engineering*, *28*, 715-722.
- Nag, S., Roy, M. B., & Roy, P. K. (2020). Optimum prioritisation of sub-watersheds based on erosion-susceptible zones through modeling and GIS techniques. *Modeling Earth Systems and Environment*, *6*, 1529-1544.
- Nandi, I., Tewari, A., & Shah, K. (2016). Evolving human dimensions and the need for continuous health assessment of Indian rivers. *Current Science*, 263-271.
- NAS (2007) River Science at the United States Geological Survey, 2010. National Academic Press, Washington, DC, p 206
- Pal, S., & Akoma, O. C. (2009). Water scarcity in wetland area within Kandi Block of West Bengal: a hydro-ecological assessment. *Ethiopian Journal of Environmental Studies and Management*, *2*(3).
- Pal, S., Let, S., & Das, P. (2012). Assessment of channel width disparity of the major rivers within Mayurakshi River Basin. *Int J Geol Earth Environ Sci*, *2*(3), 1-10.

- Pal, S., Let, S., & Das, P. (2012). Assessment of channel width disparity of the major rivers within Mayurakshi River Basin. *Int J Geol Earth Environ Sci*, *2*(3), 1-10.
- Parish, E. S., Kodra, E., Steinhaeuser, K., & Ganguly, A. R. (2012). Estimating future global per capita water availability based on changes in climate and population. *Computers & Geosciences*, *42*, 79-86.
- Pekel, J. F., Cottam, A., Gorelick, N., & Belward, A. S. (2016). High-resolution mapping of global surface water and its long-term changes. *Nature*, *540*(7633), 418-422.
- Pickett, S. T., Kolasa, J., Jones, C. G., & Willis, A. J. (1995). Ecological Understanding The Nature of Theory and the Theory of Nature. *Biological Journal of the Linnean Society*, *54*(1), 107.
- Sarkar, A. (2015). Impact of climate change on the runoff regime of an Eastern Himalayan river basin. *Global NEST Journal*, *17*(2), 323-333.
- Sarkar, A. (2015). Impact of climate change on the runoff regime of an Eastern Himalayan river basin. *Global NEST Journal*, *17*(2), 323-333.
- Sen, P. K. (1968). Estimates of the regression coefficient based on Kendall's tau. *Journal of the American statistical association*, *63*(324), 1379-1389.
- Shaeri Karimi, S., Yasi, M., & Eslamian, S. (2012). Use of hydrological methods for assessment of environmental flow in a river reach. *International journal of environmental science and technology*, *9*, 549-558.
- Singh, O., & Turkiya, S. (2013). A survey of household domestic water consumption patterns in rural semi-arid village, India. *GeoJournal*, *78*, 777-790.
- Sinha, R., Jain, V., & Tandon, S. K. (2013). River Systems and River Science in India: major drivers and challenges. *Earth system processes and disaster management*, 67-90.
- UNESCAP. (2007). Statistical yearbook for Asia and the Pacific.
- United Nations Environmental Programme Annual Report, 2008
- Van Eck, N., & Waltman, L. (2010). Software survey: VOSviewer, a computer program for bibliometric mapping. *scientometrics*, *84*(2), 523-538.
- Vörösmarty, C. J., McIntyre, P. B., Gessner, M. O., Dudgeon, D., Prusevich, A., Green, P., ... & Davies, P. M. (2010). Global threats to human water security and river biodiversity. *nature*, *467*(7315), 555-561.
- White, H. D., & Griffith, B. C. (1981). Author cocitation: A literature measure of intellectual structure. *Journal of the American Society for information Science*, *32*(3), 163-171.
- Yang, Z. F., Sun, T., Cui, B. S., Chen, B., & Chen, G. Q. (2009). Environmental flow requirements for integrated water resources allocation in the Yellow River Basin, China. *Communications in Nonlinear Science and Numerical Simulation*, *14*(5), 2469-2481.
- Zhai, C., & Ho, Y. S. (2018). A bibliometric analysis of distributed control publications. *Measurement and Control*, *51*(3-4), 113-121.
- Zhang, Q., Zhang, Z., Shi, P., Singh, V. P., & Gu, X. (2018). Evaluation of ecological instream flow considering hydrological alterations in the Yellow River basin, China. *Global and Planetary Change*, *160*, 61-74.
- Zupic, I., & Čater, T. (2015). Bibliometric methods in management and organization. *Organizational research methods*, *18*(3), 429-472.

CHAPTER 2
LITERATURE REVIEW

2. Introduction

Water is a necessary resource for the survival of both humans and other living things on the planet. In economically, water resources are considered as a multifunctional asset since they facilitate the production and consumption of a wide range of commodities and services (Wei et al. 2010 & Zuo et al. 2014). However, as an effect of accelerating socioeconomic growth and changing climates (Kashaigili et al. 2009), there are now more major global issues with water scarcity and worsening water quality, which has increased water demand for socioeconomic sectors and decreased E-flow (Wei et al. 2012). The United Nations Environment Programme (UNEP) predicts that 5 billion of the world's 7.9 billion inhabitants will live in locations where it will be difficult or challenging to fulfil basic water demands for drinking, cooking, and sanitation by 2025 (Leete el al. 2003).

Stream ecosystem health has been falling globally as a result of catchment and riparian degradation (Sheldon et al. 2012). Rapid developmental activities are primarily responsible for such degradation leading to excessive waste discharge into the river, which harms the aquatic ecology. Since the late 1990s, many rivers have lost their ecosystem functionality, and these issues have hampered the region's overall ecological development. Mayurakshi River is one of them which is an important western tributary of river Bhagirathi. It runs across 288 km through the provinces of Chhotonagpur plateau of Jharkhand and plains of Bengal having a drainage area of 5325 sq. km. This rivers plays a major role in terms of social, economic as well as ecological as it has two important civil structures- Tilpara Barrage and Massanjore Dam on it, which are now at risk for preserving the natural flow pattern throughout the channel. Other than this, some human induced activities like sand mining, river lift irrigational activities, creation of temporary khals/nullahs on the active river bed are exaggerate the problems of channel deformation (Nag et al. 2022). Numerous evaluations of river's overall health and its significance to the environment, have been conducted by many researchers mainly to prevent further degradation of the ecosystem associated with rivers- are discussed in the following manner-

2.1. Review to Literatures Based on Different Issues Related to the Mayurakshi River

Islam et al. (2023) have examines how flooding in a tropical river basin, such as the Mayurakshi River basin in India, has impacted the area's deteriorating social infrastructure and diminishing agricultural productivity. While cropping intensity, crop diversification index, and

relative relevance index have been used to assess the vulnerability of the agricultural and socio-infrastructural systems, flood frequency, depth, duration, and inundation over the Mayurakshi River basin have been used to describe the flood magnitude. The results demonstrate that more frequent floods in these areas can result in transient unemployment, which encourages labor migration, especially to Middle Eastern countries. In addition, there are some obvious problems with the infrastructure, such as crumbling kaccha homes and slick roadways. More than 90% of persons during floods developed diarrhoea as a result of consuming contaminated floodwater.

Ghosh et al. (2023) have used modern modeling techniques along with remote sensing, GIS, and investigated soil erosion over the Mayurakshi river basin. They identified the more susceptible zones for soil erosion and utilized the RUSLE model to assess the soil loss from the basin region. It has been demonstrated that soil loss is the least severe in the basin's lower plain land areas based on the features of rainfall, runoff, land use, and DEM. These findings could help the area's soil management and watershed development strategies.

Ghosh and Maiti (2021) enumerated SWAT model to quantify the sediment yields from the Mayurakshi river basin area. To determine the spatial distribution of gully erosion-prone sites, they have also included Artificial Neural Network and Random Forest analysis. ROC plot curves have been used to validate all of the used models with high reliability.

Nag et al. (2023) have made an effort to analyse the Mayurakshi River's hydro geomorphological characteristics. To explore important channel features such as channel depth-width velocity, etc., they have conducted a thorough cross-sectional field survey. The authors also attempted to compare all these variables with the field data using a few chosen hydraulic and hydrological models, with the hydraulic models providing a higher level of accuracy. The entire study was conducted using non-monsoonal flow data, primarily to show the peculiarities of stream flow during a lean season, which is thought to be the most important factor for riverine ecosystem as a whole.

Nag et al. (2022) have done an assessment on the impact of land use land cover change over the ground water resources of Mayurakshi River basin area. This research established its novelty through a proper assessment of land use land cover alteration and its impact on ground recharge zone. Land use land cover has been considered as a significant element in certain prior studies' assessments of ground water recharge zones. To measure the ground water level from

the excavated well using a TLC meter and correlate the output with remotely sensed data, a thorough field study was conducted. The entire study demonstrates the benefits of an increase in ground water level caused by the expansion of vegetation in that location. The locals have made a good effort to improve the amount of greenery, which will ultimately benefit the system for managing water resources.

Islam and Sarkar (2021) discussed in the Mayurakshi River Basin, records of flooding have been seen since 1860. When major civil structures like Massanjore Dam, Tilpara Barrage, Brahmini Barrage, Bakreswar Weir, and others were built in the riverine catchment during the post-dam period, especially in the 1950s, the high magnitude low frequency flood events dramatically changed into low magnitude high frequency flood events. They examined the nature of flood frequency using the extreme value method developed by Gumbel and Log Pearson, where they discovered a clear variation in yearly flood discharge. The analysis of flood frequency may also be useful in developing policy recommendations that reduce flooding susceptibility. With this knowledge, the development of an early warning system to safeguard the agricultural industry, thereby lowering the vulnerability of risk.

Ghosh and Maiti (2021) have created a severe soil erosion likelihood index in the subtropical monsoonal climate-dominated Mayurakshi River watershed. Soil erosion, which is currently regarded as one of the area's key environmental threats, has a significant impact on this area. For the purposes of modeling and model validation, the authors selected 70% and 30% of sample sites, respectively. Numerous environmental factors highlight the region that has been seriously damaged by soil loss, particularly in the undulating western section of the basin, and that urgent conservation measures were required.

Ghosh & Maity (2021) stated that human influence has significantly changed the physical, ecological, and aesthetic character of many rivers throughout the world. In order to evaluate ecological quality, human health, and pollution levels, scientists and researchers have developed a number of indices based on physical, biological, and chemical aspects. However, the environment the river flows through, the land use and land cover pattern along the river banks, and the many human activities that take place inside the channel all have an impact on the river's physical, biological, and chemical health. The Mayurakshi River and its surrounding surroundings have thus been subjected to fresh ecological susceptibility testing by the authors. The findings show that compared to their upstream and downstream counterparts, the middle

and lower portions of the Mayurakshi River are significantly more susceptible to environmental changes.

Islam and Ghosh (2021) declared that the lower Mayurakshi River Basin area in the Indian state of West Bengal has a high risk of flooding. In the many lower communities in the basin, floods have occurred on average a number of times since 1998. To evaluate the impact of the flood on the economic situation, the authors conducted a thorough socioeconomic study in the lower basin of Murshidabad districts. The survey report shows a progressive transformation of the economy, with seasonal unemployment, frequent property damage, and rising costs as well as a decline in crop production acting as push factors and international labour migration acting as a pull factor and boosting the economy simultaneously.

Islam and Barman (2020) analysed the capacity of each tributary basin to create flooding, which results in flood conditions in the basin's lower portion. The main technique used in this work to indicate the significance of peak flow and basin lag time with various morphometric indicators is principal component analysis (PCA). The author also created an index called the flood inducing capacity index, which measures the capacity of each sub basin to induce floods in its master stream using both morphometric and basin area co-efficient data. But in addition to this solely basin-based morphometric analysis, climatic considerations, as well as incorporation of the function of soil and vegetation, are also required in this context.

Nag et al. (2020) identified the sub basin wise erosion risk zone using a set of basin morphometric parameters. The TOPSIS (Technique for Order Preference by Similarity to Ideal Solution) model, which largely takes into account the interdependencies of all criteria utilized for the analysis, has been developed by the authors for optimal level basin management. Additionally, they have validated the model to show that the discovered sub watershed is just as susceptible to rainfall and soil erodibility as the rest of the river basin.

Debnashi and Pal (2018) have contributed yet another addition to the Mayurakshi river basin. They evaluated the Mayurakshi River Basin's gully erosion susceptibility zone. 15 distinct conditioning indicators were used to identify the gully erosion-sensitive zones using a correlation matrix and logistic regression model. The results indicate that 16% of the upper catchment area of the river is classified as an extremely sensitive zone to gully erosion, whereas the lower catchment region, which is made up of both fresh and old alluvium deposits, is classified as a lowly susceptible zone to gully erosion. These results have also been supported by a field investigation and an analysis of the ROC (receiver operating characteristic curve)

plot, which strengthens the logic of this research for the susceptibility prediction and management plan.

Mondal & Pal (2018) studied the hydrological properties of wetlands located in the lower reach of the Mayurakshi River. The wetlands are transitory in nature and periodically submerged. Due to their diminutive size, their importance in terms of hydrology and socioeconomics is sometimes disregarded. The authors concentrate on their existence and hydrological variability throughout a 14-year period (1987–2014). They have investigated the frequency of water presence using multi-spectral Landsat satellite imageries. The water presence frequency study can effectively identify the physical susceptibility as well as shrinkage in wetland inundation regions due to key human triggers factors such as river management, dry farming practices, and other developmental activities. This research also lays a strong platform for future ecological and hydrological studies, which is helpful for safeguarding and controlling the tropical monsoon climate of wetland areas.

Pal and Debanshi (2018) have investigated the Mayurakshi River Basin's susceptibility to soil erosion. They concentrated mostly on gully heads bundhs, which are reservoirs built at Massanjore Dam to prevent soil erosion and sedimentation. The investigation showed that there are extremely sensitive soil erosion zones close to the gully heads bundhs and that the massive soil loss from the region overloads and increases the vulnerability of those bundhs.

Pal (2017) analysed the effects of Tilpara Barrage, another significant civil structure on the Mayurakshi River. He recognized that the water in the reservoir had caused a backwater to form at the point where the Mayurakshi and Kushkarini Rivers converged, which had a negative impact on the carrying capacity and slope of the channel. The surrounding agricultural land has been harmed by the canal becoming inundated and by sporadic significant flood discharges. This study came to the conclusion that the upstream dam and reservoir affect the socio-ecological situation of the river basin area in addition to changing the hydro-morphological features of the channel.

Ghosh el al. (2017) assessed the river water quality using Agglomerative Hierarchical Cluster (AHC) analysis. The results indicated that the bulk of the water quality is seen to be in a favourable range, promoting the basin as having river water that is less artificially influenced by humans and more ecologically sustainable.

Pal (2016) evaluated the hydro-morphological dynamism of the Mayurakshi River's riverine environment in relation to the effects of the Massanjore dam and Tilpara Barrage. The results

of this study reveal that the attenuation of maximum water levels both during monsoon and non-monsoon seasons has dropped greatly. This study has become more relevant as a consequence of the combined use of remote sensing, GIS (Geographic Information System), and field inquiry. Furthermore, the average suspended sediment load at the dam site areas has decreased as well, and the volume of flow has decreased to 11.3% since the dam was built. Such a drop in flow volume and sediment load points to a significant channel change in the river's downstream basin.

Pal (2015) has conducted a scientific inquiry on how various climatological and geological elements operating in the area affect the morphology of an alluvial channel. He spent the last 60 years researching the surface morphology of floodplains and the characteristics of stream avulsion. To provide detailed information on the formation of floodplains and their morphology since 1955, the author combined ancient topographical maps with Landsat and SRTM (Space Shuttle Radar Topography Mission) data. The results indicate a significant shift in the Bhagirathi Mayurakshi confluence. Additionally, he said that the intricate meandering patterns of the Mayurakshi and Dwarka at their confluence were to blame for the formation of the intra-channel crevasses that gradually exposed the right bank of the Bhagirathi River.

Mukhopadhyay and Das (2013) examined the deranging characteristics of the Mayurakshi-Kuya interfluve and their effects on the basin region. The word "channel deranging" refers to the unscientific creation of new channels and the natural decomposition of old streams, which alters the drainage pattern. Due to the loss of stream energy and water velocity entering the channel, this phenomenon occurs frequently in the lower reach of any watershed (Bloom 1979; Richards 1987). The inter channel space in the Mayurakshi-Kuya interfluve area is so limited that tributaries join without taking the interfluve area of each catchment into account. According to the authors, the main causes of the degeneration of the Mayurakshi-Kuya River are channel shifting, human-induced channel piracy, and channel modification by extensive sand deposition on river beds. However, some notable positive and negative impacts have also been observed in agricultural sector like decayed river bed has been used as a fertile land which induces the crop productivity over the region, similarly scarcity of water affects the consumption of groundwater resources etc.

Pal et al. (2012) have made an effort to comprehend the thalweg line-based pattern of channel width distribution. In general, when the volume of discharge in a stream's downstream portion grows, the channel width generally widens as well (Moriswa, 1985 & 1968). However, an

asymmetry pattern in the channel width distribution has been seen in this study area. The author looked into the origins of these changes, finding that significant human interventions had a significant impact on bank stability and that the construction of dams and barrages had increased channel width and altered the channel's natural flow.

Jha and Bairagya, (2012) used the Tilpara Barrage's daily discharge data to conduct a floodplain planning study. In order to help policymakers develop a better flood management strategy for the Mayurakshi River Basin area, they used statistical analyses such as flood frequency analysis, peak discharge analysis, return period analysis, and floodplain zoning mapping.

Chowdhury et al. (2009) used a variety of thematic layers from hydro-geomorphology, land use and land cover (LULC), lineament features, drainage, soil, and slope maps in a remote sensing environment to study integrated water resource development plans. By combining all of these layers, an integrated water resource development plan has been created that identifies the best locations for the development of ground and surface water resources. Such a system could be applied in a comprehensive approach to ensure proper management of natural resources.

2.2. Review of Literatures Relevant to the Research

2.2.1. Channel Morphological Evaluation and the Flow Variability

Maurtua et al. (2023) examined the flash flood-prone Canete River basin regions in the Peruvian Pacific. Because there is a lack of hydrological data for the area, authors have mostly used morphometric analysis to predict flood-prone locations. Weighted sum analysis (WSA) was used to prioritize the study region, and the results show that around 26.08% of the entire study area is classified as a high-risk zone that needs immediate intervention to reduce the likelihood of extreme hydrological events like floods and droughts.

Sener and Arslanoglu (2023) have created a Google Earth-based program to examine a watershed's morphometry using data from stream flow and digital elevation models. This cutting-edge method of hydrology research expands the scope of how morphometric analysis can be used to characterize any watershed on a worldwide scale. This web-based program makes it possible to analyse the physical characteristics of any watershed even in the absence of data.

Govekar et al. (2023) studied the basin properties of Hirehalla sub basin of Malaprabha River based on geo-informatics application. Analysis of the linear, aerial, and relief components of basin morphometry, as well as key morphometric indices like the roughness index, form factor, and elongation ratio, can provide a clear picture of the nature of the riverine ecosystem and its sustainability.

Chen et al. (2023) evaluates the climatic factors affecting North American hydrological regimes, such as variations in surface runoff and groundwater storage. This study also offers a critical assessment of potential solutions based on local demands for effective water management. The results demonstrate that many parts of North America are susceptible to disastrous events such as severe droughts, floods, wildfires, and erratic precipitation trends. As a result, these changes are having a wide range of effects on water resources and are causing a shortage of water, which is altering the amount and quality of water in surface waters in the United States, Canada, Mexico, and other countries. Finally, the findings suggest that, in order to safeguard water flows along with cutting-edge technologies and management plans, an integrated strategy for managing water resources is required.

Ajadi and Adediji (2022) have investigated how climatic variables affect a watershed's morphometric analysis. The Shiroro drainage basin was chosen for this study because water scarcity there is a significant problem all year round. The development of contemporary geographic information systems is important for planning and management purposes since this technology makes it simple to depict the physical state of the basin in terms of extreme climatic events, their hazards, and mitigations.

Naemitabar et al. (2022) assessed basin morphometric parameters to determine the level of tectonic activity there. Using GIS-based MCA analysis, they assessed the relative tectonic activity over the Torbat Heydariyeh Kalshur basins in Iran. The primary objective of this study is to map neo-tectonic landform deformation. A single complete measure of relative tectonic activity based on 18 morphometric parameters has been developed, showing that the current research region has been significantly impacted by geo-tectonic upliftment, with the fault system being the most obvious. Such a calculation of basin priority will be useful for showing the type of tectonic separation present in a region.

Song et al. (2022) noted that the difficulty of forecasting surface runoff is critical for optimal scheduling and allocation of water resources. With the aim of analysing the impacts of climate

change on surface water resources, the authors have created a basin-scale water balance model using the Budyko-type equation. The outcome demonstrates that while high precipitation increases runoff over the basin area, an increase in temperature has an indirect proportionate effect on runoff generation. These kinds of conclusions can serve as a guide for future planning and management of water resources, including their possible expansion.

Liu et al. (2022) have examined how, in a snow-covered catchment in the United States of America, the mean annual stream flow drops as the variability of the inter-annual stream flow increases. The authors have made an effort to explain how snowfall affects stream flow variability in this article. They looked at the hydro-climatic relationships between annual stream flow and the amount of snowfall. The results indicate that as a result of the effects of global warming, snowfall will be reduced along with mean annual stream flow and inter-annual stream flow variability. Due to the asymmetric hydrological effects of snowfall in successively dry and rainy years, stream flow variability and snowfall fraction may be positively correlated. This innovative approach to comprehending the impact of second order hydro-climatic effects would aid policymakers in the management of water resources under a scenario with altered climatic conditions.

Ahrendt et al. (2022) have evaluated the variations in stream flow intensity and frequency with changes in channel conveyance in 50 river gauges of western Washington State between 1930 and 2020. Typically, changes in flooding severity and probability are correlated with variations in stream flow frequency and intensity. Changes in the river's capacity to convey water, however, can also affect the area's danger of flooding. They noticed that areas with uncontrolled rivers had experienced more moderate floods. Changes in the water flow through a channel are typical, although their size and timing vary from place to place. In rivers that are managed, this trend is lessened and in some cases completely reversed. Depending on how they are modified, channel conveyance's significance for flood risk assessment changes. The impact of conveyance changes on flood risk is equal to or larger than that of stream flow at the same site in areas with a history of landslides, extreme floods, and flow restrictions. In such a situation, analysis of both long-term and short-term channel conveyance changes will be helpful for the assessment of the vulnerability to flood hazards in any location.

Fenicia and Mc. Donnell (2022) have created a distributed perpetual model on a regional scale when conducting fieldwork is unfeasible. The Moselle watershed, which contains 26 gauged sub-catchments, was used for the study. Precipitation, evaporation, average stream flow,

lithological influences, topography, and land use control are some of the major factors that the authors included in their analysis, and observed the spatial variability of each factor in response to stream flow generation at various sub-catchments.

Ghosh et al. (2021) have investigated the eco-geomorphological behavior and flow change caused by the dam of the Damodar River in West Bengal. They concentrated on environmental flow, channel metamorphism, and the fluvial functionality of the Damodar River while taking into account flow divergence caused by dams and barrages, as well as the expansion of the local agricultural and industrial sectors. It has been reported that human-induced changes in the eco-geomorphological behaviour of the river system cause the Damodar River's functionality to swing from poor to good.

Islam and Guchhait (2020) have made an effort to pinpoint how the Farakka Barrage's construction has changed the lower Bhagirathi River's cross-sectional shape and channel efficiency. The study found that most cross-sections had changed significantly, with a larger width-depth ratio, higher channel form index, and higher areal asymmetry of the river. A total of 39 cross-sections had been evaluated at field sites utilizing more comprehensive topographical maps and satellite imageries. However, the Ajay Mayurakshi River system's massive silt intake and rapid bank erosion caused a transport-limited condition to arise, which significantly reduced channel efficiency.

Mondal et al. (2018) have created a brand-new technique called the Optimum Cross section Index (OCI) to determine the Icchamati River in West Bengal's ideal channel condition. In order to construct the areal differential asymmetry index (ADAI), they took into account 22 cross-section points from which crucial geomorphic data, such as channel depth, width, hydraulic radius, wetted perimeter, etc., were obtained. The conclusion shows that the state of the river would worsen from upstream to downstream. Here, the OCI is based on more readily accessible data such as channel width and depth, which further suggests that the model needs a more thorough review to determine the river channel.

Jhariya et al. (2018) have used MCDM approach, a multi-criteria decision-making approach (AHP-based), to prioritize vulnerable watersheds for conservation measures of soil and water. For this study, a watershed in the Bindara region that is separated into 16 smaller watersheds has been chosen. The soil and water hazard rate index has been created with the aid of remote sensing and GIS using a number of sub-indices, including soil loss, sediment yield, runoff

potentiality, etc. Combining these results indicates that soil conservation measures, particularly in SW11, are urgently needed. Mechanical interventions such as bench terraces, contour trenching, check dams, and percolation tanks may be considered useful in places of extremely high and high-priority sub-watersheds where the rate of soil erosion and sediment output is high and the slope is steep.

Aouragh and Essahlaoui (2018) have tried further to use basin morphometric features to prioritize watersheds. The authors have integrated Technique for Order Preferences by Similarity to Ideal Solution (TOPSIS), an advanced multi-criteria analysis with GIS, to study various linear and areal parameters of any watersheds as a useful tool for better planning and implementing various management programs. Based on how far they are from the ideal and anti-ideal points, this model assigns them a rating. The optimum choice in this situation must be the one that comes closest to both the positive and negative ideal solutions. The application of such a system by land planners and developers can help to conserve land and use it effectively.

Ameri et al. (2018) have conducted a comparative analysis of various multi-criteria decision-making methodologies, such as TOPSIS, VIKOR, SAW, and CF, with the goal of giving the Iranian Ghaem Shahr River basin priority in terms of soil erodibility. Each year, soil erosion harms the neighbourhood significantly by reducing crop yields and choking reservoirs with debris. Because of this, authors have examined key basin characteristics to pinpoint the location of the erosion hotspot. The results reveal that morphometric parameters are particularly helpful for identifying areas vulnerable to erosion and that the VIKOR strategy outperforms the applied MCDM approaches because it prioritizes watersheds with greater precision.

Chen and Liu (2017) emphasized the significance of river cross-section data in any form of river survey prognostic measures. The researchers looked at three different techniques for resampling the data from the original river cross-section data in both transverse and longitudinal orientations. On a river with simulated inflow and outflow data, a high-resolution, 2-dimensional hydrodynamic model was used to compare the performance of the original and resampled cross-section data. The results indicate that under low flow circumstances, the river phases in the tidal and non-tidal portions of the river are identical in both the 2D and 3D models. However, the 2D model overestimates the river phases during the high flow situation when compared to the 3D model.

Kisku et al. (2017) have investigated the water quality in relation to the variety of fish in the Paschim Medinipur area of West Bengal. Four years have been spent conducting this investigation. In addition to analyzing 76 freshwater fish species, other physio-chemical properties of the water were also examined. Given the abundance of major water bodies in the Paschim Medinipur area of West Bengal, the taxonomical and conservation study suggests that fish culture has a great deal of promise. The diversity of fish culture throughout the region, however, may be more positively impacted by good management methods and scientific culture adaptation.

Meshram and Sharma (2017) have prioritized the Shakkar River basin in Madhya Pradesh, India's watershed. They conducted an analysis of significant basin morphometric factors and, using Principal Component Analysis (PCA), prioritized watersheds. This study demonstrates how basin morphometry can be utilized to prioritize sub-watersheds using remote sensing, GIS technologies, and PCA analysis. There may be a substantial risk of soil erosion in SW 7 and SW 5. Therefore, in these locations, suitable soil conservation techniques are required to prevent future loss of land resources.

Gopinath et al. (2016) discussed the important morphometric parameters to explore the hydro-geological behaviour of any area. To explore the interrelationship between each morphometric parameters, authors have incorporated the multi criteria decision making approach. It is obvious that among all the morphometric attributes overland flow plays the crucial role in watershed prioritisation. Maximum relief and steep gradient in the eastern part of the basin shows highest flood susceptibility. Various conservational measures like check dam, man-made pools can reduce some of its vulnerability however an immediate actions must require for the high priority areas.

Schappi et al (2010) have created a digital terrain model (DTM) to better model the flow of the river and collect data on its topography. In order to thoroughly study complex riverbed features like gravel bars and river widening, writers created an algorithm using topographic data and DTM. When there is a lack of easily available river bathymetric data, this type of technique can also be quite helpful.

Chatterjee and Purohit (2009) have conducted research on the estimation and use of groundwater resources in the context of India. The estimating recharge method is based on the method of water level fluctuation and empirical standards. The classification of the assessment

units takes into account both the long-term water levels and the degree of groundwater development. In all of India, there are 5723 units; 4078 are rated safe, while 839 are deemed overexploited. The remaining things fall under the critical and semi-critical categories. India's peninsular, western, and north-western regions are where overexploitation is more prevalent. Eastern India offers a lot of potential for groundwater development in the future. In view of the groundwater situation, a periodic evaluation of groundwater resources is necessary, which would call for substantially expanding the current database.

Sreedevi et al. (2005) have conducted research on the Pageru River's drainage basin to identify the possible zones for groundwater resources in a challenging topographic area. The erosional agents of fluvial origin have had a significant impact on the subsurface lithology of the basin. This displays complicated morphometric properties in the basin shape, stream ordering characteristics, and developments of stream segments within the basin. Such watershed development plans are essential for utilizing surface water and groundwater resources in arid and semi-arid regions.

2.2.2. Impact of Land Use and Land Cover Alterations

Devanantham and Saravanan (2022) have studied a coastal district in Tamilnadu to see how the land use and cover have changed and how stable the environment is. The land use and cover forecasts for the years 2009 to 2019 and 2019 to 2030 were analyzed using the Google Earth Engine (GEE), Terrset software, and GIS tools. The authors also employed a CA Markov model to forecast the change in land usage. The study area is divided into many zones for the purpose of statistical analysis and change monitoring. In both zones, the built-up regions are expanding while the water bodies are shrinking. Additionally, it has been shown that the sparsely vegetated area is under stress and is turning into development property.

Das and Angadi (2022) noted that the quick urban growth is a big concern for local government and urban planners in tiny cities of India because of a lack of data and a poor comprehension of the chaotic urban expansion. a small-scale investigation of the Barrackpore sub district region using many Landsat pictures and methods of maximum likelihood categorization. The outcome revealed observable variations in build-up areas. The study area's build-up land has expanded more swiftly due to population pressure, as shown by the positive correlation between population growth and build-up land growth. The recommendations made in this study support environmentally responsible urban development and reasonable land use planning.

Samal and Gedam (2021) employed a novel method called OBIA (Object-Based Image Analysis) to determine the land use dynamism in the upper Bhima River basin, India, for the years 1992, 2000, and 2009. Using an open-source hydrological model called Soil and Water Assessment Tool (SWAT), authors have also attempted to simulate hydrological processes and assess the impact of land use and land cover on surface runoff, groundwater flow, lateral flow, etc. of the basin region. From the labelled images, it can be seen that there has been a significant transformation of agricultural land and wastelands into developed areas. Such a land conversion may have an impact on the capacity for runoff, water yield, and percolation at the basin and sub-basin levels. Such varying effects of land use land cover change can alter the overall hydrological processes operated within that region.

Ahmed et al. (2021) have evaluated the relationship between the change in Pakistan's land use and land cover and the evolution of groundwater quality between 2012 and 2019. The results of the analysis showed that, mostly in densely populated areas, groundwater quality declined for the year 2019 compared to the year 2012. The percentage of patients with methemoglobinemia has increased by 14% as a result of the widespread use of nitrogenous fertilizers and pesticides in the vicinity of agricultural land. Overall results indicate that the primary cause of spatiotemporal quality variations in the study region. The health administration may benefit from this kind of research in analysing changes in groundwater quality, devising site-specific policies, and creating new health laws.

Vinayak et al. (2021) used multi-layered perception Neural network-based Markov chain model (MCM) and remotely sensed data to conduct a study on the prediction of LULC changes in Mumbai city. It is possible to address a number of issues related to urbanization, climate change, and other environmental processes including flood, drought, land use issues, urban planning, etc. by comparing past and present land use and land cover with an eye toward the future. In this work, precise land use and land cover statistics for the years 1992 and 2000 were detected using Landsat satellite photos using a supervised algorithm to analyse the progress of urban development. The next step was to replicate the LULC for the year 2011 and to estimate the land use and land cover for the year 2050 using a Markov model based on a multiple perception neural network (MLPNN). The results show rapid urbanization of Mumbai city and the surrounding area with few changes to the city's coastline features. The use of this model, which is based on research, will make it possible to realize the region's goal of sustainable development.

Talukdar et al. (2020) have looked at a few machine learning techniques for the quantitative evaluation of changes in a specific area's land usage, land cover, and extension of land transformations. These input values from the satellite are further categorized and validated using a variety of methods, including the kappa coefficient, the Receiver Operational Curve (ROC), index-based validation, and the root mean square method (RMSE). The validated results demonstrate that the Random Forest (RF) algorithm offers the best accuracy out of all these. Mahalanobis Distance (MD) provides the least accurate assessment of changes in land use and cover. Such conclusions have already been reported in the literature, but the authors stress that a more thorough analysis of the RF model is needed with more sophisticated physio-climatic data.

Tewake and Fentahun (2020) Land conservation, sustainable development, and water resource management all benefit from information acquired through the detection of changes in land use and land cover. Therefore, the goal of this study is to ascertain how land use and cover have changed in the Tana basin. Land use and cover changes were identified for the years 1986, 2002, and 2018 using Landsat TM 30m resolution and advanced image processing techniques. Software such as ENVI and Arc GIS were utilized to identify the change. His analysis indicates that over the previous 32 years, both the agricultural land and the residential areas of the basin have increased significantly. Proper land management practices, integrated watershed management, and proactive community involvement should be encouraged to prevent unscientific land modifications.

Sharma et al. (2017) have published their research on the effects of changing land use and land cover on water supplies. Their study reveals that rising urbanization has a considerable impact on groundwater, which has been a major source of concern for individuals who work with groundwater resources recently. Groundwater recharge and storage are impacted by the reduction in infiltration brought on by the growth of the urban population.

Song and Deng (2017) evaluated how China's ecosystem services were affected by land use change. China has experienced a number of difficult changes over the past few decades as a result of some economic and social policy reorganization as well as the dynamic nature of land use and land cover. They examined the changes in land use and cover for the years 1988, 2000, and 2008 using the value transfer method, and the resulting ecosystem services were calculated for the study region. Ecosystem services have significantly decreased from 1988 to 2000 and 2000 to 2008, respectively. Indicators of elasticity were also created to evaluate how ecosystem

services changed in response to changes in land use and land cover. The results show that China's 1% land conversion throughout the analysed time period resulted in average changes in the value of ecosystem services of 0.15% and 0.10%, respectively.

Rwanga and Ndambuki (2017) emphasized the significance of using remote sensing and GIS to assess the land use and cover of any region. The only source from which historical landscape data can be assessed through the method of picture classification is high-resolution satellite photographs. Additional aspects include the caliber of the satellite data, classification techniques, user skill and experience, etc. The purpose of this research has been to classify and map the land use change of the Limpopo provinces of Africa using RS & GIS methodologies in order to assess how effectively the classification procedures were implemented and to judge the usefulness of the classification. Using a non-parametric approach, the categorized image demonstrates how agricultural land predominates over other types of terrain.

Khatun and Pal (2016) have concentrated on controlling the hydrological and geomorphological variables on the LULC over the Kushkarini watershed area, which is situated in the Chhotonagpur Plateau region of West Bengal. The slope, drainage pattern, water availability, soil erosion, and other factors frequently influence the various land use and cover types. Additionally, the size and socio-economic and livelihood pressures that may be present in a given area can have an impact on how diverse land use practices develop. The findings showed that every element had a varied level of influence on the development of various land use and land cover patterns throughout the research locations. However, the development of socioeconomic pressures might occasionally violate the law, severely altering the land resources. People would feel under pressure to go beyond the natural limit, which would decrease the sustainability of the environment. Rearranging land uses in this situation as much as is practical will go a long way toward eradicating the ensuing unsustainability.

Hasan et al (2016) have seen a change in the land use in and around Islamabad. Every day, new urban areas, and business, industrial, and agricultural projects are being built. So, this study's objective was to evaluate how Islamabad's land usage and land cover changed between 1992 and 2012. The results demonstrate that the amount of water, acreage used for development, and agricultural land all increased. The amount of woodland and barren land is reduced on the other side. Population expansion as well as climatic and economic change contributed to this transition. Reduced habitat quality is one of the detrimental repercussions of deforestation and fast urbanization on the ecosystem.

Sajikurnar and Remya (2015) stated that the drainage basin's runoff characteristics are significantly impacted by changes in land use and cover, and these changes in turn influence the region's surface and groundwater availability, leading to further land alteration. In order to ascertain how changes in land use and cover, even at a minor or sub basin level, affect regional runoff characteristics, the author has taken action in this instance. A promising option for this study was determined to be the SWAT (soil and water Analysis Tool) model, a flexible watershed simulation model with several GIS integration options. The model's output revealed that the forest area has a decline of 60% to 32%, respectively. Additionally, the expansion of agricultural land affects groundwater recharge and percolation rates.

Pielke et al (2011) have shown how changes in landscape architecture brought on by human land management over the course of centuries have affected surface fluxes at the local, meso, and regional scales. Using both modeled and observed data, authors have come to the conclusion that failing to take into account this forcing runs the risk of misaligning investment in strategies for climate mitigation and adaptation in places where extensive human landscape change has already occurred or will occur in the future.

Onur et al. (2009) have used remote sensing and a GIS framework to explore the dynamicity of LULC changes in a small town in Turkey. To explore the changes in land use hierarchy after adopting the Coordination of Information on the Environment (CORINE) methodology, almost 30 years' worth of Landsat data have been analysed. From 1975 to 2003, the permanent cropland had declined significantly, according to the GIS analysis of all the data, although there had been no change in the forest area due to the presence of the Olympos-Bey Mountains National Park. This type of research's main objectives are to promote healthier urban development and encourage the maximum amount of natural environment protection.

Falcucci at al. (2007) have examined the changes in Italian land use and cover and their significance for the preservation of biodiversity. Since anthropic disturbances have affected the Mediterranean region for thousands of years, it is currently one of the world's regions that has undergone the most profound change. The entire Italian peninsula has been chosen by the authors to analyse the pattern of land use changes in relation to biodiversity loss between 1960 and 2000. Areas that were intensely cultivated have seen a modern fall, whereas areas that were farmed widely have had a large drop. Mammal and other bird species followed a pattern that was quite similar throughout the same time period. While species that are frequently found in the Mediterranean are declining, forest birds, ungulates, and carnivores all rose. The knowledge

provided by these associated results may be crucial for organizing conservation efforts across the entire Mediterranean region.

2.2.3. Significance of Environmental Flow and the Riverine Ecology

Zhang et al (2023) claimed that as the economy grows, the lower Yellow River region's water resource dispute is getting worse. Increased socioeconomic water demand along with economic growth may have an impact on environmental stability in light of an ecological imprint that is unbalanced. An updated ecological footprint methodology that took soil water into account was used in this investigation. The possibilities for 2025 and 2030 in wet, normal, and arid years were estimated using 30 different scenarios as a guide for decision-makers. The findings suggest that the water supply is influenced by the amount of water resources in the lower Yellow River. When water supplies are distributed, the region with the smallest ecological imprint often benefits. When the ecological footprint of the regional water resources is the shortest, the area with the smallest ecological footprint often receives the allocation of water resources.

Su et al. (2022) indicated that the main reason for problems with water is imbalances in water supply and demand. Such an approach has been used for this study in order to conduct an empirical investigation of the sustainable use of water resources in Japan. The results show that from 1980 to 2020, both traditional and pollutant accounts of Japan's total water ecological footprint decreased, and its spatial pattern was characterized by the relationship that the rate of urbanization was negatively correlated with the size of the water ecological footprint.

Prakasam and Saravanan, (2022) have attempted to evaluate the National Green Tribunal's (NGT) environmental flow order. Environmental flow is the bare minimum flow needed to sustain a healthy ecosystem, and according to NGT's law, 15% of the average flow during the lean season is permitted. According to current ecology and environmental stability, the Larji Hydropower Dam in Kullu, Himachal Pradesh, must maintain up to 20–25% of the typical flow during the dry season. This conclusion was reached after using the flow duration curve approach to determine the scenarios during the lean season.

Houque, et al (2022) have developed a methodical search strategy to identify the prior work that has been published over the past three decades (1990-2020) on a variety of search engines and websites in order to critically examine the concept of environment flow in the context of dams and other development. The writers also failed to mention other forms of development

that impair the river's need for natural flow, such as industrialization, urbanization, the expansion of modern agriculture, etc. In this study, the Damodar River has been selected to examine how the results of the Damodar Valley Project have changed the river's natural flow and the frequency and intensity of its floods. The river in the area's urban industrial district was similarly polluted. The final outcome showed how this environmental risk has endangered aquatic life, the fish community, etc. By carefully assessing the diversity of species, flow variability, and river pollution, this review will inform readers about the long-term implications of dam-induced fluvial dynamism in the environment.

Pace et al. (2022) examined some remote sensing-based metrics to evaluate the state of the riparian vegetation area's quality and general health. The authors of this study prioritized the development of remote sensing technologies since it is expensive and time-consuming to monitor local riparian conditions in the field. The remote sensing-based indices, however, have all been independently verified by a number of field-based indicators along a stretch of a few rivers in northwest Portugal. They found a link between the quantity of dissolved inorganic nitrogen in the forest buffer area and the quality of the riparian flora. Additionally, this study found that changes in vascular plant biomass may be predicted by riparian vegetation density.

Liang et al. (2021) have used a three dimensional ecological model to conduct research on the sustainable use of water resources in the Wuhan metropolitan area. They calculated the natural capital stock's occupancy, the natural capital flow's consumption, and they examined the variables influencing the use of water resources in the development of the research metropolitan region. In order to address the sustainable use of water resources, five different indices including water ecological deficit, water ecological surplus, ecological pressure, it's pressure, its depth; size, etc., have been developed. The findings showed that while population pressure and economic growth had favourable effects on the water ecosystem footprint change, their intensity and carrying capacity had the reverse effect. Finally, a better degree of sustainable water resource utilisation can be achieved by increasing the effectiveness of water resources, utilizing them more effectively, protecting the nation's water capital stock, realizing differentiated regional development through the market economy, and implementing a water policy.

Singh et al. (2021) discussed how riparian zone management can enhance a region's riverine ecosystem. The riparian ecosystem is essential because it acts as an ecological engineer, improving the health of rivers by carrying out a number of tasks. Riparian zones also provide

a variety of other ecologically important roles that benefit human welfare. In contrast, in the contemporary context, riparian ecosystems are seriously threatened by agricultural activities, urbanization, altered river flow, and climate change. Here, the writers have covered all aspects of the riparian zone management process, including its policy framework, stakeholder participation, and public awareness. Aside from that, consider the character, purpose, and vulnerability of riparian areas.

Chua et al. (2019) have chosen the Fitzroy basin in central Queensland, which is a part of the Bioregion belt and is afflicted by the highest rates of tree mortality in Australia as a result of grazing operations close to the riparian zone. In addition to the riverine ecology, river quality has already decreased as a result of plant decline and canal pollution. The author used two approaches in this case, the Rapid Appraisal of Riparian Condition and the Australian Rivers Assessment System, Habitat Assessment, to show that the most extensive riparian zone degradation has been seen upstream in the creek area.

Yin et al. (2018) have created a novel technique for assessing the environmental flow of an urban river, which is currently seen as a top priority because most urban rivers have been transformed into straight channels with concrete channels. This may also result in the valuable species declining, disrupting the ecosystem as a whole. Regarding the longitudinal hydrological connection, they suggest three e-flow degrees (high, medium, and low), where high connection refers to maintained river flow and low scenario is where the connection is limited and e-flow are intermittently linked with some isolated ponds that can further lead to the diminishing of flows. This novel approach may efficiently guide the creation and management of e-flow supply initiatives and can deliver more precise and realistic e-flow results.

Swanson et al. (2017) said that when the riparian habitats have flora, the pollutants can be lessened, rendered less dangerous, or absorbed. Changes in water quality, aquatic life, and indicators of upstream discharge accumulation and shift in riparian functions are all caused by plants, soil, and other physical elements. As a result, a lot of riparian area pollution sources go unnoticed due to faulty and slow water quality monitoring methods. This study examined the proper operation of the following riparian and aquatic habitats and established relationships between these operations and the features of water pollution.

Wurbs and Hoffpauir (2017) developed environmental flow requirements for a small portion of its river system in accordance with a procedure required by law. These requirements are

based on flow regimes, including the size, frequency, magnitude, length, pulse, and overbank flow of flows, as well as the timing of flows required to maintain a healthy environment. This study employed the generalized Water Rights Analysis Package (WRAP), which may be used in any river system. The WRAP and WAM applied modes now have a significantly greater capacity for incorporating the e-flow demand in water allocation and related water availability modeling.

Sahoo et al. (2016) analysed various techniques for evaluating environmental flow in the lower Mahanadi basin. The river almost runs dry throughout the dry season of the year due to the building of hydropower plants and other providing services, such as water retention structures and water extraction by water users, posing a major threat to both the environment and aquatic life. As a result, river management must be done in a way that ensures flushing flow is maintained throughout the year. Here, the authors have used the Global Environmental Flow Calculator (GEFC) software to measure environmental flow using a variety of methodologies, including FDC, Tennant, Tessman, and others.

Verma et al. (2015) noted that it is customary not to acknowledge the assessment of e-flows from a single approach, which is essential for a river's longevity. Three significant hydrological models- Tennent, Tessman, and stochastic FDC—have been used by the authors of this study to estimate E-Flows on various surface waters in the Damodar basin. The construction of new water resources projects, such as the design of storage facilities and the assessment of the amount of accessible water for various uses that satisfies e-flows in the Damodar River basin, will be aided by the output recommended probabilities of 90% and 95% for 7Q50 and 7Q100.

Olley et al. (2014) have addressed the environment in Moriton Bay of Australia, which is a Ramsar, wetland that has been shown to be getting worse because of silt accumulation and nutrient shortfall from the catchment source. Reforestation of canal networks has been advocated as a way to lessen the instability seen in the research area. Additionally, the scientists used multiple linear regression analysis to create a predictive model for the estimation of sediment load. The factor that combined discharge and the percentage of the stream's length that drains remaining vegetation was the most reliable prediction. According to their findings, in order to lower the loads of sediment, phosphorus, and total nitrogen by 50% each, the channel networks beneath the dams would need to be restored.

Li et al. (2013) studied the key variables that have an impact on the Chinese river's environment. Using both quantitative and qualitative analysis, they discovered that the main

factors contributing to the significant decrease in flow caused by various impoundments and structures, deterioration of water quality, channel deformation caused by an increase in sedimentation, and changes in stream slope and river bed structure, loss of vegetation from the bank side, and loss of biodiversity are those that need immediate attention for development.

Karimi and Eslamian (2012) discussed the computer-based assessment of environmental flow in a river for which there is limited information on ecological traits and values. For the investigation of possible e-flow employing FDC curve shifting methodology, the Shahar Chai River in Iran has been selected. Using month-flow data to develop a flow duration curve, this method generates flow requirements for various river ecological parameters. According to the investigated methods, river flows need to be kept within acceptable environmental limits in order to maintain the essential function of the riverine ecosystem.

Minjan et al (2012) have stated that irresponsible water resource development in China's Hao Lino river basin must cause, among other effects, the death of rivers, declines in subterranean water levels, and the extermination of aquatic life. Fish habitat approaches are used to compute the adopted methodology, which primarily depends on the biological & hydrological qualities of the river, in order to ecological flows that will act as a safeguard to the river's health. The results show a minimal river flow to mean annual natural flow ratio of 5–13% for the Liao River as a whole, with a continuous decline in this ratio as one moves downstream. This method is effective for cross sections when the relationship between water level, discharge, and velocity is constant, but it is ineffective for sections that are subject to backwater and tidal effects.

Vyas et al. (2012) examined the state of the riverine ecosystem in the Indian Narmada River basin. A riparian buffer zone is typically made up of shrubs and other flora that have survived the region's continuous riverine flow and other significant physical causes. The authors established a methodology and thoroughly studied both river banks while taking into account the area's ecological importance. They saw that the strain of cropland and human habitation substantially hampered the floodplains and damaged the ecological stability of the area.

Yang et al. (2009) have examined various ecological management objectives and the variation in the e-flow requirements in various Yellow River basin China locations. The maximal main rule has been used to assess water consumption and compatibility based on ecosystem regionalization. National and artificial water consumption has also been identified in order to determine the environmental flow needs for integrated water resource allocation. Finally, the

findings showed that the downstream water requirement should be given top priority when developing integrated water resources plans with regard to its environmental flow requirements.

Huang et al. (2008) emphasized the significance of Wachernagel's ecological footprint model, which is a good tool for measuring the sustainable use of water resources development. However, the approach mainly focused on the production of surface water area for harvesting fish and other seafood, disregarding other essential production functions for water resources. For the purpose of analysing ecological water resources, writers have prioritized three crucial elements at this time: mean worldwide yield, global equivalent factor, and local yield factor.

2.2.4. Impact of Surface and Ground Water Quality

Uddin et al. (2023) have created an improved method for assessing water quality. The goal of the current study was to choose certain feature selection approaches in order to create a useful WQI in coastal locations. In total, 15 sets of datasets were utilized to determine the quality of the coastal waters and machine learning algorithms were employed to test each model's performance. Lastly, using deep learning techniques will enhance the capability of accurately predicting coastal water quality.

Angello et al. (2021) have suggested a novel strategy for studying water quality monitoring. The smallest Akair River in Ethiopia was chosen, and the best pollution load reduction and water quality improvement techniques were used. They noticed that the poor sanitation facilities, weak pollution management strategies, and expanding urbanization have all contributed to the reduction in water quality in Ethiopia's river systems. The management of river water life, pollution reduction, aquatic life protection, and sustainable development in the large catchment could all be improved by a pollution load management and control strategy that incorporates source-based wastewater treatment, diffuse pollution control through best management practices, and in-stream measures like cascaded rock ramp.

Bilali et al. (2021) have used the artificial intelligence application to predict and evaluate the irrigation water quality of the aquifer system. Support vector Regression (SVR) and ANN models are used in this study to forecast TDS, salinity, sodium adsorption rate (SAR), magnesium adsorption rate (MAR), and other variables using electrical conductivity, temperature, and pH as inputs. The characteristics of irrigation water quality can be predicted using these models, which could help farmers and decision-makers manage irrigation water quality.

Chen et al. (2020) applied machine learning models to a comparative evaluation of surface water quality. They highlight how the parameters chosen for the training dataset may affect the effectiveness of machine learning in forecasting the quality of the water in addition to themselves. They compared the water quality prediction performances using 10 different learning models and a large dataset of observations from China's important rivers and lakes between 2012 and 2018. The conclusion shows that larger datasets can improve the learning models' productivity and accuracy in forecasting assessments of water quality.

Jha et al. (2020) have evaluated the quality of groundwater using a fuzzy hybrid water quality index. For a thorough and affordable review, they combined fuzzy logic with a GIS-based evaluation technique. This suggested hybrid framework is illustrated on a hard rock surface in south Indian terrain using 10 prominent groundwater quality indices recorded during pre- and post-monsoon seasons. When comparing the pre-and post-monsoon seasons, the watershed's quality declines, showing a higher influx of contaminants during the monsoon season from numerous industries, mining locations, and garbage disposal sites. These results also call for strict implementation of laws to manage effluents from different sources of contamination within the research area.

Conant et al. (2019) stated that the function of surface water and groundwater and their interaction, which affects the water quantity, quality, and the health of the environment, is the basis for the management of water resources, environmental protection, and land management. In this regard, scholars have put forth a thorough framework to talk about the variables influencing the interaction of surface and groundwater, as well as how they relate to other environmental processes. In order to achieve their goal, they have chosen a few regions in southern Ontario, Canada, and have identified issues such as groundwater nutrient discharge into lakes and rivers and polluted plume water entering rivers. This case study demonstrates how the framework may be tailored to construct conceptual models, assess environmental disturbances, pinpoint knowledge gaps, and provide a framework for organizing the investigation.

Wu et al. (2019) have used statistical and multivariate methods to identify the polluting sources and significant causes of groundwater pollution in the rapidly expanding city of the Chinese Loess Plateau region. The polluting sources and their effects on the quality of groundwater have been depicted using samples collected from shallow pumping wells in Yan'an City and various multivariate techniques including Principal Component Analysis (PCA), Hierarchical Cluster

Analysis, etc. The results show that some natural processes, such as the dissolution of carbonates, silicates, and even soil leaching, are the main regulators of groundwater chemistry, with human activities to be viewed as a supporting element. Therefore, such a study is significantly more effective at determining the quality of groundwater in metropolitan areas.

Mukate et al. (2019) have created a new water quality index (WQI) that can symbolically represent the acceptability of drinking water all around the world. The reason it is known as the Integrated Water Quality Index (IWOI) is that any parameter concentration that is below the desired limit or over the legal limit contributes to the overall rise in index value. The results are produced at a 20% shortfall of the maximum permissible level and can be altered as needed by the user to alert water management of potential threats to human health from drinking water.

Shah and Joshi (2017) have developed a WQI and assessed some of the most significantly impacted parameters, such as pH, DO, BOD, EC, and TC, at three distinct sites along the Sabarmati River basin. This analysis found that the bulk of the indicators had been negatively impacted by sewage discharge into the river and human activity. Additionally, it was discovered that the main causes of the reduction in water quality were excessive anthropogenic activity, unlawful dumping of solid and liquid wastes, poor sanitation, and urban runoff.

Rahamanian et al. (2015) have conducted research on the Perak state's drinking water quality to safeguard public health. In this article, drinking water samples from diverse residential and commercial areas were analysed for a thorough physical and chemical analysis that included several heavy metals including Cu, Zn, Mg, and Cd, as well as other crucial factors like pH, Turbidity, TSS, and TDS. The National Drinking Water Quality Standard (NDWQS), a local standard, and the WHO standard values are used to validate each outcome. Overall, it was found that the water from every location was secure and appropriate for drinking. However, it is also required to take into account additional microbiological and radioactive components, such as human body fluid, in order to assess the whole scenario of the research area's water quality.

Pinto et al. (2013) have concentrated on doing a long-term qualitative analysis of river water located in southeast Australia in order to effectively monitor river health. The peri-urban landscape predominates in this area. The Hawkesbury Nepean River's natural features have grown increasingly complex as a result of the intense pressure of urbanization. For this reason, the authors tried to analyse the historical record to determine whether the effects on the river system were natural or anthropogenic. The results of the analysis showed that agricultural,

sewage, and other industrial effluents had an impact on the river's spatiotemporal fluctuations in water temperature and suspended particles. The information from this study could improve the effectiveness of river health monitoring programs in terms of time, cost, and even in a peri-urban area.

Wang et al. (2013) have researched the Yangtze Estuary's long-term morphological change between the years 1842 and 2006. They used nearly 16 nautical charts, which were then further analysed in a GIS context. The evidence shows that the estuary has been experiencing overall erosion for the past 165 years and has been affected by multiple noteworthy episodes of erosion and deposition. Although human involvement in the estuary was restricted to a few locations, such as the upstream node, it had a significant effect on the geomorphologic history as a whole.

Juahir et al. (2011) examined the surface water quality at seven different locations along Malaysia's Langat River. They included several environmental indices, such as Factor Analysis (FA), Principle Component Analysis (PCA), Hierarchical Agglomerative Cluster Analysis (HACA), etc. Their main goal was to locate the principal source of pollution that could seriously worsen the quality of the river's water. The results show that home and agricultural runoffs are mostly to blame for the decline in river water quality. In addition, industrial and municipal trash are also deposited close to the river bank, seriously polluting the waterway.

Sharma and Kansal (2011) have created a water quality index (WQI) for the Yamuna River, which is thought to be the most contaminated due to the amount of residential runoff that is seen there. Therefore, improving the river's water quality has been a big problem for environmental managers. The goal of the study was to ascertain how accurately WQI could represent the river's level of pollution throughout a ten-year period starting in 2000 and ending in 2009. Pre-monsoon, monsoon, and post-monsoon data results revealed that with the exception of Palla, all other locations' water quality slipped into the bad category and necessitated quick treatment.

Delpa et al. (2009) had reviewed the most recent interdisciplinary literature on the topic of water quality analysis in order to create a synthesis. In addition to the effects of climate change on water availability and hydrological risks, they claimed that research into the effects on water quality is only just getting started. They thought about ways to alter the physical and chemical characteristics of natural water and how that might affect the quality of drinking water. Additionally, it has been found that urban, industrial, and other human activities are closely related to water consumption and that these activities may indirectly worsen surface water

quality due to climate change. The main point that can be made is that when the quality of drinking water diminishes as a result of climate change, more situations arise where potentially harmful health impacts could exist.

Boyacioglu & Boyacioglu (2007) have chosen the Buyuk Meanders River basin and its tributaries in Turkey for the examination of river water quality using environmental data. Eleven factors have been chosen, and samples have been taken at 17 different locations to determine the water quality. Factor analysis was performed to pinpoint the key components that explain the correlations between the observations. The findings indicated that agricultural uses significantly impacted the quality of the water.

Panda et al. (2006) have used R-mode factor analysis and cluster analysis to analyse the Mahanadi River's and estuary water quality. These multivariate analyses are often used to describe and rate the quality of water, and they are useful for showing temporal and seasonal changes brought on by both anthropogenic and natural factors. The results of research using the R-Mode factor indicate that nutrition input from humans is what reduces the DO and pH levels of water, albeit the magnitude of this impact varies depending on whether the water is fresh or salty and throughout different times of the year. This study aims to show that depending on the system, the relative influence of various water quality indicators varies. This study highlights the necessity and importance of these concepts for the efficient management of freshwater and estuarine systems.

References

- Abijith, D., Saravanan, S. (2022). Assessment of land use and land cover change detection and prediction using remote sensing and CA Markov in the northern coastal districts of Tamil Nadu, India. *Environ Sci Pollut Res 29*, 86055–86067. https://doi.org/10.1007/s11356-021-15782-6
- Ahmad, W., Iqbal, J., Nasir, M.J. *et al.* (2021). Impact of land use/land cover changes on water quality and human health in district Peshawar Pakistan. *Sci Rep 11*, 16526. https://doi.org/10.1038/s41598-021-96075-3
- Ahrendt, S., Horner-Devine, A. R., Collins, B. D., Morgan, J. A., & Istanbulluoglu, E. (2022). Channel Conveyance Variability can Influence Flood Risk as Much as Stream flow Variability in Western Washington State. Water Resources Research, 58(6), e2021WR031890.
- Ajadi, S. A., & Adedeji, O. (2022). Assessing the Influence of Climatic Factors on the Morphometric Analysis of Shiroro Drainage Basin using Remote Sensing and GIS Techniques. *World Scientific News*, *172*, 131-143.
- Ameri, A. A., Pourghasemi, H. R., & Cerda, A. (2018). Erodibility prioritization of sub-watersheds using morphometric parameters analysis and its mapping: A comparison among TOPSIS, VIKOR, SAW, and CF multi-criteria decision making models. *Science of the Total Environment*, *613*, 1385-1400.
- Angello, Z.A., Behailu, B.M., Tränckner, J. (2021). Selection of Optimum Pollution Load Reduction and Water Quality Improvement Approaches Using Scenario Based Water Quality Modeling in Little Akaki River, Ethiopia. *Water*. *13*(5):584. https://doi.org/10.3390/w13050584
- Aouragh, M. H. & Essahlaoui, A. (2018). A TOPSIS approach-based morphometric analysis for sub-watersheds prioritization of high Oum Er-Rbia basin, Morocco. *Spatial Information Research*, *26*, 187-202.
- Asif, Z., Chen, Z., Sadiq, R. et al. (2023). Climate Change Impacts on Water Resources and Sustainable Water Management Strategies in North America. *Water Resour Manage.* 37, 2771–2786, https://doi.org/10.1007/s11269-023-03474-4
- Bilali, A.E., Taleb, A., Brouziyne, Y. (2021). Groundwater quality forecasting using machine learning algorithms for irrigation purposes. *Agricultural Water Management. 245*, 106625, ISSN 0378-3774, https://doi.org/10.1016/j.agwat.2020.106625.
- Boyacioglu, H., Boyacioglu, H. (2007). Surface Water Quality Assessment by Environmetric Methods. *Environ Monit Assess 131*, 371–376. https://doi.org/10.1007/s10661-006-9482-4
- Chatterjee, R., & Purohit, R. R. (2009). Estimation of replenishable groundwater resources of India and their status of utilization. Current Science, 96(12), 1581–1591. http://www.jstor.org/stable/24104886
- Chen, K., Chen, H., Zhou, C., Huang, Y., Qi, X., Shen, R., Liu, F., Zuo, M., Zou, Z., Wang, J., Zhang, Y., Chen, D., Chen, X., Deng, Y., Ren, H. (2020). Comparative analysis of surface water quality prediction performance and identification of key water parameters using different machine learning models based on big data, *Water Research. 171*,115454, ISSN 0043- 1354,https://doi.org/10.1016/j.watres.2019.115454.
- Chen, W. B., Liu, W. C. (2017). Modeling the Influence of River Cross-Section Data on a River Stage Using a Two-Dimensional/Three-Dimensional Hydrodynamic Model. *Water*, *9*, 203. https://doi.org/10.3390/w9030203

- Chowdary, V. M., Ramakrishnan, D., Srivastava, Y. K., Chandran, V., & Jeyaram, A. (2009). Integrated water resource development plan for sustainable management of Mayurakshi watershed, India using remote sensing and GIS. *Water resources management*, *23*(8), 1581-1602.
- Chua, E.M., Wilson, S.P., Vink, S., Flint, N. (2019). The influence of riparian vegetation on water quality in a mixed land use river basin. *River Res Applic. 35*, 259– 267. https://doi.org/10.1002/rra.3410
- Conant, B., Robinson, C.E., Hinton, M.J., Russell, H.A.J. (2019). A framework for conceptualizing groundwater-surface water interactions and identifying potential impacts on water quality, water quantity, and ecosystems, *Journal of Hydrology. 574*, 609-627, ISSN 0022-1694, https://doi.org/10.1016/j.jhydrol.2019.04.050.
- Das, S., Angadi, D.P. (2022). Land use land cover change detection and monitoring of urban growth using remote sensing and GIS techniques: a micro-level study. *Geo Journal* 87, 2101–2123. https://doi.org/10.1007/s10708-020-10359-1
- Debanshi, S., & Pal, S. (2020). Assessing gully erosion susceptibility in Mayurakshi river basin of eastern India. *Environment, Development and Sustainability*, *22*, 883-914.
- Delpla, I., Jung, A.V., Baures, E., Clement, M., Thomas, O. (2009). Impacts of climate change on surface water quality in relation to drinking water production, *Environment International. 35*, (8), 1225-1233, ISSN 0160-4120, https://doi.org/10.1016/j.envint.2009.07.001.
- Falcucci, A., Maiorano, L. & Boitani, L. (2007). Changes in land-use/land-cover patterns in Italy and their implications for biodiversity conservation. *Landscape Ecol.* 22, 617–631. https://doi.org/10.1007/s10980-006-9056-4
- Fenicia, F., & McDonnell, J. J. (2022). Modeling streamflow variability at the regional scale:(1) perceptual model development through signature analysis. Journal of Hydrology, 605, 127287.
- Ghosh, A. & Maiti, R. (2021). Development of new Ecological Susceptibility Index (ESI) for monitoring ecological risk of river corridor using F-AHP and AHP and its application on the Mayurakshi river of Eastern India, *Ecological Informatics*, Volume 63, 101318, ISSN 1574-9541 https://doi.org/10.1016/j.ecoinf.2021.101318.
- Ghosh, A. & Maiti, R. (2021). Soil erosion susceptibility assessment using logistic regression, decision tree and random forest: study on the Mayurakshi river basin of Eastern India. *Environ Earth Sci,* 80, 328 (2021). https://doi.org/10.1007/s12665-021-09631-5
- Ghosh, A., Rakshit, S., Tikle, S., Das, S., Chatterjee, U., Pande, C.B., Alataway, A., Al-Othman, A.A., Dewidar, A.Z., Mattar, M.A. (2023). Integration of GIS and Remote Sensing with RUSLE Model for Estimation of Soil Erosion. *Land*, 12(1):116. https://doi.org/10.3390/land12010116
- Ghosh, S., Chaudhury, S., & Manoj, K. (2017). An Appraisal of the Mayurakshi River System Water Quality–the Agrarian Basin. *Int. J. Agric. Environ. Sci*, *4*(4), 53-59.
- Ghosh, S., Hoque, M., Saha, U. D, Islam, A. (2022). Assessment of dam-induced changes in eco-geomorphological behaviour and fluvial functionality in the Damodar River, West Bengal, India. *AQUA - Water Infrastructure, Ecosystems and Society* 1 June, 71 (6): 722–750. https://doi.org/10.2166/aqua.2022.003
- Gopinath, G., Nair, A. G., Ambili, G. K., & Swetha, T. V. (2016). Watershed prioritization based on morphometric analysis coupled with multi criteria decision making. *Arabian Journal of Geosciences*, *9*, 1-17.

- Govekar, P., Gudagur, J. T. & Asode, A.N. (2023). Morphometric analysis of Hirehalla Sub-basin of Malaprabha River, Northern Karnataka using geoinformatics techniques. *Journal of Geomatics*, *17*(1), 121–130. https://doi.org/10.58825/jog.2023.18.1.9
- Hassan, Z., Shabbir, R., Ahmad, S.S. et al. (2016). Dynamics of land use and land cover change (LULCC) using geospatial techniques: a case study of Islamabad Pakistan. *Springer Plus* 5, 812.https://doi.org/10.1186/s40064-016-2414-z
- Hoque, M.M., Islam, A. & Ghosh, S. (2022). Environmental flow in the context of dams and development with special reference to the Damodar Valley Project, India: a review. *Sustain. Water Resour. Manag*. 8, 62. https://doi.org/10.1007/s40899-022-00646-9
- Huang, L. N., Zhang, W. X., Jiang, C. L., & Fan, X. Q. (2008). Ecological footprint method in water resources assessment. *Acta Ecologica Sinica*, *28*(3), 1279-1286.
- Islam, A. & Sarkar, B. (2021). Analysing flood history and simulating the nature of future floods using Gumbel method and Log-Pearson Type III: The case of the Mayurakshi River Basin, India. Bulletin of Geography. *Physical Geography Series*, 19. 43-69. 10.2478/bgeo-2020-0009.
- Islam, A., & Ghosh, S. (2021). Economic transformation in the wake of flood: a case of the lower stretch of the Mayurakshi River Basin, India. *Environ Dev Sustain.* 23, 15550–15590. https://doi.org/10.1007/s10668-021-01310-6
- Islam, A., Deb Barman, S. (2020). Drainage basin morphometry and evaluating its role on flood-inducing capacity of tributary basins of Mayurakshi River, India. *SN Appl. Sci*. 2, 1087. https://doi.org/10.1007/s42452-020-2839-4
- Islam, A., Ghosh, S., Sarkar, M., Barman, S.D., Shit, P.K., Rahman, A. (2023). Agrarian and Socio-Infrastructural Vulnerability in the Wake of Flood: An Example from the Mayurakshi River Basin, India. In, et al. Floods in the Ganga–Brahmaputra–Meghna Delta. *Springer Geography. Springer, Cham*. https://doi.org/10.1007/978-3-031-21086-0_10
- Islam, A., Guchhait, S.K. (2020). Characterizing cross-sectional morphology and channel inefficiency of lower Bhagirathi River, India, in post-Farakka barrage condition. *Nat Hazards*. 103, 3803–3836. https://doi.org/10.1007/s11069-020-04156-9
- Jha, M.K., Shekhar, A., Jenifer, M.A. (2020). Assessing groundwater quality for drinking water supply using hybrid fuzzy-GIS-based water quality index, *Water Research.179*, 115867, ISSN 0043-1354, https://doi.org/10.1016/j.watres.2020.115867.
- Jha, V. C., & Bairagya, H. (2012). Floodplain planning based on statistical analysis of Tilpara Barrage discharge: a case study on Mayurakshi River Basin. *Caminhos de Geografia*, *13*(43), 326-346.
- Jhariya, D.C., Kumar, T. & Pandey, H.K. (2018). Watershed Prioritization Based on Soil and Water Hazard Model Using Remote Sensing, Geographical Information System and Multi-Criteria Decision Analysis Approach, *Geocarto International*, 10.1080/10106049.2018.1510039
- Juahir, H., Zain, S.M., Yusoff, M.K. et al. (2011). Spatial water quality assessment of Langat River Basin (Malaysia) using environmetric techniques. *Environ Monit Assess. 173*, 625–641. https://doi.org/10.1007/s10661-010-1411-x
- Karimi, S., Yasi, S. M. & Eslamian, S. (2012). Use of hydrological methods for assessment of environmental flow in a river reach. *Int. J. Environ. Sci. Technol. 9*, 549–558. https://doi.org/10.1007/s13762-012-0062-6

- Kashaigili, J. J., Rajabu, K., & Masolwa, P. (2009). Freshwater management and climate change adaptation: experiences from the Great Ruaha River catchment in Tanzania. *Climate and Development*, *1*(3), 220-228.
- Khatun, S., & Pal, S. (2016). Control of Hydrological and Geomorphic Characteristics on Land Use Land Cover of Kushkarni River Basin of East India. *International Journal of Engineering Science and Computing*, 6(7), 8505–8515.
- Kisku, S., Chini, D.S., Bhattacharya, M., Kar, A., Parua, S., Das, B.K., Patra, B.C. (2017). A cross-sectional study on water quality in relation to fish diversity of Paschim Medinipur, West Bengal, India through geoinformatics approaches, *The Egyptian Journal of Aquatic Research*, Volume 43, Issue 4, 2017, Pages 283-289, ISSN 1687-4285, https://doi.org/10.1016/j.ejar.2017.12.001.
- Leete, R., Donnay, F., Kersemaekers, S., Schoch, M., & Shah, M. (2003). Global population and water. *UNFPA report on Population and Development Strategies Series*.
- Li, Q., Song, J., Wei, A. et al. (2013). Changes in major factors affecting the ecosystem health of the Weihe River in Shaanxi Province, China. *Front. Environ. Sci. Eng. 7*, 875–885. https://doi.org/10.1007/s11783-013-0568-2
- Liang, D., Lu, H., Feng, L., Qiu, L., He, L. (2021). Assessment of the Sustainable Utilization Level of Water Resources in the Wuhan Metropolitan Area Based on a Three-Dimensional Water Ecological Footprint Model. *Water*, *13*, 3505. https://doi.org/10.3390/w13243505
- Liu, Z., Wang, T., Han, J., Yang, W., & Yang, H. (2022). Decreases in mean annual stream flow and interannual stream flow variability across snow-affected catchments under a warming climate. *Geophysical Research Letters*, 49(3), e2021GL097442.
- Meshram, S. G. & Sharma, S. K. (2017). Prioritization of watershed through morphometric parameters: a PCA-based approach. *Applied Water Science*, 7, 1505-1519.
- Minjian, C., Gaoxu, W., Huali, F., Liqun, W. (2012). The Calculation of River Ecological Flow for the Liao Basin in China, *Procedia Engineering. 28*, 715-722, ISSN 1877-7058, https://doi.org/10.1016/j.proeng.2012.01.796.
- Mondal, D. & Pal, S. (2018). Monitoring dual-season hydrological dynamics of seasonally flooded wetlands in the lower reach of Mayurakshi River, Eastern India, *Geocarto International*, 33:3, 225-239, DOI: 10.1080/10106049.2016.1240720
- Mondal, M., Ghosh, S. & Satpati, L.N. (2018). Optimum cross section index (OCI): a new approach for identification of an optimum channel—a case study of the Ichamati River, India. *Arab J Geosci*. 11, 333. https://doi.org/10.1007/s12517-018-3667-3
- Mukate, S., Wagh, V., Panaskar, D., Jacobs, J.A., Sawant, A. (2019). Development of new integrated water quality index (IWQI) model to evaluate the drinking suitability of water, *Ecological Indicators.101*, 348-354, ISSN 1470-160X, https://doi.org/10.1016/j.ecolind.2019.01.034.
- Mukhopadhyay, S., & Das, P. (2013). Channel deranging and its impact: a study on Mayurakshi-Kuya interfluve, Santal Pargana and Birbhum Districts, Jharkhand and West Bengal. *Journal of Indian Geomorphology*, *2*, 37-45.
- Naemitabar, M., Asadi, M.Z. & Karami, M. (2022). Morphometric analysis for the assessment of relative tectonic activity using GIS-based multi-criteria analysis (case study: Torbat Heydariyeh Kalshur Basins, Iran). *Arab J Geosci*. 15, 1037. https://doi.org/10.1007/s12517-022-09993-5

- Nag, S., Biswas Roy, M. & Roy, P. (2020). Optimum Prioritisation of Sub-watersheds based on Erosion Susceptible Zones through Modelling and GIS Techniques. *Modeling Earth Systems and Environment*, 6. 10.1007/s40808-020-00768-z.
- Nag, S., Karmakar, S., Roy, M. B., & Roy, P. K. (2023). A Combined use of Hydraulic and Hydrological Model to Characterise Channel Hydro-Geomorphology of a Tropical River Basin of West Bengal, India.
- Nag, S., Roy, M. B., & Roy, P. K. (2022). Study on the functionality of land use land cover over the evaluation of groundwater potential zone: A fuzzy AHP based approach. *Journal of Earth System Science*, 131(3), 146.
- Olley, J., Burton, J., Hermoso, V., Smolders, K., McMahon, J., Thomson, B., and Watkinson, A. (2015). Remnant riparian vegetation, sediment and nutrient loads, and river rehabilitation in subtropical Australia. *Hydrol. Process.* 29, 2290– 2300. doi: 10.1002/hyp.10369.
- Onur, I., Maktav, D., Sari, M., & Kemal Sönmez, N. (2009). Change detection of land cover and land use using remote sensing and GIS: a case study in Kemer, Turkey. *International Journal of Remote Sensing*, 30(7), 1749–1757. https://doi.org/10.1080/01431160802639665
- Pace, G., Gutiérrez-Cánovas, C., Henriques, R., Carvalho-Santos, C., Cássio, F., Pascoal, C. (2022). Remote sensing indicators to assess riparian vegetation and river ecosystem health, *Ecological Indicators. 144*, 109519, ISSN 1470-160X, https://doi.org/10.1016/j.ecolind.2022.109519.
- Pal, R. (2015). Channel Avulsion Archives and Morphological Readjustment near the Bhagirathi-Mayurakshi Confluence in the Lower Gangatic Plain, West Bengal, India. *J. Environ. Earth Sci*, *5*(3), 67-75.
- Pal, S. (2016). Impact of Massanjore dam on hydro-geomorphological modification of Mayurakshi river, Eastern India. *Environment, development and sustainability*, *18*, 921-944.
- Pal, S. (2017). Impact of Tilpara barrage on backwater reach of Kushkarni River: a tributary of Mayurakshi River. *Environment, Development and Sustainability*, *19*, 2115-2142.
- Pal, S. (2017). Impact of Tilpara barrage on backwater reach of Kushkarni River: a tributary of Mayurakshi River. *Environment, Development and Sustainability*, *19*, 2115-2142.
- Pal, S., & Debanshi, S. (2018). Influences of soil erosion susceptibility toward overloading vulnerability of the gully head bundhs in Mayurakshi River basin of eastern Chottanagpur Plateau. *Environment, Development and Sustainability*, *20*, 1739-1775.
- Pal, S., Let, S., & Das, P. (2012). Assessment of channel width disparity of the major rivers within Mayurakshi River Basin. *Int J Geol Earth Environ Sci*, *2*(3), 1-10.
- Panda, U.C., Sundaray, S.K., Rath, P., Nayak, B.B., Bhatta, D. (2006). Application of factor and cluster analysis for characterization of river and estuarine water systems – A case study: Mahanadi River (India), *Journal of Hydrology. 331*, 3–4, 434-445, ISSN 0022-1694, https://doi.org/10.1016/j.jhydrol.2006.05.029.
- Pielke, R.A., Sr., Pitman, A., Niyogi, D., Mahmood, R., McAlpine, C., Hossain, F., Goldewijk, K.K., Nair, U., Betts, R., Fall, S., Reichstein, M., Kabat, P. and de Noblet, N. (2011). Land use/land cover changes and climate: modeling analysis and observational evidence. *WIREs Clim Change*, 2: 828-850. https://doi.org/10.1002/wcc.144

- Pinto, U., Maheshwari, B. L., & Ollerton, R. L. (2013). Analysis of long-term water quality for effective river health monitoring in peri-urban landscapes--a case study of the Hawkesbury-Nepean river system in NSW, Australia. *Environmental monitoring and assessment*, *185*(6), 4551–4569. https://doi.org/10.1007/s10661-012-2888-2
- Portuguez-Maurtua M, Arumi, J. L., Stehr, A., Lagos, O., Chávarri-Velarde, E., Rivera-Ruiz, D. (2023). Mapping of Areas Vulnerable to Flash Floods by Means of Morphometric Analysis with Weighting Criteria Applied. *Water*. 15(6):1053. https://doi.org/10.3390/w15061053
- Prakasam, C., Saravanan, R. (2022). Ecological flow assessment using hydrological method and validation through GIS application, *Groundwater for Sustainable Development. 19*, 100841, ISSN 2352-801X, https://doi.org/10.1016/j.gsd.2022.100841.
- Rahmanian, N., Ali, S.H., Homayoonfard, M., Ali, N., Rehan, M., Sadef, Y., & Nizami, A.S. (2015). Analysis of Physiochemical Parameters to Evaluate the Drinking Water Quality in the State of Perak, Malaysia. *Journal of Chemistry.*1-10.
- Ralph, A., Wurbs, R., Hoffpauir, J. (2017). Environmental flow requirements in a water availability modeling system. *Sustainability of Water Quality and Ecology, 9* (10), 9-21, ISSN 2212-6139, https://doi.org/10.1016/j.swaqe.2016.05.003.
- Rwanga, S.S. and Ndambuki, J.M. (2017). Accuracy Assessment of Land Use/Land Cover Classification Using Remote Sensing and GIS. *International Journal of Geosciences*, 8, 611-622. https://doi.org/10.4236/ijg.2017.84033
- Sahoo, S., Khare, D., Mishra, P., Behera, S., Krishan, R. (2016). A Comparative Study on Environmental Flows Assessment Methods in Lower Reach of Mahanadi River. *International Journal of Engineering Trends and Technology*. 32. 82-90. 10.14445/22315381/IJETT-V32P215.
- Sajikumar, N., Remya, R.S. (2015). Impact of land cover and land use change on runoff characteristics. *Journal of Environmental Management*, 161, 460-468, ISSN 0301-4797, https://doi.org/10.1016/j.jenvman.2014.12.041.
- Samal, D.R., Gedam, S. (2021). Assessing the impacts of land use and land cover change on water resources in the Upper Bhima river basin, India, *Environmental Challenges*, Volume 5, 100251, ISSN 2667-0100, https://doi.org/10.1016/j.envc.2021.100251.
- Schäppi, B., Perona, P., Schneider, P., Burlando, P. (2010). Integrating river cross section measurements with digital terrain models for improved flow modelling applications, *Computers & Geosciences*, Volume 36, Issue 6, Pages 707-716, ISSN 0098-3004, https://doi.org/10.1016/j.cageo.2009.12.004.
- Şener, M., Arslanoğlu, M.C. (2023). Morphometric analysis in Google Earth Engine: An online interactive web-based application for global-scale analysis, *Environmental Modelling & Software*, Volume 162, 105640, ISSN 1364-8152, https://doi.org/10.1016/j.envsoft.2023.105640.
- Shah, K.A., Joshi, G.S. (2017). Evaluation of water quality index for River Sabarmati, Gujarat, India. *Appl Water Sci.7*, 1349–1358. https://doi.org/10.1007/s13201-015-0318-7
- Sharma, D., Kansal, A. (2011). Water quality analysis of River Yamuna using water quality index in the national capital territory, India (2000–2009). *Appl Water Sci 1*, 147–157. https://doi.org/10.1007/s13201-011-0011-4
- Sharma, P., Gupta, G., Prabhakar, P., Tiwari, S., Kathait, P., Pathak, Y., Mishra, N. & Kumar, S. (2017). Land Use Land Cover Change Impact on Water Resources- A

Review. *International Journal of Advances in Engineering & Scientific Research*. 4. 7-14. 10.5281/zenodo.569714.

- Sheldon, F., Peterson, E. E., Boone, E. L., Sippel, S., Bunn, S. E., & Harch, B. D. (2012). Identifying the spatial scale of land use that most strongly influences overall river ecosystem health score. *Ecological Applications*, *22*(8), 2188-2203.
- Singh, R., Tiwari, A., Singh, G. (2021). Managing riparian zones for river health improvement: an integrated approach. *Landscape and Ecological Engineering. 17*. 3. 10.1007/s11355-020-00436-5.
- Song, P., Wang, C., Ding, D., Sun, J., Kong, L., Lu, M., Lei, X., Wang, H. (2022). Evaluating the impact of climate change on surface water resources in the upper Ganjiang River Basin, China. *Journal of Water and Climate Change* 1 March, 13 (3): 1462–1476. https://doi.org/10.2166/wcc.2022.258
- Song, W., & Deng, X. (2017). Land-use/land-cover change and ecosystem service provision in China. *Science of the Total Environment*, 576, 705-719.
- Sreedevi, P.D., Subrahmanyam, K. & Ahmed, S. (2005). The significance of morphometric analysis for obtaining groundwater potential zones in a structurally controlled terrain. *Env Geol* 47, 412–420. https://doi.org/10.1007/s00254-004-1166-1
- Su, Y., Zheng, Q., & Liao, S. (2022). Spatio-Temporal Characteristics of Water Ecological Footprint and Countermeasures for Water Sustainability in Japan. *International journal of environmental research and public health*, *19*(16), 10380. https://doi.org/10.3390/ijerph191610380
- Swanson, S., Kozlowski, D., Hall, R., Heggem, D., & Lin, J. (2017). Riparian proper functioning condition assessment to improve watershed management for water quality. *Journal of soil and water conservation*, *72*(2), 168–182. https://doi.org/10.2489/jswc.72.2.168
- Talukdar, S., Singha, P., Mahato, S., Pal, S., Liou, S., Rahman, Y.A. (2020). Land-Use Land-Cover Classification by Machine Learning Classifiers for Satellite Observations—A Review. *Remote Sens. 12*, 1135. https://doi.org/10.3390/rs12071135
- Tewabe, D. & Fentahun, T (2020). Assessing land use and land cover change detection using remote sensing in the Lake Tana Basin, Northwest Ethiopia, *Cogent Environmental Science*, 6:1, DOI: 10.1080/23311843.2020.1778998
- Uddin, M.G., Nash, S., Rahman, A., Olbert, A.I. (2023). Assessing optimization techniques for improving water quality model, *Journal of Cleaner Production. 385*, 135671, ISSN 0959-6526, https://doi.org/10.1016/j.jclepro.2022.135671.
- Verma, R.K., Murthy, S., Tiwary, R. K. (2015). Assessment of Environmental Flows for Various Sub-Watersheds of Damodar River Basin Using Different Hydrological Methods. *Int J Waste Resour 5*, 182.
- Vinayak, B., Lee, H.S., Gedem, S. (2021). Prediction of Land Use and Land Cover Changes in Mumbai City, India, Using Remote Sensing Data and a Multilayer Perceptron Neural Network-Based Markov Chain Model. *Sustainability*, *13*, 471. https://doi.org/10.3390/su13020471
- Vyas, V., Kumar, A., Wani, S. G., & Parashar, V. (2012). Status of riparian buffer zone and floodplain areas of River Narmada, India. *International journal of environmental sciences*, *3*(1), 659-674.
- Wang, Y., Dong, P., Oguchi, T., Chen, S., Shen, H. (2013). Long-term (1842–2006) morphological change and equilibrium state of the Changjiang (Yangtze) Estuary,

China, *Continental Shelf Research, 56*, 71-81, ISSN 0278-4343, https://doi.org/10.1016/j.csr.2013.02.006.

- Wei, S., Yang, H., Abbaspour, K., Mousavi, J., & Gnauck, A. (2010). Game theory based models to analyze water conflicts in the Middle Route of the South-to-North Water Transfer Project in China. *Water research, 44*(8), 2499-2516.
- Wei, S., Yang, H., Song, J., Abbaspour, K. C., & Xu, Z. (2012). System dynamics simulation model for assessing socio-economic impacts of different levels of environmental flow allocation in the Weihe River Basin, China. *European journal of operational research, 221*(1), 248-262.
- Wu, J., Li, P., Wang, D., Ren, X., & Wei, M. (2020). Statistical and multivariate statistical techniques to trace the sources and affecting factors of groundwater pollution in a rapidly growing city on the Chinese Loess Plateau. *Human and Ecological Risk Assessment: An International Journal*, *26*(6), 1603-1621.
- Yang, Z.F., Sun, T., Cui, B.S., Chen, B., Chen, G.Q. (2009). Environmental flow requirements for integrated water resources allocation in the Yellow River Basin, China. *Communications in Nonlinear Science and Numerical Simulation. 14*, (5), 2469-2481, ISSN 1007-5704, https://doi.org/10.1016/j.cnsns.2007.12.015.
- Yin, X., Yang, Z., Zhang, E., Xu, Z., Cai, Y., Yang, W. (2018). A New Method of Assessing Environmental Flows in Channelized Urban Rivers. *Engineering. 4*. 10.1016/j.eng.2018.08.006.
- Zhang, S., Li, H., Li, C., Yi, Y., Wang, X., Liu, Q. (2023). Allocation of water resources in the lower Yellow river based on ecological footprint. *Frontiers in Earth Science. 10*. ISSN=2296-6463, https://www.frontiersin.org/articles/10.3389/feart.2022.1018980
- Zuo, D., Xu, Z., Wu, W., Zhao, J., & Zhao, F. (2014). Identification of stream flow response to climate change and human activities in the Wei River Basin, China. *Water Resources Management*, *28*, 833-851.

CHAPTER 3
RESEARCH DESIGN

3. Significance of Eco-environmental Hydrological Studies

Eco-environmental quality analysis refers to an assessment of the entire ecological and environmental assemblage or some of its constituent parts in a chosen area by choosing pertinent elements like geology, land resources, water resources, environment, and economy within a specified temporal and spatial scope. Since Doxiadis first coined the term "Ekistics" in the 1950s, developed nations have begun to statistically analyse and evaluate the quality of the eco-environmental condition (Mukherjee et al.1979, Pacione 2003). For many years, the development of evaluation indicator systems and measurement procedures was the main emphasis of eco-environmental research. The foundation for establishing eco-environmental quality assessment is a suitable indicator system, in which the indicators can be chosen from a variety of environmental features, infrastructure, and social-economic components. Eco-environmental studies address various aspects of qualification and quantification. The majority of research are based on quantitative methods that employ equations or models to determine specific indicators of community, economy, and environment, and that allow for the assessment of the influence of human activities and the environment as a whole on ecosystem variance. Analytical hierarchy process (Cao et al. 2012), fuzzy evaluation (Chen et al. 2013), principal component analysis (Keshavarzi & Kumar 2019), BP neural network (Zhao et al. 2019), support vector machine (SVM) model (Wang et al. 2021), and set pair analysis (He et al. 2021) are the most often used quantitative evaluation techniques for the assessment of eco-environmental studies. Meanwhile, improvements in computer technology make the transition from physical representation to spatial analysis has become easier. For example, Jing et al. (2020) analysed the ecological environment quality of the Aibi Lake Wetland Nature Reserve in Xinjiang, China, using the RSEI model and RS technology. Using spatial statistics, Fu et al. (2017) evaluated the Songhua River's coastline condition. Xin and Liu (2022) used the GIS spatial analysis approach, the NAR neural network model, spatial auto regression, and a spatially weighted regression model to investigate the driving forces behind eco-environmental protection and high-quality development in the Yellow River Basin, China. They said that the phrase "eco-environmental" refers to the establishment and application of some strategies that have successfully promoted ecological conservation as well as contributing to the sustainable development of a region. In recent years, study on eco-environmental protection and high-quality development of a watershed has emerged as an increasingly popular subject and has drawn more academic attention, as it directly or indirectly influences the region's total economic prosperity. The inevitable expansion of social and economic forces is sometimes

given priority over ecological and environmental development. Many social and economic development elements have profited from this, including widespread and enormous high-tech businesses, scientific and technological innovation, the creation of massive municipal structures, and amusement parks that lag behind the area's ecological and environmental prospects. As a result, it is necessary to identify and implement several measures that have effectively promoted ecological protection and contributed to the region's sustainable development. Despite the extensive research, there are still some limitations in the evaluation of regional eco-environmental quality. For example, external interference and data uncertainty result in indicators of evaluation that are not fully complete, and subjectivization and fuzziness in the weighing of indicators can affect the nonlinearity and non-normality of the indicator system.

3.1.Need for Research in this Area

Water resources are composite assets from an economic perspective that offer a range of products and services for human consumption and production (Wei et al. 2010; Zuo et al. 2014). However, excessive socioeconomic activity and human involvement in recent years have severely degraded the ecosystem in riverine areas, and the need to restore and maintain the river basin area has garnered a lot of attention.

To sustain the global hydrologic change, a river's ecological and environmental health evaluation is quite important. The quantity and quality of water flows necessary to maintain freshwater and the riverine ecology, as well as the human livelihood and wellbeing that depend on these ecosystems, are defined by the environmental health assessment. In the context of certain hydrological and ecological conditions, a river's ecological functions must be maintained for it to flow sustainably. Ecological processes in a large river are governed by flow variability. However, the recent global climate change is anticipated to bring about a global vicious cycle on the water supplies. The impact of climate change combined with population growth and economic development has significantly changed a river's flow pattern. Regarding its flow pattern, water quality, availability of water, etc., a river's health faces a number of ecological and environmental issues. West Bengal has already begun to confront the water crisis. West Bengal experienced 11% less rainfall in 2014 than its average monthly rainfall during the monsoon season, which runs from June to September. According to the Irrigation and Waterways Directorate (2014), the post-monsoon rainfall in October 2014 was 65% below average, which was also very poor. The availability of different water footprints, such as green

water, and blue water, is still decreasing. In the past 20 years, India's overall water supply per person dropped from 4000m^3 to 1869m^3 (UNEP, 2008). Since the economy of West Bengal is built on agriculture, the demand for water in the agricultural and energy sectors would take up the largest percentage of the state's water supply. According to projections, West Bengal's water consumption will increase from 7.71 mm in 2000 to 10.98 mm in 2025, creating a 59% shortfall from a 38% surplus (Bhuin, 2014). Rivers have lost their carrying capacity as a result of extensive human interference. The natural flow of water and river beds can occasionally be encroached upon by unplanned industrial growth, siltation, and sedimentation. In West Bengal, many rivers, including the Saraswati and Behula, have already dried up. Therefore, it is crucial to research how surface water invasion affects communities at both the regional and local levels. In this hypothetical situation, an attempt has been made to evaluate the water resources that are currently available or how climate change can affect the West Bengali Mayurakshi river basin's water supply.

The Mayurakshi River (length 288 km) is an important western tributary of the Bhagirathi. Its catchment area (5325 sq. km) is located in the transitional region between the Chotonagpur plateau and the Bengal basin, two mega physiographic provinces (Bhattacharya, A. 2013). This river has a long geological history with significant tectonic influences because of its geographic effect. There are remnants of evidence from at least three erosion surfaces, suggesting the tectonic movements are still active (Chakrabarti 1970). However, in the Anthropocene, structural restrictions brought about by dams and barrages, namely the Massanjore Dam and Tilpara Barrage, are clearly shown as having control over the Mayurakshi River basin. Physically, the Mayurakshi River Basin is made up of highlands on the Chhotonagpur Plateau that border the hot and humid Rarh plain in Birbhum and Murshidabad districts. West Bengal experiences very unpredictable rainfall patterns, which heavily rely on the state's main economic activity, agriculture. Such a hydro-climatic situation encourages a variety of extreme hydrological occurrences, such as floods and droughts, and it also hinders agricultural production. After gaining independence in 1951, the Bengal Government launched the Mayurakshi Reservoir Project and Canal Irrigation System with funding from the Canadian Government in order to adapt to such hydrological events and increase the agriculture yield of this area. It is the first significant irrigation project West Bengal has undertaken after gaining independence. In the beginning, it was only irrigated between the Mayurakshi and Brahmani rivers in the north and the Ajoy Rivers in the south. The vast population of Birbhum, Murshidabad, and Bardhaman districts benefits most from the increase in irrigated areas. The

mass population of that region has benefited greatly from the overall advantages of the construction of the Massanjore Dam and Tilpara Barrage, which are regarded as pillars of the economic development of that region. Unfortunately, the region has not been able to follow the path of sustainable growth and development in recent years. Such construction activities have reduced carrying capacity and may cause significant changes in river cross sections. The Mayurakshi River has changed dramatically during the past ten years as a result of development activity. The mainstream is being impounded by several dams, barrages, and reservoirs, which not only disrupt its natural flow pattern but also structurally control it. The river's primary flow is now maintained within a constrained area of active channels, and it is insufficient to meet the environmental flow requirements for enhancing or restoring the overall condition of the riverine ecosystem. The downstream channel has undergone extensive fluvial change, and irregular channel geometry, variation in channel width, and depth have all been observed. In the high, middle, and lower reaches of the basin, no correct geometric trend has been followed, which encourages uneven channel design and processes. (Nag et al. 2023). The dam reservoir modifies the flow regimes and sediment budget, affecting agriculture and soil erosion in the region, resulting in significant sediment deposition in the lower course of the Mayurakshi River. Another significant issue in the reservoir is siltation, which lowers its capacity and submerges the area around it. The submergence and absence of floodwater near the dammed area also have a significant impact on the channel floodplain, the riparian zone, and aquatic species. In-stream sedimentation, population growth, the conversion of agricultural land, and sand mining operations inside the active river bed are the main causes of the loss of riparian covering and aquatic ecosystems (Plate No. 3.1a-f). From the field study, authors observed unscientific sand mining has been going on the river bed in progressive way for which the channel shape, size and its natural flow is getting hampered. Such changes in channel configuration, continues narrowing and widening of channel may disturb the normal hydro-morphological rhythm of the river (Pal et al. 2012).

In addition, the physiochemical characteristics of the river water are also changed by dam construction. The process of trapping silt and nutrients alters the water's temperature and turbidity in the downstream section of the river, affecting the aquatic community. Beside this, this river has a significant impact on the basin's social, ecological, and economic development. About 90% of the population in this region, which is mostly made up of farming areas, relies on agriculture for a livelihood (Chakraborty 2015). For their irrigation needs, they heavily rely on water from rivers and canals. However, because of the yearly unpredictability of

rainfall, the main channel water and other sources of surface water are becoming less abundant (Pal et al. 2012). As a result, the current aquifer system is under tremendous pressure due to the excessive use of groundwater through the drilling of wells and submersible pumping (Plate no. 3.1e-f). Such situation further give rise to the water scarcity, which is primarily seen in the lower stretch of Mayurakshi river basins. The installation of a significant number of pumping wells close to the river bank may have decreased water infiltration, causing the fall of groundwater table in the river basin area. Due to its history of disastrous floods and water inundations, the majority of Birbhum district still struggles with water scarcity, especially during the dry season. (Department of Irrigation and Waterways, 2006).

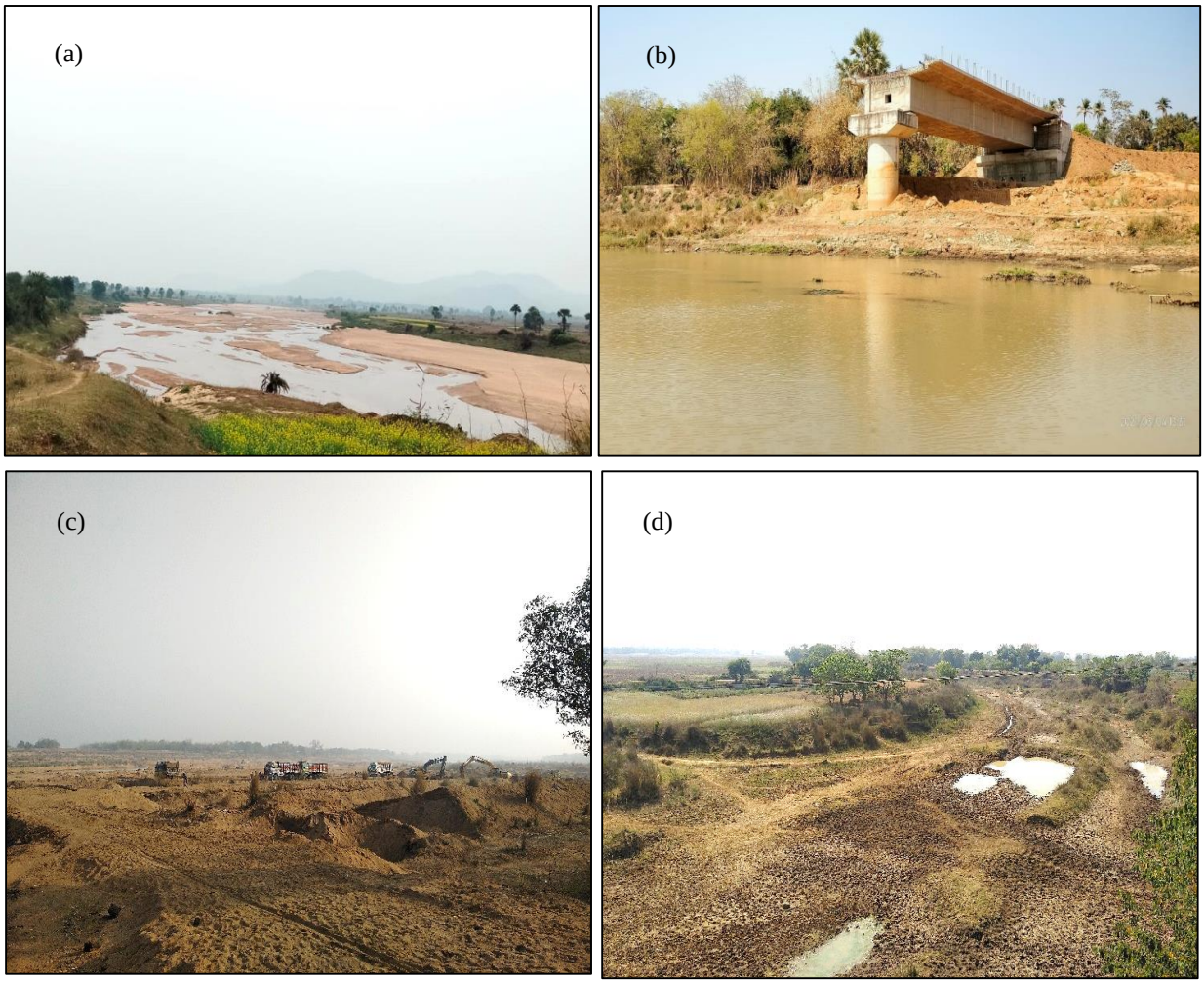

Plate No. 3.1 *Field Observations Regarding Mayurakshi River and Riparian Health Degradation (a) In stream channel sedimentation (b) Loss of riparian cover due to bridge constructions (c) Sand mining activity on the river bed (d) Channel bed deformation (e) Excessive Use of Groundwater by Submersible Shallow Pump (f) Crop Land Converted into Seasonal Fallow Land due to Lack of Water for Irrigational Purposes*

Plate No. 3.1 *Continued*

The planners and developers must pay the necessary attention to such fluvial metamorphosis in the environment caused by dams. In order to avoid further deterioration in the ecosystem functions of the Mayurakshi River, it is important to take into account the physical health of the catchment and restore the ecological balance of the riparian area.

3.2. Research Gap

In the last two decades, a significant amount of scientific study has been published on the assessment of ecological and environmental flow or control of river flows to mitigate the effects of hydrologic modification. A study was undertaken by Yang, Z. F. et al. (2008) to identify the ecologically necessary flow levels taking into account several ecological functions for a sustainable water resource allocation plan and management approach. Unreasonable water resource development causes the depletion of channels, declines in groundwater levels, the destruction of aquatic habitats, etc. In order to determine the minimal river flow necessary to maintain the low flow channel and the aquatic ecology, Minjian C. et al. (2012) conducted a study on the Liao basin in China in 2012. In order to examine prospective environmental flows in a river reach of the Shahr Chai River in Iran, Karimi. S.S. and Eslamian. S. (2012) conducted a study using a newly developed hydrological technique called Flow Duration Curve shifting. The results were also contrasted with those from the other methods to confirm the necessary flow to preserve the fundamental operations of the river ecosystem. However, the direct effects of human activity on river channels through flow fluctuation and water use patterns have not yet been fully addressed. However, Pal et al. (2012) investigated changes in channel instability and asymmetry in channel width that show a high positive association with human activities.

Ghosh and Pal (2015) provide an illustration of the influence of dams and barrages on river flow characteristics and the subsequent changes in the region's flood behaviour. These studies might not provide a thorough assessment of the effects of ecological or environmental disturbances brought on by physical imbalance in the watershed. Any river system that experiences such physiological changes may endanger the ecological equilibrium of the region as well as the riparian ecology. Therefore, a significant gap in scientific assessment has been found that integrates the evaluation of river health encompassing its physical, biological, and social behaviour.

In a nutshell, the structure and functions of each river are evaluated to determine its overall health. The physical state of any river is mostly covered by its morphology, while its chemical and biological makeup are covered by its physiology. The physical state of the river also includes changes in its hydrological behaviour, channel migration and shifting, changes in its path, and related phenomena like flooding and river bank erosion. The ecological significance of the river water is included in the physiological condition of the river and its surrounding riparian area. Thus, a thorough hydrological assessment incorporates fluvial geomorphology, river hydrology, and environmental as well as ecological perspectives, which is limited in Indian scenario. It is important to note that human activity has the potential to alter all of the aforementioned aspects of river health. In light of this, the current study places particular emphasis on the development of holistic methodologies through the integration of multidisciplinary data (physical, ecological, and social) that have a great potential to determine the issues causing overall river health degradation and to produce some potential conclusions that could aid in rebuilding the ecological and environmental balance of the river basin area.

3.3. Research Hypothesis

The entire research work are carried out by considering some of the research hypothesis as mentioned below-

- Massanjore Dam and Tilpara Barrage are the only two significant river impoundment structures that are largely thought to be responsible for any form of changes in Mayurakshi River.
- The long-term historical stream flow data of Massanjore Dam and Tilpara Barrage, which was obtained from the government agency, was regarded as an unregulated flow and had no impact on the results of hydrological simulation.

- The output of the hydrological evaluation is unaffected by some outliers and missing data observed in the secondary dataset of daily discharge, which have been substituted by the average value of the corresponding months of the particular year.
- The riparian area of the Mayurakshi River Basin has been designated within a 100 m buffer zone because it possesses all of the distinctive features of the regional riparian vegetation.

3.4. Research Objectives

In accordance with previously published research, the Mayurakshi River Basin's extreme climatic and hydrologic variability, combined with such structural impoundments on the river, have caused a decrease in water availability, which has led to a decrease in the minimum flow necessary to maintain the estuarine ecosystem of the Mayurakshi River Basin area. This poses a serious risk to the overall health condition of the river. As a result, focus should be placed on monitoring the environmental and ecological value of the Mayurakshi River Basin area using a number of physical, biological, and social indicators that will precisely reflect the outcomes necessary to maintain the freshwater ecosystem of the Mayurakshi River basin area. To achieve such goal, the following aspects of the work scope must be taken into account.

3.4.1. Scope of Research

The scope of the entire research work has been divided into three phases, as mentioned below-

Assessment of Physical Indicators-

- Preparation of hydro-geological and hydro-morphological databases of the study area, which have a significant impact over the water resources scenario of the region.
- Identification of possible trend and magnitude of long term hydro-climatological dataset of the Mayurakshi River basin area. This study also includes the determination of possible correlation between rainfall frequency, intensity and duration over the basin area.
- Assessment of water resources vulnerability in terms of both surface and ground water using multiple indicators representing the water availability in the Mayurakshi basin area.
- Investigation of hydro-geomorphological behaviour of the Mayurakshi river with due emphasis on its consistency and variability in river discharge and velocity in different segments of the river during the low flow season.

- Study the impact of Land use land cover change on different hydrological processes in a temporal scale of 32 years of the study area. Along with this, an application of multi-layer perception neural network approach to examine the potentiality impact of future land use land cover dynamism over the study area.

Assessment of Ecological Indicators-

- Estimation of hydrological fluxes (water budget) and stream flow simulation at a high spatial and temporal resolution using SWAT model.
- Quantification of ecosystem service values and functions of the study area in response to the impact of exploitation of natural and urban land resources.
- Assessment of the quality of riparian vegetation, to ensure the environmental and ecological integrity of the fluvial ecosystem of the study area.
- Assessment and evaluation of Environmental Flow of the study area using different methods and determination of quantity of flow required for sustaining the surrounding ecosystem.
- Investigation of the current state of the physical, chemical, and biological quality of surface and ground water resources in order to determine the impact of pollution load in the Mayurakshi River and adopt appropriate measures to keep potable water safe for human use.

Assessment of Social Indicators-

- A perception study of the river bank dwellers with respect to the impact of various social, environmental and ecological view on the Mayurakshi River and its surroundings.

3.5. Novelty of Research

The term "hydrological studies" often refers to the qualitative and quantitative evaluation of the available water resources that are at risk as a result of extreme circumstances witnessed by climatological events around the world. In contrast, anthropogenic activities are equally to blame for the depletion of surface water resources. These elements not only limit the availability of water but also have an impact on its quality. Such difficulties can severely undermine the balance of the environment. In terms of the previous study, there are relatively few studies that will emphasize both the physical and ecological aspects of the river basin. In

this situation, the novel approach of the current research places special emphasis on the development of comprehensive strategies through the combination of multifaceted indicators (physical, ecological, and social) which holds considerable potentiality for discovering the challenges causing overall river ecosystem deterioration and come up with a few possible conclusions that could help in restoring the ecological and social equilibrium of the river basin area.

References

- Annual flood report, Irrigation and Waterways Directorate, Government of West Bengal, May 2014
- Bhattacharyya, A. (2013). Evaluation of hydro genomic characteristics of flood in the Mayurakshi river basin of eastern India.
- Bhuin, P. K. (2014). Sustainable water resource management in West Bengal: A review. *Bhatter College Journal of Multidisciplinary Studies*, *4*, 94-104.
- Cao, D. Y., Huang, C. L., Wu, J., Li, H. T., & Zhang, Y. D. (2012). Environment carrying capacity evaluation of coal mining in Shanxi Province. *Advanced Materials Research*, *518*, 1141-1144.
- Chakraborty, A. (2015). Study on growth of major agricultural crops in Birbhum district. *J. Agric. Vet. Sci*, *2*(1), 63-66.
- Chakraborty, S. C. (1970). Some consideration on the evolution of physiography of Bengal. *Geography Institute. Presidency College, Calcutta*, 20-21.
- Chen, J., Ma, L., & Zhang, H. (2013). A new method for mining area ecological environment assessment based on credibility measure. *Kybernetes*, *42*(1), 55-66.
- Fu, B., Li, Y., Wang, Y., Campbell, A., Zhang, B., Yin, S., ... & Jin, X. (2017). Evaluation of riparian condition of Songhua River by integration of remote sensing and field measurements. *Scientific reports*, *7*(1), 2565.
- Ghosh, K. G., & Pal, S. (2015). Impact of dam and barrage on flood trend of lower catchment of Mayurakshi river basin, eastern India. *European Water*, *50*, 3-23.
- He, G., Bao, K., Wang, W., Zhu, Y., Li, S., & Jin, L. (2021). Assessment of ecological vulnerability of resource-based cities based on entropy-set pair analysis. *Environmental technology*, *42*(12), 1874-1884.
- *http://www.india-wris.nrsc.gov.in*
- Jing, Y., Zhang, F., He, Y., Johnson, V. C., & Arikena, M. (2020). Assessment of spatial and temporal variation of ecological environment quality in Ebinur Lake Wetland National Nature Reserve, Xinjiang, China. *Ecological Indicators*, *110*, 105874.
- Journal of Irrigation and Waterways Department, 2006
- Keshavarzi, A., & Kumar, V. (2019). Ecological risk assessment and source apportionment of heavy metal contamination in agricultural soils of Northeastern Iran. *International journal of environmental health research*, *29*(5), 544-560.
- Minjian, C., Gaoxu, W., Huali, F., & Liqun, W. (2012). The calculation of river ecological flow for the Liao Basin in China. *Procedia Engineering*, *28*, 715-722.
- Mukherjee, M., Ray, A. K., & Rajyalakshmi, C. (1979). Physical quality of life index: Some international and Indian applications. *Social Indicators Research*, *6*, 283-292.
- Nag, S., Karmakar, S., Roy, M. B., & Roy, P. K. (2023). A Combined use of Hydraulic and Hydrological Model to Characterise Channel Hydro-Geomorphology of a Tropical River Basin of West Bengal, India.
- Pacione, M. (2003). Urban environmental quality and human wellbeing—a social geographical perspective. *Landscape and urban planning*, *65*(1-2), 19-30.
- Pal, S., Let, S., & Das, P. (2012). Assessment of channel width disparity of the major rivers within Mayurakshi River Basin. *Int J Geol Earth Environ Sci*, *2*(3), 1-10.

- Shaeri Karimi, S., Yasi, M., & Eslamian, S. (2012). Use of hydrological methods for assessment of environmental flow in a river reach. *International journal of environmental science and technology*, *9*, 549-558.
- United Nations Environmental Programme Annual Report, 2008
- Wang, Y., Wu, X., He, S., & Niu, R. (2021). Eco-environmental assessment model of the mining area in Gongyi, China. *Scientific Reports*, *11*(1), 17549.
- Wei, S., Yang, H., Abbaspour, K., Mousavi, J., & Gnauck, A. (2010). Game theory based models to analyze water conflicts in the Middle Route of the South-to-North Water Transfer Project in China. *Water research*, *44*(8), 2499-2516.
- Xin, Y., & Liu, X. (2022). Coupling driving factors of eco-environmental protection and high-quality development in the yellow river basin. *Frontiers in Environmental Science*, *10*, 951218.
- Yang, Z. F., Sun, T., Cui, B. S., Chen, B., & Chen, G. Q. (2009). Environmental flow requirements for integrated water resources allocation in the Yellow River Basin, China. *Communications in Nonlinear Science and Numerical Simulation*, *14*(5), 2469-2481.
- Zhao, K., He, T., Wu, S., Wang, S., Dai, B., Yang, Q., & Lei, Y. (2019). Application Research of Artificial Neural Network in Environmental Quality Monitoring. *International Journal of Pattern Recognition and Artificial Intelligence*, *33*(12), 1959039.
- Zuo, D., Xu, Z., Wu, W., Zhao, J., & Zhao, F. (2014). Identification of streamflow response to climate change and human activities in the Wei River Basin, China. *Water Resources Management*, *28*, 833-851.

CHAPTER 4
METHODOLOGICAL FRAMEWORK

4. Introduction

Research is a methodical process of inquiry that involves gathering data, documenting important information, and then analysing and interpreting that data and information in accordance with appropriate procedures established by particular academic and professional disciplines. This chapter primarily focuses on the methodology employed in the current study to establish the facts and figures of the Mayurakshi River's ecological and environmental significance. Figure 4.1 depicts the overall methodological structure of this study, which may be split into three phases: pre-field, field, and post-field work. The next section provides a thorough, systematic discussion of each phase.

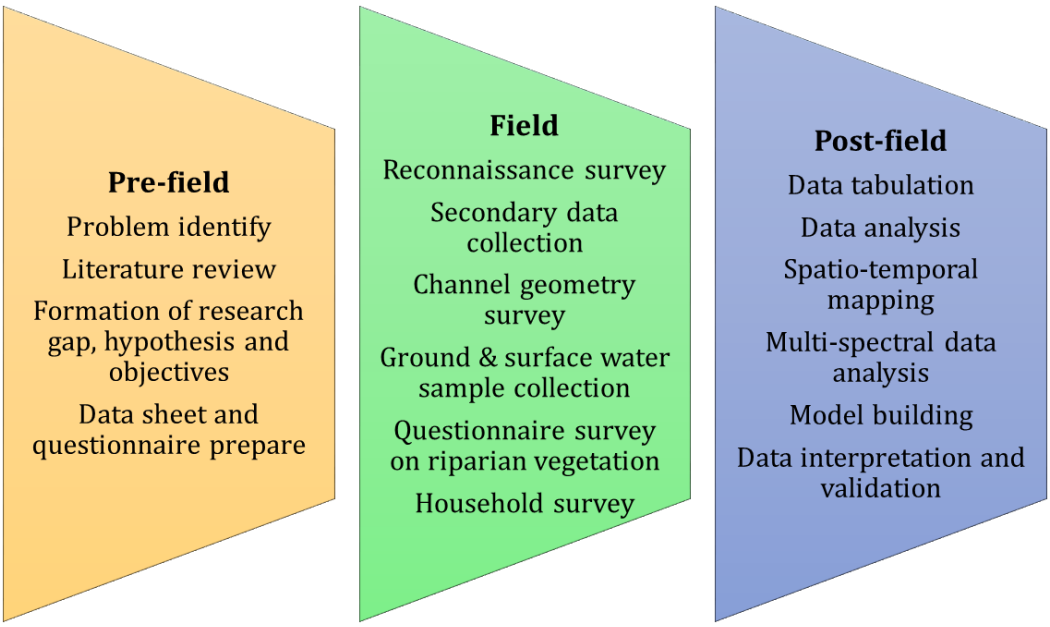

Figure 4.1 *Methodological Framework used in this Research*

4.1. Pre-field Work

This pre-fieldwork phase of a research entails the planning, setup, and groundwork that must be done before commencing actual fieldwork. This stage is essential for making research well-designed, practical, and morally upright. During the pre-fieldwork stage, the following actions and factors has been taken into account:

For the purpose of gathering background information on the subject area, a thorough reconnaissance study has been conducted. The main issues with the research area's overall environmental relevance have been determined from this survey. This stage involves a thorough review of the published literature, which includes books, journals, articles,

governmental publications, and even newspapers. The creation of the research gap and research questions has been made possible by studying the previously published works on the Mayurakshi River. After that, a thorough study proposal that included appropriate research questions, objectives, methodology, and anticipated results had been developed. At this level, the relevant maps and secondary data have been gathered from various private and public sectors. These include soil maps from the National Bureau of Soil Survey and Land Use Planning (NBSS & LUP), hydro-meteorological dataset from the Indian Meteorological Department, Pune, Government of India (https://www.imdpune.gov.in/), topographical maps from Survey of India, geological maps from the Geological Society of India (GSI), and geomorphological and other thematic layers from the BHUVAN website (https://bhuvan.nrsc.gov.in/home/index.php). The Central Water Commission (CWC), Government of India, and the Irrigation and Waterways Department, Government of West Bengal, have provided historical river gauge data. Developing the relevant questionnaires and other data sheets for gathering the essential primary data for this research is another crucial step in this phase. Other than that, several multi spectral high resolution satellite imageries have also been downloaded for further analysis from USGS Earth Explorer website (https://earthexplorer.usgs.gov/).

4.2. Field Work

This study could be of two forms, depending on its purpose: a survey of physical things or a study of socioeconomic elements. A region's physical characteristics include its topography, terrain and slope characteristics, river or drainage characteristics, physical and chemical characteristics of the soil, and type of vegetation, among others. In this research, authors have conducted a Differential Global Positioning System (DGPS) survey to measure the cross-sectional bed profile across the 14 selected sections of the river Mayurakshi during the month of December, 2021.During this survey Post Processed Kinematic Survey (PPK) method has been applied by which the measured elevation data has been calibrated with reference to its closest permanent/local benchmark point using Trimble Business Centre software in post survey period (Plate No. 4.1a-b). The measurement of flow velocity in each section has been done using Current Meter instrument. It is regarded as most convenient instrument in hydrometry which measures at a point flow of water in a particular depth. (Subramanya 2008).The bank full height of each survey sites has been identified by visualising the demarcation of floodplain areas, water mark on the riparian vegetation zone and also from the local dwellers. Slope is another important parameter for the construction of cross profiles. It is

the ratio of vertical gradient to its horizontal distance (Sen 1993). Here, to calculate the longitudinal slope, vertical gradient and equivalent horizontal distance of a particular channel has been measured using Google Earth Pro software. Other important channel features like channel depth, width, thalweg point have been measured with the help of measuring staff and tape. Furthermore, the investigation on soil properties in terms of its conductivity and infiltration properties has been carried out through Vertical Electrical Sounding (VES) survey and soil infiltrometer test over the river basin area (Plate No. 4.1c-d). For a qualitative analysis of both ground and surface water, the samples have been collected by a random sampling method from the concerned area of the studied region. Following the steps outlined in APHA (2012), the samples were collected, transferred and analysed in the laboratory of School of water Resources Engineering, Jadavpur University.

To explore the socio-economic scenario of a study area, a researcher has to collect some primary data by door to door survey. This study interprets the perception of local people regarding their surrounding environment, the condition of Mayurakshi River and its associated riparian vegetation. This study employed an indirect survey methodology and incorporated qualitative research as part of the surveying procedure by asking the locals. First, a questionnaire survey form was created to collect data. Later, other researchers visited the study area with some people to interview them directly. There were both closed- and open-ended questions on the survey form. In the first section of the survey, participants were asked to self-report their socio-demographic information. In the second phase, a thorough questionnaire survey has been carried out of over 230 respondents, most of whom live close to riverbank areas and have knowledge of the surroundings and local dynamics.

4.3. Post-field Work

A research project's post-fieldwork phase signifies the transition from data gathering to data analysis, interpretation, and synthesis. This stage is essential for integrating the unprocessed fieldwork data into valuable insights and findings. In this phase, all collected secondary information has processed, tabulated and analysed individually depending on their purpose of objective to this research. Several spatial and temporal mapping techniques has been executed through advanced remote sensing software system. Various multi-criteria decision making model has been applied for a periodical and scientifically assessment. For a detailed qualitative and quantitative analysis, various statistical tools were also used in this research like SPSS, Matlab, R software etc. Finally, to determine the consistency of analysed output or to establish

the viability and reliability of the study, each quantitative variables have been validated with the primary filed observed dataset.

Plate No. 4.1 *Field Work (a) DGPS Survey (b) Channel Thalweg Measurement (c) VES Survey (d) Soil Infiltration Test*

References

- Sen PK (1993) Geomorphological analysis of drainage basins. Univ of Burdwan Burdwan: 5
- K. Subramanya (2008) Engineering Hydrology. 3rd Edition, Tata McGraw-Hill Publishing, New Delhi
- APHA (2012) Standard Methods for the Examination of Water and Waste Water. 22nd Edition, American Public Health Association, American Water Works Association, Water Environment Federation.

CHAPTER 5
DESCRIPTION OF THE STUDY AREA

5. Introduction

Understanding the geophysical state of the river basin is necessary for a scientific and logical response to various river problems as well as for proper planning and design of water resources projects. The river, its shape, and how it interacts with the shaded area are all a reflection of the existing relief, topography, litho-tectonic-structural characteristics, prevailing climate, presence and state of soil and vegetation. All of these components and variables serve as an indication and multidimensional mirror on which the geomorphic environment, in particular, is reflected. The purpose of this chapter is to give a comprehensive overview of the Mayurakshi River Basin area, including its geographic location and the physical landscape of the study area.

5.1. Locational Description

Mayurakshi River is an important western tributary of the Bhagirathi River, which drains from the region of Jharkhand to the Bengal plain area. It covers an area about 5325 sq. km having a longitudinal extent of 86°84'–88°22' E to latitudinal extend of 23°64'–24°62' N. It has its origin on the Trikut hill, about 16km from Deoghar in Jharkhand, India. It flows through Deoghar, Dumka and Jamtara district of Jharkhand and then through the districts of Birbhum and Murshidabad in West Bengal and finally drains into the river Bhagirathi (Fig. 5.1). This 288km long river makes some important tributaries on both side of its flowing route like Dhobi, Motihara, Tepra, Matihara, Bhurbhuri, Siddheswari, Bhamri, Pusaro, Main channel, Bara Nadi, Kushkarini and Kuya river. Physiographically, the river basin comprises of fringe part of the highland of the Chhotonagpur Plateau and the Rarh plain of the Birbhum and Murshidabad districts of West Bengal, which experiences hot and humid climatic conditions throughout the year (Pal 2015).

Since the time of independence, Mayurakshi River has been playing an important role both to the state of Jharkhand and West Bengal. Two major structures that had been impounded on this river i.e., Massanjore dam and Tilpara barrage (Fig. 5.2) and its adjoining canal system, are the prime reason behind the success of agricultural development in West Bengal (Annual flood report 2016). Mayurakshi Reservoir Project and Canal Irrigation System are the first major irrigation project in West Bengal after independence which were started by the Bengal Government with the financial assistance of the Canada Government. The fruitfulness of this project was very much reflected through the enhancement of crop productivity by which a huge

number population of Birbhum, Murshidabad, and Bardhaman districts are benefited (Annual Flood Report, 2016).

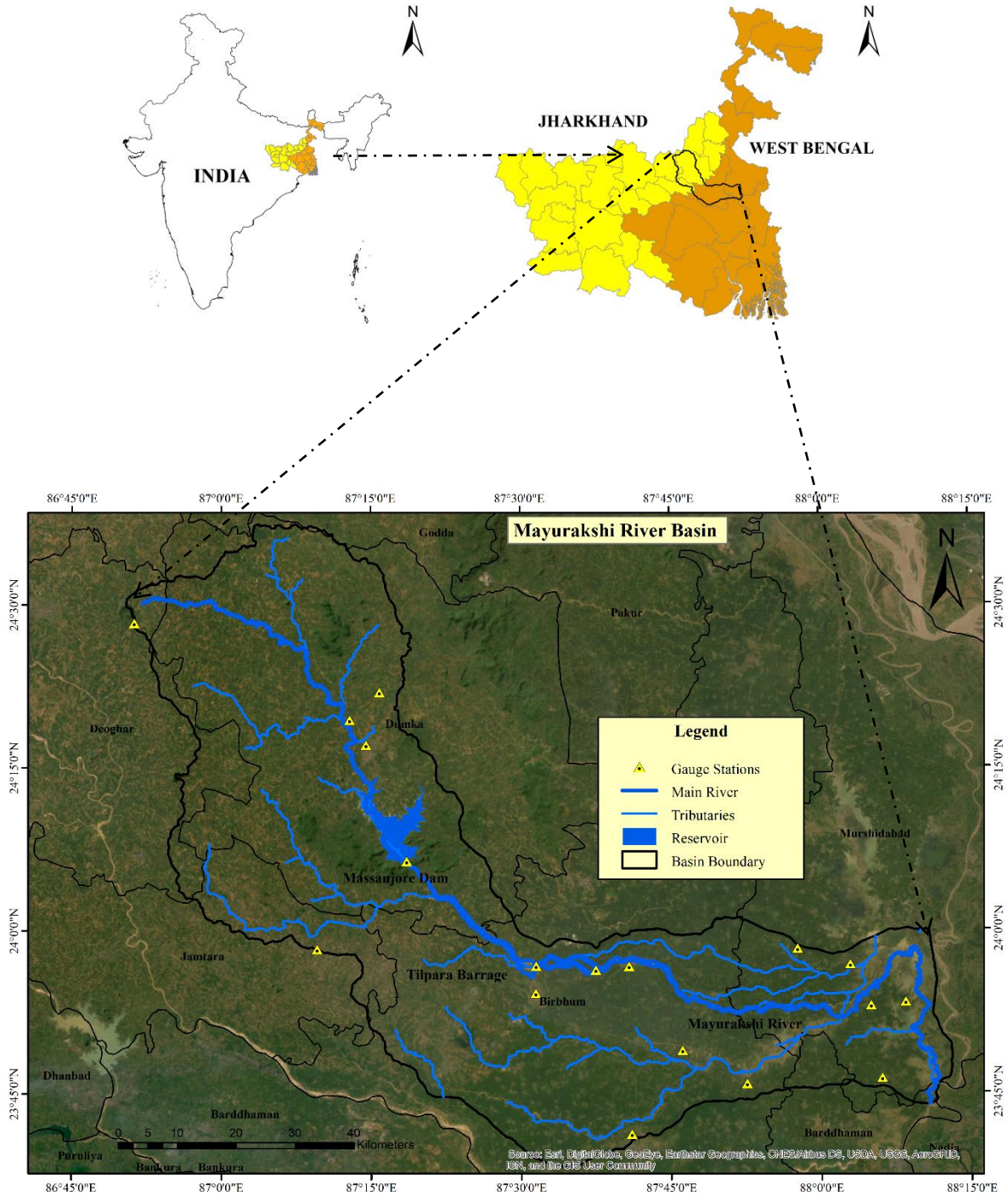

Figure 5.1 *Location Map of the Study Area*

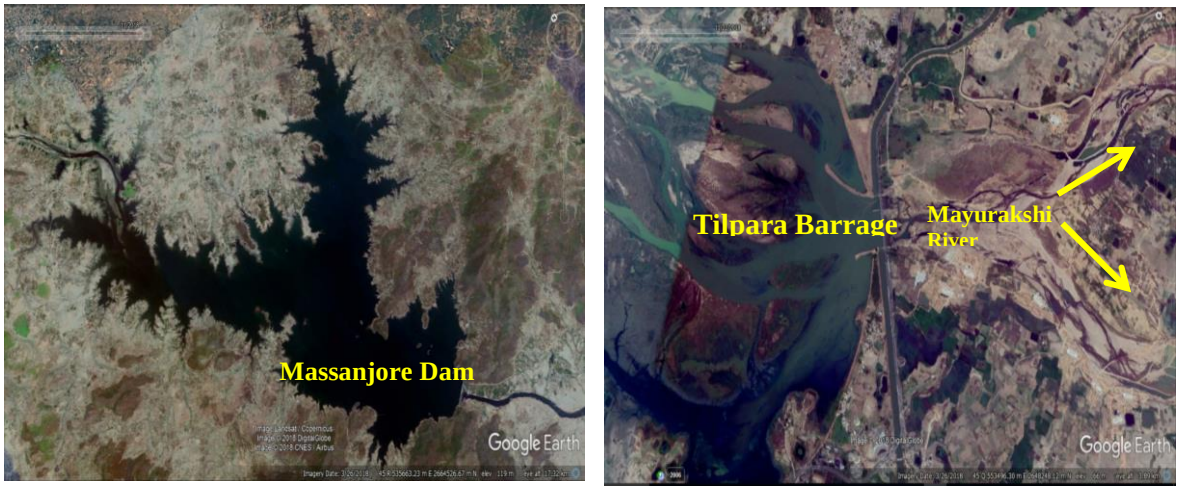

Figure 5.2 *Google Earth View of Massanjore Dam and Tilpara barrage*

5.2. Physical Set-up of Study Area

Investigation of the root cause of a problem in an area or to plan and manage those problems in a scientific way, understanding of the geo-physical and environmental condition is a pre-requisite. A river, which passes through various stages of developmental activities, from youth to mature stage is the reflection of the existing relief properties, dominance various geological and geomorphological characteristics prevailing to this area. All these factors are very much interconnected with each other which might resultant towards any kind of geographical changes in an area. So, this chapter focussed on to infer the characteristics of such independent variables which are controlling the physical nature of the river basin.

5.2.1. The Physiography

Mayurakshi River basin has been located within the transitional zone between two mega physiographic provinces namely the Chhotonagpur plateau and the Bengal basin (Pal and Debanshi 2018). The basin has been characterised by numerous flat-topped hills and undulating plateau cover. The Trikut hill is the highest peak in this region having the elevation of about 750m, located in the Dumka district of Jharkhand. Other important isolated hills are Nawadih, Makra pahar, Punch pahar etc. situated in this region. Physiographically, the Mayurakshi river basin has been divided into three catchment zones- upper catchment, middle catchment and lower catchment (Fig. 5.3). A section line has been drawn from the highest elevation to the lowest elevation of the basin to observe the break of slope and physiographic division of the river basin (Fig. 5.4).

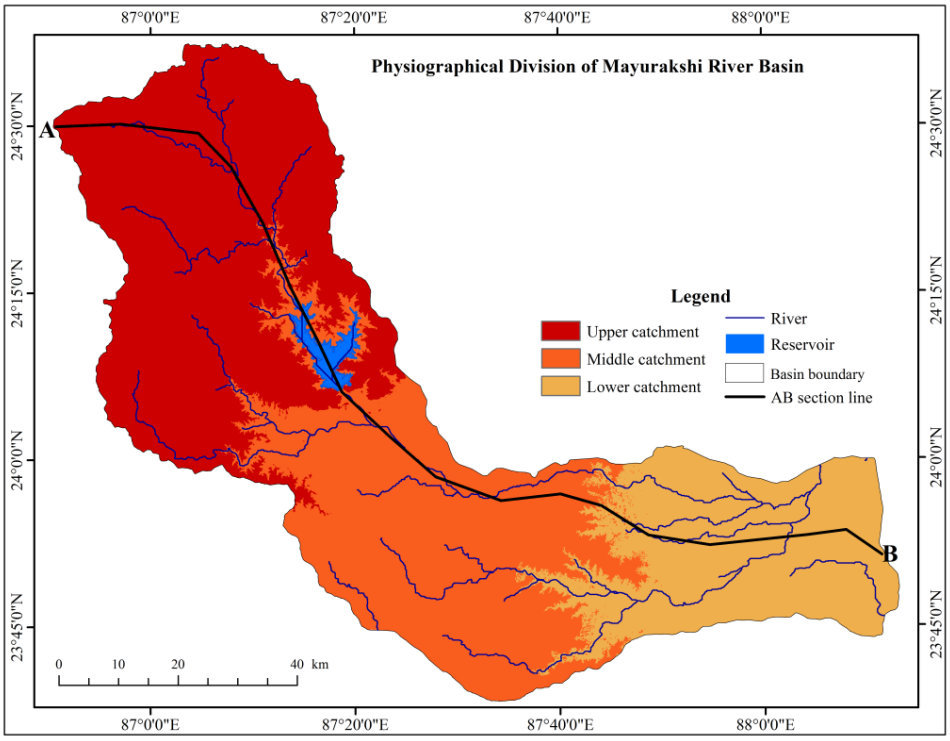

Figure 5.3 *Physiographic Division of the Mayurakshi River Basin Area*

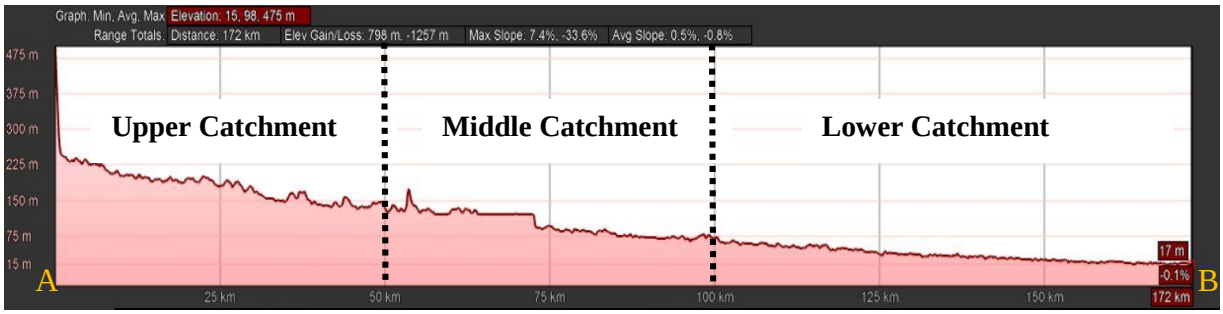

Figure 5.4 *Long Profile of the Mayurakshi River*

The upper and middle part of the catchment is characterized by rugged topography which is the effect of continuous active denudational activities (Nag et al. 2022). Several small rocky hillocks, commonly known as patland in Chhotonagpur, are very much dominant over this region. The lower catchment of the Mayurakshi river basin lies within the Rarh plain of Birbhum, Murshidabad and a small part of Burdwan districts of West Bengal. A huge variation in relief properties has been observed from upper to the lower catchment of the river basin. This zone is dominated by low lying topography with numerous rivers, gullies etc. Wetlands and swampy lands are also very common in this lower part of the river basin area. Figure 5.5 shows the relative relief map of the study area, where the high relief area has been concentrated

within the area of rounded flat-topped hills. Whereas the low relief area has been lied on the lower catchment area having more or less plain topography with numerous rills and gullies.

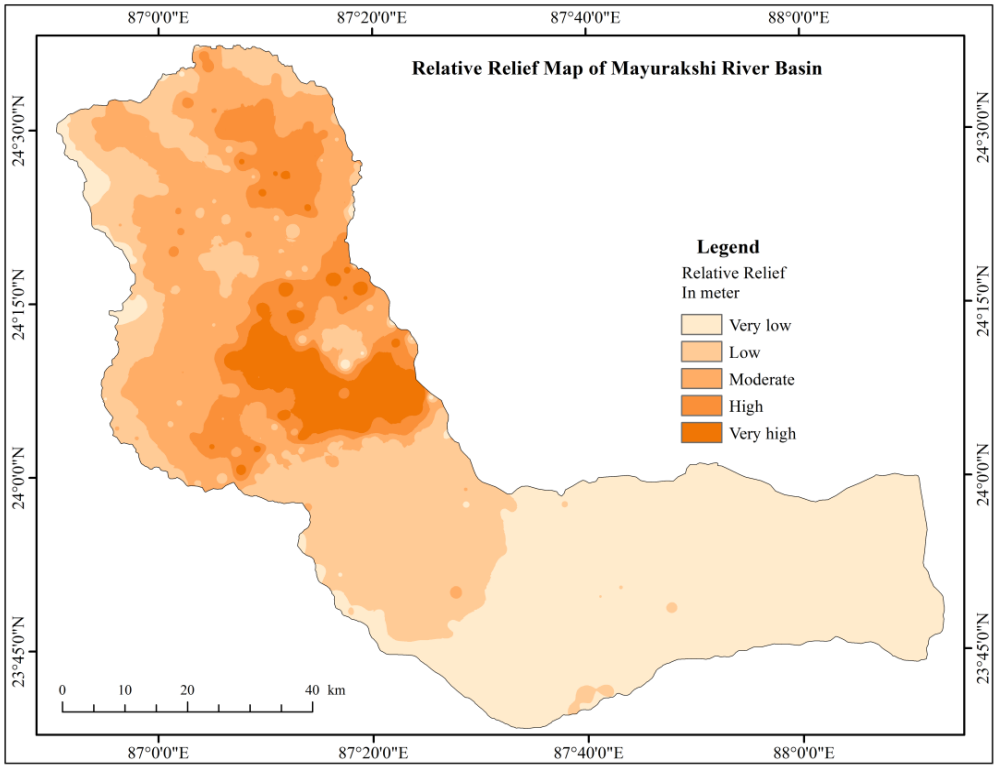

Figure 5.5 *Relative Relief Map of the Mayurakshi River Basin Area*

5.2.2. Slope

The Mayurakshi River has been originated from the Trikut hill of Jharkhand, located in the north western part of the river basin. The western part of the river basin is primarily dominated with unconsolidated and consolidated rocky materials which are regarded as the extension of Chhotonagpur plateau region and in the eastward direction of the basin, the hills are become lower in Birbhum Rarh plain and in Murshidabad the land becomes variation less in terms its topography when the river valley becomes narrower and it merges with the Gangetic delta. The general slope of the river basin is from north western to eastern direction (Fig. 5.6).

The contour map of the river basin (Fig. 5.7) shows the actual gradient of the slope is from upper to the lower part of the basin (NW-E). The contour map reveals the highest contour of the river basin is 240m located in north western part and the lowest contour is 20m located in the eastern most part of the basin.

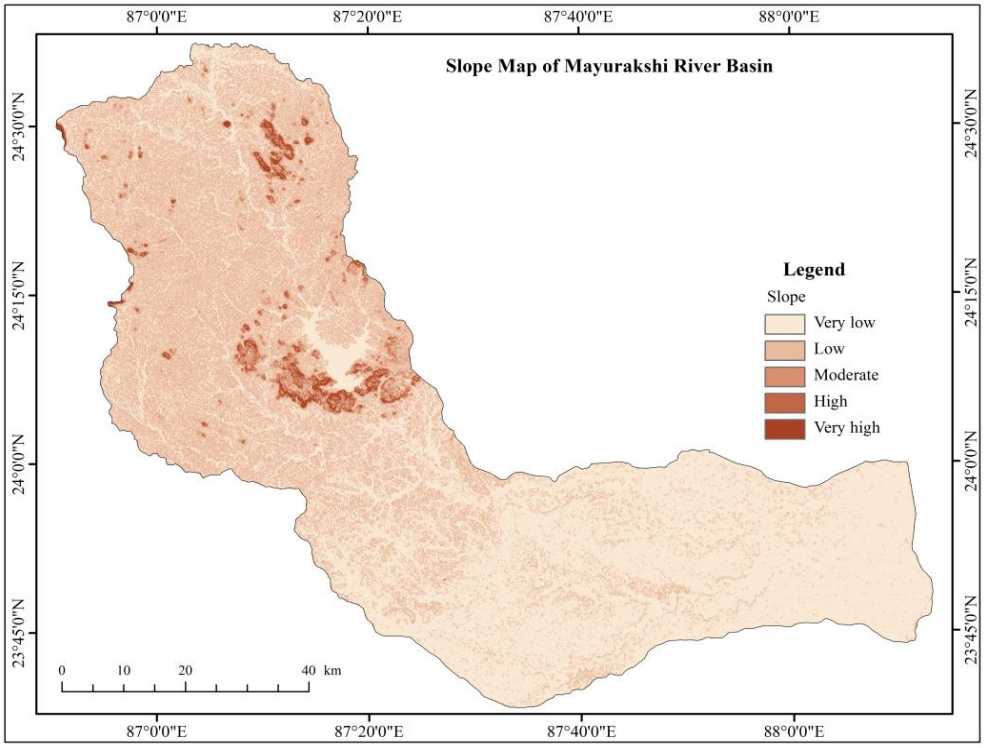

Figure 5.6 *Slope Map of the Mayurakshi River Basin Area*

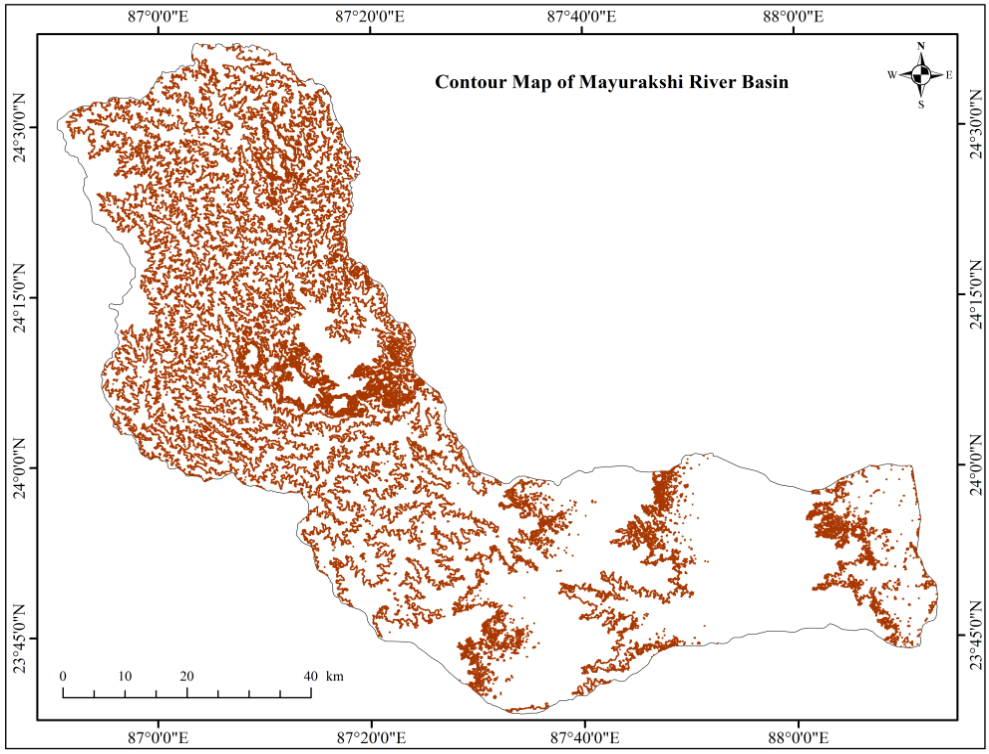

Figure 5.7 *Contour Map of the Mayurakshi River Basin Area*

5.2.3. Geology

The geological map of the study area has been taken from the Geological Survey of India (GSI) having a scale of 1:50,000 (Fig. 5.8). In the Mayurakshi River basin area, the upper catchment has been composed of granite and gneiss formation, which is the extended portion Chhotonagpur plateau shield region. Several remnant hillocks were observed in this area which has been composed of granulite and megmatite. Geologically, this area has basaltic intra trappen bed. The middle and the lower part of the catchment has lies on the West Bengal state covering some portion of Birbhum, Murshidabad and Burdwan districts. These areas of the Mayurakshi river basin has been composed of Gondwana sedimentaries with Rajmahal traps. Sub recent lateritic and alluviam composition has been observed in the lower reach of the river basin. Older alluvial deposits cover the major position of the area. They are coarse and generally reddishly coloured, lies in calcareous & limonitic concretions. Newer alluvium is mostly confined along the present drainage channels & in poor in calcareous matter. It gradually merges in the east into the flood plain of the Bhagirathi basin.

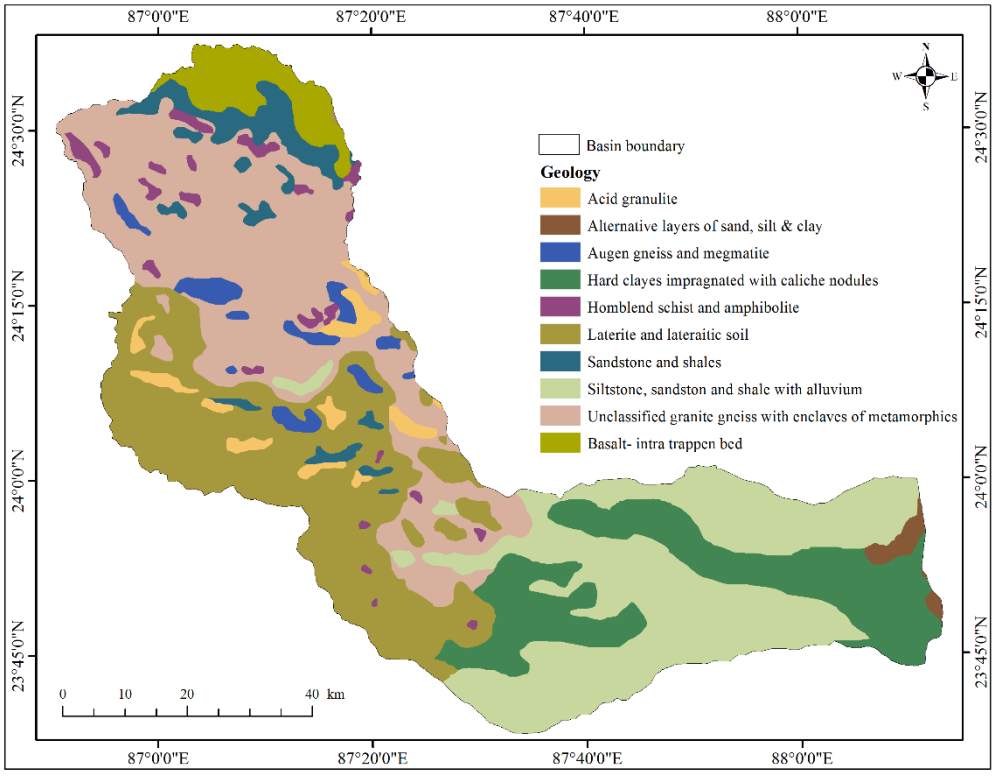

Figure 5.8 *Geological Map of the Mayurakshi River Basin Area*

5.2.4. Geomorphology

Geomorphology is the science of landforms which deals with the landforms processes in the earth surface and generates topographic variations (Kumar and Krishna 2016). The geomorphological map of the study area has been downloaded from Bhuvan website (*https://bhuvan.nrsc.gov.in/bhuvan_links.php*) in 1:50,000 scale (Fig. 5.9). The study area has several geomorphic units like anthropogenic terrain, denudation and structural origin of low and moderate dissected hills and valleys, the denudational origin of pediment peneplain complex, and fluvial origin of older and active flood plains. Among them, about 33.09% of the study area has been embedded with the pediment pediplain complex landform. Several denudational activities, including weathering of rocks, the formation of moderate to low dissected hills, and small patches of anthropogenic terrains, are very much observable in this region (Nag et al. 2022). Around this rocky landscape, fabrication of the Massanjore dam is classified under the anthropogenic terrain feature of the study area. Whereas the lower part of the river basin has been characterized by the alluvium flood plain. The lower part of the river basin has been characterized by fluvial origin alluvium flood plain. Active alluvium flood plain has been associated within the active channel area whereas in the other part older flood plain has been distributed. This older flood plain gradually merges with the portion of the Gangetic delta region where the Mayurakshi River merges with the river Bhagirathi and fluvial origin active flood plain forms.

5.2.5. Soil

The Mayurakshi River basin consists of seven different types of soil texture classes, which has been taken from the office of the National Bureau of Soil Survey and Land Use Planning (Fig. 5.10). The upper part of the basin is mainly composed of fragile coarse loamy to fine loamy soils. The presence of granitic and gneiss formation makes the soil more acidic in nature. In the middle part of the loamy to gravelly loamy soils are dominant one. The water holding capacity is very low in this soil. Some of the small patches of fine soil with clayey surface have also been observed. The lower part of the basin mainly the Birbhum Rarh plain is characterized by lateritic soil. Dominant of such loamy soils makes the region more susceptible to rills and gully erosion. In further eastern side of the basin, continuous deposits of fluvial alluvium by the rivers hamper the development of soil profile. Fine textured clay to clayey loamy has been observed in this region.

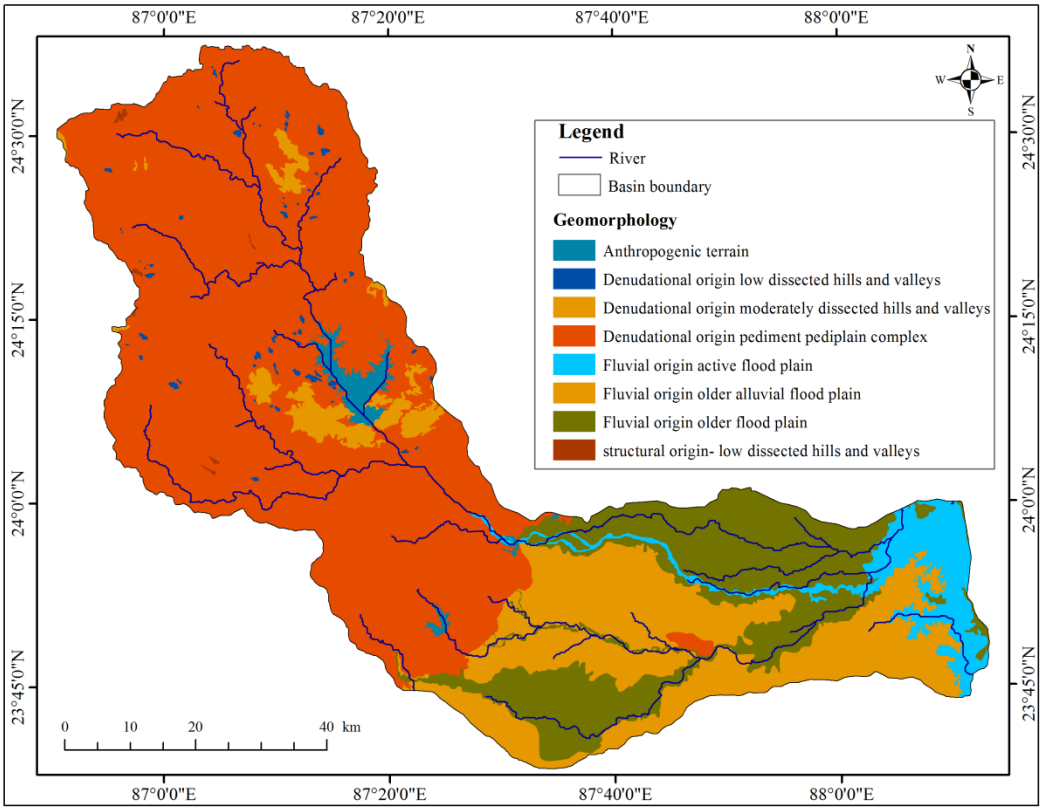

Figure 5.9 *Geomorphological Map of the Mayurakshi River Basin Area*

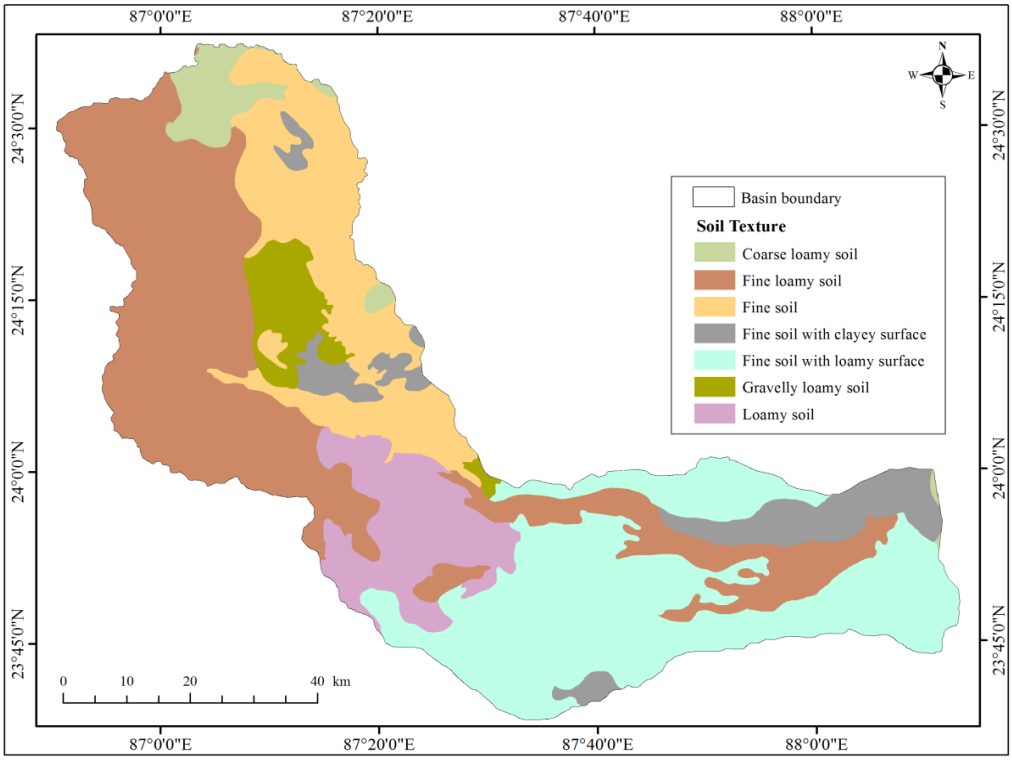

Figure 5.10 *Soil Texture Map of the Mayurakshi River Basin Area*

5.2.6. Land Use Land Cover

Classification of land use land cover of a region is an important approach to understand how the land utilization pattern can influence the hydrological processes. The response of groundwater recharge into the aquifer system is highly varied with individual land use classes. Like in forest cover areas the process of infiltration will increase than in built-up areas which reduces the water penetration and increases the surface runoff as well (Mishra et al. 2014). Following such relation, supervised classifications have been carried out on Landsat satellite imageries using a maximum likelihood algorithm for 2000 and 2018 (Fig. 5.11). Total eleven classes have been classified for both the period; these are- Dense vegetation, Laterite exposer, River/ water bodies, Reservoirs, Sand bar, Agricultural land, Wet fallow land, Dry fallow land, Wasteland, Settlement, Homestead with plantation. The whole classification methodology has been done in ERDAS Imagine 9.2 software using AOI and signature editor tool. To know the accuracy of each classification, Kappa co-efficient has been calculated (0.89 for 2000 and 0.93 for 2018) which shows that the generated land use land cover maps and the output of accuracy assessments are comparable with each other (Shen et al. 2013; Li et al. 2014).

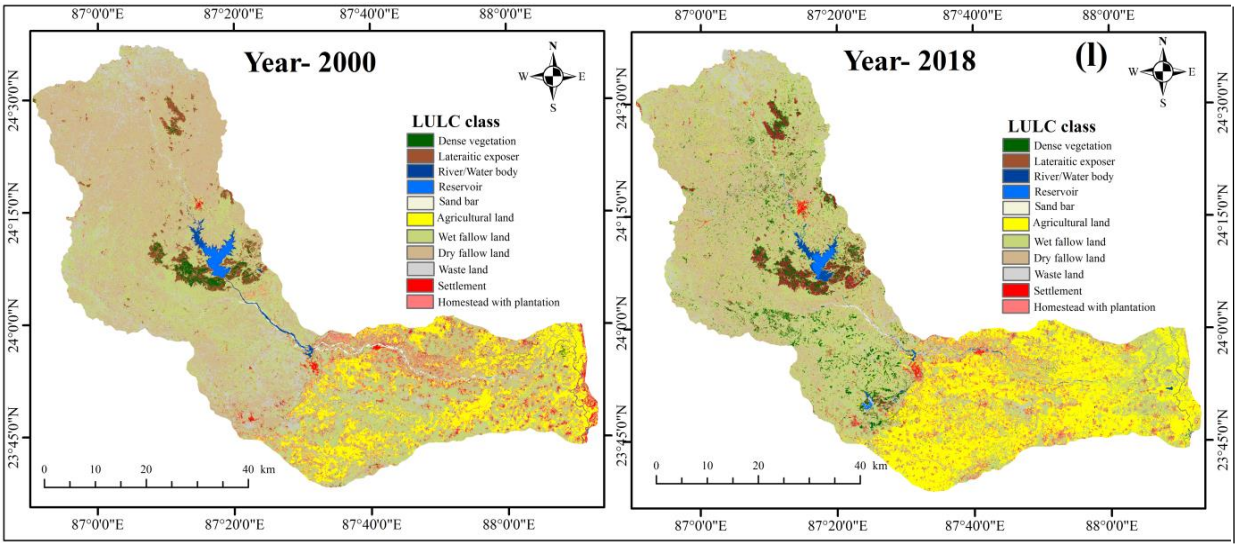

Figure 5.11 *Land Use Land Cover Map for 2000 and 2018*

Changes in the areal statistics of each land use land cover class from the period of 2000 to 2018 have been studied to understand the quantitative changes in land-use practices and their effect on the groundwater recharging process over the study area. The result presented in table 5.1 depicts that the agricultural land has been increased by 635.36 sq. km (10.9%) to 1366.80 sq. km (10.9%) with a positive change of 731.44 sq. km (12.57%) while the dry fallow land and wasteland area have been decreased by 2055.75 sq. km (35.27%) to 970.83 sq. km (16.67%) and 414.97 sq. km (7.12%) to 280.07 sq. km (4.81%) respectively. The result also suggests that within the time of 18 years the settlement has also accelerated from 124.87 sq. km (2.14%) to 174.30 sq. km (2.14%) with a positive change of 0.85% of the total area. The rapid growth of population could be the reason for the expansion of agricultural land as well as wet fallow land of the study area.

Table 5.1 *Areal Statistics of Land Use Land Cover Classes from 2000 to 2018*

LULC classes	**Year 2000** **Area in sq. km (%)**	**Year 2018** **Area in sq. km (%)**	**Area changes** **(sq. km)**	**Area changes (%)**
Dense vegetation	53.55 (0.92)	214.97 (3.69)	161.42	2.77
Laterite exposer	125.49 (2.15)	145.83 (2.50)	20.34	0.35
River/ water bodies	51.87 (0.89)	80.58 (1.38)	28.71	0.49
Reservoirs	31.02 (0.53)	18.61(0.32)	-12.41	-0.21
Sand bar	22.45 (0.39)	6.53 (0.11)	-15.92	-0.27
Agricultural land	635.36 (10.90)	1366.80 (23.47)	731.44	12.57
Wet fallow land	2012.08 (34.52)	2373.37 (40.75)	361.29	6.23
Dry fallow land	2055.75 (35.27)	970.83 (16.67)	-1084.93	-18.60
Waste land	414.97 (7.12)	280.07 (4.81)	-134.89	-2.31
Settlement	124.87 (2.14)	174.30 (2.99)	49.43	0.85
Homestead with plantation	301.38 (5.17)	196.89 (3.38)	-104.49	-1.79
Total	**5828.78 (100)**	**5828.78 (100)**		

5.3. Climatological Condition of the Study Area

In a recent past, the dynamic changes in climatic factors like rainfall, temperature, evapotranspiration affects the hydrological cycle severely. According to some relevant research reports, global warming resulting the rise in global temperature and reduction in the frequency of the wet season aggravates the shortage of surface and ground water resources

(Treidel et al. 2012). Besides of some human activities like land use modification or other hydraulic engineering action (dam or barrages), the potential changes in global climatic factors plays a crucial role in stream flow modification. In this context, the quantification of major climatic components like temperature and rainfall are essential mainly to visualise the nature of surface water resources in order to plan and manage it for our future environment (IPCC, 2013).

5.3.1. Temperature

The study area is comprised of fringe part of the highland of the Chhotonagpur plateau and the Rarh plain of Birbhum and Murshidabad districts of West Bengal, which experiences hot and humid climatic conditions throughout the year (Pal 2015). For better understanding, a spatial distribution map of mean annual temperature of Mayurakshi River Basin area (Fig. 5.12) has been prepared using 40 years (1980-2021) temperature data downloaded from Indian Meteorological Department (IMD) website (*https://www.imdpune.gov.in/*) having a resolution of 0.5° * 0.5°. The observed mean temperature of the basin is about 25-30°c, whereas the maximum average temperature is reached up to 35-45°c, mainly during the summers season. The figure also represents the southern part of the basin (Birbhum) experienced maximum average temperature in 40 years of time span.

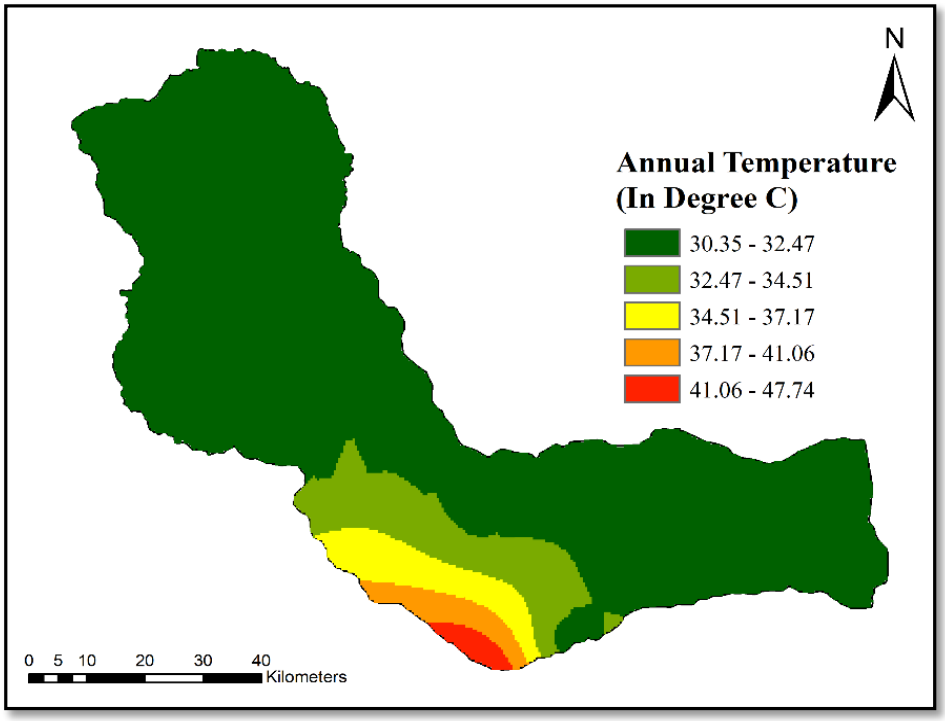

Figure 5.12 *Mean Annual Temperature of Mayurakshi River Basin Area for the Period of 1980-2021*

5.3.2. Rainfall

Mayurakshi is a non-perennial river which indicates its life is primarily depends on monsoonal rainy season and specifically the major source of flowing water is the down pouring huge monsoonal rainfall from the upper part of the plateau region (Roy 2013). The rainfall pattern is highly erratic in nature. The Maximum amount of rain occurs during the month of June to October having a mean annual rainfall of 1400 mm (Chaudhury 1966). On the contrary, during the dry season, almost no flow condition prevails in every stretch of the river making it non-perennial in nature.

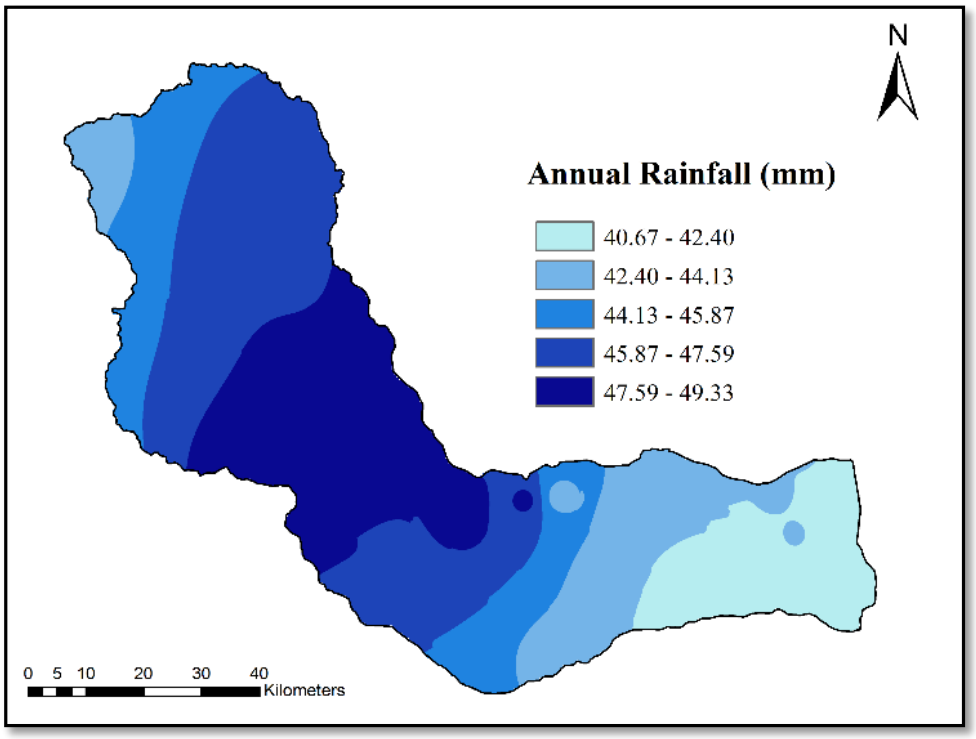

Figure 5.13 *Mean Annual Rainfall of Mayurakshi River Basin Area for the Period of 1980-2021*

A surface layer of 40 years (1980-2021) mean annual rainfall map has also prepared using IMD provided dataset having 0.5° *0.5° resolution (Fig. 5.13). The figure shows that the maximum annual rainfall is concentrated over the middle catchment area, whereas the decadal rainfall distribution map of 2010 and 2017 (Fig. 5.14) depicts the erratic nature of rainfall occurs within the study area. It ranges from 800-1600 mm over the basin area, out of which about 80% of rainfall occurs within a monsoonal month (June to October).

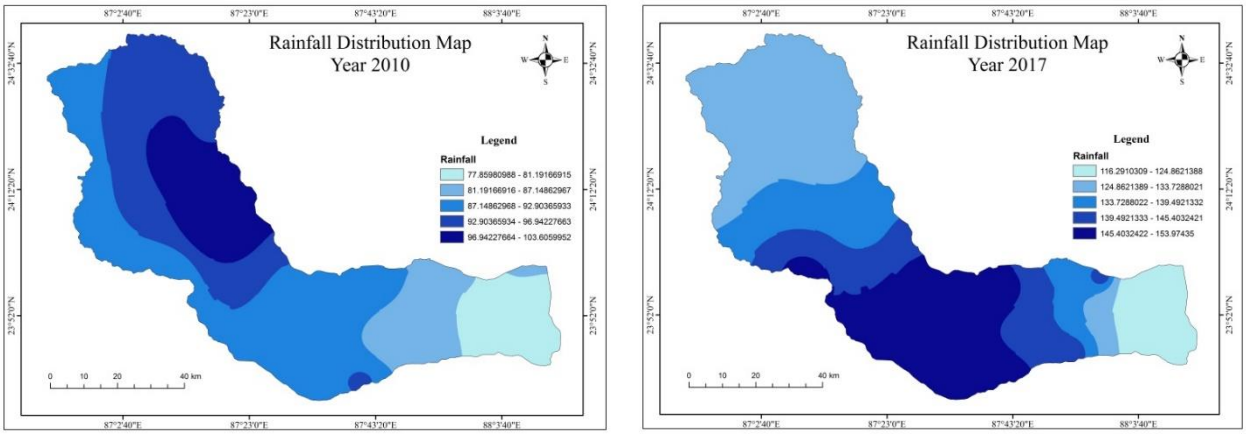

Figure 5.14 *Decadal Rainfall Distribution Map of Mayurakshi River Basin Area*

5.4. Hydrological Condition of the Study Area

5.4.1. Watershed and Sub-Watersheds

The Mayurakshi River is an important rain fed river of Jharkhand and West Bengal and also recognise as an important western tributary of Bhagirathi River. The 288 km long river has its catchment area about 5325 sq. km, lays within the transitional zone between two mega physiographic provinces namely the Chhotonagpur plateau and the Bengal basin. The major tributaries are Dhobi, Motihara, Tepra, Matihara, Bhurbhuri, Siddheswari, Pusaro, Kushkarini, Kuya etc. The network of the stream has been extracted from the rectified topographical maps provided by Survey of India and the boundaries of each sub watersheds were demarcated on the basis of contour values and the stream flow direction. The digitization of drainage line, watershed boundaries have been performed in GIS environment using Arc GIS 10.3 software. The whole river basin has been divided into 12 sub-watersheds (SW) represented as SW1 to SW12 and the name of the sub-watersheds (Fig. 5.15). The whole drainage network forms a dendritic pattern mainly in the upper part of river basin.

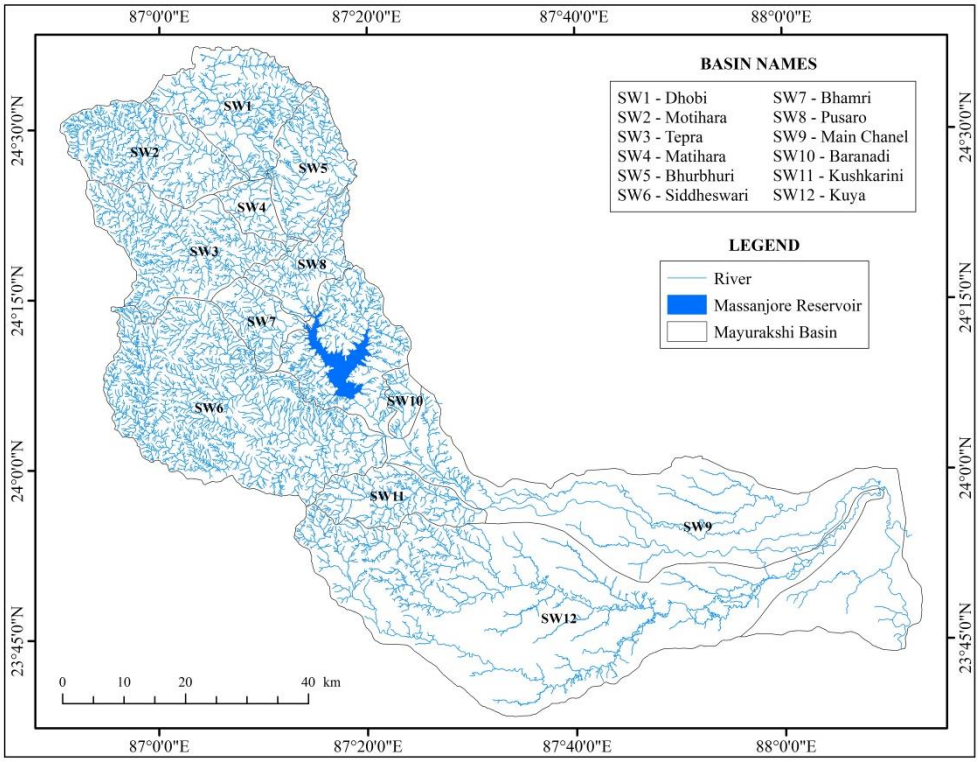

Figure 5.15 *Drainage Map of the Mayurakshi River Basin Area*

Since from the time of independence, Mayurakshi River has been playing an important role to the state of Jharkhand and West Bengal. Two major structures that had been impounded on this river i.e., the Massanjore dam and Tilpara barrage, are the major factor for the development of agricultural activities in West Bengal (Annual flood report 2016). But several problems related channel degeneration has been encountered by various researchers. Day by day the channel changes its original morphometric pattern which has mainly led by the human intervention within the river. Continues narrowing and widening of the channel may disturb the normal hydro-morphological rhythm of the river (Pal et al. 2012). Furthermore, the problem of soil cover degradation has been also very much dominating within the upper part of Mayurakshi river basin area (Pal and Debanshi 2018). Inadequate forest cover, uncontrolled grazing land and presence of hard rock areas coupled with a high drainage density of that region generate more soil erosion over this area (Chowdary et al. 2013) which in turn degrades the overall basin condition.

5.4.2. Flow Direction & Accumulation

Flow direction is an important hydrological tool which is mainly used to explore the properties of any surface in terms of its ability to determine the direction of flow from a particular point to its neighbouring point. It is a raster based function where elevation is taken as a surface layer and based on the slope of that area, it produce a raster output containing the direction of flow

movement from each pixel to its neighbouring one. The code used to determine the direction of flow is represented in figure. 5.16 (Qin et al. 2007)

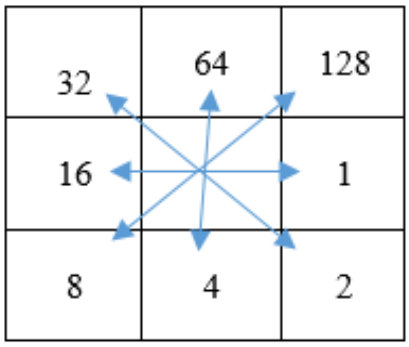

Figure 5.16 *Coding used for Flow Direction Raster*

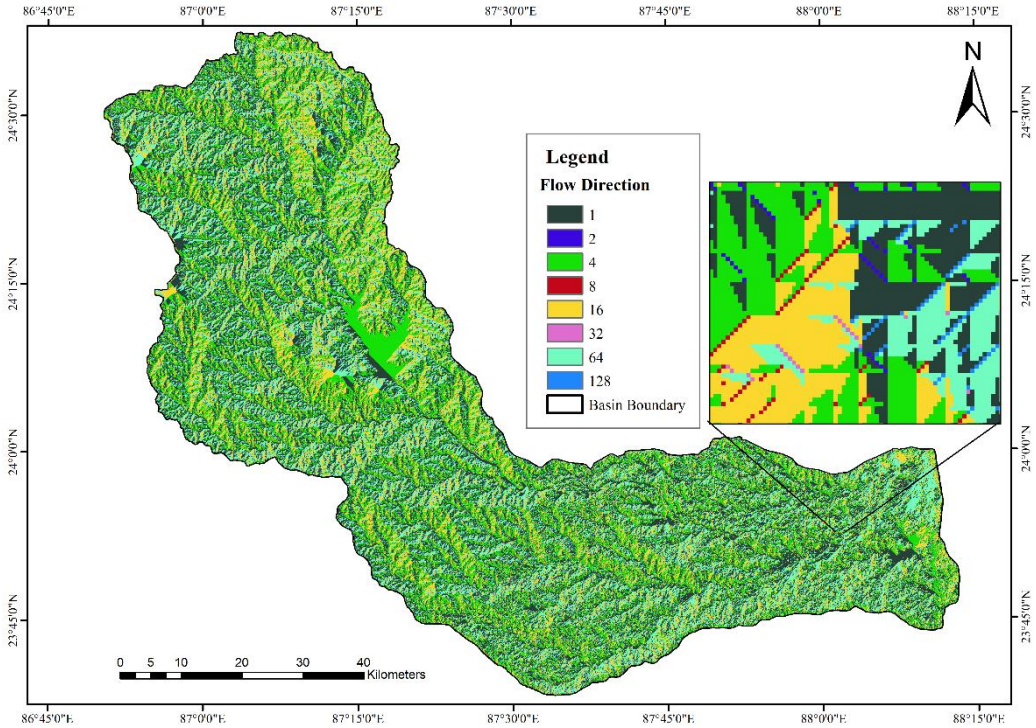

Figure 5.17 *Flow Direction Map of the Mayurakshi River Basin Area*

In an ArcGIS environment, the flow direction of an area is easily derived using the spatial analyst tool from Arc toolbox. The flow direction map of the study area is represented in the following figure (Fig. 5.17)

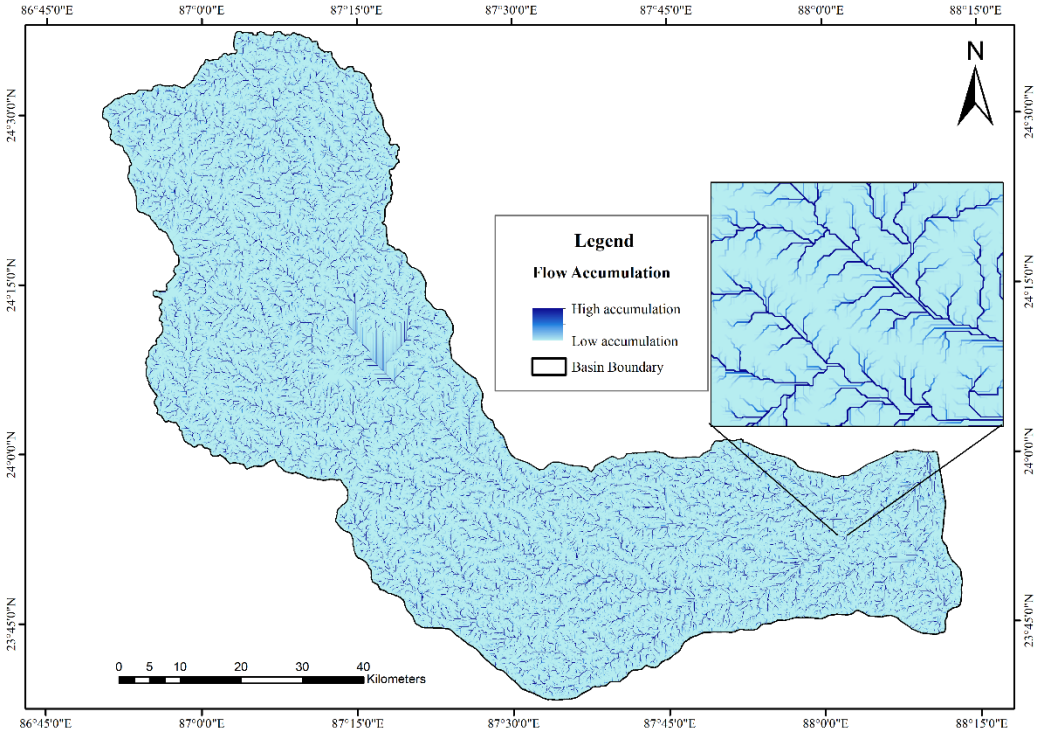

Figure 5.18 *Flow Accumulation Map of the Mayurakshi River Basin Area*

Using flow direction raster as a surface layer, the accumulation of flow of the Mayurakshi River basin has also been generated (Fig. 5.18). The legend depicts the value of each cells that flow into its steepest neighbouring cells. From this raster layer, the network of streams has been generated as the application of this flow accumulation window is the foremost step to delineate the stream network of an area.

References

- Annual flood report 2016 Irrigation and waterways directorate. Government of West Bengal. https ://wbiwd .gov.in/uploa ds/ANNUAL_FLOOD REPOR T_2016.pdf.
- Chaudhury, A. K. (1966). On the meteorological conditions responsible for heavy rainfall in Ajay catchment Area. *Indian J Meteorol Geophys*, *17*, 127-132.
- Chowdary, V. M., Chakraborthy, D., Jeyaram, A., Murthy, Y. K., Sharma, J. R., & Dadhwal, V. K. (2013). Multi-criteria decision making approach for watershed prioritization using analytic hierarchy process technique and GIS. *Water resources management*, *27*, 3555-3571.
- Kumar, A., & Krishna, A. P. (2018). Assessment of groundwater potential zones in coal mining impacted hard-rock terrain of India by integrating geospatial and analytic hierarchy process (AHP) approach. *Geocarto International*, *33*(2), 105-129.
- Li, C., Wang, J., Wang, L., Hu, L., & Gong, P. (2014). Comparison of classification algorithms and training sample sizes in urban land classification with Landsat thematic mapper imagery. *Remote sensing*, *6*(2), 964-983.
- Mishra, N., Khare, D., Gupta, K. K., & Shukla, R. (2014). Impact of land use change on groundwater—a review. *Advances in Water Resource and Protection*, *2*(28), 28-41.
- Nag, S., Roy, M. B., & Roy, P. K. (2022). Study on the functionality of land use land cover over the evaluation of groundwater potential zone: A fuzzy AHP based approach. *Journal of Earth System Science*, *131*(3), 146.
- Pal, R. (2015). Channel Avulsion Archives and Morphological Readjustment near the Bhagirathi-Mayurakshi Confluence in the Lower Gangatic Plain, West Bengal, India. *J. Environ. Earth Sci*, *5*(3), 67-75.
- Pal, S., & Debanshi, S. (2018). Influences of soil erosion susceptibility toward overloading vulnerability of the gully head bundhs in Mayurakshi River basin of eastern Chottanagpur Plateau. *Environment, Development and Sustainability*, *20*, 1739-1775.
- Pal, S., Let, S., & Das, P. (2012). Assessment of channel width disparity of the major rivers within Mayurakshi River Basin. *Int J Geol Earth Environ Sci*, *2*(3), 1-10.
- Qin, C., Zhu, A. X., Pei, T., Li, B., Zhou, C., & Yang, L. (2007). An adaptive approach to selecting a flow-partition exponent for a multiple-flow-direction algorithm. *International Journal of Geographical Information Science*, *21*(4), 443-458.
- Roy, S., & Mistri, B. (2013). Estimation of peak flood discharge for an ungauged river: a case study of the Kunur River, West Bengal. *Geography journal*, *2013*.
- Shen, Z., Lu, C., Yin, R., & Qi, J. (2013). Land cover changes in northeast China from the late 1970s to 2004. *Applied ecology and environmental research*, *11*(1), 67-78.
- Stocker, T. F., Qin, D., Plattner, G. K., Alexander, L. V., Allen, S. K., Bindoff, N. L., ... & Xie, S. P. (2013). Technical summary. In *Climate change 2013: the physical science basis. Contribution of Working Group I to the Fifth Assessment Report of the Intergovernmental Panel on Climate Change* (pp. 33-115). Cambridge University Press.
- Treidel, H., Martin-Bordes, J. L., & Gurdak, J. J. (Eds.). (2011). *Climate change effects on groundwater resources: a global synthesis of findings and recommendations*. CRC Press.

CHAPTER 6

ASSESSMENT OF THE PHYSICAL INDICATORS OF THE STUDY AREA

6. Introduction

The state of a river's morphology and physiology is the definition of river health. The anatomy of a river is predominantly concerned with its physical condition, whereas its physiology is concerned with its chemical and biological conditions. The physical condition of the river also includes the river's changing hydrological behaviour, channel shifting and migration, river course change, flood and river bank erosion, and similar occurrences. This chapter discusses recent developments in our understanding of the physical characteristics of the Mayurakshi River basin. Its primary goals are to investigate the nature of hydrological, physiological, and climatological aspects and offer policymakers a scientific foundation for enhancing the overall river management status. It including the long term analysis of rainfall and temperature, characterisation of channel morphometry, channel hydraulics, estimation of available surface and ground water resources along with its predominant land use land cover of the study area.

6.1. Spatio-temporal Trend Analysis of Annual Air Temperature and Precipitation of Mayurakshi River Basin Area

Air temperature and rainfall are two important physical determinants that describes the climatic variability of any region. The variation among them can causes a drastic changes both in water resources and in agricultural production of an area. The hydrologic cycle depends heavily on precipitation, and variations in its pattern would have a direct impact on the region's water resources, changing the spatial and temporal distribution of runoff, soil moisture, and groundwater reserves. Additionally, the frequency and amount of rain directly affect river discharge. Krishnan et al. (2016) stated that Hydrodynamic and thermal regime of rivers, stream flow, surface runoff, and the freshwater environment are all affected by variations in rainfall and temperature.

Due to their extreme spatial and temporal variability at various local, regional, and global scal es, rainfall and temperature trends must be examined in order to comprehend climate variabili ty and change. However, because to their interdependence (correlation), precipitation and temperature are extremely challenging to model together in a single simulation (Shukla et al. 1977; Tanarhte et al. 2012). Time series analysis or the spatial and temporal trend analysis

using long term meteorological data can facilitate to understand the extent and magnitude of climatic alteration both in field of water resources and agricultural development (Gadefaw et al. 2018; Nikumbh et al. 2019). There are numerous methodologies to detect the trend in any hydro-metrological datasets including both parametric and non-parametric techniques. Linear regression, cumulative sum, Mann-Kendall test, Sen's slope, Spearman's rho test are the most popular methods in non-parametric trend analysis used by several researcher in around the world (Alifujiang et al. 2020; Sang et al. 2014; Gocic et al. 2013; Rahman et al. 2016).In order to detect a substantial trend in time series data, non-parametric tests are the best option because they can preserve outliers that should only be an autonomous prerequisite (Suheila et al. 2011). These statistically-based trend analysis techniques, however, do not identify the magnitude of the trends at high, medium, or low levels in a single calculation step. Besides of this monotonic trend identifying techniques, Sen (2012) came up with an innovative trend analysis (ITA) method that not only looks at the trends of hydrological and meteorological factors but also uses flexible graphical techniques to find hidden trends in low, medium, and high value categories. Numerous studies in the field of hydro-meteorological science, such as rainfall, evaporation, temperature, stream flow etc. have already made use of the Innovative Trend Analysis technique as a result of its innovative features and graphical illustrations (Das et al. 2020; Mandal et al. 2020; Cui et al. 2017; Tabari et al. 2011; Machiwal and Jha 2012).

The climate in the Mayurakshi River basin area is typically quite hot and humid. This available water resources are already being impacted by an identified anomaly in the quantity of mean monthly precipitation (Pal et al. 2012). In addition, the recent sharp decline in freshwater supplies can exacerbate the issue of groundwater level decline and poorer crop productivity (Nag et al. 2022). Therefore, this study focussed on the identification of possible trend and magnitude of 40 years (1980-2020) temperature and precipitation data in 30 different meteorological stations of Mayurakshi river basin area (Fig. 6.1) using Innovative Trend Analysis (ITA) technique and also verify the output with the traditional method of Mann Kendall (MK) test (Mann 1945; Kendall 1975). To estimate the changes in slope of the trend, Sen's slope estimator (Şen 1968) has also been implemented.

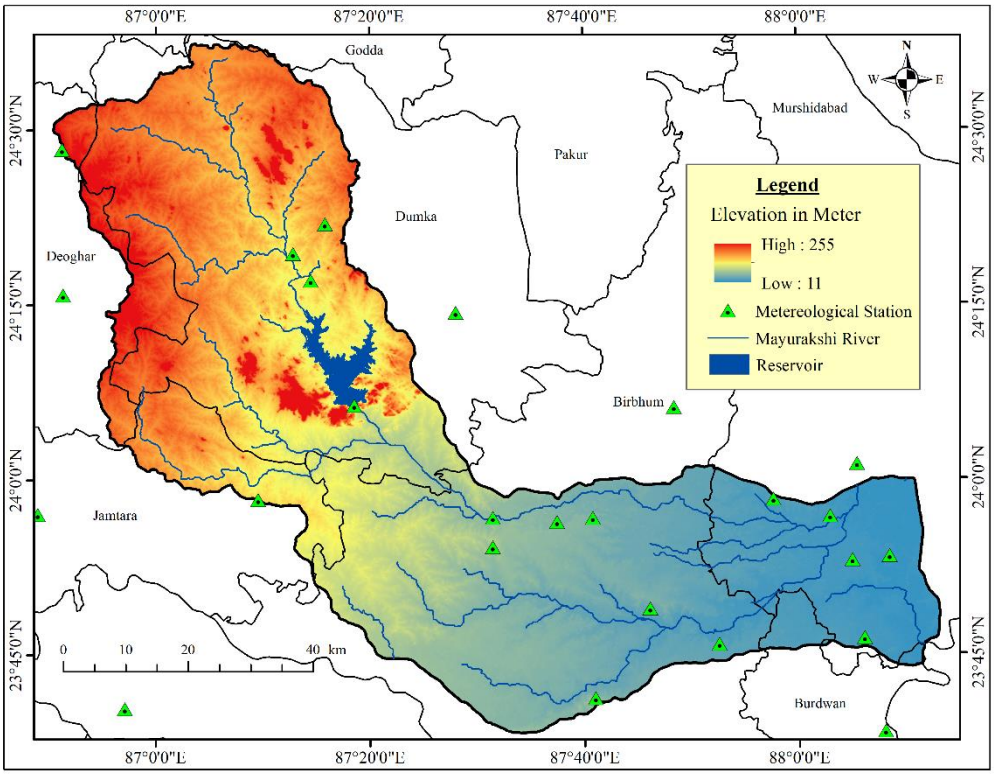

Figure 6.1 *Location of the Meteorological Stations along with the Digital Elevation Model of Mayurakshi River Basin Area*

6.1.1. Data Source

The meteorological datasets used in this study has been obtained from the official website of Indian Meteorological Department (IMD) (*https://www.imdpune.gov.in/*) for the period of 1980 – 2020 having a resolution of 0.5*0.5 degree. For the station wise datasets, total 30 rain and river gauge stations have been considered in and around the Mayurakshi River basin area and estimation of mean monthly data of temperature and precipitation has been done. The descriptive statistics of the collected data of temperature and precipitation including mean, standard deviation, skewness, kurtosis, variance and coefficient of variation respectively have been presented in tabular format (Table 6.1 and 6.3)

6.1.2. Methodology

- **Mann Kendall (MK) Test**

Mann-Kendall (MK), a nonparametric conventional trend analysis technique, has been used to achieve the goal of this study, specifically to identify the type of trend from the long-term time series data of temperature and precipitation in the Mayurakshi River Basin area. It is the most

widely used technique that can identify the significance of the trend within a various hydro-meteorological datasets, regardless of the presence or absence of outliers or missing values (Dong et al. 2020). It just provides an overview of whether a monotonic rising or downward trend is seen in a given dataset. The magnitude of the slope cannot be estimated through this method.

The MK Z statistics has been calculated using the following equation:

$$Z = \begin{cases} \frac{S-1}{\sqrt{VAR(S)}}, if\ S > 0 \\ 0, \qquad\quad if\ S = 0 \\ \frac{S+1}{\sqrt{VAR(S)}}, if\ S > 0 \end{cases} \tag{6.1}$$

Where, the variance of S is determined by the following equation:

$$VAR(S) = \left\{n(n-1)(2n+5) - \sum_{t=1}^{g} \alpha(\alpha-1)(2\alpha+5)\right\}/18 \tag{6.2}$$

Here, n indicates total number of data points, g denotes the number of tied group within a dataset where the α represents the extent of α^{th} ties number.

Similarly the S variance of MK test has been computed in a following manner-

$$S = \sum_{j=1}^{n-1} \sum_{k=j+1}^{n} Sign\left(Y_k - Y_j\right) \tag{6.3}$$

Where, Y_k and Y_j represents data at the time of k and$j$.

In this MK test, a positive Z values indicate an upward trend, while negative Z values indicate a downward trend. If the standardised statistic Z is greater than 2.58, the trend is significant at the 99% confidence level; if it is greater than 1.96, it is significant at the 95% confidence level; if it is greater than 1.65, it is significant at the 90% confidence level, and so on (Farlie 1971).

- **Sen's Slope Estimator**

The magnitude of trend from the MK test has been separately calculated for 40 years mean annual temperature and precipitation data using Sen's Slope estimator (Sen 1968). It can demonstrate the magnitude of the rate of change in trend over time. From N pairs of data, the slope can be determined as follows:

$$Q_n = \frac{x_k - x_j}{k - j}, n = 1,2,3 \ldots\ldots N, k > j \quad (6.4)$$

Where Q_n represents slope andx_k, x_j represents the observed data at the time of k and$j$.

- **Innovative Trend Analysis (ITA) Test**

Using this advanced technique for graphical trend analysis, the traditional MK test result has been confirmed. Innovative Trend Analysis (ITA) is a novel method for detecting trends that is capable of displaying hidden patterns that were present in the dataset and can also be deciphered from the ITA graphs (Pour et al. 2020).

In this technique, the collected time series dataset are divided into two equal halves and arranged them in ascending order. Then the first half of the arranged dataset are being plotted in X axis and the second half of the same on Y axis within a Cartesian co-ordinate system (Alifujiang et al. 2020). A 1:1 straight line (45°) has also been constructed within a scatter plot showing a trendless/ no-trend line. No trend in a dataset has been represented if the scatter points are completely align with the 45° line. Whereas scatter plots above or below the straight line exhibits an increasing or decreasing trend respectively. The quantification in the change of slope has been calculated by the following formula:

$$D = \frac{1}{n}\sum \frac{10(y - x)}{\bar{x}} \quad (6.5)$$

Where D indicate the trend in a dataset, n is the number of each series, $\bar{x}$ denote the mean of the 1st series of the dataset (x) and y, x indicates the consecutive sub series. Here, all the variables are finally multiplied by 10 mainly to compare the output with MK test (Mandal et al.2021)

Table 6.1 *Descriptive Statistics of 40 years Air Temperature of Mayurakshi River Basin Area*

Sl. No	Station	Location		Elevation (m)	Annual Temperature (°C)					
		Latitude	Longitude		Mean (mm)	SD*	Variance	CV (%)*	C_s*	C_k*
1	Tilpara	23.94854	87.52383	63.66	31.86	0.52	0.025	1.62	1.90	7.41
2	Suri	23.90475	87.52383	80.01	31.86	0.52	0.025	1.62	1.90	7.41
3	Shyambati	23.68847	87.68438	64.44	31.86	0.52	0.025	1.62	1.90	7.41
4	Shekhampur	23.81585	87.77063	44.70	31.86	0.52	0.025	1.62	1.90	7.41
5	Salar	23.77339	88.10368	23.47	31.78	0.49	0.021	1.54	1.75	10.98
6	Sainthia	23.94854	87.68173	47.60	31.86	0.52	0.025	1.62	1.91	7.41
7	Narayanpur	23.89016	88.14084	20.61	31.78	0.49	0.021	1.54	1.75	10.98
8	Massanjore	24.10644	87.31153	101.54	31.44	0.63	0.046	2.01	1.49	2.21
9	Maharo	24.32671	87.21466	150.91	31.44	0.63	0.046	2.01	1.49	2.21
10	Kundahit	23.97375	87.16026	153.23	31.81	0.52	0.133	1.62	-4.36	27.21
11	Kultore	23.94323	87.62467	52.07	31.86	0.52	0.025	1.62	1.90	7.41
12	Kirnahar	23.76543	87.87413	35.27	31.86	0.52	0.025	1.62	1.90	7.41
13	Kandi	23.94589	88.04928	26.20	31.78	0.49	0.021	1.54	1.75	10.98
14	Jama	24.36784	87.26243	168.56	31.44	0.63	0.045	2.01	1.49	2.21
15	Dumka	24.28694	87.24385	156.04	31.44	063	0.045	2.01	1.49	2.21
16	Bharatpur	23.88618	88.08112	18.52	31.78	0.49	0.021	1.54	1.75	10.98
17	Kuli	23.97243	87.95905	27.28	31.85	0.52	0.024	1.62	2.02	8.18
18	Khushiyari	24.47234	86.85657	344.05	31.27	0.60	0.063	1.91	1.28	0.54
19	Deoghar	24.47941	86.69218	252.29	31.27	0.60	0.063	1.91	1.28	0.54
20	Haripur	24.26552	86.85484	197.94	31.27	0.60	0.063	1.91	1.28	0.54
21	Jamtara	23.95088	86.81768	188.08	31.43	0.68	0.063	2.16	1.23	0.72
22	Asansol	23.67689	86.95379	120.96	31.43	0.68	0.063	2.16	1.23	0.72
23	Durgapur	23.52134	87.31263	107.86	54.29	0.52	0.025	1.62	1.90	7.41
24	Satkahonia	23.59911	87.49469	64.41	54.29	0.52	0.025	1.62	1.90	7.41
25	Katwa	23.6433	88.13282	20.32	31.78	0.49	0.022	1.54	1.64	9.47
26	Berhampore	24.09936	88.26362	22.12	21.53	0.55	0.028	1.75	1.98	5.32
27	Ranagram	24.02335	88.09039	24.83	31.53	0.55	0.028	1.75	1.98	5.32
28	Tarapur	24.10643	87.80757	39.63	31.44	0.63	0.046	2.01	1.49	2.21
29	Shikaripur	24.24254	87.46464	145.31	31.44	0.63	0.046	2.01	1.49	2.21
30	Sikatia	24.83647	87.15354	98.68	31.44	0.63	0.046	2.01	1.49	2.21

*SD= Standard deviation, CV (%) = Co-efficient of variation, C_s= Skewness, C_k= Kurtosis

6.1.3. Result and Discussion

- **Variability and Trends in Air Temperature**

In order to investigate long-term (1980–2020) trends in annual temperature, this study compared the output of innovative trend analysis (ITA), an advanced graphical method of trend detection, with a conventional nonparametric statistical approach that is Mann-Kendall (MK) test. Figures show the spatial distribution, temporal variability, change of slope in MK test and ITA test analysis of mean annual temperature in Mayurakshi River Basin area. The average annual temperature in Mayurakshi River Basin ranged from 30.35°C to 47.74°C, as indicated in the figure 6.2a with a CV ranges from 1.54% to 2.05% (Fig. 6.2b).

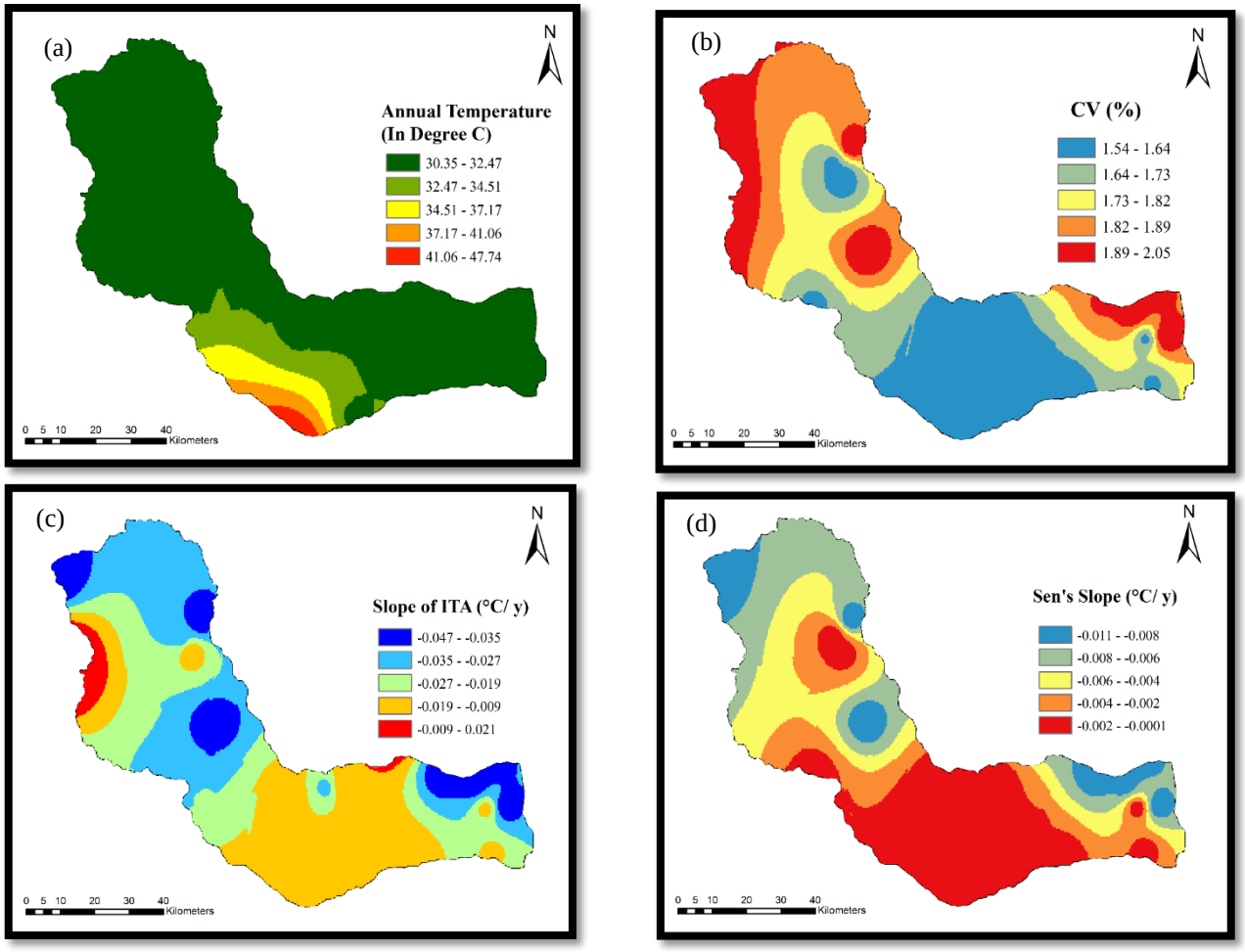

Figure 6.2 *Surface Layer of 40 Years of Annual Temperature (a) Distribution Map (b) Co-efficient of Variance map (c) Innovative Trend Analysis Slope Map (d) Sen's Slope Map*

Table.6.2 *Detailed Output of Annual Temperature Trend Analysis of Mayurakshi River Basin Area*

Sl. No	Station	p-Value	Z Statistics	MK tau	Sen's Slope	IT Slope (D)	ITD
1	Tilpara	***0.0104***	-2.5608[A]**	-0.2765	-0.00012	-0.016	⬇
2	Suri	***0.0104***	-2.5608[A]**	-0.2765	-0.00012	-0.016	⬇
3	Shyambati	***0.0104***	-2.5608[A]**	-0.2765	-0.00012	-0.016	⬇
4	Shekhampur	***0.0104***	-2.5608[A]**	-0.2765	-0.00012	-0.016	⬇
5	Salar	***0.0013***	-3.210[A]***	-0.3422	-0.00045	-0.0098	⬇
6	Sainthia	***0.0057***	-2.763[A]***	-0.2979	-0.00014	-0.016	⬇
7	Narayanpur	***0.0013***	-3.210[A]***	-0.3422	-0.00045	-0.0098	⬇
8	Massanjore	***0.0026***	-5.149[A]***	0.5483	-0.01154	-0.044	⬇
9	Maharo	***0.0026***	5.149[A]***	0.5483	-0.01154	-0.044	⬇
10	Kundahit	***0.0086***	-2.621[A]***	-0.2816	-0.00015	-0.0316	⬇
11	Kultore	0.086	-2.621[R]***	-0.2816	-0.00015	-0.0316	⬇
12	Kirnahar	0.086	-2.621[R]***	-0.2816	-0.00015	-0.0316	⬇
13	Kandi	0.0876	-2.621[R]***	-0.2816	-0.00015	-0.0098	⬇
14	Jama	***0.0026***	-5.149[A]***	0.5483	-0.01154	-0.044	⬇
15	Dumka	***0.0026***	-5.149[A]***	0.5483	-0.01154	-0.044	⬇
16	Bharatpur	0.0876	-2.621[R]***	-0.2816	-0.00015	-0.0098	⬇
17	Kuli	***0.0101***	-2.569[A]**	-2.7736	-0.00012	-0.015	⬇
18	Khushiyari	***0.00037***	-3.557[A]***	-0.3791	-0.01185	-0.048	⬇
19	Deoghar	***0.00037***	-3.557[A]***	-0.3791	-0.01185	-0.048	⬇
20	Haripur	***0.00037***	-3.557[A]***	-0.3791	-0.01185	-0.048	⬇
21	Jamtara	***0.00017***	3.759[A]***	-0.4005	-0.0081	0.049	⬆
22	Asansol	***0.00017***	3.759[A]***	-0.4005	-0.0081	-0.049	⬇
23	Durgapur	***0.01229***	2.504[A]**	-0.2697	-0.00012	0.016	⬆
24	Satkahonia	***0.01229***	-2.504[A]**	-0.2697	-0.00012	-0.016	⬇
25	Katwa	***0.00145***	-3.183[A]***	-0.3391	-0.00045	-0.011	⬇
26	Berhampore	***0.00021***	-3.704[A]***	-0.3947	-0.00574	-0.030	⬇
27	Ranagram	***0.00021***	-3.704[A]***	-0.3947	-0.00574	-0.030	⬇
28	Tarapur	***0.0026***	-5.131[A]***	-0.5463	-0.01154	-0.044	⬇
29	Shikaripur	***0.0026***	5.131[A]***	-0.5463	-0.01154	0.044	⬆
30	Sikatia	***0.0026***	-5.131[A]***	-0.5463	-0.01154	-0.044	⬇

Note: Bold and Italic font denotes statistically significant trend exists within the dataset; [A]: Accepted the alternative hypothesis (Ha); [R]: Rejected the null hypothesis (H0); *Trend at the 90% confidence level; **Trend at the 95% confidence level; ***Trend at the 99% confidence level; ITD: Innovative Trend Detection.

The ITA graphs of annual temperature has been presented in figure 6.3 represents station wise trend within the study area where the table shows a detailed output of MK test, p-value, Z statistics, MK tau, Sen's slope and IT slope (D) of the analysed long term time series data of annual temperature. The constructed ITA graphs and ITA slope (Fig. 6.3) indicate that approximately 23% of the stations are statistically significant at a 95% confidence level, with 90% of the basin area exhibiting a decreasing trend. Only three stations exhibits positive trend namely Jamtara, Durgapur and Shikaripur, which are located in the upper part of the basin area. However, ITA identifies the few significant decreasing trends missed by the MK test, validating this method's ability to detect unseen trends in the data series. The MK test data showed that more than half (83.33%) of the regions had declining trends over the course of the investigation (Table 6.2). Such declining trend in annual average temperature also affect the pattern and distribution of annual rainfall over the basin area.

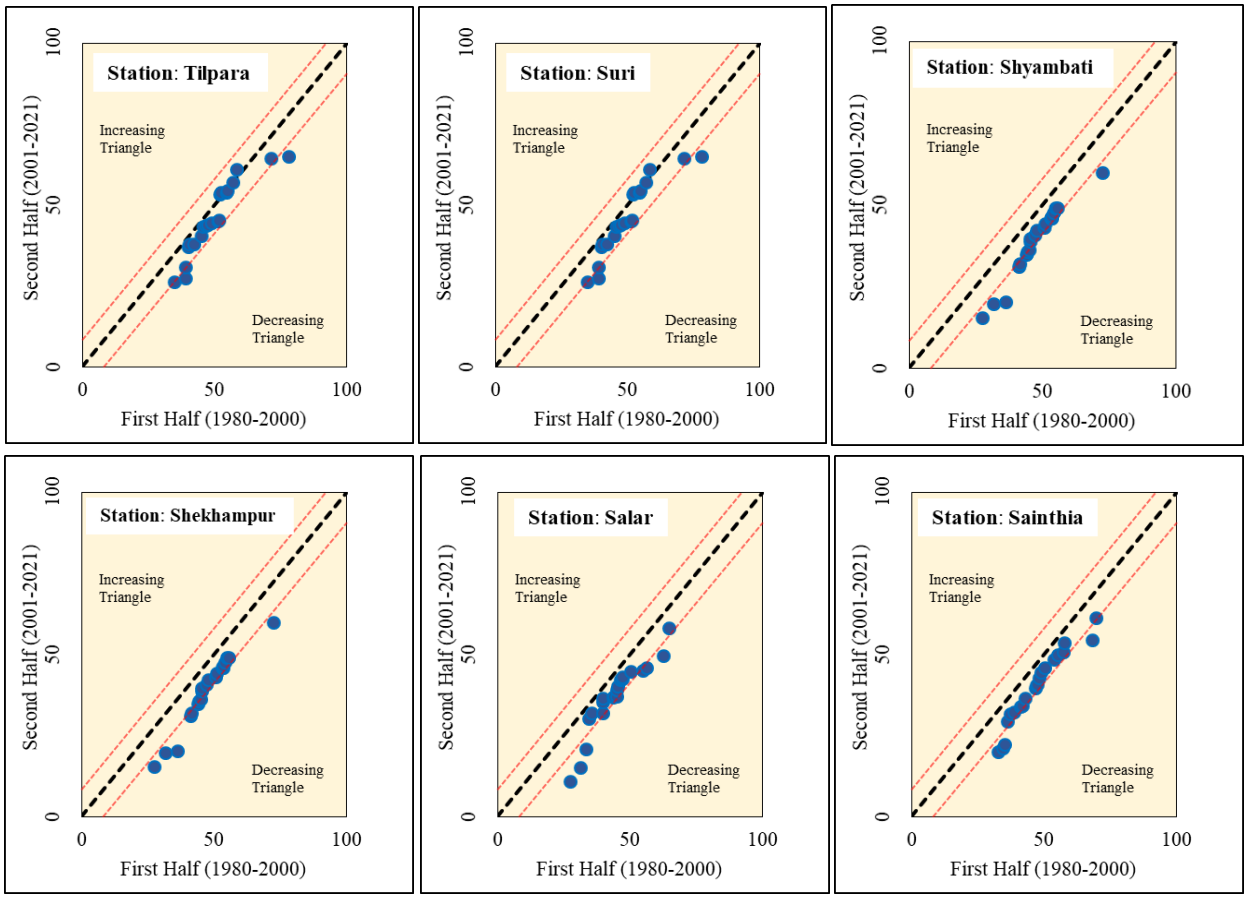

Figure 6.3 *Station Wise Plots of Innovative Trend Analysis of Annual Temperature for the period of 1980-2000 (First half) and 2001-2021 (Second half)*

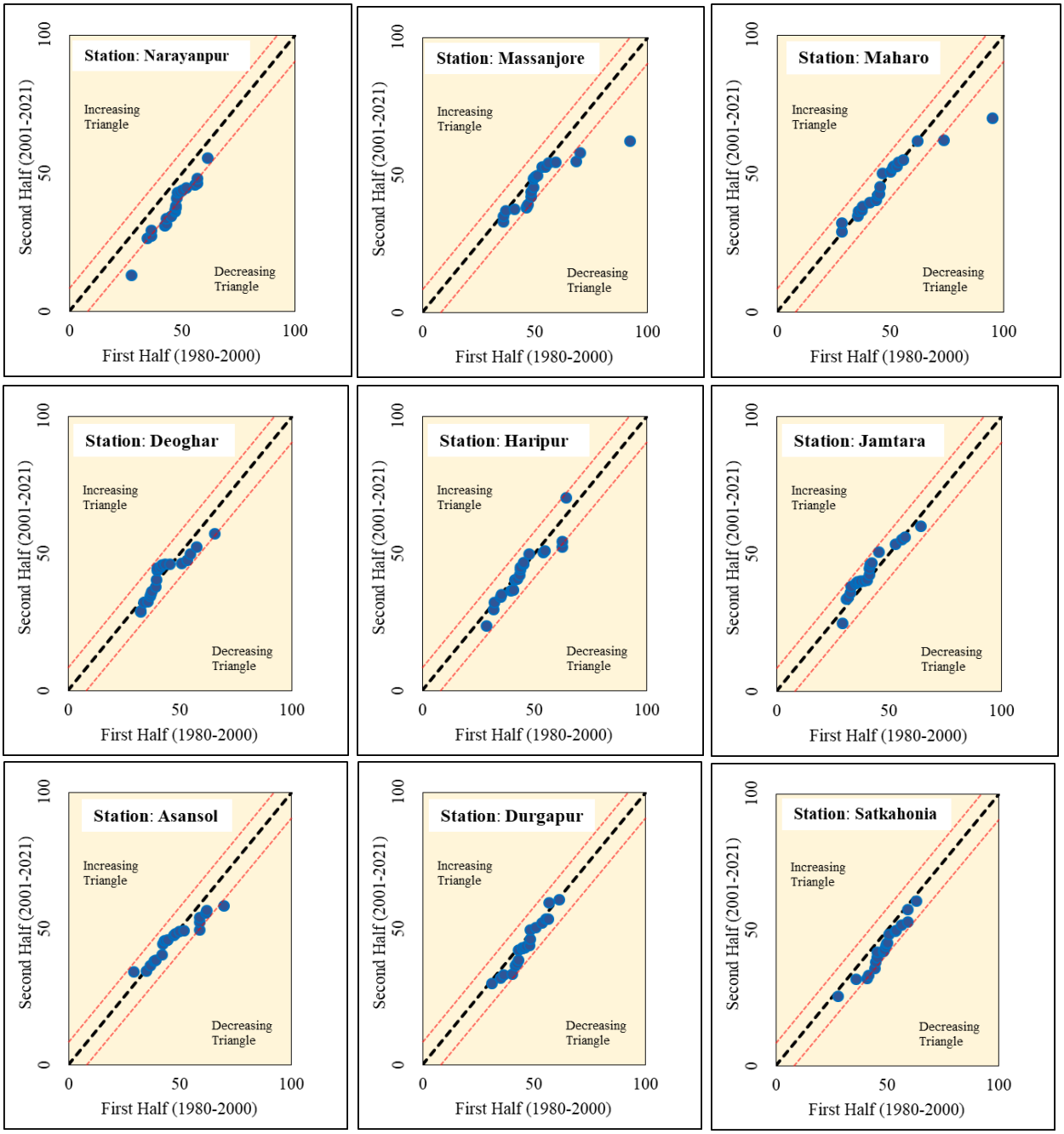

Figure 6.3 *Continued*

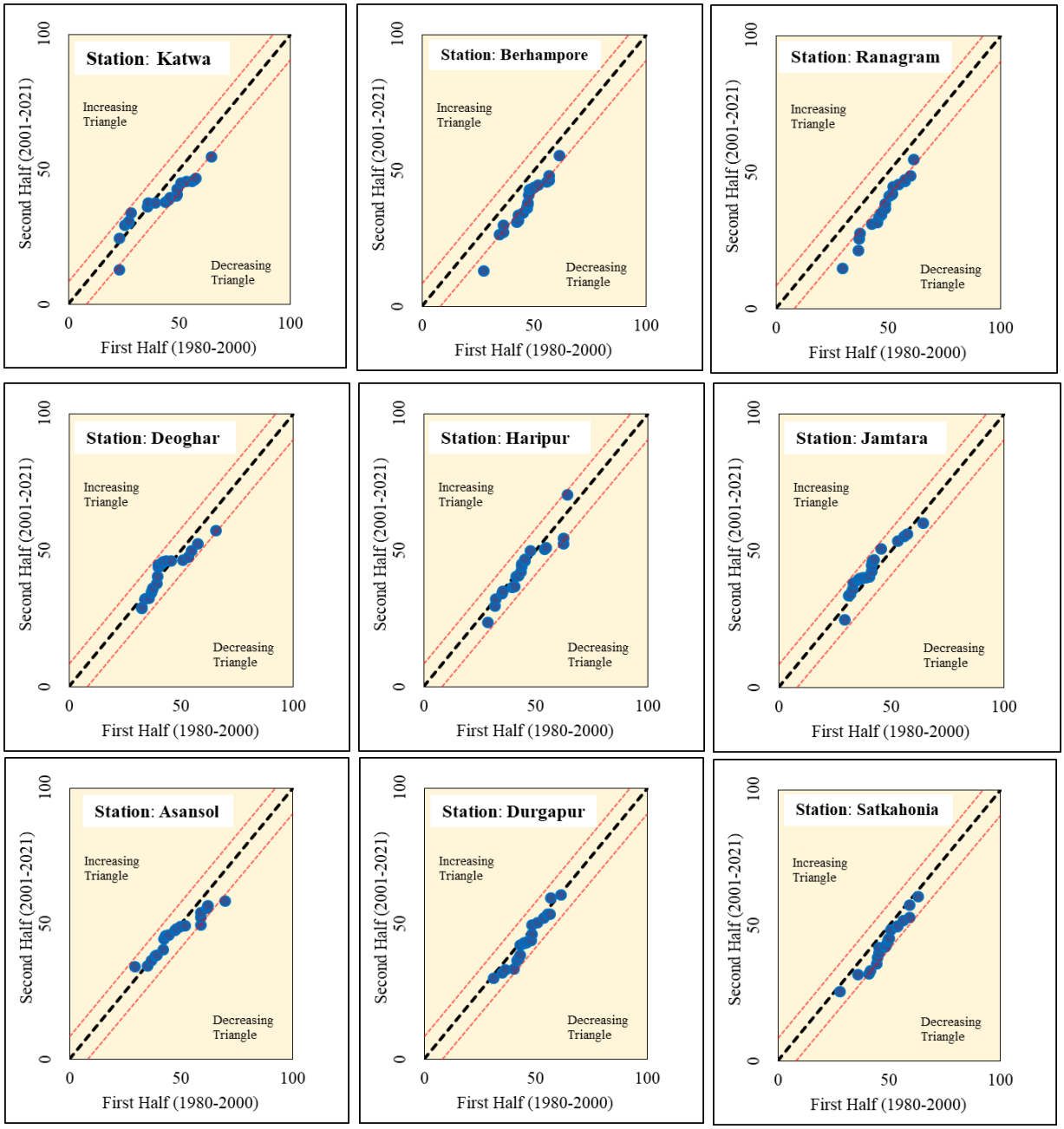

Figure 6.3 *Continued*

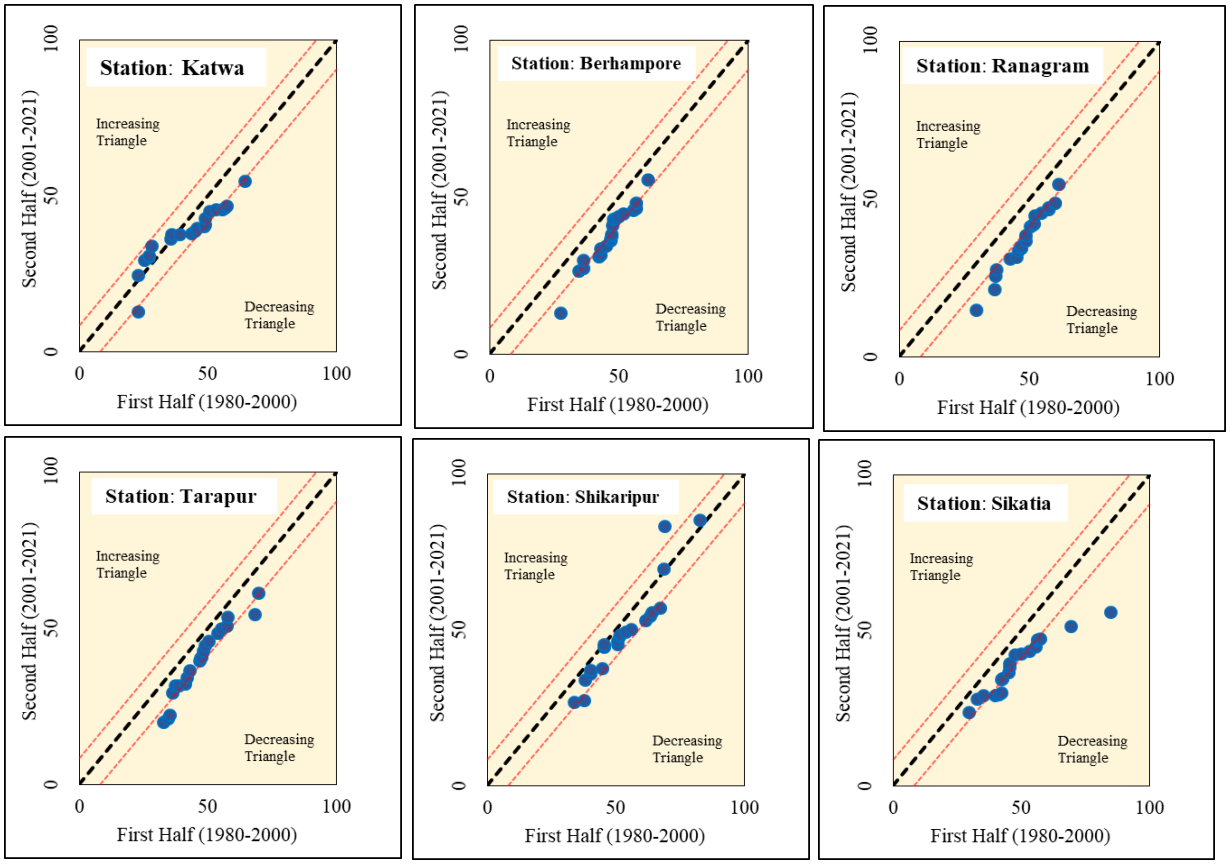

Figure 6.3 *Continued*

- **Variability and Trends in Rainfall**

The analysis of long term annual rainfall using both MK test and ITA test, has been presented in table 6.3. Figure 6.5 shows station wise ITA trend lines of mean annual rainfall of the Mayurakshi River basin area. Rainfall variability over the study area has been noted in previous studies (Nag et al.2022). The value of CV as shown in figure 6.4b, represents the lower portion of the basin area witnessing the highest variation in rainfall (28.14%), and the middle and some portions of the upper reach experiencing the lowest variation in rainfall (5.05%) over a 40-year period.

One of the most frequent natural disasters in the Mayurakshi River is flooding, which is mostly caused by a massive water release from the Siddheswari tributary. The largest concentration of mean annual rainfall over the middle half of the basin area further contributed to this surge of river discharge into the main river (Fig. 6.4a). Additionally, the computed Z statistics in the MK test (Table 6.4) show that 5% of the region is under the 95% confidence level and 13% of

the stations exhibit a significant trend at 99% confidence level. Some of the station shows significant monotonic trends whereas some shows a non-monotonic trends in their rainfall distribution over the study area. Except for the four meteorological stations Haripur, Durgapur, Jamtara, and Shikaripur, the ITA Slope in this trend analysis shows that 86.66% of the stations have experienced a decline in their mean annual rainfall over the past 40 years. Such a decreasing trend in long term precipitation has a social and economic impact on the hydrological health of the catchment as a whole.

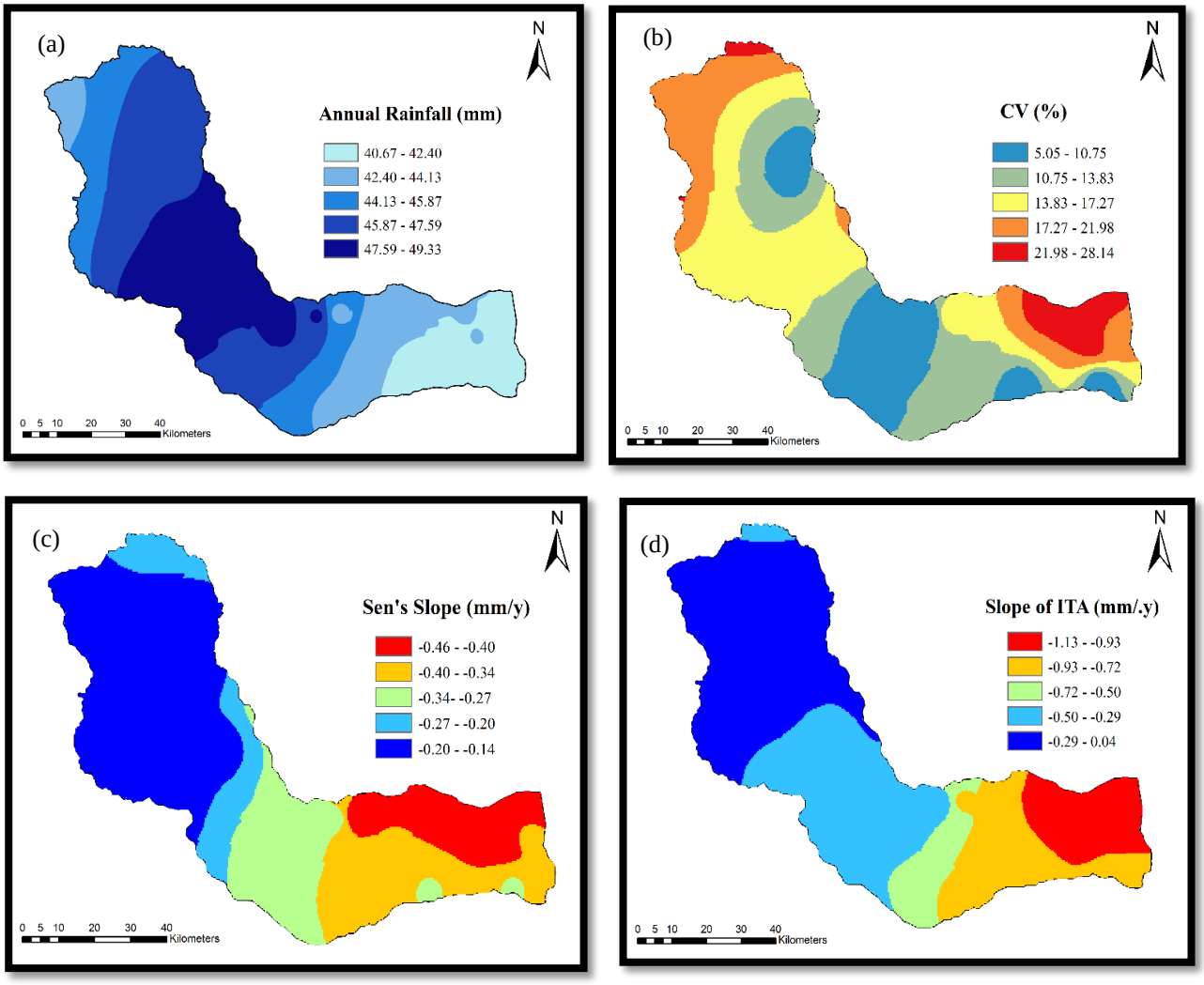

Figure 6.4 *Surface Layer of 40 Years of Annual Rainfall (a) Distribution Map (b) Co-efficient of Variance map (c) Innovative Trend Analysis Slope Map (d) Sen's Slope Map*

Table 6.3 *Descriptive Statistics of 40 years Annual Rainfall of Mayurakshi River Basin Area*

Sl. No	Station	Location			Annual Rainfall (mm)					
		Latitude	Longitude	Elevation (m)	Mean (mm)	SD*	Variance	CV (%)*	C_s*	C_k*
1	Tilpara	23.94854	87.52383	63.66	48.01	3.14	119.17	6.55	0.41	0.54
2	Suri	23.90475	87.52383	80.01	48.01	3.14	119.17	6.55	0.41	0.54
3	Shyambati	23.68847	87.68438	64.44	43.12	5.74	118.69	13.31	-0.33	1.11
4	Shekhampur	23.81585	87.77063	44.70	43.12	5.74	118.69	13.31	-0.33	1.11
5	Salar	23.77339	88.10368	23.47	40.67	2.05	119.83	5.04	-0.34	1.13
6	Sainthia	23.94854	87.68173	47.60	43.44	7.35	130.27	16.92	0.10	0.02
7	Narayanpur	23.89016	88.14084	20.61	41.86	7.66	93.89	18.30	-0.49	0.67
8	Massanjore	24.10644	87.31153	101.54	49.19	8.07	120.11	16.41	1.45	4.55
9	Maharo	24.32671	87.21466	150.91	47.43	4.51	168.19	9.51	1.26	3.18
10	Kundahit	23.97375	87.16026	153.23	49.19	8.07	120.11	16.41	1.45	4.55
11	Kultore	23.94323	87.62467	52.07	48.01	3.14	119.17	6.55	0.41	0.54
12	Kirnahar	23.76543	87.87413	35.27	40.67	2.05	119.83	5.04	-0.34	1.13
13	Kandi	23.94589	88.04928	26.20	42.51	11.96	108.63	28.15	-0.44	0.03
14	Jama	24.36784	87.26243	168.56	47.43	4.51	168.19	9.51	1.26	3.18
15	Dumka	24.28694	87.24385	156.04	47.43	4.51	168.19	9.51	1.26	3.18
16	Bharatpur	23.88618	88.08112	18.52	42.51	11.96	108.63	28.15	-0.44	0.03
17	Kuli	23.97243	87.95905	27.28	42.51	11.96	108.63	28.15	-0.44	0.03
18	Khushiyari	24.47234	86.85657	344.05	42.77	8.07	83.10	18.87	0.83	0.63
19	Deoghar	24.47941	86.69218	252.29	42.77	8.07	83.10	18.87	0.83	0.63
20	Haripur	24.26552	86.85484	197.94	43.53	11.45	101.75	26.31	0.58	0.38
21	Jamtara	23.95088	86.81768	188.08	42.02	5.96	78.06	14.19	0.62	-0.01
22	Asansol	23.67689	86.95379	120.96	46.98	3.31	78.59	7.04	0.33	-0.20
23	Durgapur	23.52134	87.31263	107.86	45.13	0.94	67.62	2.07	0.09	-0.60
24	Satkahonia	23.59911	87.49469	64.41	45.73	5.12	75.89	11.20	-0.21	-0.15
25	Katwa	23.6433	88.13282	20.32	39.96	0.90	122.92	2.25	-0.14	-0.24
26	Berhampore	24.09936	88.26362	22.12	41.87	7.66	93.57	18.30	-0.49	0.69
27	Ranagram	24.02335	88.09039	24.83	42.51	11.96	108.63	28.15	-0.44	0.03
28	Tarapur	24.10643	87.80757	39.63	43.38	7.35	131.46	16.94	0.10	-0.01
29	Shikaripur	24.24254	87.46464	145.31	51.18	16.01	198.42	31.29	0.65	0.27
30	Sikatia	24.83647	87.15354	98.68	43.35	23.12	136.93	53.33	1.09	2.71

*SD= Standard deviation, CV (%) = Co-efficient of variation, C_s= Skewness, C_k= Kurtosis

Table 6.4 *Detailed Output of Annual Rainfall Trend Analysis of Mayurakshi River Basin Area*

Sl. No	Station	p-Value	Z Statistics	MK tau	Sen's Slope	IT Slope	ITD
1	Tilpara	***0.045***	1.99[A]**	-0.200	-0.32	-0.394	⬇
2	Suri	***0.045***	1.99[A]**	-0.200	-0.32	-0.394	⬇
3	Shyambati	***0.0029***	2.98[A]***	-0.298	-0.387	-0.887	⬇
4	Shekhampur	***0.0029***	2.98[A]***	-0.298	-0.387	-0.887	⬇
5	Salar	***0.0079***	-2.66[A]***	-0.266	-0.334	-0.848	⬇
6	Sainthia	***0.0035***	-2.92[A]***	0.292	-0.461	-0.787	⬇
7	Narayanpur	***0.0012***	-3.23[A]***	0.323	-0.388	-0.936	⬇
8	Massanjore	0.2743	-1.09[R]	0.109	-0.147	-0.492	⬇
9	Maharo	0.2443	-1.164[R]	-0.117	-0.172	-0.156	⬇
10	Kundahit	0.2743	-1.093[R]	-0.109	-0.147	-0.492	⬇
11	Kultore	***0.0455***	-1.999[A]**	-0.200	-0.322	-0.394	⬇
12	Kirnahar	***0.0081***	-2.658[A]***	-0.266	-0.334	-0.848	⬇
13	Kandi	***0.0062***	-3.422[A]***	-0.342	-0.463	-1.126	⬇
14	Jama	0.2443	-1.164[R]	-0.117	-0.172	-0.156	⬇
15	Dumka	0.2443	-1.164[R]	-0.117	-0.172	-0.156	⬇
16	Bharatpur	***0.0006***	-3.422[A]***	-0.342	-0.463	-1.126	⬇
17	Kuli	***0.0006***	-3.422[A]***	-0.342	-0.463	-1.126	⬇
18	Khushiyari	0.237	-1.182[R]	-0.118	-0.174	-0.263	⬇
19	Deoghar	0.237	-1.182[R]	-0.118	-0.174	-0.263	⬇
20	Haripur	0.142	1.466[R]	0.147	0.219	0.164	⬆
21	Jamtara	0.575	-0.559[R]	-5.673	-0.053	0.247	⬆
22	Asansol	0.493	-0.684[R]	-6.914	-0.098	-0.145	⬇
23	Durgapur	0.119	-1.555[R]	-0.156	-0.194	0.232	⬆
24	Satkahonia	***0.0213***	-2.302[A]**	-0.230	-0.304	-0.497	⬇
25	Katwa	0.0799	-1.751[R]*	-0.175	-0.288	-0.473	⬇
26	Berhampore	***0.0012***	-3.226[A]***	-0.322	-0.387	-0.933	⬇
27	Ranagram	***0.00062***	-3.422[A]***	-0.342	-0.463	-1.126	⬇
28	Tarapur	***0.0035***	-2.915[A]***	-0.299	-0.465	-0.799	⬇
29	Shikaripur	***0.016***	-2.409[A]**	-0.241	-0.439	0.353	⬆
30	Sikatia	***0.0074***	-2.675[A]***	-0.268	-0.403	-1.010	⬇

Note: Bold and Italic font denotes statistically significant trend exists within the dataset; [A]: Accepted the alternative hypothesis (Ha); [R]: Rejected the null hypothesis (H0); *Trend at the 90% confidence level; **Trend at the 95% confidence level; ***Trend at the 99% confidence level; ITD: Innovative Trend Detection.

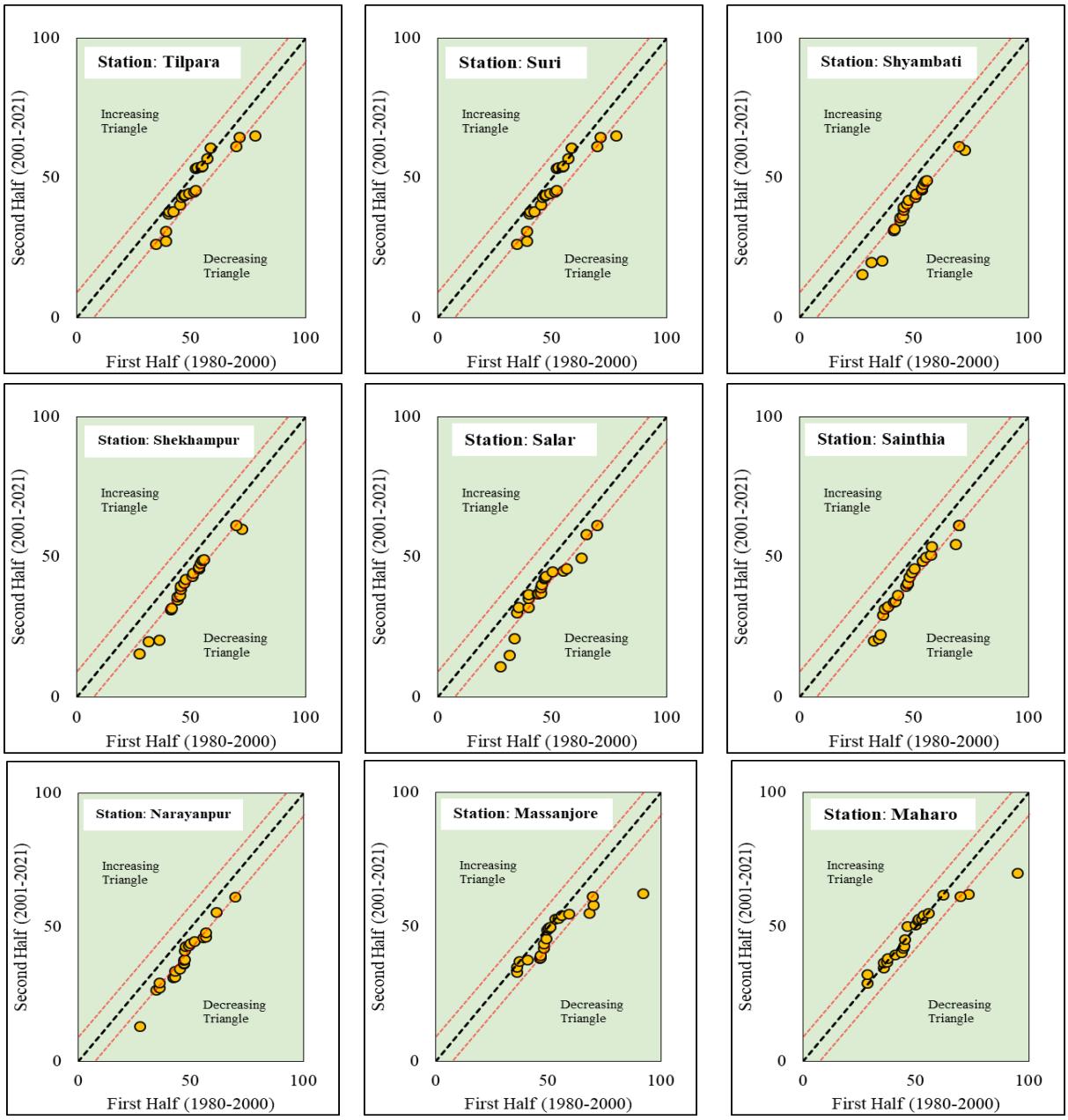

Figure 6.5 *Station Wise Plots of Innovative Trend Analysis of Annual Rainfall for the period of 1980-2000 (First half) and 2001-2021 (Second half)*

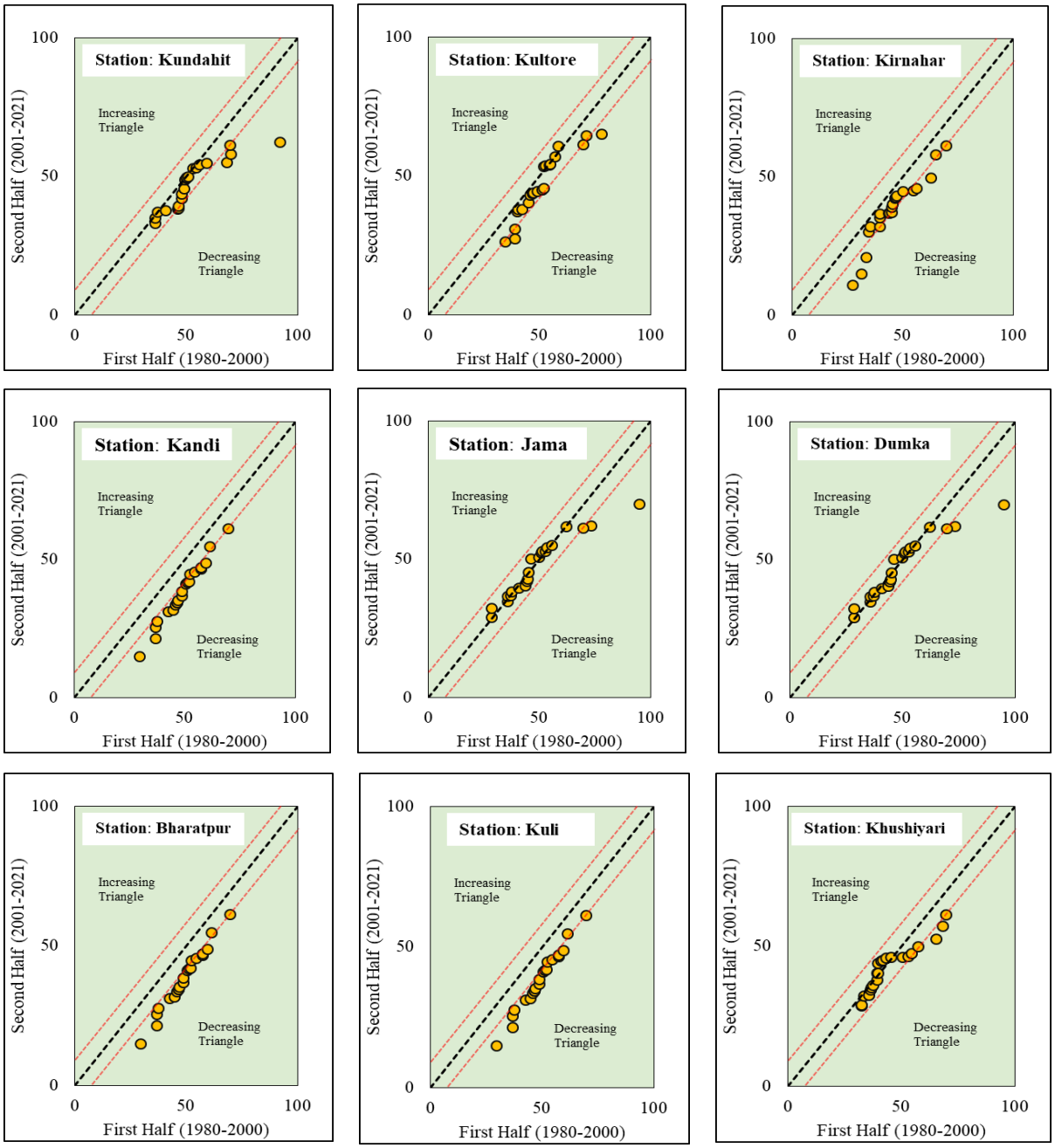

Figure 6.5 *Continued*

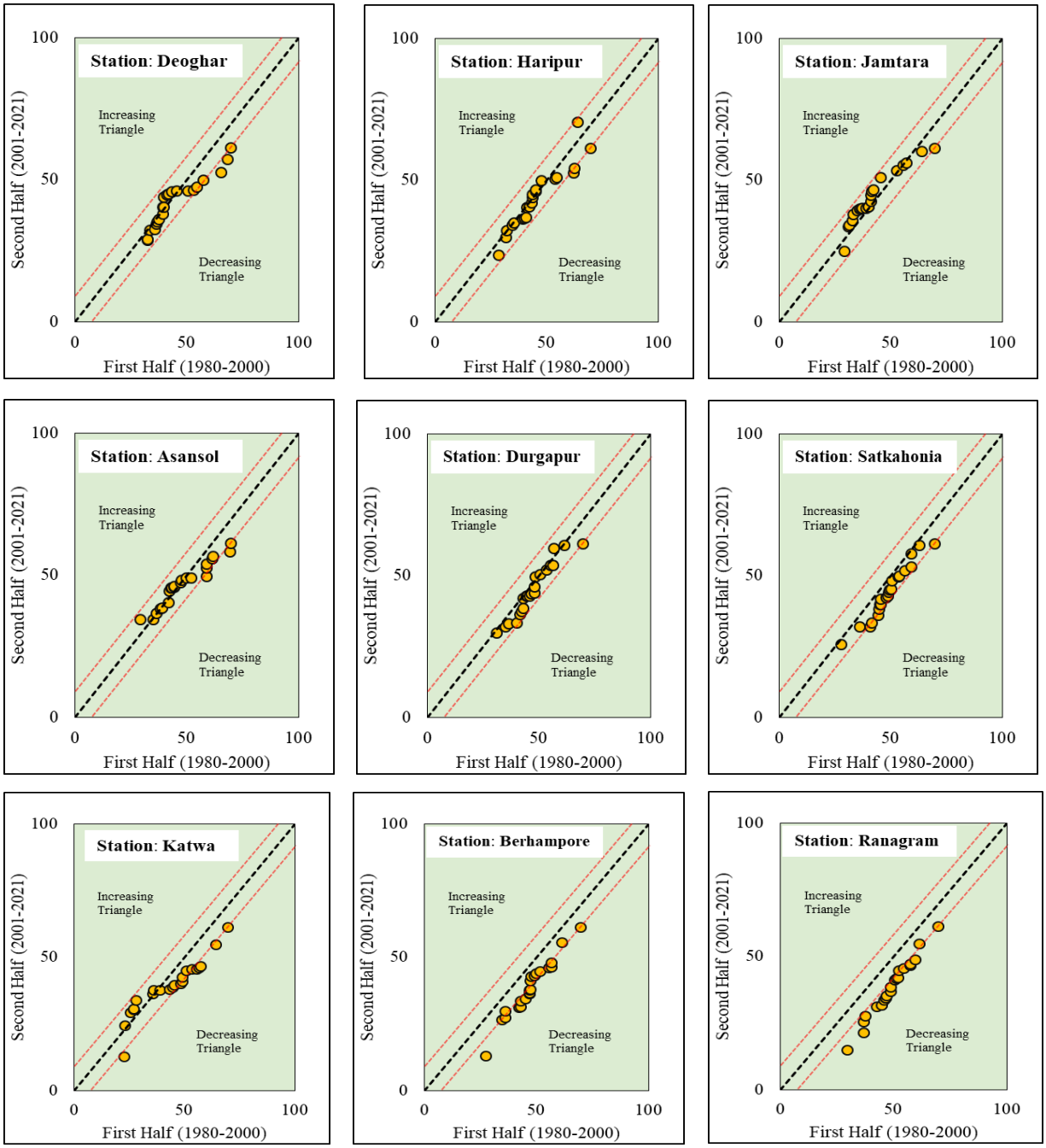

Figure 6.5 *Continued*

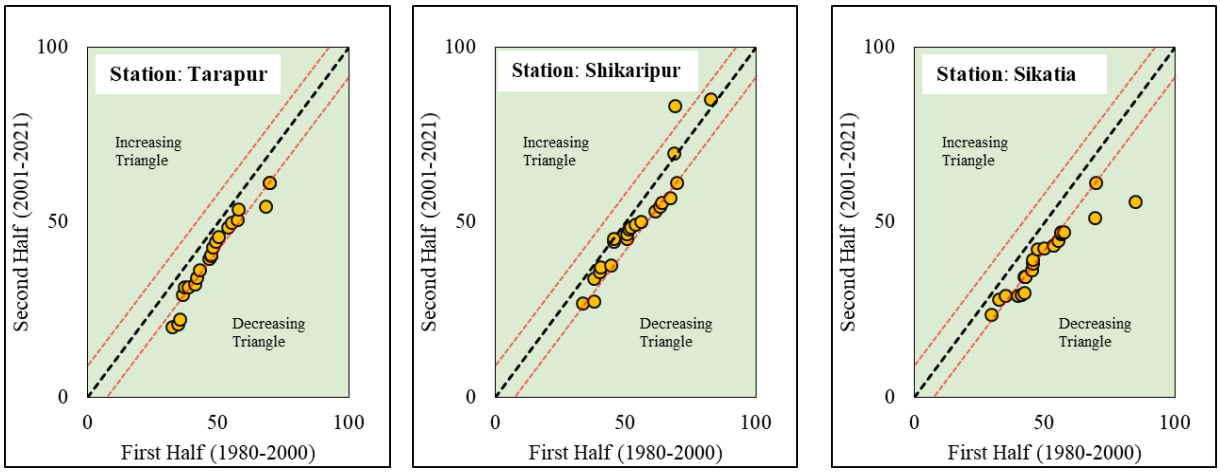

Figure 6.5 *Continued*

6.1.4. Conclusion

This study investigated the spatial and temporal characteristics of temperature and precipitation in Mayurakshi River Basin area. By analysing the trend, it had been possible to conclude that the results of ITA and MK test exhibited a similar trend for all stations and time scales, and the Z statistic confirmed its dependability. Overall a decreasing trend has observed in both the case of mean annual temperature and precipitation over a time period of 40 years at 95% of confidence level. In the long run such kind of evaluation of hydro-meteorological conditions at a regional scale can be helpful for regional-scale planning about the status of flood and drought in any region, which will ultimately be beneficial for agricultural development.

6.2. Construction of Intensity-Duration-Frequency (IDF) Curve

In water resources engineering, the intensity–duration–frequency (IDF) relationship of rainfall amounts is one of the most frequently used methods for planning, designing, and operating water resources projects (Elsebaie 2012). This IDF curves are graphical illustrations that indicate the amount of precipitation that descends in drainage regions over a particular time period (Dupont and Allen, 2000). Effects of rising temperatures on the hydrologic cycle alter the intensity and duration of precipitation and may increase the frequency of extreme precipitation occurrences. Such extreme rainfall events are further lead to deterioration of water quality, property damage, and potential fatalities from flooding. At this point, estimating the prospective implications of climate change and researching the impact of historical statistics on rainfall events (in terms of intensity, duration, and return period) are required. A representation of IDF curve is one of the best choice that can graphically depicts the possibility that a given rainfall intensity and duration will occur at a specific location. With modern remote sensing and satellite data, it is simple to construct IDF curves at various return periods to determine the relationship between rainfall depth duration and frequency in any region (Awadallah et al. 2011).

The major goal of this work is to create IDF curves for the Mayurakshi River basin area in order to determine the correlation between rainfall frequency, intensity, and duration. To doing so, the whole river stretch has been split into three parts based on the steepness of the terrain. The 12 hydro-meteorological stations in the study area were then put into these three groups (upper, middle, and lower) based on their location (Fig. 6.1). The first step for the generation of IDF curve is prepare a frequency distribution table, mainly to figure out the function of the probability distribution of rain intensity exceedance for each time. In this study, two significant probability distributions for frequency analysis—the Gumbel distribution of frequency and the Log Pearson type III probability distribution—have been utilised at various time intervals (2,10,25,50,100 years) and for various durations (10,20,30,60,120,180,360,720,1440 min). In addition, the IDF equation was computed for the estimation of rainfall intensity at a particular interval and return period and also to detect the best fit frequency distribution a goodness of fit test has also been executed. The details methodology have been presented in figure 6.6.

6.2.1 Data Source

One and only primary data for this study is rainfall data, which has been downloaded from the official website of Indian Meteorological Department (IMD) Pune at a daily basis having a resolution of 0.5*0.5 degree for the period of 1980-2020 and then the analysed data has been further analysed to calculate the maximum annual rainfall of each station of the study area.

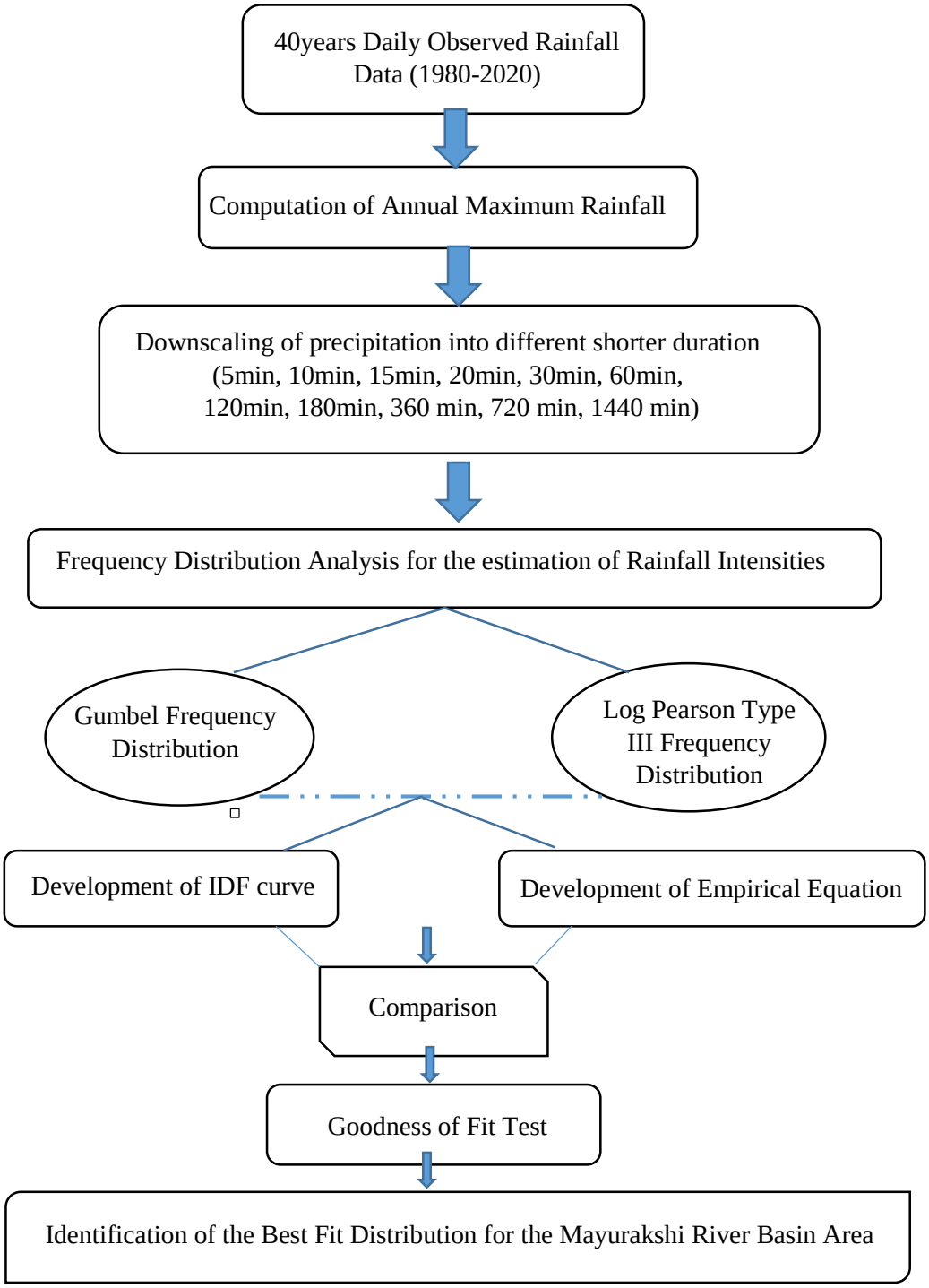

Figure 6.6 *Methodological Chart of Intensity Duration Frequency Curve*

6.2.2. Methodology

- **Generation of the IDF curves**

In this study, two widely used frequency analysis approaches namely Gumbel distribution and LPT III distribution has been executed using maximum annual precipitation data (Millington et al. 2011).

- **Gumbel Frequency Distribution**

The Gumbel theory of distribution is most frequently employed for IDF analysis due to its effectiveness for representing maximum. It is relatively simple and only uses of severe occurrences or peak values of rainfalls. In this model, the computation of frequency precipitation (P_T) in a certain return and duration has been done using the given formula-

$$P_T = P_{ave} + KS \tag{6.6}$$

Here, K is defined as Gumbel frequency factor, calculated using the following formula-

$$K = -\frac{\sqrt{6}}{\pi}\left[0.5772 + \ln\left[\ln\left[\frac{T}{T-1}\right]\right]\right] \tag{6.7}$$

Here, P_{ave} is referred as mean annual maximum precipitation at a specific duration of rainfall, which is calculated using the following as given below-

$$P_{ave} = \frac{1}{n}\sum_{i=n}^{n} P_i \tag{6.8}$$

Where, P_i indicate the maximum value of rainfall and n is the number of years of records. The standard deviation of rainfall (S) event has been calculated using the given equation-

$$S = \left[\frac{1}{n-1}\sum_{i=1}^{n}(P_i - P_{ave})^2\right]^{1/2} \tag{6.9}$$

S represents the standard deviation of the data set P. When multiplied by the standard deviation, the frequency factor (K), which is an indicator of the return period and sample size, produces the deviation of the expected return period rainfall from the mean. Finally, the rainfall intensity, I (in mm/h) for return period T is derived from

$$I_t = \frac{P_t}{T_d} \tag{6.10}$$

The computed Precipitation frequency (P_t), intensities (I_t) for different time duration (T_d) in hours and different return period for 12 different gauge stations of Mayurakshi River basin area using Gumbel frequency distribution method has been presented in annexure 1.

- **Log Pearson Type (LPT) III Frequency Distribution**

LPT III distribution implies logarithms forms of the measured values, which are used to calculate the rainfall intensity at various durations and return periods. The LPT III method is used to obtain the frequency of precipitation in a similar way to the Gumbel method and the mean and standard deviation has also obtained from the logarithmic data. The following is the concise expression for this later distribution.

$$P^* = \log(P_i) \tag{6.11}$$

$$P_T^* = P_{ave}^* + K_T S^* \tag{6.12}$$

$$P^*{}_{ave} = \frac{1}{n}\sum_{i=n}^{n} P^* \tag{6.13}$$

$$S^* = \left[\frac{1}{n-1}\sum_{i=1}^{n}(P^* - P^*{}_{ave})^2\right]^{1/2} \tag{6.14}$$

Here, P^* is the logarithmic transformation of P_i, similarlyP_T^*, $P^*{}_{ave}$ and S^* are same as defined in earlier section of Gumebl distribution. K_T is the the pearson frequency factor can be affected by the skewness coefficient (C_S) and return period (T).

In LPT III, the coefficient of skewness is calculated by the given equation

$$C_S = \frac{n\sum_i^{ni}(P_i^* - P^*{}_{ave})^3}{(n-1)\quad(n-2)\quad(S^*)^3} \tag{6.15}$$

$K_T$values can be obtained from numerous hydrology references, such as Chow (1988).

The computed Precipitation frequency (P_T^*), intensities (I_t) for different time duration (T_d) in hours and different return period for 12 different gauge stations of Mayurakshi River basin area using LPT III distribution has been shown in annexure 1.

- **Derivation of IDF Equation**

The IDF formulae are empirical equations that show the link between the maximum amount of precipitation as a dependent variable and the length of time and frequency of that precipitation as independent variables (Chow 1988, Burke and Burke 2008). There are some necessary steps for developing an equation to suit the calculation of rainfall intensity for a certain recurrence interval and specific rainfall period, which primarily depends on the results from the IDF curves.

By using the logarithmic conversion, the equation may be changed into a linear equation, allowing all of its associated parameters to be calculated (Chow 1988, Al Hassoun 2011), as mentioned below

$$I = \frac{CT_r^m}{T_d^e} \tag{6.16}$$

Using the logarithmic function to obtain

$$\log I = \log K - e \log T_d \tag{6.17}$$

Where, K= CT_r^m and e denotes the slope of the trend line.

- **Goodness of Fit Test**

The purpose of the test is to determine the extent to which the expected frequencies from the hypothesised distributions fit with the observed frequency of occurrence in a sample. In this study, The Root Mean Square Error (RMSE) test-based goodness-of-fit test is used to determine which probability distribution best fits the data (Alam et al. 2018). Despite the fact that it is commonly recognised that the lower the RMSE, the better the model performance, the RMSE is beneficial since it reveals inaccuracies in the units of the element of concern, which aids in data interpretation. It has been derived from the given formula-

$$RMSE = \sqrt{\frac{1}{n}\sum_{i=1}^{n}\left[R_{obs} - R_{exp}\right]^2} \tag{6.18}$$

Where, R_{obs} is the observed rainfall depth, R_{exp} is expected rainfall depth from those two probability distribution model and n is total number of data at a station.

6.2.3. Results and Discussion

In this study, long term daily rainfall data (1980-2020) have been utilised for the computation of maximum annual rainfall and other statistical indices (mean, standard deviation) for various duration (10,20,30,60,120,180,360,720,1440 min) and return period (2,5,10,25,50,100 year) of Mayurakshi River Basin area. For a more concise examination of the relationship between rainfall depth and duration, the study area has been divided into three catchment segments based on the basin's physiography. Then, the basin's meteorological stations are categorised based on their position above the basin. Total 12 meteorological stations were selected for the point wise extraction of the daily data and which was then downscaled into different shorter

duration using conventional formula as given by Indian Meteorological department (IMD) (Rashid et al. 2018).

Upper Catchment

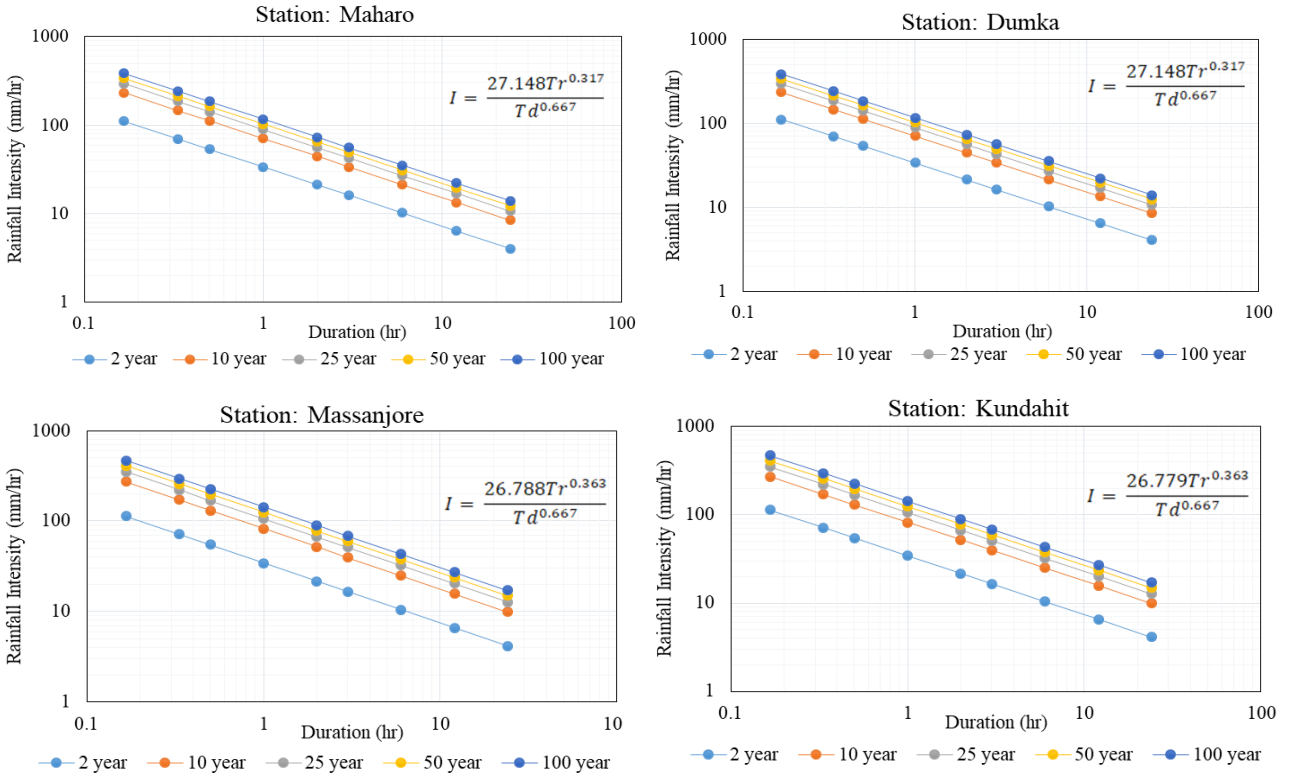

Middle Catchment

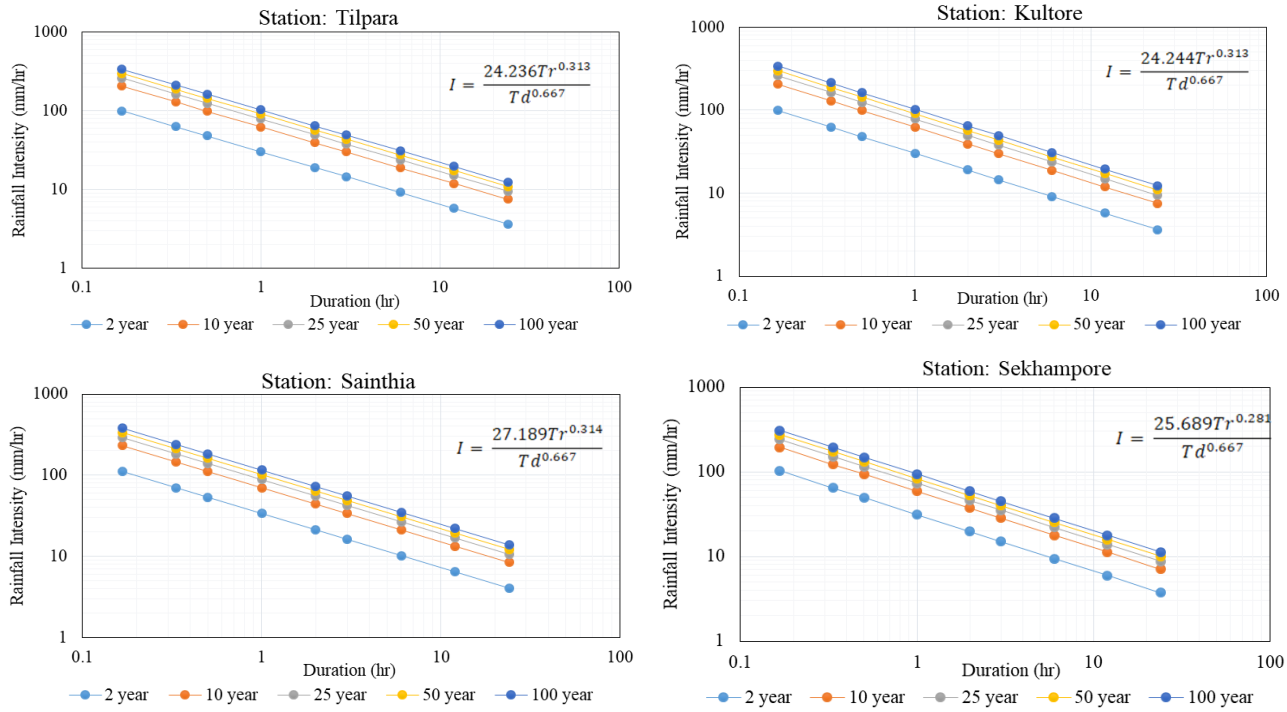

Figure 6.7 *IDF curves by Gumbel Method for Different Gauge Stations of Mayurakshi River Basin Area*

Lower Catchment

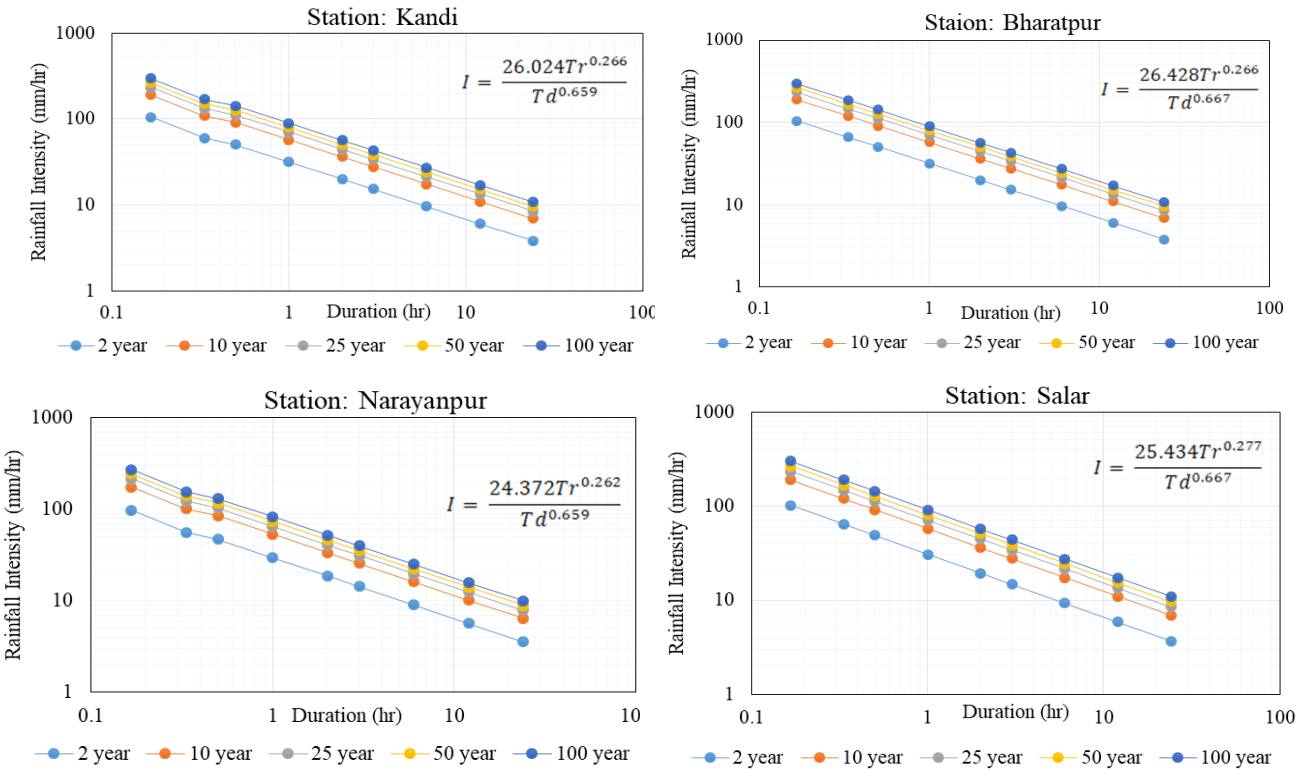

Figure 6.7. *Continued*

Two important probability distribution methods, namely the Gumbel distribution of frequency and Log Pearson's Type III probability distribution model, have been used to investigate the rainfall intensity duration of the study area. Both of the aforementioned techniques have also been used to create station-wise IDF curves, as shown in figure 6.7 from the Gumbel distribution and figure 6.8 from the LPT III distribution. The overall output shows that, the estimated amount of rainfall goes up as the return period increases, whereas the rainfall intensities tend to decrease as the duration of the rainfall stays constant throughout all return times. The frequency of rainfall events tends to be accompanied by an increase in their intensity. The results that were produced using the two distinct methodologies are quite consistent with one another. Although the findings achieved by the Gumbel method are slightly greater than those obtained by the Log Pearson III approach. This is also demonstrated by the parameters of the equation that was created in order to calculate the rainfall intensity using the two different approaches (Table 6.5).

Upper Catchment

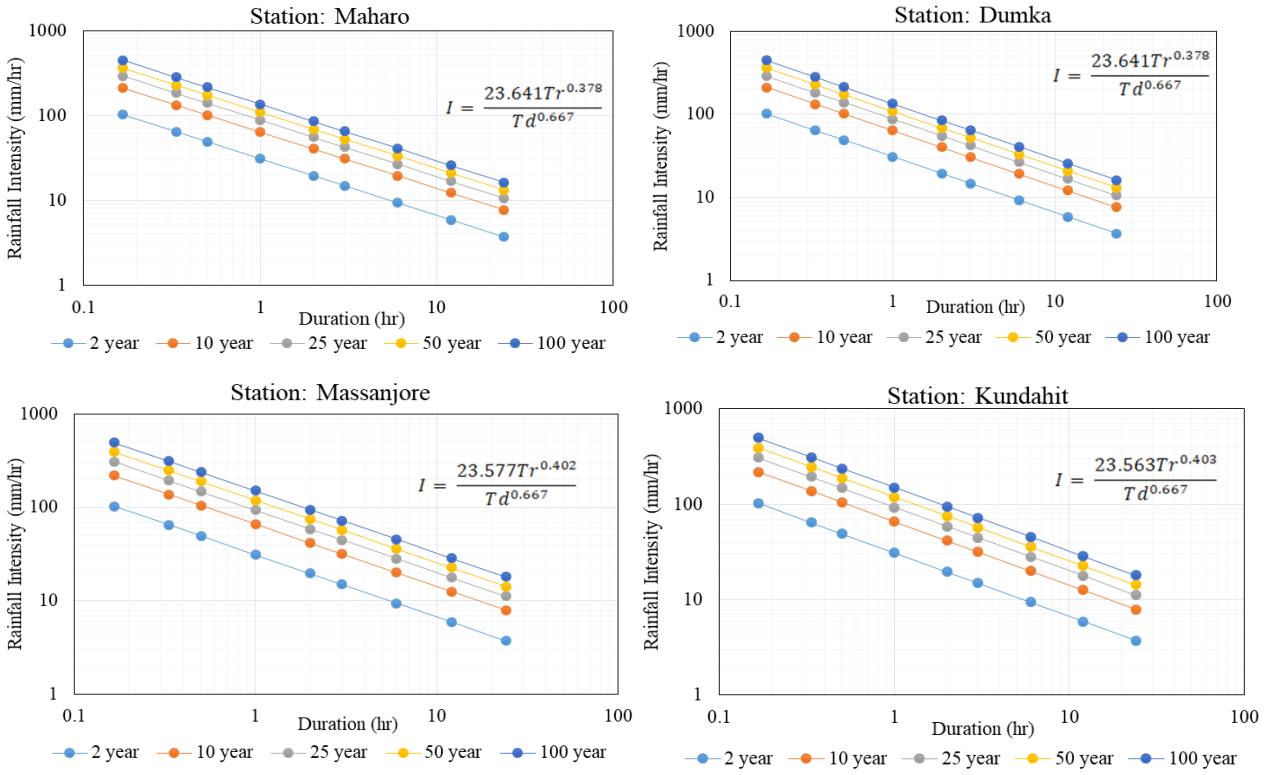

Middle Catchment

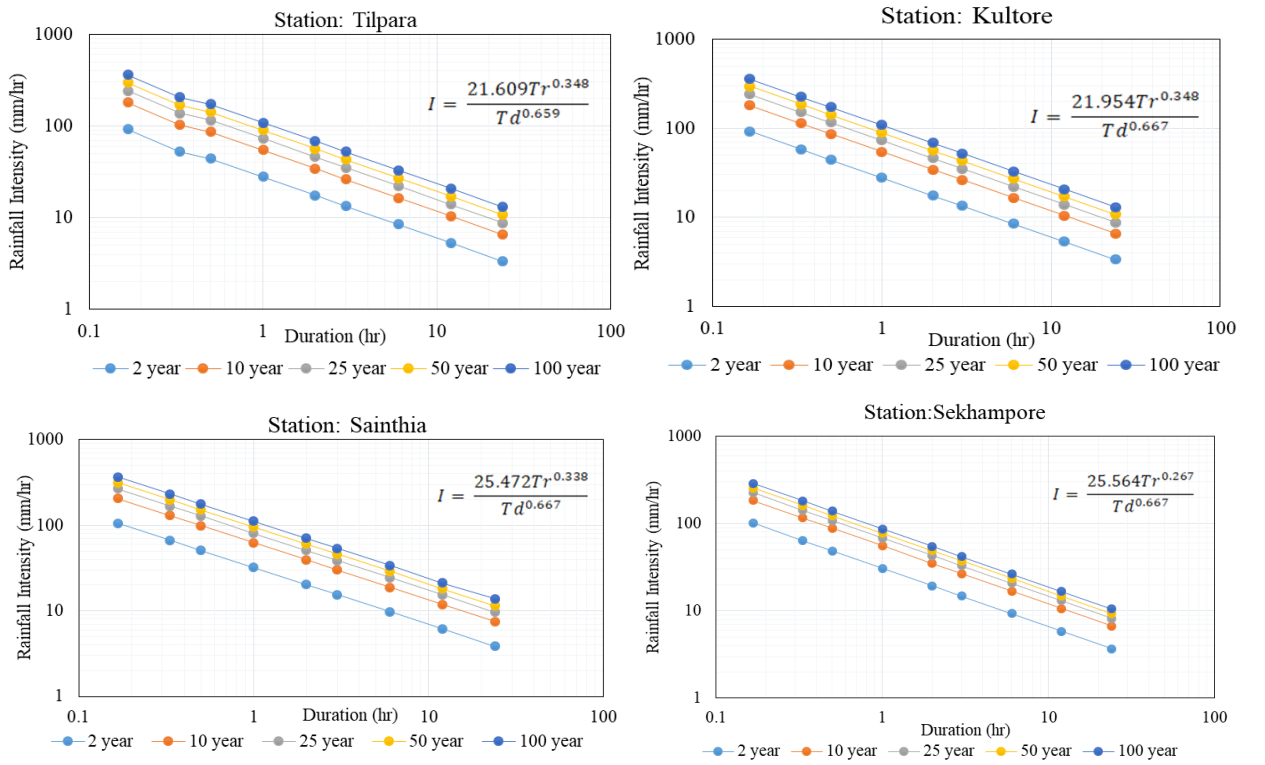

Figure 6.8 *IDF curves by LPT III method for Different Gauge Stations of Mayurakshi River Basin Area*

Lower Catchment

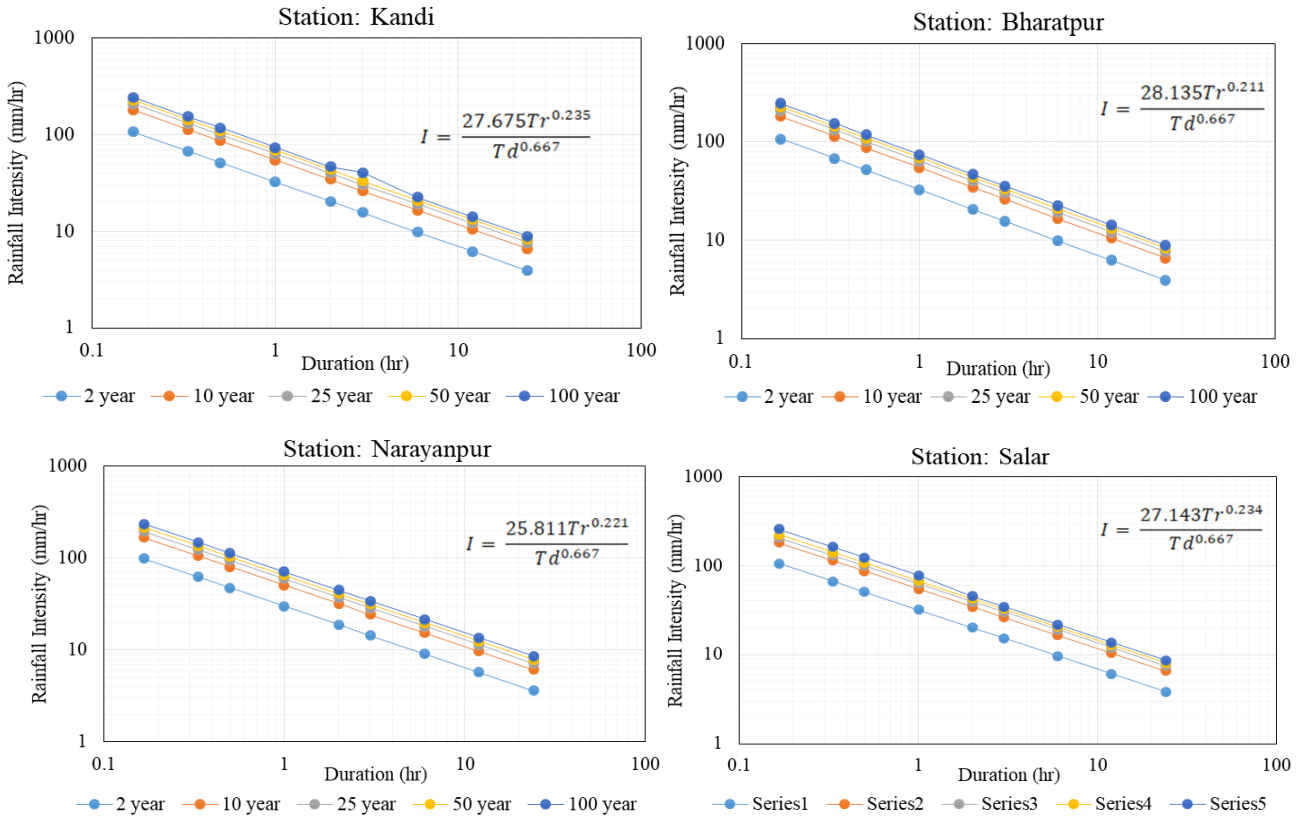

Figure 6.8 *Continued*

In addition, goodness-of-fit tests were utilised in order to appraise the data based on the correlation coefficient and to identify the methodology that produced the most accurate statistical distribution. Table 6.6 shows the output of root mean square error goodness of fit test which denote the correlation coefficient resembles a strong between the observed and expected variable and Log Pearson Type III test gives the better accuracy with respect to the previous one and can be used to predict any extreme rainfall event in future.

Table 6.5 *The Values of the Parameters that are used in the Development of IDF Curve Formulas in 3 Different Provinces of Mayurakshi River Basin*

Provinces	Rain Gauge Stations	Parameters	Method of Frequency Distribution Function	
			Gumbel Method	LPT III Method
Upper Catchment		C	27.148	23.641
	Maharo	m	0.3167	0.3781
		e	0.667	0.667
		C	27.148	23.641
	Dumka	m	0.3167	0.3781
		e	0.667	0.667
		C	26.788	23.577
	Massanjore	m	0.3628	0.4023
		e	0.667	0.667
		C	26.779	23.563
	Kundahit	m	0.3629	0.403
		e	0.667	0.667
Middle Catchment		C	24.236	21.609
	Tilpara	m	0.3129	0.3483
		e	0.667	0.659
		C	24.244	21.954
	Kultore	m	0.3128	0.3481
		e	0.667	0.667
		C	27.189	25.472
	Sainthia	m	0.3137	0.3384
		e	0.667	0.667
		C	25.689	25.564
	Sekhampore	m	0.2813	0.2665
		e	0.667	0.667
Lower Catchment		C	26.024	27.675
	Kandi	m	0.2656	0.2346
		e	0.659	0.667
		C	26.428	28.135
	Bharatpur	m	0.2655	0.2109
		e	0.667	0.667
		C	24.372	25.811
	Narayanpur	m	0.2624	0.2207
		e	0.659	0.667
		C	25.434	27.143
	Salar	m	0.2769	0.2335
		e	0.667	0.667

N.B: The parameters used in estimation of the IDF equations based on the rainfall (mm), Rainfall intensities (mm/h) for different return period (years).

Table 6.6 *Summary of the Root Mean Square Error (RMSE) for Different Rain Gauge Stations of Mayurakshi River Basin Area*

Provinces	Rain Gauge Stations	Gumbel Method		LPT III Method	
		RMSE in mm	RMSE in %	RMSE in mm	RMSE in %
Upper Catchment	Maharo	14.561	9.58	7.861	8.56
	Dumka	14.561	9.58	7.861	8.56
	Massanjore	21.221	11.03	7.403	7.47
	Kundahit	21.224	11.21	7.399	7.45
Middle Catchment	Tilpara	12.576	10.64	7.746	10.33
	Kultore	12.572	9.57	6.119	8.00
	Sainthia	14.200	11.36	8.312	10.17
	Shekhampore	9.988	12.54	8.545	12.39
Lower Catchment	Kandi	9.817	12.67	7.522	11.81
	Bharatpur	8.831	13.99	8.685	13.69
	Narayanpur	8.949	10.64	7.537	12.61
	Salar	9.464	10.33	6.483	10.26

6.2.4. Conclusion

The IDF curves for rainfall established in this work are extremely helpful in estimating rainfall intensity for use in flood planning and allocating water supplies. Using the most effective methods for generating probability distribution functions, this study compiled a database of Mayurakshi River Basin's historic rainfall intensities. It was shown that in most return periods, the results obtained using the two distributions are fairly similar and follow the same pattern. In contrast to Gumbel's method, the results from the log-Pearson type III approach are slightly more favourable. The constructed IDF rainfall curve also proves that the rainfall intensity calculated by the adopted methods and the values estimated by the calibrated formula matched well, with a correlation coefficient of more than 0.99 in almost every cases. Therefore it can be concluded that, the planning and ideal design of hydraulic structures, as well as future flood hazard studies, will be made possible and guaranteed by the accurate and reliable calculation of IDF curves.

6.3. Morphological Character of the Channel

The quantitative analysis of morphometric parameters is incredibly useful for river basin evaluation, soil and water conservation, and micro-level natural resource management. The discipline of river morphology is concerned with the physical characteristics of river channels, including their shape, size, and behaviour. It is also essential for comprehending how rivers function and how they are affected by natural and anthropogenic changes (Chorley 1969). Such morphometric study of a drainage basin can be accomplished by measuring the linear features, channel network gradient, and contributing ground slopes of the drainage basin (Nautiyal 1994). Morphometric study of a basin can be improved by using advanced tools such as RS (Remote Sensing) and Geographical Information System (GIS), as traditional measurement of these characteristics is time-consuming and inefficient (Sharma et al. 2010; Nag. et al. 2020)

6.3.1. Database & Methodology

Mayurakshi river basin has been delineated using Survey of India (SOI) toposheets (scale 1:50,000). All these maps are geographically rectified assigning Universal Transverse Mercator (UTM), WGS 1984 datum and 45N zone projection system and finally mosaicked with the help of Arc GIS 10.3 software system. The network of the stream has been extracted from the rectified topographical maps and the boundaries of the sub watersheds were demarcated on the basis of contour values and the stream flow direction. The digitization of drainage line, watershed boundaries and preparation of all the thematic layers of morphometric analysis has been performed in GIS environment using Arc GIS 10.3 software. The whole river basin has been divided into 12 sub-watersheds (SW) represented as SW1 to SW12 and the name of the sub-watersheds are mentioned in figure 6.9a.

Table 6.7 *Details of the Used Datasets*

Data type	Details	Source
Topographical Maps(1:50,000)	72L/ 14, 72L/15, 72L/16, 72P/2, 72P/3, 72P/4, 72P/6, 72P/7, 72P/8, 72P/16, 73M/1, 73M/5, 73M/9, 73M/10, 73M/13, 73M/14, 76M/6, 79A/1, 79A/2	Survey of India (SOI)
SRTM DEM	Resolution- 30m	USGS Earth explorer (https://earthexplorer.usgs.gov/)
TRMM Gridded Precipitation Data	Grid size 0.25º * 0.25º	GESDISC website (https://disc.gsfc.nasa.gov/)

The important parameters of morphometric analysis are being calculated for individual sub watersheds of the study area. Among the parameters considered, basin slope and relief properties have been calculated using Digital Elevation Model (DEM) of Shuttle Radar Topography Mission (SRTM) having 30m spatial resolution (Fig. 6.9a) as downloaded from USGS website (https://earthexplorer.usgs.gov/). The detailed information of the used datasets has been shown in Table 6.7.The fundamental parameters of morphometric analysis through various linear, relief and areal aspects for individual sub watersheds have been calculated using standard formulae as mentioned in table 6.8.

Table 6.8 *Morphometric Parameters with Formulae*

Sl. No		Morphometric Parameters	Formula	References
1	LINEAR	Stream Order (u)	Hierarchical order	Strahler (1964)
2		Bifurcation Ratio (Rb)	Rb = Nu / Nu+1 Where, Nu=Number of stream segments present in the given order, Nu+1= Number of segments of the next higher order	Schumn (1956)
3		Mean Bifurcation Ratio (Rbm)	Rbm = Average of bifurcation ratios of all orders	Strahler (1957)
4		Drainage Density (Dd)	Dd=L/A Where, L=Total length of stream (km), A= Area of basin (sq. km).	Hortan (1945)
5		Stream frequency (Fu)	Fu=N/A Where, N=Total number of stream, A=Area of basin(sq. km)	Horton (1945)
6		Texture ratio (T)	T=N1/P Where, N1=Total number of first order stream, P=Perimeter of basin (km)	Horton (1945)
7		Constant of channel maintenance (C)	$C = \frac{A}{\sum_{i-n}^{i=1} L_u}$ A= Area of basin (sq. km), L_u= Total stream length of all orders (km)	Horton (1945)
8		Length of Overland Flow(Lo)	Lo=1/2D km Where, D=Drainage density (km/sq. km)	Horton (1945)
9		Infiltration Number (If)	If= Fs* Dd Fs= Stream frequency and Dd= Drainage density(km/sq. km)	Faniran (1968)
10		Drainage Intensity(Di)	Di= L_u / A L_u= Total stream length of all orders (km) A= Area of basin (sq. km)	Horton (1945)
11	AREAL	Elongation ratio (Re)	Re=√(Au/π)/ Lb Where, A=Area of basin (sq. km), π=3.14, Lb=Basin length (km)	Schumn (1956)
12		Circulatory ratio (Rc)	Rc=4πA/P2 Where A= Area of basin (sq. km), π=3.14, P= Perimeter of basin (km)	Miller (1953)
13		Form factor (Rf)	Rf=A/(Lb)2 Where, A=Area of basin (sq. km), Lb=Basin length (km)	Horton (1945)
14		Shape factor (Bs)	Bs= Lb2/A Lb2=Square of basin length (km), A= Area of basin (sq. km)	Nooka Ratnam et al. (2005)
		Compactness co-efficient (Cc)	$Cc = \frac{P}{\sqrt[2]{\pi A}}$ P= Perimeter of basin (km), A= Area of basin (sq. km)	Horton (1945)
15	RELIEF	Basin Relief (Bh)	Vertical distance between the lowest and highest points of basin.	Schumn (1956)
16		Basin Slope (S)	S = H / Lb Where H= Basin relief (m) and Lb= Basin length (km)	Miller (1953)
17		Ruggedness Number (Rn)	Rn=Bh*Dd Where, Bh=Basin relief, Dd=Drainage density(km/sq. km)	Schumn (1956)
18		Dissection Index (DI)	DI = H / Ra Where, H = Basin relief (m) and Ra = Absolute relief (m)	Dov Nir (1957)

6.3.2. Results and Discussions of Morphometric Analysis

- **Analysis of Linear Parameters**

Linear parameters includes stream order (u), stream frequency (Fu), drainage density (Dd), drainage intensity (Di), mean bifurcation ratio (Rbm), texture ratio (T), length of overland flow (Lo), constant of channel maintenance (C), infiltration number (If) has been calculated using different algorithm as shown in table 6.8.

- ***Stream Order (u)*** is one of the significant parameter for morphometric analysis. Here Strahler's method (1964) of stream ordering has been implemented (Fig. 6.9b), which is the modified version of Horton's method. Here, Mayurakshi river basin has been recognised as 7^{th} order basin. Each stream of a specific stream order has its own basin area from which the streams receive water. Presence of more first and second order streams indicates high relief and gradient condition, favourable for erosional processes as in the case of sub watersheds located in the upper part of the river basin like SW1, SW2 etc.
- ***Stream Frequency (Fu)*** is another important parameter which reflects the lithological character of a drainage basin. It is the ratio between stream order and drainage basin area (Aouragh and Essahlaoui 2018). Like stream order, high stream frequency is characterized by high relief condition and vice versa. In this study, the stream frequency varies from 0.84 to 4.05. Higher value of stream frequency has been found in SW2 associated with rocky surface with steep slopes whereas lower value denotes lower ground slope area observed in SW12 which promotes low runoff and low risk of erosion.
- ***Drainage Density (Dd)*** is another important parameter for the evaluation of erosion susceptibility. It is a measurement of total stream length in a per unit area. This index quantitatively express the characteristics of physiographic condition on which the amount of runoff, permeability of soil, development of stream network and rate of erosion varies from place to place. In Mayurakshi basin area the value of drainage density ranges from 0.68 to 1.93 km/ sq. km (Table 6.9). In the upper part of the basin, due to the dominance of 1^{st} and 2^{nd} order streams and steep slope, the high drainage density has been found in SW6 (1.93 km/ sq. km) depicting more dissected topography and the lower drainage density has been observed in the low relief area in lower part of the basin in SW9 (0.68 km/ sq. km) (Fig. 6.9c).
- ***Drainage Intensity (Di)*** defines as the ratio between stream frequency and drainage density of an area (Faniran 1968). This parameter has a direct relationship with erodibility (Nitheshnirmal et al. 2019). High drainage intensity and rocky nature of topography makes the

region more vulnerable to erosion while Low value of Di indicates least denudation activities over the region. Here, SW12 and SW9 have lowest drainage intensity value and SW1 and SW2 experiences high drainage intensity indication the region as more susceptible to erosion (Table 6.9).

- ***Mean Bifurcation Ratio (Rbm)*** shows the ratio of the number of stream segments of given order to the number of segments of the next higher stream order. It is closely relate with the branching pattern of stream segments. Here the mean bifurcation ratio varies from 3.15 (SW9) to 1.20 (SW1) depicting geologically least disturbed watershed (Table 6.9). Also the bifurcation ratio has the direct relation to the runoff and erosion potential of an area. According to that, the SW9 and SW7 are more vulnerable to erosion.
- ***Texture Ratio (T)*** is also known as drainage texture, which implies on the spacing between each drainage line of the watershed. It also has a positive relation with the denudation processes operated within that region. In Mayurakshi river basin, the value of texture ratio ranges in between 20.38 in SW6 to 2.34 in SW12 (Table 6.9). According to the classification by Smith (1950) the SW6 has fallen under the very fine texture category indicating highest risk of erosion whereas SW12 has the lowest texture ratio denoting least susceptible to erosion.
- ***Length of overland Flow (Lo)*** defines the length of running water over the surface before it gets concentrated into the definite channel. Overland flow is significantly affected by the soil character of the particular area. It directly relates with the slope and relief of the region. Within a low slope area, the overland flow is less and vice versa. In this study, high Lo observed in SW6 (0.97) indicating fragile soil and low Lo observed in SW9 (0.34) where the soil is alluvium in nature denoting low risk of erosion (Fig. 6.9f).
- ***Constant of Channel Maintenance (C)*** defines the ratio between drainage areas to total length of all streams as it is the reciprocal of drainage density of that area. It expresses the significance of drainage area required to maintain a unit of stream length. Here, the minimum C value has been observed in SW12 (0.36) and the highest value has been observed in SW9 (1.47) (Table 6.9). According to Ameri et al. (2018) this parameter has a direct relation to erosion. So the result suggests that SW9 have higher risk of erosion than others.
- ***Infiltration Number (If)*** also expresses the risk of erosional activities within the drainage basin area. It has an indirect relationship with the runoff factor. The lower values of infiltration number indicate low infiltration which enhances the runoff and erosional process. Depending on the character of soil the amount of infiltration and permeability varies. From the table 6.9, the maximum infiltration number has been observed as 7.77 for SW2 and lowest value found as 0.57 for SW9. Therefore the SW2 has the high potential for erodibility.

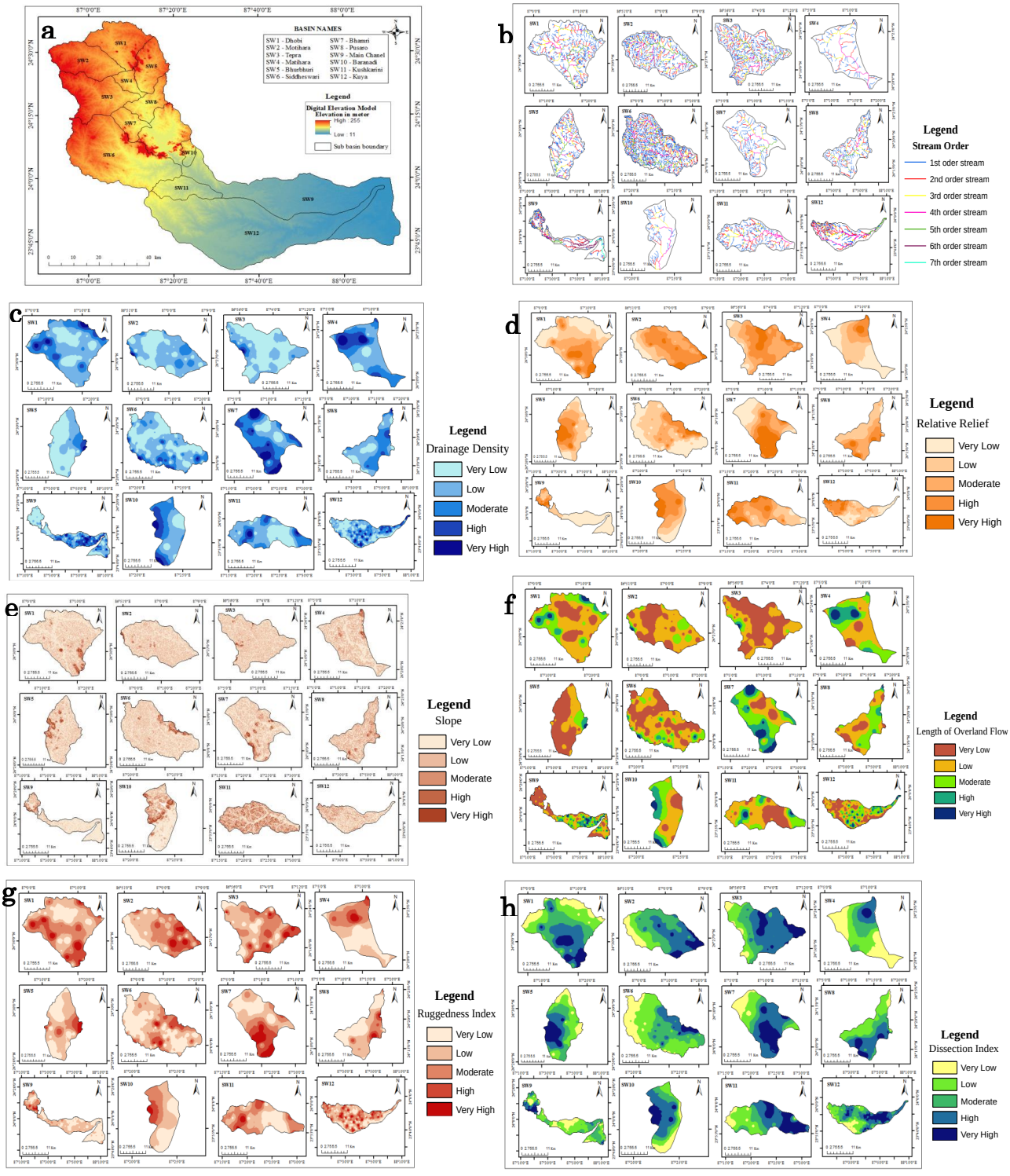

Figure 6.9 *Morphometric parameters (a) Digital elevation model (b) Stream order (c) Drainage density (d) Relative relief (e) Slope (f) Length of overland flow (g) Ruggedness index (h) Dissection index*

Table 6.9 *Extraction of Linear, Areal and Relief Parameters of Mayurakshi River Basin Area*

Basin Parameters	SW1	SW2	SW3	SW4	SW5	SW6	SW7	SW8	SW9	SW10	SW11	SW12
*u	5	5	5	4	5	6	5	5	7	4	4	5
Fu	2.78	4.05	3.51	2.02	2.60	3.43	2.39	2.75	0.84	2.64	2.31	0.36
Dd	1.34	1.92	1.79	1.33	1.59	1.93	1.56	1.65	0.68	1.55	1.59	1.24
Di	2.07	2.11	1.96	1.52	1.63	1.78	1.54	1.67	1.23	1.71	1.45	0.13
Rbm	1.20	1.92	2.03	1.68	2.13	2.14	2.17	1.73	3.15	1.75	1.66	1.86
T	10.30	16.00	13.24	3.32	8.37	20.38	5.39	5.86	3.38	3.97	6.02	2.34
Lo	0.37	0.96	0.90	0.67	0.80	0.97	0.78	0.82	0.34	0.77	0.79	0.37
C	0.75	0.52	0.56	0.75	0.63	0.52	0.64	0.61	1.47	0.65	0.63	0.36
If	3.73	7.77	6.29	2.69	4.15	6.64	3.73	4.54	0.57	4.08	3.67	1
Re	0.72	0.63	0.64	0.59	0.65	0.65	0.76	0.59	0.41	0.65	0.54	0.47
Rc	0.54	0.61	0.46	0.46	0.60	0.50	0.54	0.38	0.13	0.56	0.46	0.34
Rf	0.41	0.31	0.32	0.27	0.34	0.34	0.45	0.28	0.13	0.34	0.23	0.17
Bs	2.46	3.22	3.12	3.71	2.96	2.98	2.21	3.60	7.48	2.98	4.38	5.72
Cc	0.28	0.27	0.27	0.41	0.30	0.22	0.35	0.36	0.26	0.43	0.33	0.21
Bh	89.99	66.75	68.99	69.98	77.99	164.00	90.98	130.98	166.78	117.41	18.69	46.99
S	37.23	42.30	32.19	29.37	33.69	34.56	28.97	28.57	32.20	28.49	5.55	11.70
Rn	3.73	7.77	6.29	2.69	4.15	6.64	3.73	4.54	0.57	4.08	3.67	1
DI	0.89	1	1	0.66	0.75	1	0.73	0.99	0.99	0.77	0.50	0.98

* Stream Order (u), Stream Frequency (Fu), Drainage Density (Dd), Drainage Intensity (Di), Mean Bifurcation Ratio (Rbm), Texture Ratio (T), Length of Overland Flow (Lo), Constant of Channel maintenance (C), Infiltration Number (If), Elongation Ratio (Re), Circularity Ratio (Rc), Form Factor (Rf), Shape Factor (Bs), Compactness Co-efficient (Cc), Basin Relief (Bh), Slope (S), Ruggedness Index (Rn), Dissection Index (D)

- **Analysis of Areal Parameters**

Elongation Ratio (Re), Circularity Ratio (Rc), Form Factor (Rf), Shape Factor (Bs) and Compactness Co-efficient (Cc) have been taken from the areal parameters of the morphometric analysis.

- ***Elongation Ratio (Re)*** analyse the basin properties in terms of its shape, size, that has been effected by geological condition of the prevailing area. It also reveals different hydrological scenarios of a river basin which are often used for watershed management. Depending on various rock type Re can be classified into four groups like circular (0.9-1.0), oval (0.8-0.9), less elongated (0.7-0.8), elongated (0.5-0.7), highly elongated (<0.5). It has a direct impact on flood discharge and peak flow of a basin. More elongated basin has been characterised by low peak flow for longer duration enhancing the erosional activities whereas round to circular basin has been characterised by high peak flow for short duration. In this regard the value of Re is minimum (0.41) for SW9 fallen under more elongated basin with more susceptible to erosion and the maximum value (0.72) for SW1 indicate less elongated shape of basin with low risk of erosion (Table 6.9).

- ***Circularity Ratio (Rc)*** describes the shape of the drainage basin. It may also be affected by various parameters like slope, vegetation cover, climate, soil etc. Higher value of Rc indicate more circular basin whereas low Rc denotes elongated drainage area (Ameri et al. 2018). Here the Rc values varies from 0.13 to 0.61 where the SW9 has the lowest Rc value indicating more elongating and more erosion prone sub watershed of Mayurakshi river basin shown in table 6.9.

- ***Form Factor (Rf)*** is another parameter from areal aspect which also depicts the shape of a basin. It is a dimensionless index. It has an inverse relation with the basin denudation activity. In the study area, low value of Rf has been observed in SW9 (0.13) and highest value has been observed in SW7 (0.45) (Table 6.9). So the SW9 has been categorised under high erosion prone area whereas SW7 fall under low erosion prone area.

- ***Shape Factor (Bs)*** is an important parameter that effects on the amount of discharge, flow, run off and sediment generation from the watershed. In case of erosional activities, an elongated watershed had highest potential of erosion than the circular watershed. Among all the 12 sub watersheds of Mayurakshi river basin, the shape of SW9 has been more elongated than others. Accordingly the highest Bs value for SW9 (7.48) denotes the high risk of erodibility whereas the sub watersheds having low value of Bs like SW1 (2.46), SW6 (2.98) shows low risk of erodibility within Mayurakshi river basin area (Table 6.9).

- ***Compactness Co-efficient (Cc)*** is also regarded as an important parameter in this study. This parameter behave as same as the Bs and Rf. Here, SW6, SW12, SW2 and SW3 obtained lower Cc value indicating more elongated basin in shape and highest risk of erosion activities (Table 6.9).

- **Analysis of Relief Parameters**

Relief parameters that are considered for the study of sub-watershed prioritisation are Basin Relief (Bh), Slope (S), Ruggedness Index (Rn) and Dissection Index (DI).

- ***Basin Relief (Bh)*** is one of the major parameter to understand the formation of drainage pattern within a region. It expresses the elevation difference between highest and lowest point of an area. The basin relief also depicts the nature of topography on which the river flows. Depending on the variation of slope, the relief varies significantly affecting the processes of basin development. It has a direct correlation with the erosional processes. Among all the sub watersheds of Mayurakshi river basin , SW11 obtained minimum value i.e., 18.69 m reflecting

lower risk of erosion and maximum value of relief (166.78 m and 164.00 m) has been observed in SW9 and SW6 respectively (Fig. 6.9d), indicating high risk of erosion (Table 6.9).

- ***Slope (S)*** is another dominant morphometric parameter for the study of erosion susceptible zone. It signifies the nature of stream flow, basin runoff which may affects the various erosional processes. In Mayurakshi river basin, minimum slope value (5.55º) has been noticed in SW11 and highest value (42.30º) has been observed in SW2 (Fig. 6.9e). Increase of slope in an area represents more rugged topography, generates more runoff and makes the region more prone to erosion. Accordingly as the result suggests SW2 has the highest potentiality of erosion and SW11 has low risk of erosion (Table 6.9).

- ***Ruggedness Index (Rn)*** depicts the relationship between basin relief and drainage density of a particular area. This index also reveals the nature of topography of a region. High value of Rn represents more rugged topography and vice versa. It has a direct relation with basin erodibility. From the figure 6.9g it has been observed that maximum value of Rn (7.77) observed in SW2 representing the area more susceptible to erosion whereas lower value of Rn (0.57) found in SW9 suggests low risk of erosion (Table 6.9).

- ***Dissection Index (DI)*** has also been related with the relief as well as slope of the region. It affects the whole physiography reflecting the degree of vertical erosion by fluvial processes dominated over the region. The value of dissection index ranges between zero (absences of dissection) to one (vertical cliff). In this study area (Fig. 6.9h) higher value of dissection index i.e. 1 has been found in SW2, SW3 depicting more risk of erosion and in SW11 lower value of DI (0.50) represents low risk erosion over the area (Table 6.9).

6.3.3. Hypsometric Analysis

Hypsometric analysis is an effective technique for assessing and comparing the geomorphic evolution of distinct landforms, irrespective of their root cause that are regulating landscape evolution including tectonics, climate, and lithology variation etc. It is an expression of non-dimensional distribution of relative basin elevations with the relative area of the drainage basin (Strahler, 1957). The shape of the curve determines the erosion potentiality of the basin, its stages of topographic evolution and also explained the sequential changes in the slope of the original basin. The convex upward curve denotes a "Youthful Stage", 'S' shaped curve which is concave in upward and convex in the downward elevation of the land represents a "Mature Stage" and an upward concave shaped curve represents an "Old Stage" of land evolution with distorted peneplains (Strahler,1957). Langbein and Basil established the concept of hypsometry in 1947, and Strahler (1952) expanded it to include the percentage of area-altitude curve and

the hypsometric integral. The volume of the original basin that is still un-weathered is expressed as a percentage by the hypsometric integral (HI), which may be derived from the area under the curve. According to Pike and Wilson (1971) HI is a representation of elevation-relief ratio of a drainage basin, which has been regarded as a useful tool for the assessment of basin health. This index is calculated by using the following equation-

$$HI = \frac{h_{mean} - h_{min}}{Basin\ Relief} \quad (6.19)$$

Where, h_{mean} (m) is the mean elevation, and h_{min} (m) is the minimum height of the area. The value of HI, which has obtained by using the above mentioned formula, is classified as follow-

HI= >0.6 (Youthful Stage)

HI= 0.6-0.35 (Mature Stage)

HI= <0.35 (Old stage)

In this study, Hypsometric curve and the calculation of Hypsometric Integral (HI) has been carried out for all the sub-watersheds of Mayurakshi River Basin using SRTM digital elevation model (30m resolution) with the help of Arc GIS 10.3 software system.

- **Results of Hypsometric analysis**

The hypsometric curve of all the sub-watersheds (SW) of Mayurakshi River basin has been plotted and represented in figure 6.10. The comparison between all the plotted graphs and the calculated integral values depicts that the whole Mayurakshi drainage system has progressed into the old monadnock stage from mature stage of erosion. In addition to expressing the stages of landscape evolution, these curves reveal information about the nature of the underlying strata. In this case, the lithological characteristics of the SW2 (Motihara) and SW3 (Tepra) are primarily dominated by the presence of metamorphosed rocks like granite, gneiss, amphibolite which are more resistant to erosion compared to the basalt and alluvial rock surface. However, the assessment made from the values of hypsometric integral indicates that the sub-watersheds which are in youthful stage (HI>0.6) located within a zone of higher elevation and slope, which further triggered the rate of erosion along with sediment generation. Reducing such sediment influx and raising the groundwater level necessitate the installation of artificial recharge structures at desirable locations within the sub-basins (Babu el a. 2012; Singh et al. 2008). Similar kind of observations has also been noticed in the sub-watershed prioritisation using

Technique for Order Preference by Similarity to Ideal Solution (TOPSIS) model, discussed as follows.

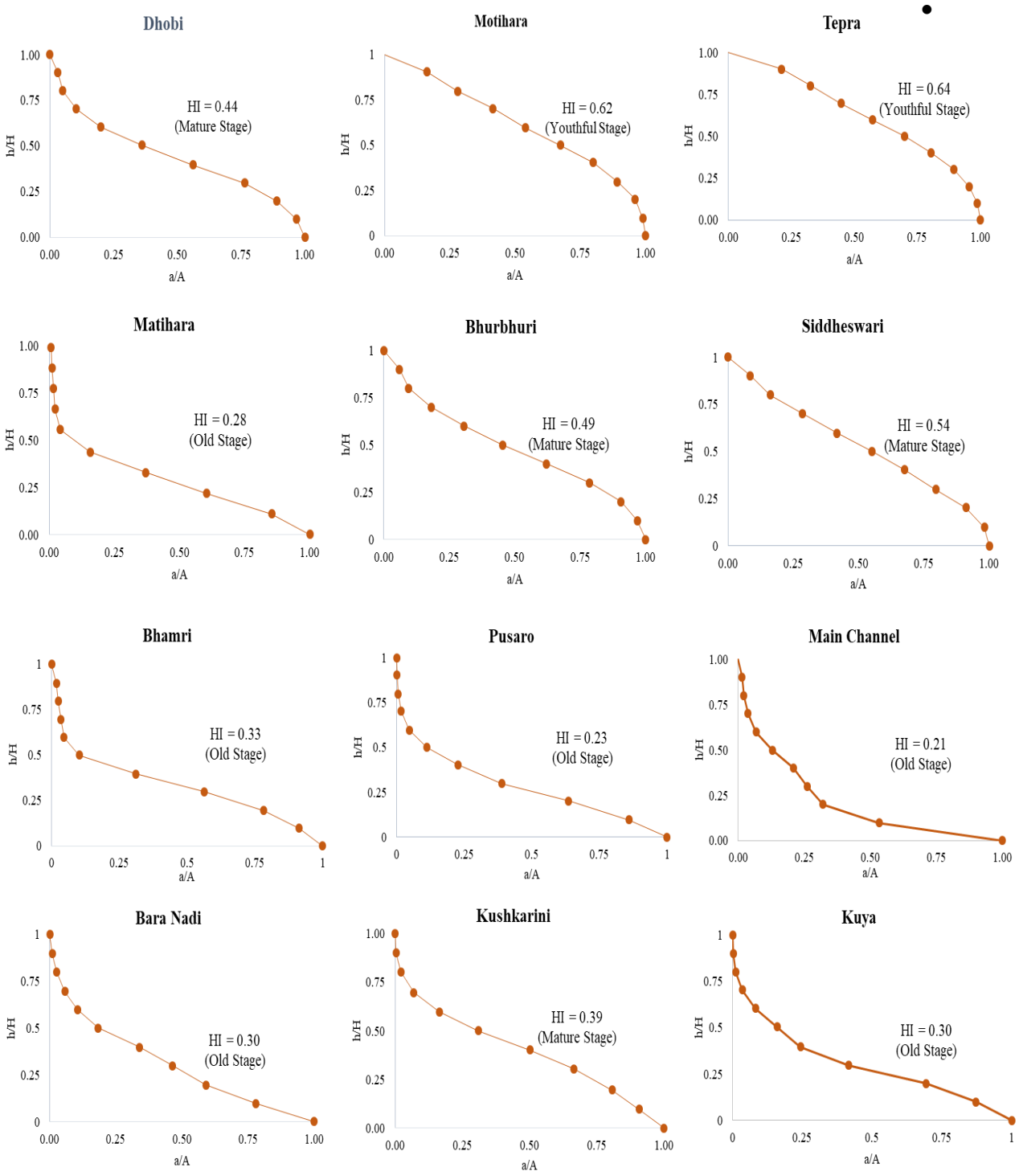

Figure 6.10 *Hypsometric Curve with Hypsometric Integral Values of the Sub-watersheds of Mayurakshi River Basin*

6.4. Identification of Erosion Susceptible Zones using Morphometric Analysis

In recent time the Mayurakshi River changes its original morphometric pattern which was mainly led by the human intervention. From the field study, authors observed unscientific sand mining has been going on the river bed in progressive way for which the channel shape, size and its natural flow is getting hampered (Plate no. 6.1). Such changes in channel configuration may accelerate the erosional processes and is disturbing the stability of the river bed. Several problems related channel degeneration has also been encountered by various researchers. Continues narrowing and widening of channel may disturb the normal hydro-morphological rhythm of the river (Pal et al. 2012). Furthermore, the problem of soil degradation is quite observable within the upper part of Mayurakshi river basin area (Pal and Debanshi 2018). Dispersed forest cover, uncontrolled grazing land and presence of hard rock terrain coupled with high drainage density are the reasons which accelerate soil erosion over the area which in turn degrades the overall basin condition (Chowdary et al. 2008). Therefore, it is significant to determine which sub watershed comes under which priority zone in order to conserve soil and water resources to diminish the erosional hazards and maintain its health condition in a sustainable way.

In reference to that, drainage morphometric parameters have been taken as criteria for addressing the erosion susceptible zones within the river basin. The morphometric parameters of a basin broadly include linear, relief and areal aspects. The quantification of all these aspects is very important as it provides an idea about the erosional characteristics. Of these some parameters have direct and indirect relation with erodibility (Farhan and Anaba 2016) and are recognised as erosion assessment parameters (Ameri et al. 2018; Aouragh and Essahlaoui 2018). In the present work, such 18 important morphometric parameters have been taken from linear, relief and areal aspects to evaluate the erosion susceptibility in the study area as shown in the table 6.8.

Plate No. 6.1 *Mayurakshi River Bed Condition due to Excessive Sand Mining in 2019*

6.4.1. Methodology

For the prioritization of the sub-watersheds based on the erosion susceptibility, MCDM technique of TOPSIS model has been implemented. In TOPSIS model the alternatives have been prioritized on the basis of distance from the positive ideal solution (PIS) and negative ideal solution (NIS). 18 morphometric parameters (Table 6.8) have been taken as input criteria of this respective multi criteria decision making process. The validation of the model has been done by calculating the rainfall erosivity factor (R factor) of the study area for which TRMM monthly gridded rainfall data of 0.25º * 0.25º which has been obtained from GESDISC website (https://disc.gsfc.nasa.gov/), taken as an input for the calculation rainfall erosivity index (R factor). The flow chart of the methodology is shown in figure 6.11.

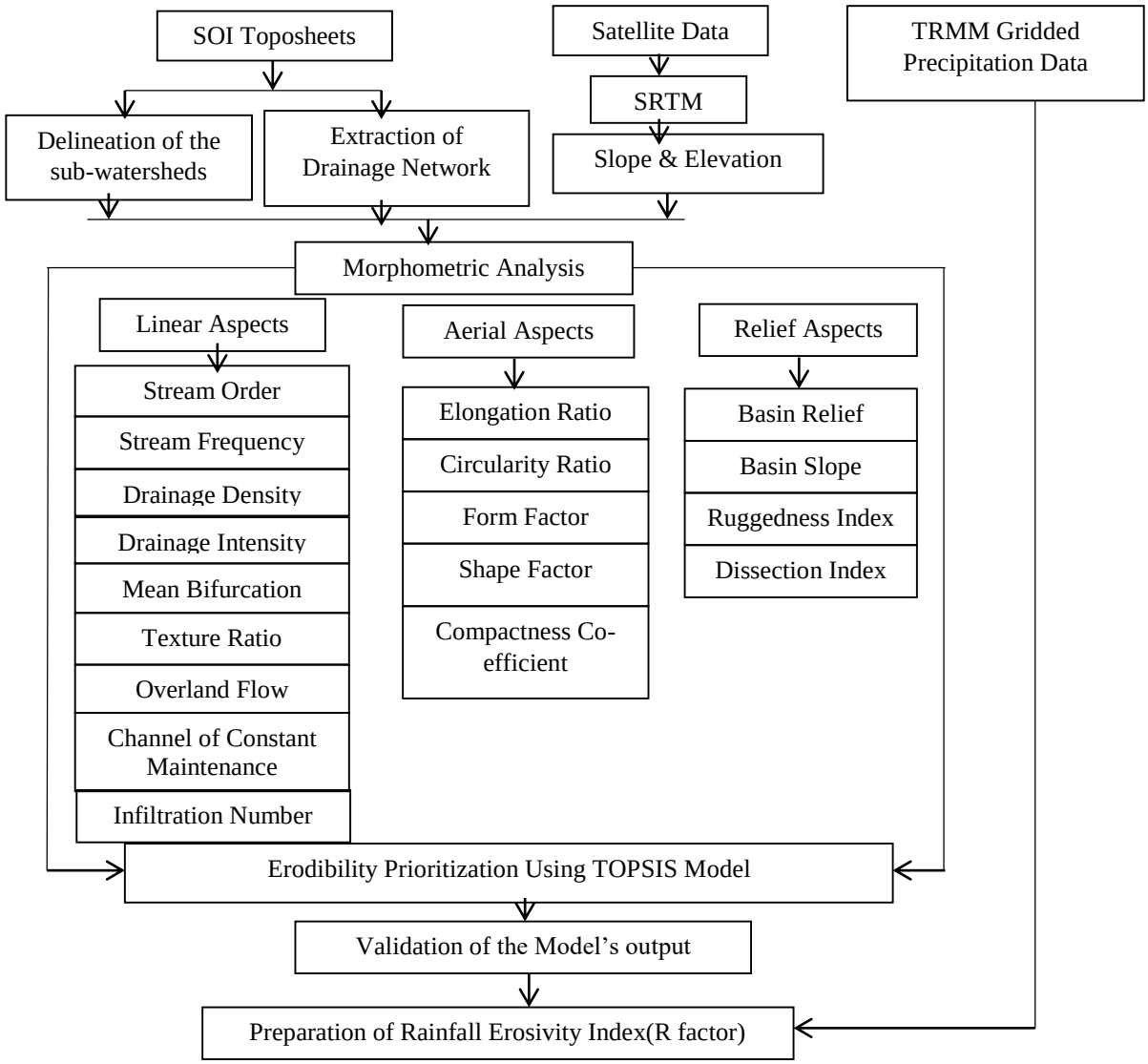

Figure 6.11 *Flow Chart Showing the Methodology for the Assessment of Erosion Susceptible Zone in Mayurakshi River Basin Area*

- **TOPSIS Model**

Technique for Order Preference by Similarity to Ideal Solution (TOPSIS) model has been proposed by Hwang and Yoon (1981) and has been widely used for prioritization of the alternatives. In this model the alternatives has been ranked on the basis of euclidean distance from the positive ideal solution (PIS) and negative ideal solution (NIS). These distances have been termed as closeness co-efficient factor. In the final output of this model, the superior alternative should be placed more close to the positive ideal solution and has the farthest distance from the negative ideal solution. The method has been executed under following steps-

In the first step, Shannon (1948) entropy method has been executed here to calculate the weight of the each parameter using the following equation.

$$Wj = \frac{1-ej}{\sum_{j=i}^{m}(1-ej)} \tag{6.20}$$

Where, Wj is the weight of the j-th criteria.

In the 2nd step, to find out the best possible alternative having lower risk of erosivity, calculation of closeness co-efficient (Cli_+) has been done using the following equation (Aouragh and Essahlaoui 2018).

$$Cli_+ = \frac{S_{j-}}{Si_+ + S_{i-}} \tag{6.21}$$

Where, Cli_+ is the closeness co-efficient and $Si_+, S_i-$is the euclidean distance from positive ideal and negative ideal solution that have been calculated by the following equations.

$$Sj+= \sqrt{\sum_{j=1}^{n}(Vij - Vj^+)^2}\ ; i = 1,2,3,..,m \tag{6.22}$$

$$Sj-= \sqrt{\sum_{j=1}^{n}(Vij - Vj^-)^2}\ ; i = 1,2,3,..,m \tag{6.23}$$

Where, Vj^+ and Vj^- is positive ideal and negative ideal solution.

6.4.2. Calculation of Rainfall Erosivity Index (R factor) to validate the Model's Output

In this study, to validate the output of TOPSIS model rainfall erosivity index (R factor) has been calculated. This index indicates the energy of rainfall which is associated with the rate of erosion. The calculation has been carried out using Modified Fourier Index (MFI) by Arnoldus (1980), Wischmeir and Smith (1978) as shown in following equation.

$$MIF = \sum \frac{Pi^2}{Pt} \quad (6.24)$$

Where, MIF denotes Modified Fourier Index, Pi is monthly precipitation (mm) of the i-th month and Pt indicate annual precipitation (mm). In such juncture, TRMM gridded monthly precipitation data (0.25º * 0.25º) has been downloaded from GESDISC website (https://disc.gsfc.nasa.gov/). The data has been downloaded as a raster file in NETCDF format and then it has been extracted by the point features of 25 river and rain gauges stations in Mayurakshi river basin area. Finally, mean monthly rainfall has been calculated using raster calculator tool of Arc GIS 10.3 to compute the index.

Followed by this, the Rainfall Erosivity Index (R factor) has been determined using the following equation.

$$R = 1.735 * 10^{(1.5 \log MIF - 0.8188)} \quad (6.25)$$

Where, R represent as a Rainfall Erosivity Index (MJ mm ha-1 h-1 y-1) and MIF refers a Modified Fourier Index.

6.4.3. Prioritisation of Sub Watersheds using TOPSIS Model

Based on extensive literature survey and environmental condition of the study area, 18 drainage morphometric parameters (Table 6.8) have been selected as independent variables for prioritisation of erosion susceptible zone in the sub-watersheds of Mayurakshi river basin area using TOPSIS model. The analysis of drainage morphometric attributes clearly indicates the nature of the basin in terms of its slope, topography, runoff and other erosional properties. Here the selected parameters from linear aspects are stream order (u), stream frequency (Fu), drainage density (Dd), drainage intensity (Di), mean bifurcation ratio (Rbm), texture ratio (T), length of overland flow (Lo), constant of channel maintenance (C), infiltration number (If), from areal aspects are Elongation Ratio (Re), Circularity Ratio (Rc), Form Factor (Rf), Shape Factor (Bs) and Compactness Co-efficient (Cc) and from relief aspects are Basin Relief (Bh), Slope (S), Ruggedness Index (Rn) and Dissection Index (DI) has been utilised to execute the methodology. The interrelationship among the parameters helps to explore the erosional characteristics of a drainage basin area. Some of the parameters from linear aspects have positive relation with erodibility like drainage density, stream frequency etc. while few areal parameters are signifying negative relation with erodibility for example elongation ration, circularity ratio etc. Higher value of linear parameters indicates higher the erosional risk whereas higher value of areal parameters indicates lower erosional dominancy (Amiri et al.

2019). Following such relationship among the parameters, a successful implementation of TOPSIS model has been done for prioritising the sub watersheds in terms of erodibility.

In such case, at first a decision matrix (Table 6.9) has been prepared which is considered as a preliminary method in a multi criteria decision making approach. Next to avoid the unitary biasness from the decision matrix a vector normalising process has been implemented here. After that, Shannon (1948) Entropy method has been applied to calculate the weight of the each parameter using Eq. (6.20). This method has been very much applicable when the decision makers have objective views on each criterion. Here the sum of the weights are has been always equal to 1 as there is no such need to give importance scale to the criteria, so that the inconsistency in the judgement of weight preference can be avoided. In the next step weighted normalised decision matrix has been prepared as shown in table 6.10. The determination of positive ideal solutions (Vj^+) and negative ideal solutions (Vj^-)has also been done using Eqs. (6.22) and (6.23). In this study, the parameters having best performance value represents the low risk of erosion has been taken as positive ideal solution (Vj^+) and the parameters denoting worst performance in terms of erosion has been considered as a negative ideal solution (Vj^-). The positive ideal solutions (Vj^+) and negative ideal solutions (Vj^-)of each criterion is shown in table 6.11. Finally, closeness co-efficient (Cli_+) index has been calculated for the individual criterion using the Eq. (6.21) depending on which the priority ranking of the sub-watersheds has been done in an ascending order and the final map has been prepared shown in figure 6.12a. The result of $Sj + Sj -$, and Cli_+ has been tabulated as shown in table 6.12. The final score of TOPSIS model shows that the lowest rank (Rank 1) has been assigned to SW11 having the highest Cli_+ value (0.679) suggesting as an best alternative in terms of lower risk of erosion whereas SW6 has obtained highest rank (Rank 12) having lowest Cli_+ value (0.365), indicating as worst alternative in terms of highest susceptibility towards erosion. Besides such ranking of all sub-watersheds of the study area, a priority wise classification has also been done based on basin erodibility (Fig. 6.12b), which includes very less priority class, less priority class, moderate priority class, high priority class, and very high priority class. The basin falling under the different priority classes has been given in a tabular format (Table 6.13).

Table 6.10 *Calculated Weighted Normalised Decision Matrix for Morphometric Parameters of Mayurakshi River Basin Area*

Basin Parameters	*u	Fu	Dd	Di	Rbm	T	Lo	C	If	Re	Rc	Rf	Bs	Cc	Bh	S	Rn	DI
SW1	0.016	0.017	0.013	0.021	0.009	0.017	0.007	0.017	0.014	0.019	0.019	0.022	0.010	0.016	0.014	0.020	0.012	0.009
SW2	0.016	0.025	0.019	0.021	0.014	0.026	0.019	0.012	0.028	0.017	0.021	0.016	0.013	0.015	0.011	0.023	0.013	0.010
SW3	0.019	0.022	0.017	0.020	0.015	0.022	0.018	0.013	0.023	0.017	0.016	0.017	0.012	0.015	0.011	0.017	0.013	0.010
SW4	0.013	0.012	0.013	0.015	0.013	0.005	0.013	0.017	0.010	0.016	0.016	0.014	0.015	0.023	0.011	0.016	0.010	0.006
SW5	0.016	0.016	0.016	0.016	0.016	0.014	0.016	0.014	0.015	0.018	0.021	0.018	0.012	0.017	0.013	0.018	0.013	0.007
SW6	0.019	0.021	0.019	0.018	0.016	0.033	0.019	0.012	0.024	0.018	0.017	0.018	0.012	0.012	0.026	0.019	0.033	0.010
SW7	0.016	0.015	0.015	0.015	0.016	0.009	0.015	0.015	0.014	0.021	0.019	0.024	0.009	0.020	0.015	0.016	0.015	0.007
SW8	0.016	0.017	0.016	0.017	0.013	0.010	0.016	0.014	0.017	0.016	0.013	0.014	0.014	0.020	0.021	0.016	0.022	0.010
SW9	0.023	0.005	0.008	0.012	0.023	0.006	0.007	0.034	0.002	0.011	0.005	0.007	0.030	0.015	0.027	0.017	0.012	0.009
SW10	0.013	0.016	0.015	0.017	0.013	0.006	0.015	0.015	0.015	0.018	0.019	0.018	0.012	0.024	0.019	0.015	0.019	0.007
SW11	0.013	0.014	0.016	0.015	0.012	0.009	0.016	0.014	0.013	0.015	0.016	0.012	0.018	0.019	0.003	0.003	0.003	0.005
SW12	0.016	0.002	0.027	0.001	0.029	0.004	0.027	0.008	0.004	0.013	0.012	0.009	0.023	0.012	0.008	0.006	0.013	0.009

* Stream Order (u), Stream Frequency (Fu), Drainage Density (Dd), Drainage Intensity (Di), Mean Bifurcation Ratio (Rbm), Texture Ratio (T), Length of Overland Flow (Lo), Constant of Channel maintenance (C), Infiltration Number (If), Elongation Ratio (Re), Circularity Ratio (Rc), Form Factor (Rf), Shape Factor (Bs), Compactness Co-efficient (Cc), Basin Relief (Bh), Slope (S), Ruggedness Index (Rn), Dissection Index (DI).

It is evident from the result (Fig. 6.12b) that the upper part of Mayurakshi river basin has been highly affected by erosional hazards as SW6 namely River Siddheswari comes under the high priority class of erosion (Table 6.13). Improper land use practices, rocky terrain condition are mainly responsible for such kind of soil degradation within the upper part of the basin. Not only this, the predominance of 1st order streams coupled with high drainage density, slope, sparse vegetation cover associated with coarse laterite fragile soil makes that sub-watershed (SW6) more prone to erosion (Pal and Debanshi 2018). Besides, the temperature variation induces the weathering processes causing extensive soil erosion. Thus priority based conservation measures should be carried out in each sub watersheds which will help the stakeholders and policy makers to undertake sustainable conservation technique to protect the river basin system by reducing the erosion related problems.

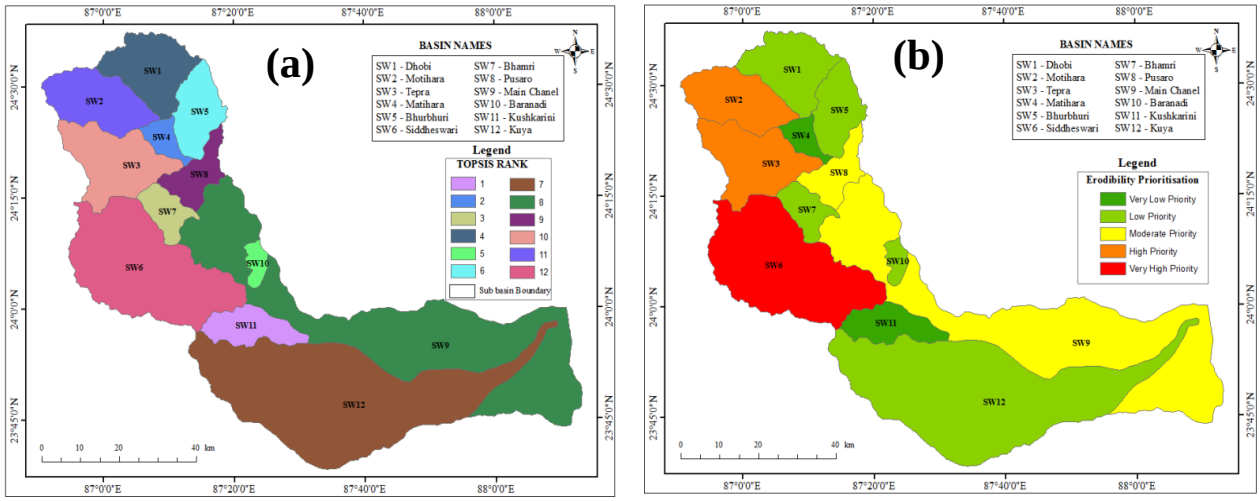

Figure 6.12 *TOPSIS Model Output (a) Ranking of Sub-watersheds (b) Prioritisation of Sub-watersheds based on Erosion Susceptibility of Mayurakshi River Basin Area*

6.4.4. Validation of Model's Output

TOPSIS is one of the finest multi criteria decision making method through which each criteria has been ranked based on their euclidean distance in respect of it ideal best and worst situation. In this study, the output suggests five levels of priority classes related to erosion susceptibility of all the sub-watersheds in Mayurakshi river basin. To validate the same, rainfall erosivity index (R factor) has been calculated using GIS techniques. The R factor defines the kinetic energy produced by raindrops in a per unit area, which enhance the entrainment of soil and amount of runoff. Direct impact of raindrops has been more effective on bare soil surface and produces more soil loss over the region (Prasannakumar et al. 2012). However this may vary from one region to other depending on the characteristics of soil properties, texture, particle

size distribution etc. Other than that, the intensity of rainfall may also affect the detachment of soil from the topsoil area. Various past literatures reveals that, minimum 20 to 25 year rainfall data should be considered to assess the pattern of rainfall and soil erosivity factor (Yjjou et al. 2014) where the output mainly describes the relative scenario of the erodibility over the region. In this study, high precipitation variability has been observed from 1998 to 2018 over the study area (Table 6.14). To visualise the current scenario of rainfall-runoff erosivity, mean monthly precipitation data of 2018 has been considered for the calculation of R factor.

The output of this analysis reveals that the SW6 has been fall under the area of very high rainfall erosivity zone whereas the other sub watersheds have been categorised under the low rainfall erosivity zone (Fig. 6.13). The result has clearly validates the output of TOPSIS method where the same watershed (SW6) has been identified under very high erosion prone area. Hence it can be concluded that the extremities of climatic events like variation of precipitation and temperature may alter the nature of basin erosive characteristics significantly. Such type of correlation technique helps in watershed erodibility prioritisation through morphometric analysis and also it plays an effective role in implementing micro watershed planning and management measures at a ground level in a very cost effective and socially acceptable manner.

Table 6.11 *Extraction of Ideal Positive Solution (Vj+) and Ideal Negative Solution (Vj-)*

	u	Rbm	Bh	Dd	Rn	DI	S	Lo	Fu	T	Rf	Rc	Re	Bs	Cc	C	Di	If
VJ+	0.013	0.009	0.003	0.007	0.003	0.005	0.003	0.007	0.002	0.004	0.024	0.021	0.021	0.030	0.024	0.008	0.021	0.002
VJ-	0.023	0.029	0.027	0.027	0.033	0.010	0.023	0.027	0.025	0.033	0.007	0.004	0.011	0.009	0.012	0.034	0.001	0.028

Table 6.12 *Prioritisation of Sub-watersheds of Mayurakshi River Basin Area*

	SW1	SW2	SW3	SW4	SW5	SW6	SW7	SW8	SW9	SW10	SW11	SW12
Sj +	0.041	0.055	0.048	0.032	0.040	0.066	0.039	0.045	0.051	0.040	0.031	0.048
Sj −	0.057	0.048	0.048	0.060	0.055	0.038	0.056	0.049	0.061	0.055	0.065	0.063
Cli_+	0.584	0.467	0.497	0.655	0.570	0.365	0.590	0.520	0.543	0.579	0.679	0.565
Priority Ranking	4	11	10	2	6	12	3	9	8	5	1	7

Table 6.13 *Result of Prioritisation Carried out for Each Sub-watersheds of Mayurakshi River Basin Area*

Sl. No	**Priority Classes**	**Sub-watersheds**	**Name of the sub-watersheds**
1	Very Low	SW 4, SW 11	Matihara, Kushkarini
2	Low	SW 1, SW 5, SW7, SW 10, SW 12	Dhobi, Bhurbhuri, Bhamri, Bara Nadi, Kuya
3	Moderate	SW 8, SW 9	Pusaro, Main Channel
4	High	SW 2, SW 3	Motihara, Tepra
5	Very High	SW 6	Siddheswari

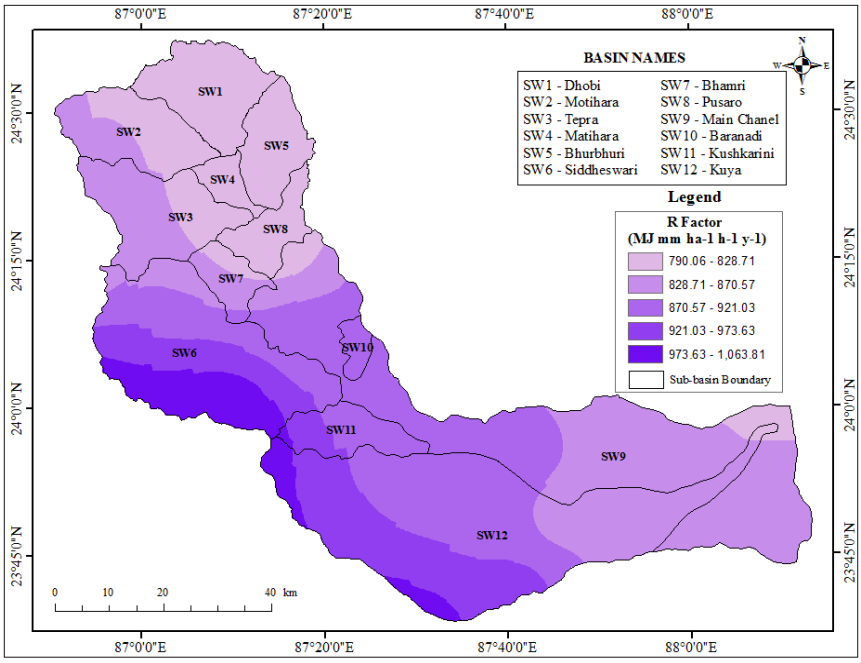

Figure 6.13 *Rainfall Erosivity Index of Mayurakshi River Basin of 2018*

Table 6.14 *Variation in Mean Annual Rainfall Data in Mayurakshi River Basin Area*

Year	Mean Rainfall (mm)
1998	150.3895
1999	187.5294
2000	152.0502
2001	121.5765
2002	118.6057
2003	106.8847
2004	120.4113
2005	110.6999
2006	117.0064
2007	152.9821
2008	120.4865
2009	108.0819
2010	90.99676
2011	139.0523
2012	100.6012
2013	122.7641
2014	96.78836
2015	113.5384
2016	109.286
2017	137.5944
2018	95.05
Mean	122.4917
Standard Deviation	23.55924
Coefficient of Variation (%)	19.23334

6.4.5. Conclusions

The present study emphasises on prioritisation of sub watersheds based on drainage morphometric parameters. The usefulness of all these parameters has been represented here as an effective erosion assessment factors, which has been validated by computing rainfall erosivity factor. 18 morphometric parameters have been calculated for each of the sub watersheds of Mayurakshi river basin, which reflects their individual response towards addressing erosional characteristics of the respective sub watersheds. Identification of erosion susceptible zones has been made based on the calculated morphometric parameters. MCDM method of TOPSIS has been applied to rank the sub watersheds according to their vulnerability towards soil erosion. For proper and impartial judgement in TOPSIS model, Shannon entropy method has been used to calculate the weight of the individual parameters. Finally the result of TOPSIS model shows five levels of priority classes like very high, high, moderate, low and very low priority class, where the SW6 fall under high priority classes in term its erodibility and SW11 has been ranked under low risk of erosion class. This output of the TOPSIS model has also been validated by mean monthly precipitation data of the year 2018 through calculating the R factor. The result signifies that the kinetic energy of raindrops higher over the SW6, making the region more susceptible towards soil loss from that zone.

Overall this study concludes that the study of basin properties is an important approach as it can effect on the land management over the area. Degradation and aggradation of land resources are dependent on various independent variables which may affect our societal livelihood system. Due to improper land use practices or the loss of fertile land cover, crop production may affect significantly. In Mayurakshi river basin area, the upper part of the basin has majorly dominated with mono crop cultivation because of the presence of more arable land and removal of topsoil cover. So, to maintain our physical environment and a sustainable societal livelihood such kind of identification and prioritisation is necessary. Various statistical models and application of remote sensing GIS technologies can help in the decision making process for the formulation of effective soil conservation plan to enhance the land capability and agricultural productivity at a micro scale level in a long run. In future research, further issues can be addressed for the identification of vulnerable areas using detailed study on soil texture, permeability, its cohesiveness and temporal changes in land use land cover pattern with modern MCDM techniques to increase its sustainability than degradation.

6.5. Application of Hydraulic and Hydrological Model to Study the Hydro-Geomorphological Behaviour of the Channel

A series of cross profiles reveals the fundamental hydro-geomorphological behaviour of a channel. The cross-section of a channel is function of its shape, size, flow, sediments that are moved through the section and deposited around the river bank (Leopold et al. 1964). The cross-section of a natural channel is characterised by irregularly outlined width, mean flow depth and a volume of discharge which are assumed to get balanced with the underlying topography to form a stable reach irrespective of the scour and fill of river bed (Mistry 1972; Petts 1979). The study of channel geometry and the hydro-geomorphological behaviour may be monitored as a key concern for the scientific management of a river health (Richards 1982; Williams and Wolman 1984). In river hydraulics, the geometry of a cross section changes more frequently than a longitudinal profile. Any alteration in water discharge or sediment flow induces a noticeable change in channel geometry (Swamee et al. 2000; Singh 2003; Basu et al. 2005; Lord et al. 2009). Such changes are mainly driven by the human intervention on river bed. Construction of various civil structures like dam, barrages, rail or road bridges, creation of temporary nala's for irrigation purposes and excessive sand extraction from the active channel are the major catalyst behind the degradation of channel geometric properties resulting channel in-efficiency to carry enough water for a long run (Mc Manamay and Bevelhimer 2013). Channel efficiency is largely dependent on the channel adjustment. In recent time, controlled or human regulated flow pattern is very much observed across the world. Most of rivers are being impounded with dam and barrages, which are not able met the sustainable development strategies (Pal 2016). Unfortunately, the main flow of river is now maintained within a narrow active channel area. River loses its natural flow due to the construction of water holding structures and also disturbed the movement of sediment, nutrient to the downstream on which the fluvial community depends (Ghosh and Guchhait 2016). In Ganga Bramhaputra Delta, the alteration in channel geometry due to anthropogenic intervention is well documented. Pal and Debanshi (2018) discussed the changes in channel morphology due to construction of Massanjore Dam and Tilpara Barrages in the Mayurakshi River. Not only the controlled flow, scouring activity near the dam area generate a huge aggradation of sediment which may chock the downstream channel width significantly (Mondal et al. 2018). Mitra and Singh (2018) noted the gradual shifting in flood duration during the post dam period of Damodar River. Moreover, the effect of post Farakka Barrage Project on the Bhagirathi Hugli River is worth mentioning.

All the studies stated above indicates the channel hydro-geomorphological changes due to various constructional activities on the river bed. Estimation of river discharge is a major component of river hydraulics mainly when the understanding of its spatio-temporal dynamism is unacquainted to ourselves. The measurement of available surface water resources and the temporal heterogeneity of flow magnitude, frequency both during peak and lean flow period is crucial for the assessment of flood or drought like situation under changed climate scenarios (Xu et al. 2018). Rivers with such civil structures like dam or barrages, have their own gauge stations to monitor and document the daily records. But in West Bengal, most of the rivers are ungauged due to some environmental or financial limitations or rivers having monitoring station does not maintain the data properly. However, the direct measurement of river discharge using traditional gauging system or to via installing instrument are some points not suitable in remote or inaccessible areas along the river reach and thereby various indirect methodologies are becoming useful and feasible. Various indirect approaches such as the development of rating curves, stage discharge estimations, graphical or artificial intelligence, and other statistical applications have already been used in several studies to estimate the discharge quantity in connection to channel geometry parameters. In order to represent discharge as a function of hydraulic radius and longitudinal water slope rather than just water level, Leonard et al. (2000) suggested a modified variant of the Manning equation. Tabata and Hickin (2003) used the 'inter-channel hydraulic geometry' model on Columbia River (Canada) and observed the changes in channel discharge capacity due to alteration in channel flow pattern. To assess the potential for reliable lean season flows in the San and Barah watersheds of Orissa, Pandey and Ramasastri (2003) applied various flow duration curve methods using daily/weekly/monthly discharge data. Using the support vector approach, developed by Sivapragasam and Muttil (2005) and based on the idea of linear regression on a higher dimensional feature space, the rating curves have been expanded. According to the findings, the support vector method is more precise than the ANN method for extrapolating rating curves. Using the idea of isovel contours, Rahimpour and Maghrebi (2006) evaluated the discharge in rectangular channels with composite roughness. While Maghrebi and Ball (2006) created a novel method for estimating the discharge based on a single point of measurement utilizing normalized isovel contours. The implications of rating curve uncertainty on hydraulic model calibration have been researched by Domeneghetti et al. (2012). Singh et al. (2014) calculated the discharge in natural rivers using Tsallis entropy. This approach is based on mean discharge and two generic conditional probabilities. Hasanpour Kashani et al. (2015) investigated the use of several neural network techniques in the Turkish Kizilirmak River. The

outcomes showed that the ANFIS model outperformed all other models in terms of efficiency. In order to predict the rating curve, Londhe and Panse-Aglave (2015) used three distinct data-driven techniques: nonlinear regression (NLR), artificial neural networks (ANN), and model tree (MT) methods. Compared to the other models, the MT model is more accurate. Above all, an accurate measurement of river hydraulics (width, depth, slope etc.) from field survey and compare the result with various multi-variate open channel flow equation gives the better output in discharge estimation (Sichangi et al., 2016; Hoque et al. (2022).

The present study examines the changes in the hydro-geomorphological properties of the Mayurakshi River channel. Currently, Massanjore Dam and Tilpara Barrage are the only river gauges measuring the inflow and discharge of water from the dam each day. This study attempts to fill the gap of insufficient stream flow databases for sparsely gauged river basins (e.g., Mayurakshi River), by choosing 14 cross-sectional sites to illustrate channel geometry and the nature of lean period flow velocity and discharge scenarios. Hence, the study aims at estimating lean period discharge using two classical hydraulic and hydrological algorithms and validating the calculated values against field observed discharge data through different statistical measures like MAPE, RMSE and NRMSE analysis (Maghrebi & Ahmadi 2017). Nevertheless, this study will ensure the benefit of field work besides the usage of such established numerical methodologies for estimating the hydraulic properties of a channel. The output of such research work will not only bring interests to the local stakeholders, but also make a significant contribution to the international science.

6.5.1. Study Area

Mayurakshi River is an important western tributary of Bhagirathi River which drains from the region of Jharkhand to the Bengal plain area. It covers an area about 5325 sq. km having a longitudinal extent of 86°84'–88°22' E to latitudinal extend of 23°64'–24°62' N. This 288km long river makes some important tributaries on the both side of its flowing route like Dhobi, Motihara, Tepra, Matihara, Bhurbhuri, Siddheswari, Bhamri, Pusaro, Main channel, Bara Nadi, Kushkarini and Kuya river. Since this river lies within a zone of tropical environment (Roy 2013), the major source of flowing water is the down pouring huge monsoonal rainfall from the upper part of the plateau region. The Maximum amount of rain occurs during the month of June to October having a mean annual rainfall of 1400 mm (Chaudhury 1966). On the contrary, during dry season, almost no flow condition prevails in every stretch of the river making it non-perennial in nature. Despite of this, installation of major anthropogenic civil structures like

dam, barrages making the natural flow of river more controlled (Islam and Sarkar 2021). Adding to this, some other unscientific activities like excessive sand mining, creation of temporary recharge pools /nullahs (Patra 2008) on the river bed, are also exaggerate the problems of channel deformation by altering the channel geometry (Nag et al. 2022).

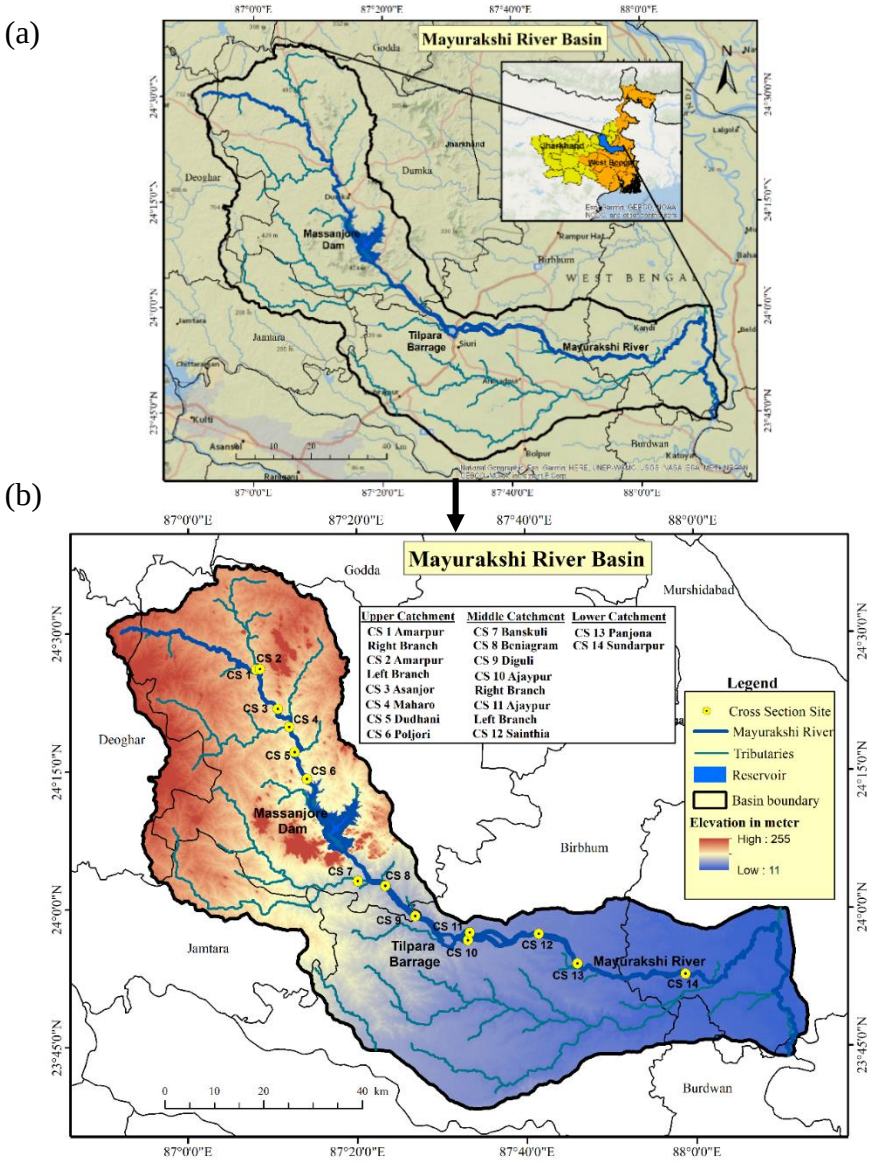

Figure 6.14 *Location of the Study Area (a) Study Area (b) Location of the Cross-section Sites Over the Mayurakshi River Basin*

Therefore, it is essential to examine the channel hydro-geomorphological properties and quantification of lean period river discharge of water to preserve the holistic benefits of Massanjore dam, Tilpara barrage and its adjoining canal system which is enjoyed by the mass population living in the floodplain area of the Mayurakshi River without hampering its future

fluvial environment. To fulfil the objective of this research, 14 different cross profiles are selected from the upstream to downstream of the river Mayurakshi as shown in figure 6.15.

6.5.2. Materials and Methods

The present research work is totally based on both primary and secondary data collection procedure. To study the channel cross sectional properties, authors have conducted an intensive field survey comprised of 14 different cross-sectional sites from the upstream of the river near Amarpur, Dumka, Jharkhand to the downstream of Sundarpur, Murshidabad during the month of December, 2021 (Fig. 6.14). The selection of each survey sites has been totally based on its locational importance in terms of sites near the upstream and downstream portions of dam and barrages, confluence point of important tributaries, channel closer to densely populated areas etc. The measurement of flow velocity in each section has been done using Electromagnetic Current Meter instrument (Hach FH950 Portable Flow Meter, Range = 0 - +20 ft/s). It is regarded as most convenient instrument in hydrometry which measures at a point flow of water in a particular depth following the principle of Faraday's law of electromagnetic induction. (Subramanya 2008). According to this law, a conductor (water) that passes through the magnetic field produces a voltage that is linearly proportional to the flow velocity. As with conventional current meter, the sensor is guided through the measurement cross-sections using the wading rod. To determine the velocity of each section, almost 50 (channel width 585 m) to 25 (channel width 88 m) number of verticals have been considered, of which the distance between each vertical has not been larger than the $1/20^{th}$ of total width of stream (River & Creek 2023). In this case, most of the study site represents less than 1m of the channel depth of water. In light of this, the mean velocity for each sampling site along the Mayurakshi River was determined by placing the instrument at a height of 0.9D (average of typical range 0.85D-0.95D) (Perzyna 2016) from the river bed for 1 minute, during which 20 separate flow velocity values were obtained at 2-second intervals (Saha et al. 2020). The weighted mean of these 20 values has been calculated to determine the average maximum velocity of the particular section. Furthermore, to determine the depth where average velocity of the flow channel occurs, the Vanoni's formula (1941) has been executed which is mentioned as below.

$$v(y) = V + \frac{1}{K}\sqrt{gdS_o\left(1 + 2.3log\frac{y}{d}\right)} \qquad (6.26)$$

Where, $v(y)$ is the velocity of water at the depth y from the free surface, V is the depth-averaged velocity, K is the von Karman constant (~0.4), d is the hydraulic mean depth of channel, S_o is the slope of the channel (dimensionless) and y is the distance from the bottom of the channel.

Finally, after applying a 1/7th power law function as mention in equation (), the average velocity had been determined subsequently (Knight et al. 2010).

$$v(y) = V_{max}\left(\frac{y}{d}\right)^{1/7} \tag{6.27}$$

Authors have also conducted a Differential Global Positioning System (DGPS) survey to measure the cross-sectional bed profile across the 14 selected sections of the river Mayurakshi. During this survey Post Processed Kinematic Survey (PPK) method has been applied by which the measured elevation data has been calibrated with reference to its closest permanent/local benchmark point using Trimble Business Centre software in post survey period (Shouny et al. 2017). In this regard, three permanent benchmarks such as 144.96 m at Dumka Railway station, 67.44 m at Suri Railway station and 48.365 m at Sainthia Railway station have been used. Using that calibrated elevation data, each cross profiles have been constructed to depict the nature of channel geometry. The bank full height of each survey sites has been identified by visualising the demarcation of floodplain areas, water mark on the riparian vegetation zone and also from the local dwellers. Slope is another important parameter for the construction of cross profiles. It is the ratio of vertical gradient to its horizontal distance (Sen 1993). Here, to calculate the longitudinal slope, vertical gradient and equivalent horizontal distance of a particular channel has been measured using Google Earth Pro software. Other important channel features like channel depth, width, thalweg point have been measured with the help of measuring staff and tape.

In case of secondary data collection, rainfall plays a major source of runoff generation over a basin area which contributes maximum amount of river flow and discharge accordingly. Here, maximum rainfall intensity (cm/h) has been taken into consideration for the estimation of discharge using Kinematic Wave Parameter (KWP) method, for which 31 days (December, 2021) rainfall data has been collected from the official website of Indian Meteorological Department (IMD) (www.imdpune.gov.in) having a resolution of 0.25*0.25 degree (about 27.75 km).

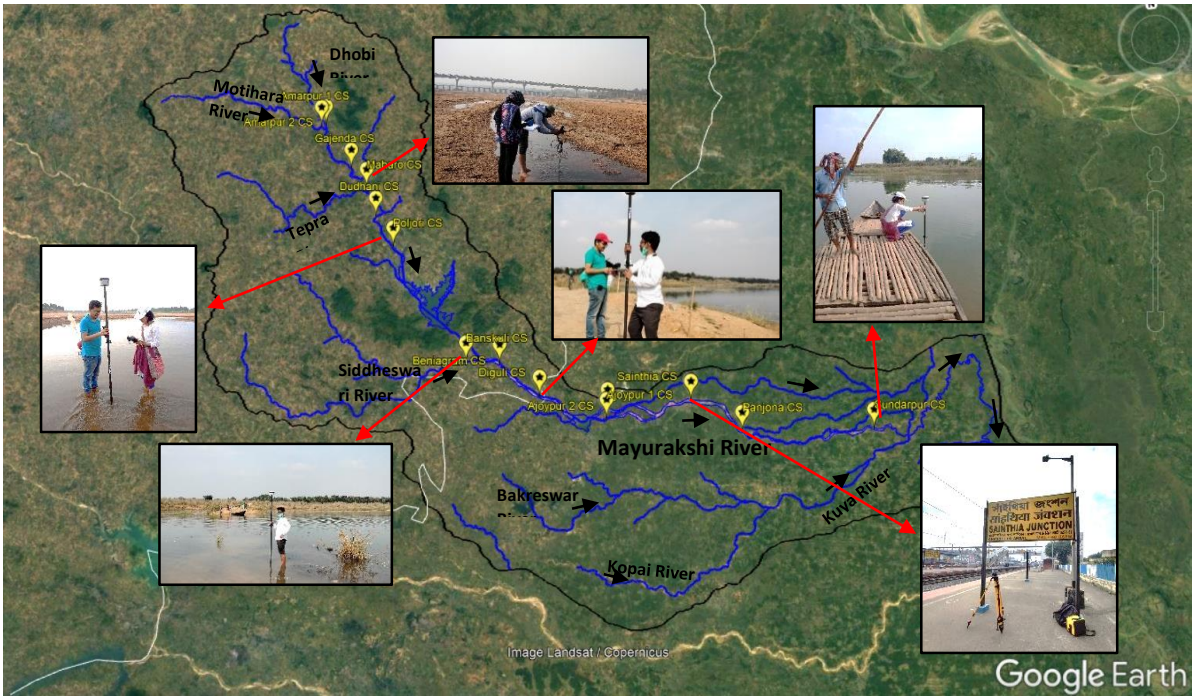

Figure 6.15 *Google Earth View of the Cross-section Sites with Some Field Photographs over the Mayurakshi River*

- **Application of Manning's equation for Discharge Estimation**

In this study, a combination of hydraulic and hydrological method of discharge estimation has been executed. The main aim behind this approach is to determine the scientifically accepted and cost-effective way for the calculation of river discharge during post field survey period.

Manning's equation of flow is regarded as one of the most versatile and can widely be used in the analysis of open channel flow where channel bed roughness has been incorporated for the estimation of flow velocity (Summerfield 1991; Leonard et al. 2000; Darabad et al. 2023). This equation includes channel area, hydraulic radius, manning's roughness coefficient and longitudinal bed slope to determine the flow rate of the channel. The manning's equation defines the mean flow velocity (v) using the following equation (Manning 1891).

$$v = \frac{k\left(R_h{}^{2}/_{3} * S^{1}/_{2}\right)}{n} \tag{6.28}$$

Where, k is the unit conversion factor (k=1 in SI unit and 1.486 in English unit).

Depending on the shape of the cross-sectional area, the hydraulic radius (R_h) and wetted perimeter (P) varies significantly. In this study, the cross profiles of each channel in the Mayurakshi River exhibit uneven channel bed profiles, and the entire channel flow area may be split into a number of small trapezoidal segments, as can be seen in figure 6.16a and 6.16b.

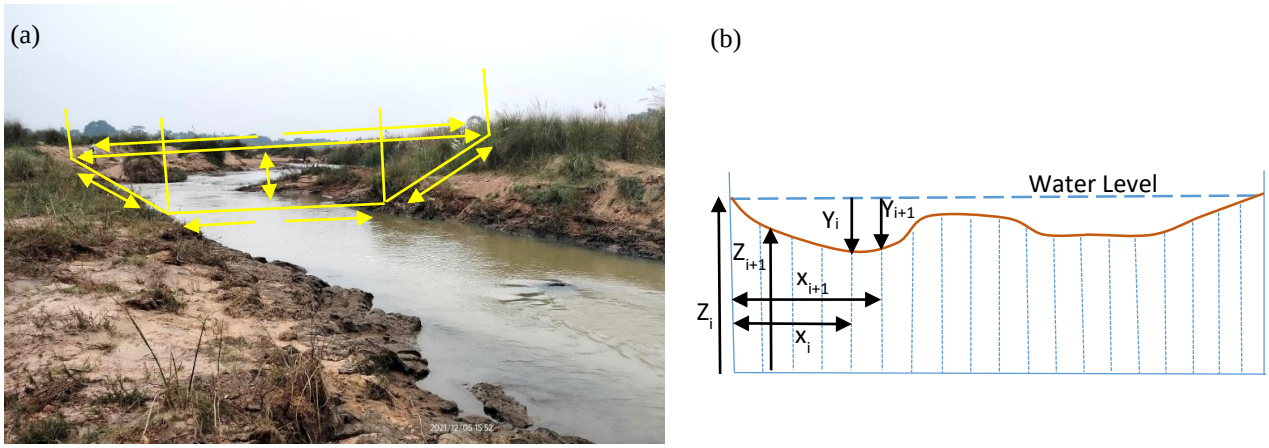

Figure 6.16 *(a) Trapezoidal Cross-section of Mayurakshi River (b) A Schematic Representation of an Open Cross-section Channel*

Hydraulic Radius (R_h) is an important parameter for Manning's equation (Roy 2013). For an open channel cross-section, hydraulic radius (R_h) is often expressed as-

$$R_h = {}^{A}/_{P} \tag{6.29}$$

Where A represents cross-sectional area of flow. To calculate the area of flow, the entire river cross-section has been divided into n numbers of small trapezoids (Fig. 3b) and using the following trapezoidal rule (equation) the cross-section area of a channel has been determined.

$$A = \frac{\sum_{i=1}^{n}(y_i+y_{i+1})(x_{i+1}-x_i)}{2} \tag{6.30}$$

Where, y_i represents water depth at i^{ih} point and xi represents distance of that point from the river bank.

And P is the wetted perimeter of a channel cross-section which can be expressed as-

$$P = \sum_{i=1}^{n}\sqrt{(z_{i+1}-z_i)^2+(x_{i+1}-x_i)^2} \tag{6.31}$$

Where, z_i represents the reduced level of i^{th} point.

Manning's Roughness Co-efficient (n) is another major input for Manning's flow calculation. It is a representation of channel friction or roughness applied to the flow by the bed surface (Manning 1891; Bloom 2009). The n value is often selected from the table as given by Chow (1964). In other way, numerous researchers have attempted to assign Manning's roughness co-efficient in a natural channel by comparing it cross-sectional area, values of sand particles in river bed profile etc (Chow 1959; Yen 2002). In this work, Manning's roughness co-efficient

(n) has been obtained by comparing the Manning and Darcy– Weisbach equations (Chin 2020) which has been mentioned below.

$$\frac{R_h{}^{1}/_{6}}{n} = \sqrt{\frac{8g}{f}} \tag{6.32}$$

Where, R_h is the hydraulic radius of the channel, g is the acceleration due to gravity (9.8 m/s^2) and f is the friction factor. Often, f is calculated from the formulas as mentioned below.

$$\frac{1}{\sqrt{f}} = -2\log_{10}\left(\frac{ks}{12R_h}\right), \text{ for rough flow condition} \tag{6.33}$$

The friction factor of a channel is affected by the relative roughness of flow (smooth, transitional or rough). In our case of study, mostly rough flow conditions ($\frac{u_* k_s}{\nu} > 70$) prevail in most of the cross sections of the channel, that has been determined based on the shear velocity (u), equivalent sand roughness (ks) and kinematic viscosity (ν) of water.

The average particle size distribution of the channel bed material determines the value of ks in this situation. It is responsible for the resistance that affects the channel's flow. The equivalent sand roughness has been determined by using the following formula (Raul Lopez et al. 2008).

$$ks = 6.1D_{50} \tag{6.34}$$

where, D_{50} is the mean particle size diameter (mm) of river bed material that has been computed from the sieve analysis and grain size distribution of the materials collected from the river bed of the study area (Table 6.15).

Table 6.15 *Computed Data Showing the Analysis of Mean Particle Size Diameter (D50), Equivalent Sand Roughness (Ks) And Manning's Roughness Co-efficient (N) of Each Cross-section Sites of Mayurakshi River*

Site Name	Mean particle size diameter in mm (D_{50})	Equivalent sand roughness (ks)	$\frac{u_* k_s}{\nu}$	Flow type	Friction factor (f)	Manning's Roughness Co-efficient (n)
Amarpur right branch	3.2	0.01952	No Water			
Amarpur left branch	3.2	0.01952				
Asanjor	3	0.01830	788.47	Rough	0.078	0.0212
Maharo	2.2	0.01342	761.90	Rough	0.063	0.0196
Dudhani	1.7	0.01037	289.74	Rough	0.040	0.0182
Poljori	1.8	0.01098	317.72	Rough	0.040	0.0184
Banskuli	2.1	0.01281	490.36	Rough	0.073	0.0198
Beniagram	1.1	0.00671	163.34	Rough	0.033	0.0169
Diguli	0.95	0.00580	199.74	Rough	0.036	0.0165
Ajaypur right branch	0.55	0.00336	53.28	Rough	0.028	0.0152
Ajaypur left branch	0.42	0.00256	38.54	Rough	0.027	0.0146
Sainthia	0.5	0.00305	63.70	Rough	0.023	0.0152
Panjona	0.35	0.00213	62.81	Rough	0.024	0.0143
Sundarpur	0.54	0.00329	143.87	Rough	0.016	0.0164

- **Application of Kinematic Wave Parameter (KWP) for Discharge Estimation**

Lighthill and Whitham (1955) developed the kinematic wave theory based on the investigation of flood routing in long rivers. It is a simplified approach that measures the channel form, dimension and flow conditions of water in open channels, such as rivers, streams etc. In a mild-slope channels like Mayurakshi River, this method is especially helpful for immediately predicting flow parameters and studying flow behaviour (Adhikari et al. 2023). It is crucial to remember that the kinematic wave equation is a concise model that functions effectively in some flow scenarios, especially shallow and gently variable flows. A set of partial differential equations, such as the Saint-Venant equations (SVE) or the shallow water equations (SWE), can be used to simulate the gradually varying flow (GVF). The continuity equation and the momentum equation, which combine to form the Saint Venant equations, are written as follows.

$$\frac{\partial Q}{\partial x} + \frac{\partial A}{\partial t} = 0 \tag{6.35}$$

$$S_f = s_0 - \frac{\partial y}{\partial x} - \frac{v}{g}\frac{\partial v}{\partial x} - \frac{1}{g}\frac{\partial v}{\partial t} \tag{6.36}$$

Here, equations (6.35) and (6.36) are based on the principles of conservation of mass and momentum, respectively where the term $\frac{\partial y}{\partial x}$ and $\frac{v}{g}\frac{\partial v}{\partial x}$ refers to the changes in potential and kinetic momentum whereas the term $\frac{1}{g}\frac{\partial v}{\partial t}$ denotes the regional acceleration of the flowing

stream. Consecutively, from the output of Eq.6.35 and Eq. 6.36, Henderson's (1966) developed an equation for the looped rating curve as mentioned below:

$$Q = CA\sqrt{R\left(s_0 - \frac{\partial y}{\partial x} - \frac{v}{g}\frac{\partial v}{\partial x} - \frac{1}{g}\frac{\partial v}{\partial t}\right)} \tag{6.37}$$

Hysteresis in the rating curve can be described by the inclusion of inertial and pressure terms, and the formulation of the Kinematic Wave equation results from the exclusion of inertial terms in Eq. (11) (Adhikari et al. 2023). Kinematic Wave equation is an important rainfall dependent model where the amount of rainfall is being transformed into overland sheet flow and can be modelled as channel discharge when it reaches to its outlet (Mohammadi et al. 2012). On a trapezoidal channel, the generation of surface runoff is dependent on the slope of the flow path (S_Ω) and the amount of rainfall produce over an area. Therefore, an estimation must be made for the calculation of rainfall intensity (i) (cm/h) over an area. Finally, Rodriguez-Iturbe et al. (1979) had demonstrated kinematic wave equation for the estimation of flow velocity (v_Ω) using following equation

$$v_\Omega = 0.665\alpha_\Omega^{0.6}(i * A)^{0.4} \quad , \qquad \alpha_\Omega = \frac{S_\Omega^{0.5}}{nB^{2/3}} \tag{6.38}$$

Where, A denoted as drainage basin area in sq. km, B is the mean flow width of the cross profile, i is the rainfall intensity (cm/h), n is the manning's roughness co-efficient and S_Ω is the % of slope of the main river at the drainage basin outlet.

- **Evaluation of Model Performance**

There are a number of statistical analyses that are frequently used to determine the level of accuracy or error function in any kind of dataset. Here, to identify the performance of the proposed hydrological and hydraulic models, the Mean Absolute Percentage Error (MAPE), Root Mean Square Error (RMSE) and the Normalized Root Mean Square Error (NRMSE) were evaluated based on the estimated discharge ($\hat{y}i$) and the observed data (yi) are given as follows (Maghrebi and Ahmadi 2017).

$$MAPE = \frac{100}{n}\sum_{i=1}^{n}\left|\frac{y_i - \hat{y}_i}{y_i}\right| \tag{6.39}$$

$$RMSE = \sqrt{\sum_{i=1}^{n}\frac{(y_i - \hat{y}_i)^2}{n}} \tag{6.40}$$

$$NRMSE = \frac{\sqrt{\frac{1}{n}\sum_{i=1}^{n}(y_i - \hat{y}_i)^2}}{y_{max} - y_{min}} \quad (6.41)$$

6.5.3. Results

- **Channel Hydro-geomorphological Properties**

In this study, authors have selected 14 different locations from upstream to downstream of the Mayurakshi River. Elevation data has been collected using Differential Global Positioning System (DGPS). The purpose of this study is to construct channel cross profiles to depict the geometrical aspects of the river. As noted by Knighton (1998), the general shape of any cross-section is a function of its depth (d), width (w), area (A), velocity (v) discharge (Q), wetted perimeter (P), hydraulic radius (R_h), and its width depth ratio (w:d). Figure 6.18(a)-(n) shows the lean period channel configuration of the studied 14 cross profiles of different sites of the Mayurakshi River.

Authors have also tried to analyse the necessary hydraulic relationships between important variables that are discussed as follows.

- **Width-Depth Variation**

Table 6.16 shows important channel geometrical characters of the Mayurakshi River Basin. Width and depth of a channel are the most important structural variables which shows an interrelated nature of existence in every cross section of a channel (Mondal et al. 2018). Since width does not change with time, it is an independent variable. However, the depth of a channel varies based on its flow. In general, depth and width of a channel both are increases in downward but in case of Mayurakshi River, no definite trend has been observed among them. There has been found to have an unusually extended nature of river width (585 m) around Beniagram, which lies upstream of the Mayurakshi River. The main causes of such fluctuation in channel width are a significant increase in the volume of water released from the Massanjore Dam. Another fact is that a sizable amount of water from the Siddheswari River, a tributary of the Mayurakshi, is discharged here as well and widens the channel width significantly (Plate no. 6.2). Additionally, a noticeable narrowing of the channel (349 m) has been seen close to the left and right branches of the Mayurakshi River in Ajaypur, which are situated downstream of the Tilpara Barrage. The existence of civil structures controls the flow of water into the channel's downstream parts and is also accountable for modifying the morphology of the channel. Similar to this, a reversal condition has also been noted in the Mayurakshi River's channel depth alterations. The downpour of water from tributaries like River Siddheswari and

Kuya has been witnessed close to the downstream part of Sundarpur, resultant an abrupt increase in channel depth (7.31 m) significantly. While an upstream portion near Asanjor (2.99 m) and Maharo (2.21 m) has shown a drop in channel depth because of the braided-like channel structure and shoal deposition from the fragile bed topography of the study area (Bhattachrayay 2013). Figure 6.17 shows such asymmetric behaviour in channel depth from upstream to downstream of River Mayurakshi.

- **Variation in Hydraulic Radius (R_h)**

Hydraulic Radius is a measurement of channel flow efficiency that can control the amount of fluid discharge of a channel and also determine the ability to move sediments (Spark 1960). It is the ratio between cross sectional area with its length of wetted perimeter. This hydraulic mean depth can vary with the shape of the cross section. In a trapezoidal section, higher value of hydraulic radius denotes an improved condition of channel efficiency because of the increased velocity in a greater cross-sectional area. Such situation is very much obvious in an upper course of a channel but in this study area, an inverse picture has been noticed. With increasing distance from the upstream to downstream, the value of hydraulic radius gradually increases. This shows the downstream of the river is more efficient in terms of greater amount of discharge of water.

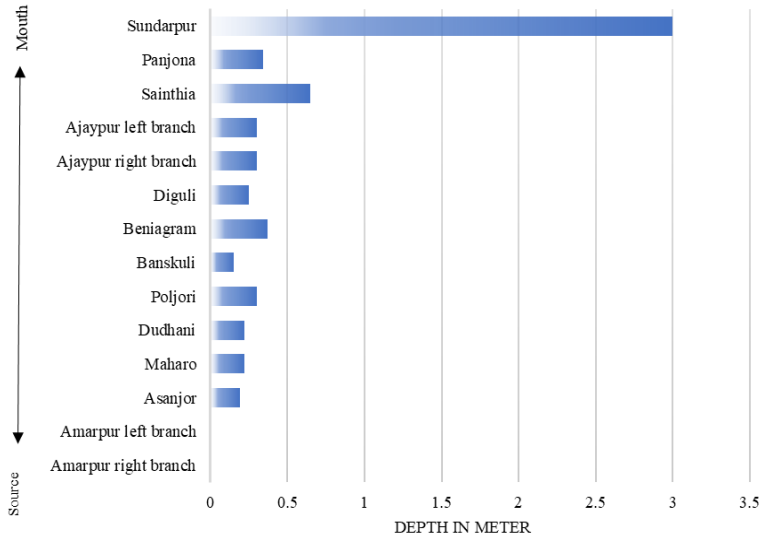

Figure 6.17 *Variation in Channel Depth from Upstream to Downstream of Mayurakshi River during Post-monsoon Season*

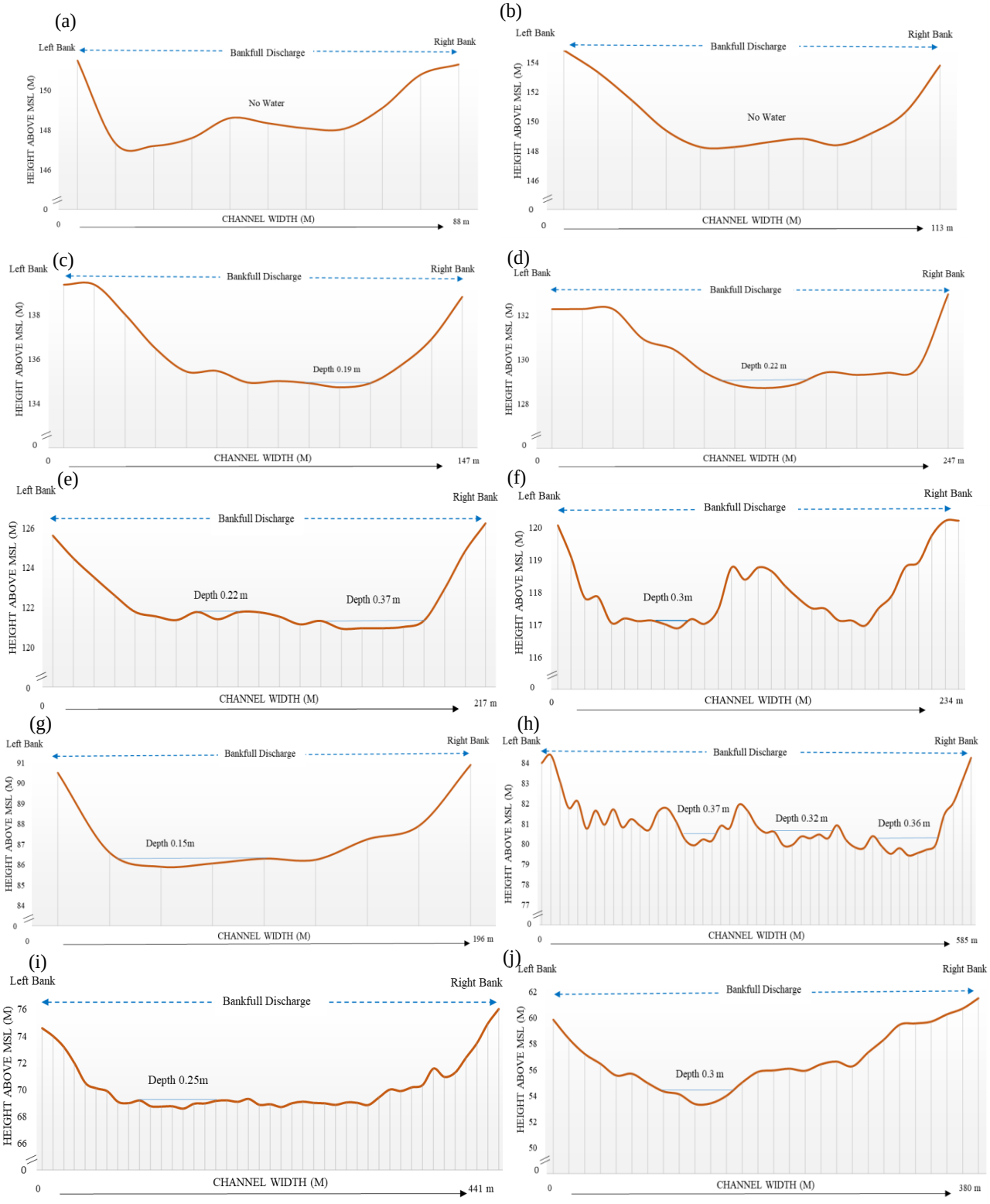

Figure 6.18 *Channel configuration of 14 different cross-sectional sites of the Mayurakshi River Basin (a) Amarpur right branch (CS 1), (b) Amarpur left branch (CS 2), (c) Asanjor (CS 3), (d) Maharo (CS 4), (e) Dudhani (CS 5), (f) Poljori (CS 6), (g) Banskuli (CS 7)*

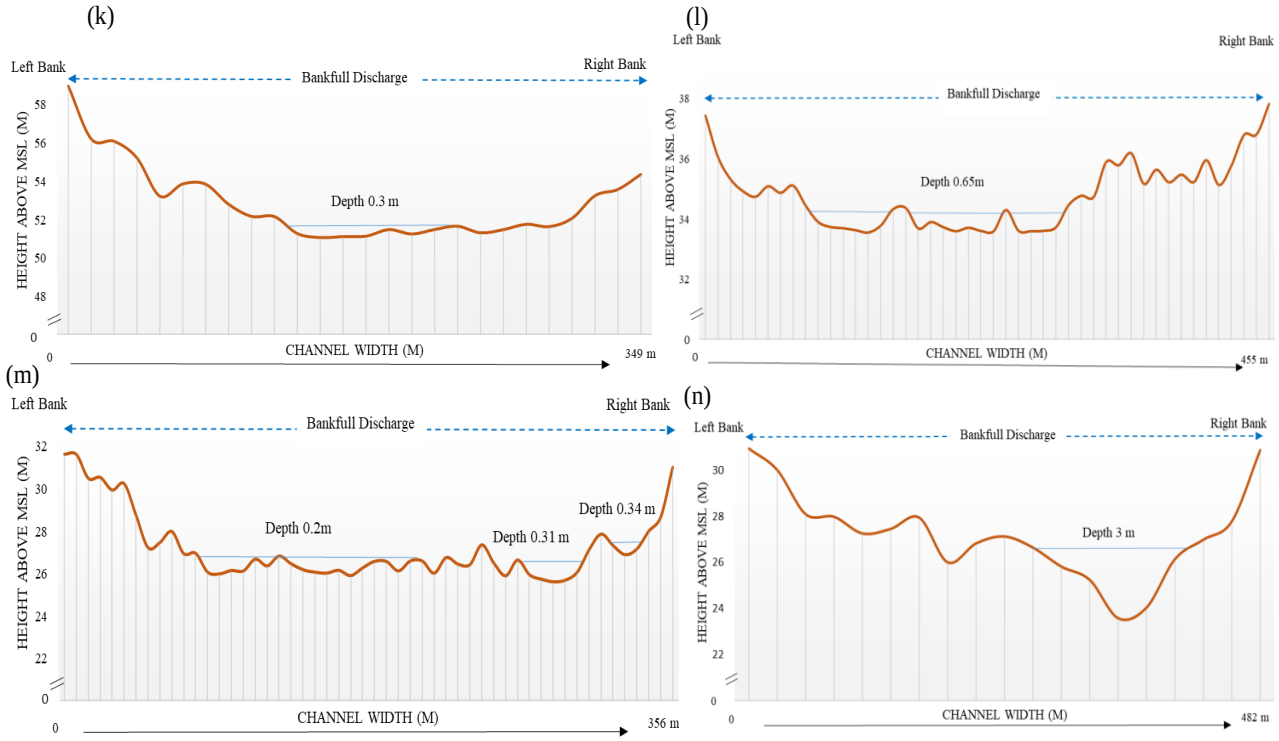

Figure 6.18 *Continued*

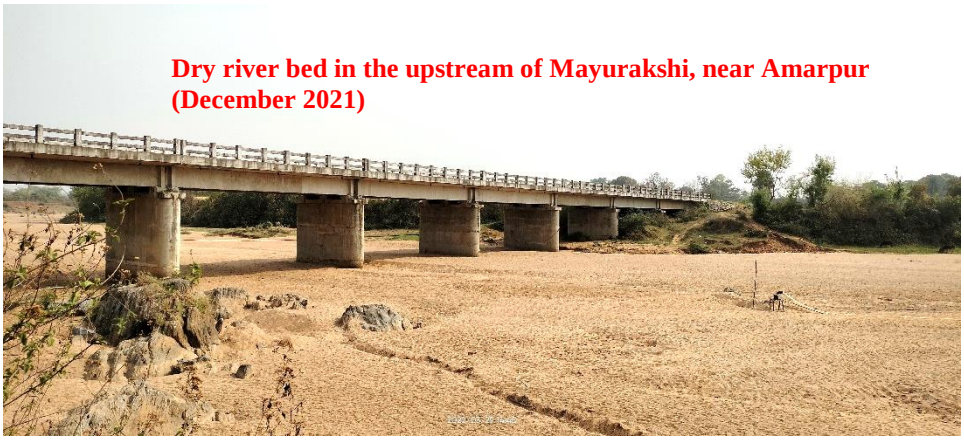

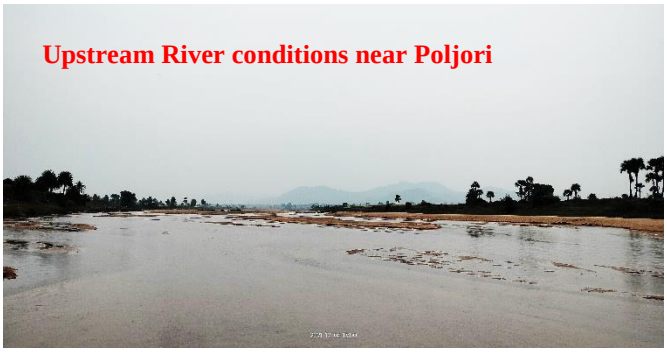

Plate No. 6.2 *Upstream Condition of Mayurakshi River during Post Monsoon Season, 2021*

Table 6.16 *Important Geometrical Character of Cross-Sectional Sites of the Mayurakshi River Basin during Post-Monsoon Season*

Sl. No	Course	Location	Total channel width (in m)	Total flow width (in m)	Bank to thalweg width (in m)		Channel Depth (in m) (Bank to Bank)		Maximum depth of Water (in m)	Longitudinal Slope (in %)	Wetted Perimeter (in m)	Hydraulic Radius (in m)	Total flow area (in sq. m)	Total channel area (in sq. m)
					From left bank	From right bank	Maximum	Average						
1	Upper course	Amarpur right branch	88	No Water	No Water		4.09	2.18	No Water	0.22	No Water	No Water	No Water	283.72
2		Amarpur left branch	113	No Water			4.50	2.44	No Water	0.22	No Water	No Water	No Water	385.38
3		Asanjor	147	42	105	42	2.99	1.45	0.19	0.2	41.38	0.095	3.93	147
4		Maharo	247	16.7	63	184	2.21	0.73	0.22	0.3	16.70	0.110	1.84	247
5		Dudhani	217	69	69	148	4.67	3.30	0.37	0.03	69.05	0.266	18.39	217
6		Poljori	234	37	65	169	2.69	1.36	0.30	0.03	37.33	0.286	10.66	234
7	Middle course	Banskuli	196	28	25	171	4.62	2.99	0.15	0.2	28.33	0.075	2.12	196
8		Beniagram	585	183	253	332	4.57	3.03	0.37	0.02	182.88	0.303	55.46	585
9		Diguli	441	113	56	385	5.97	4.34	0.25	0.06	112.90	0.203	22.88	441
10		Ajaypur right branch	380	48	106	274	6.43	2.98	0.30	0.01	48.12	0.258	12.42	380
11		Ajaypur left branch	349	49	191	158	7.92	6.12	0.30	0.01	49.56	0.232	11.48	349
12		Sainthia	455	98	180	275	3.88	2.54	0.65	0.01	98.60	0.446	44.02	455
13	Lower course	Panjona	356	164	261	95	5.39	3.80	0.34	0.03	164.05	0.295	48.44	356
14		Sundarpur	482	54	465	17	7.31	3.58	3.0	0.01	54.53	1.952	106.46	482

- **Velocity Distribution**

During lean period of study, the flow velocity of the Mayurakshi River is not uniformly distributed throughout the channel. Not only the flat broader channel shape, there are some other considerations for which the inconsistency in flow velocity pattern has been observed. The data retrieved from the field study using current meter shows, the average velocity of the upstream section of the river is very low than the lower reach of the river. In Asanjor (CS 3), the depth of water is very minimum (0.19 m) for which the hydraulic radius become low and because of the higher surface roughness, the velocity of the channel has reduced to 0.223 m/s (Table 6.17). Whereas in Dudhani (CS 5) and Diguli (CS 9), the middle and lower reach of the river shows a comparatively high average velocity i.e., 0.37 m/s and 0.43m/s respectively. In this region, the flow momentum of the river got also affected by the huge down pouring of water to the Mayurakshi River via its tributaries like Tepra and Siddheswari. These two rivers carry huge volume of water during monsoon season and create a flood like situation near the adjoining areas of the Mayurakshi River (Pal and Debanshi 2018). Next to this, Poljori (CS 6), just above the Massanjore Dam, the velocity of river water reduces significantly (0.11m/s) as a result of stagnant water with no flow condition. But from the area down below the Tilpara Barrage, the average flow velocity of the channel has been increased significantly. At Sundarpur (CS 14), due to an abrupt increase of hydraulic radius, the flow velocity increases significantly upto 0.85 m/s. Although the non-uniformity of the velocity distribution throughout the river is catalysed by the presence of bridges in Sainthia (CS 12), sand heap formation in the river bed near Asanjor (CS 3), Banskuli (CS 7), Sainthia (CS 12) and confine the normal shape and flow of the river.

- **Application of Hydraulic and Hydrological Model for Discharge Estimation**

In this study, the estimation of lean period discharge has been presented in a three-way - field observed discharge data, calculated discharge using two important model- Manning's method and Kinematic Wave Parameter (KWP) method. These two methods have been taken into consideration as it includes the in-stream channel geometry, channel roughness, longitudinal slope and also the amount of rainfall which are mainly responsible for the generation of runoff contributing discharge over an area (Roy 2013).

- **Estimation of Discharge from Field Survey**

Table 6.16 shows field observed discharge data for the selected 14 cross sections of the Mayurakshi River. This method of discharge estimation consists of the measuring the area of cross-section and the velocity using current meter. The entire river cross-section has been divided into n numbers of small trapezoids and the cross-section area of a channel has been determined using the trapezoidal rule. Using an area-velocity or conventional current meter method, the volume of flow released from several sites of the Mayurakshi River during the post-monsoon period has been determined (Subramanya 2008). This analysis reveals a significant increase in discharge, primarily in the downstream of the river. The Mayurakshi River's lower reach receives a significant amount of water from tributaries like the Kuya and Dwaraka, which causes the river discharge around Panjona (CS 13) and Sundarpur (CS 14) to increase during the lean season by up to 90.9 cumec and 26.9 cumec, respectively. Beniagram (CS 8), which is close enough to the Massanjore Dam, has also observed a notable rise in the amount of water. A significant release of water from the dam effectively widens the channel flow (183 m) and increases the channel's water discharge (13.25 m3/s) significantly. Apart from the tributary inputs, the river's downstream segment has additionally encountered a number of additional causes behind the variation in the volume of river discharge. The proportion of water passing through the lower watershed must increase since water from various sources has been added gradually. It can be attributed to the effect of downstream irrigational activities, where the additional water generated from surface irrigation eventually flows into the mainstream and contributes to greater discharge into the lower catchment (Mukhopadhyay & Das 2013). Additionally, Nag et al. (2022) have emphasized that a combination of rising urbanization and declining plant cover can result in increased surface runoff into streams. The loss of vegetation in the area might reduce the soil's capacity to absorb water, which may have an impact on the basin's overall hydro-morphological situation.

Table 6.17 *Lean Period Velocity Measurement Using Current Meter at Different Cross-Sections of the Mayurakshi River*

Sl. No	Course	Location	Area of Flow (in sq. m)	Measured Average Velocity (in m/s)	Discharge (in m^3/s)
1	Upper course	Amarpur right branch	No Water		
2		Amarpur left branch			
3		Asanjor	3.93	0.223	0.877
4		Maharo	1.84	0.38	0.698
5		Dudhani	18.39	0.371	6.822
6		Poljori	10.66	0.114	1.216
7	Middle course	Banskuli	2.12	0.225	0.478
8		Beniagram	55.46	0.239	13.254
9		Diguli	22.88	0.428	9.791
10		Ajaypur right branch	12.42	0.187	2.322
11		Ajaypur left branch	11.48	0.196	2.249
12		Sainthia	44.02	0.263	11.577
13	Lower course	Panjona	48.44	0.556	26.933
14		Sundarpur	106.46	0.854	90.918

- **Estimation of Discharge using Manning's Equation Method**

Table 6.18 shows the required parameters for calculating river discharge using Manning's equation. It is the most important hydraulic model that consists the estimation of hydraulic radius and wetted perimeter of each section. Another important consideration of Manning's equation is the channel roughness co-efficient. The uniqueness of this work is lied on calculating the Manning's 'factor using the channel friction factor and equivalent sand roughness instead of selecting the 'n' value from the table given by Chow (1964). All these parameters have been calculated using various convenient equations as mentioned in the methodology section. The result of this study has significantly coincided with the field observed discharge data with a little variation. In CS 5 (Dudhani), the Manning's derived discharge is 18.39 cumec where the field observed data shows 6.82 cumec volume of water passes during post-monsoon season. Similarly in a downstream location like in CS 13 (Panjona) the observed discharge is 26.33 m^3/s and the calculated discharge shows a slightly higher value of 48.44 m^3/s in a lean period of study.

- **Estimation of Discharge using Kinematic Wave Parameter (KWP) Method**

It is a major hydrological model which is totally based on the amount of rainfall intensity, generating the surface runoff as discharge over the river basin area. As the field has been carried out on a post monsoon month of December, authors have calculated the rainfall intensity in cm/h based on those corresponding 31 days daily rainfall data. Table 6.19 represent the result of discharge estimation using this method which shows a comparative higher value of discharge

from the field observed measurements. For example, in Beniagram (CS 8) the estimated discharge from Kinematic Wave equation is 23.37 m^3/s, whereas in case field observed discharge data shows 13.25 m^3/s. The use of total rainfall for determining rainfall intensity for the study area is the primary cause of such discharge variation. Due to the minimal effective precipitation (total precipitation-infiltration loss) during the post-monsoon season, total rainfall has been utilized as a key input for assessing the intensity of the rainfall (Singh 2017). As a result, the discharge estimated by the Kinematic Wave model is greater than the discharge discovered by the field experiment.

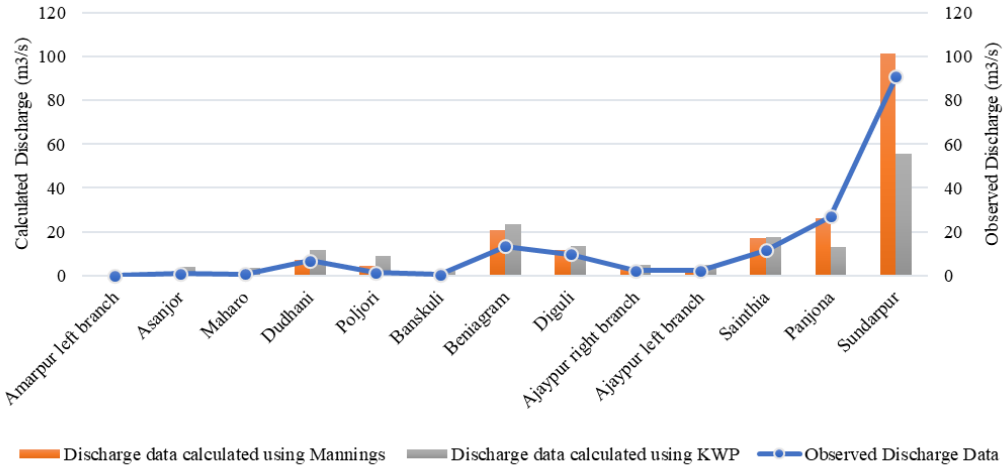

Figure 6.19 *Comparison between the Applied Models with Respect to the Field Observed Discharge Data in the Mayurakshi River*

- **Model Performance Evaluation**

In this section, authors compared all these calculated data derived from Manning's equation and Kinematic Wave parameter method, with the observed data collected during the field study conducted in post monsoon season. The results demonstrate good consistency between the measured discharge levels and Manning's discharge estimation output (Fig. 6.19). Using a variety of statistical indicators, such as MAPE, RMSE, and NRMSE, the proposed approaches (Manning's and KWP) are evaluated in order to determine their performance in comparison to the data acquired during the field survey. The output shows a good accuracy of 60.16%, 30.53%, and 0.05 in MAPE, RMSE, and NRMSE respectively (Table 6.20), has been found to make the performance of the proposed Manning's equation technique more reliable.

Table 6.18 *Lean Period Discharge Estimation of Different Cross Section Sites of the Mayurakshi River Using Manning's Equation*

Sl. No	**Course**	**Location of Cross-Section**	**Longitudinal Slope (in %)**	**Area of Flow (in sq. m)**	**Hydraulic Radius (in m) (R_h)**	**Manning's Roughness Co-efficient (n)**	**Manning's Velocity (in m/s) (v)**	**Discharge (in m^3/s)**
1		Amarpur right branch	0.22			No Water		
2		Amarpur left branch	0.22					
3	Upper course	Asanjor	0.2	3.93	0.095	0.0212	0.438	1.723
4		Maharo	0.3	1.84	0.110	0.0196	0.641	1.178
5		Dudhani	0.03	18.39	0.266	0.0182	0.394	7.248
6		Poljori	0.03	10.66	0.286	0.0184	0.409	4.363
7	Middle course	Banskuli	0.2	2.12	0.075	0.0198	0.401	0.851
8		Beniagram	0.02	55.46	0.303	0.0169	0.377	20.922
9		Diguli	0.06	22.88	0.203	0.0165	0.512	11.722
10		Ajaypur right branch	0.01	12.42	0.258	0.0152	0.267	3.314
11		Ajaypur left branch	0.01	11.48	0.232	0.0146	0.259	2.970
12		Sainthia	0.01	44.02	0.446	0.0152	0.384	16.909
13	Lower course	Panjona	0.03	48.44	0.295	0.0143	0.537	26.011
14		Sundarpur	0.01	106.46	1.952	0.0164	0.954	101.525

Table 6.19 *Lean Period Discharge Estimation of Different Cross Section Sites of the Mayurakshi River Using Kinematic Wave Parameter (KWP)*

Sl. No	**Course**	**Location of Cross-Section**	**Contributing Drainage Basin Area in sq. km (A)**	**Intensity of Rainfall in cm/hr (i)**	**Longitudinal Slope in % (S_Ω)**	**Manning's Roughness Co-efficient (n)**	**Mean Flow Width of the channel in m (B)**	**Alpha (α_Ω)**	**Flow Velocity in m/s (v_Ω)**	**Discharge in m^3/s**
1	Upper course	Amarpur right branch	466	0.05	0.22	No Water				
2		Amarpur left branch	485	0.05	0.22					
3		Asanjor	684	0.05	0.2	0.0212	42	0.17205	0.9502	3.74
4		Maharo	917	0.05	0.3	0.0196	16.7	0.42362	1.8346	3.37
5		Dudhani	1385	0.05	0.03	0.0182	69	0.05581	0.6412	11.79
6		Poljori	1437.98	0.05	0.03	0.0184	37	0.08393	0.8315	8.87
7	Middle course	Banskuli	811.46	0.028	0.2	0.0198	28	0.24166	0.9893	2.10
8		Beniagram	2807	0.028	0.02	0.0169	183	0.02549	0.4215	23.37
9		Diguli	2886	0.016	0.06	0.0165	112.85	0.06261	0.5842	13.37
10		Ajaypur right branch	1560	0.016	0.01	0.0152	48	0.04921	0.3953	4.91
11		Ajaypur left branch	1560	0.016	0.01	0.0146	49	0.05059	0.4019	4.61
12		Sainthia	3168	0.016	0.01	0.0152	98	0.03047	0.3936	17.34
13	Lower course	Panjona	3205	0.0042	0.03	0.0143	164	0.03974	0.2716	13.16
14		Sundarpur	1293	0.049	0.01	0.0164	54	0.04217	0.5230	55.68

Table 6.20 *Result of Model Performance Analysis*

Applied models	**MAPE (%)**	**RMSE (%)**	**NRMSE**
Manning's equation	60.16	30.53	0.05
Kinematic Wave Parameter	184.98	85.28	0.13

Plate No. 6.3 *Human intervention on the Mayurakshi River (a) No flow condition of river during dry season (b) Fragmented flow pattern in the downstream of Tilpara Barrage during dry season (c) Unscientific sand extraction from the river bed (d) Construction of temporary recharge pools/nullahs for river lift irrigation (e)Disturbed channel flow due to bridge construction, near Sainthia, Birbhum (f) Channel shape and size deformation due to active human interventions (g) Human induced temporary bridges are hampered the natural flow velocity of the channel, near Sainthia, Birbhum.*

6.5.4. Discussions

The hydro-geomorphological studies of the Mayurakshi River reveal a general asymmetry in the structural variables (channel with-depth) observed from the upstream to downstream of the river, which further exemplifies the nature of channel dynamism that may reduce the stream's capacity to carry enough water in the future. Other than the water influx from the dam, barrages, and neighbouring rivers, various man-made causes are also accountable for the change in channel behaviour. Plate no. 6.3 displays some of the field-observed evidence in this regard. The river flow path in the vicinity of Sundarpur (CS 14) has undergone significant changes due to human activity. By impounding various structures like big pipes and stones, people have hindered the natural flow of the river and have utilized the river water for brick kiln industries, fishing operations, etc. As a result, the flow area and velocity in the channel have been artificially boosted, creating a paradoxical appearance of the river. A similar circumstance can be seen near Sainthia village (Plate no. 6.3g). Additionally, the river's natural flow has also been hampered by the practice of sand mining from the riverbed, which has also destroyed the area's channel bed morphology.

Additionally, this study attempted to compare the river discharge data obtained from fieldwork with the discharge amount estimated by Manning's and Kinematic wave equations. The lack of secondary data significantly hinders watershed planning, which has led many hydrologists to adopt various indirect approaches to estimate the quantity of river discharge. In this work, Manning's equation and the Kinematic Wave Parameter (KWP) are two crucial hydraulic and hydrologic models that have been used to calculate the Mayurakshi River's lean season discharge volume. There are several different techniques for estimating river discharge from an ungauged basin or in situations where it is more difficult to acquire real data owing to geographical or economic constraints. But in this case, just these two models have been chosen due to their geomorphic methodology and worldwide feasibility (Roy & Mistri 2013). In the fields of fluid dynamics and open-channel hydraulics, Manning's equation is a fundamental frequently employed formula. This method is especially advantageous when it is difficult to acquire precise direct measurements of flow rate. Another key concept is the kinematic wave equation, which can be applied to describe how water flows through a river or channel by focusing only on the variation in flow depth over time. This equation is particularly useful for calculating discharge when the flow behaviour is comparatively shallow and swift (Singh 2017). Finally, to compare the proposed models with the field-observed discharge data and to evaluate the effectiveness of the proposed models, a number of statistical metrics have

been examined. The results demonstrate that Manning's equation exhibits the least error function with good accuracy in all scenarios of MAPE, RMSE, and NRMSE assessment. However, the importance of gathering actual data through field measurements has been highlighted in this work, which helps to ensure the accuracy and dependability of discharge estimates derived by other approaches.

6.5.5. Conclusion

The current study includes a lean period hydro-geomorphological analysis of the Mayurakshi River, which is indeed crucial for developing an effective plan for managing the surface water supplies needed to maintain the local ecology and ecosystem. This study also shows how different hydrological and hydraulic models may be used to predict the quantity of river flow in a river basin that is not gauged or within the constraints of the limited amount of available dataset. Along with this, every aspect of channel geometry has been physically evaluated during the field survey by selecting 14 different cross-sectional sites along the Mayurakshi River. Additionally, all hydro-geomorphological aspects of the channel geometry were assessed during a field inspection at 14 different cross-sectional locations along the Mayurakshi River. The analysis demonstrates that the width and depth of the cross profiles in the Mayurakshi River do not adhere to the typical hydrologic pattern. Due to the presence of the Tilpara Barrage and Massanjore Dam, the channel's upper portion has a broader width. Additionally, the tributaries' continued input of water boosts the momentum of the flow and deepens the channel in the lower sections of the main river. In terms of velocity, throughout the examined lean season, it exhibits an increasing trend (0.52 m/s near Sundarpur) downstream of the river. Using several statistical metrics, such as MAPE, RMSE, and NRMSE, the performance evaluation of the employed models revealed that the estimated and measured river discharge had an acceptable degree of agreement. The results show that the model based on Manning's equations has the lowest error function for estimating discharge during a lean phase. Despite numerous model flaws, the study's main goal has been accomplished. Thus, it can be inferred that the manning equation in the examined river achieves reliable results for more effectively calculating river discharge during lean periods.

6.6. Assessment of Available Surface Water Resources

Water bodies are an essential part of the Earth's system. Surface water observation is a functional prerequisite for understanding ecological and hydrological systems. Water contributes to the conservation of biodiversity in riparian or wetland environments by acting as habitats for an abundance of plant and animal species. In addition to being essential to ecosystems as a crucial part of the hydrologic cycle, it also has an impact on many aspects of society, including the production of electricity, drinking water, agriculture, transportation, and industrial uses (Vörösmarty et al. 2010).

Surface water bodies are dynamic in that they diminish, swell, or alter their appearance or flow direction over time due to a variety of natural and human-induced factors (Scanlon et al. 2007). Typically, alterations in the volume of surface water have negative effects. Extreme flooding may occur when surface water levels rise rapidly, and a similar drought condition would predominate when a region's water supply is inadequate. Consequently, it is necessary to accurately detect the presence of surface water, ascertain its extent, calculate its volume, and monitor its dynamics. Satellite remote sensing data are advantageous in monitoring the water resources in many regions because field investigations of water bodies are challenging owing to costs and logistics (Alsdorf & Lettenmaier 2003). Currently, radar and optical remote sensing data, such as ENVISAT, Sentinel-1, and other optical remote sensing data, such as the Landsat series, spot, and WorldView series (Sinha et al. 2015) are commonly utilised to extract water bodies. Among all, Landsat data series are widely used for the extraction of various surface water features like rivers, lake, because of the added benefits of high resolution, extended time series, and being free to the user (Yao et al. 2019).

Among the various water extracting methodology using remote sensing, the thresholding techniques gain immense popularity as it can be useful for both single and multibands to distinguish water from non-water features effectively (Huang et al. 2018; Yang et al. 2015). Although the results are usually influenced by the shadows of mountains. So, this method can only be used in places with a relatively flat topography (Bangira et al. 2019). In this present work, authors have tried to extract the surface water bodies from Mayurakshi River Basin area, which is primarily dominated by moderate to low relief features. Several band ratio approaches are being adopted for the implementation of different index based surface water extract methods. The adopted indices are Normalised Difference Water Index (NDWI), Normalised Difference Moisture Index (NDMI), Modified Normalised Difference Water Index (MNDWI),

Water Ratio Index (WRI), and Automated Water Extraction Index (AWEI). To compare the accuracy of all indices, 500 sample points have been selected randomly over the study are and compare the output of each indices with Google Earth Pro imagery. Lastly a Principal Component Analysis (PCA) have been performed combining all these indices to achieve the best visual reflectance of surface water bodies over the Mayurakshi River Basin area.

6.6.1. Data Used

This research focuses on quantifying surface water bodies (natural, artificial, and recharge pools) in relation to how their size, number, and distribution throughout geography have changed over time, from 2000 to 2018. For the years 2000 and 2018, the Landsat series of satellite images including ETM+ images (Landsat 7 ETM+) and OLI images (Landsat 8_OLI; Yamazaki et al. 2015) were used to achieve this goal. The satellite images were freely downloaded from the United States Geological Survey (USGS) Earth Explorer website (www.earthexplorer.usgs.gov). The two acquired Landsat imageries were resampled to 30 m and geo-referenced at the Universal Transverse Mercator projection system (zone: 45° N, datum: WGS-84) beforehand. Along with that, all of the satellite images were pre-processed with the radiometric calibration tool in ENVI, which changed the digital number (DN) image to top-of-atmosphere (TOA) reflectance. To remove variances in light illumination and cloudiness, the images were chosen for the same season (Pre-Monsoon) and similar dates.

6.6.2. Methods

The authors have chosen a number of water-based indices for the detection of both natural and man-made recharge pools within the study area, along with their spatial and temporal variation. All the image processing and the extraction of water and non-water points have been done using ArcGIS software package 10.3.1 and Environment for Visualizing Images (ENVI) software version 5.3. Lastly the Principal Component Analysis (PCA) has been performed in TNT Mips 2014 software.

- **Normalized Difference Water Index (NDWI)**

In 1996, the Normalised Difference Water Index (NDWI) was developed. It is identical to the normalised difference vegetation index (NDVI). Landsat TM's two-band spectral water indices utilise the near-infrared and green bands. The NIR band has a high water absorption and the green band has a strong water reflection. Consequently, NDWI took advantage of this benefit, and the following formula can be used to calculate NDWI:

$$NDWI = \frac{Green-NIR}{Green+NIR} \tag{6.42}$$

Where, Green and NIR (near infrared band) surface reflectance bands.

- **Modified Normalized Difference Water Index (MNDWI)**

Xu (2006) made the new version of the NDWI. Instead of the Near Infra-Red band, this method used the Middle Infra-Red band. This algorithm effectively eliminates background noises caused by both natural and manmade sources. Water was represented by positive numbers, whereas noise was shown by negative ones. It has been calculated using the following equation:

$$MNDWI = \frac{Green-SWIR}{Green+SWIR} \tag{6.43}$$

- **Normalized Difference Moisture Index (NDMI)**

Hardisky et al. 1984, and Gao 1996 were the first to use NDMI to extract biomass and vegetation moisture content. Multiple investigations demonstrated that NDMI outperforms NDVI. The values range between 1 and + 1, with high values indicating a high water content. Consequently, the NDMI derived from Landsat TM reflectance images were directly compared for detecting the moisture content of features. The equation is

$$NDMI = \frac{NIR-SWIR1}{NIR+SWIR1} \tag{6.44}$$

- **Water Ratio Index (WRI)**

It is a newly developed index for the extraction of surface water bodies. In 2010, Shen and Li created this index, which uses a total of four spectral reflectance bands. The ratio of the total spectral reflectance of the two visible bands (green and red) to the total spectral reflectance of the near-infrared and middle infrared band (MIR) is known as the spectral reflectance ratio. The following equation is used for the detection of surface water bodies:

$$WRI = \frac{Green+Red}{NIR+SWIR} \quad (6.45)$$

After computing all the above mentioned indices, Principal Component Analysis (PCA)has been performed to identify the best indices to achieve best surface reflectance for the detection of surface water bodies over the study area.

- **Automated Water Extraction Index (AWEI)**

Feyisa et al. (2014) created the AWEI_nsh (for no shadow) and AWEI_sh (for shadow) versions of the Automated Water Extraction Index. Where shadows pose little to no threat, the AWEI_nsh is employed. It successfully eliminates non-water pixels and black accumulation areas. While shadows remain the main challenge in extracting water bodies, the AWEI_sh was developed to increase accuracy, which has been executed in this study using the following equation:

$$AWEI_{sh} = (Blue + 2.5 * Green - 1.5 * (NIR + SWIR1) - 0.25 * SWIR2) \quad (6.46)$$

- **Accuracy Assessment**

For any scientific modelling, it is necessary to conduct an accuracy assessment for evaluation the purposes. Using the high-resolution imagery provided by Google Earth, surface water bodies can be readily distinguished from non-water areas (Zhai et al. 2015). Here visual interpretation has been done by choosing 500 random sample points and overlapped the indices outputs on the Google Earth Pro satellite imagery, where MNDWI index shows the closest overview rather than others.

6.6.3. Results and Discussion

The effectiveness of different water indices for the detection of surface water bodies has been evaluated here. The results of the five of the most popular multiband indexes, are shown in the accompanying figure 6.20. It has also been analysed from the visual study that not a single method was able to extract surface water in the entire scene with better accuracy. To find out the better surface reflectance and distinguish water from non-water bodies, authors have executed a Principal Component Analysis (PCA) using TNT Mips software. Combining all the analysis of water indices, the output of PCA analysis represents a better visibility of all surface water bodies located over the study area (Fig. 6.21). This analysis also denotes that, from all the adopted indices applied for the extraction of natural and man-made water features, MNDWI

have the highest accuracy for both period of study while comparing with the Google Earth imagery.

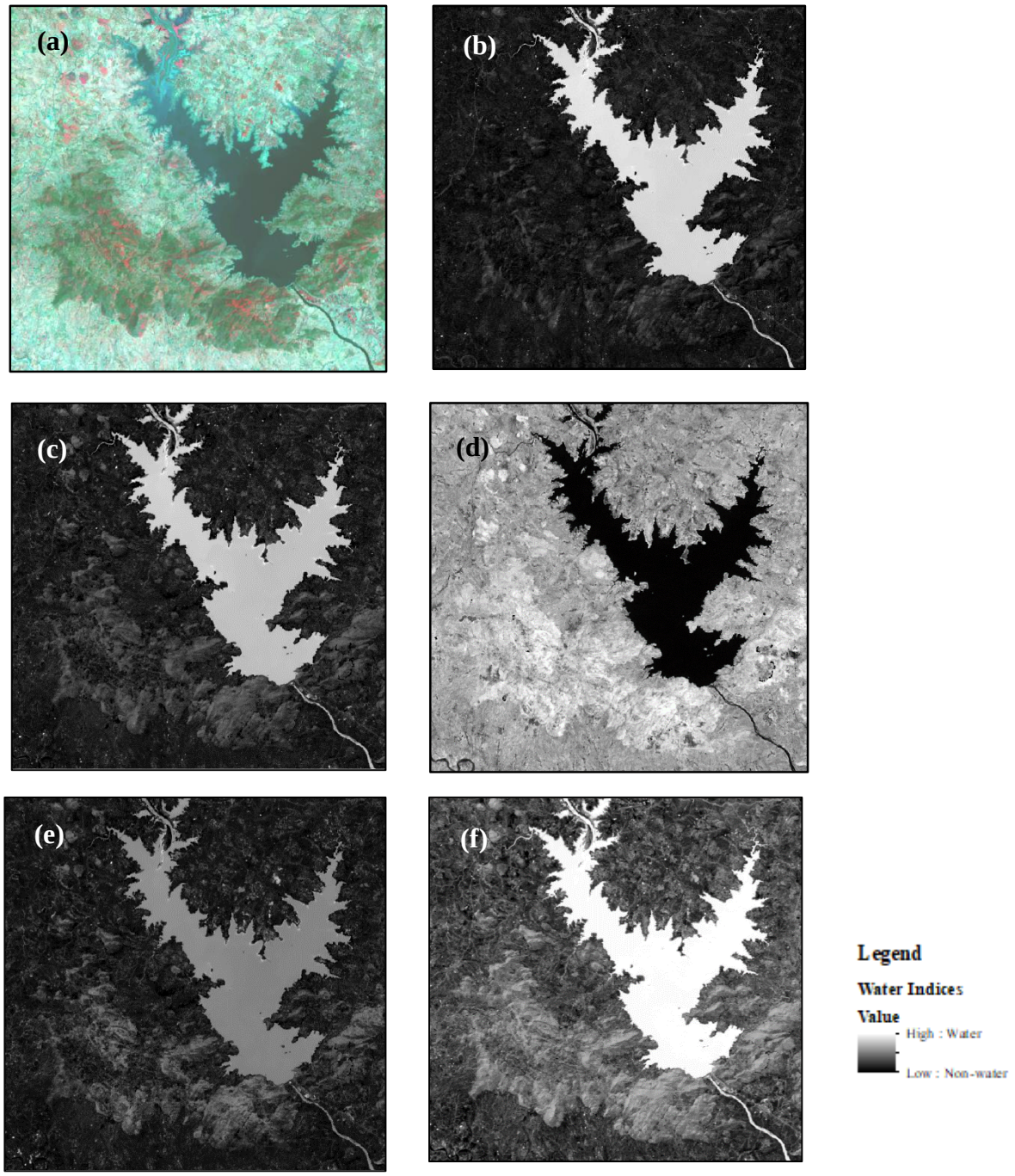

Figure 6.20 *Visualisation of Surface Water Bodies of Massanjore Dam Area (a) Landsat 8 OLI image (b)NDWI (c) MNDWI (d) NDMI (e) WRI (f) AWEI results*

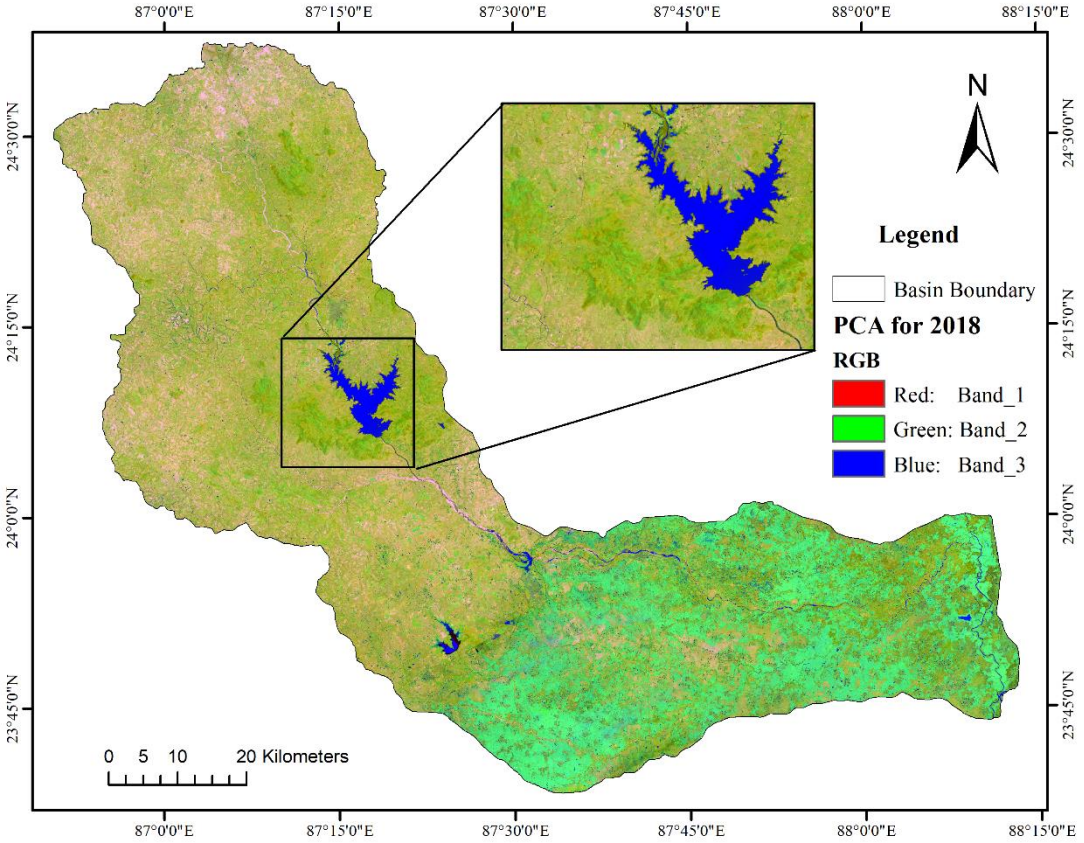

Figure 6.22 *Extracted Surface Water Bodies from Principal Component Analysis of the Mayurakshi River Basin Area*

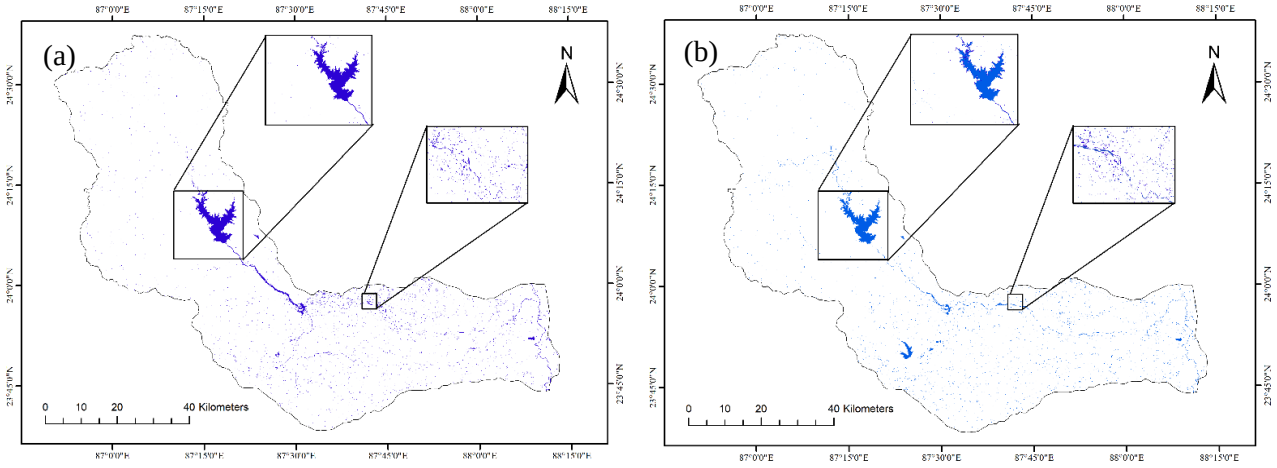

Figure 6.21 *Extracted Surface Water Bodies of Mayurakshi River Basin Area (a) 2000 year (b) 2018 year*

Figure 6.22 shows the extracted surface water bodies of Mayurakshi River Basin area for the year of 2000 and 2018. Visually it has been observed from both the images that the number of water bodies have been significantly increased from the year 2000 to 2018. The maximum increase has been noticed in the lower part of the basin area, where mainly the man-made recharge pools have grown up, to satisfy the irrigational demand during the pre-monsoon

season. Other than that, Bakreswar Dam has also been constructed on the river Bakreswar, a main tributary of Mayurakshi. This reservoir also serves surface water to their periphery areas through the canal system of Mayurakshi River. Such growing demand of irrigational water has continuously rise up mainly because of the recent year fall of groundwater level over the basin area (Nag et al. 2022).

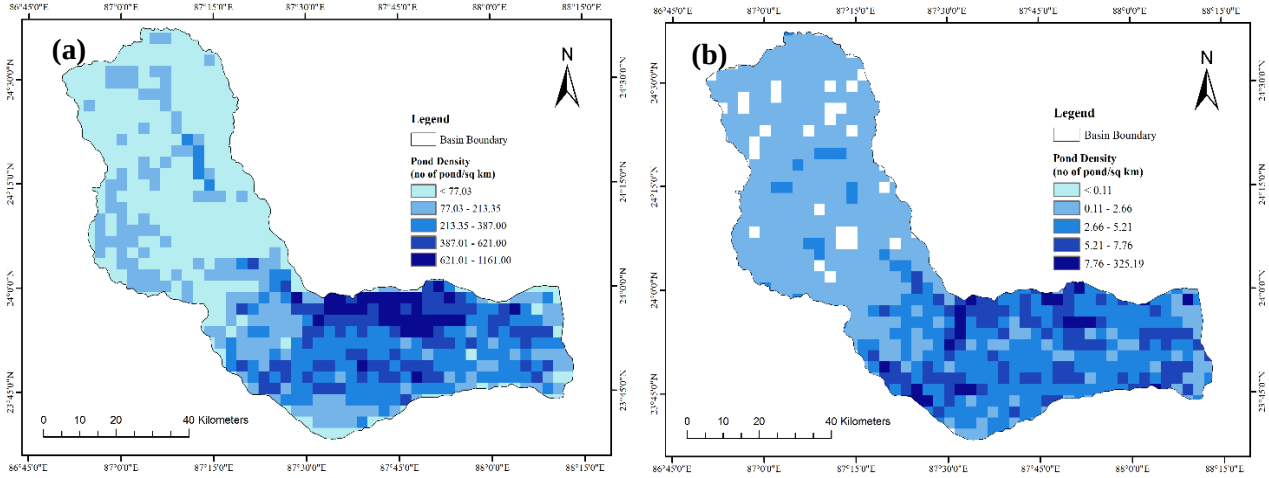

Figure 6.23 *Pond Density of Mayurakshi River Basin Area (a) Year 2000 (b) Year 2018*

However, the distribution of surface water bodies from 2000 to 2018 does not correspond to the output of pond density for those years. The figure 6.23 illustrates the results of an analysis of pond density carried out across the Mayurakshi River basin in 2000 and 2018. This research demonstrates that while there has been an increase in the dispersion of water bodies, but pond density of the corresponding year decreases over the study area. This scenario is primarily responsible for the rising need for irrigational water, which is why farmers and other local stakeholders are creating temporary recharge pools and nullahs to meet the farmers' day-to-day needs, particularly during the warm summer months. This kind of non-scientific approach to the construction of water-saving buildings not only poses a threat to the overall health of the topography but also makes it more likely that the lower half of the basin will become inundated with water during the monsoon season.

6.6.4. Conclusion

In order to effectively study the ecological and hydrological processes, it is required to characterise the dynamics of surface water. The advantages of remote sensing technology in the acquisition of information about Earth observation at a variety of geographical, temporal, and thematic scales make it possible to watch the dynamics of surface water in a way that is

both effective and efficient. In this work, the applicability of employing OLI data obtained from the Landsat 8 satellite to locate surface water bodies in both urban and rural settings using a variety of water indices was studied. The findings demonstrated that the MNDWI has a higher degree of accuracy than other methods when it comes to the overall precision of water extraction from OLI imagery over the course of both years. All of these applications, whether mentioned here or not, have substantially aided research in numerous related disciplines, including eco-hydrological studies and water resources management. In addition to shedding light on the effects of climate change and climate oscillation on surface water distribution, they will also aid in capturing the effects of humans on surface water resource distribution. In an era of global warming and fresh water scarcity, it is critical to restore water sources such as ponds not only for the survival of poor people, but also to adapt to the changing climatic and meteorological conditions. The emphasis should be on increasing pond water retention capacity as well as physical rehabilitation of small tank systems through institutional reforms. To keep these multipurpose water bodies in excellent shape, both physical and governance issues must be addressed.

6.7. Assessment of Groundwater Recharge Potential Zone

Deciphering the groundwater potential zones has become a global concern for hydro-geologist, hydraulic engineer, and environmental scientists around the world. Groundwater can be regarded as an important freshwater resource for both rural and urban areas (Hossein 2004). The occurrence of groundwater in any region may be influenced greatly by various hydro-geomorphic-geological formations, presence of drainage network, soil properties, lineament density, temperature, precipitation, etc. (Singh et al. 2011; Şener et al. 2018). It also plays a significant role by fulfilling the daily need of human beings, maintaining the ecosystem, and also in various activities of economic development (IPCC 2013). Despite these natural factors, some of the human-induced factors like rapid population growth, urbanization, and improved standard of living may lead to overutilization of groundwater resources resultant substantial decline in groundwater level (Qadir et al. 2019). In India, 60% of wells are facing a major water table lowering issue, which accelerates the scenario of water scarcity all over India (CGWB 2016). Likewise in rural areas, the existed groundwater may fail to reach the demand of farmers to fulfil the requirements in irrigational activities. Due to a lack of scientific knowledge, they cater to their need by extracting groundwater through excessive pumping (CWC 2016). Such unplanned and unmanaged use of groundwater has put an effect on the existing aquifer system, resulting in rapid declination of groundwater storage. Because of this fact, the shortage of water has been considered the biggest threat to our environment and the society.

Despite this huge dependency on groundwater extraction, changes in land use land cover pattern influences groundwater recharge condition (Halder et al. 2020). At such a juncture, study the effectiveness of land use land cover changes is essential to understand the overall hydrological status of a region. Several driving forces alter the present land cover and land use management of a region. Climate change is considered an important causal factor behind such modification of land-use changes. Longer and more frequent temperature and precipitation anomalies can increase the regional water demand and induce the alteration in vegetation pattern, which is ultimately manifested by desertification (Owuor et al. 2016). Gee et al. (1992) and Scanlon et al. (2005) have studied that the enhancement of green cover increased groundwater recharge rate, while the areas having impervious surface cover leading to create more runoff than infiltration resulting in an urban flood syndrome. Scanlon et al. (2005) has also analysed that the alteration of drainage network has been associated with the nature of land

management practices of a particular region. Overutilization of land resources including overgrazing, tillage structure can also modify the hydro-physical properties of soil and hamper the soil pore space distribution resulting in a reduction of infiltration rate and groundwater enrichment (De Waroux and Lambin 2012; Price et al. 2010). Besides this, with the population explosion, the growth of urbanization and industrialization are also going hand in hand which gives rise to form more build-up areas inducing poor evapotranspiration and low groundwater recharge (Mishra et al. 2014).

Due to such above-mentioned outcomes, it is essential to understand the effect of land use land cover changes in response to the groundwater enrichment into the aquifer system. Various hydrological models have been successfully developed to study the land resource modifications or to stimulate the impact of land use land cover over a catchment area. Among them, Storm Water Management Model (SWMM) (Huber et al. 1988), Soil and Water Assessment Tool (SWAT) (Arnold et al. 1998), Hydrological Simulation Program- Fortran (HSPF) (Zhang and Ross 2015) have profoundly been utilized. In addition, the application of remote sensing and GIS technologies plays a significant role in the evaluation of resource potential zones which are becoming more cost-effective and less time-consuming as well. Much of the past literature shows (Table 6.21) huge application of remote sensing and GIS technologies for extracting various hydrogeological and hydro-morphological information to delineate the groundwater potential zone, where the assignment of weights for each parameter has been done by various methods. In a recent decade, applications of various bivariate and multivariate statistical approaches like Frequency Ratio (Moghaddam et al. 2015), Logistic Regression (Pourtaghi and Pourghasemi 2014), Certainty Factor (Razandi et al. 2015) are extensively used in delineating groundwater potential zones but some drawbacks are observed within this assumption making process (Sener et al. 2018). To overcome the inefficiencies in decision-making processes, the wise use of multi-criteria decision-making (MCDM) processes has made such predictive decision-making easier and accurate. Analytical Hierarchical Process (AHP) is one of the most commonly used MCDM techniques for any kind of predictive model analysis (Chenini et al. 2010; Adiat et al. 2012; Rahmati et al. 2015). In this work, the Fuzzy AHP technique has been executed to decipher the groundwater potential zone in the study area. This process is the modified version of the traditional AHP model which has been developed by Saaty (Ayhan 2013). The fuzzy logic-based AHP model is primarily based on a fuzzy set of theory, where the parameters form a pairwise comparison matrix in a hierarchical order, for which it has been

regarded as a powerful MCDM tool to solve problems that depend on multiple criteria. Owing to this unique characteristic of this method, the present work aims to (1) decipher groundwater potential zones in the Mayurakshi river basin area for 2000 and 2018 based on 13 parameters adopting Fuzzy AHP technique coupling with remote sensing and GIS, and (2) study the functionality between the selected potential parameters which can have a more controlling power in targeting the groundwater rich zone with the temporal shifting of groundwater potential zones of the study area. No such previous studies have been done regarding the functionality study on the potential parameters, which have more power to accelerate and manage the recharge potential sites of groundwater resources.

Table 6.21 *Past Literature on Groundwater Potential Zone Analysis*

Authors	**Location**	**R**	**S**	**G**	**GM**	**L**	**Soil**	**LD**	**DR**	**GWT**	**DD**	**Rain**	**LULC**
Chenini *et al.* (2010)	International			✓				✓			✓		
Preeja *et al.* (2011)	National		✓	✓	✓		✓	✓			✓		✓
Magesh *et al.* (2012)	National	✓	✓	✓			✓	✓			✓		
Agarwal *et al.* (2013)	National		✓	✓	✓		✓	✓		✓	✓	✓	✓
Rahmati *et al.* (2014)	International		✓			✓		✓			✓	✓	
Razandi *et al.* (2015)	International	✓	✓			✓			✓	✓	✓	✓	
Jhariya *et al.* (2016)	National		✓	✓	✓		✓	✓		✓	✓	✓	✓
Tiwari *et al.* (2017)	National		✓			✓	✓			✓	✓		✓
Patra *et al.* (2018)	National	✓	✓	✓	✓		✓			✓	✓	✓	✓
Mallikarjun *et al.* (2018)	National		✓	✓	✓						✓	✓	✓
Sener *et al.* (2018)	International		✓			✓	✓	✓			✓	✓	✓
Kordestani *et al.* (2018)	International	✓	✓			✓			✓		✓		✓
Costa *et al.* (2019)	International		✓	✓			✓	✓			✓	✓	✓
Dar *et al.* (2020)	International		✓		✓	✓		✓			✓	✓	✓

*R= Relief, S= Slope, G= Geology, GM= Geomorphology, L= Lithology, LD= Lineament density, DR= Distance from river, GWT= Groundwater table, DD= Drainage density, LULC= Land use land cover

6.7.1. Study Area

Mayurakshi River is an important tributary of the Bhagirathi River, which flows through the states of Jharkhand and West Bengal, India (Figure 6.24). It covers an area of 5325 sq. km and is bounded by 23º64´N to 24º62´N latitude and 86º84´E to 88º22´E longitude. About 288 km long Mayurakshi River has 12 major tributaries, which are Dhobi, Motihara, Tepra, Matihara, Bhurbhuri, Siddheswari, Bhamri, Pusaro, Main channel, Bara Nadi, Kushkarini, and Kuya river. Physiographically, the river basin comprises of fringe part of the highland of Chotanagpur Plateau and the Rarh plain of Birbhum and Murshidabad districts of West Bengal, which experiences hot and humid climatic conditions throughout the year (Pal 2015). The rainfall pattern is highly erratic, with the maximum amount of rainfall during the monsoon season. To reduce the dependency on monsoonal rainfall and enhance the crop productivity of this region, Mayurakshi Reservoir Project and Canal Irrigation System were started by the Bengal Government with the financial assistance of the Canada Government. It is the first major irrigation project in West Bengal after independence by which a huge number population of Birbhum, Murshidabad, and Bardhaman districts are benefited (Annual Flood Report, 2016).

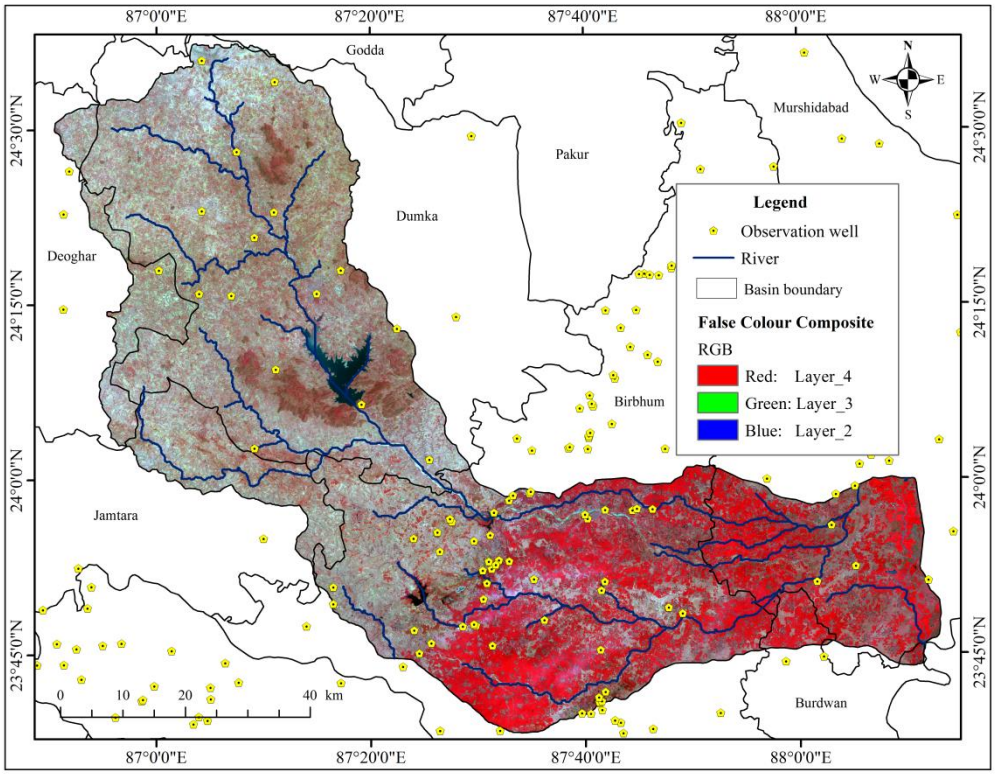

Figure 6.24 *Location Map of the Study Area with Observation Wells*

The present study area is primarily dominated by cropland areas, where about 90% of the population are engaged in agricultural activities for their livelihood (Chakraborty 2015). They are highly dependent on the river and canal water to fulfil their irrigational need. But due to the seasonal variability of rainfall, the main channel water and other sources of surface water are drying up (Pal et al. 2012). As a consequence, excessive use of groundwater via dug wells and submersible pumping has created immense pressure on the existing aquifer system (Plate no. 6.4a). For this, the identification of groundwater potential zones is the objective of this study. In such a context of hydrological crisis, many cultivable lands are being converted into fallow lands, which are now only used for single crop production (Plate no. 6.4b). Such kind of alteration in land-use patterns from agricultural land to fallow land or the expansion of settlement and bare land surfaces certainly affects the groundwater recharge process and the potential areas of groundwater resources accordingly.

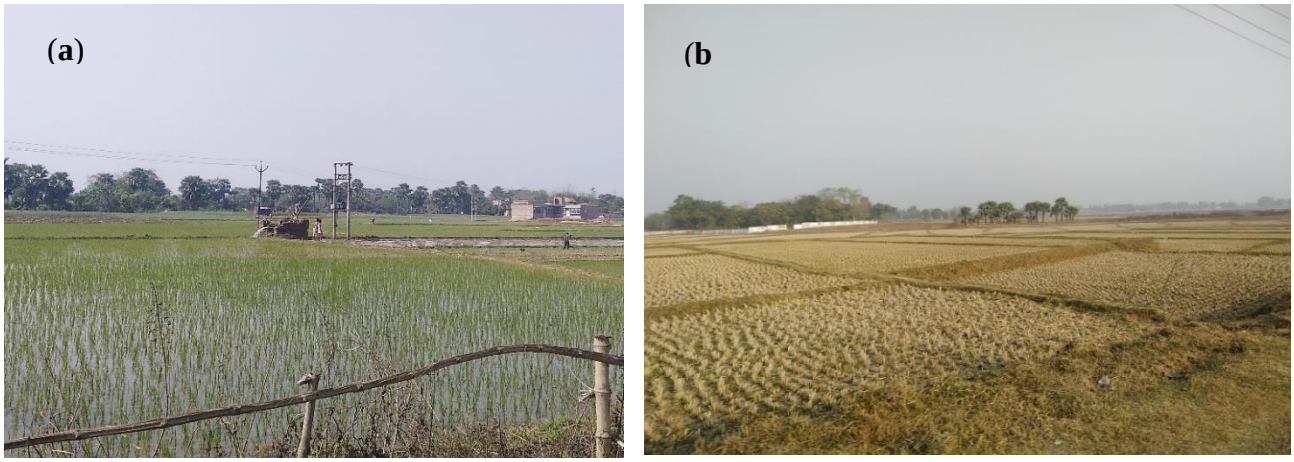

Plate No. 6.4 *(a) Excessive Use of Groundwater by Submersible Shallow Pump, (b) Crop Land Converted into Seasonal Fallow Land due to Lack of Water for Irrigational Purposes*

6.7.2. Methodology

The methodology involved in this study has been shown in the given flow chart (Figure 6.25), which involves the following steps: (1) preparation of groundwater potential zone inventory maps; (2) Land Use Land Cover (LULC) map classification for 2000 and 2018; (3) Accuracy assessment of the classified LULC maps; (4) application of Fuzzy AHP method to delineate groundwater potential zones for the above mentioned period; (5) validation of groundwater resource potential maps; (6) Evaluation of the groundwater potential zones and its spatiotemporal changes for 18 years; (7) study the functionality of LULC over the groundwater resource potential zones of the study area.

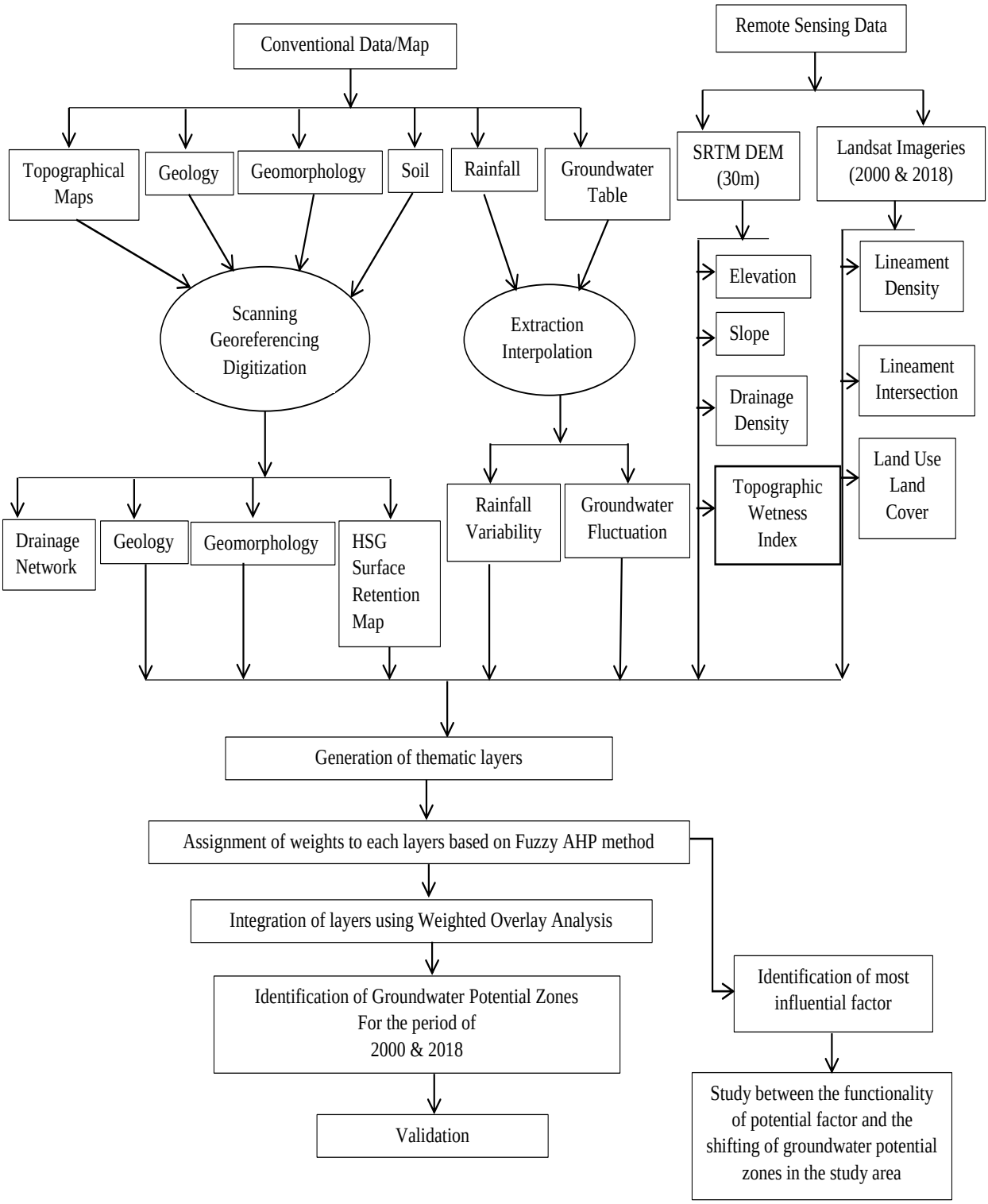

Figure 6.25 *Methodological Flow Chart of the Study*

Table 6.22 *Details of the Used Dataset*

Data type	Details of data	Sources	Time period	Used for
Topographical Maps(1:50,000)	72L/ 14, 72L/15, 72L/16, 72P/2, 72P/3, 72P/4, 72P/6, 72P/7, 72P/8, 72P/16, 73M/1, 73M/5, 73M/9, 73M/10, 73M/13, 73M/14, 76M/6, 79A/1, 79A/2	Survey of India (SOI)	1972	Drainage network
SRTM DEM	Resolution- 30m	USGS Earth explorer (https://earthexplorer.usgs.gov/)	2005	Relief, Slope, Drainage Density, Topographic Wetness Index
TRMM Gridded Precipitation Data	Grid size 0.25º × 0.25º	GESDISC website (https://disc.gsfc.nasa.gov/)	2000 and 2018	Rainfall variability
Satellite Imagery	Path: 139 Row: 43 and 44 Resolution: 30 m	USGS Earth explorer (https://earthexplorer.usgs.gov/)	2000 and 2018	Lineament Density, Lineament Intersection, Land Use Land Cover
Geological Map	Scale 1: 2, 50,000	Geological Survey of India (https://www.gsi.gov.in)	--	Geology
Geomorphological map	Scale 1: 50, 000	BHUVAN (https:// bhuvan.nrsc.gov.in/bhuvan_links.php)	--	Geomorphology
Soil Data	Scale 1: 2, 50,000	National Bureau of Soil Survey and Land Use Planning	--	Hydrological Soil Group, Surface Retention
Groundwater Level Data	Pre and post monsoon well data	Central Groundwater Board (http://cgwb.gov.in/)	2000 and 2018	Groundwater fluctuation

- **Data Source and Preparation of the Thematic Layers**

This study emphasizes the functionality of land use land cover on the evaluation of groundwater potential zone. To fulfil the objective and assess the impact of land-use alteration on groundwater resources, Landsat 7 Enhanced Thematic Mapper Plus (ETM+) and Landsat 8 Operational Land Imager (OLI) (https://earthexplorer.usgs.gov/) has been used to classify each land use class by applying maximum likelihood supervised classification method in ERDAS Imagine 9.3 software. The spatial and temporal resolutions of the used datasets have been mentioned in table 6.22.

In the next step, the delineation of groundwater potential zones for 2000 and 2018 has been executed using 13 different hydrogeological and hydro-geomorphological parameters which are very much influential to identify the potential areas of groundwater resources in any region (Jhariya et al. 2016). These are- relief, slope, geology, geomorphology, lineament density, lineament intersection, hydrological soil group, surface retention, drainage density, topographical wetness index, rainfall variability, land use land cover, and groundwater table fluctuation. All these parameters have been classified into two sub-types i.e. subjective parameters and objective parameters. Subjective parameters are those which cannot be directly perceived like geology, geomorphology, and rainfall condition of an area; while the objective parameter defines the parameters that can be directly perceived and quantified as well as land use land cover of a region. Using various conventional datasets and satellite imageries, the development of the thematic layers of each parameter has been done in a GIS environment. Survey of India (SOI) topographical maps have been used to prepare the base map of the study area. All these maps were georeferenced and digitized in Arc GIS 10.3 software, through which the network of streams has been extracted. The relief, slope, topographic wetness index, and drainage density map have been generated from Shuttle Radar Topography Mission (SRTM) digital elevation model (DEM) having a 30m resolution. To calculate the rainfall variability of the study area, TRMM monthly gridded rainfall data ($0.25^{o} \times 0.25^{o}$) has been retrieved from the GESDISC website (https ://disc.gsfc.nasa.gov/) for 20 rain gauge stations and the map has been prepared using Arc GIS 10.3 software by applying inverse distance weight (IDW) method. The geology and geomorphological aspects of the river basin have been studied from the map produced by the Geological Survey of India (GSI) (https://www.gsi.gov.in) and BHUVAN thematic services of National Remote Sensing Centre (NRSC) (https:// bhuvan.nrsc.gov.in/bhuvan_links.php) of Hyderabad, having a scale of 1: 2, 50,000 and 1: 50, 000 respectively. Soil map has been obtained from National Bureau of Soil Survey and Land

Use Planning (NBSSLUP) having a scale of 1: 2, 50, 000. The map has been geographically rectified and digitized in a GIS environment to classify the various soils into Hydrological Soil Group (HSG), developed by Soil Conservation Service (SCS). In addition, extraction of the lineament features has been performed through visual interpretation of the Landsat satellite imageries to produce lineament density and lineament interaction map of the study area. Seasonal groundwater level data has been acquired from the website of Central Groundwater Board (CGWB) (http://cgwb.gov.in/) from where 62 observation wells of the study area and other wells from the adjoining parts has been selected to retrieve the water table data in pre and post-monsoon season. Finally, the fluctuation map of the groundwater table depth has been analysed using the IDW tool in Arc GIS 10.3 software.

- **Land Use Land Cover Classification**

Classification of land use land cover of a region is an important approach to understand how the land utilization pattern can influence the hydrological processes. The response of groundwater recharge into the aquifer system is highly varied with individual land use classes. Like in forest cover areas the process of infiltration will increase than in built-up areas which reduces the water penetration and increases the surface runoff as well (Mishra et al. 2014). Following such relation, supervised classifications have been carried out on Landsat satellite imageries using a maximum likelihood algorithm for 2000 and 2018. Total eleven classes have been classified for both the period; these are- Dense vegetation, Laterite exposer, River/ water bodies, Reservoirs, Sand bar, Agricultural land, Wet fallow land, Dry fallow land, Wasteland, Settlement, Homestead with plantation. The whole classification methodology has been done in ERDAS Imagine 9.2 software using AOI and signature editor tool.

- **Accuracy Assessment**

Accuracy assessment is an important part of land use land cover classification, as it reveals the performance of the classification having correctly classified classes. In this study, a non-parametric Kappa statistical analysis (k) has been done, which calculates the overall classification accuracy (OCA), producer's accuracy (PA), user's accuracy (UA), and generates the kappa coefficient index (k). Here, the overall classification accuracy has been assessed for the land use land cover maps for both 2000 and 2018, using the following formula (Cohen 1960)

$$k = \frac{P_o - P_e}{1 - P_e} \qquad (6.47)$$

where, P_o=relative observed agreement, P_e= hypothetical probability of chance agreement

- **Application of Fuzzy AHP Method to Delineate Groundwater Potential Zones**

In this study, Fuzzy Analytical Hierarchical Process (FAHP) technique has been employed for the decision-making analysis of various parameters selected to explore the groundwater potential zones in the Mayurakshi river basin area. The fuzzy extension of the AHP method has been proven as a more consistent decision-making method that solves the hierarchical fuzzy problems compared to the AHP method (Laarhoven and Pedrycz 1983; Buckley 1985a/b; Chang 1996). However, there are some other methods rooted within the scope of the FAHP technique. To fulfil the objective of the present work, Buckley's method of FAHP technique has been implemented, where every criterion has been evaluated through linguistic variables (Table 6.23) and the determination of fuzzy weights has been done based on the geometric mean method. The steps of the method are summarized as follow:

Step 1: Construction of fuzzy pairwise comparison matrix by assigning linguistic variables (Table 6.23) among all the criteria. The result of constructed fuzzy pairwise matrix ($\tilde{A}$) shown in equation 6.48.

$$\tilde{A}=\begin{bmatrix} \tilde{1} & \tilde{a}_{12}\cdots & \tilde{a}_{1n} \\ \tilde{a}_{21} & \tilde{1} \;\vdots & \tilde{a}_{2n} \\ \vdots & \vdots\ddots & \vdots \\ \tilde{a}_{n1} & a_{n2\ldots} & \tilde{1} \end{bmatrix}=\begin{bmatrix} \tilde{1} & \tilde{a}_{12}\cdots & \tilde{a}_{1n} \\ 1/\tilde{a}_{21} & \tilde{1} \;\vdots & \tilde{a}_{2n} \\ \vdots & \vdots\ddots & \vdots \\ 1/\tilde{a}_{n1} & 1/a_{n2\ldots} & \tilde{1} \end{bmatrix} \quad (6.48)$$

Step 2: Computation of fuzzy geometric mean ($\tilde{r}_i$) to each of the criteria using equation 6.49.

$$\tilde{r}_i = [\tilde{a}_{i1} \quad \otimes \ldots\ldots\ldots \otimes \quad \tilde{a}_{in}]^{1/n} \quad (6.49)$$

where, $\tilde{a}_{1n}$ is the fuzzy value of the ith criterion to the criterion nth.

Step 3: In the next step, calculation of the fuzzy weight of each criterion ($\widetilde{W}_i$) has been done executing the following equation 6.50.

$$\widetilde{W}_i = \tilde{r}_i \otimes (\tilde{r}_1 \oplus \tilde{r}_2 \oplus \ldots\ldots \oplus \tilde{r}_n)^{-1} \quad (6.50)$$

Step 4: Next the fuzzy weight ($\widetilde{W}_i$) numbers are needed to be de-fuzzified by the method of the center of the area using equation 6.51.

$$M_i = \frac{l_{w_i} + m_{w_i} + u_{w_i}}{3} \quad (6.51)$$

Step 5: In the final step, a normalization of the fuzzy weight (N_i) has been done by equation 6.52.

$$N_i = \frac{M_i}{\sum_{i=1}^{n} M_i} \quad (6.52)$$

Table 6.23 *Linguistic Variables for Constructing Pairwise Comparison Matrix*

Saaty scale	Linguistic variable	Triangular fuzzy number	Triangular fuzzy reciprocal number
1	Equal	(1, 1, 1)	(1, 1, 1)
3	Moderately Importance	(2, 3, 4)	(1/4, 1/3, 1/2)
5	Strongly Importance	(4, 5, 6)	(1/6, 1/5, 1/4)
7	Very Strongly Importance	(6, 7, 8)	(1/8, 1/7, 1/6)
9	Extremely Importance	(9, 9, 9)	(1/9, 1/9, 1/9)
2	Intermediate Values	(1, 2, 3)	(1/3, 1/2, 1)
4		(3, 4, 5)	(1/5, 1/4, 1/3)
6		(5, 6, 7)	(1/7, 1/6, 1/5)
8		(7, 8, 9)	(1/9, 1/8, 1/7)

Executing the above-mentioned steps, the weight of each criterion has been calculated and the result declares the criteria having the highest weight are the most influential than criteria having the lowest weight. The pair-wise comparison matrix and derived normalized weight of the 13 selected parameters are presented in table 6.24. Finally, incorporating the weight and ranking of each parameter a dimensionless groundwater potential index (GWPI) has been created which reveals the land-use specific potential groundwater resources sites of the study area. Such kind of estimation of past and present land use land cover alteration with respect to the changes in groundwater recharge potential sites are prerequisites for the development of proper land use planning and management for the betterment of future land capability and water resources scenario as well.

The GWPI of the Mayurakshi river basin area has been generated computing the following formula-

$$GWPI = [R * R_w + S * S_w + G * G_w + LD * LD_w + LI * LI_w + GM * GM_w + HSG * HSG_w + TWI * TWI_w + Dd * Dd_w + Rv * Rv_w + GWF * GWF_w + LULC * LULC_w + Sr * Sr_w] \quad (6.53)$$

where, $GWPI$ denote Groundwater Potential Index, R is the Relief, S is the Slope, G is the Geology, LD is the Lineament Density, LI is the Lineament Intersection, GM is the Geomorphology, HSG is the Hydrological Soil Group, TWI is the Topographic Wetness Index, Dd is the Drainage Density, Rv is the Rainfall Variability, GWF is the Groundwater Fluctuation, $LULC$ is the Land Use Land Cover, Sr is the Surface Retention and the subscript w indicate the weight of the respective parameters. All the thematic layers have been reclassified and combined in a GIS platform using the weighted overlay analysis method. Afterward, Jenks natural break classification method has been adopted to classify the output into five qualitative classes like very high, high, moderate, low, and very low groundwater potential zone to ensure the maximum homogeneity between each criterion.

- **Validation**

For validating the output of the FAHP model, the groundwater potential zone has been verified with the water level data obtained from the CGWB website for the year 2000 and field observed water level data for 2018. The water level in mbgl has been measured using Temperature, Water Level, and Conductivity meter (TLC) from different dug wells located within the river basin area.

6.7.3. Results and Discussions

- **Areal Changes in Land Use Land Cover Map from 2000 to 2018**

A strong relationship exists between land utilization and groundwater resource management. The association between every land-use practice can have an irreversible impact on the aquifer system, as it controls the movement of water into the ground surface (www.gwp.org). In this study, 11 land use land cover classes have been identified from the image classification for both 2000 and 2018 (Fig. 6.26l). To know the accuracy of each classification, Kappa co-efficient has been calculated (0.89 for 2000 and 0.93 for 2018), which shows that the generated land use land cover maps and the output of accuracy assessments are comparable with each other (Shen et al. 2013; Li et al. 2014). Changes in the areal statistics of each land use land cover class from the period of 2000 to 2018 have been studied to understand the quantitative changes in land-use practices and their effect on the groundwater recharging process over the study area. The result presented in table 6.25 depicts that the agricultural land has been increased by 635.36 sq. km (10.9%) to 1366.80 sq. km (10.9%) with a positive change of 731.44 sq. km (12.57%), while the dry fallow land and wasteland area have decreased by 2055.75 sq. km (35.27%) to 970.83 sq. km (16.67%) and 414.97 sq. km (7.12%) to 280.07 sq. km (4.81%) respectively. The result also suggests that within the time of 18 years, the settlement has also accelerated from 124.87 sq. km (2.14%) to 174.30 sq. km (2.14%) with a positive change of 0.85% of the total area. The rapid growth of population could be the reason for the expansion of agricultural land as well as wet fallow land of the study area. From the above-mentioned explanation, it is also clear that the reduction in dry fallow land, wasteland, and increase of the settlement, agricultural land, and water bodies have put an effect on the recharging capacity in groundwater storage of the study area (Elmahdy et al. 2017).

Table 6.24 *Pairwise Comparison Matrix and Derived Normalized Weight of the Selected 13 Parameters*

	***R**	**S**	**G**	**LD**	**LI**	**GM**	**HSG**	**TWI**	**Dd**	**Rv**	**GWF**	**LULC**	**Sr**	**Normalised Weight**
R	(1,1,1)	(9,9,9)	(1,1,1)	(6,7,8)	(6,7,8)	(9,9,9)	(1,1,1)	(2,3,4)	(9,9,9)	(2,3,4)	(6,7,8)	(1/9, 1/9,1/9)	6,7,8	0.1581
S	1/9, 1/9, 1/9	(1,1,1)	(1,1,1)	1/9, 1/9, 1/9	1/6,1/7, 1/8	(1,1,1)	(1,1,1)	4,5,6	9,9,9	2,3,4	4,5,6	1/9, 1/9,1/9	9,9,9	0.0508
G	(1,1,1)	(1,1,1)	(1,1,1)	1/6,1/7,1/8	1/6,1/7, 1/8	(1,1,1)	6,7,8	1/2,1/3, 1/4	4,5,6	(1,1,1)	1/6,1/7,1/8	1/9, 1/9, 1/9	6,7,8	0.0399
LD	1/6,1/7,1/8	9,9,9,	6,7,8	(1,1,1)	9,9,9,	(1,1,1)	2,3,4	2,3,4	6,7,8	(1,1,1)	9,9,9,	1/2,1/3,1/4	4,5,6	0.1253
LI	1/6,1/7,1/8	6,7,8	6,7,8	1/9, 1/9,1/9	(1,1,1)	(1,1,1)	(1,1,1)	2,3,4	6,7,8	(1,1,1)	9,9,9,	1/2,1/3,1/4	4,5,6	0.0805
GM	(1/9, 1/9,1/9)	1,1,1	1,1,1	1,1,1	1,1,1	(1,1,1)	2,3,4	4,3,2	2,3,4	1,1,1	4,5,6	1/6,1/7,1/8	4,5,6	0.0623
HSG	(1,1,1)	(1,1,1)	1/6,1/7, 1/8	1/2,1/3,1/4	(1,1,1)	1/2,1/3, 1/4	(1,1,1)	1/2,1/3, 1/4	1/6,1/7, 1/8	(1,1,1)	(1/9, 1/9,1/9)	1/4,1/5,1/6	(1/9, 1/9,1/9)	0.0200
TWI	1/2,1/3,1/4	1/4,1/5, 1/6	2,3,4	1/2,1/3,1/4	1/2,1/3, 1/4	2,3,4	2,3,4	(1,1,1)	4,5,6	2,3,4	4,5,6	1/4,1/5,1/6	4,5,6	0.0652
Dd	(1/9, 1/9,1/9)	(1/9, 1/9,1/9)	1/4,1/5, 1/6	1/6,1/7,1/8	1/6,1/7, 1/8	1/2,1/3, 1/4	6,7,8	1/4,1/5, 1/6	(1,1,1)	9,9,9	(1/9, 1/9,1/9)	1/4,1/5,1/6	6,7,8	0.0306
Rv	1/2,1/3,1/4	1/2,1/3, 1/4	(1,1,1)	(1,1,1)	(1,1,1)	(1,1,1)	(1,1,1)	1/2,1/3, 1/4	(1/9, 1/9,1/9)	(1,1,1)	(1/9, 1/9,1/9)	(1/9, 1/9,1/9)	6,7,8	0.0288
GWF	1/6,1/7,1/8	1/4,1/5, 1/6	6,7,8	(1/9, 1/9,1/9)	(1/9, 1/9,1/9)	2,3,4	9,9,9	1/4,1/5, 1/6	9,9,9	9,9,9	(1,1,1)	1/4,1/5,1/6	9,9,9	0.0554
LULC	9,9,9	9,9,9	9,9,9	2,3,4	2,3,4	6,7,8	4,5,6	4,5,6	4,5,6	9,9,9	4,5,6	(1,1,1)	6,7,8	0.2706
Sr	1/6,1/7,1/8	1/9, 1/9, 1/9	1/6,1/7, 1/8	1/4,1/5,1/6	1/4,1/5, 1/6	1/4,1/5, 1/6	9,9,9	1/4,1/5, 1/6	1/6,1/7, 1/8	1/6,1/7, 1/8	1/9, 1/9, 1/9	1/6,1/7,1/8	(1,1,1)	0.0124

Table 6.25 *Areal Changes in Land Use Land Cover Classes in the Study Area from 2000 to 2018*

LULC classes	Year 2000 Area in sq. km (%)	Year 2018 Area in sq. km (%)	Area changes (sq. km)	Area changes (%)	Nature of changes in relation with groundwater recharge potentiality
Dense vegetation	53.55 (0.92)	214.97 (3.69)	161.42	2.77	Positive
Laterite exposer	125.49 (2.15)	145.83 (2.50)	20.34	0.35	Negative
River/ water bodies	51.87 (0.89)	80.58 (1.38)	28.71	0.49	Positive
Reservoirs	31.02 (0.53)	18.61(0.32)	-12.41	-0.21	Negative
Sand bar	22.45 (0.39)	6.53 (0.11)	-15.92	-0.27	Negative
Agricultural land	635.36 (10.90)	1366.80 (23.47)	731.44	12.57	Positive
Wet fallow land	2012.08 (34.52)	2373.37 (40.75)	361.29	6.23	Positive
Dry fallow land	2055.75 (35.27)	970.83 (16.67)	-1084.93	-18.60	Positive
Waste land	414.97 (7.12)	280.07 (4.81)	-134.89	-2.31	Positive
Settlement	124.87 (2.14)	174.30 (2.99)	49.43	0.85	Negative
Homestead with plantation	301.38 (5.17)	196.89 (3.38)	-104.49	-1.79	Negative
Total	**5828.78 (100)**	**5828.78 (100)**			

Conditioning Factors to Delineate Groundwater Potential Zones

- **Relief (R)**

The relief of any region plays a major role in the assessment of groundwater prospect zone. It has a direct relation with the surface runoff and overland flow. In a steep relief area, the number of runoff increases than the rate of infiltration and percolation, which tend the region low recharge capable from the low relief region. The relative relief of the study area varies from 166 meters to less than 20 meters (Fig. 6.26a). The upper part of the basin comprises some rocky hillocks formed due to the effect of active denudational activity, whereas the lower part of the study area characterized by low lying topography having numerous rills and gullies represents a homogenous plain surface, which permits more water retention and recharging capacity into the groundwater storage. Based on the nature of the relief of the study area, the calculated weightage (0.158) has been assigned to the parameter shown in table 6.24.

- **Slope (S)**

The slope is another important parameter influencing the occurrence and movement of groundwater significantly. An area having a high slope has been categorized as a poor recharge potentiality due to a low rate of infiltration and high runoff (Kumar and Krishna 2016). Other than that, the steep slope area permits more overland flow towards the gentle slopy region to enrich the groundwater storage. Here, the slope map of the study area has been prepared using SRTM DEM (30 m resolution) and classified into five classes ranging from less than 1 to 42 degrees. As observed from figure 6.26b, the general trend of the slope of the basin is from the

north-west to the eastern direction. The assigned weight to this parameter has been shown in table 6.24.

- **Geology (G)**

The geology of a region plays a critical role by providing important information regarding the hydrogeological aspects on which the nature of groundwater recharge potentiality has been dependent (Chowdhury 2010). Geologically, the studied river basin has been composed of 10 different geological units namely Acid granulite, Alternative layers of Sand, Silt and Clay, Augen gneiss and megmatite, Hard clays impregnated with caliche nodules, Homblend schist and amphibolite, Laterite and lateritic soil, Sandstones, and shales, Siltstone, sandstone and shale with alluvium, Unclassified granite gneiss with enclaves of metamorphic and Basalt intra-trappen bed (Fig. 6.26c). A major portion of the study area has been covered with the unclassified granitic and gneiss formation which may be considered as an extended portion of the Chhotonagpur Plateau shield region. Similarly, basaltic intratrappean bed and sub recent lateritic and alluvium composition have also been observed in the lower part of the river basin which exhibits a good groundwater prospect in the study area. The calculated weight of this parameter has been presented in table 6.24.

- **Lineament Density (LD)**

Lineaments are the geologically linear features that can give a better prediction to identify the potential groundwater recharge zone (Rao et al. 2001). Such features are the surface expression of faults, cracks, and joints that occurs within the bedrock and induce the movement of groundwater. So, mapping of lineament features is very much beneficial to explore the groundwater prospect zone. Using high-resolution satellite imageries, such as linear curvatures can be easily determined (Pradhan et al. 2006).

In this study, Landsat 8 has been used to extract the lineament features, and a grid-based lineament density mapping has been done using Arc GIS software (Kumar and Krishna 2016; Sener et al. 2018). The density map has been classified into five classes where the value ranges from 0 (no lineament) to 2.70 km/sq. km (very high lineament density) (Fig. 6.26d). The highest density observed in the upper part of the basin suggests the good prospect of groundwater recharge than the lower part having the least lineament density. Accordingly, the weight has been determined for this parameter shown in table 6.24.

- **Lineament Intersection (LI)**

Joining points of two or more linear features are demarcated as a lineament intersection point. Such intersection points are denoted as a more permeable zone which may provide an easy path for groundwater movement. From figure 6.26e it has been observed that the upper part of the river basin has been dominated with closely spaced lineament intersection points that enable the region more capable of groundwater recharge than the lower part of the basin having a long distance from the intersection points. The assigned weight to the parameter has been shown in table 6.24.

- **Geomorphology (GM)**

Geomorphology is the science of landforms that deals with the landforms processes in the earth's surface and generates topographic variations. The study of various morphological units plays an imperative role to assess the groundwater potential zone as it can control the surface and subsurface flow of groundwater (Kumar and Krishna 2016). The study area has several geomorphic units like anthropogenic terrain, denudation and structural origin of low and moderate dissected hills and valleys, the denudational origin of pediment peneplain complex, and fluvial origin of older and active flood plains (Fig. 6.26f). Among them, about 33.09% of the study area has been embedded with the pediment pediplain complex landform. Several denudational activities, including weathering of rocks, the formation of moderate to low dissected hills, and small patches of anthropogenic terrains, are very much observable in this region. Around this rocky landscape, fabrication of the Massanjore dam is classified under the anthropogenic terrain feature of the study area. Whereas the lower part of the river basin has been characterized by the alluvium flood plain. Due to the higher porosity, permeability, and water retention capacity of any alluvium and flood plain deposition has been considered for potential groundwater resource area whereas the areas comprised of residual hills and rocky topography, which encourages high surface runoff properties may be unsuitable for the development of potential groundwater resource area hence weightage has been assigned accordingly (Table 6.24).

- **Hydrological Soil Group (HSG)**

The amount of surface water penetration within the aquifer system has been highly dependent on the soil type of the area. It can regulate the rate of infiltration and percolation into the soil, depending on which the groundwater level varies. Based on infiltration, runoff and major soil

texture characteristics, the soil map of the study area has been prepared using NBSSLUP soil map (scale 1:2,50, 000) and classified into four classes (A, B, C, and D) of hydrological soil group as developed by the Soil Conservation Services (SCS) of the USA in 1969. The characteristics of four HSG related to the groundwater recharging capacity are represented in table 6.26.

Such classification of soil groups may reflect the nature of runoff potentiality and groundwater recharge capability of a particular area. The study area has been categorized into four HSG as shown in figure 6.26g. The river basin has been majorly dominated with the group C soil type indicating an average infiltration rate with moderate low potential of the groundwater resource. The assigned weight of this parameter has been given in table 6.24.

Table 6.26 *Relationship between Hydrological Soil Groups and Groundwater Potentiality*

Hydrological Soil Group	Type	Runoff potentiality	Groundwater recharge potentiality
A	Deep, well-drained sands and gravels	Low	High
B	Moderately drained, moderately fine to moderately fine texture	Moderately low	Moderately high
C	Moderately fine to fine texture	Moderately high	Moderately low
D	Clay soils, soils with a high water table	High	Low

- **Topographic Wetness Index (TWI)**

Topographic Wetness Index is a compound topographic index that quantifies several hydrological processes controlled by the prevailing topography (Schillaci et al. 2015). This index has been developed by Beven and Kirkby (1979) depending on the idea of water distribution and accumulation on different terrain conditions. In this study using SRTM DEM (30 m resolution), TWI has been calculated in Arc GIS 10.3 software. Figure 6.26h shows a higher value of TWI indicates high water accumulated area considered for a good groundwater potential zone. Whereas the areas having low TWI values are regarded as dry and poor groundwater potential zone as well. The calculated fuzzy weight of this factor has been shown in table 6.24.

- **Drainage Density (D_d)**

Drainage Density is another important parameter for the evaluation of groundwater potentiality of a region. This index quantitatively expresses the nature of terrain conditions on which the amount of runoff, permeability of the soil, development of stream network varies from place to place (Nag et al. 2020). It depends on several factors like underground bedrock structure,

amount of rainfall, soil properties, slope, types of vegetation, etc. From the groundwater recharge point of view, drainage density has an indirect relation with the infiltration of groundwater to the aquifer system. Here, five classes of drainage density have been observed ranging from 0.00008 km/ sq. km to 0.0011 km/sq.km (Fig. 6.26i). Following the inverse relationship between drainage density and groundwater recharge potentiality, the area having a high D_d value considered for poor groundwater potential zone and area having low D_d value is suitable for rich ground resources due to high rate of infiltration and permeability. The assigned weightage of the parameter has been presented in table 6.24.

- **Rainfall Variability (Rv)**

Rainfall is the major source of groundwater recharge in any region. The variation in the amount of rainfall may control the infiltration of water into the aquifer system. Therefore, spatio-temporal variation in the amount of rainfall has been crucial for the evaluation of groundwater potential zone.

In this work, the thematic layers of rainfall variability have been prepared for 2000 and 2018 to study the temporal variation of rainfall distribution and its impact on potential groundwater resource evaluation. The monthly gridded rainfall data has been downloaded from the TRMM website (https://disc.gsfc.nasa.gov/) for 20 rain gauge stations and applying the method of IDW in Arc GIS software, the monthly average rainfall variability map has been generated. The output map has been categorized into five classes shown in figure 6.26j. Significant changes have been observed in the distribution of maximum average rainfall amount which has shifted from the north-eastern part to the south-eastern part of the basin between the periods of 2000 to 2018. Such temporal shifting in rainfall distribution patterns can affect the groundwater recharging condition accordingly. The assigned weight in this regard has been shown in table 6.24.

- **Groundwater Table Fluctuation (GWF)**

Analysis of groundwater fluctuation is an important aspect in the study of groundwater management. Variation in groundwater table is affected by both natural processes including the lean amount of rainfall and anthropogenic activities like over-pumping of groundwater. To understand the impact of seasonal groundwater fluctuation on the assessment of groundwater potential zone over the study area, pre, and post-monsoon groundwater level data has been downloaded for 62 observation wells for 2000 and 2018 which are monitored by the Central

Groundwater Board (CGWB). In West Bengal, pre-monsoon water table data has been collected in April and post-monsoon data has been retrieved during November (Patra *et al.* 2018). Such seasonal fluctuation analysis may enable us to understand the natural and anthropogenic stresses in groundwater recharge in a specific area. By registering the geographical locations of all the observation wells in a GIS platform, the spatial distribution map of groundwater table fluctuation for the year 2000 and 2018 has been prepared (Fig. 6.26k).

In this study, the maximum groundwater fluctuation for both 2000 and 2018 has been observed in the lower part of the basin where extensive uses of submersible shallow pumping can be very much seen to fulfil the demand of irrigation need. The assigned weight of this parameter has been shown in table 6.24.

- **Land use land cover (LULC)**

In the case of groundwater recharge potentiality, land use land cover of a region plays a vital role as after the rainfall events the initial penetration of water into the aquifer depends upon the types of land use land cover of that particular region. Here, the classified Landsat satellite imageries of land use land cover for 2000 and 2018 (Fig. 6.26l) shows that agricultural land and wet fallow land are highly noticeable over the study area which allows more groundwater to percolate into the aquifer, whereas the presence of dry fallow land and increase in settlement area can hinder the recharging process. The assigned weight of this parameter has been presented in table 6.24 accordingly.

- **Surface Retention (S_r)**

Surface retention is also known as surface storage which defines a portion of storm rainfall that becomes stored in a surface depression and has maximum retention capacity depending on the nature of the soil, vegetation, and land use land cover of that particular area (Subramanya 1984). It has been calculated just one step before the runoff calculation based on the SCS curve number (CN) method using the Eq. 6.54

$$S = \frac{25400}{CN} - 254 \qquad (6.54)$$

where S denote surface retention, CN represents curve number and 254 is used as a constant value to express the surface retention in mm.

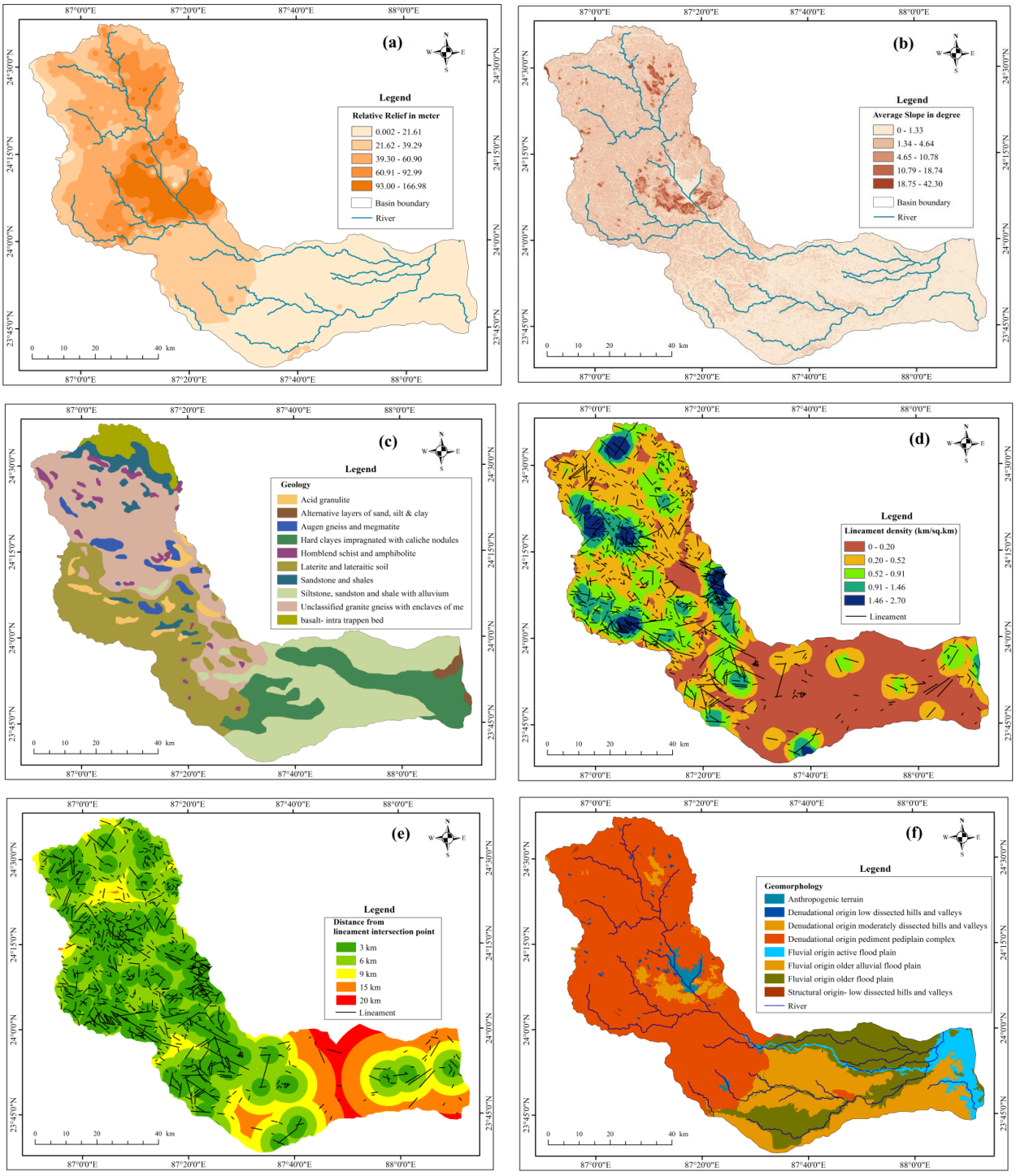

Figure 6.26 *Influential factors for the generation of groundwater potential zonation map of the Mayurakshi river basin: (a) Relief, (b) Average slope, (c) Geology, (d) Lineament Density, (e) Lineament Intersection, (f) Geomorphology, (g) Hydrological Soil Group, (h) Topographic Wetness Index, (i) Drainage Density, (j) Rainfall Variability, (k) Groundwater Fluctuation, (l) Land Use Land Cover, (m) Surface Retention*

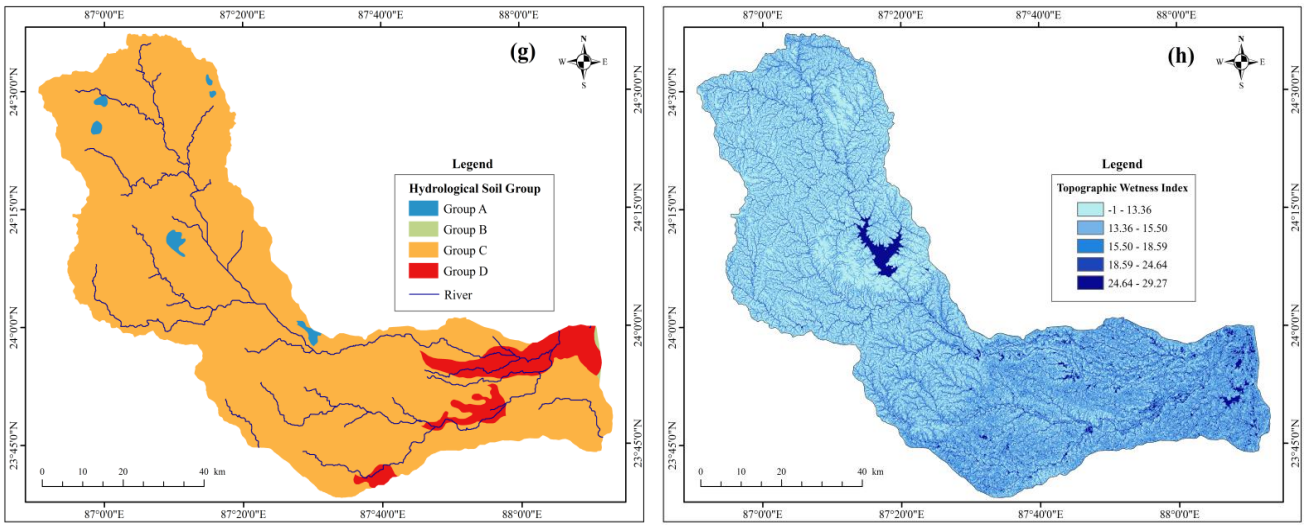

Figure 6.26 *Continued*

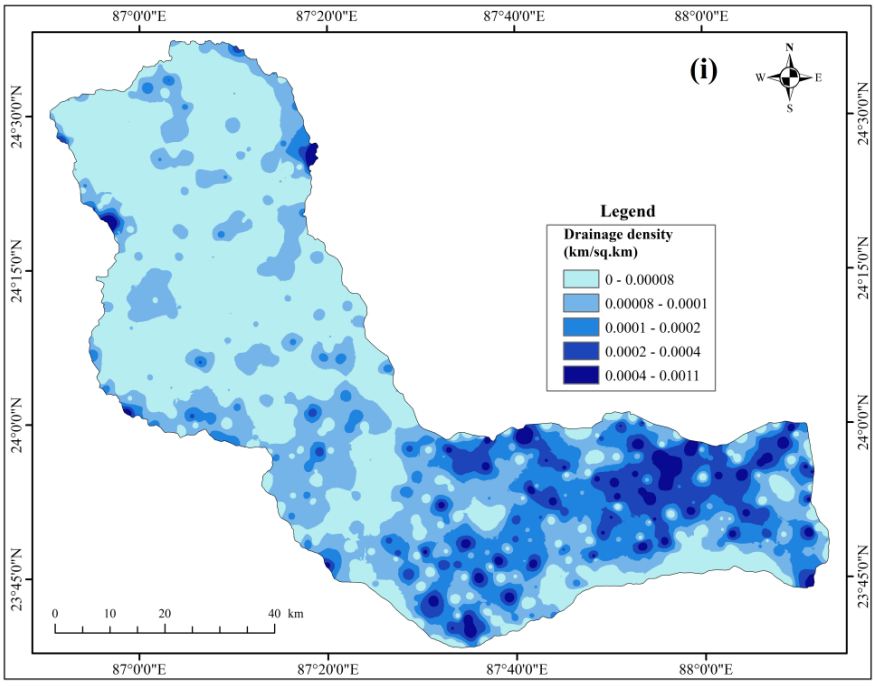

Figure 6.26 *Continued*

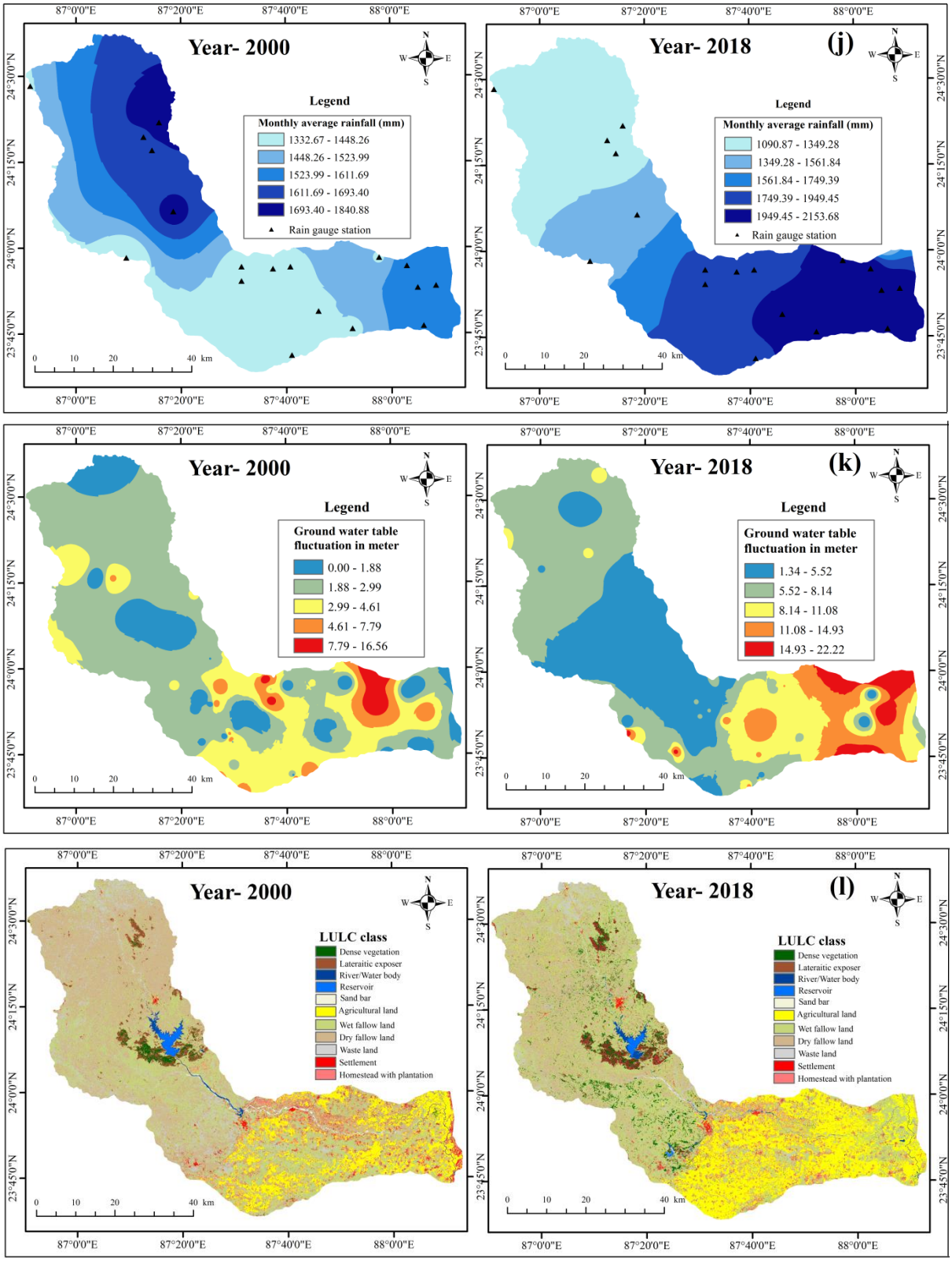

Figure 6.26 *Continued*

In this study, the surface retention of the river basin has been calculated based on the classified pre-monsoonal land use land cover map for 2000 and 2018. Hence, because of the very low precipitation in both period, the spatial distribution of surface runoff generated from each land use land cover cannot be quantified. For such reason, surface retention from each land use land cover has been calculated and represented in the surface layer shown in figure 6.26m. It has a direct relation with the penetration of water into the storage. The highest S_r value has been observed around the natural vegetation, wet fallow land indicating maximum water storage and high groundwater recharge as well. Another significant observation has been made that with the temporal changes in the areal extent of each LULC class; the surface storage capacity will also change and affect the groundwater recharging system accordingly. So the analysis of surface retention has been considered as an impactful criterion to explore the groundwater prospect zone in this present work and the assigned weight has been presented in table 6.24.

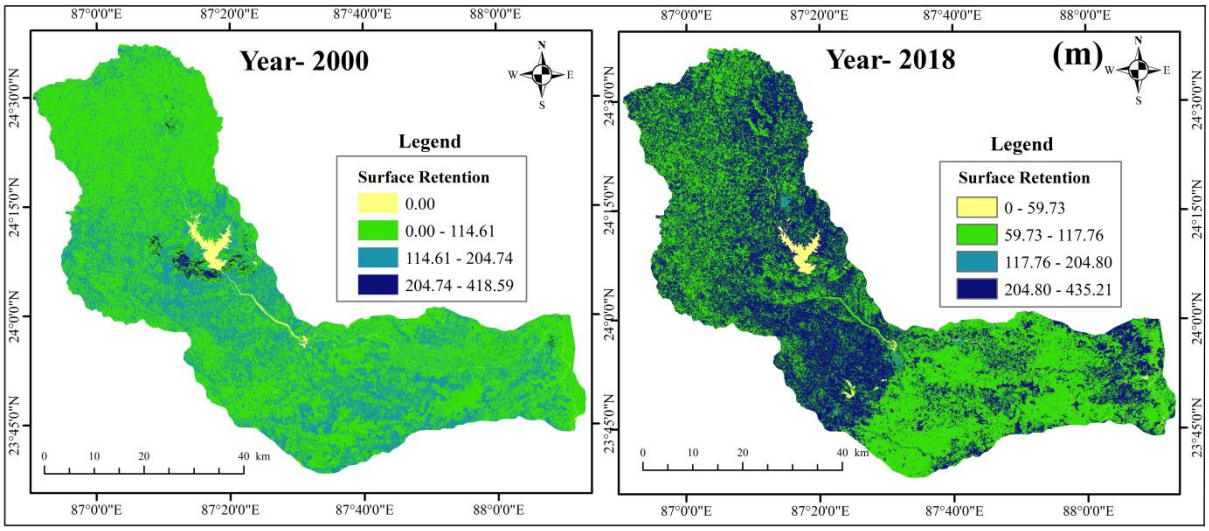

Figure 6.26 *Continued*

- **Evaluation of Groundwater Potential Zone and Its Spatio-Temporal Variations for the Year 2000 & 2018**

The evaluation of groundwater potential zones in the Mayurakshi River basin area has been executed using 13 different influential factors that have a control on the movement of groundwater. The relationship between each parameter with the occurrence of groundwater or the prospect zone of groundwater has been discussed in detail from where some of the parameters reveal an uncertain nature of the occurrence. A significant temporal variability has been observed in the distribution of mean annual rainfall, the occurrence of groundwater fluctuation around the study area. Similarly changes in the areal extent of each land use land cover classes along with the nature of surface retention capacity have also been discovered.

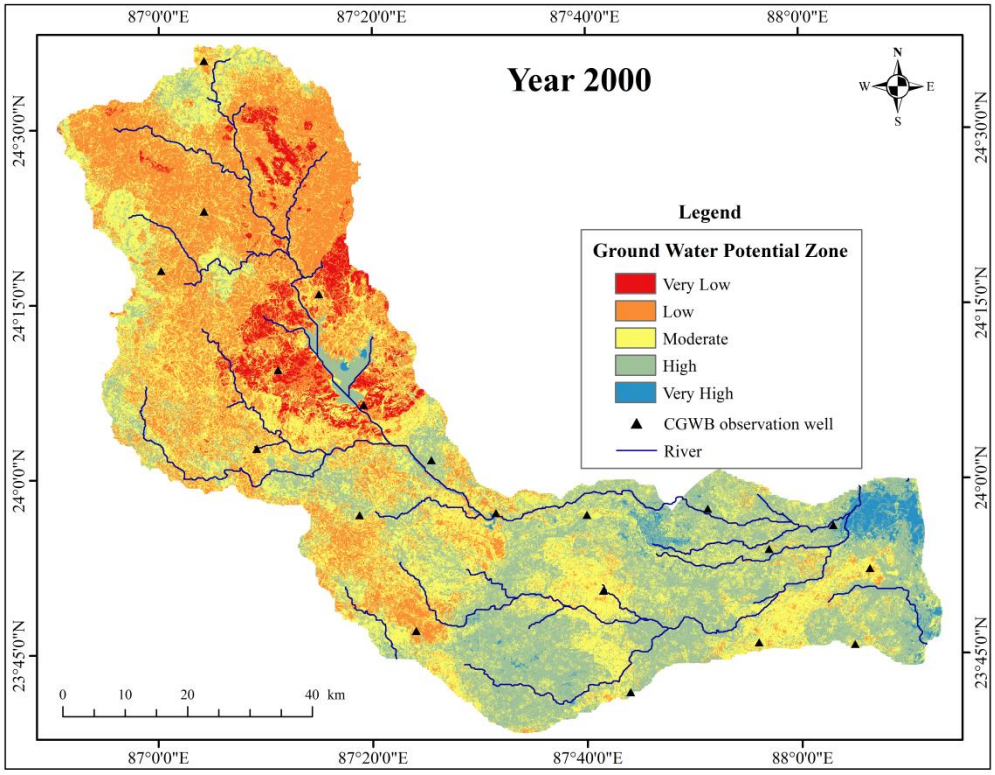

Figure 6.27 *Groundwater Potential Zones of Mayurakshi River Basin for the Period of 2000*

Such kind of temporal modifications in the characteristics of groundwater controlling parameters may shift the potential zone of groundwater resources from one year to another. In this backdrop, to avoid the variable nature of the influential parameters, analyse of rainfall, groundwater table fluctuation, land use land cover, and surface retention have been studied for the year 2000 and 2018 and taken as an input parameter to explore the groundwater potential zones for the respective period.

The groundwater potential zone index maps for both years have been generated using the weighted overlay analysis method in Arc GIS software assigning the equation 6.53. The weight of the selected 13 parameters has been calculated adopting the methodologies of the FAHP technique. The calculated normalized weight of each parameter has been derived from the pairwise comparison matrix and presented in table 6.24, where land use land cover has got the maximum weightage (0.2706) followed by relief (0.1581), lineament density (0.1253), and so on. However, the presence of water bodies, a drainage network may be considered as a vital source of groundwater recharge, but the increase of drainage network in a particular area may create drainage congestion which promotes more surface runoff and restrict the penetration of water into the aquifer (Patra et al. 2018). The generated groundwater potential map of the study area for 2000 and 2018 has been classified into five classes namely very low, low, moderate,

high, and very high potential zone (Fig. 6.27 & 6.28). The result for the year 2000 revealed that 244.85 sq. km (4.2%) are accounted for the very low potential zone, 1572.15 sq. km (26.97%) area shows low potential zone, 2166.73 sq. km (37.17%) area fallen under the moderate potential zone, 1656.64 sq. km (28.42%) area under the high potential zone and 188.39 sq. km (3.23%) area comprised of the very high potential zone.

On the other hand, a remarkable change has been observed in every class of ground potential zone map for the year 2018. The resultant classification shows 109.78 sq. km (1.88%), 427.08 sq. km (7.33%) and 2304.55 sq. km (39.54%) areas have been accounted for very low, low and moderate potential zone while the area of 2609.38 sq. km (44.77%) and 377.97 sq. km (6.48%) have been categorized under high and very high groundwater potential zone. Such areal changes in groundwater potential zone from 2000 to 2018 are presented in a graphical format shown in figure 6.29.

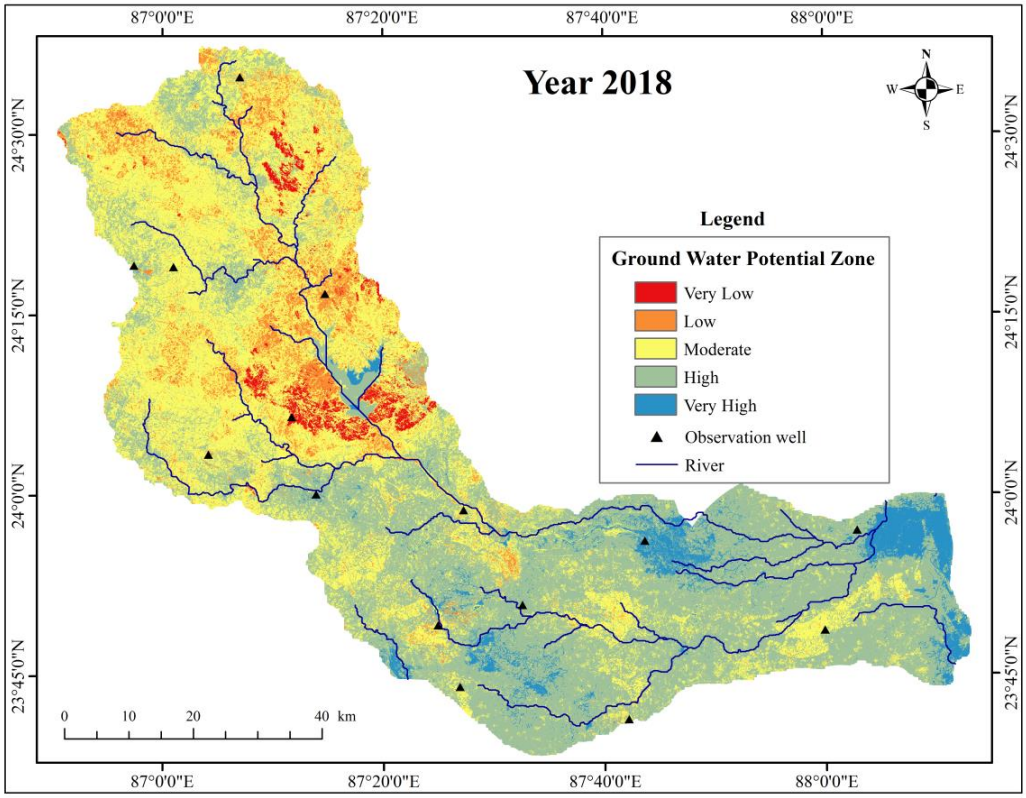

Figure 6.28 *Groundwater Potential Zone map of Mayurakshi River Basin for the Period of 2018*

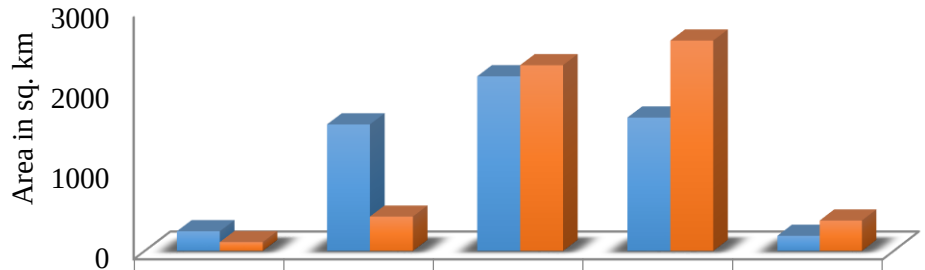

	Very Low	Low	Mode rate	High	Very High
Area in sq.km (2000)	244.85	1572.15	2166.73	1656.64	188.39
Area in sq.km (2018)	109.78	427.08	2304.55	2609.38	377.97

Figure 6.29 *Areal Changes in Groundwater Potential Zone from the year 2000 to 2018*

- **Validation of Groundwater Potential Zonation Map**

In this study, the groundwater resource potential map has been delineated using the FAHP technique integrated with remote sensing and GIS. After calculating the normalized weightage of each parameter applying the pairwise comparison matrix, the potential map of groundwater resources has been generated through weightage overlay analysis in a GIS environment. The output map of groundwater potential zone for the year 2000 and 2018 generated through the FAHP analytical method has been validated with the Central Ground Water Boards (CGWB) monitored dug well (Table 6.27) and field observed groundwater level data (Table 6.28) from different dug wells located within the river basin area respectively. Considering the seasonally monitored CGWB well data, the water level fluctuation (meter) has been calculated from the pre and post-monsoonal water level data. The results show that very high to high groundwater potential zone for 2000 has coincided with the lower water level fluctuation values (0.62 to 1.43 m) indicating higher recharge potentiality from the surface whereas the low to very low potential zone of groundwater has coexisted with the higher water level fluctuation values (2.22 to 12.5 m) signifying the region as a low groundwater resource potential zone.

Similarly, the accuracy of the groundwater potential map of 2018 has been validated with the field observed water level data. The field survey has been carried out during the pre-monsoon season of 2018 and the observation wells have been selected randomly over the study area. The authors were collected data from 15 observation dug wells of which the location of each well has been captured using Global Positioning System (GPS) and also shown in the final potential map of groundwater resources. The water level has been measured with the help of the

Temperature, Water Level and Conductivity meter (TLC) (Plate no. 6.5) in meter below the ground level (mbgl). The collected data shows that the groundwater level of a well is about 0.79 mbgl falls under the class of high groundwater resource potentiality where the main land use is associated with agricultural land that hinders the surface runoff and is favourable for groundwater recharge. In the areas which exhibit dry fallow land, a water level of about 7.41 mbgl has been observed which falls under the class of low groundwater resource potential zone. Such correlated results for both the year 2000 and 2018 may exhibit a significant validation of the predictive model outputs of groundwater resource potential zone of the study area.

Table 6.27 *Validation of GWPZ map of 2000 with CGWB Retrieved Groundwater Level Data of Mayurakshi River Basin*

Sl. No	Well Type	Latitude	Longitude	Water Level Fluctuation (m)	Location on GWPZ Map (2000)
1	Dug Well	23.84167	87.69167	3.43	Low
2	Tube Well	23.90000	87.95000	12.5	Very Low
3	Tube Well	23.87167	88.10667	6.4	Low
4	Dug Well	23.69639	87.73333	3.05	Moderate
5	Dug Well	24.26667	87.25000	2.66	Low
6	Dug Well	24.60000	87.07083	6.5	Low
7	Dug Well	23.78528	87.40056	1.43	Very High
8	Dug Well	24.38472	87.07083	2.42	Low
9	Tube Well	23.95806	87.85472	0.7	Very High
10	Dug Well	23.93333	88.05000	0.7	High
11	Dug Well	23.95333	87.52500	3.5	Low
12	Dug Well	23.76667	87.93333	1.29	High
13	Dug Well	24.15833	87.18611	1.84	Moderate
14	Dug Well	24.10833	87.31944	3.43	Very Low
15	Dug Well	24.04583	87.15278	2.22	Low
16	Dug Well	24.30000	87.00389	4.44	Low
17	Dug Well	23.95083	87.31278	3.09	Low
18	Dug Well	24.02917	87.42500	1.08	High
19	Dug Well	23.95000	87.66667	0.62	Very High
20	Dug Well	23.76333	88.08278	2.24	Moderate

Table 6.28 *Validation of GWPZ Map of 2018 with Field Observed Groundwater Level Data of Mayurakshi River*

Sl. No	Well Type	Latitude	Longitude	Groundwater Level (mbgl)	Location on GWP Map (2018)
1	Dug Well	23.739820	87.448777	1.11	High
2	Dug Well	23.850218	87.541340	2.61	Moderate
3	Dug Well	23.982395	87.452177	3.3	Moderate
4	Dug Well	23.815273	87.418316	1.02	High
5	Dug Well	23.941282	87.731337	0.85	Very High
6	Dug Well	23.689432	87.699238	3.65	Moderate
7	Dug Well	23.951197	88.051704	0.71	Very High
8	Dug Well	23.817328	87.996867	2.09	High
9	Dug Well	24.112474	87.193479	7.41	Very Low
10	Dug Well	24.284320	87.247694	5.30	Low
11	Dug Well	24.317493	87.011318	3.35	Moderate
12	Dug Well	24.583573	87.114358	1.29	High
13	Dug Well	24.056057	87.070285	0.7	High
14	Dug Well	24.319411	86.956838	4.98	Low
15	Dug Well	24.006438	87.231777	4.85	Low

Plate No. 6.5 *Water level measurement from a dug well using Temperature, Water Level and Conductivity Meter (TLC)*

6.7.4. Study the Functionality of Land Use Land Cover over the Shifting of Groundwater Potential Zone

Alteration in Land Use Land Cover (LULC) over some time has been considered as one of the crucial factors behind the modification of global environmental changes (Sun et al. 2011). In the context of climate change and population growth, groundwater resources have become fundamental natural resources that are continuously diminishing due to the effect of uncontrolled extraction of groundwater resources that exceeds the natural recharge of groundwater. Furthermore, the deterioration of natural vegetation and loss of pasture lands are also intensifying the lower rate of groundwater recharge into the aquifer system (Latifovic et al. 2010). At such juncture understanding the nature of LULC changes is essential to know the hydrological response of a river basin area.

In this work, classification of LULC map for different years (2000 & 2018) and delineation of groundwater prospect zone over the Mayurakshi river basin area for those respective years have been done through pairwise comparison matrix of FAHP technique. Integrating 13 different parameters, the final potential map of groundwater resources has been generated, which further have been classified into five classes from very low to very high potential zone. The quantitative assessment of groundwater potential maps (Fig. 6.27 & 6.28) demonstrate that within 18 years, a significant increase in high to very high potential areas and a decrease in low to very low potential areas have been observed which may enhance the overall groundwater resource scenario over the Mayurakshi River basin area. In the year 2000, lower potential zone of groundwater resources has been observed mainly in the upper part of the basin area, which became transformed into high groundwater resource potential zone in 18 years' time span. Likewise, during the studied time period, the high groundwater potential zone has also increased its spatial and areal extent around the lower reach of the river basin area. Such kind of symbiosis between groundwater potential zones with other criteria may vary from one place to another depending on the relationship between favourable parameters of groundwater occurrences (Trinidad et al. 2017 and Patra et al. 2018).

To identify the same, an attempt has been taken to identify the interaction between the temporal shifting of groundwater resource potential zone with the parameters which can have a more controlling power in targeting the resource potential area. As per the methodology adopted to calculate the weight of each parameter, land use land cover has been received the maximum weightage value (0.27) and has regarded as one of the effective parameters controlling the

groundwater potentiality over the Mayurakshi River basin area. However, among all the 13 selected parameters for this study, some of the parameters are characterized by temporal variability of occurrences like rainfall, groundwater level, and land use land cover in respect to the delineation of groundwater resource potential zones. The analysis shows along with the variability of rainfall, groundwater, or surface retention capacity of the soil, land use land cover has been recognized as the most dominant factor responsible for the temporal shifting of groundwater potential zone. It has been regarded as an important objective parameter through which any kind of resource management can be implemented. Various kinds of human-induced activities are the primary driving forces leading to the alteration in any hydrological processes over a region (Bonansea 2016; Yin et al. 2017 and Wang et al. 2014).

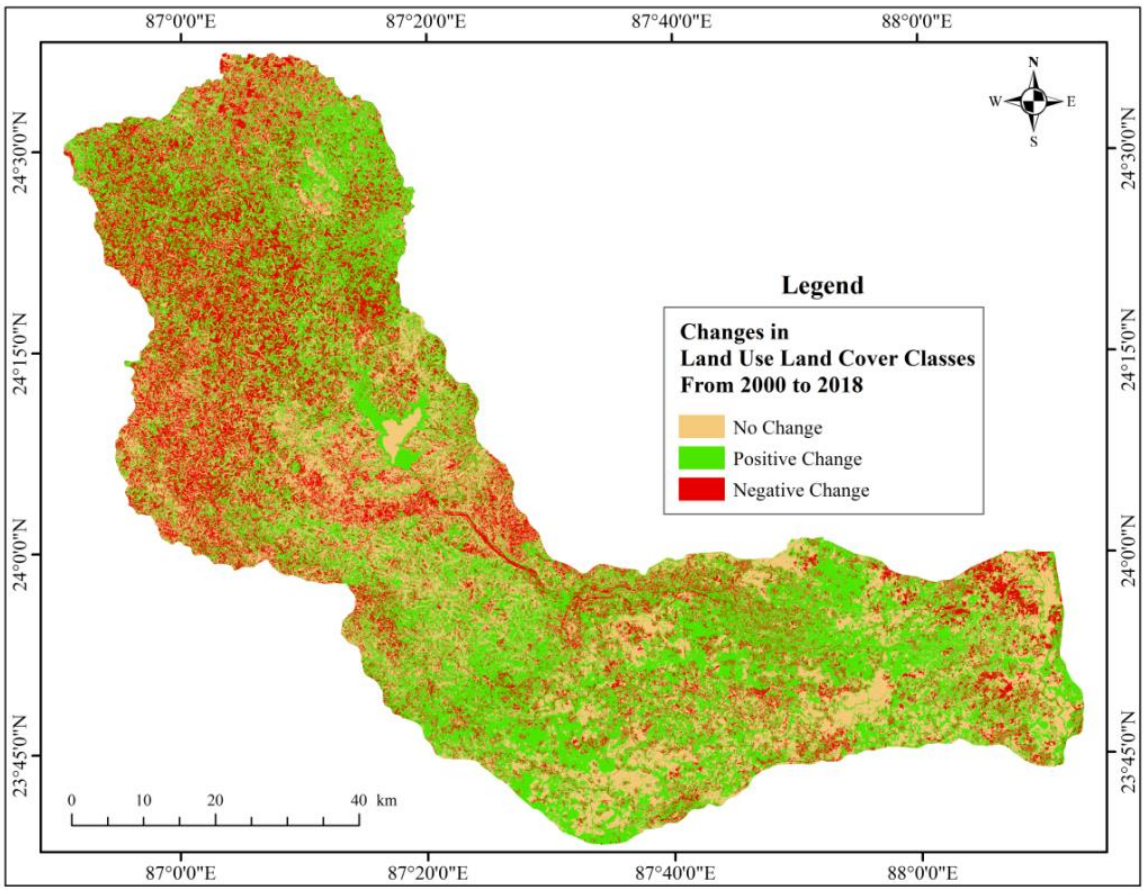

Figure 6.30 *Land Use Land Cover Reconfiguration Map from the Year 2000 to 2018*

The basic functionality of LULC over the identification of groundwater prospect zone can be visualized through a transformation study on land use land cover of the study area. A spatial distribution map of land use land cover reconfiguration has been prepared (Fig. 6.30) and classified into 3 different classes related to groundwater potential zones such as no change, positive change, and negative change. In figure 6.30 no change depicts no transformation in

land use land cover classes, positive change indicates the transformation of one class to another which may induce the recharge potentiality and enrich the groundwater storage like a wasteland to agriculture land. Whereas the negative changes indicate the transformation of that classes which may restrict the penetration of water and enhance the runoff over the area, for example, dense vegetation to settlement. The classified output map shown in figure 6.30 shows 41% of the total area has been exemplified with positive changes in LULC located in the lower part of the basin while 26% of the total area has accounted for negative changes and other 33% has identified as a no change in land use of the study area. As noted from the research of Gurnell et al. (2016) conversion of wasteland to cropland encourages the water infiltration rate into the soil and modifies the groundwater recharge capacity. However, unscientific alteration of the natural landscape (forest to settlement) has an unfavourable impact on both global and local surface-groundwater resources. A similar kind of result has been reported from the present study where high recharge potential areas have coincided with the positive transformation of land use and areas having the lower potentiality of groundwater resources have been surrounded by negative changes of landscape and have also been detrimental to the ecosystem. Such kind of correlative studies depicts the importance of the selection of land use land cover class in the evaluation of groundwater prospect zone, from which the variability of land use land cover and its influence over the identification of groundwater potential zone can easily be explored.

6.7.5. Conclusion

The movement of groundwater and its recharge potentiality is very much linked with the prevailing landscape above it. Increasing population generates more pressure on land and water resources. Local people are converting natural land cover into settlement areas which leading to create more impervious land cover affecting the natural infiltration processes into the aquifer. Besides this, the expansion of green cover over a region induces more water to percolate and encourages the groundwater recharge process. The present study is an attempt to assess the functionality of land use land cover change over the evaluation of groundwater potential zone with an area of 5828.78 sq. km in the Mayurakshi River basin area. The

quantitative assessment of the groundwater potential map for the period of 2000 to 2018 profoundly shows a positive transformation of recharge potential zone which indicates an improvement of overall groundwater recharging capacity over the river basin area. Among all the 13 influencing parameters, LULC plays a major role in such favourable shifting (low potential to high potential) of groundwater potential zone. Within a period of 18 years, the positive transformation of land use practices (wasteland to agricultural land) accelerates the penetration of water into the aquifer system and increases the resource potentiality for future uses. The very low potential region has only concentrated over the areas of rocky exposers where the land cannot be utilized for any sustainable uses. The lower level of groundwater fluctuation has also been found in some villages of study area mainly due to the fact of wise use land resources over the area. Within a zone of the middle and lower catchment, the conversion of wasteland to forest and seasonal fallow land to agricultural land have been observed which may promote more infiltration and reduces the seasonal variability of groundwater fluctuation. However, the temporal variability of rainfall patterns has also been very much prominent over the study area. Furthermore, in recent times, local farmers are used extracting groundwater using shallow submersible pumps to meet the demand for water for irrigational purposes which may affect groundwater storage and reduce the future potentiality of groundwater resources.

Such kind of correlated studies between human-induced factors and resource management can prove the selection of suitable parameters for the evaluation of groundwater potentiality and to maintain the environmental viability sustainably. Besides, the wise use of remote sensing and GIS applications coupled with FAHP based approach can satisfy the result of groundwater resource evaluation for this study and can also be helpful for the evaluation of proper resource utilization from higher prospect areas and development of environment-friendly management plans for the low prospectus areas of groundwater resources as well.

6.8. Estimation of Surface Runoff

Rainfall and runoff are the most important hydrologic components in the assessment of water resources of a drainage basin. A drainage basin is a hydrological unit that accompanied by natural ridges that allow precipitation-caused runoff to drain in a well-defined pattern of streams streaming within watershed boundaries. Rainfall is the principal source of runoff is essentially needed to meet a variety of requirements, including those for agriculture, hydropower, industries, the climate, and environmental systems.

However the amount and frequency of rainfall generated runoff is mainly depends on the features of the rainfall event, such as its intensity, duration, and dispersion. In addition to these aspects of rainfall, there are a number of catchment-specific elements that directly affect the frequency and amount of runoff including the catchment type, slope, and vegetation cover of the soil. As a function of soil type and land use, Curve Number (CN) offers an empirical relationship for estimating initial abstraction and runoff with respect to the nature and characteristics of soil and land use of the region (Srinivas et al. 2018). A major drop in freshwater availability may occur in the future decades due to rapid population increase, polluting of surface water, climate change, and erratic and inadequate precipitation. In such juncture, proper quantification and conservation of rainfall runoff will lead to effective use of water for agricultural, residential usage, industrial use, power generation, and so on, and so the resources may be managed successfully. There are various ways to calculate runoff from rainfall, including the rational technique, the Green-Ampt method, and the SCS-CN method, however the SCS-Curve Number method continues to be the most commonly employed method as it primarily depends on the soil type, antecedent soil moisture (AMC), and land use/land cover (LULC) of the particular area (Jaafar et al. 2019). The National Resources Conservation Service (NRSC), United States Department of Agriculture (USDA), developed the Soil Conservation Service-Curve Number (SCS-CN) method in 1969. It is a straightforward, reliable, and stable conceptual method for estimating direct runoff depth based on storm rainfall depth. The runoff curve number has been determined using a combination of the soil type, soil group, and Antecedent Soil Moisture Condition (AMC). In the current investigation, all three antecedent soil moisture conditions (AMC-I, AMC-II, and AMC-III) were utilised.

In this study, the surface runoff has been calculated for each sub-watersheds of Mayurakshi River basin and for a comparative analysis different time period has been selected like 1989,

2000, 2010, 2018 and 2021 for the assessment of surface runoff generation from the study area. Among the several land use classes, agricultural land is the most dominant one as it covers the maximum portion of the study area. Furthermore, the presence of fallow land and other impermeable structures reduces the ability of water to permeate and interrupts groundwater recharge possibilities over the region. Therefore, in the field of management and evaluation of water resources, evaluation of surface runoff plays a crucial role in determining the capacity of land potentiality as well as the health status of the river basin area.

6.8.1. Data Used and Methodology

For the assessment of surface runoff over the research area, numerous datasets were needed. The boundaries of each sub-watershed in the Mayurakshi River basin have been defined using Survey of India Topographical maps at a scale of 1:50,000. Data on daily observed precipitation has been gathered for the years 1989, 2000, 2010, 2018, and 2021 from the official website of the Indian Meteorological Department (IMD). USGS Earth Explorer-downloaded Landsat satellite images were used to create the land use land cover map of the study area for the aforementioned years. The National Bureau of Soil Survey's and Land Use Planning (NBSS & LUP) West Bengal soils sheets and a national atlas and thematic mapping organization's soil region map with various soil types were used to prepare the soil texture map of the study area.

The first stage in estimating surface runoff is to identify major land use land cover (LULC) over the research area. A total of 5 LULC maps were created from high resolution Landsat imagery, with 11 major land use classes dominating over the region. (Mentioned in the previous section). A necessary thematic layer of soil type (Fig. 6.32) was collected from the National Bureau of Soil Survey and Land Use Planning (NBSS and LUP) since soil texture is crucial for determining the hydrologic soil group. Using Arc GIS software, hydrological soil group (HSG) maps of the research area are created based on soil texture (Fig. 6.33). The soil's minimum infiltration rate determines the HSG's four groups, which are designated as Groups A, B, C, and D. To identify the land use and soil group for each polygon and define every land-use class area under the same soil group for given CN values, the overlay operation is carried out using the land use map and hydrologic soil group map. Within the boundaries of the basin, the CN of each distinct land use-soil group is determined using the conventional SCS curve number approach.

- **Estimation of Curve Number (CN)**

To describe the combined hydrologic effects of soil, land use, agricultural land treatment class, hydrology and antecedent soil moisture, SCS developed an indicator called Runoff Curve Number (CN). From soil surveys, site inspections, and land use maps, these elements can be evaluated. A runoff curve number is therefore described as:

$$S = \frac{25400-254}{CN} \tag{6.55}$$

Here, S is defined as the prospective maximum retention, which depends on the complex relationship between soil-vegetation-land use and the catchment area's prior moisture condition. SCS has expressed S (in mm) in terms of the dimensionless parameter CN, which is related to S and is represented as

$$CN = \frac{25400}{S+254} \tag{6.56}$$

The CN (a dimensionless number between 0 and 100) is derived from a formula based on land-use/land-cover (LU/LC), hydrological soil group (HSG), and Antecedent moisture conditions (AMC). The value of CN was derived from the table estimated by the Technical release (United States Department of Agriculture (USDA), Natural Resources Conservation Service, 1986).

Then, the Weighted Curve Number (CN_w) has been calculated for each sub-basins of Mayurakshi, using the following equation

$$CN_w = \frac{\sum(CN*A_i)}{A} \tag{6.57}$$

Where, A_i is the area with the CN while A is the total basin area.

Finally, the deviation of CN value under different AMC conditions has been assigned using the formulae listed below

$$Q = \frac{(P-(0.3S))^{\wedge 2}}{(P+(0.7S))} \tag{6.58}$$

Where, Q is defined as the surface runoff (in mm) and P is amount of rainfall observed in the respective AMC period.

6.8.2. Result and Discussion

In this research, surface runoff of the Mayurakshi River basin area was estimated using an integrated GIS-based rainfall-runoff modelling, allowing for more efficient watershed

management. The runoff generating process is incredibly intricate, nonlinear, dynamic, and influenced by a wide range of interrelated physical phenomena (Kumar et al. 2021). For effective management and development of water resources, detailed runoff assessment is done. Here, the SCS-Curve Number (CN) technique has been employed for the estimation of rainfall-runoff relationship over the study area.

- **Land Use Land Cover (from 1989 to 2021)**

The basin consists of various land use/land cover classes (as discussed in the previous section), and current research reveals that agriculture is the dominant land use class in the region under study period. Among the various land-use categories, fallow land and open waste land play a vital role in surface runoff.

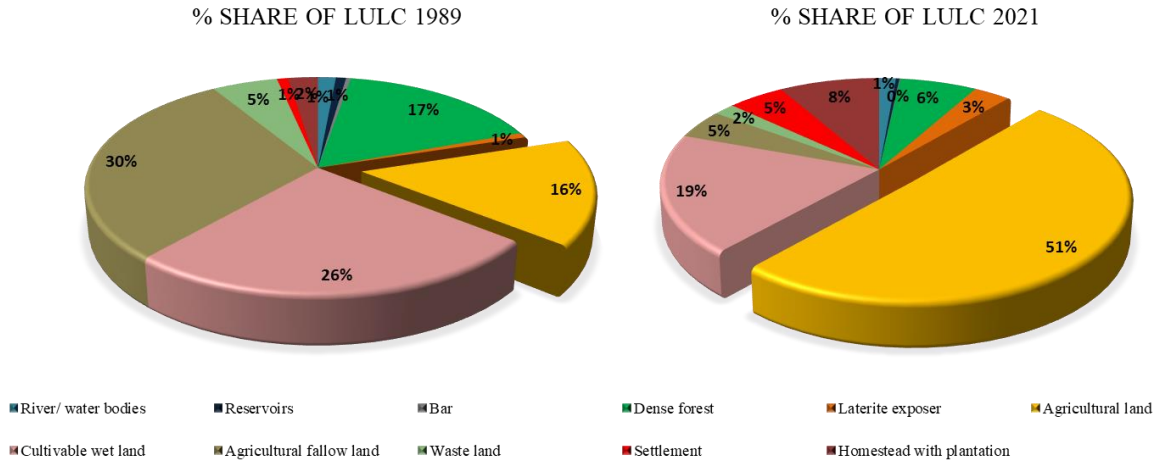

Figure 6.31 *Percentage Share of Land Use Land Cover Area of Mayurakshi River Basin for the Year 1989 & 2021*

Figure 6.31 depicts the percentage share of each land use classes for 1989 and 2021. The years 1989 and 2021 have been selected as the beginning and conclusion points of the study period in order to examine the most dramatic changes in land use classes during that time period. In the year 1989, just 16% of the land with respect to the total basin area that was utilised as agricultural land across the Mayurakshi basin. This is in contrast to the current scenario, which shows that more than 50% of the land area has been covered with crop land. This abrupt change in the agricultural area causes increased surface runoff and less infiltration throughout the region. Similarly, the settlement area has been expanded from (53.86 sq. km in 1989) to (283.96 sq. km in 2021).Population growth has led to an increase in the demand for urban infrastructure to meet people's requirements, which in turn has led to an increase in impervious surfaces, which impacts the water circulation of an area. With this increase in imperviousness, generated

surface discharge remains on the surface rather than being absorbed. Rapid urbanisation is associated with numerous adverse climatic effects, including urban heat island effect, urban inundation, and pollution (Sood et al. 2021).

- **Hydrological Soil Group (HSG) and Estimation of Curve Number (CN)**

The soil map of the research area, generated from NBSSLUP (scale 1:2,50, 000) (Fig. 6.30), has been classified into four classes (A, B, C, and D) of hydrological soil group as determined by the Soil Conservation Services (SCS) of the USA in 1969 based on infiltration, runoff, and key soil texture features. Such classification of soil groups may reflect the nature of runoff potentiality and groundwater recharge capability of a particular area. The study area has been classified into four HSG as shown in figure 6.33. The river basin has been majorly dominated with the soil group of C indicating average infiltration with moderately low potential of groundwater recharge.

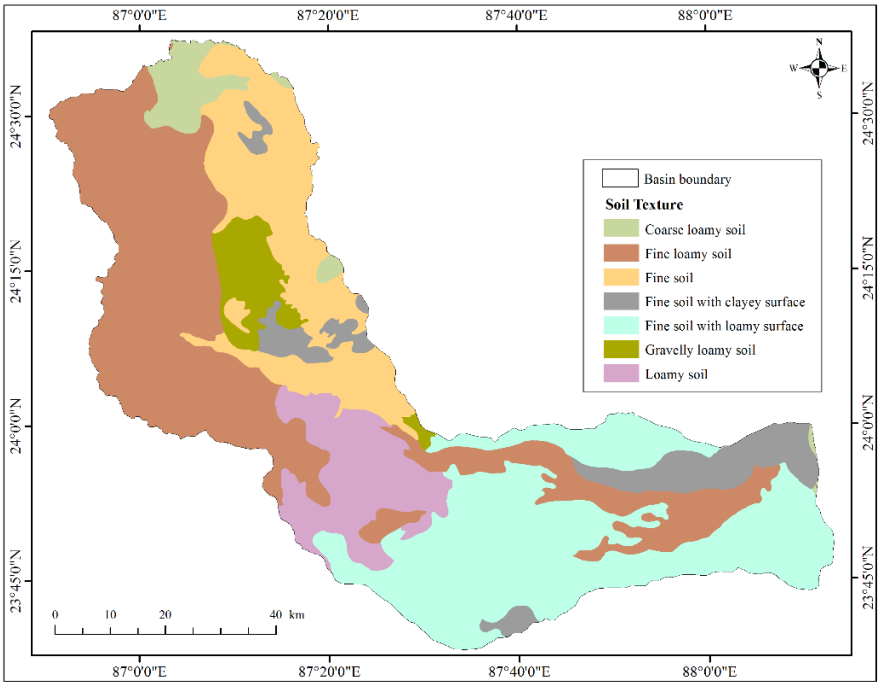

Figure 6.32 *Soil Texture Map of the Mayurakshi River Basin Area*

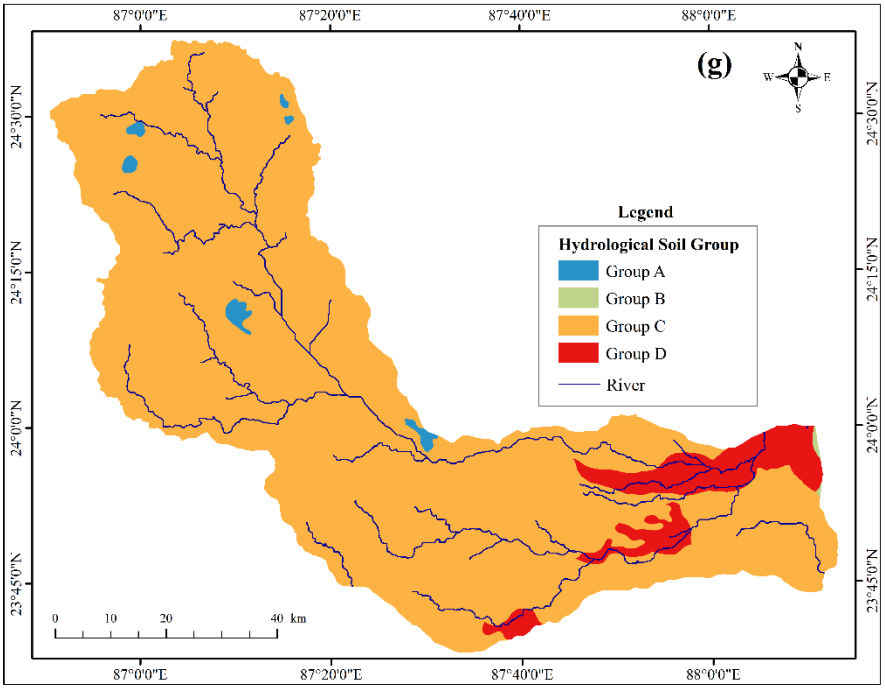

Figure 6.33 *Hydrological Soil Group Map of the Mayurakshi River Basin Area*

The dimensionless number run-off index Curve Number (CN) is calculated based on the hydrological soil group, land-use class, hydrological situation, and precedent moisture state (AMC). Each soil type is assigned a hydrologic soil category of Group A, B, C, or D based on its infiltration characteristics. The CN values can range from 1 to 100. The greater CN values indicate a greater runoff. The Overlay analysis (Union) executed on the soil, land use map, and hydrological soil group map generated in Arc GIS 10.3. This result is used to calculate the total area-weighted curve number for the study area. The calculated weighted CN number, which is finally utilised to estimate surface retention and surface runoff of the research region, is computed for each sub-basin of the Mayurakshi River basin for antecedent moisture state (AMC) of I, II, and III (Fig. 6.34).

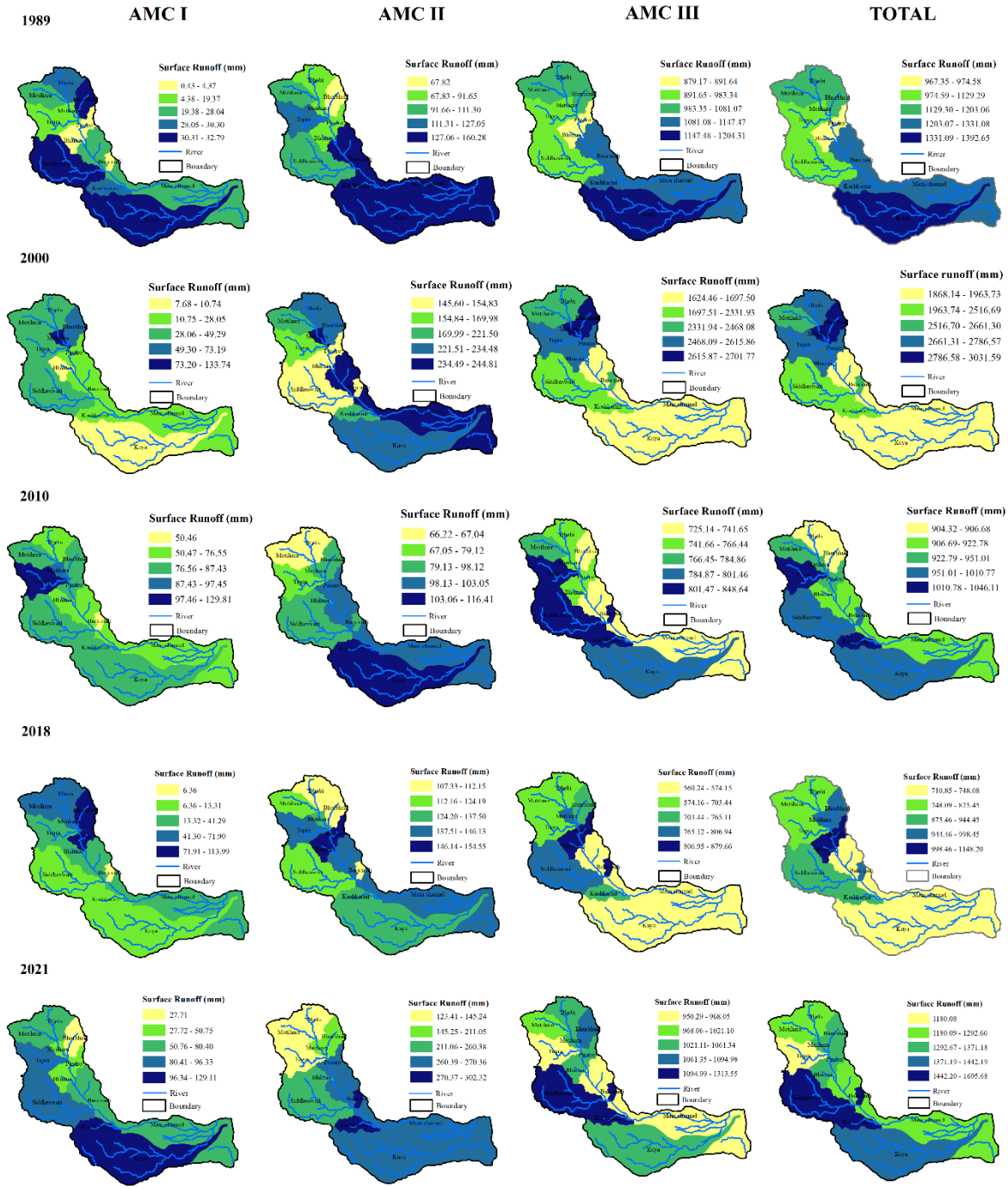

Figure 6.34 *SCS Curve Number Generated Runoff Map of the Mayurakshi River Basin Area*

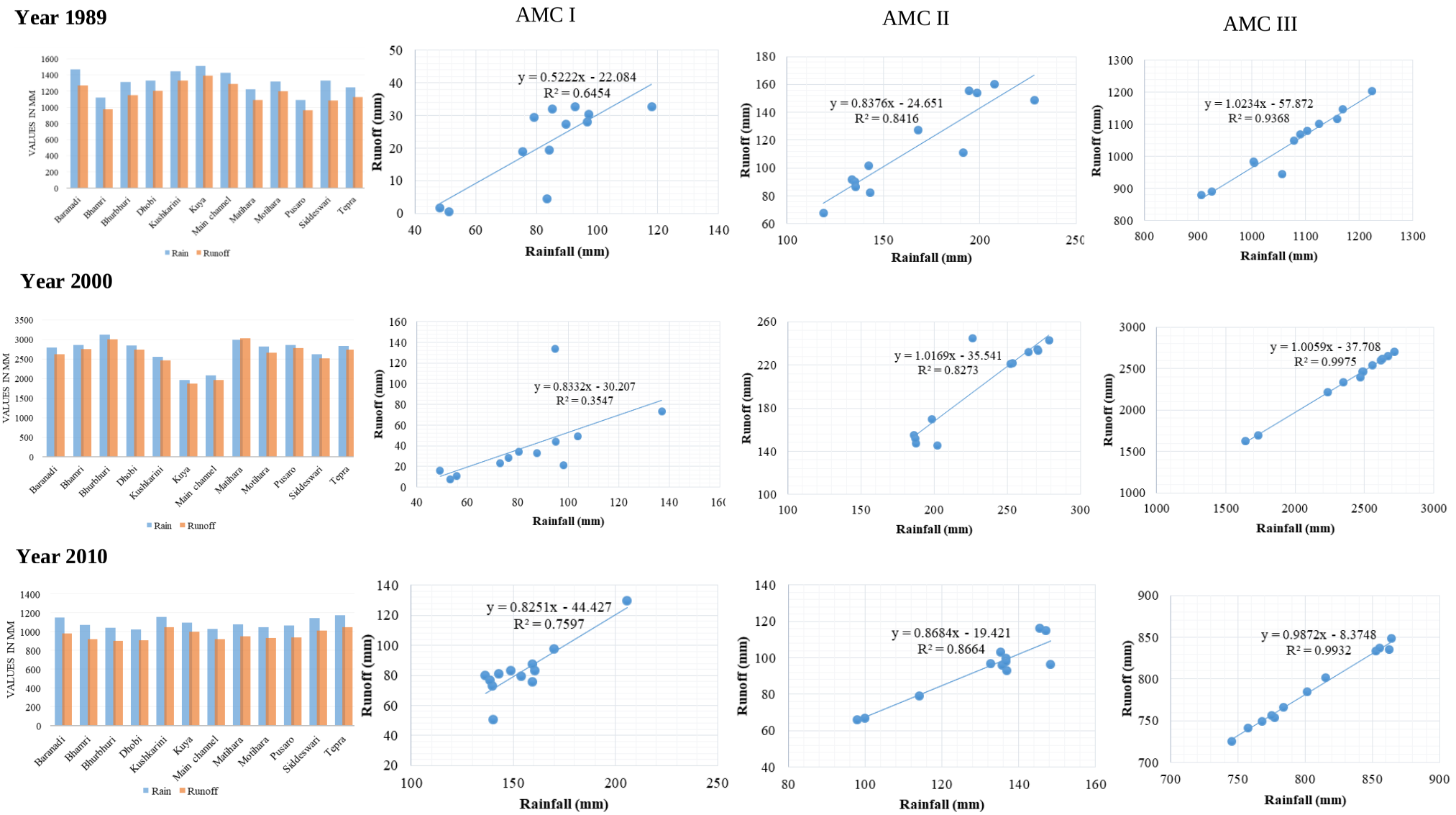

Figure 6.35 *Correlation between Rainfall and Runoff of the Mayurakshi River Basin Area for the period of 1989, 2000, 2010, 2018 and 2021*

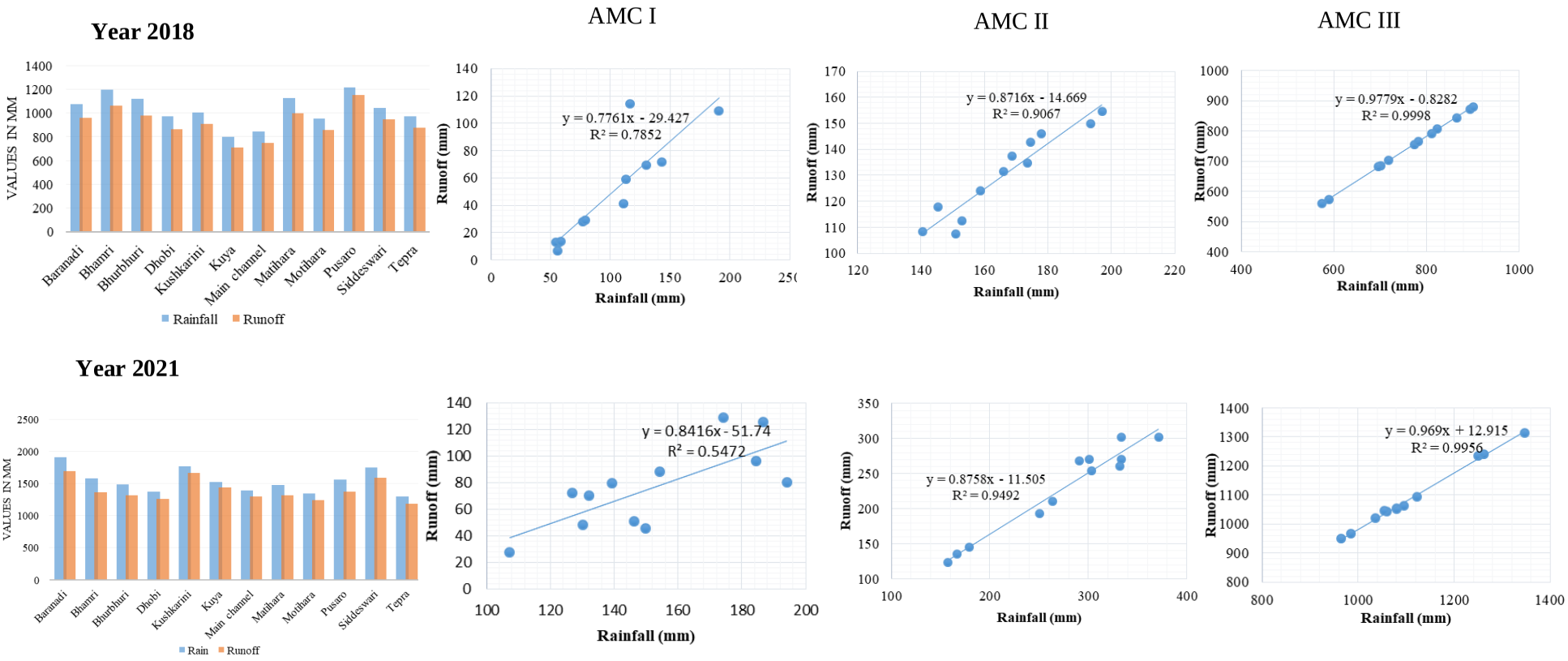

Figure 6.35 *Continued*

The figure 6.34 depicts the spatial distribution of surface runoff for the various AMC conditions of the study area during the years 1989, 2000, 2010, 2018, and 2021. From 1989 to 2021, the output indicates that the basin area's total surface runoff has substantially increased, affecting the middle to lower reaches of the basin. More precisely, the sub basins Siddheswari, Kushkarini, and Kuya have consistently produced the highest surface discharge. Because of their physiographic location, topographic slope, and large riverine flow of water, those areas are more prone to surface runoff as well as erosion and flooding.

The main factor generating surface runoff from each sub-basin of the Mayurakshi River basin area is the volume, intensity, and frequency of rainfall. The increased inflow of water from the Ajay Mayurakshi River caused a flood situation across the study region in 2000, which resulted in significant amounts of surface runoff. As a result, the highest amount of rainfall, which was measured at 2744.22 mm, and the highest amount of surface runoff, which was measured at 2701.77 mm has been observed during the same season of the year 2000. A scatter plot with a correlation function and a comparative bar diagram have been created to specifically demonstrate the relationship between rainfall and runoff. The scatter plots with the co-relation function, as depicted in figure 6.35, has also demonstrated a similar result. AMC II and III conditions exhibit a significant upward trend in nearly every year of the study period. It demonstrates that the anticipated surface discharge is directly proportional to the precipitation in the region.

6.8.3. Conclusion

According to the findings of this study, the SCS-CN method combined with GIS methodologies is useful for estimating runoff. This strategy can also be utilised efficiently in watershed management. The collected results show variation in runoff potential with diverse land use/land cover and varying soil conditions in the study area. The majority of the river basin has a high curve number of more than 80, indicating substantial runoff in the Mayurakshi River basin. The soil in the study area is divided into four hydrological soil categories A, B, C, and D based on its infiltration rate. The majority of the studied area is covered by hydrological soil group C, according to the soil map.

The majority of the sub-basins in the Mayurakshi River basin show high curve number values of greater than 80, which denote strong runoff. Siddheswari, Kuya and Kushkarini sub-basins of Mayurakshi River that are most susceptible to runoff are those with high rates of soil erosion and low infiltration rates. Due to the highest amount of rainfall, the monsoon season of 2010 saw the highest total surface runoff volume of the Mayurakshi River basin at 3031.59 mm. Finally, the Soil Conversations Service – Curve Number (SCS-CN) method has been demonstrated to be superior, requiring less time and having the capacity to manage large data sets and a larger environmental region to identify potential artificial recharge structure sites.

6.9. Land use land Cover Analysis

Landform vis-à-vis geomorphic characteristics widely control on the land use and land cover of a particular region. The earth surface is undergoing rapid land use and land cover changes due to various natural phenomena and socio economic activities. Human activities, such as urbanisation processes and policies for social and economic development at local to regional scales, can be reflected in the spatial pattern of land use (Redman 1999). For the best management of natural resources, it is important to comprehend how changes in land use and land cover (LULC) affect the hydrologic cycle. It also has a significant role in energy and water balance of a region (Samal and Gedam, 2021). Urbanisation, deforestation, and shifting agricultural practises have produced a significant impact on hydrologic processes like interception, infiltration rate, and evapotranspiration, and therefore on water resources over the past few decades. The change in land use, the alteration of water channels, and the construction of river impoundments for artificial storage are all examples of how this modification can have an effect on the natural flow mechanism of a river system. Because the majority of these shifts take place in a wide variety of different configurations, it can be challenging to determine the impacts on hydrological components in isolation (Salmoral et al. 2015). As a result, examining the impact of LULC on hydrological processes may provide a better knowledge of the phenomena, allowing policymakers to make better, more sustainable decisions when executing watershed development plans for a specific region.

The ecological health of a river basin can be inferred by studying the watershed processes that shape it and the manner in which they shift through time and space. Land use management at the watershed scale is essential because changes in land use at large scales may disrupt the local biological equilibrium of the region. This kind of reshaping of the environment can be found in abundance along the Mayurakshi river basin and the areas that surround it; as a result, the region is extremely susceptible to both flooding and drought. The Mayurakshi River system, which includes significant tributaries such as Dwarka, Brahmani, Kopai, and Bakreswar, is more susceptible to flood hazards. (Islam & Sarkar, 2021). All of these rivers have extremely low flows all year long. However, during the monsoon season, this river system exhibits a swift current and causes serious flood damage, affecting the livelihoods of residents in the affected area. In addition, a drainage congestion has been reported in the lower portion of the Mayurakshi basin, which exacerbates both the inundation scenario and the channel network diversion (Islam and Ghosh, 2021). These types of environmental hazards are caused by human activity, such as by constructing temporary recharge pools, khals/nullahs, altering

the channel flow pattern, and extreme sand extraction from riverbeds (Nag et al. 2022). As a result, a proven understanding of land use change and hydrological processes at the watershed scale can be used to prevent unintended consequences in a watershed. At this point, the investigation focuses on the shift of land use and land cover that has occurred over the course of 32 years in the Mayurakshi River basin area.

In this discipline, remote sensing and Geographical Information Systems (GIS) are regarded as effective tools for providing accurate and timely data on the spatial distribution of land use/land cover changes over large areas. In this study, more than 30 years land use alteration has been studied with their temporal variability, gain and loss in major land use classes along with the accuracy assessment of each land use land cover classification. The selected study periods are 1989, 2000, 2010, 2018 and 2021. In this regards, authors have used high spectral resolution Landsat images and evaluate the each year through land use land cover classification with the maximum likelihood method (Lillesand and Kiefer 2000) and change detection analysis using ERDAS Imagine software system.

6.9.1. Data and Methodology

The major data used in this study were high resolution Landsat Thematic Mapper satellite imageries for the year of 1989, 2000, 2010, 2018 and 2021, have been downloaded from the USGS Earth Resources Observation Systems data centre (https://earthexplorer.usgs.gov/). The study area consists of two distinct scenes (Path/Row 139/43 & 139/44) and all satellite imageries are collected during the same season (post monsoon) in order to acquire cloud-free images for the corresponding years. The details of the used dataset have been represented in table 6.29.

Table 6.29 *Details of the Satellite Data used in this Study*

Satellite	Sensor	Path and Row	Date of acquisition	Spatial resolution	Source
Landsat 5	TM		04/12/1989		USGS Earth Resources
Landsat 5	TM	139/43	31/10/2000		Observation Systems
Landsat 7	ETM+	&	04/11/2010	30m	
Landsat 8	OLI	139/44	18/11/2018		
Landsat 8	OLI		02/11/2021		

TM: Thematic Mapper, ETM+: Enhanced Thematic Mapper, OLI: Operational Land Imager, USGS: United States Geological survey

- **Pre-processing and Image Classification**

Classification of land use land cover of a region is an important approach to understand how the land utilization pattern can influence the hydrological processes. In this study, Images from the post-monsoon season were selected, which are known for their clear skies, vigorous plant growth, full water bodies, and completely sown croplands. No atmospheric corrections were necessary because there was no haze or cloud cover in any of the images. The only pre-processing techniques used in this work include geo-referencing and image enhancement. Finally a supervised classification with maximum likelihood method has been executed for the classification of each satellite imageries using ERDAS Imagine 9.2 software. All the images were classified separately and total 11 classes were identified namely dense forest, lateritic exposer, river/water bodies, reservoirs, sand bar, agricultural land, wet fallow land, dry fallow land, waste land, settlement, and homestead with plantation. After image classification, all the classified imageries are then exported into Arc GIS software for further analysis required for this study.

- **Accuracy Assessment**

Validating the satellite imageries that have been digitally categorised requires accuracy assessment. It is the process used to compare classification results to the presumed-accurate geographic reference data (Richards 2006). In this study, a nonparametric Kappa statistical analysis (k) has been done, which calculates the overall classification accuracy (OCA), producer's accuracy (PA), user's accuracy (UA), and generates the kappa coefficient index (k). Here, the overall classification accuracy has been assessed for the all studied land use land cover maps using the following formula (Cohen 1960):

$$k = \frac{P_o - P_e}{1 - P_e} \tag{6.59}$$

where, P_o=relative observed agreement, P_e= hypothetical probability of chance agreement. A classification accuracy rating of greater than 70% can be considered satisfactory, while a kappa value of one (1) indicates perfect agreement and a value of zero (0) indicates no agreement. The majority of applications can tolerate kappa values greater than 0.75 as indicating an excellent or very good agreement. After accuracy evaluation and correction, the class specific area of each image has been determined within a remotely sensed environment.

6.9.2. Results and Discussions

- **Analysis of LULC Image Classification and Accuracy Assessment**

Classification of land use land cover of a region is an important approach to understand how the land utilization pattern can influence the hydrological processes. In response to that supervised classifications have been carried out on Landsat satellite imageries using a maximum likelihood algorithm for the study period of 1989, 2000, 2010, 2018 and 2021. The whole classification methodology has been done in ERDAS Imagine 9.2 software using AOI and signature editor tool. All the classified land use land cover maps shows an optimum level of accuracy like 0.96, 0.87, 0.95, 0.81 and 0.81 for the respective years of 1989, 2000,2010, 2018 and 2021 (Table in Annexure II). The output of the land use land cover classification maps for the respective years has been shown in figure 6.36. Similarly the areal coverage with the percent of land use and land cover has been summarised in table 6.30 and figure 6.37.The areal statistics also confirmed that the total area of Mayurakshi River basin is about 5828.78 sq. km. The areal statistics as presented in table 6.30 shows that, in the year of 1989, the dominancy of agricultural fallow land (1736.18 sq. km or 29.79%) is greater than the cultivable wet land (1498.81 sq. km or 25.71%) followed by the agricultural land of 914.83 sq. km (15.70%) over the study area. However, a reversal picture has been observed in the following years of image classification, showing a considerable decrease in both amount in area and percentage has been notified in agricultural fallow land (15.31% in the year 2000 to 4.71% in 2018) which is supplemented by the growth and development of agricultural land from 914.83 sq. km (15.71%) in 1989 to 2220.83 sq.km (38.10%) and 2992.41 sq.km (51.34%) in the year of 2021 over the basin area. This result is due to the expansion of human settlement with their growing need increases the overall agricultural production so as to increase the land coverage with agricultural land over the study area. The growth of the settlement has also been observed from the percentage share of settlement and homestead with plantation from 0.91% (52.86 sq. km) to 3.16% (183.96 sq.km) and 2.44% (142.21 sq.km) to 8.51% (495.81 sq.km) from 1989 to 2021. (Table 6.30)

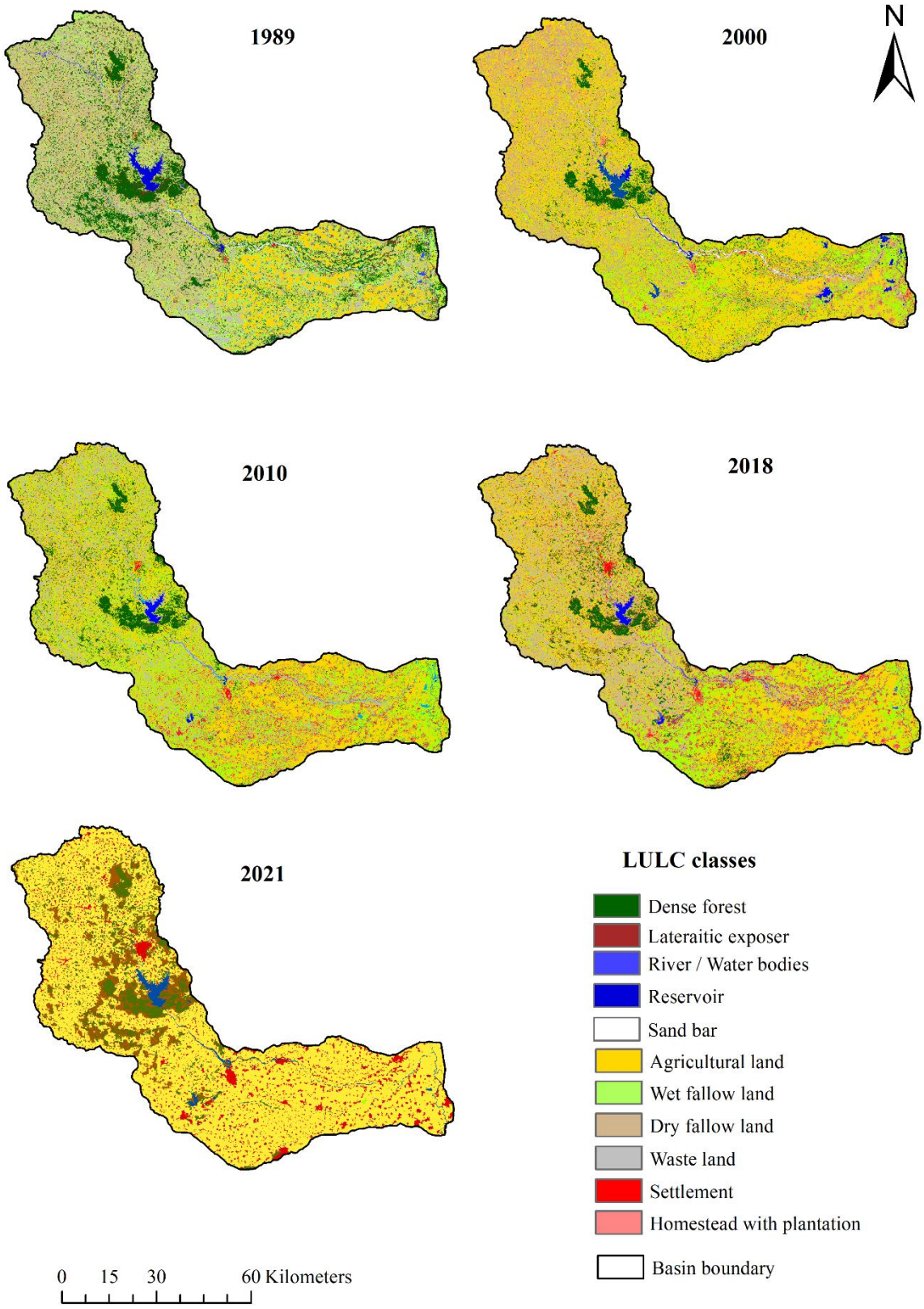

Figure 6.36 *Classified Land Use Land Cover Maps of Mayurakshi River Basin Area*

Table 6.30 *Areal Statistics of Land Use Land Cover Classes of Mayurakshi River Basin Area*

LULC Classes	1989		2000		2010		2018		2021	
	Area in		Area in		Area in		Area in		Area in	
	Sq. km	%	Sq. km	%	Sq. km	%	Sq. km	%	Sq. km	%
River/ water bodies	85.33	1.46	88.52	1.52	88.47	1.52	84.88	1.46	82.34	1.41
Reservoirs	48.53	0.83	36.48	0.63	29.77	0.51	23.86	0.41	17.58	0.30
Sand Bar	22.54	0.39	43.67	0.75	10.03	0.17	4.05	0.07	3.07	0.05
Dense forest	971.49	16.67	435.35	7.47	440.37	7.56	372.82	6.40	382.63	6.56
Laterite exposer	42.68	0.73	16.99	0.29	13.72	0.24	107.21	1.84	184.41	3.16
Agricultural land	914.83	15.70	2220.83	38.10	1909.63	32.76	2947.09	50.56	2992.41	51.34
Wet fallow land	1498.81	25.71	1919.76	32.94	1839.76	31.56	1203.63	20.65	1113.05	19.10
Dry fallow land	1736.18	29.79	892.34	15.31	524.98	9.01	274.33	4.71	264.38	4.54
Waste land	313.33	5.38	96.04	1.65	408.51	7.01	186.12	3.19	109.14	1.87
Settlement	52.86	0.91	66.03	1.13	215.74	3.70	135.81	2.33	183.96	3.16
Homestead with plantation	142.21	2.44	12.78	0.22	347.80	5.97	488.99	8.39	495.81	8.51
TOTAL	5828.78	100.00	5828.78	100.00	5828.78	100.00	5828.78	100.00	5828.78	100.00

Table 6.31 *Areal Changes of Land Use Land Cover Classes of Mayurakshi River Basin Area*

LULC Classes	Areal Change								32 years net change		
	(1989-2000)		(2000-2010)		(2010-2018)		(2018-2021)		(1989-2021)		
	Sq. km	%	Sq. km	%	Sq. km	%	Sq. km	%	Sq. km	%	Change type
River/ water bodies	3.19	0.05	-0.05	0.00	-3.59	-0.06	-2.54	-0.04	-2.99	-0.05	Negative
Reservoirs	-12.05	-0.21	-6.71	-0.12	-5.90	-0.10	-6.28	-0.11	-30.95	-0.53	Negative
Sand Bar	21.13	0.36	-33.64	-0.58	-5.99	-0.10	-0.98	-0.02	-19.47	-0.33	Negative
Dense forest	-536.14	-9.20	5.02	0.09	-67.55	-1.16	9.81	0.17	-588.86	-10.10	Negative
Laterite exposer	-25.68	-0.44	-3.27	-0.06	93.49	1.60	77.20	1.32	141.73	2.43	Positive
Agricultural land	1306.00	22.41	-311.19	-5.34	1037.46	17.80	45.32	0.78	2077.58	35.64	Positive
Wet fallow land	420.95	7.22	-80.00	-1.37	-636.13	-10.91	-90.58	-1.55	-385.76	-6.62	Negative
Dry fallow land	-843.85	-14.48	-367.36	-6.30	-250.65	-4.30	-9.95	-0.17	-1471.80	-25.25	Negative
Waste land	-217.29	-3.73	312.47	5.36	-222.40	-3.82	-76.98	-1.32	-204.19	-3.50	Negative
Settlement	13.17	0.23	149.71	2.57	-79.93	-1.37	48.15	0.83	131.10	2.25	Positive
Homestead with plantation	-129.43	-2.22	335.02	5.75	141.19	2.42	6.82	0.12	353.60	6.07	Positive

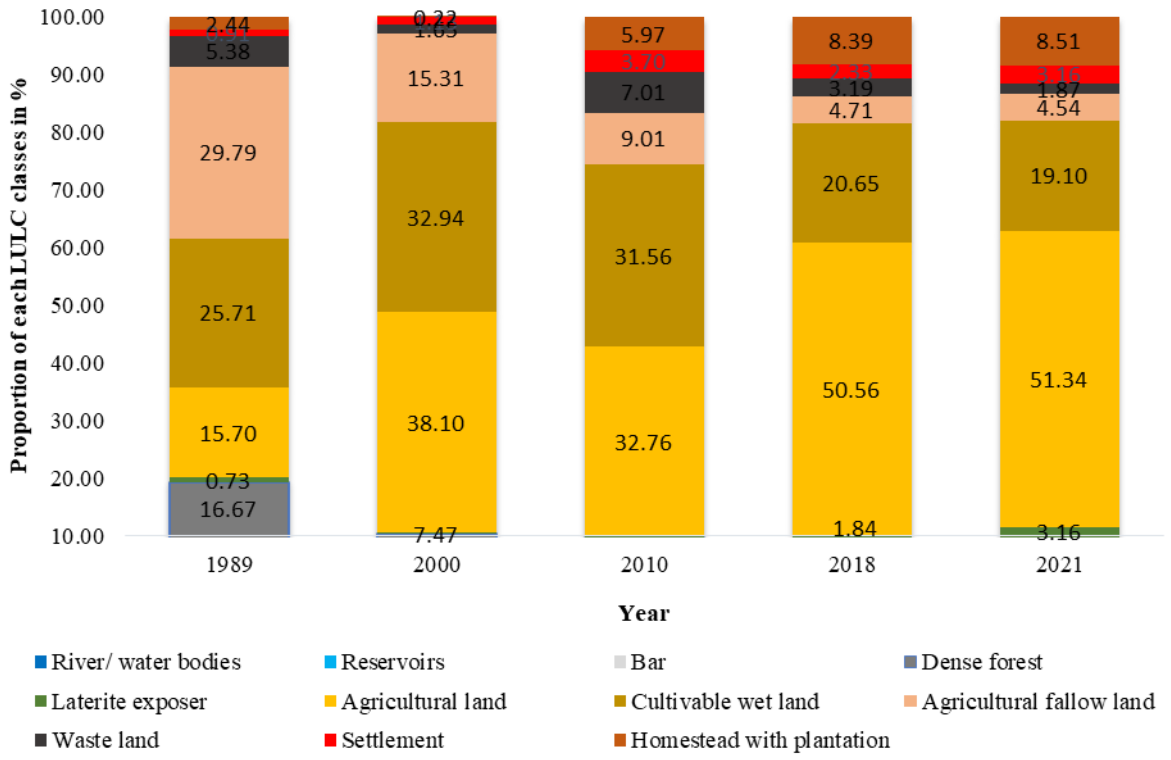

Figure 6.37 *Percentage of Areal Coverage of Land Use Land Cover Classes of Mayurakshi River Basin Area*

- **Areal Change Detection of Land Use Land Cover Analysis**

Remote sensing image-based methods for detecting changes in land use and land cover have been widely used in LUCC research, natural resource management, and environmental monitoring and protection (Zhang et al. 2014). Changes in the areal statistics of each land use land cover classes from the period of 32 years (1989 to 2021) have been studied and summarised in table 6.31, mainly to understand the quantitative changes in land-use practices and their effect on the environmental process operated within the study area. A comparative bar diagram has also been constructed for better visual interpretation of the 32 years land use dynamism over the study area (Fig. 6.38). Considering the changing pattern of Land use land cover from 1989 to 2000, the quantity of agricultural land and cultivable wet land has increased by 22.41% (1,306 sq. kilometres) and 7.22% (420.95 sq. kilometres), respectively. In addition, settlement classes have experienced a substantial increase, from 13.17 sq. kilometres in 1989 to 48.15 sq. kilometres in 2021. In contrast, from 1989 to 2000, there was a drop in land use land cover classes in dense forest (9.20%), agricultural fallow land (14.48%), and waste land (3.73%). Such a changing trend was not observed over the remainder of the study period. The occurrence of an exceptional flood event in the year 2000 (Pal 2012) resulted in a significant

decline in agricultural land (5.34%), cultivable wet fallow land (1.37%), and agricultural fallow land (6.3%) across the Mayurakshi River basin area. In contrast, non-productive land uses, such as waste land, have increased by 5.36%. Since then, similar patterns of land use have been abolished. According to the analysis of changes in the Mayurakshi River basin's land use and cover from 2010 to 2018, agricultural land witnessed the largest increase in area changed (+1037.46 sq. km) relative to the basin's total area, while agricultural fallow land shrank noticeably (-4.30%). This is due to the fact that both the human population and the need for agricultural products have increased in the study area. On the other hand, the amount of dense forest has decreased by 1.16 percent (67.55 sq. kilometres) in just 18 years (from 2010 to 2018). The changing land use from thick forest to farmland is because the study area is getting more people and becoming more urban. Despite the fact that in recent years, 2021, a 0.17 percent increase in the dense forest has been observed, this is primarily due to the efforts of the local population and various governmental and non-governmental organisations to increase the region's vegetation. During fieldwork, the authors also observed similar activities near the Labhpur and Bolpur region blocks, where abandoned waste lands or transient agricultural fallow lands are converted and classified as belonging to the social forestry region. The categories agricultural land (35.64 sq. km), lateritic exposer (2.43 sq. km), settlement (2.25 sq. km), and homestead with plantation (6.07 sq. km) have undergone the most significant positive changes over the entire 32-year study period (1989-2021). In contrast, dense forest coverage and area of livestock or waste lands have decreased by 10% and 25%, respectively, indicating that the majority of forest and fallow land in the Mayurakshi Basin is being converted into settlement and agricultural land.

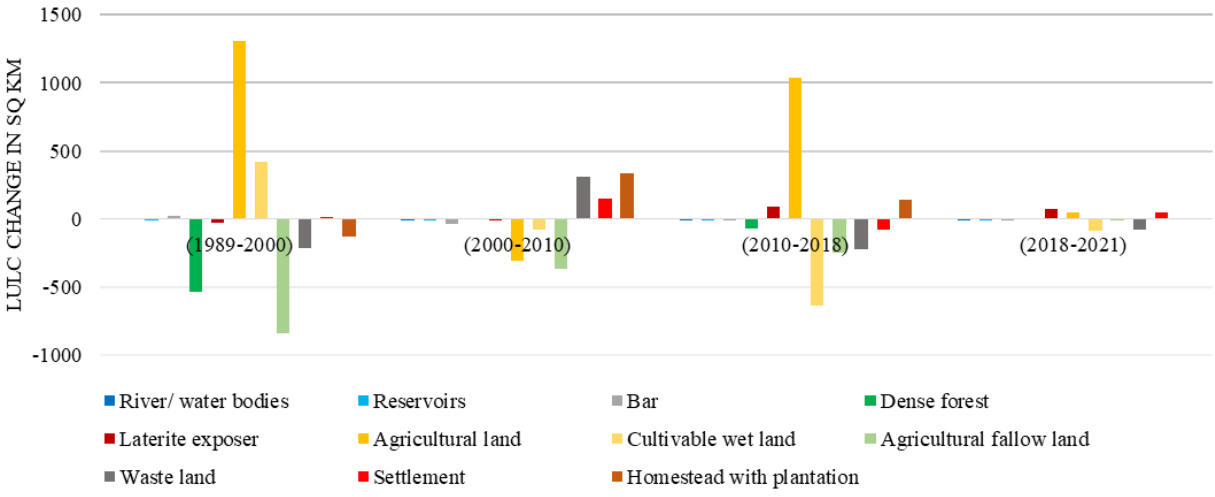

Figure 6.38 *Areal Changes in 32 years Land Use Land Cover of Mayurakshi River Basin Area*

In response to the remarkable transformation in all the eleven land use land cover classes of the study area, a change type map of the 32 years land use land cover analysis has been prepared focussing on the overall river basin health status both in terms of physical and economical perspective. Figure 6.39 shows the 32 years land use land cover map which has been categorised into 3 types. Based on concept of sustainable land use and maintaining the basin health status, any conversion from productive to non-productive land use class can be referred as negative change, for example conversion of agricultural land to waste land. On the other hand, a positive change indicates the conversion of waste or fallow land into dense forest or crop land. No change indicates the unaltered land use land cover classes within a time span of 32 years over the study area. It has been observed from the output that, majority of the land area (37%) has been categorised in negative change group whereas 27% of area has reported under positive change type, reflecting the degradation of natural resources in expanse of the growth of population and cultivable land areas in Mayurakshi River basin area.

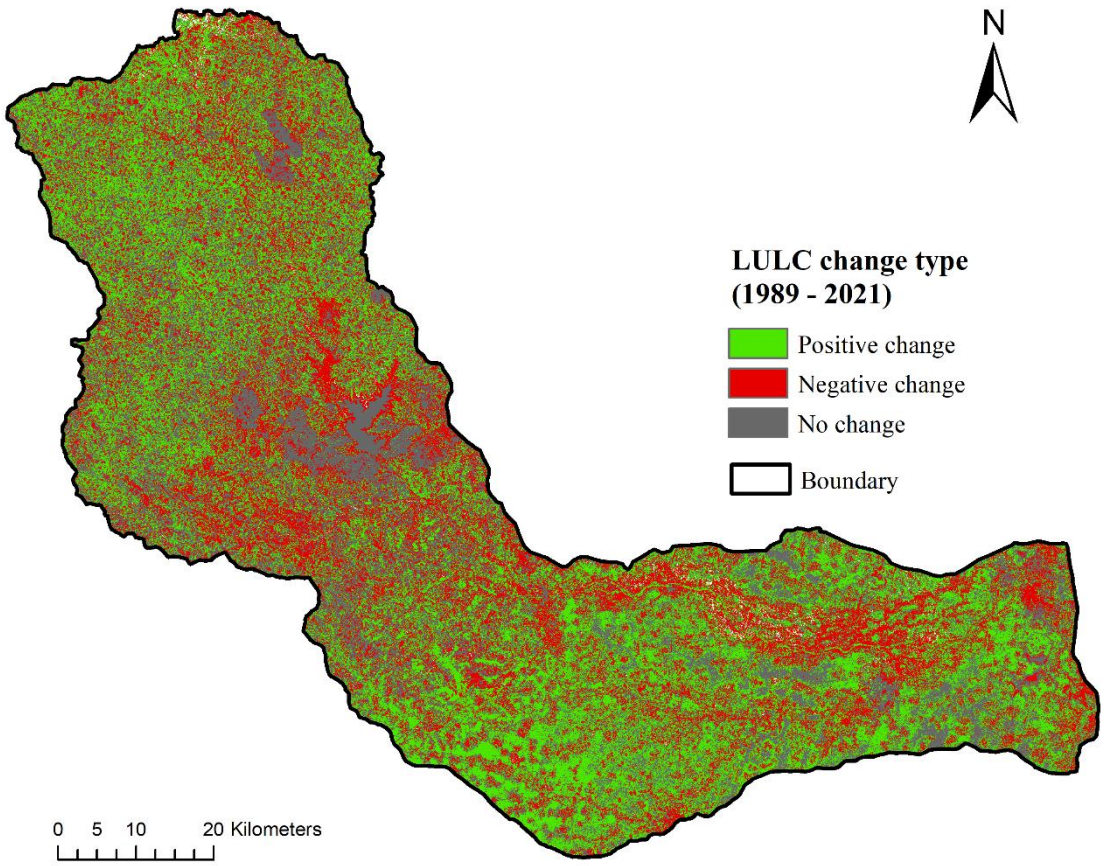

Figure 6.39 *Land Use Land Cover Reconfiguration Map from the year 1989 to 2021*

- **Land Use Land Cover Change Matrix**

A conversion matrix of land use land cover change plays a vital function in the field of land use land cover analysis in illustrating both the nature and direction of land use alteration during a given time period. This matrix generates 'to' and 'from' land use changes that have occurred over a 32-year period. (Table 6.32). The most important conclusion that can be derived from the table is that approximately 527 sq. kilometres of cultivable wet land are being converted to agricultural land, indicating an increase in the land capacity of the region with the highest crop yield. In a comparable manner the conversion of dry fallow to agricultural land accounted for 300.65 sq. kilometres, and the conversion of wet fallow to settlement and homestead with plantation constitute for 414 sq. kilometres and 207.59 sq. kilometres, respectively. Population pressure, agricultural and settlement expansions, and urbanisation are typically the main drivers of LULC changes in the studied area. These factors have a long-term impact on the overall basin health including the hydrological processes such rainfall pattern, evapotranspiration, runoff, and infiltration of the study area.

Table 6.32 *32 Years (1989-2021) Land Use Land Cover Transformation of the Mayurakshi River Basin Area*

		Year 2021 (Area in sq.km)											
	LULC Class Name	River/ Water	Reservoir	Sand Bar	Dense Forest	Lateritic Exposer	Agricultural Crop Land	Cultivated Wet Land	Dry Fallow Land	Waste Land	Settlement	HSP	Total (1989)
Year 1989	River/Water	**18.43**	0.0081	30.53	--	--	0.32	4.88	3.22	--	--	1.49	58.88
	Reservoir	2.51	--	--	--	--	2.013	4.76	--	0.03	28.70	6.12	44.14
	Sand Bar	7.44	--	--	0.082	--	0.21	7.14	3.69	0.04	3.93	--	22.54
	Dense Forest	--	0.9576	0.0027	**299.27**	6.83	--	--	--	--	--	--	307.06
	Lateritic Exposer	0.03			2.58	--	3.64	2.85	0.036	13.30	19.07	1.16	42.66
	Agricultural Crop Land		0.0009	28.21	101.83	3.82	**842.75**	363.78	--	84.75	2.26	0.17	1427.59
	Cultivated Wet Land	0.4005	--	--		--	526.60	**0.42**	320.04	29.56	413.68	207.59	1498.29
	Dry Fallow Land	996.89	--	--	16.74	114.02	300.65	--	**532.90**	--	--	--	1961.20
	Waste Land	7.85	0.42	--	1.74	166.26	12.57	136.91	--	**0.04**	--	--	325.80
	Settlement	--	--	--	1.49	--	17.54	--	1.54	8.47	**13.19**	2.02	44.27
	HSP	--	--	--	8.32	33.49	--	49.88	0.009	--	--	**4.67**	96.37
	Total (2021)	1033.54	1.39	58.74	432.07	324.42	1706.30	570.62	861.43	136.20	480.84	223.23	5828.78

* Bold letters shows the no change area

6.10. Future Prediction of Land Use and Land Cover (LULC) using CA-Markov Chain Model (CA-MCM)

The primary forces behind LULC changes include social variables like population growth and physical elements like physiography (Zubair 2019). Understanding, analysing, and simulating LULC change transitions is essential for many planning and management tasks. The growth of decision-making depends on the observation of past and present LULC changes as well as the prediction of future changes. Recent advancements in remote sensing techniques and integration with geographic information systems (GIS) are able to provide accurate information that permits determining the area and pattern of changes in LULC from the past to the present and predicting the future (Nath et al. 2018). This study focuses on a comparative analysis of past, present, and future predictions of LULC, for implementing a sustainable land use policy of the Mayurakshi river basin area, in order to address the issues associated with the deterioration in river basin health, urban growth, modification of climate, environmental processes, land use problems, food security, urban planning, etc. Various empirical models (Cromley and Hanink 1999), evolutionary models (Sahebgharani 2016), SLEUTH (Zhou et al. 2019), cellular automata (CA)-Markov chain model (MCM) (Abdulrahman and Ameen 2020), artificial neural network/multiple perceptron neural network (ANN/MLPNN)-based model (Saputra and Lee 2019) are just a few of the models that have been used in previous studies to analyse and predict the future land use pattern. Among them the CA Markov chain model (CA-MCM) is a popular choice since it adopts spatial and temporal aspects of LULC dynamics into account, as well as establishes a correlation between land use efficiency, relative change in land use type, land use transfer matrix data, and relevant indicators, and evaluates the execution of policies (Vinayak et al. 2021 and Zubair 2019).

In this study, authors have employed CA Markov model for predicting the future land use dynamism over the Mayurakshi River basin area, mainly to decipher the complex scenario of land use land cover alteration along with their future trend. The potential application of the CA Markov model in an urban setting not only provides a robust method for analysing temporal dynamics among LULC classes based on transition probabilities (Sang et al. 2011), but also determines local norms via the CA spatial filter or transition potential maps projecting for future land use scenarios (Singh et al. 2015).

6.10.1. Data Used

In this study, Sentinel-2 land use land cover time series data has been accessed via Microsoft's Planetary Computer and ESRI, for a temporal period of 2017, 2019 and 2021 at a spatial resolution of 10 meter (https://livingatlas.arcgis.com/landcover/). All of these maps were generated by Impact Observatory's deep learning AI land classification model using more than 5 billion manually annotated Sentinel-2 pixels developed by the National Geographic Society (Karra et al. 2021). The annual land use and land cover map of the study area has been classified into the following classes: River/Water, Natural vegetation, Wet fallow land, Agricultural land, Settlement, Bare land, and Pasture land, with a class definitions displayed in a tabular format (Table 6.33).

Table 6.33 *Details of the Land Use Categories used in this Study*

Sl. no	Land use classes	Description
1	River/Water	Rivers, ponds, lakes and reservoirs
2	Natural vegetation	Scrubland, Grassland, Evergreen, Deciduous and mixed type of forests
3	Wet fallow land	Seasonally flooded area that is a mix of grass/shrub/trees/bare ground or heavily irrigated and inundated agricultural land
4	Agricultural land	Human planted/plotted cereals, grasses, crop lands
5	Settlement	Residential or industrial build-up areas
6	Bare land	Areas of rock or soil with very sparse to no vegetation for the entire year
7	Pasture land	Open areas covered in homogenous grasses with little to no taller vegetation, moderate to sparse cover of bushes, shrubs and tufts of grass

The authors have used historical land use data to anticipate future land use patterns and create forecasts for the years 2031, 2041, and 2051. In order to achieve this goal, it was necessary to assess a number of spatial drivers, including the analysis of elevation, slope, rivers, and dynamic transportation networks. For the evaluation of elevation and slope data, Shuttle Radar Topography Mission (SRTM) data were used. Additionally, the river network of the research area was retrieved from the digital elevation model. Similar to this, the vector dataset of roads and settlements includes the dynamic layer of the transport network extracted using the Open Street Map (OSM) (https://www.openstreetmap.org/) database.

6.10.2. Methodology

- **Future Scenario Predictions Using CA-Markov Chain Model**

CA-Markov, an open-structured spatial model, is frequently employed to improve the accuracy of land cover simulations and forecast potential future land-use scenarios for a region. In this

study, the Land Change Model (LCM) module of TerrSet 18.31, designed by Clark Lab, was employed for the prediction of future LULC of the Mayurakshi River basin area. This model uses multi layer perceptron neural network approach (MLPNN) which considers the historical alterations in LULC with spatial explanatory variables for the evaluation of future trend of LULC over a region.

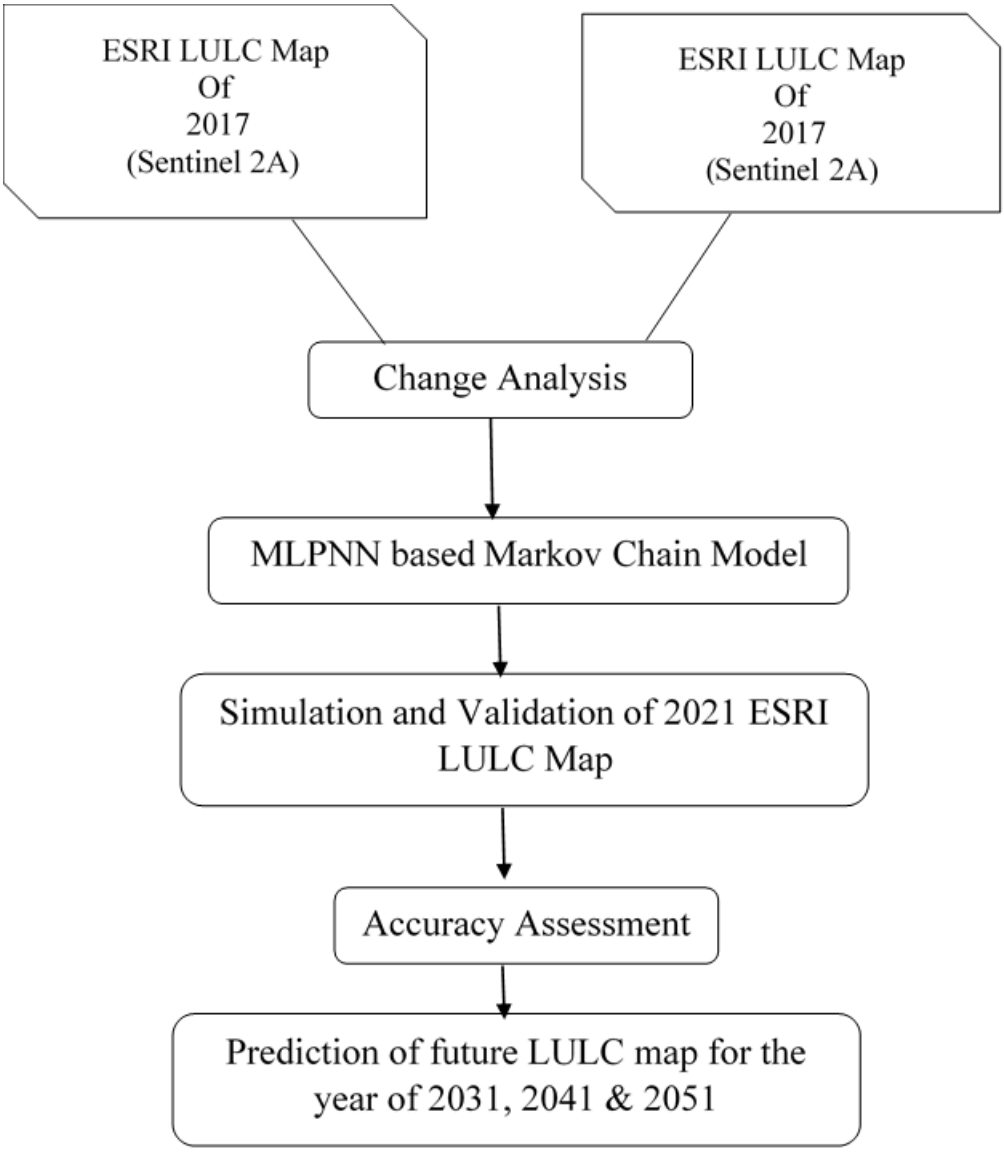

Figure 6.40 *Detailed Methodology Used in CA-Markov Chain Model*

The current research integrates an analysis of LULC from 2017 to 2019 and uses the resulting probability transition models for each year to simulate LULC in 2021. Here, the LULC map for 2021 has been taken into consideration for validation. After the LULC transition from 2017 to 2019 was successfully calibrated and optimised, validation of the simulated output for 2021

was carried out using the 2021 land use and land cover data from ESRI. Similar to this, the CA-Markov chain algorithm has been optimised to simulate future LULC scenarios of Mayurakshi River basin area for the year 2031, 2041, and 2051 (Fig. 6.40). A few transitional potential maps, such as the elevation map, slope map, distance from road, river, and main urban centres of the research area, were also developed as spatial drivers to increase the performance of the land change module of the Markov model. In addition, some significant maps of land use transitions were created based on the maximum amount of land alteration anticipated in 2021. These maps show the transitions from natural vegetation and range land to agricultural land, agricultural land to settlement, and natural vegetation and agricultural land to range land. All of these maps served as a bridge to the sub model at a later point (Fig. 6.41). The third and fourth polynomial functions have been used to build each transitional map during this process because they provide the finest situation for illustrating the shifting patterns of each class.

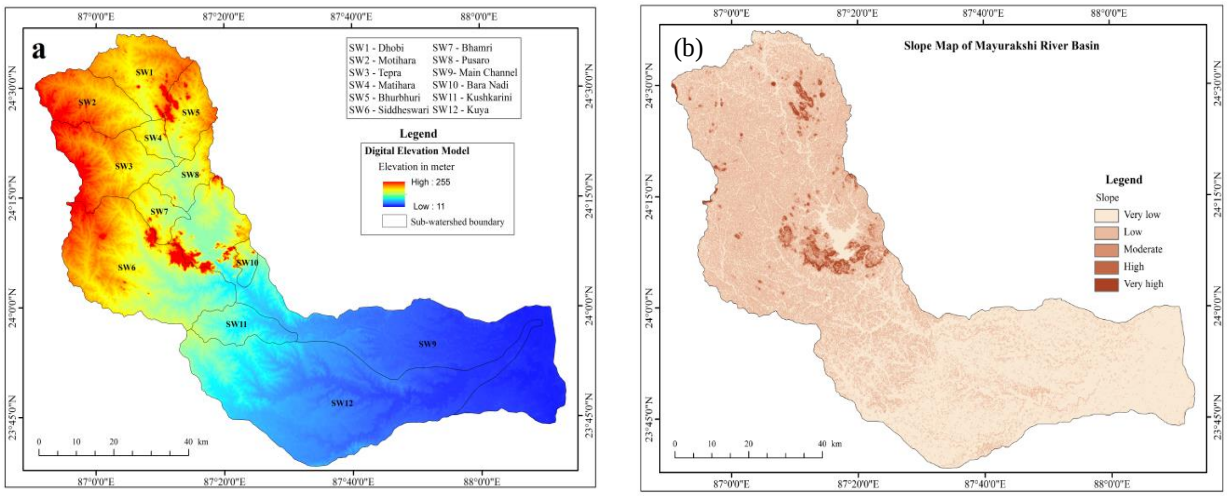

Figure 6.41 *CA-Markov Model Transition Potential Maps (a) Digital Elevation Model (b) Slope Map (c) Euclidean Distance Map from River (d) Euclidean Distance Map from Road (e) Euclidean Distance Map from Urban Areas (f) Spatial trend of Change Map from Natural Vegetation to Agricultural Land (g) Spatial trend of Change Map from Natural Vegetation to Pasture Land (h) Spatial trend of Change Map from Pasture Land to Agricultural Land (i) Spatial trend of Change Map from Agricultural Land to Settlement (j) Spatial trend of Change Map from Agricultural Land to Pasture Land*

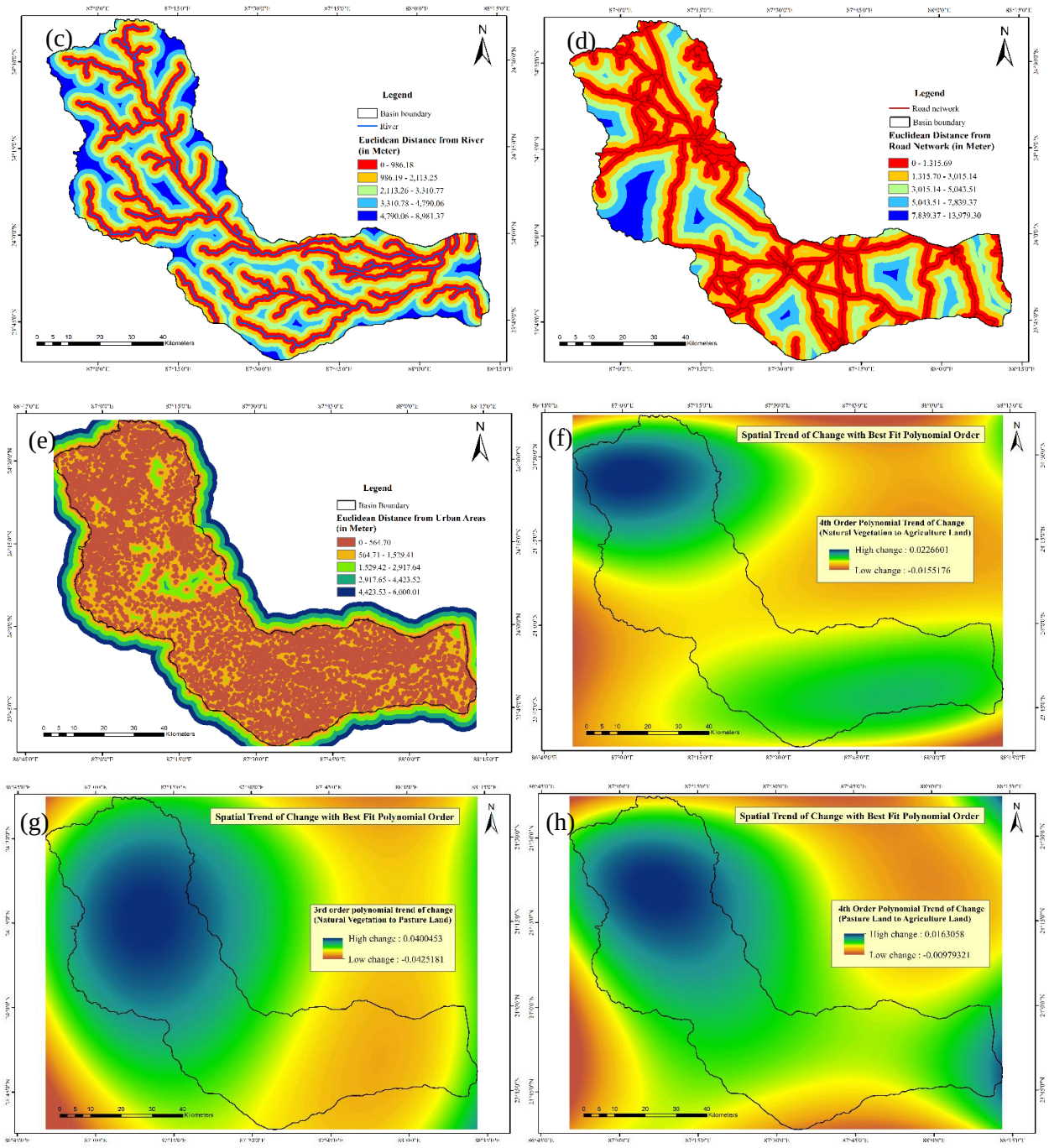

Figure 6.41 *Continued*

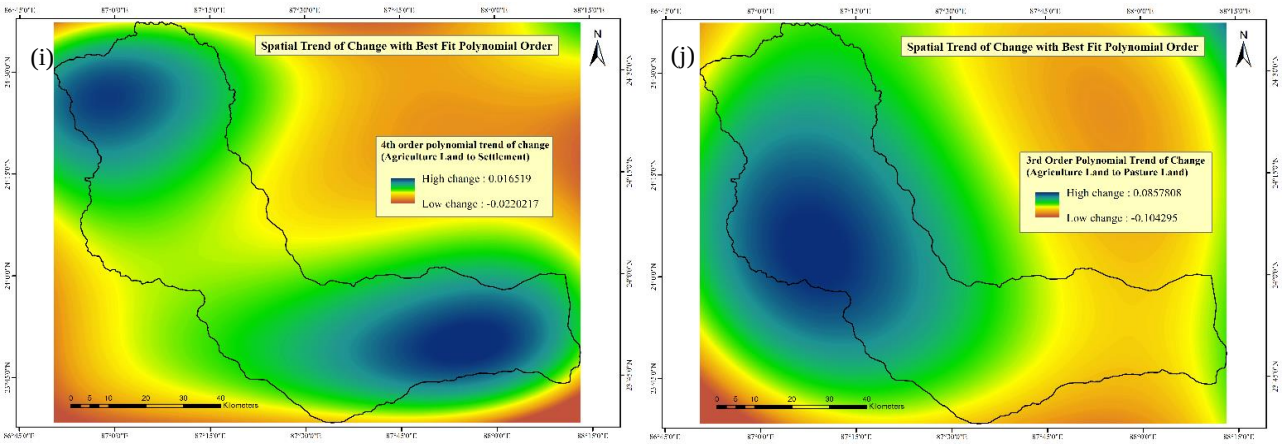

Figure 6.41 *Continued*

- **Accuracy Assessment**

The MCM was used to calculate the total amount of changes in the LULC pattern after the construction of transition potential maps and LULC maps, and it was then used to assess the changes that occurred during the course of prediction. This model has also been helpful includes calculating the transition probability matrix, which shows the probability that a member of one LULC class will switch to a member of every other class within the anticipated time period. In order to estimate the future spatial pattern of LULC, transition probabilities and prospective transition maps were produced. In this study, the simulated LULC of 2021 has been validated with the real LULC received from the ESRI LULC map. For validation as well as accuracy assessment, the kappa index statistics were used to compare the maps that were actually drawn with those that were anticipated. Four alternative kappa index calculations were made for the validation: kappa for no information (k_{no}), kappa for stratum level location ($k_{location\ strata}$), kappa for grid cell level location ($k_{location}$), and kappa for standard (Vinayak et al. 2021). All this validation processes has already been embedded within the Terrset software's Validation Module.

6.10.3. Result and Discussions

- **ESRI LULC Change Analysis**

The Mayurakshi River basin area's classified land use and land cover map for the years 2017, 2019, and 2021 are shown in figure 6.42. The LULC map produced by ESRI shows that during the study period, agricultural land predominance has been very perceptible in the study area. As shown in figure 6.43, about 4256.83 sq. km of the total area was devoted to agriculture in 2017, and in 2019 and 2021, that amount climbed to 4327.81 sq. km and 4389.86 sq. km,

respectively. Similar types of growth have been seen in settlement classes, where 333.94 sq. kilometres in 2017 increased to 423.38 sq. kilometres and 448.34 sq. kilometres in 2019 and 2021, respectively. On the other hand, the research region has seen a noticeable decline in the overall statistics of natural vegetation. The overall amount of natural vegetation has shrunk from 584 sq. kilometres in 2017 to 280 sq. kilometres in 2021. The changes in the surrounding environment for the other groups during the course of the four-year study period, such as wet fallow land and bare land, are insignificant.

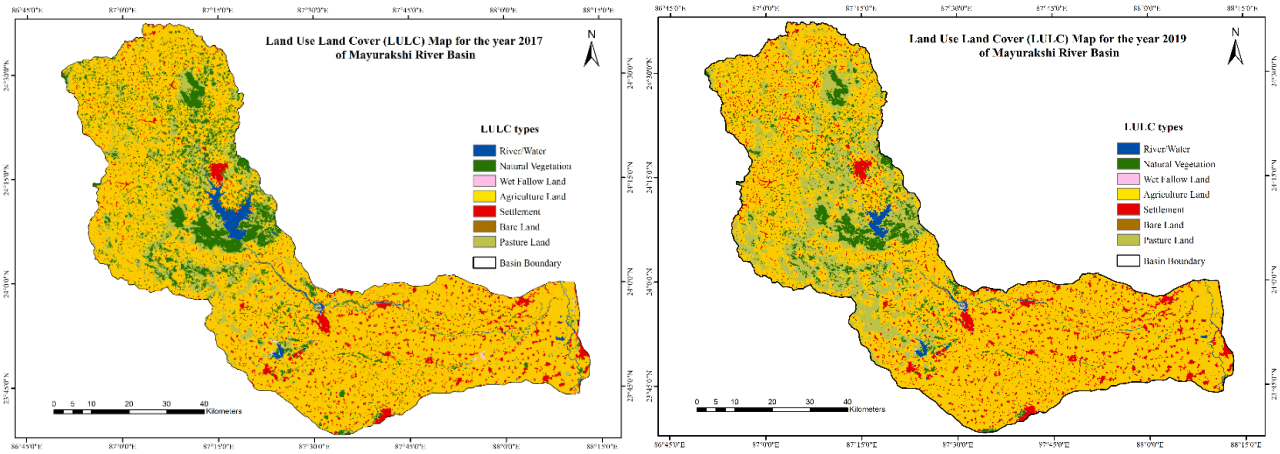

Figure 6.42 *ESRI Produced Land Use Land Cover Map of the Mayurakshi River Basin Area for the period of 2017 & 2019*

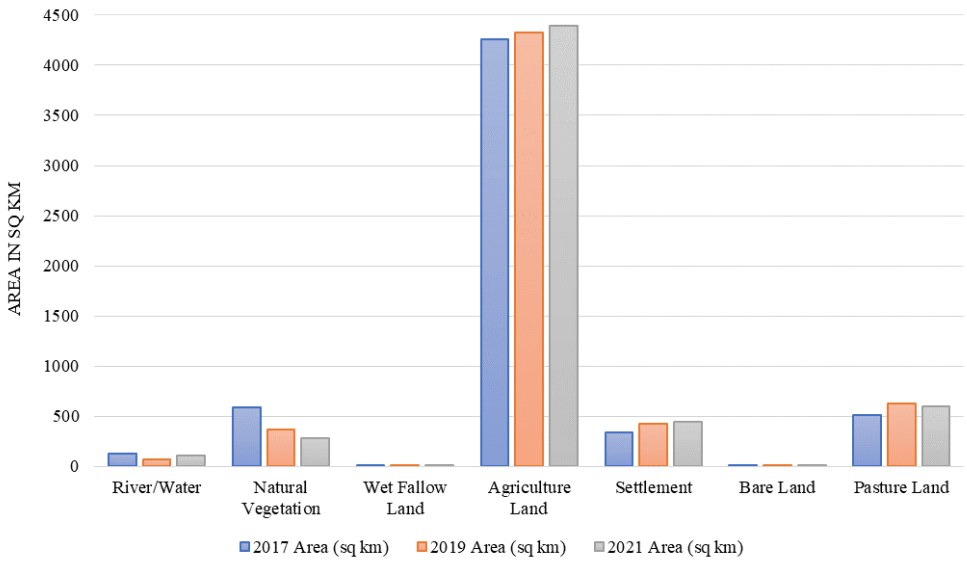

Figure 6.43 *Areal Coverage in Individual Land Use Classes for the Period of 2017, 2019 and 2021*

➢ Prediction and Validation of LULC for 2021

Figure 6.44 illustrates how the LULC of 2017 and 2019 were used in this work to replicate the LULC of the year 2021. The MLPNN-based MCM has been used for this purpose, and the computed transition potentials show greater than 90% accuracy for all classes. Figure 6.45 shows percentage-wise area data of the observed and projected LULC for 2021, and to evaluate the model's predicting competence, an accuracy evaluation has been carried out, showing about the same model output.

The comparative bar graph displays the similarities and contrasts between the maps in 2021 for the areas of existing and projected land-use classes. The river, wet fallow land, bare land and pasture land seemed nearly same on both the reference and projected result for 2021. With the exception of natural vegetation, agricultural land and settlement, the reference and simulated areal statistics were nearly comparable for the land use categories in which they differed slightly.

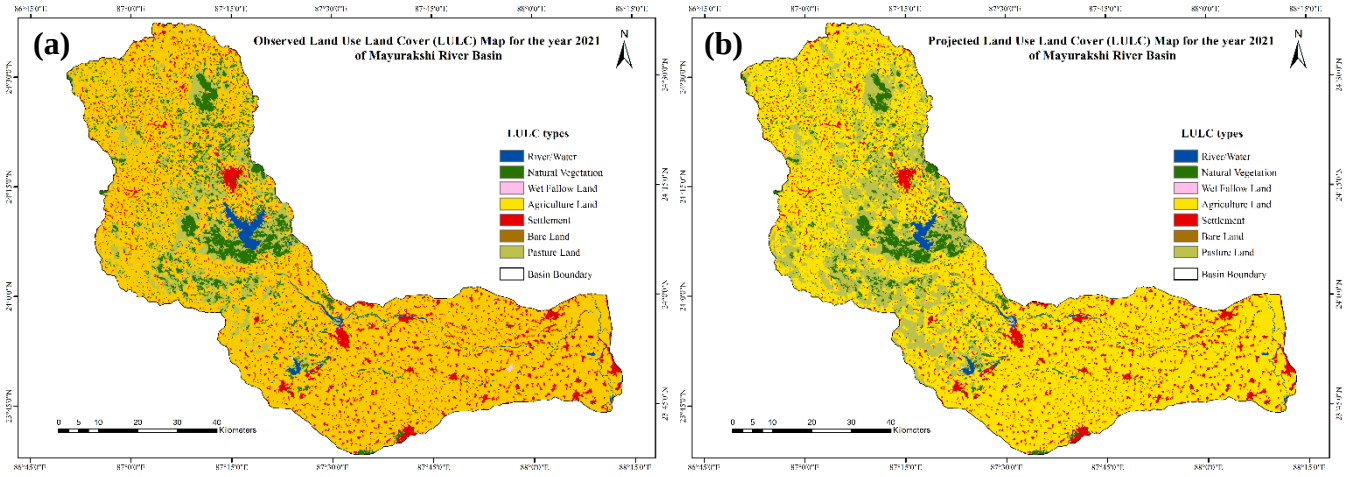

Figure 6.44 *(a) Observed and (b) Projected LULC map of Mayurakshi River basin area for the year 2021*

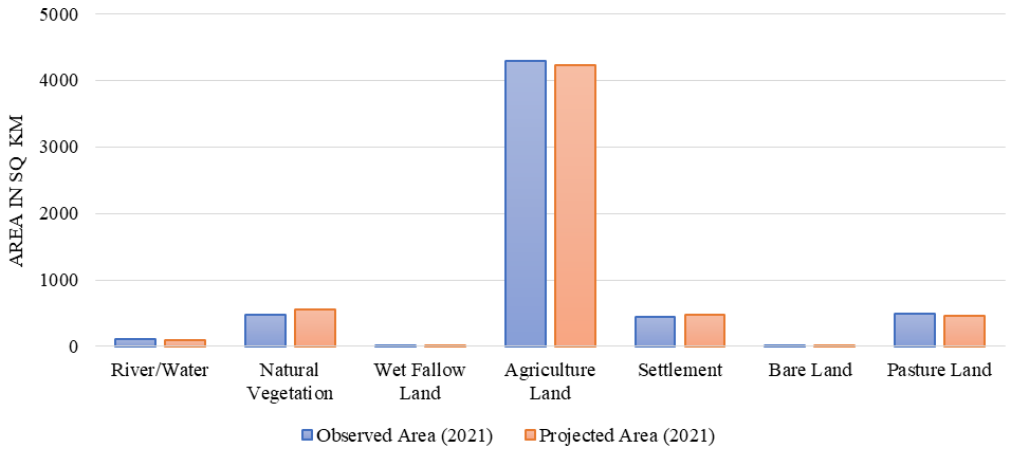

Figure 6.45 *Areal Changes of Observed and Predicted Land use Land Cover Classes for the Year of 2021*

- **Projected Land Use Pattern for the Year 2031, 2041 and 2051**

In the prediction of 2051 LULC (Fig. 6.46c), the transition potentials and transition probabilities in Table estimated from the 2017–2019 LULC data were utilized. Table 6.34 indicates that in the future (2051), every classes were equally contributed to the conversion into the settlement. On the other hand, wet fallow land has leading the most (0.5004) in changing into the agricultural land over the study area.

An area wise comparative study has also been executed (Table 6.35 and Fig. 6.47) showing the LULC statistics for the year of projected 2021, 2031, 2041 and 2051 along with the observed result of 2021 LULC. The result shows that compared to 2021, the total area under settlement, pasture land would be increased by 561.38 sq. km, 2025.13 sq. km respectively. However, between the time span of 2021 to 2051, land under river or water, agricultural land and natural vegetation is expected to reduce rapidly from 103 to 70.91 sq. km, 4289.86 to 2898.82 sq. km and 480.45 to 260.32 sq. km respectively. These alterations in the future pattern of LULC are maybe the response of ongoing and proposed development of this region in the various sectors like industrial, infrastructure, transportation, etc.

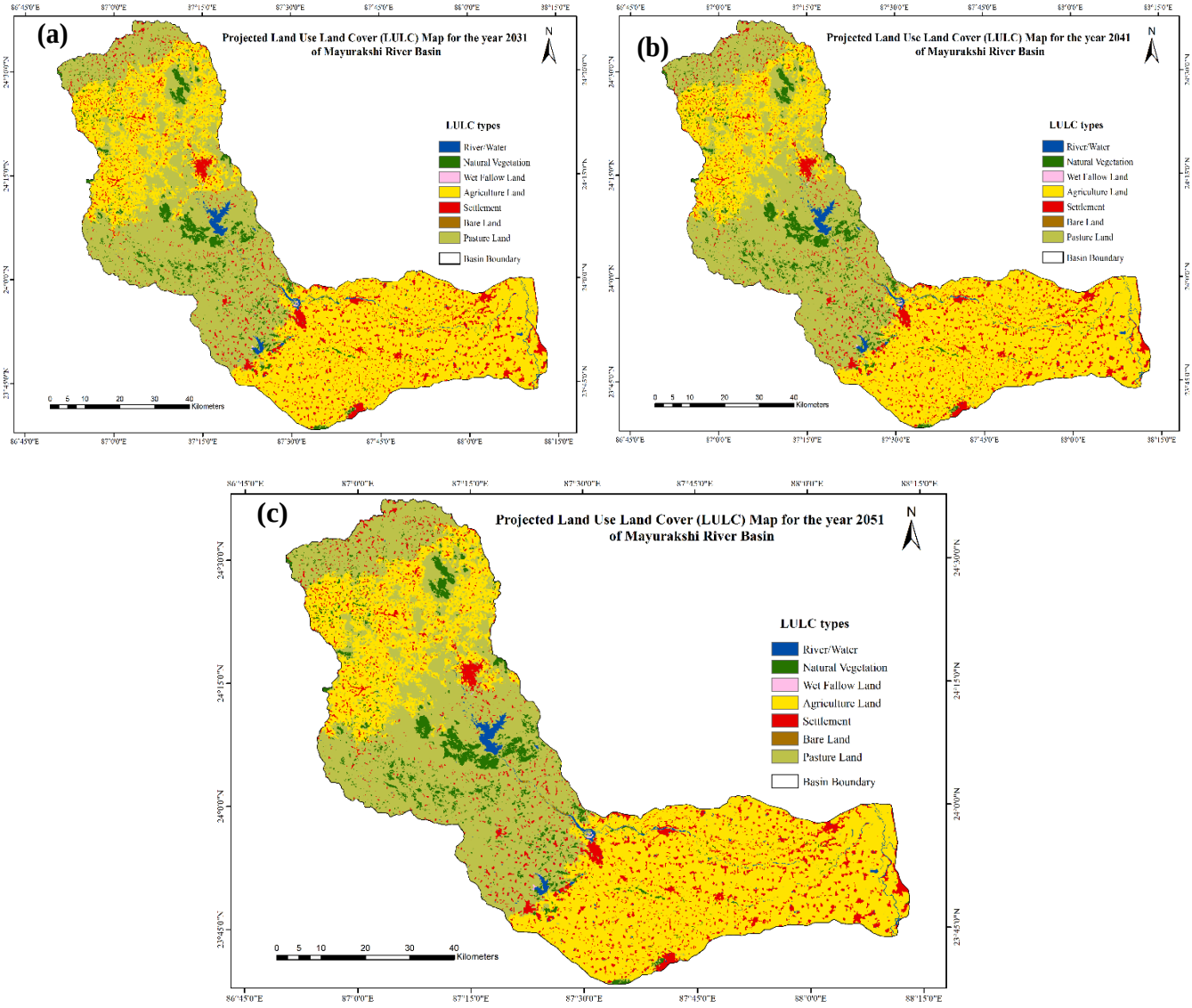

Figure 6.46 *Predicted Land Use Land Cover Map of Mayurakshi River basin area (a) Year 2031 (b) Year 2041 (c) Year 2051*

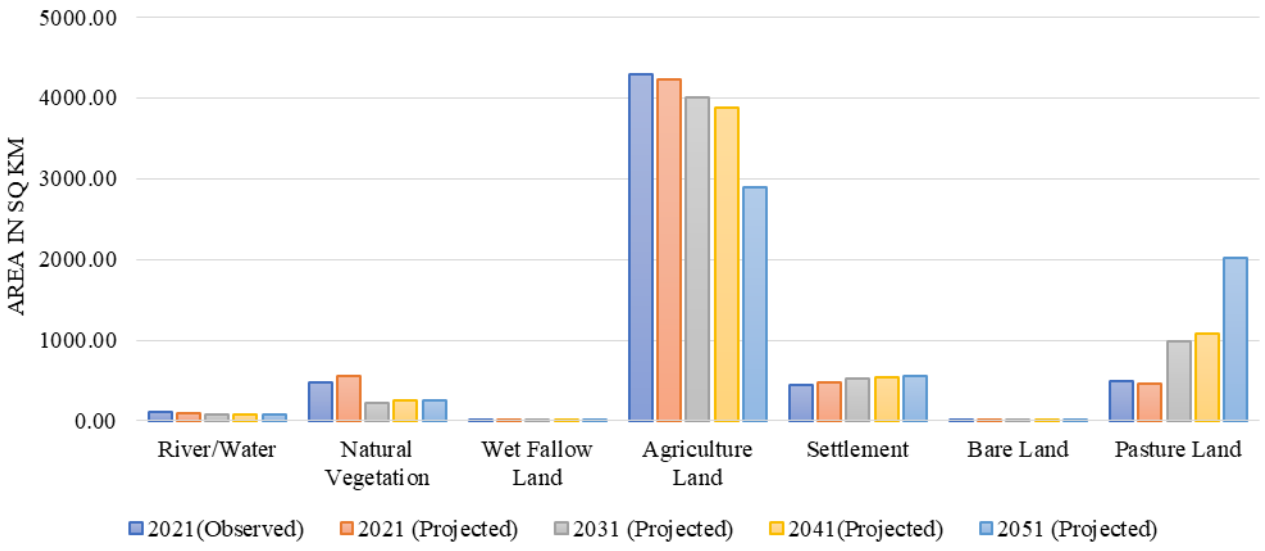

Figure 6.47 *Comparative Analysis of Areal Changes in Observed and Projected Land Use Land Cover Classes in Mayurakshi River Basin Area*

Table 6.34 *Markov Transitional Probability Matrix of LULC 2051 Used For Simulation of This Study*

LULC classes	River/Water	Natural vegetation	Wet fallow land	Agricultural land	Settlement	Bare land	Pasture land
River/Water	0.0024	0.0173	0.0003	0.4746	0.1972	0.0003	0.2821
Natural vegetation	0.0024	0.0181	0.0003	0.4978	0.2189	0.0003	0.2854
Wet fallow land	0.0024	0.0173	0.0003	0.5004	0.2006	0.0003	0.2813
Agricultural land	0.0024	0.0172	0.0003	0.4995	0.2000	0.0003	0.2803
Settlement	0.0019	0.0117	0.0002	0.2921	0.5037	0.0002	0.1902
Bare land	0.0024	0.0177	0.0003	0.4934	0.2012	0.0003	0.2848
Pasture land	0.0024	0.0180	0.0003	0.4745	0.2191	0.0003	0.2854

Table 6.35 *Areal statistics of Land Use Land Cover Analysis of the Projected Years of 2031, 2041 and 2051*

Land cover types	Year 2021		Year 2031 (Projected)	Year 2041(Projected)	Year 2051 (Projected)
	Observed	Projected			
River/Water	103.00	97.80	72.91	70.91	70.91
Natural Vegetation	480.45	548.52	223.27	249.25	260.32
Wet Fallow Land	2.75	2.34	1.94	1.69	1.61
Agriculture Land	4289.86	4227.80	4012.01	3875.11	2898.82
Settlement	448.34	478.78	523.38	544.25	561.38
Bare Land	2.22	2.11	3.90	4.01	4.32
Pasture Land	495.81	465.06	985.05	1077.23	2025.13
TOTAL	**5822.41**	**5822.41**	**5822.41**	**5822.41**	**5822.41**

6.10.4. Conclusion

The goal of the current study is to comprehend how past and anticipated LULC patterns have changed from 2017 to 2051. This investigation was conducted using an integrated strategy that used GIS, remote sensing, and an MLPNN-based MCM model. The numerous meteorological and environmental processes may shift as a result of projected future LULC changes over Mayurakshi River basin area. For instance, the rapid growth of metropolitan areas can change the region's leaf area index, albedo, and sky view factor, which can change the micrometeorology of the study area by interfering with the interaction between the ground and the atmosphere.

Therefore, it is essential to create some policies and strategies that can reduce the negative consequences brought on by those changes in order to meet the goals for sustainable development and urban planning. Additionally, different stakeholders, including urban planners, meteorologists, and policy-makers, will benefit from the spatial data gathered from these types of studies in order to construct the local and regional scale plans necessary for sustainable development.

References

- Abdulrahman, A. I., & Ameen, S. A. (2020). Predicting Land use and land cover spatiotemporal changes utilizing CA-Markov model in Duhok district between 1999 and 2033. *Academic Journal of Nawroz University*, *9*(4), 71-80.
- Adiat, K. A. N., Nawawi, M. N. M., & Abdullah, K. (2012). Assessing the accuracy of GIS-based elementary multi criteria decision analysis as a spatial prediction tool–a case of predicting potential zones of sustainable groundwater resources. *Journal of Hydrology*, *440*, 75-89.
- Agarwal, E., Agarwal, R., Garg, R. D., & Garg, P. K. (2013). Delineation of groundwater potential zone: An AHP/ANP approach. *Journal of earth system science*, *122*, 887-898.
- Aher, P., Adinarayana, J., & Gorantiwar, S. D. (2013). Prioritization of watersheds using multi-criteria evaluation through fuzzy analytical hierarchy process. *Agricultural Engineering International: CIGR Journal*, *15*(1), 11-18.
- Alam, M. A., Emura, K., Farnham, C., & Yuan, J. (2018). Best-fit probability distributions and return periods for maximum monthly rainfall in Bangladesh. *Climate*, *6*(1), 9.
- AlHassoun, S. A. (2011). Developing an empirical formulae to estimate rainfall intensity in Riyadh region. *Journal of King Saud university-engineering sciences*, *23*(2), 81-88.
- Alifujiang, Y., Abuduwaili, J., Maihemuti, B., Emin, B., & Groll, M. (2020). Innovative trend analysis of precipitation in the Lake Issyk-Kul Basin, Kyrgyzstan. *Atmosphere*, *11*(4), 332.
- Alsdorf, D. E., & Lettenmaier, D. P. (2003). Tracking fresh water from space. *Science*, *301*(5639), 1491-1494.
- Ameri, A. A., Pourghasemi, H. R., & Cerda, A. (2018). Erodibility prioritization of sub-watersheds using morphometric parameters analysis and its mapping: A comparison among TOPSIS, VIKOR, SAW, and CF multi-criteria decision making models. *Science of the Total Environment*, *613*, 1385-1400.
- Amiri, M., Pourghasemi, H. R., Arabameri, A., Vazirzadeh, A., Yousefi, H., & Kafaei, S. (2019). Prioritization of flood inundation of Maharloo Watershed in iran using morphometric parameters analysis and TOPSIS MCDM model. In *Spatial modeling in GIS and R for earth and environmental sciences* (pp. 371-390). Elsevier.
- Annual flood report 2016 Irrigation and waterways directorate. Government of West Bengal. https ://wbiwd .gov.in/uploa ds/ANNUAL_FLOOD REPOR T_2016.pdf.
- Aouragh, M. H., & Essahlaoui, A. (2018). A TOPSIS approach-based morphometric analysis for sub-watersheds prioritization of high Oum Er-Rbia basin, Morocco. *Spatial Information Research*, *26*, 187-202.
- Arabameri, A., Pradhan, B., Pourghasemi, H. R., & Rezaei, K. (2018). Identification of erosion-prone areas using different multi-criteria decision-making techniques and GIS. *Geomatics, Natural Hazards and Risk*, *9*(1), 1129-1155.
- Arami, S. A., Alvandi, E., Frootandanesh, M., Tahmasebipour, N., & Sangchini, E. K. (2017). Prioritization of watersheds in order to perform administrative measures using fuzzy analytic hierarchy process. *Journal of the Faculty of Forestry Istanbul University*, *67*(1), 13-21.
- Arnold, J. G., Srinivasan, R., Muttiah, R. S., & Williams, J. R. (1998). Large area hydrologic modeling and assessment part I: model development 1. *JAWRA Journal of the American Water Resources Association*, *34*(1), 73-89.

- Arnoldus, H. M. J. (1980). An approximation of the rainfall factor in the Universal Soil Loss Equation. *An approximation of the rainfall factor in the Universal Soil Loss Equation.*, 127-132.
- Ayhan, M. B. (2013). A fuzzy AHP approach for supplier selection problem: A case study in a Gear motor company. *arXiv preprint arXiv:1311.2886*.
- Ayman G, A., Mohamed, E., Ashraf, E., & Hesham, E. (2011). Developing intensity-duration-frequency curves in scarce data region: an approach using regional analysis and satellite data. *Engineering*, *2011*.
- Azizi, A., Aikhuele, D. O., & Souleman, F. S. (2015). A fuzzy TOPSIS model to rank automotive suppliers. *Procedia Manufacturing*, *2*, 159-164.
- Babu, K. J., Sreekumar, S., Arish, A., & Midhun, K. P. (2014). Hypsometry and geomorphic development of a watershed: A case study from South India. *İnternational journal of science and research*, *3*(10).
- Basu, S. R., Ghosh, A., & De, S. K. (2005). Meandering and cut-off of the river Bhagirathi. *Geomorphology and environmental sustainability. Concept Publishing Company, New Delhi*, 20-37.
- Beven, K. J., & Kirkby, M. J. (1979). A physically based, variable contributing area model of basin hydrology/Un modèle à base physique de zone d'appel variable de l'hydrologie du bassin versant. *Hydrological sciences journal*, *24*(1), 43-69.
- Bhattacharya, R. K., Das Chatterjee, N., & Das, K. (2019). Multi-criteria-based sub-basin prioritization and its risk assessment of erosion susceptibility in Kansai–Kumari catchment area, India. *Applied Water Science*, *9*, 1-30.
- Biswas, S., Sudhakar, S., & Desai, V. R. (1999). Prioritisation of subwatersheds based on morphometric analysis of drainage basin: A remote sensing and GIS approach. *Journal of the Indian society of remote sensing*, *27*, 155-166.
- Bjerklie, D. M., Dingman, S. L., Vorosmarty, C. J., Bolster, C. H., & Congalton, R. G. (2003). Evaluating the potential for measuring river discharge from space. *Journal of hydrology*, *278*(1-4), 17-38.
- Bloom L (2009) Geomorphology, a Systematic Analysis of Late Cenozoic Landforms, PHI Learning Private, New Delhi, India, 3rd edition.
- Buckley, J. J. (1985). Fuzzy hierarchical analysis. *Fuzzy sets and systems*, *17*(3), 233-247.
- Burke, C. B., & Burke, T. T. (2008). Storm Drainage Manual. *Indiana LTAP*.
- Central Ground Water Board 2018 Ministry of water resources, river development and ganga rejuvenation, government of India (2017–2018); *ground water year book- India* 2017-2018
- CGWB Report 2016 http://cgwb.gov.in. Last retrieved September 2020.
- Chakraborty, A. (2015). Study on growth of major agricultural crops in Birbhum district. *J. Agric. Vet. Sci*, *2*(1), 63-66.
- Chang, D. Y. (1996). Applications of the extent analysis method on fuzzy AHP. *European journal of operational research*, *95*(3), 649-655.
- Chaudhry MH (1993) Open-Channel Flow. Prentice-Hall, Inc.
- Chaudhury, A. K. (1966). On the meteorological conditions responsible for heavy rainfall in Ajay catchment Area. *Indian J Meteorol Geophys*, *17*, 127-132.
- Chenini, I., Mammou, A. B., & El May, M. (2010). Groundwater recharge zone mapping using GIS-based multi-criteria analysis: a case study in Central Tunisia (Maknassy Basin). *Water resources management*, *24*, 921-939.
- Chorley, R. J. (1969). Introduction to Fluvial Processes. Bungay.
- Chow VT (1959) Open-Channel Hydraulics, McGraw-Hill, New York, NY, USA.

- Chowdary, V. M., Chakraborthy, D., Jeyaram, A., Murthy, Y. K., Sharma, J. R., & Dadhwal, V. K. (2013). Multi-criteria decision making approach for watershed prioritization using analytic hierarchy process technique and GIS. *Water resources management*, *27*, 3555-3571.
- Chowdary, V. M., Ramakrishnan, D., Srivastava, Y. K., Chandran, V., & Jeyaram, A. (2009). Integrated water resource development plan for sustainable management of Mayurakshi watershed, India using remote sensing and GIS. *Water resources management*, *23*(8), 1581-1602.
- Chowdhury, A., Jha, M. K., & Chowdary, V. M. (2010). Delineation of groundwater recharge zones and identification of artificial recharge sites in West Medinipur district, West Bengal, using RS, GIS and MCDM techniques. *Environmental Earth Sciences*, *59*, 1209-1222.
- Cohen, J. (1960). A coefficient of agreement for nominal scales. *Educational and psychological measurement*, *20*(1), 37-46.
- Cromley, R. G., & Hanink, D. M. (1999). Coupling land use allocation models with raster GIS. *Journal of geographical systems*, *1*, 137-153.
- Cui, L., Wang, L., Lai, Z., Tian, Q., Liu, W., & Li, J. (2017). Innovative trend analysis of annual and seasonal air temperature and rainfall in the Yangtze River Basin, China during 1960–2015. *Journal of Atmospheric and Solar-Terrestrial Physics*, *164*, 48-59.
- da Costa, A. M., de Salis, H. H. C., Viana, J. H. M., & Leal Pacheco, F. A. (2019). Groundwater recharge potential for sustainable water use in urban areas of the Jequitiba River Basin, Brazil. *Sustainability*, *11*(10), 2955.
- Dar, T., Rai, N., & Bhat, A. (2021). Delineation of potential groundwater recharge zones using analytical hierarchy process (AHP). *Geology, Ecology, and Landscapes*, *5*(4), 292-307.
- Das, J., Rahman, A. S., Mandal, T., & Saha, P. (2021). Exploring driving forces of large-scale unsustainable groundwater development for irrigation in lower Ganga River basin in India. *Environment, Development and Sustainability*, *23*, 7289-7309.
- David A. Chin (2020) Water-resources Engineering. 4th Edition, Pearson Prentice Hall publisher, United States of America
- De Waroux, Y. L. P., & Lambin, E. F. (2012). Monitoring degradation in arid and semi-arid forests and woodlands: The case of the argan woodlands (Morocco). *Applied Geography*, *32*(2), 777-786.
- Debelo, G., Tadele, K., & Koriche, S. A. (2017). Morphometric analysis to identify erosion Prone areas on the upper blue Nile using Gis (Case Study of Didessa and Jema Sub-Basin, Ethiopia). *International Research Journal of Engineering and Technology*, *4*(8), 1773-1784.
- Dong, Z., Jia, W., Sarukkalige, R., Fu, G., Meng, Q., & Wang, Q. (2020). Innovative trend analysis of air temperature and precipitation in the jinsha river basin, china. *Water*, *12*(11), 3293.
- Dupont, B. S., Allen, D. L., & Clark, K. D. (2000). Revision of the rainfall-intensity-duration curves for the Commonwealth of Kentucky. Kentucky Transportation Center, College of Engineering, University of Kentucky. *Econ. Geogr*, *47*, 438-451.
- Elmahdy, S. I., & Mohamed, M. M. (2018). Monitoring and analysing the Emirate of Dubai's land use/land cover changes: An integrated, low-cost remote sensing approach. *International Journal of Digital Earth*, *11*(11), 1132-1150.
- Elsebaie, I. H. (2012). Developing rainfall intensity–duration–frequency relationship for two regions in Saudi Arabia. *Journal of King Saud University-Engineering Sciences*, *24*(2), 131-140.

- Faniran, A. (1968). The index of drainage intensity: a provisional new drainage factor. *Aust J Sci*, *31*(9), 326-330.
- FAO, F. (2015). Agriculture Organization: Status of the World's Soil Resources (SWSR)–Main Report. *Food and Agriculture Organization of the United Nations and Intergovernmental Technical Panel on Soils, Rome, Italy*.
- Farhan, Y., & Anaba, O. (2016). A remote sensing and GIS approach for prioritization of Wadi Shueib Mini-Watersheds (Central Jordan) based on morphometric and Soil erosion susceptibility analysis. *Journal of Geographic Information System*, *8*(1), 1-19.
- Farlie, D. J. G. (1971). Rank correlation methods.
- Feyisa, G. L., Meilby, H., Fensholt, R., & Proud, S. R. (2014). Automated Water Extraction Index: A new technique for surface water mapping using Landsat imagery. *Remote sensing of environment*, *140*, 23-35.
- Gao, B. C. (1996). NDWI—A normalized difference water index for remote sensing of vegetation liquid water from space. *Remote sensing of environment*, *58*(3), 257-266.
- Gedefaw, M., Yan, D., Wang, H., Qin, T., Girma, A., Abiyu, A., & Batsuren, D. (2018). Innovative trend analysis of annual and seasonal rainfall variability in Amhara regional state, Ethiopia. *Atmosphere*, *9*(9), 326.
- Gee, G. W., Campbell, M. D., Campbell, G. S., & Campbell, J. H. (1992). Rapid measurement of low soil water potentials using a water activity meter. *Soil Science Society of America Journal*, *56*(4), 1068-1070.
- Getirana, A. C. V., Bonnet, M. P., Roux, E., Calmant, S., Rotunno Filho, O. C., & Mansur, W. J. (2009). Hydrological monitoring of large poorly gauged basins: a new approach based on spatial altimetry and distributed rainfall-runoff model. J. Hydrol, 379, 205-219.
- Ghosh, S., & Guchhait, S. K. (2016). Dam-induced changes in flood hydrology and flood frequency of tropical river: a study in Damodar River of West Bengal, India. *Arabian Journal of Geosciences*, *9*, 1-26.
- Gocic, M., & Trajkovic, S. (2013). Analysis of changes in meteorological variables using Mann-Kendall and Sen's slope estimator statistical tests in Serbia. *Global and planetary change*, *100*, 172-182.
- Gonzalez-Trinidad, J., Junez-Ferreira, H. E., Pacheco-Guerrero, A., Olmos-Trujillo, E., & Bautista-Capetillo, C. F. (2017). Dynamics of land cover changes and delineation of groundwater recharge potential sites in the Aguanaval aquifer, Zacatecas, Mexico. *Applied Ecology & Environmental Research*, *15*(3).
- Gurnell, A. M., Corenblit, D., García de Jalón, D., González del Tánago, M., Grabowski, R. C., O'hare, M. T., & Szewczyk, M. (2016). A conceptual model of vegetation–hydrogeomorphology interactions within river corridors. *River research and applications*, *32*(2), 142-163.
- Halder, S., Roy, M. B., & Roy, P. K. (2020). Fuzzy logic algorithm based analytic hierarchy process for delineation of groundwater potential zones in complex topography. *Arabian Journal of Geosciences*, *13*, 1-22.
- Hardisky, M. A., Daiber, F. C., Roman, C. T., & Klemas, V. (1984). Remote sensing of biomass and annual net aerial primary productivity of a salt marsh. *Remote Sensing of Environment*, *16*(2), 91-106.
- Hoque, M. M., Islam, A., & Ghosh, S. (2022). Environmental flow in the context of dams and development with special reference to the Damodar Valley Project, India: a review. *Sustainable Water Resources Management*, *8*(3), 62.

- Horton, R. E. (1945). Erosional development of streams and their drainage basins; hydrophysical approach to quantitative morphology. *Geological society of America bulletin*, *56*(3), 275-370.
- Huang, C., Chen, Y., Zhang, S., & Wu, J. (2018). Detecting, extracting, and monitoring surface water from space using optical sensors: A review. *Reviews of Geophysics*, *56*(2), 333-360.
- Hussein, M. T. (2004). Hydrochemical evaluation of groundwater in the Blue Nile Basin, eastern Sudan, using conventional and multivariate techniques. *Hydrogeology Journal*, *12*, 144-158.
- Hwang, C. L., Yoon, K., Hwang, C. L., & Yoon, K. (1981). Methods for multiple attribute decision making. *Multiple attribute decision making: methods and applications a state-of-the-art survey*, 58-191.
- IPCC, A. (2013). Climate change 2013: the physical science basis. *Contribution of working group I to the fifth assessment report of the intergovernmental panel on climate change*, *1535*.
- Islam, A., & Ghosh, S. (2021). Economic transformation in the wake of flood: a case of the lower stretch of the Mayurakshi River Basin, India. *Environment, development and sustainability*, *23*(10), 15550-15590.
- Islam, A., & Sarkar, B. (2020). Analysing flood history and simulating the nature of future floods using Gumbel method and Log-Pearson Type III: the case of the Mayurakshi River Basin, India. *Bulletin of Geography. Physical Geography Series*, (19), 43-69.
- Jaafar, H. H., Ahmad, F. A., & El Beyrouthy, N. (2019). GCN250, new global gridded curve numbers for hydrologic modeling and design. *Scientific data*, *6*(1), 145.
- Jain, S. K., & Kumar, P. (2014). Environmental flows in India: towards sustainable water management. *Hydrological Sciences Journal*, *59*(3-4), 751-769.
- Javed A, Khanday M, Ahmad R (2020) Prioritization of sub-watersheds based on morphometric and land use analysis using Remote Sensing and GIS techniques. Journal of the Indian Society of Remote Sensing.37(2):261-274.
- Jhariya, D. C., Kumar, T., & Pandey, H. K. (2020). Watershed prioritization based on soil and water hazard model using remote sensing, geographical information system and multi-criteria decision analysis approach. *Geocarto International*, *35*(2), 188-208.
- Jhariya, D. C., Kumar, T., Gobinath, M., Diwan, P., & Kishore, N. (2016). Assessment of groundwater potential zone using remote sensing, GIS and multi criteria decision analysis techniques. *Journal of the Geological Society of India*, *88*, 481-492.
- Karra, K., Kontgis, C., Statman-Weil, Z., Mazzariello, J. C., Mathis, M., & Brumby, S. P. (2021, July). Global land use/land cover with Sentinel 2 and deep learning. In *2021 IEEE international geoscience and remote sensing symposium IGARSS* (pp. 4704-4707). IEEE.
- Kendall, M. G. (1975). Rank Correlation Measures; Charles Griffin Book Series.
- Knight DW, McGahey C, Lamb R, Samuels PG (2010) Practical Channel Hydraulics. CRC Press Inc. Boca Raton, FL.
- Knighton AD (1998) Fluvial forms and processes. Oxford univ press, Inc., New York, USA
- Kordestani, M. D., Naghibi, S. A., Hashemi, H., Ahmadi, K., Kalantar, B., & Pradhan, B. (2019). Groundwater potential mapping using a novel data-mining ensemble model. *Hydrogeology journal*.

- Krishnan, R., Sabin, T. P., Vellore, R., Mujumdar, M., Sanjay, J., Goswami, B. N., ... & Terray, P. (2016). Deciphering the desiccation trend of the South Asian monsoon hydroclimate in a warming world. *Climate dynamics*, *47*, 1007-1027.
- Kumar, A., & Krishna, A. P. (2018). Assessment of groundwater potential zones in coal mining impacted hard-rock terrain of India by integrating geospatial and analytic hierarchy process (AHP) approach. *Geocarto International*, *33*(2), 105-129.
- Kumar, A., Kanga, S., Taloor, A. K., Singh, S. K., & Đurin, B. (2021). Surface runoff estimation of Sind river basin using integrated SCS-CN and GIS techniques. *HydroResearch*, *4*, 61-74.
- Langhein, W.B. (1947). Topographic characteristics of drainage basins. U.S. Geological survey. Water supply paper. 986. 157159.
- Latifovic, R., Pouliot, D., & Nastev, M. (2010). Earth observation based land cover for regional aquifer characterization. *Canadian water resources journal*, *35*(4), 433-450.
- Leopold, L. B. (1). Wolman M g, Miller JP (1964) Fluvial Processes in Geomorphology. *Freeman. San Francisco, London*, *1*, 522.
- Li, C., Wang, J., Wang, L., Hu, L., & Gong, P. (2014). Comparison of classification algorithms and training sample sizes in urban land classification with Landsat thematic mapper imagery. *Remote sensing*, *6*(2), 964-983.
- Lillesand, T., Kiefer, R. W., & Chipman, J. (2015). *Remote sensing and image interpretation*. John Wiley & Sons.
- López, R., & Barragán, J. (2008). Equivalent roughness of gravel-bed rivers. *Journal of Hydraulic Engineering*, *134*(6), 847-851.
- Lord, M. L., Germanoski, D., & Allmendinger, N. E. (2009). Fluvial geomorphology: Monitoring stream systems in response to a changing environment.
- Machiwal, D., Jha, M. K., Machiwal, D., & Jha, M. K. (2012). Analysis of Streamflow Trend in the Susquehanna River Basin, USA. *Hydrologic time series analysis: Theory and practice*, 181-200.
- Magesh, N. S., Chandrasekar, N., & Soundranayagam, J. P. (2012). Delineation of groundwater potential zones in Theni district, Tamil Nadu, using remote sensing, GIS and MIF techniques. *Geoscience frontiers*, *3*(2), 189-196.
- Mallikarjun A, Vallakeerthi J 2018 Investigation of Groundwater Potential Zones Using RS & GIS In Western Part Of Krishnagiri District.
- Mandal, T., Das, J., Rahman, A. S., & Saha, P. (2021). Rainfall insight in Bangladesh and India: climate change and environmental perspective. *Habitat, Ecology and Ekistics: Case Studies of Human-Environment Interactions in India*, 53-74.
- Mandal, T., Sarkar, A., Das, J., Rahman, A. S., & Chouhan, P. (2021). Comparison of classical Mann–Kendal test and graphical innovative trend analysis for analyzing rainfall changes in India. In *India: Climate Change Impacts, Mitigation and Adaptation in Developing Countries* (pp. 155-183). Cham: Springer International Publishing.
- Mann, H. B. (1945). Nonparametric tests against trend. *Econometrica: Journal of the econometric society*, 245-259.
- Manning, R. (1891). On the flow of water in open channels and pipes: Institute of Civil Engineers of Ireland Transactions, v. 20.
- McFeeters, S. K. (1996). The use of the Normalized Difference Water Index (NDWI) in the delineation of open water features. *International journal of remote sensing*, *17*(7), 1425-1432.
- McManamay, R. A., & Bevelhimer, M. S. (2013). A holistic framework for environmental flows determination in hydropower contexts. *ORNL/TM-2013/159. Oak Ridge National Laboratory*.

- Miller, V. C. (1953). *A quantitative geomorphic study of drainage basin characteristics in the Clinch Mountain area, Virginia and Tennessee* (Vol. 3). New York: Columbia University.
- Millington, N., Das, S., & Simonovic, S. P. (2011). The comparison of GEV, log-Pearson type 3 and Gumbel distributions in the Upper Thames River watershed under global climate models.
- Mishra, N., Khare, D., Gupta, K. K., & Shukla, R. (2014). Impact of land use change on groundwater—a review. *Advances in Water Resource and Protection*, *2*(28), 28-41.
- Mistry, R. E. (1972). Navigational problems and hazards in the port of Calcuta. In *The Bhagirathi-Hooghly Basin—proceedings of the interdisciplinary symposium* (pp. 168-173).
- Mitra, S., & Singh, A. (2018). Assessment of environmental flow requirements of damodar river basins by using flow duration indices method–a case study. *International Journal of Hydrology*, *2*(3), 281-283.
- Moghaddam, D. D., Rezaei, M., Pourghasemi, H. R., Pourtaghie, Z. S., & Pradhan, B. (2015). Groundwater spring potential mapping using bivariate statistical model and GIS in the Taleghan watershed, Iran. *Arabian Journal of Geosciences*, *8*, 913-929.
- Mohammadi, A. A. (2012). Regional model presentation for peak discharge estimation in ungauged drainage basin using geomorphologic, Synyder, SCS and triangular models (case study: Kan drainage basin). *Caspian Journal of Environmental Sciences*, *10*(1), 91-102.
- Molla, T., & Sisheber, B. (2017). Estimating soil erosion risk and evaluating erosion control measures for soil conservation planning at Koga watershed in the highlands of Ethiopia. *Solid Earth*, *8*(1), 13-25.
- Mondal, M., Ghosh, S., & Satpati, L. N. (2018). Optimum cross section index (OCI): a new approach for identification of an optimum channel—a case study of the Ichamati River, India. *Arabian Journal of Geosciences*, *11*, 1-19.
- Mundetia, N., Sharma, D., & Dubey, S. K. (2018). Morphometric assessment and sub-watershed prioritization of Khari River basin in semi-arid region of Rajasthan, India. *Arabian Journal of Geosciences*, *11*, 1-18.
- Nag, S., Roy, M. B., & Roy, P. K. (2020). Optimum prioritisation of sub-watersheds based on erosion-susceptible zones through modeling and GIS techniques. *Modeling Earth Systems and Environment*, *6*, 1529-1544.
- Nag, S., Roy, M. B., & Roy, P. K. (2022). Study on the functionality of land use land cover over the evaluation of groundwater potential zone: A fuzzy AHP based approach. *Journal of Earth System Science*, *131*(3), 146.
- Nath, B., Niu, Z., & Singh, R. P. (2018). Land Use and Land Cover changes, and environment and risk evaluation of Dujiangyan city (SW China) using remote sensing and GIS techniques. *Sustainability*, *10*(12), 4631.
- Nautiyal, M. D. (1994). Morphometric analysis of a drainage basin using aerial photographs: a case study of Khairkuli Basin, District Dehradun, UP. *Journal of the Indian Society of Remote Sensing*, *22*, 251-261.
- Nikumbh, A. C., Chakraborty, A., & Bhat, G. S. (2019). Recent spatial aggregation tendency of rainfall extremes over India. *Scientific reports*, *9*(1), 10321.
- Nir, D. (1957). The ratio of relative and absolute altitudes of Mt. Carmel: a contribution to the problem of relief analysis and relief classification. *Geographical Review*, *47*(4), 564-569.

- Nitheshnirmal, S., Thilagaraj, P., Rahaman, S. A., & Jegankumar, R. (2019). Erosion risk assessment through morphometric indices for prioritisation of Arjuna watershed using ALOS-PALSAR DEM. *Modeling Earth Systems and Environment*, *5*, 907-924.
- Nooka Ratnam, K., Srivastava, Y. K., Venkateswara Rao, V., Amminedu, E. K. S. R., & Murthy, K. S. R. (2005). Check dam positioning by prioritization of micro-watersheds using SYI model and morphometric analysis—remote sensing and GIS perspective. *Journal of the Indian society of remote sensing*, *33*, 25-38.
- Owuor, S. O., Butterbach-Bahl, K., Guzha, A. C., Rufino, M. C., Pelster, D. E., Díaz-Pinés, E., & Breuer, L. (2016). Groundwater recharge rates and surface runoff response to land use and land cover changes in semi-arid environments. *Ecological Processes*, *5*(1), 1-21.
- Pai, D. S., Rajeevan, M., Sreejith, O. P., Mukhopadhyay, B., & Satbha, N. S. (2014). Development of a new high spatial resolution (0.25× 0.25) long period (1901-2010) daily gridded rainfall data set over India and its comparison with existing data sets over the region. *Mausam*, *65*(1), 1-18.
- Pakhmode, V., Kulkarni, H., & Deolankar, S. B. (2003). Hydrological-drainage analysis in watershed-programme planning: a case from the Deccan basalt, India. *Hydrogeology Journal*, *11*, 595-604.
- Pal, R. (2015). Channel Avulsion Archives and Morphological Readjustment near the Bhagirathi-Mayurakshi Confluence in the Lower Gangatic Plain, West Bengal, India. *J. Environ. Earth Sci*, *5*(3), 67-75.
- Pal, S. (2016). Impact of Massanjore dam on hydro-geomorphological modification of Mayurakshi river, Eastern India. *Environment, development and sustainability*, *18*, 921-944.
- Pal, S., & Debanshi, S. (2018). Influences of soil erosion susceptibility toward overloading vulnerability of the gully head bundhs in Mayurakshi River basin of eastern Chottanagpur Plateau. *Environment, Development and Sustainability*, *20*, 1739-1775.
- Pal, S., Let, S., & Das, P. (2012). Assessment of channel width disparity of the major rivers within Mayurakshi River Basin. *Int J Geol Earth Environ Sci*, *2*(3), 1-10.
- Pandey, R. P., & Ramasastri, K. S. (2003). Estimation of lean season water availability in streams with limited data. *Journal of the Institution of Engineers. India. Civil Engineering Division*, *84*(nov), 149-152.
- Patra, S., Mishra, P., & Mahapatra, S. C. (2018). Delineation of groundwater potential zone for sustainable development: A case study from Ganga Alluvial Plain covering Hooghly district of India using remote sensing, geographic information system and analytic hierarchy process. *Journal of Cleaner Production*, *172*, 2485-2502.
- Petts, G. E. (1979). Complex response of river channel morphology subsequent to reservoir construction. *Progress in Physical Geography*, *3*(3), 329-362.
- Pike, R. J., & Wilson, S. E. (1971). Elevation-relief ratio, hypsometric integral, and geomorphic area-altitude analysis. *Geological Society of America Bulletin*, *82*(4), 1079-1084.
- Pour, S. H., Abd Wahab, A. K., Shahid, S., & Ismail, Z. B. (2020). Changes in reference evapotranspiration and its driving factors in peninsular Malaysia. *Atmospheric Research*, *246*, 105096.
- Pourtaghi, Z. S., & Pourghasemi, H. R. (2014). GIS-based groundwater spring potential assessment and mapping in the Birjand Township, southern Khorasan Province, Iran. *Hydrogeol J*, *22*(3), 643-662.

- Pradhan, B., Singh, R. P., & Buchroithner, M. F. (2006). Estimation of stress and its use in evaluation of landslide prone regions using remote sensing data. *Advances in Space research*, *37*(4), 698-709.
- Prasannakumar, V., Vijith, H., Abinod, S., & Geetha, N. J. G. F. (2012). Estimation of soil erosion risk within a small mountainous sub-watershed in Kerala, India, using Revised Universal Soil Loss Equation (RUSLE) and geo-information technology. *Geoscience frontiers*, *3*(2), 209-215.
- Preeja, K. R., Joseph, S., Thomas, J., & Vijith, H. (2011). Identification of groundwater potential zones of a tropical river basin (Kerala, India) using remote sensing and GIS techniques. *Journal of the Indian Society of Remote Sensing*, *39*, 83-94.
- Price, K., Jackson, C. R., & Parker, A. J. (2010). Variation of surficial soil hydraulic properties across land uses in the southern Blue Ridge Mountains, North Carolina, USA. *Journal of hydrology*, *383*(3-4), 256-268.
- Qadir, J., & Singh, P. (2019). Land use/cover mapping and assessing the impact of solid waste on water quality of Dal Lake catchment using remote sensing and GIS (Srinagar, India). *SN Applied Sciences*, *1*(1), 25.
- Rahman, M. A., Yunsheng, L., & Sultana, N. (2017). Analysis and prediction of rainfall trends over Bangladesh using Mann–Kendall, Spearman's rho tests and ARIMA model. *Meteorology and Atmospheric Physics*, *129*(4), 409-424.
- Rahmati, O., Nazari Samani, A., Mahdavi, M., Pourghasemi, H. R., & Zeinivand, H. (2015). Groundwater potential mapping at Kurdistan region of Iran using analytic hierarchy process and GIS. *Arabian Journal of Geosciences*, *8*, 7059-7071.
- Rao, N. S., Chakradhar, G. K. J., & Srinivas, V. (2001). Identification of groundwater potential zones using remote sensing techniques in and around Guntur town, Andhra Pradesh, India. *Journal of the Indian Society of Remote Sensing*, *29*, 69-78.
- Razandi, Y., Pourghasemi, H. R., Neisani, N. S., & Rahmati, O. (2015). Application of analytical hierarchy process, frequency ratio, and certainty factor models for groundwater potential mapping using GIS. *Earth Science Informatics*, *8*, 867-883.
- Redman, C. L. (1999). Human dimensions of ecosystem studies. *Ecosystems*, 296-298.
- Richards KS (1982) Rivers, form and process in alluvial channels. Methuen, London
- Richards, J. A., & Jia, X. (2006). Interpretation of hyperspectral image data. *Remote sensing digital image analysis: An introduction*, 359-388.
- Rodríguez-Iturbe, I., Devoto, G., & Valdés, J. B. (1979). Discharge response analysis and hydrologic similarity: the interrelation between the geomorphologic IUH and the storm characteristics. *Water Resources Research*, *15*(6), 1435-1444.
- Roy, J., Adhikary, K., & Kar, S. (2019). Credibilistic TOPSIS model for evaluation and selection of municipal solid waste disposal methods. In *Advances in Waste Management: Select Proceedings of Recycle 2016* (pp. 243-261). Springer Singapore.
- Roy, S., & Mistri, B. (2013). Estimation of peak flood discharge for an ungauged river: a case study of the Kunur River, West Bengal. *Geography journal*, *2013*.
- Sahebgharani, A. (2016). Multi-objective land use optimization through parallel particle swarm algorithm: case study baboldasht district of Isfahan, Iran. *Journal of Urban and Environmental Engineering*, *10*(1), 42-49.
- Salmoral, G., Willaarts, B. A., Troch, P. A., & Garrido, A. (2015). Drivers influencing streamflow changes in the Upper Turia basin, Spain. *Science of the total environment*, *503*, 258-268.
- Samal, D. R., & Gedam, S. (2021). Assessing the impacts of land use and land cover change on water resources in the Upper Bhima river basin, India. *Environmental Challenges*, *5*, 100251.

- Sang, L., Zhang, C., Yang, J., Zhu, D., & Yun, W. (2011). Simulation of land use spatial pattern of towns and villages based on CA–Markov model. *Mathematical and Computer Modelling*, *54*(3-4), 938-943.
- Sang, Y. F., Wang, Z., & Liu, C. (2014). Comparison of the MK test and EMD method for trend identification in hydrological time series. *Journal of Hydrology*, *510*, 293-298.
- Saputra, M. H., & Lee, H. S. (2019). Prediction of land use and land cover changes for north sumatra, indonesia, using an artificial-neural-network-based cellular automaton. *Sustainability*, *11*(11), 3024.
- Sayadi, M. K., Heydari, M., & Shahanaghi, K. (2009). Extension of VIKOR method for decision making problem with interval numbers. *Applied Mathematical Modelling*, *33*(5), 2257-2262.
- Scanlon, B. R., Jolly, I., Sophocleous, M., & Zhang, L. (2007). Global impacts of conversions from natural to agricultural ecosystems on water resources: Quantity versus quality. *Water resources research*, *43*(3).
- Scanlon, B. R., Reedy, R. C., Stonestrom, D. A., Prudic, D. E., & Dennehy, K. F. (2005). Impact of land use and land cover change on groundwater recharge and quality in the southwestern US. *Global Change Biology*, *11*(10), 1577-1593.
- Schillaci C A B, and J Kropacek 2015 Chapter 2.4.2: Terrain analysis and landform recognition;, in Geomorphological Techniques; In: *British Society for Geomorphology*. 18.
- Schumm, S. A. (1956). Evolution of drainage systems and slopes in badlands at Perth Amboy, New Jersey. *Geological society of America bulletin*, *67*(5), 597-646.
- Sen, P. K. (1968). Estimates of the regression coefficient based on Kendall's tau. *Journal of the American statistical association*, *63*(324), 1379-1389.
- Sen, P. K. (1993). Geomorphological analysis of drainage basins.
- Şen, Z. (2012). Innovative trend analysis methodology. *Journal of Hydrologic Engineering*, *17*(9), 1042-1046.
- Şener, E., Şener, Ş., & Davraz, A. (2018). Groundwater potential mapping by combining fuzzy-analytic hierarchy process and GIS in Beyşehir Lake Basin, Turkey. *Arabian Journal of Geosciences*, *11*, 1-21.
- Shannon, C. E. (1948). A mathematical theory of communication. *The Bell system technical journal*, *27*(3), 379-423.
- Shen, L., & Li, C. (2010, June). Water body extraction from Landsat ETM+ imagery using adaboost algorithm. In *2010 18th International Conference on Geoinformatics* (pp. 1-4). IEEE.
- Shen, Z., Lu, C., Yin, R., & Qi, J. (2013). Land cover changes in northeast China from the late 1970s to 2004. *Applied ecology and environmental research*, *11*(1), 67-78.
- Shukla, J., & Misra, B. M. (1977). Relationships between sea surface temperature and wind speed over the central Arabian Sea, and monsoon rainfall over India. *Monthly Weather Review*, *105*(8), 998-1002.
- Sichangi, A. W., Wang, L., Yang, K., Chen, D., Wang, Z., Li, X., ... & Kuria, D. (2016). Estimating continental river basin discharges using multiple remote sensing data sets. *Remote Sensing of Environment*, *179*, 36-53.
- Singh, C. K., Shashtri, S., Singh, A., & Mukherjee, S. (2011). Quantitative modeling of groundwater in Satluj River basin of Rupnagar district of Punjab using remote sensing and geographic information system. *Environmental Earth Sciences*, *62*, 871-881.
- Singh, O., Sarangi, A., & Sharma, M. C. (2008). Hypsometric integral estimation methods and its relevance on erosion status of north-western lesser Himalayan watersheds. *Water Resources Management*, *22*, 1545-1560.

- Singh, S. K., Mustak, S., Srivastava, P. K., Szabó, S., & Islam, T. (2015). Predicting spatial and decadal LULC changes through cellular automata Markov chain models using earth observation datasets and geo-information. *Environmental Processes*, *2*, 61-78.
- Singh, V. P. (2003). On the theories of hydraulic geometry. *International journal of sediment research*, *18*(3), 196-218.
- Sinha, S., Jeganathan, C., Sharma, L. K., & Nathawat, M. S. (2015). A review of radar remote sensing for biomass estimation. *International Journal of Environmental Science and Technology*, *12*, 1779-1792.
- Smith, K. G. (1950). Standards for grading texture of erosional topography. *American journal of Science*, *248*(9), 655-668.
- Sood, A., Ghosh, S. K., & Upadhyay, P. (2021). Impact of land cover change on surface runoff. *Advances in Remote Sensing for Natural Resource Monitoring*, 150-169.
- SPARKS, B. (1960). Geomorphology.–371 págs.
- Srinivas, R., Singh, A. P., & Deshmukh, A. (2018). Development of a HEC-HMS-based watershed modeling system for identification, allocation, and optimization of reservoirs in a river basin. *Environmental monitoring and assessment*, *190*, 1-18.
- Strahler, A. N. (1957). Quantitative analysis of watershed geomorphology. *Eos, Transactions American Geophysical Union*, *38*(6), 913-920.
- Strahler, A. N. (1964). Quantitative geomorphology of drainage basin and channel networks. *Handbook of applied hydrology*.
- Strahler, A. N., & Chow, V. T. (1964). Handbook of applied hydrology. *Quantitative geomorphology of drainage basins and channel networks*, 39-76.
- Subramanya, K. (2008). *Engineering hydrology*. McGraw-Hill.
- Suhaila, J., Jemain, A. A., Hamdan, M. F., & Zin, W. Z. W. (2011). Comparing rainfall patterns between regions in Peninsular Malaysia via a functional data analysis technique. *Journal of hydrology*, *411*(3-4), 197-206.
- Sun, Z., Guo, H., Li, X., Huang, Q., & Zhang, D. (2011, May). Effect of LULC change on surface runoff in urbanization area. In *Proceedings of the ASPRS 2011 Annual Conference, Milwaukee, Wisconsin, May* (Vol. 1, No. 5).
- Suresh, M., Sudhakar, S., Tiwari, K. N., & Chowdary, V. M. (2004). Prioritization of watersheds using morphometric parameters and assessment of surface water potential using remote sensing. *Journal of the indian society of remote sensing*, *32*, 249-259.
- Swamee, P. K., Mishra, G. C., & Chahar, B. R. (2000). Comprehensive Design of Minimum Cost IrrigationCanal Sections. *Journal of irrigation and drainage engineering*, *126*(5), 322-327.
- Tabari, H., Marofi, S., Aeini, A., Talaee, P. H., & Mohammadi, K. (2011). Trend analysis of reference evapotranspiration in the western half of Iran. *Agricultural and forest meteorology*, *151*(2), 128-136.
- Tabata, K. K., & Hickin, E. J. (2003). Interchannel hydraulic geometry and hydraulic efficiency of the anastomosing Columbia River, southeastern British Columbia, Canada. *Earth Surface Processes and Landforms: The Journal of the British Geomorphological Research Group*, *28*(8), 837-852.
- Tanarhte, M., Hadjinicolaou, P., & Lelieveld, J. (2012). Intercomparison of temperature and precipitation data sets based on observations in the Mediterranean and the Middle East. *Journal of Geophysical Research: Atmospheres*, *117*(D12).
- Te Chow, V., Maidment, D. R., & Mays, L. W. (1988). *Applied hydrology*.
- Thorne, C. R. (1992). MA Summerfield 1991. Global Geomorphology. An Introduction to the Study of Landfornis. xxii+ 537 pp. Harlow: Longman; New York: John Wiley Inc.

Price£ 17.99 (paperback). ISBN 0 582 30156 4 (Longman), 0 470 21666 2 (Wiley). *Geological Magazine*, *129*(3), 379-380.

- Tiwari, A. K., Lavy, M., Amanzio, G., De Maio, M., Singh, P. K., & Mahato, M. K. (2017). Identification of artificial groundwater recharging zone using a GIS-based fuzzy logic approach: a case study in a coal mine area of the Damodar Valley, India. *Applied Water Science*, *7*, 4513-4524.
- Van Laarhoven, P. J., & Pedrycz, W. (1983). A fuzzy extension of Saaty's priority theory. *Fuzzy sets and Systems*, *11*(1-3), 229-241.
- Velasquez, M., & Hester, P. T. (2013). An Analysis of Multi-Criteria Decision Making Methods International Journal of Operations Research Vol. 10.
- Vinayak, B., Lee, H. S., & Gedem, S. (2021). Prediction of land use and land cover changes in Mumbai City, India, using remote sensing data and a multilayer perceptron neural network-based Markov chain model. *Sustainability*, *13*(2), 471.
- Vörösmarty, C. J., McIntyre, P. B., Gessner, M. O., Dudgeon, D., Prusevich, A., Green, P., ... & Davies, P. M. (2010). Global threats to human water security and river biodiversity. *nature*, *467*(7315), 555-561.
- Vulević, T., Dragović, N., Kostadinov, S., Simić, S. B., & Milovanović, I. (2015). Prioritization of Soil Erosion Vulnerable Areas Using Multi-Criteria Analysis Methods. *Polish Journal of Environmental Studies*, *24*(1).
- Wang, R., Kalin, L., Kuang, W., & Tian, H. (2014). Individual and combined effects of land use/cover and climate change on Wolf Bay watershed streamflow in southern Alabama. *Hydrological Processes*, *28*(22), 5530-5546.
- Williams, G. P., & Wolman, M. G. (1984). *Downstream effects of dams on alluvial rivers* (Vol. 1286). US Government Printing Office.
- Wischmeier, W. H., & Smith, D. D. (1978). *Predicting rainfall erosion losses: a guide to conservation planning* (No. 537). Department of Agriculture, Science and Education Administration.
- Xu, H. (2006). Modification of normalised difference water index (NDWI) to enhance open water features in remotely sensed imagery. *International journal of remote sensing*, *27*(14), 3025-3033.
- Xu, M., Kang, S., Chen, X., Wu, H., Wang, X., & Su, Z. (2018). Detection of hydrological variations and their impacts on vegetation from multiple satellite observations in the Three-River Source Region of the Tibetan Plateau. *Science of the total environment*, *639*, 1220-1232.
- Yamazaki, D., Trigg, M. A., & Ikeshima, D. (2015). Development of a global~ 90 m water body map using multi-temporal Landsat images. *Remote Sensing of Environment*, *171*, 337-351.
- Yang, Y., Liu, Y., Zhou, M., Zhang, S., Zhan, W., Sun, C., & Duan, Y. (2015). Landsat 8 OLI image based terrestrial water extraction from heterogeneous backgrounds using a reflectance homogenization approach. *Remote Sensing of Environment*, *171*, 14-32.
- Yao, F., Wang, J., Wang, C., & Crétaux, J. F. (2019). Constructing long-term high-frequency time series of global lake and reservoir areas using Landsat imagery. *Remote Sensing of Environment*, *232*, 111210.
- Yazdi, J., Salehi Neyshabouri, S. A. A., Niksokhan, M. H., Sheshangosht, S., & Elmi, M. (2013). Optimal prioritisation of watershed management measures for flood risk mitigation on a watershed scale. *Journal of Flood Risk Management*, *6*(4), 372-384.
- Yen, B. C. (2002). Open channel flow resistance. *Journal of hydraulic engineering*, *128*(1), 20-39.

- Yin, J., He, F., Xiong, Y. J., & Qiu, G. Y. (2017). Effects of land use/land cover and climate changes on surface runoff in a semi-humid and semi-arid transition zone in northwest China. *Hydrology and Earth System Sciences*, *21*(1), 183-196.
- Yjjou, M., Bouabid, R., Hmaidi, A. E., Essahlaoui, A., & ABASSI, M. (2014). Modeling water erosion via GIS and the universal soil loss equation in the Oum Er-Rbia watershed. *The International Journal of Engineering and Science (IJES)*, *3*(8), 83-91.
- Zhai, K., Wu, X., Qin, Y., & Du, P. (2015). Comparison of surface water extraction performances of different classic water indices using OLI and TM imageries in different situations. *Geo-spatial Information Science*, *18*(1), 32-42.
- Zhang, J., & Ross, M. (2015). Hydrologic modeling impacts of post-mining land use changes on streamflow of Peace River, Florida. *Chinese Geographical Science*, *25*, 728-738.
- Zhang, Q., Xu, C. Y., Zhang, Z., Chen, Y. D., Liu, C. L., & Lin, H. (2008). Spatial and temporal variability of precipitation maxima during 1960–2005 in the Yangtze River basin and possible association with large-scale circulation. *Journal of Hydrology*, *353*(3-4), 215-227.
- Zhang, T., Zhang, X., Xia, D., & Liu, Y. (2014). An analysis of land use change dynamics and its impacts on hydrological processes in the Jialing River Basin. *Water*, *6*(12), 3758-3782.
- Zhang, X., Wu, B., Ling, F., Zeng, Y., Yan, N., & Yuan, C. (2010). Identification of priority areas for controlling soil erosion. *Catena*, *83*(1), 76-86.
- Zhou, Y., Varquez, A. C., & Kanda, M. (2019). High-resolution global urban growth projection based on multiple applications of the SLEUTH urban growth model. *Scientific Data*, *6*(1), 34.
- Zubair, H. (2019, October). Prediction of land use and land cover (LULC) changes using CA-Markov model in Mamuju Subdistrict. In *Journal of Physics: Conference Series* (Vol. 1341, No. 8, p. 082033). IOP Publishing.

CHAPTER 7

ASSESSMENT OF THE ECOLOGICAL INDICATORS OF THE STUDY AREA

7. Introduction

The health and condition of aquatic ecosystems are evaluated using ecological indicators of surface water conditions. The ecological integrity of water bodies and the potential effects of pollution or other disruptions are both essential information that these indicators offer. This chapter discusses the indicators that have an impact on the ecological functions carried out in surface water, such as the evaluation of indicators of water availability, the quality of riparian vegetation, the assessment of ecosystem services, the evaluation of water quality, etc. Scientists, environmental organizations, and governments can better understand aquatic ecosystem health, spot possible problems, and take appropriate action to lessen any harmful effects by tracking and evaluating these indicators over time.

7.1. Application of SWAT Hydrological Model on Mayurakshi River Basin

Quantifying the accessibility of freshwater resources is of vast importance. This is a result of the need to estimate water allocations at different spatiotemporal scales and is supported by ongoing climate and socioeconomic changes (Xu and Singh 2004). In this regard, hydrological models are essential for comprehending the behaviour and responses of watersheds (Bárdossy and Singh 2008). Watershed development that promotes sustainable conservation of hydrological components such as discharge, groundwater, percolation, lateral flow, and evapotranspiration, etc., requires accurate stream flow simulation.

The timing and geographical locations of the water users have an impact on the regional and temporal distribution of the water availability across basins (Van Oel et al. 2009). In particular, irrigation along river basins reduces water output downstream. A change in water use at one level or sector directly affects the availability and productivity of water for other levels or sectors or users, despite the effects of climate change and the difficulties they provide to the water supply. In order to meet the demands of the rapidly expanding population and economy (Vairavamoorthy et al. 2008; Ridoutt et al. 2009), as well as the expansion of irrigated areas (Wada et al., 2011), it is crucial to develop techniques and quantify water for the agricultural, industrial, and domestic sectors. One of the best ways to estimate water availability is to use hydrologic models with precise data sets from the hydro-meteorological, socio-economic (such as population and GDP), technological (such as energy and household consumption and electricity production), and agricultural (such as the number of livestock and irrigated areas) domains.

Hydrologic models have emerged as a new accomplishment for effectively predicting water availability and distribution systems under different demand loading and operating conditions. Arnold and Allen (1996) describe deterministic process-based models like the Soil and Water Assessment Tool (SWAT) as a semi-distributed hydrological model that works on a daily time scale. Because of its semi-distributed physical development, it can be used to model watershed hydrology, sediment, and nutrient transport and behaviour (Srinivasan et al. 1998). Extensive studies of SWAT's practical applications have proven that it is an efficient method for simulating a hydrological system that allows for a great deal of leeway in terms of the data that is available (Somura et al. 2009; Singh and Saravanan, 2020; Bhatt et al. 2020). This paper aims to estimate water availability in the Mayurakshi River Basin using the SWAT hydrological model, along with simple but effective techniques and observed hydro-meteorological data. This will inform farmers, decision-makers, and policymakers about the quantity of available water in the Mayurakshi River Basin, as well as the strategies for enhancing sustainable agricultural and productivity, improving human livelihood, and ensuring food security. This study also utilised Remote Sensing, Geographic Information System, and the Markov Chain Model to analyse and predict future LULC change patterns, as well as the SWAT model to evaluate soil and water. Watershed modelling is a concept that combines geospatial methods with hydro-meteorological information. The United States Department of Agriculture (USDA) introduced SWAT as a physically based model that can assist in evaluating a river's stream flow based on climate datasets. In this study, SWAT model has been chosen to study the statistical correlation between observed and simulated stream-flow data in order to enhance human welfare and protect the environment. The available spatio temporal hydro-meteorological data for different rain gauge stations (rainfall, temperature, evapotranspiration etc.) and the long term stream flow datasets of the two important gauging station (Masanjore Dam and Tilpara Barrage) were used to simulate and calibrate the model. The precise goals that directed data gathering and analysis included the following:

- Stream flow simulation and calibration utilising historical observed discharge data (daily) from the Massanjore Dam and Tilpara Barrage, two significant river gauge stations located within the Mayurakshi River Basin area.
- Determination of model’s uncertainty and sensitive parameters by conducting SUFI-2 algorithm of SWAT-CUP analysis, which are crucially accountable for the adjustment of hydrologic response of the river basin.

- Quantification and prediction of water balance components based on the studied simulated (2021) and anticipated (2031) hydrological flow models.
- Estimation of several water resources availability indicators including Blue and Green water flow and storage, together with its spatio temporal variability analysis at a sub basin level of the study area.

7.1.1. Input Data

In this study, hydrological modelling was conducted using high resolution satellite images and a variety of observed information which are listed and also presented in table 7.1.

Table 7.1 *Summary of Data Used In Model Development, Calibration and Validation in Mayurakshi River Basin*

<table>
<tr><th colspan="2">Data used</th><th>Period of record</th><th>Supplying agency</th><th>Primary use</th></tr>
<tr><td colspan="2">ALOS PALSAR DEM (cell size: 12.5*12.5m)</td><td>--</td><td>Alaska Satellite Facility</td><td rowspan="5">Model Input</td></tr>
<tr><td colspan="2">Soil (1:2,50,000)</td><td>--</td><td>FAO</td></tr>
<tr><td colspan="2">Land use land cover</td><td>2021 & 2031</td><td>ESRI and CA-Markov model predicted</td></tr>
<tr><td colspan="2">Meteorological data</td><td rowspan="2">1980-2021</td><td rowspan="2">IMD</td></tr>
<tr><td>Minimum and maximum temperature (resolution: 1°*1°)</td><td>Daily precipitation (resolution: 0.25°*0.25°)</td></tr>
<tr><td colspan="2" rowspan="2">Daily stream flow data</td><td>Tilpara Barrage (1992-2019)</td><td>Irrigation & Waterways, Suri, Govt. of West Bengal</td><td rowspan="2">Model calibration & validation</td></tr>
<tr><td>Massanjore Dam (1983-2017)</td><td>CWC, Govt. of India</td></tr>
</table>

- **Meteorological Data**

Five meteorological parameters are required for SWAT analysis: daily precipitation, minimum and maximum temperature, wind speed, sun radiation, and relative humidity. The Indian Meteorological Department (IMD), Government of India, provided the daily precipitation, minimum and maximum air temperature data for the years 1980–2021 used in the present research. over the purpose of gathering gridded temperature (resolution: 1°*1°) and precipitation (resolution: 0.25°*0.25°) data over the aforementioned study period, a total of thirty weather stations located within and surrounding the study region (Fig. 7.1) have been taken into consideration. Global Weather Data for SWAT (http://globalweather.tamu.edu/) was used to gather the remaining data, which included solar radiation, relative humidity, and wind speed. Furthermore, SWAT's weather generator (WGEN) projected datasets (till 2050) have also been utilised for the assessment of future hydrological response of the river basin.

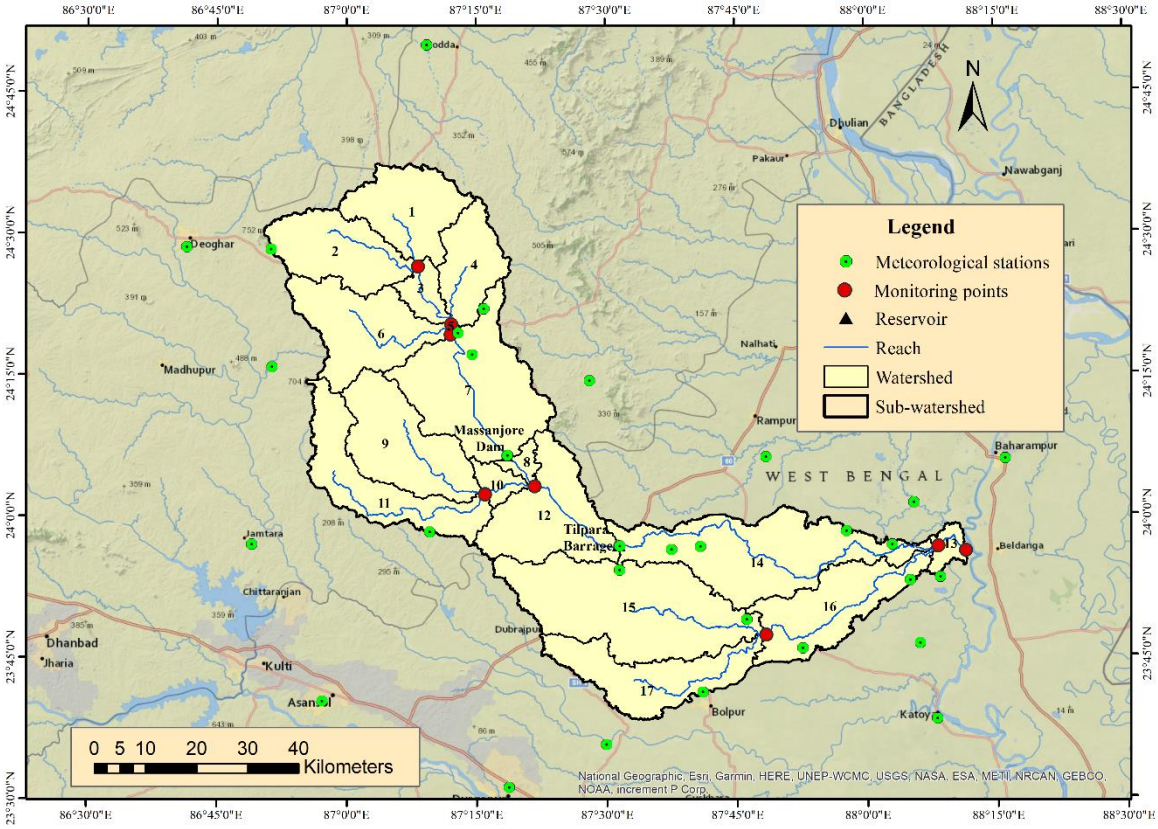

Figure 7.1 *Location Map of the Study Area Used in SWAT Model*

- **Digital Elevation Model (DEM), Land Use Land Cover (LULC), Slope and Soil Data**

The topography of the watershed was described using a DEM. Any point in a given area is presented in a DEM with its elevation at a certain spatial resolution. Most watershed characteristics, including watershed boundary (catchment area), watershed drainage patterns, slope, aspect, and sloping length of terrain, were obtained using the Advanced Land Observing Satellite-1 (ALOS) PALSAR Digital Elevation Model with 12.5 m resolution, which was downloaded from the Alaska Satellite Facility (ASF) Distributed Active Archive Centre (DAAC) (Fig. 7.2). The DEM of the research region is also used to determine drainage features such as channel slope, length, and width.

Hydrologic modelling and comprehending the earth as a system both depend on analysis of land use and cover, which is crucial for many planning and management tasks. In order to build a worldwide cover LULC map (LULC 2020-ESRI) with a resolution of 10 m, the Environmental Systems Research Institute (ESRI) has deployed a deep learning segmentation

model. They created a worldwide map of land use and cover at the national and local levels using high definition Sentinel-2 satellite imageries and cutting-edge AI algorithms. From the global LULC map of the ESRI dataset, the 2021 land use map for the Mayurakshi River basin area has been extracted (Fig. 7.3) where a total of seven primary land use land cover classes were identified namely water/river (WATR), natural vegetation (FRST), wet fallow land (WETF), agricultural land (AGRL), settlement (URHD), bare land (BARR) and pasture land (RNGE). When analysing the potential future water balance situation, the SWAT model simulation additionally included a CA-Markov model-generated land use and land cover for the research area for the year 2031 (Fig. 7.4). Terrset 18.3.1 software, developed by Clark Lab, has been used for assessing probable future forecasts in the land use and land cover situation over the research region utilising a multi-layer perception neural network method (MLPNN) of the Land Change Model (LCM). The table 7.2 below shows the areal coverage for each class of LULC for the years 2021 and 2031.

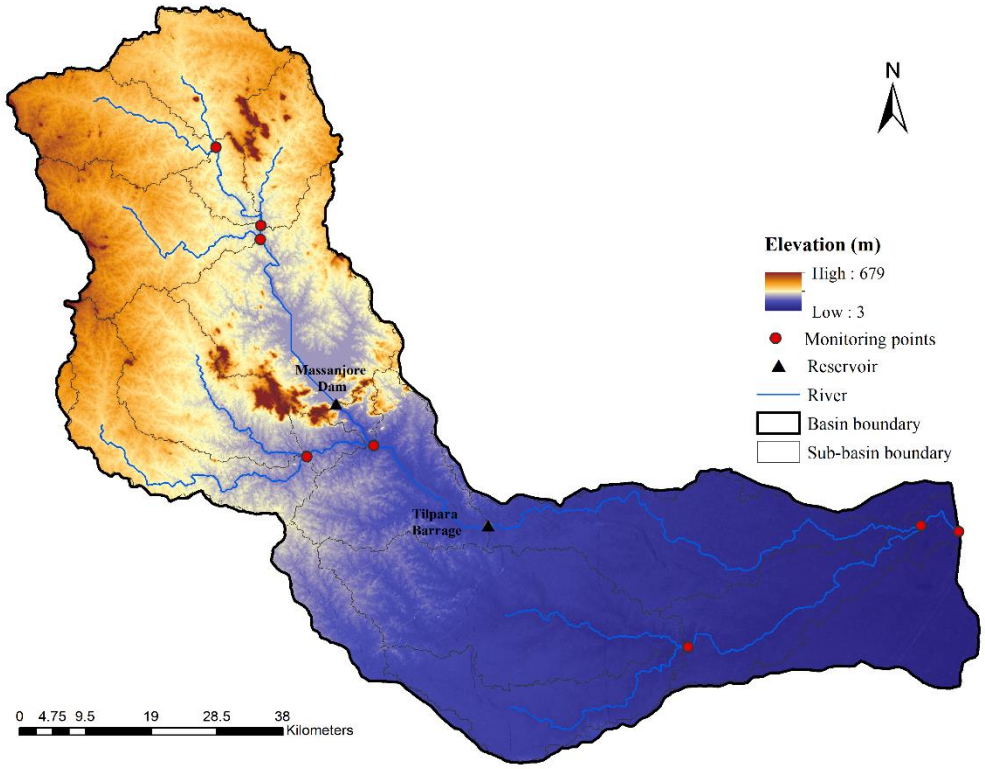

Figure 7.2 *Digital Elevation Model of Mayurakshi River Basin Area*

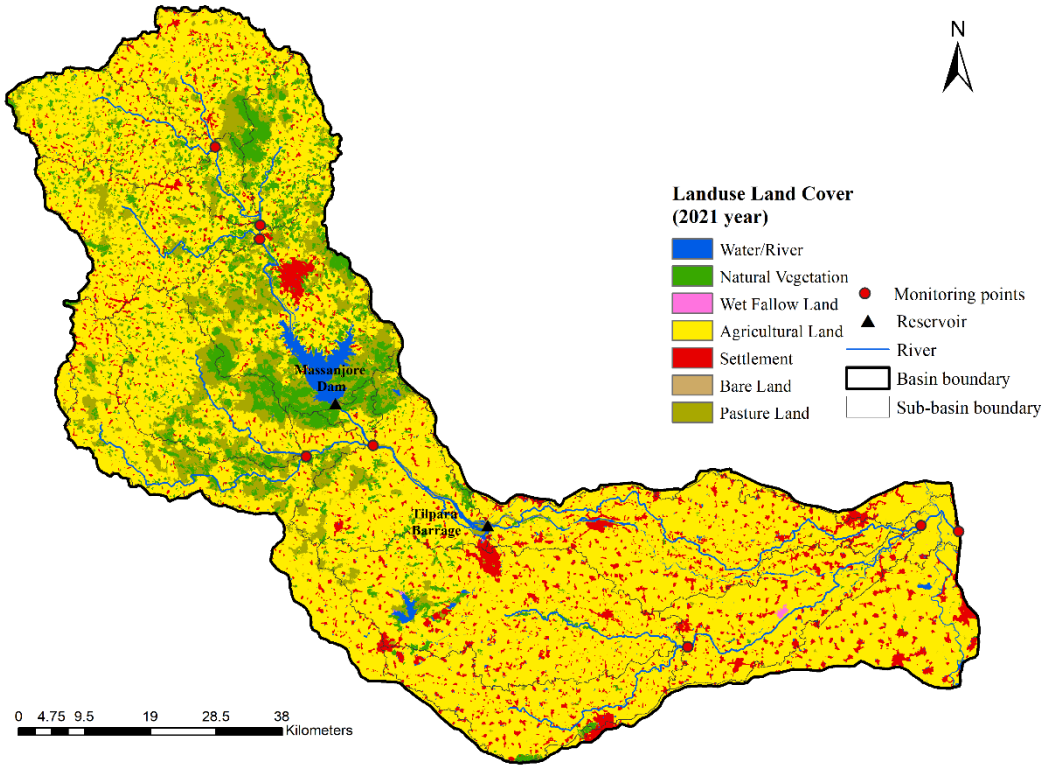

Figure 7.4 *ESRI Generated Land Use Land Cover Map (2021) of the Mayurakshi River Basin Area*

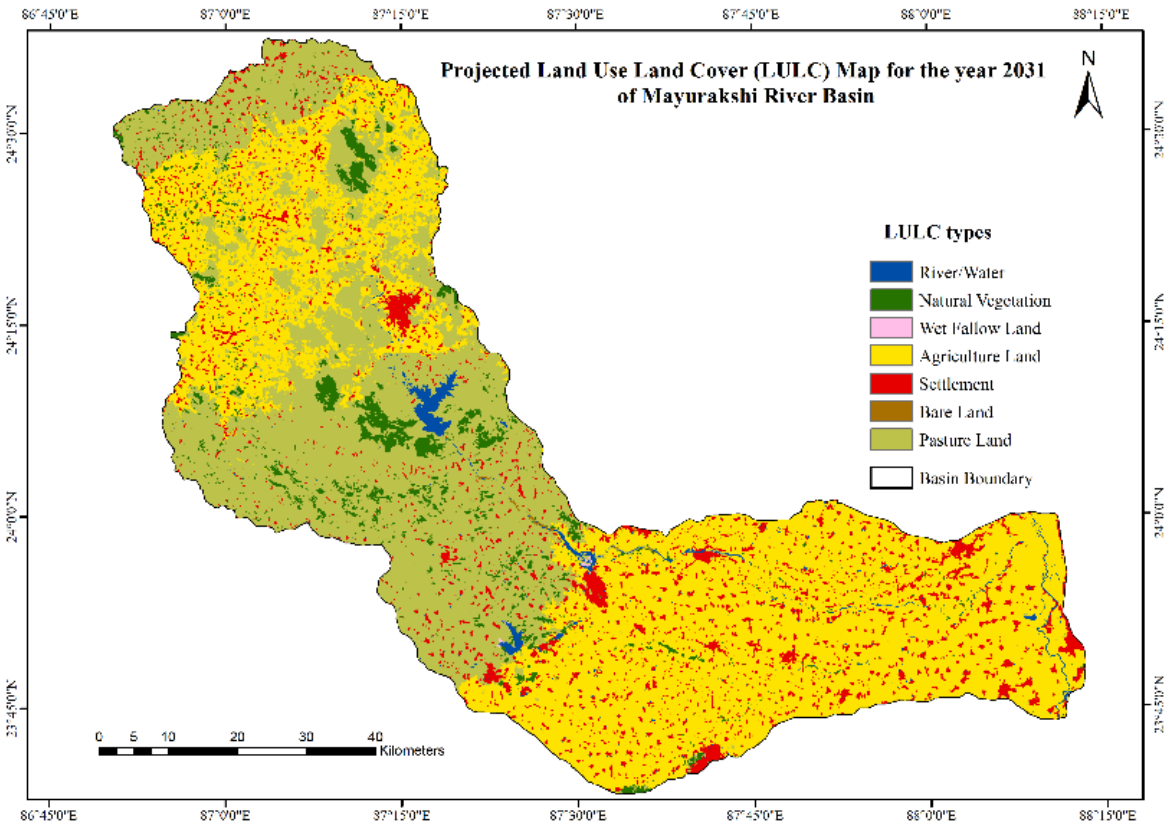

Figure 7.3 *CA-Markov Model Produced Land use Land Cover Map (2031) of the Mayurakshi River Basin Area*

Table 7.2 *Areal Statistics of Land Use Land Cover Classes for the Year 2021 and 2031*

LULC Classes	Year 2021		Year 2031	
	Area (sq. km)	% of area	Area (sq. km)	% of area
Water/River	102.99	1.76901	72.91	1.25
Natural Vegetation	480.45	8.2517	223.27	3.83
Wet Fallow Land	2.75	0.047192	1.94	0.03
Agricultural Land	4289.86	73.6784	4012.01	68.91
Settlement	448.34	7.70019	523.38	8.99
Bare Land	2.22	0.03806	3.90	0.07
Pasture Land	495.81	8.51549	985.05	16.92
TOTAL AREA	**5822.41**	**100**	**5822.41**	**100**

The soil map used as model input has been generated by integrating the higher-resolution Digital Soil Map of the World (DSMW) published by the Food and Agriculture Organisation (FAO), in 1974 (Fig. 7.5). Following that, utilising the FAO-UNESCO Digital Soil Map of the World (DSMW) (http://www.fao.org/geonetwork), which provides soil data with a resolution of 5 km, the different soil types were initialised. In the study catchment, four different soil classes were found, and then the relevant lookup table has been manually created (Table 7.3).

In order to accurately simulate hydrological processes, slope is one of the most crucial variables to take into account. Arc SWAT involves the integration of land slope classes with various land uses and soil types in the sub-watersheds to categorise the sub-watershed into different

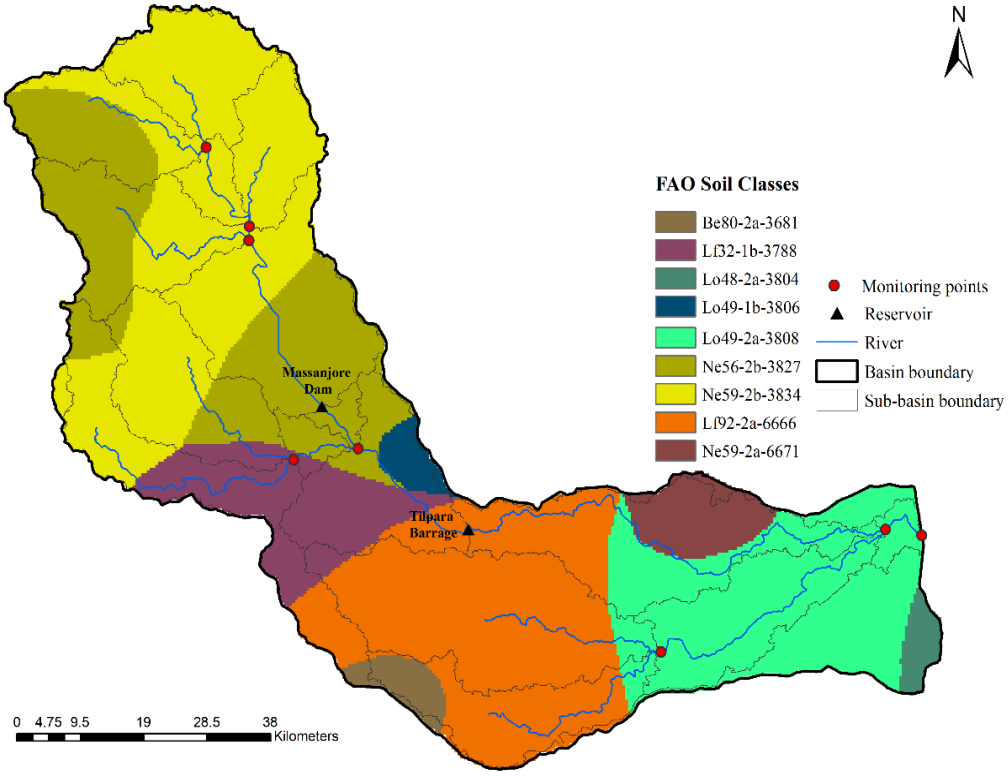

Figure 7.5 *FAO Soil Map of the Mayurakshi River Basin Area*

hydrologic response units (HRUs). In this work, the slope map of the study region was created using the ALOS-PALSAR DEM and categorised into five classes with a maximum value of 134 and an average value of 7.8.

Table 7.3 *Detailed Characteristics of FAO Soil Classes of Mayurakshi River Basin Area*

FAO Soil unit	Dominant soil type	Associated soil type	Associated soil texture class	Associated slope class	Area in sq. km (%)
Be80-2a-3681	Cambisols	Eutric Cambisols	Medium textured	Level to undulating	1.23
Lf32-1b-3788	Luvisols	Ferric Luvisols	Coarse textured	Rolling to hilly	8.04
Lo48-2a-3804	Luvisols	Orthic Luvisols	Medium textured	Level to undulating	3.05
Lo49-1b-3806	Luvisols	Orthic Luvisols	Coarse textured	Rolling to hilly	1.16
Lo49-2a-3808	Luvisols	Orthic Luvisols	Medium textured	Level to undulating	10.40
Ne56-2b-3827	Nitosols	Eutric Nitosols	Medium textured	Rolling to hilly	20.65
Ne59-2b-3834	Nitosols	Eutric Nitosols	Medium textured	Rolling to hilly	29.25
Lf92-2a-6666	Luvisols	Ferric Luvisols	Medium textured	Level to undulating	22.91
Ne59-2a-6671	Nitosols	Eutric Nitosols	Medium textured	Level to undulating	3.31

- **Hydrological Data**

The simulated hydrological model of Mayurakshi River has been calibrated using historical data on daily stream flow collected from gauge stations at Massanjore Dam and Tilpara Barrage over periods of 34 years (1983 - 2017) and 27 years (1992 - 2019), respectively. All of the data had been acquired from the Central Water Commission (CWC), Government of India, and the Irrigation and Waterways Department, Government of West Bengal (WB), respectively. The simulation and calibration technique were carried out independently for the aforementioned time period, followed by a warm-up period of three years.

7.1.2. Methodology

The Soil and Water Assessment tool (SWAT), has been considered as one of the most contemporary hydrological modelling technique, which was collaboratively created by the Agricultural Experiment Station and the United States Department of Agriculture-Agricultural Research Service (USDA-ARS). This can also gain access to land management practises that have an impact on streams, soil, and chemicals in unregulated areas (Arnold et al. 1998). The hydrologic operations in the model replicate water, sediment, nutrient, pesticide, and bacterial yields as outputs and employ topography, land-use, soil, and climatic data as inputs (Neitsch et al. 2011; Krysanova and White 2015). In the current study, daily rainfall is used to determine

surface runoff using the NRCS-CN method. The Penman-Monteith approach was utilised to determine potential evapotranspiration (PET), and the Muskingum method was employed to route channel flow. There are two types of aquifers that make up the groundwater component of SWAT: shallow and deep. The shallow aquifer is replenished by the soil profile and helps to maintain stream flow. The water that enters the deep aquifer is lost from the system and is not taken into account in the water budget. The hydrological mechanism of the SWAT model simulation can be tested using the water balance equation, which is represented as:

$$SW_t = SW + \sum_{i=1}^{t}(R_i - Q_{surf} - ET_i - P_i - QR_i) \quad (7.1)$$

Where, SW_t is the final soil water content (mm), SW is the initial soil water content (mm), t is time (days), R_i is the volume of rainfall (mm), Q_{surf} is the value of surface runoff (mm), ET_i is the value of evapotranspiration (mm), P_i is the value of percolation (mm) and QR_i is the value of return flow.

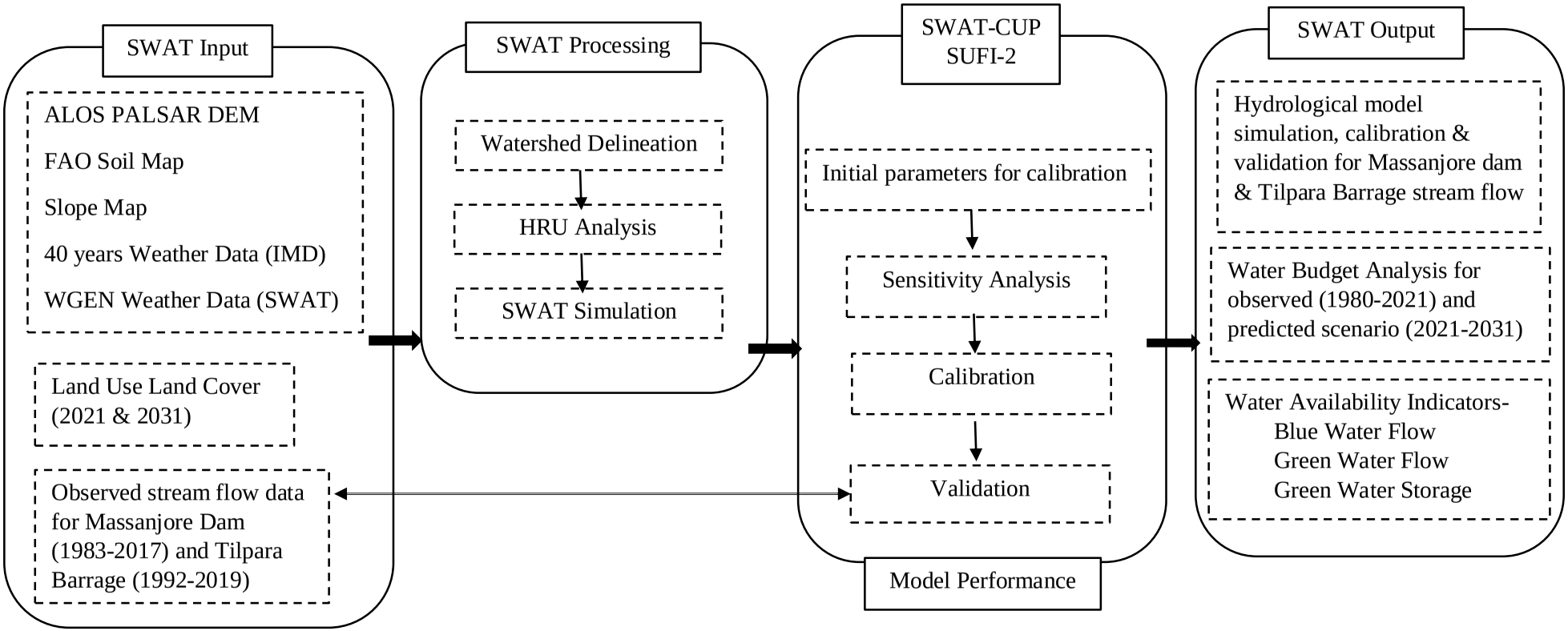

Figure 7.6 *Flow Structure of SWAT Model Setup, Calibration and Validation of Stream Flow in Mayurakshi River Basin*

- **SWAT Model Set-Up**

The configuration of the model is intended to create a hydrological simulation for the Mayurakshi River basin. To set up the model for these goals, the Arc SWAT extension of the SWAT version 2009 has been utilised. In order to set up the model, the following procedures were followed: (1) Watershed Delineation; (2) Hydrological Response Unit (HRU) analysis; (3) Write input tables; (4) SWAT simulation; and (5) Calibration using SWAT-CUP. Figure 7.6 displays the methodology's step-by-step instructions and flowchart.

With a defined threshold area to later join the stream network, the Arc SWAT watershed delineator tool was initially used to divide the entire basin into sub-basins based on DEM and the river's exhaust arrangement. Additionally, these sub-basins are split up into a number of hydrologic response units (HRUs), each of which has its own class of soil, slope, and land use. In this study, 15% of the threshold value for land use, slope, and soil have been employed to obtain a reasonable number of HRUs within each sub-basin. The Mayurakshi River basin has been divided into 54 HRUs and 17 sub-basins (Fig. 7.1). The input data for each sub-watershed was classified as weather, distinctive areas of land cover, soil, and sub-basin management. The "WGS_1984_UTM_Zone_49N" coordinate system was used to project all of the layers. Lookup tables, space databases, and attribute databases were used to link different soil and land use categories. The sub-catchment layer was superimposed over the HRU layer by reclassifying the soil types, layers, and uses, as well as the land cover and slope classes. Finally, the hydrological simulation has been performed for each sub-watersheds and based on the water balance ratios and model performance statistics, the availability of water within the sub-watersheds has also been assessed.

- **Model Calibration and Uncertainty Analysis**

Model calibration is a methodical procedure that involves altering model parameters to make sure that the behaviour of the observed system is as closely matched to the measured behaviour as possible (Gupta et al. 1998). The Sequential Uncertainty Fitting (SUFI-2) approach was used in this study for calibration and uncertainty analysis. It was carried out using the free software SWAT-CUP (Abbaspour et al. 2007), with multiple iterations to re-adjust the parameters to better suit the observed data. The main advantage of SUFI-2 algorithm is that it compensates for all types of uncertainty, including uncertainty in input variables such as rainfall, uncertainty in model conception, uncertainty in model parameters, and uncertainty in measured or observed data (Dhami et al. 2018). By comparing the observed stream flow discharges to the simulated

discharges in the hydrometric station under consideration, monthly stream flow records were used in this study to calibrate the SWAT model of the Mayurakshi River basin for the time periods of 1983 to 2007 (Massanjore Dam) and 1992 to 2010 (Tilpara Barrage).

The 95% prediction uncertainty (95PPU) band is used to measure uncertainty. The p-factor and r-factor are used to assess the effectiveness of model simulation and uncertainty assessment. The p-factor, which ranges from 0 to 1, shows the proportion of measured data that is captured by the 95% prediction uncertainty (95PPU), with 1 denoting 100% bracketing of the measured data within model prediction uncertainty and 0 denoting higher output uncertainty. Whereas, the ratio between the average width of the 95% probability band and the standard deviation of the measured variable is known as the r-factor. As a result, SUFI-2 aims to place the majority of the measured data (high p-factor, maximum 100%) into the narrowest range of the r-factor (minimum 0) (Abbaspour 2011).

To evaluate model performance, both graphical and statistical methods should be used (Nyeko 2015). A visual examination of the disparities between the hydrographs of simulated and observed data was carried out in this work because relying just on performance measures can be deceptive and lead to unrealistic simulations (Daggupati et al. 2015). It is possible to compare observed and simulated datasets visually and directly using graphical tools, such as stream flow hydrographs, and to identify trends in flow size and time fluctuations. In addition to this, based on statistical indicators, the degree of concordance between the simulated and observed data has also been assessed which includes Nash-Sutcliffe efficiency (NSE) (Eq. 7.2), Percent of bias (PBIAS) (Eq. 7.3) Co-efficient of determination (R^2) (Eq. 7.4) and Root Mean Square Error (RMSE) (Eq. 7.5). NSE calculates the ratio of the residual variance to the variance of the observed data, with a range of 0 to 1(Nash and Sutcliffe 1970). Values 0.0 imply that the mean observed value is a better predictor than the simulated value, which indicates inadequate performance, whereas values between 0.0 and 1.0 are typically regarded as acceptable levels of performance (Moriasi et al. 2007). PBIAS is a statistical error index that is frequently used to assess the performance of models. It assesses the typical tendency of the simulated data to differ from their observed counterparts in size or shape. According to Gupta et al. (1999), the ideal value of PBIAS is 0.0, with positive values denoting model overestimation and negative values denoting model underestimation. The fraction of variance in measured data is described by R^2. R^2 ranges from 0 to 1, and values larger than 0.5 are normally regarded as acceptable (Moriasi et al. 2007). The mathematical representation of all these measures are mentioned as follows-

$$NSE = 1 - \frac{\sum_{i=1}^{n}(Q_i^{obs} - Q_i^{sim})^2}{\sum_{i=1}^{n}(Q_i^{obs} - \overline{Q^{obs}})^2} \quad (7.2)$$

$$PBIAS = 100 * \frac{\sum_{i=0}^{n}(Q_i^{obs} - Q_i^{sim})}{\sum_{i=0}^{n} Q_i^{obs}} \quad (7.3)$$

$$R^2 = \frac{\left[\sum_{i=0}^{n}(Q_i^{obs} - \overline{Q^{obs}})(Q_i^{sim} - \overline{Q^{sim}})\right]^2}{\sum_{i=1}^{n}(Q_i^{obs} - \overline{Q^{obs}})^2 \sum_{i=1}^{n}(Q_i^{sim} - \overline{Q^{sim}})^2} \quad (7.4)$$

$$RMSE = \frac{\sqrt{\sum_{i=1}^{n}(Q_i^{obs} - Q_i^{sim})^2}}{\sum_{i=1}^{n}(Q_i^{obs} - \overline{Q^{obs}})^2} \quad (7.5)$$

Where, Q^{obs} and Q^{sim} stands for observed and simulated stream flow and $\overline{Q^{obs}}$ and $\overline{Q^{sim}}$ are the mean value of observed and simulated stream flow respectively, for a specific time (i) and n number of observations.

- **Model Validation**

After calibration, model validation involves putting the calibrated model to the test by examining field observations (the data that did not include utilised in calibration) with the model predictions and preserving the values of all input parameters. Considering the fact that validation should cover the entire period of stream flow recording, in this study, the model has been validated through graphical representation using data from 2008 to 2017 and 2011 to 2019 for the selected basin outlets (Massanjore Dam and Tilpara Barrage gauging site) respectively and were compared to discharge data collected during the same time period.

7.1.3. Results & Discussion

- **Evaluation of SWAT Hydrological Model for Mayurakshi River Basin Area**

In this study, the hydrological response of the Mayurakshi River basin area has been established through the execution of SWAT hydrological model calibration and validation utilising daily observed stream flow discharge data from the examined region. The Massanjore Dam gauging station (Upstream-Basin outlet 7) and the Tilpara Barrage (Downstream-Basin outlet 12) have been selected as study sites based on the data accessibility for the hydrological modelling of the area. For the model simulation, a total of 34 years (1983-2017) of stream flow data for the Massanjore Dam and 27 years (1992-2019) of stream flow data for Tilpara Barrage were incorporated. However, the available data is typically split into two groups: calibration data and validation data. The data from 1992–2008 and 2009–2019 are used for the calibration and

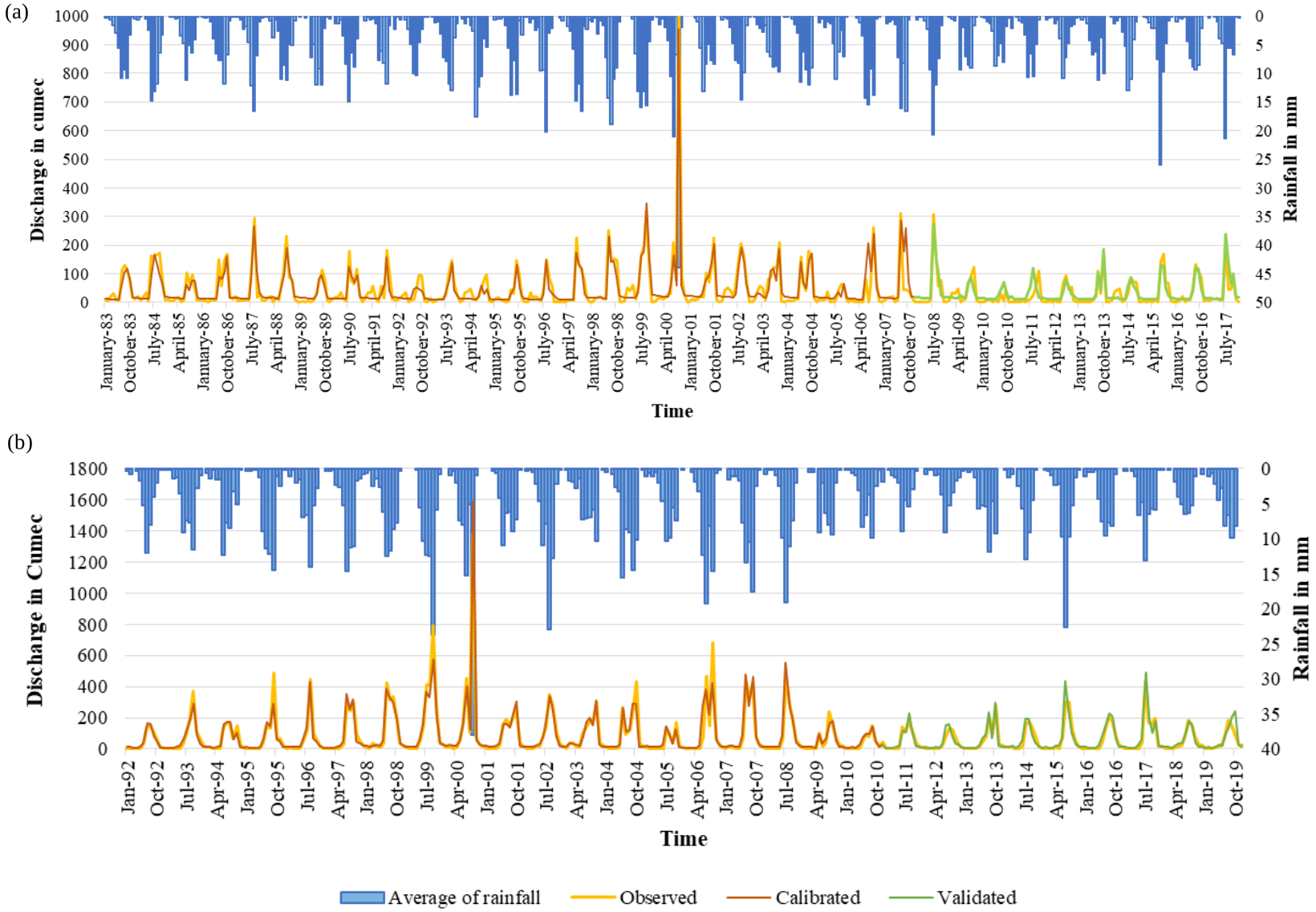

Figure 7.7 *Observed and Modelled Monthly Hydrographs of (a) Massanjore Dam for the Calibration Period (1983-2007) and Validation Period (2008-2017); (b) Tilpara Barrage for the Calibration Period (1992-2008) and Validation Period (2009-2019)*

validation of the stream flow simulation at the Massanjore Dam gauge station, while the data from 1983–2007 and 2008–2017 are used for the same purposes for the stream flow calibration at Tilpara Barrage. The first three years of data from both upstream (1980-1982 for Massanjore Dam) and downstream (1989-1991 for Tilpara Barrage) stations were used as a warm-up period for the execution of SWAT model. Based on this, the SWAT model for both of the basin outputs has been successfully calibrated, validated, and the relevant statistical information has also been assessed. The hydrographs created are displayed in figure 7.7 (a) and (b), demonstrating that peak flow timings tend to be accurately predicted for both stations and that the simulated monthly stream flow patterns are also similar to those of measurements respectively. The modelled stream flow characteristics of the investigated catchments show a rapid increase in stream flow discharge (1053.25 cumec at Massanjore Dam and 1380 cumec at Tilpara Barrage) has occurred during the month of September 2000. This was due to the arrival of a prolonged rainfall storm close to the upstream portion of the basin, which results in a significant water release from the upstream of Massanjore Dam towards the downstream of Tilpara Barrage, triggering a severe flood disaster (Islam et al. 2020). With a history of flooding in Mayurakshi, highest loss (40% of the whole basin area) was documented during this flood episode (Pal 2010).

Table 7.4 summarises the findings of statistical indicators for evaluating the model's calibration effectiveness for the two stations (Massanore Dam & Tilpara Barrage). The NSE, PBIAS, R^2, and RMSE parameters for the Massanjore Dam were 0.84, -2.8, 0.84, 0.4, and 0.93, -3.3, 0.93, 0.27 for the Tilpara Barrage. The NSE values reveal a strong goodness-of-fit throughout the whole calibration and validation period for both outlets. The association between the daily observed and simulated discharge of the Massanjore Dam and the Tilpara Barrage is shown in figure 7.8 and 7.9 respectively, which also depicts the estimated R^2 value has been extremely near to the model's R^2 value, confirming a very significant agreement between the variables. The percent of bias (PBIAS) for both stations has been determined to be -2.8 and -3.3 for Massanjore and Tilpara gauging stations, accordingly. The negative PBIAS value implies that the calibration of the Massanjore Dam was less underestimated than the Tilpara barrage, although both values are satisfactory (Moriasi et al., 2007).

In addition to these indications, the calibration period's uncertainty analysis has also been carried out by calculating the p-factor and r-factor for each of the two gauge stations under study. The Massanjore Dam station's p-factor during the calibration period was 0.80, meaning that the 95PPU band was used to bracket 80% of the recorded stream flow data while the r-

factor reached 0.87 as well (Table 7.4). Similarly, the 95PPU band bracketed 77% of the collected data at the Tilpara Barrage Station (p-factor = 0.77; r-factor, 0.97). According to earlier studies (Abbaspour et al. 2015; Schuol et al. 2008), the findings of stream flow simulations are regarded to have acceptable levels of uncertainty when the p-factor is greater than 0.75 and the simultaneous r-factor is less than 1.5. The SUFI-2 algorithm can therefore be inferred to be capable of accurately representing observed stream flow for both calibration as well as validation periods. However, a detailed study of the findings of the uncertainty analysis reveals that all the observed data are displaying regulated flow values for both stations as they have been purposefully restricted, which may be attributed to limitations in the SWAT simulation model and related uncertainties.

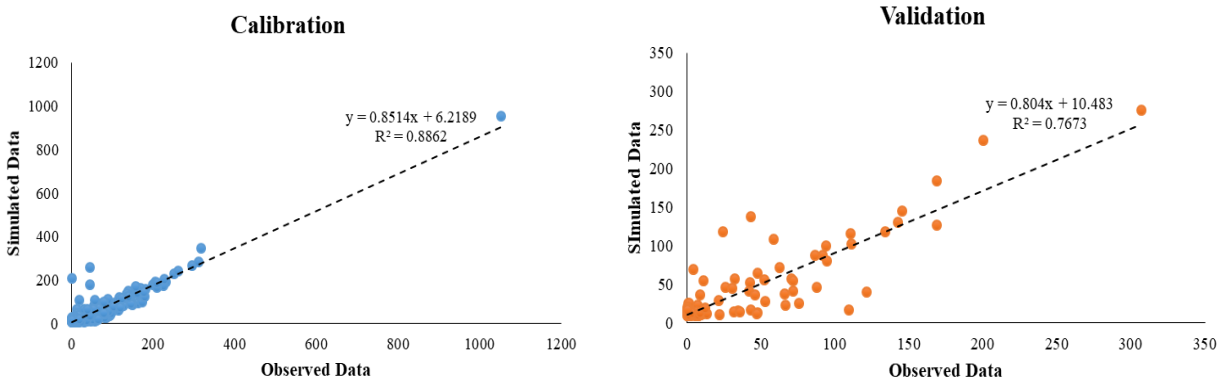

Figure 7.8 *Scatter plots of Calibrated and Validated Models of Massanjore Dam*

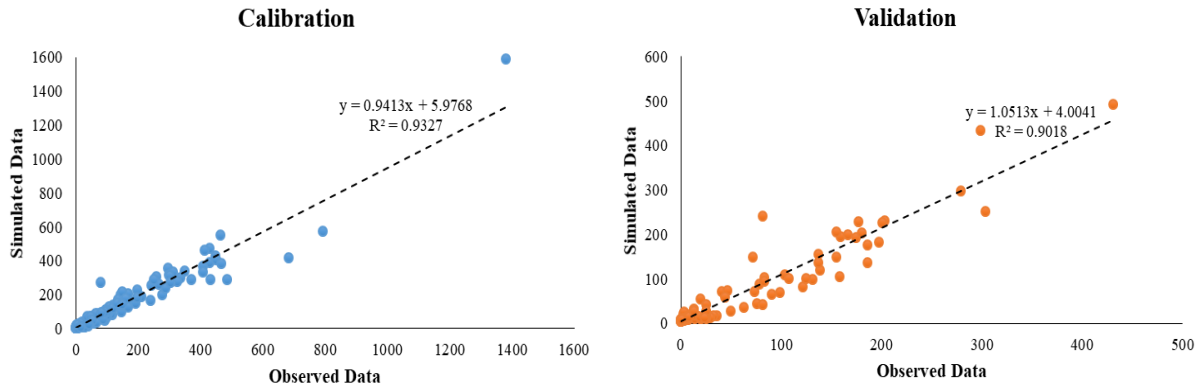

Figure 7.9 *Scatter plots of Calibrated and Validated Models of Tilpara Barrage*

Table 7.4 *Summary of statistics for the Model Evaluation*

Performance index	Massanjore Dam (Basin outlet 7) n= 437	Tilpara Barrage (Basin outlet 12) n=182
Nash-Sutcliffe efficiency (NSE)	0.84	0.93
Percent of bias (PBIAS) (%)	-2.8	-3.3
Co-efficient of determination (R^2)	0.84	0.93
Root Mean Square Error (RMSE)	0.4	0.27
P-factor	0.80	0.77
R-factor	0.87	0.97

*n= best simulation

- **Sensitivity Analysis**

Sensitivity analysis has been carried out in this study for two of the examined catchment's outlets, primarily to detect the model's output's variability in response to changes in its input parameters. Using 24 tentative parameters, the SUFI-2 technique has been used during model calibration in order to determine the most sensitive parameters. Sequential uncertainty fitting, also known as SUFI-2 (Sequential Uncertainty Fitting), is a thorough optimisation and gradient search technique that has a global search function and may calibrate numerous parameters at once. It also takes into account the unpredictability of the input data, model parameters, and model structure (Khatun et al. 2018). After 500 simulations and numerous iterations, the calibration of the monthly discharge showed extremely good performance (0.75>NSE>1.00) for both stations, and an optimisation of the most vulnerable parameters was created (Fujita et al. 2022). The 437 simulations (n=437) for Massanjore and the 182 (n=182) for Tilpara gauge station yielded the best fitting values of all the specified parameters out of 500. In table 7.5, the parameters used for the sensitivity analysis are listed along with the highest, lowest, and best fitted standards.

For stream flow measurement, the global sensitivity assessment has been addressed using two statistics (the t-stat and p-value). Sensitive parameters were identified as those with higher t-stat values and lower p values (Huijuan Bo et al. 2020). For both of the analysed basin outputs (Massanjore and Tilpara) (Figure 7.10a and b), ALPHA_BNK, CN2, CH_K2, CH_COV1, and ESCO have been identified as the most sensitive parameters in the current study at the 0.05 level of importance. The alpha factor (days) for bank storage that may have further impacted the main channel or reach inside the sub basin is indicated by the sensitivity of ALPHA_BNK. The sensitivity of CN2 shows rapid changes in land use classifications, whereas CH_K2 shows rapid changes in the main channel's hydraulic conductivity as a result of the bidirectional interaction between stream flow and groundwater, which makes the river bed less impervious.

Comparable to the soil erodibility factor used in the USLE equation, the value CH_COV1 denotes the channel erodibility factor. It is a result of the materials in the natural channel bed. Due to significant channel scouring (Islam et al. 2020) and sand mining across the riverbed (Nag et al. 2020), reduced vegetation in riparian areas, and the increasing sensitivity of these characteristics, the main channel is becoming less resistant to erosion. The sensitivity of ESCO denotes the soil evaporation compensation factor, allowing for a range in the amount of groundwater that can be dug up to satisfy evaporative demand.

(a)

Parameter Name	t-Stat	P-Value
9:V__ALPHA_BNK.rte	15.365636164	0.000000000
1:R__CN2.mgt	-7.453435754	0.000000000
8:V__CH_K2.rte	-3.236558685	0.001294330
22:R__CH_COV1.rte	3.075836656	0.002220207
6:V__ESCO.hru	-1.979178157	0.048372948
14:R__EPCO.bsn	1.733206207	0.083707988
11:R__SOL_K(..).sol	-1.653701003	0.098848949
16:R__EVLAI.bsn	-1.565418915	0.118150650
5:V__GW_REVAP.gw	-1.520670087	0.129008011
13:V__SFTMP.bsn	1.520092940	0.129152959
19:R__GW_SPYLD.gw	1.493254208	0.136034576
17:R__REVAPMN.gw	1.475935390	0.140623815
4:V__GWQMN.gw	1.215820641	0.224657145
21:R__SOL_ALB(..).sol	1.183656635	0.237141028
18:R__RCHRG_DP.gw	0.891965916	0.372862820
24:R__PLAPS.sub	0.832883092	0.405329241
7:V__CH_N2.rte	-0.828557212	0.407771135
15:R__OV_N.hru	-0.436775639	0.662472546
3:V__GW_DELAY.gw	-0.433767094	0.664654515
2:V__ALPHA_BF.gw	-0.325868969	0.744667003
20:V__SURLAG.bsn	-0.319605161	0.749408181
12:R__SOL_BD(..).sol	-0.144157187	0.885437488
23:R__CH_WDR.rte	0.109593022	0.912778429
10:R__SOL_AWC(.....	0.021350127	0.982975323

(b)

Parameter Name	t-Stat	P-Value
9:V__ALPHA_BNK.rte	16.492664578	0.000000000
1:R__CN2.mgt	-5.641328273	0.000000029
8:V__CH_K2.rte	-5.047225798	0.000000640
22:R__CH_COV1.rte	2.569025445	0.010502732
6:V__ESCO.hru	-2.064503295	0.039512308
5:V__GW_REVAP.gw	-1.876969063	0.061135046
11:R__SOL_K(..).sol	-1.838172879	0.066661184
7:V__CH_N2.rte	-1.810810208	0.070801875
13:V__SFTMP.bsn	1.581686141	0.114386834
3:V__GW_DELAY.gw	-1.566075259	0.117996925
16:R__EVLAI.bsn	-1.470043914	0.142211907
17:R__REVAPMN.gw	1.392368403	0.164462332
4:V__GWQMN.gw	1.316571110	0.188617313
19:R__GW_SPYLD.gw	1.176856790	0.239842063
14:R__EPCO.bsn	1.158564227	0.247215998
18:R__RCHRG_DP.gw	1.138453976	0.255504825
15:R__OV_N.hru	-1.053864476	0.292480737
21:R__SOL_ALB(..).sol	0.931067496	0.352291613
24:R__CH_WDR.rte	0.840456837	0.401075145
23:R__PLAPS.sub	0.476633862	0.633842051
10:R__SOL_AWC(.....	-0.332266852	0.739834341
20:V__SURLAG.bsn	0.231950942	0.816676011
12:R__SOL_BD(..).sol	-0.192383747	0.847523844
2:V__ALPHA_BF.gw	0.121355239	0.903460988

Figure 7.10 *Global Sensitivity Analysis (a) Massanjore Dam (b) Tilpara Barrage*

Table 7.5 *SWAT Input Parameters Used For the Calibration of Stream Flow of Mayurakshi River Basin*

No	Parameters	Ext.	Description	Unit	Adjustment	LB	UB	FV
			Parameters controlling water balance					
1	PLAPS	sub	Precipitation lapse rate	ºC/km	r	-1000.00	1000.00	-694.00
2	ESCO	hru	Soil evaporation compensation factor	--	r	0.0000	1.0000	0.4350
3	EPCO	hru	Plant uptake compensation factor	--	r	0.0000	1.0000	0.9990
4	EVLAI	bsn	Leaf area index at which no evaporation occurs from water surface	--	r	0.0000	10.000	1.8900
5	SFTMP	bsn	Snowfall temperature	ºC	v	-5.0000	5.0000	-2.0300
			Parameters controlling surface water response					
6	CN2	mgt	SCS runoff curve number	--	r	-0.20	0.20	-0.1124
7	SURLAG	bsn	Surface runoff lag time	--	v	0.0000	24.0000	15.6240
8	OV_N	hru	Manning's "n" value for overland flow	--	r	0.0000	30.0000	1.83000
			Parameters controlling sub-surface water response					
9	ALPHA_BF	gw	Baseflow alpha factor	days	v	0.0000	1.0000	0.72700
10	ALPHA_BNK	gw	Baseflow alpha factor for bank storage	--	v	0.0000	1.0000	0.41700
11	GW_DELAY	gw	Groundwater delay	days	v	30.000	450.00	216.899
12	GWQMN	gw	Threshold depth of water in the shallow aquifer required for return flow to occur	mm	v	0.0000	2.0000	1.91400
13	GW_REVAP	gw	Groundwater "revap" coefficient	--	v	0.0000	0.20000	0.07420
14	REVAPMN	gw	Threshold depth of water in the shallow aquifer for "revap" to occur	mm	r	0.0000	500.000	99.5000
15	RCHRG_DP	gw	Deep aquifer percolation fraction	--	r	0.0000	1.0000	0.8810
16	GW_SPYLD	gw	Specific yield of the shallow aquifer	m3/m3	r	0.0000	0.4000	0.2036
			Parameters controlling soil's physical properties					
17	SOL_AWC	sol	Available water capacity of the soil layer	--	r	0.0000	1.0000	0.2610
18	SOL_K	sol	Saturated hydraulic conductivity	--	r	0.0000	2000.00	10.000
19	SOL_BD	sol	Moist bulk density	--	r	0.9000	2.50000	2.0824
20	SOL_ALB	sol	Moist soil albedo	--	r	0.0000	0.25000	0.19025
			Parameters controlling channel's physical properties					
21	CH_N2	rte	Manning's "n" value for the main channel	--	v	-0.0100	0.30000	0.07463
22	CH_K2	rte	Effective hydraulic conductivity in main channel alluvium	--	v	-0.0100	500.000	17.49035
23	CH_COV1	rte	Channel erodibility factor	--	r	-0.0500	0.6000	0.08975
24	CH_WDR	rte	Channel width-depth ratio	--	r	0.0000	10000.00	6290.00

Ext: Extension, R: Replace by value, V: Multiply by value, LB: Lower bound, UB: Upper bound, FV: Final val

- **Water Balance Analysis**

Utilising the SWAT model, water balance serves as an essential component and impetus for watershed study. In this study, water balance components have been found for the whole model calibration period (1983–2021) and tabulated using the SWAT output files. The mean annual contribution of each component has been evaluated and is shown in table 7.7 to illustrate the total water budget scenario. The SWAT weather-generated (WGEN) climatic data (2020–2050) and a CA-Markov model–generated future projected land use information for 2031, have also been used as an input to analyse a possible future state of water availability over the research area. The overall health state of the catchment in terms of its hydrological responsiveness will be confirmed through a comparative examination of both the existing and anticipated scenarios of water balance over the Mayurakshi River basin. The results of both analyses are represented in a pie diagram (Fig.7.11).

Table 7.6 *Mean Annual Water Balance Components*

Parameters	Type of flow	Observed (2021)	Projected (2031)
		Mean value (mm)	Mean value (mm)
Precipitation	Inflow	1432.4	1404.7
Evapotranspiration	Outflow	578.4	542.1
Potential Evapotranspiration		1236.8	1231.1
Surface Runoff		566.44	613.73
Lateral Flow		6.98	7.77
Return flow		241.39	205.11
Shallow Aquifer Storage		280.14	241.85
Deep Aquifer Recharge		14.01	12.09
Total Water Yield		853.52	863.35

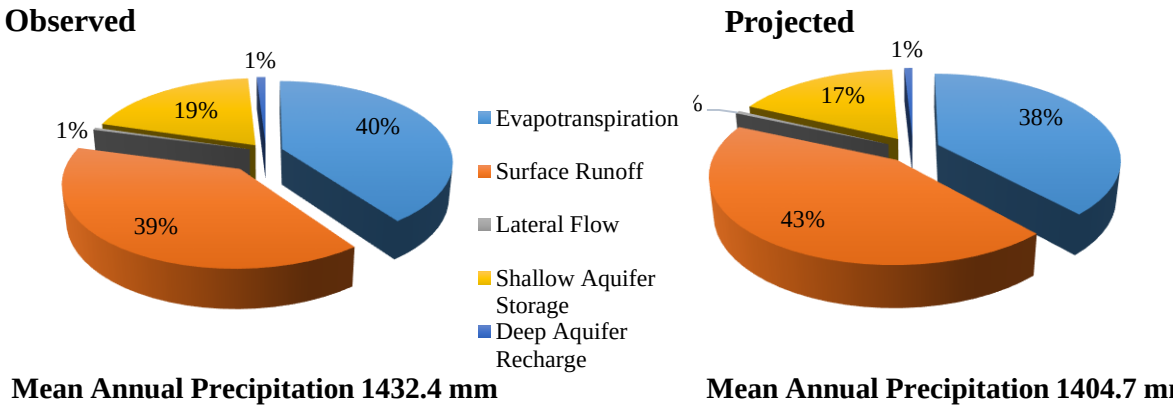

Figure 7.11 *Water Balance Ratios for Observed (2021) and Projected (2031) Period of Study*

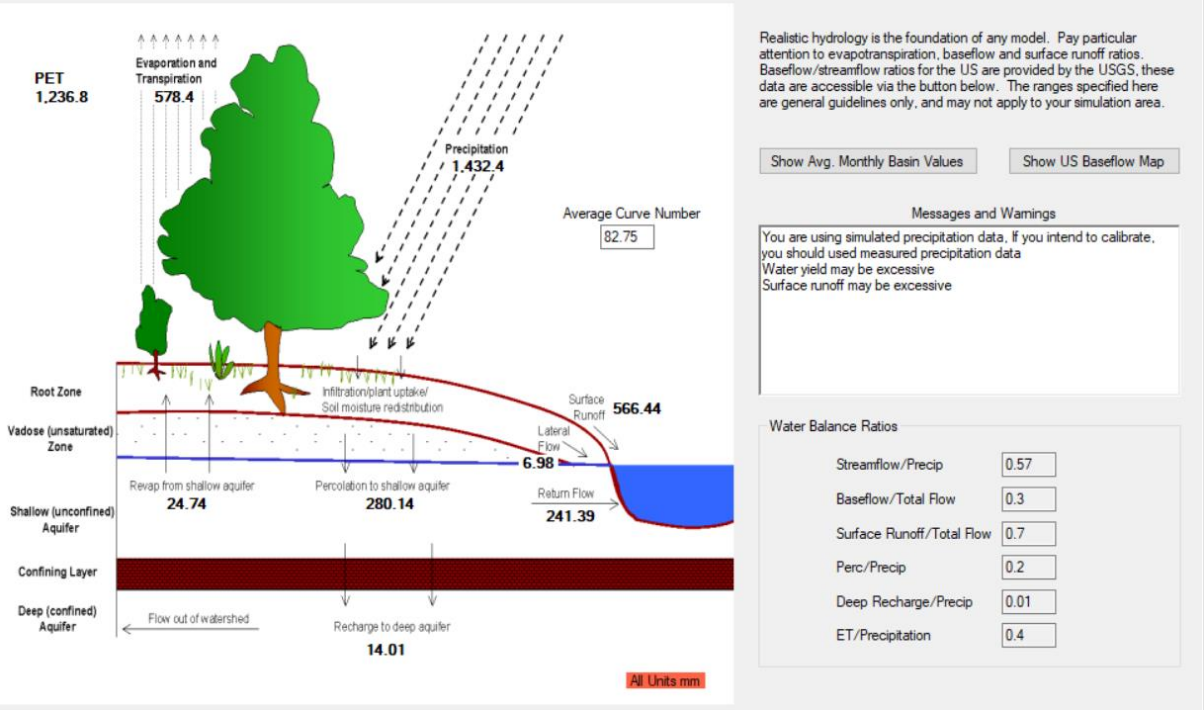

Figure 7.12 *Water Budget Analysis for the Observed Period (1983-2021) of Study*

The result shows (Fig. 7.12 & 7.13), over the past 38 years, the watershed received an average of 1432.4 mm of precipitation per year. Evapotranspiration is the greatest water balance component, accounting for approximately 578.4 mm (40%) of catchment water loss. The remainder is split between the percolation tank (the unsaturated zone, the shallow unconfined aquifer, and the deep confined aquifer) and discharge (surface runoff, lateral flow, and return flow). Surface runoff, however, makes up more than 90% of the total discharge when the ratio of the discharge components is simply taken into account (Table 7.6). This suggests that farmers will more likely have to rely on runoff, either by collecting it and storing it in ponds or reservoirs for use during the dry season for supplemental irrigation from the surface rather than extracting water from below ground. The estimated 280.14 mm and 14.01 mm contributions to the shallow and deep aquifers, respectively, equal 20% and 1% of the annual precipitation. In addition to this, the amount of water that may percolate into the soil and contribute to aquifers depends on the soil's ability to hold water. It is estimated that 294.15 mm, or 20.5% of the annual precipitation, percolates into the percolation tank, which is made up of the unsaturated zone, the shallow unconfined aquifer, and the deep confined aquifer. 17% of the water in this percolation tank evaporates as a return flow, supplying the watershed outlet while only 1% of the recharge of the deep aquifer is in the shallow and unsaturated aquifers (Table 7.6), which are more easily accessible. This proved that in several watershed areas where

groundwater is being used from shallow wells for dry season farming, causing a sharp decline in the level of groundwater (Nag et al. 2022).

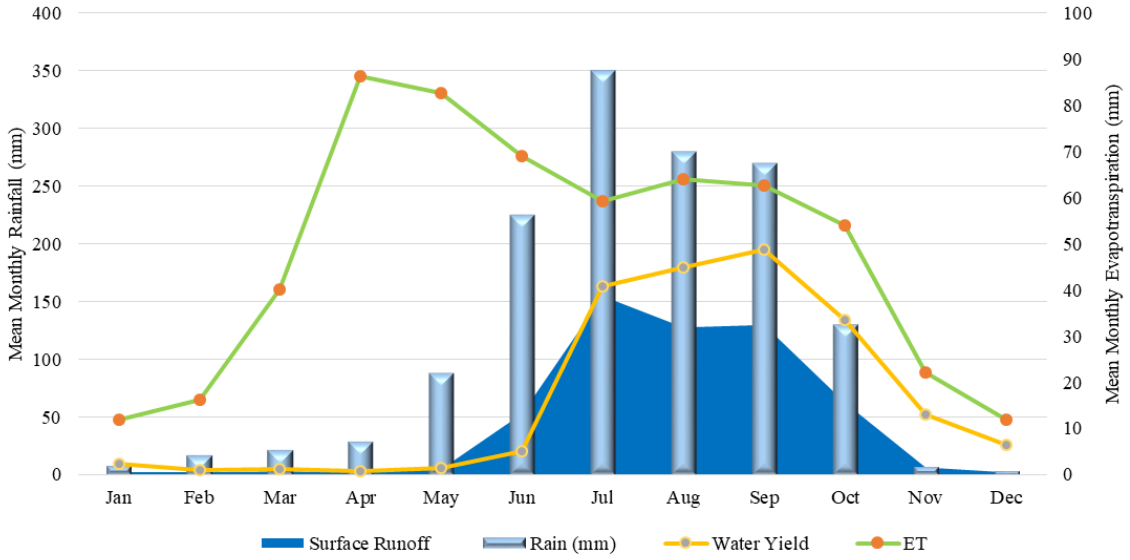

Figure 7.13 *Monthly Water Budget Analysis for the for the Observed Period (1983-2021) of Study*

In the study, future anticipated values of critical hydrologic elements were computed and shown in figure 7.14 & 7.15, where it is clear that precipitation had a considerable impact on surface runoff and lateral subsurface flow. A considerably lower mean annual precipitation (1404.7 mm) than the previous historical period has been projected for the ten-year simulated time span (2021-2031). The future scenario also predicts a significant drop in mean annual evapotranspiration, which has been measured at 542.1 mm or 38% of the mean precipitation. Such a significant drop in evapotranspiration can be attributed to a decrease in vegetation cover (46.47% in 2031) (Table 6.35 in chapter 6). The decrease in canopy interception, percolation, and evapotranspiration, as well as the rise in runoff, were signs that the soil's ability to hold water had diminished. Additionally, the water's ability to flow downward is limited by the increase of settlement (116.74% in 2031) (Table 6.35 in chapter 6) and other impermeable surfaces on the surface. This suggests a reduced penetration rate with increased surface runoff generation (Neitsch et al. 2011). The amount of surface runoff that will be accounted for during the upcoming years is predicted to be around 613.73 mm, or 44% of the total precipitation.

It is important to observe that the annual fluctuations in precipitation are compatible with the changes in water yield values (including overland flow, lateral flow, and base flow). Water yield, which includes shallow groundwater (base flow), lateral soil flow, and overland flow, is the stream flow produced at the entire catchment outlet. Because the SWAT model implies that water entered the deep aquifer flowing out of the catchment, the water yield was 826.69 mm,

which is equal to the total water yield of 838.78 mm minus that of deep groundwater recharge (12.09 mm) (Arnold et al. 1993). Such a circumstance demonstrates that there is less groundwater in relation to precipitation, which should be a fact considering the current rate of population expansion.

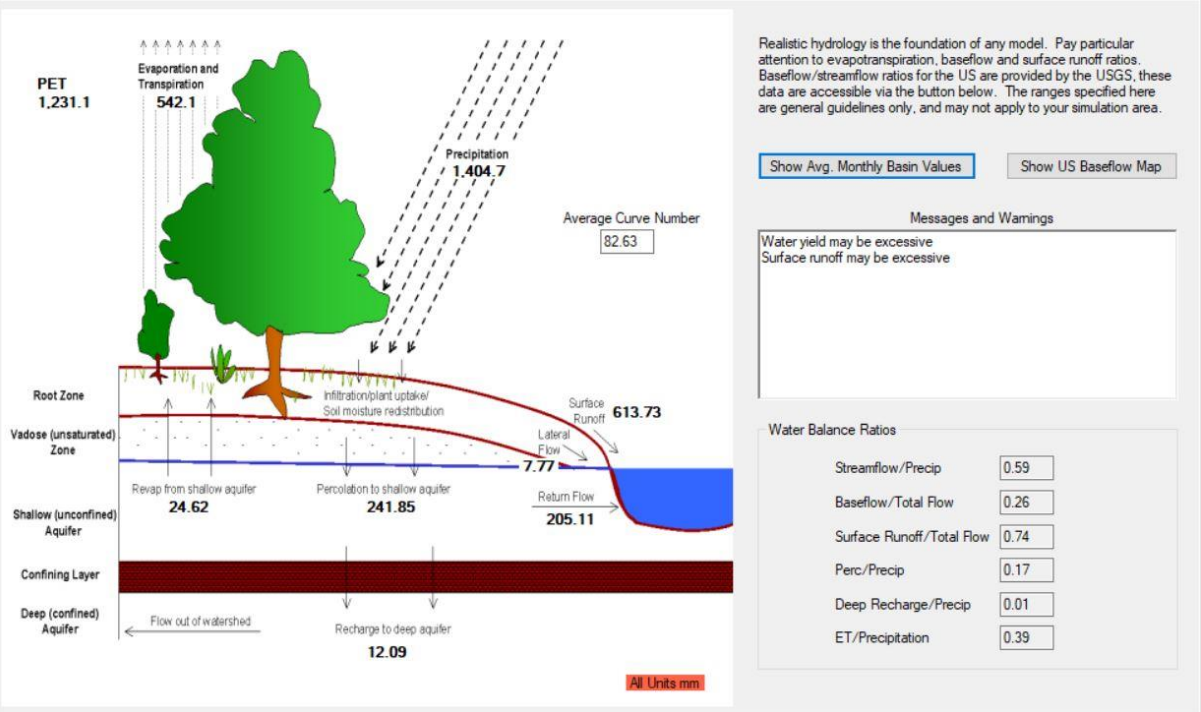

Figure 7.14 *Water Budget Analysis for the Projected Period (2020-2050) of Study*

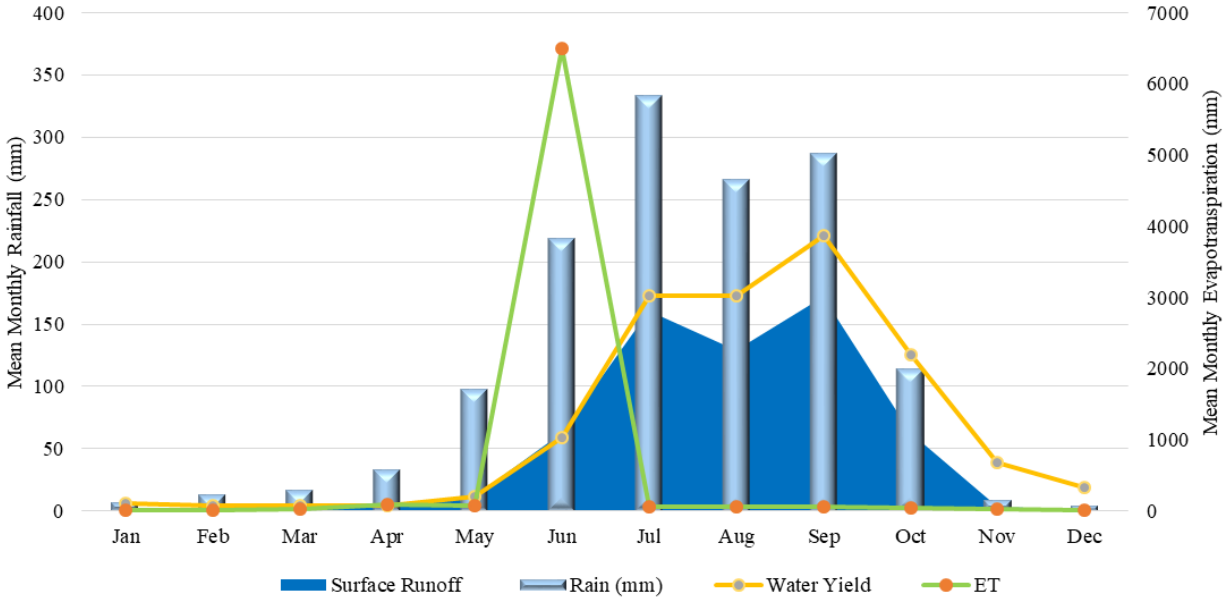

Figure 7.15 *Monthly Water Budget Analysis for the for the Projected Period (2020-2050) of Study*

Future research on the topic is required to examine the impact of potential climate change scenarios. Although large and extensive data sets have been employed here to guarantee accurate and consistent performance, their applicability is constrained in some ways including the river discharge is confined to only two gauge stations, there is a scarcity of consistent meteorological data, and so on. As a result, more research should be done to enhance the simulation using data from many sites' stream flows and fine resolution soil data.

- **Assessment of Water Availability Indicators**

This study has quantified key elements of the water cycle at the sub-basin level of the Mayurakshi River basin using the calibrated SWAT outputs. These include blue water flow (water yield plus deep aquifer recharge), green water flow (actual and potential evapotranspiration), and green water storage (soil moisture) (Fig. 7.16). This study can provide strategic information about accessible internal renewable water resources, which is required for long-term planning of a region's food and water availability, among other issues. A detailed output of the model calibration for 38 years (1983–2021) using the Sequential Uncertainty Fitting algorithm (SUFI–2) algorithm includes monthly sub-basin water balance components (precipitation, snowmelt, percolation, soil water content, PET, actual ET, surface runoff, base-flow, and water yield) for 17 sub-basins and daily stream flow records for 17 reaches. A subset of this content has been taken to investigate the spatiotemporal trends in the aforementioned indicators of the availability of water resources. Based on the Swat Data, Water yield (SURQ) and deep aquifer recharge (DA_RCHG) were added together to compute blue water flow. Whereas, the actual evapotranspiration (ET) and soil water (SW) content, respectively, were linked to green water flow and storage (Faramarzi et al. 2009). To demonstrate the temporal fluctuation of blue and green water, an inter-annual coefficients of variation (CV) are also offered.

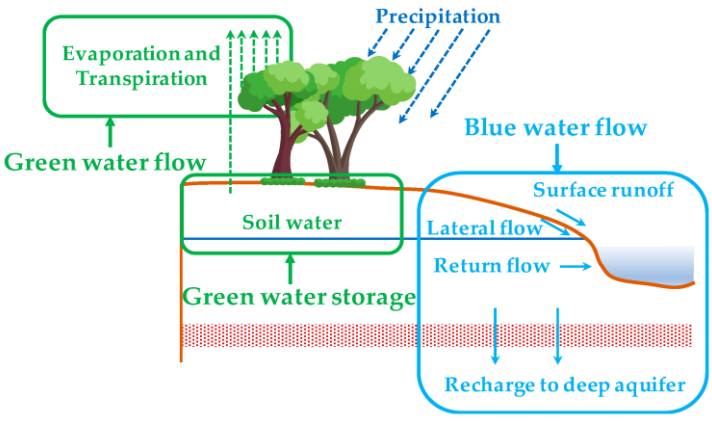

Figure 7.16 *Schematic Diagram Showing Important Water Availability Indicators (Yuan et al. 2019)*

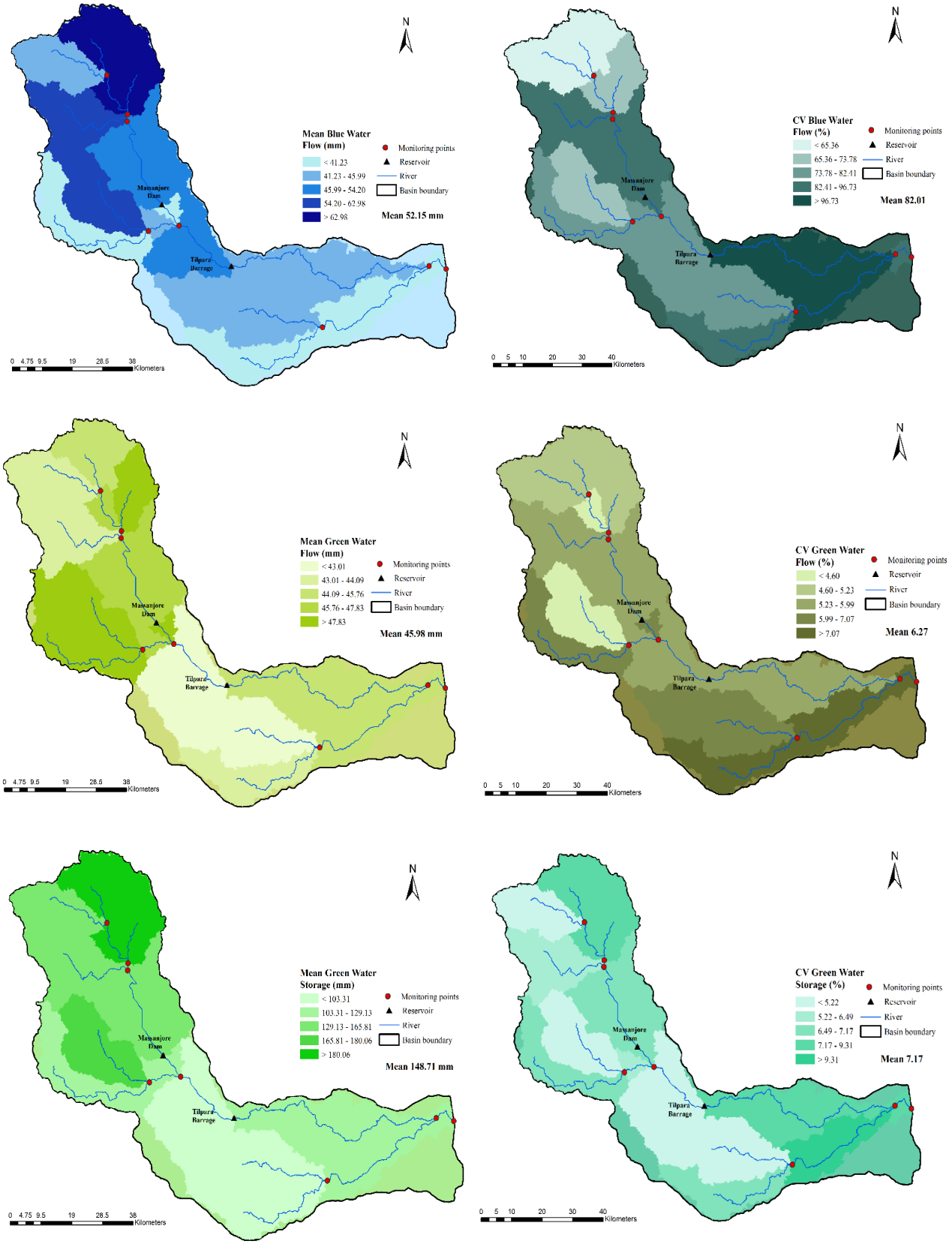

Figure 7.17 *Surface layers of Water Availability Indicators along with the Annual Co-efficient of Variation calculated Using Calibrated SWAT Model (1983-2021) of the Mayurakshi River Basin Area*

The long-term mean values (1983–2021) for all of these variables at the sub-basin level are depicted in figure 7.17, which shows their spatial variability across the study area. The Mayurakshi River basin's northwest corner, which falls under the sub-watershed of Dhobi and Bhurbhuri, has the highest blue water flow, with an average value of more than 62 mm. Such high blue water flow is primarily caused by presence of steep slopes, the existence of lineaments, and subsurface fissures over the regions. A second belt with values above average (greater than 52 mm) is found in the sub-watersheds of Tepra and a small portion of Siddheswari, while the downstream of the examined catchment exhibits the least amount of blue water flow, not reaching 40 mm. The region's mean precipitation is completely aligned with the spatial variance of the green water flow, which is represented spatially in the research area (Fig. 7.17). The highest value is mostly centred in the basin's south-western region, with a mean green water flow of 45.98 mm. The highest mean rainfall within this zone encourages higher evapotranspiration and highest green water flow from this area. In contrast, the Mayurakshi River's downstream portion has the lowest green water flow. This could be a result of the lack of vegetation in this area. The green water storage of the study region varies from 100 to less than 180 mm, with the upper basin having a greater value and the intermediate to lower basins having a low value throughout the period of the study. The minimal amount of green water storage, which denotes the absence of water in the soil profile, is frequently related to the local soil characteristics. Similarly, the lower portion of the basin, which is made up of sandstone, shale, and alluvial soil, also exhibits the trait of limited water holding capacity. The reliability of each water resources indicator from year to year is represented by the maps of the inter-annual coefficient of variation (CV) in figure 7.17. A location experiencing harsh weather conditions and less dependability for the water supplies available is indicated by a higher value of CV. Lower CV areas can be regarded as having higher availability for water supplies over a region. It can be seen that the upper Mayurakshi River basin exhibits greater variability in mean precipitation as well as blue water resources. Additionally, the downstream areas of the basin face a higher rate of unpredictability in terms of the flow and storage of green water, which can support the presence of highly permeable soil and a lack of green cover within this region.

7.2.4. Conclusion

The process-based semi-distributed hydrologic model SWAT, which incorporates agricultural, climatological, and hydrological processes all at once, was used to conduct the entire study. To improve the accuracy of the model outputs, extensive calibration, validation, sensitivity, and uncertainty evaluations were carried out. For more than 30 years, the daily observed river discharge information was used to calibrate the model. To characterise model uncertainty, the 95% prediction uncertainty range for the outputs was calculated using SUFI-2. Presentation of the freshwater availability as a 95PPU band is helpful for the management and planning of water resources in each region and across the nation because it takes into account the conceptual model uncertainty (e.g., inter-basin water transfer, water use), input data uncertainty, and parameter uncertainty in such a large-scale hydrological model. It has been further noted that the inclusion of data from two gauge stations for calibrating the model was discovered to be crucial for an accurate accounting of the Mayurakshi River's hydrological behaviour.

The characteristics of a crucial water balance component and indications of water resources availability are further explained in this work. The availability of water resources, including internal renewable blue water, present and potential ET, and soil water, was calculated for the Mayurakshi River at sub-basin and monthly temporal resolutions. In the context of long-term water resources planning and assessment, the underlying sub-basin water balance data, in particular blue and green water resources, can demonstrate its value for decision-making by national, regional, or trans-boundary water management agencies.

7.2. Assessment of Riparian Vegetation Health Quality of Mayurakshi River Basin Area

Riverine environments are crucial ecotones that link terrestrial and aquatic ecosystems and offer a variety of ecosystem services. They are morphologically and compositionally unique from neighbouring ecosystems as they maintain high levels of biodiversity. In order to sustain stream health and protect its biological services, this channel's floodplain structure and connectivity are essential to preserve. Riparian zones are areas of transition between aquatic and forest ecosystems containing a variety of microhabitats (Rykken et al. 2007) for both terrestrial and aquatic populations, hence supporting bio diverse communities (Ramey & Richardson 2017). The riverine zone is primarily distinguished by a high level of spatial as well as temporal uncertainty, which is caused by bioclimatic, geomorphological, and land-use conditions and is greatly influenced by time, such as natural or anthropogenic impacts (Dufour et al. 2019). According to Naiman et al. (2010), riverine vegetation provides a wide range of ecological services. These regions are crucial in the reduction of nonpoint contributors to pollution and nutrients by filtering (Zalewski et al. 2003); and they may remove more than 90% of the nitrate from the underground water that runs across them (Hunter et al. 2006). They also provide bank stabilisation to prevent floods (Carter & Anderson 2020). Additionally, they are capable of entangling sedimentation runoff from the surface, enhancing the resilience of the banks, and so reducing future soil loss to streams (Price & Lovett 1999). By providing shade for aquatic habitats, this plant also helps to control the temperature of those systems (Pusey & Arthington 2003). Despite the fact that all of the services offered by these ecosystems have important ecological functions, riparian forests are one of the world's most vulnerable ecosystem types (Tockner and Stanford 2002).

One of the main causes of degradation of riparian forests is alteration in land use and cover (Mondal and Patel 2018). The removal of native riparian forests in favour of exotic plantations, expansion of agricultural lands, and urban areas has resulted in significant negative effects on the structure and function of the riparian cover. As a consequence, the resulting changes in cover structure have posed serious threats to the ecological environment of rivers, the integrity of the fluvial environment, and the survival of human cultures that depend on them (Fierro et al. 2017). It also has an impact on the preservation and support of the essential mechanisms involved in the ecological system that have ability to organise themselves (Barkmann et al. 2001). Other anthropogenic activities including the building of dams, livestock grazing in riparian forests, and the channelization of streams and rivers were additional disruptions to this

type of ecosystem that resulted in the total destruction and significant decline in the width and perceived "quality" of riparian forests (Miller et al. 2006). Such concerns are most obvious near riverine habitats due to rich productivity and a connection to rivers, resulting in strong demand for exploitation.

Advanced hydro-morphological approaches to river management now focus on the structure, evolution, and dynamic morphology of hydrologic systems over time (Belletti et al. 2015). According to Newson and Large (2006), these emphasise analysing the physical stream's traits and processes as the foundation for stream restoration. Several techniques have been developed to assess various riverine properties and components. Physical habitat assessment is done using indices such the Riparian Channel and Environmental Inventory (RCE) (Petersen 1992) and the Index of Stream Condition (ISC) (Ladson et al. 1999). The Morphological Quality Index (MQI) (Rinaldi et al. 2013) and the Hydro-morphological Quality Assessment (IHG) (Ollero et al. 2011) are used to assess morphological connectivity, while The Nature Conservancy (2009) guidelines are typically used to assess changes to the hydrological regime. The EU Water Framework Directive proposes utilising biological indicators along with hydro-morphology and physicochemical analyses to categorise the stream's ecological status for the riparian habitat and ecology elements (Vidal-Abarca et al. 2016; Rodrigues et al. 2019). As a result, numerous methods for assessing and quantifying the quality of riparian vegetation have been developed, including the River Habitat Survey (Raven et al., 1998), System for Evaluating Rivers for Conservation (Boon et al. 1998), Qualitat del Bosc de Ribera (QBR) Index (Munne et al. 2003), Rapid Appraisal of Riparian Condition (Jansen et al. 2005) etc.

In this respect, the current review focussed on the evaluation and examination of the changing condition of the riparian ecosystems in the Mayurakshi River Basin area between the years of 1989 and 2021. Three key indices have been used for this purpose: the Riparian Strip Quality Index (RSQI), the Qualitat del Bosc de Ribera (QBR) Index, and the Normalised Difference Vegetation Index (NDVI). Finally, an Overall Riparian Health Quality Score (ORHQS) has been assigned to the main channel after computing all of these field-based and satellite image-based indices. The findings of the study can be applied to future rehabilitation, restoration, or preservation initiatives, watershed planning, or general riparian forest management.

7.2.1. Delineation of Riparian Zone of the Study Site

Delineating the riparian region by separating the main river from the corresponding floodplain zone is crucial before computing the approved indices for evaluating the riparian quality.

Following Munne et al. 2003 (Fig. 7.18) and based on the presence of fluvial terraces, the dominance of riparian flora, and natural evidence of bank-full discharge zone, a 100 m buffer area has been selected here as the Mayurakshi river's riparian zone.

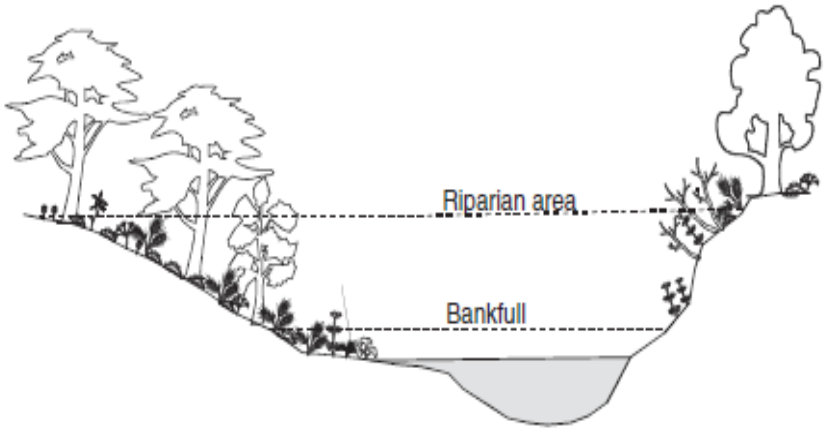

Figure 7.18 *Demarcation of Riparian Zone (Munne et al. 2003)*

A total of 23 monitoring sites have been established along the main Mayurakshi channel by segmenting the river's length (288 km) at intervals of 10 km (Fig. 7.19). During the time of field survey, each sampling site was confirmed and examined for its route accessibility, and a Garmin eTrex 10 Global Positioning System (GPS) was used to record its precise location worldwide. Only 8% of the investigated riparian zone is covered by natural vegetation, with agricultural cropland accounting for 74% of the total area, indicating a greater rate of human land exploitation. Shorea robusta (sal), Pterocarpus marsupium (Piasal), Terminalia tomentosa (asan), Anogeissus latifolia (dhaw), Terminalia bellerica (bahera), Dalbergia sissoo, etc., are native plants found in this region's tropical deciduous forest. While Eucalyptus and Akashmoni, together with other varying species, are primarily planted in the areas of degraded forest land or waste land (Annual Forest Report, Government of West Bengal).

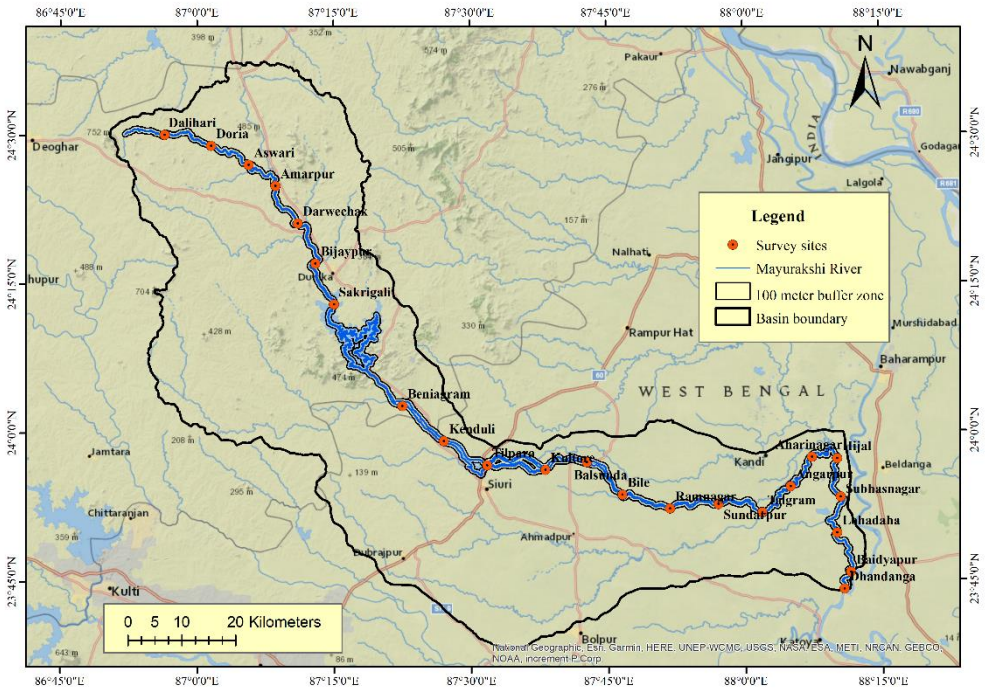

Figure 7.19 *Location of the Survey Sites along the Mayurakshi River*

7.2.2 Material and Methods

The details of the selected indices to monitor the riparian vegetation quality has been discussed in the following section and a methodological flow chart has been shown in figure 7.20.

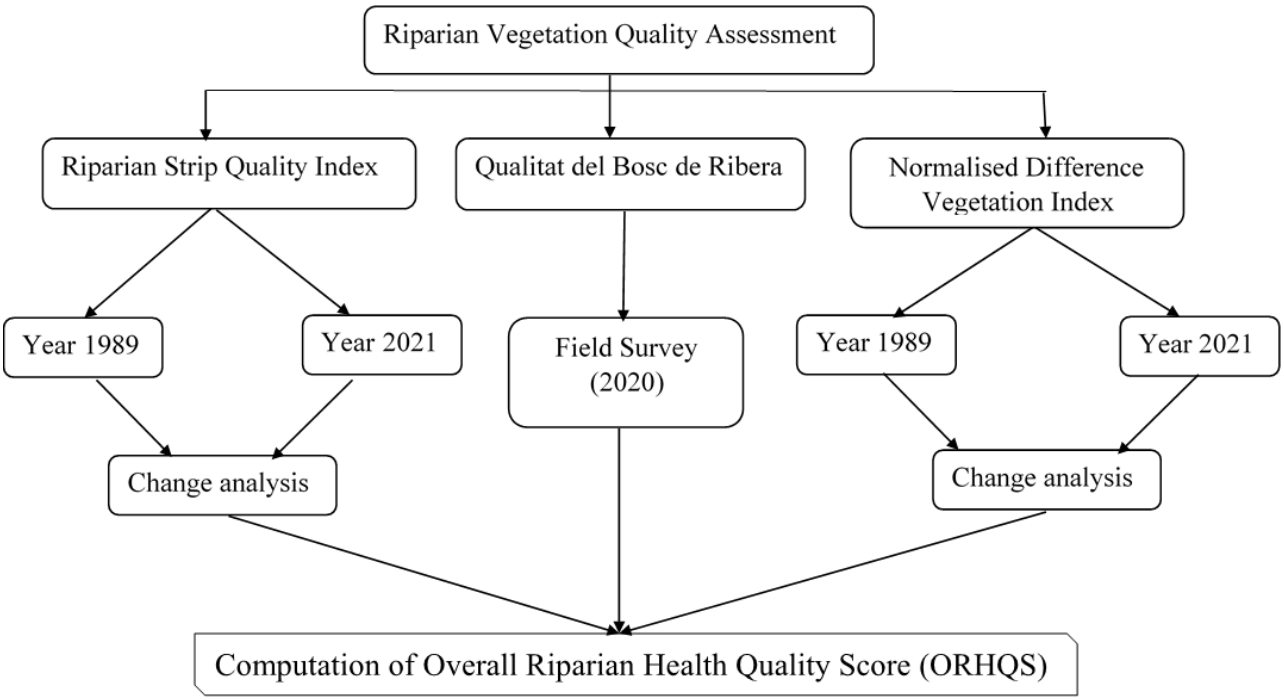

Figure 7.20 *Methodological Chart of the Riparian Study*

- **Riparian Strip Quality Index (RSQI)**

The RSQI assesses the ecological value of riparian areas, which have a substantial impact on the health and functionality of rivers (Saha et al. 2020). It can also be used to confirm regulatory compliance and track changes in riparian habitats. It is frequently employed for illustrating ecological landscapes of watershed riparian habitats. According to Saint-Jacques and Richard's (1998) technique, it is calculated using weighted riparian land cover classes as mentioned in the following equation:

$$RSQI = \frac{\sum(\%LU_i * W_i)}{10} \quad (7.6)$$

Where, LU_i represents % of land use area within the riparian zone and W_i is the weight factor of the corresponding land use class.

According to the weights assigned to each land use class in accordance with Saint-Jacques and Richard (1998), the computed RSQI values ideally range from 17 (low quality) to 100 (high quality). According to the standards established by Saint-Jacques and Richard (1998), the weighting for each land use was determined as follows: forest (10), shrubs (8.2), herbaceous vegetation (5.8), crops (1.9), bare soil (1.7), infrastructure (1.9), bedrock (3.8), and logging areas (4.3). The weighting of each land use class specified in the study region has undergone a few modest adjustments for example settlement areas were given the same weight as infrastructure, while wet fallow, and rivers were designated as logging areas, agricultural lands received the weight designated for crops, and pasture lands and bare soil retained their original weights.

- **Land Use Land Cover Classification**

Using Landsat satellite images from 1989 and 2021, a supervised classification has been carried out in the ERDAS Imagine 9.2 programme to observe a difference in the quality of the riparian vegetation along the chosen 100 metre buffer areas of the River Mayurakshi. Images from the post-monsoon season, which are well-known for their clear skies and rapid plant growth, clear water body visibility, and fully sowed crop land, were chosen for this purpose. In the riparian area of the Mayuraskhi River, all seven primary land use classes were identical after a supervised categorization using the maximum likelihood method. These include settlements, bare land, natural vegetation, seasonal wet fallow land, rivers and other bodies of water, agricultural land, and pasture land (Fig 7.21).

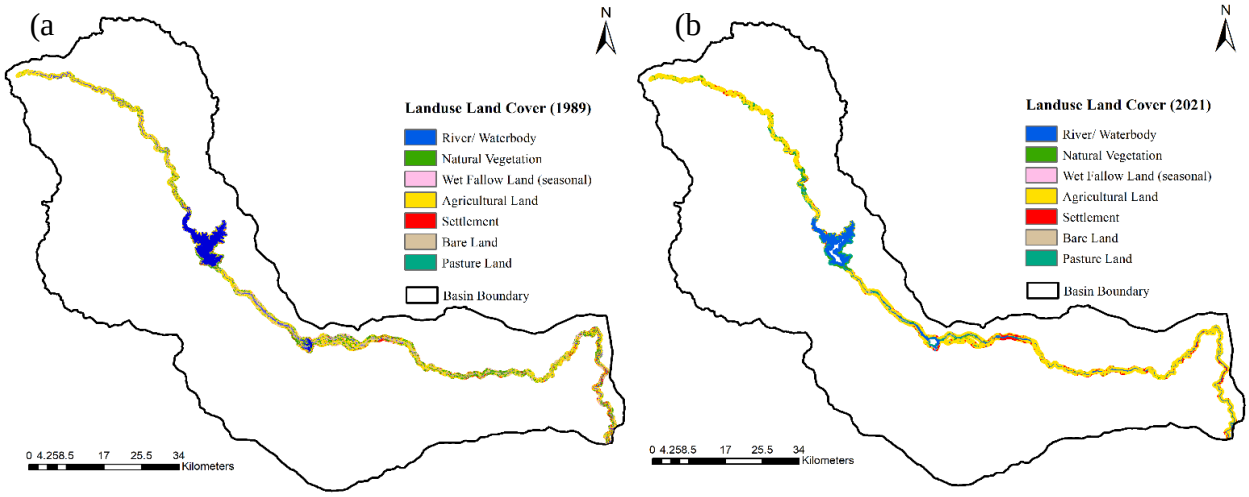

Figure 7.21 *Land Use Land Cover Map of the Mayurakshi River's Riparian Zone (a) 1989 (b) 2021*

➢ Qualitat del Bosc de Ribera (QBR) Index

The 'Qualitat del Bosc de Ribera' (or 'Riparian Forest Quality') index, so named after its Catalan abbreviation, creates a methodology that incorporates biological and physical characteristics of the river and its floodplain and can be utilised for the analysis and monitoring of riparian vegetation. This indicator is an easy way to assess the quality of riparian habitat through a field survey. It was created to be utilised in Spanish Mediterranean streams (Munne et al. 1998), but numerous authors have modified it to fit various geographical contexts (Kazoglou et al. 2010; Sirombra & Mesa 2012), while keeping the assessment process and core framework intact. According to Zhao et al. (2016), the QBR index evaluates riparian forest stands explicitly and serves as an acceptable substitute for measuring the habitat quality of river banks. It takes into account important riparian vegetation characteristics such total riparian vegetation cover, cover structure, cover quality, and channel changes like anthropogenic landscape interventions. It also considers variations in the river's geomorphology from its headwaters to its lower stages. All these sub-indices are originally scored with one of four values (0, 5, 10 or 25), and according to the scheme, intermediate values cannot be assigned into this. The final QBR score is then obtained by summing up of these four sub-indices. It is classified into five habitat quality classes with corresponding specified colours (Munne et al. 2003), as shown in table 7.7. This field-based visual assessment approach, which may be finished in 10 minutes depending on the observer's experience, is used to measure these disparities in an easy, quantifiable manner. However, it is impossible to completely prevent any biasness in observer's decision that was evident in the field survey. The precise field survey methodology—including the sampling

strategy, the number of observations, and the locals' perceptions on the quality of the riparian vegetation—will be covered in the following chapter (Chapter 8).

Table 7.7 *Classes of habitat quality and associated scores for the QBR index (Munne et al. 2003)*

Riparian Habitat Class	QBR Score	Colour
Riparian habitat in natural condition, excellent quality	≥95	Blue
Some disturbance, good quality	75-90	Green
Disturbance important, fair quality	55-70	Yellow
Strong alteration, poor quality	30-50	Orange
Extreme degradation, very poor quality	≤25	Red

- **Normalized Difference Vegetation Index (NDVI)**

The normalised difference vegetation index (NDVI), which has been proven to be the best vegetation index for evaluating vegetation density in numerous studies, was used to estimate and map the density of riparian forests throughout the entire study region (Barakat et al. 2018). For this purpose, high resolution satellite images have been used for this, and the plant cover and resilience of the examined region have been calculated (Mohamed 2016) as follows:

$$NDVI = \frac{NIR-RED}{NIR+RED} \quad (7.7)$$

Where, NIR stands for near-infrared reflectance (0.85-0.88 m) and RED for red reflectance (0.64-0.67 m). The value of the NDVI ranges from -1 to +1, with greater NDVI values being associated with dense vegetation where the lower values of NDVI is typically associated with no vegetation cover such as bare rocks, and infrastructural entities (Gupta et al. 2021).

7.2.3. Results & Discussion

- **Riparian Strip Quality Assessment**

In order to demonstrate the changing nature of the riparian vegetation quality throughout a selected floodplain zone of the Mayurakshi River, the RSQI has been separately assessed for two different time periods (1989 & 2021). A reach-wise (total of 23 reaches) calculation of the riparian strip quality index has been completed and is shown in figure 7.22 using two separately categorised LULC maps (LULC 1989 & 2021, Fig. 7.21) for the riparian strip width of 100 metres from the bank line of the main river.

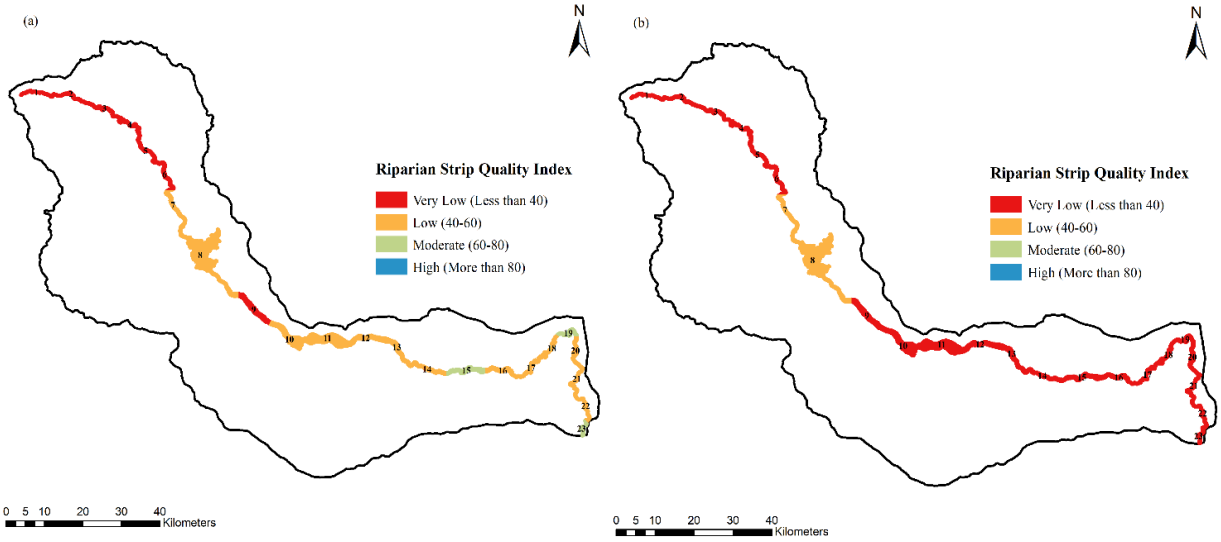

Figure 7.22 *Riparian Strip Quality Index of the Mayurakshi River's Riparian Zone (a) 1989 (b) 2021*

According to the equivalent figure of RSQI for 1989, none of the 23 sites went into the high RSQI category, with just 30% of them falling into the very low category, 57% falling into the low category, and 13% showing moderate conditions. However, the RSQI map for the year 2021 demonstrate that the reaches of the downstream part, which were previously classified (RSQI 1989) under low to moderate quality of riparian zone, have now been transformed into the very low category of riparian strip quality. Only 2% of the studied reach showed low riparian strip quality over the region. This 2% of the region is restricted to the Massanjore Dam's highlands and plateau areas, where land is unsuited for any kind of construction activity and, as a result, no further loss in riparian forest has been noted. However, the other part of the studied corridor experienced a noticeable change in the quality of riparian vegetation during the past 32 years. It has mostly been observed in the downstream region, where the riparian zone has been primarily destroyed for the expansion of new settlements and agricultural land. Such findings are precisely consistent with the findings given by Fierro et al. (2017) and

Woodward et al. (2018) that conversion of riparian forest to agricultural land is the primary factor contributing to the decline of the riparian environment.

- **Assessment of Riparian Vegetation Quality**

In this study, the QBR assessment has been used to validate the results of the high resolution satellite imagery-driven riparian quality assessment. This index has gained a lot of popularity due to its field-based applicability and has been adopted by many researchers for their own study areas (Colwell and Hix 2008; Sirombra and Mesa 2012; Castro-Lopez et al. 2019). This simple field-based visual assessment technique assigns scores to the state of the plant cover near to the channel by combining the biological and geomorphic characteristics of the riparian zone (Saha et al. 2020).

The final QBR score has been gathered for the 23 sites of the studied riparian corridor (100 metre width), incorporating every significant aspect of QBR (Total riparian cover, cover structure, cover quality, and channel alteration components), conducting a questionnaire survey and estimating all scores combined. The results demonstrate that the QBR's final value ranges from 10 (Sundarpur; reach 15) to 90 (Baidyapur; reach 22), with a mean value of 36 (Table 7.8 and Fig. 7.23). In accordance with Munne et al.'s (2003) methodology, a spatial map of the QBR index was created based on the site score, which was then divided into several habitat quality classes denoted by different colours. According to the results, 44% of the sites were classified as "very poor quality," 39% as "poor quality," 13% as "fair riparian quality," and only 1%, or Baidyapur (Downstream), has been designated as "good riparian quality," which refers to as having little to no disturbance in the riparian zone. Surprisingly none of the sites fell into the good riparian quality (QBR score 95) group, indicating that there had been minimal to significant degradation observed at every riparian zone location River Mayurakshi

Table 7.8 *Details of the Riparian Quality of the Studied Sites of Mayurakshi River Based on QBR Values*

Reach No	Site Name	TRC Score	CS Score	CQ Score	CA Score	Final QBR Score	QBR Category	Disturbances	Remarks
1	Dalihari	0	0	25	25	50	Poor	Agricultural land	Moderate riparian vegetation cover
2	Doria	0	0	5	10	15	Very poor	Extensive agricultural activity besides the active channel	Scanty vegetation cover over banks, no flow condition on the river
3	Aswari	0	10	10	25	45	Poor	Presence of large floating vegetation, agricultural activity besides the active channel	Sparse vegetation mainly covered by hassocks, almost no flow condition
4	Amarpur	5	10	10	25	50	Poor	Unscientific water withdrawal activity from the river bed, agricultural activity	Scanty vegetation cover, completely dried river bed with huge sand deposition
5	Darwechak	0	0	5	5	10	Very poor	Human habitation, agricultural activity beside the active channel	Poor riparian vegetation cover completely dried river bed with huge sand deposition
6	Bijaypur	5	10	10	0	25	Very poor	Flow affected by ongoing sand mining activity	Sparse vegetation cover, presence of settlement within the riparian zone
7	Sakrigali	0	5	0	5	10	Very poor	Presence rock and boulders within the active channel	Scanty riparian cover on both side of the river bank, agricultural activity on the river terrace
8	Beniagram	0	0	5	5	10	Very poor	Channelized river, flow mainly restricted by the presence of large floating vegetation	Extensive agricultural activity on both side of the river bank, very poor vegetation cover
9	Kenduli	0	5	0	10	15	Very poor	Sand heap formation within the active river bed, extensive agricultural activity	Very poor vegetation cover, riparian vegetation removed from the bank for growing agriculture
10	Tilpara	5	5	10	10	30	Poor	Bridge and barrage	Discontinuous flow, agricultural activity, moderate riparian vegetation cover
11	Kultore	0	10	5	5	20	Very poor	Discontinuous flow condition on both the channel by the presence of hassocks, over bank deposition during flood	Scanty vegetation cover, extensive agricultural pressure on the both side of the river bank, river bank often affected by flash floods
12	Balsunda	10	10	10	5	35	Poor	Channelized flow, river crossings, bridge	Moderate riparian cover, huge population pressure, evidences of pollution from garbage dumping on the active channel

Reach No	Site Name	TRC Score	CS Score	CQ Score	CA Score	Final QBR Score	QBR Category	Disturbances	Remarks
13	Bile	25	10	10	25	70	Fair	Agricultural activities	Good vegetation growth on both side of the riparian belt, sustained flow in the channel
14	Ramnagar	5	5	5	0	15	Very poor	Agricultural activities over the active river bed	Human habitation, vegetation removed from the river bank
15	Sundarpur	0	0	5	5	10	Very poor	Bridge, extensive agricultural activity on the active river bed	Very poor coverage of vegetation, human habitation, sustained flow in the channel, vegetation removed from both the banks
16	Talgram	0	0	5	25	30	Poor	Agricultural activities beside the active channel	Confluence with Bakreswar river, reduced channel depth due to sedimentation, sparse vegetation
17	Angarpur	0	5	5	10	20	Very poor	Extensive agricultural activities on both side of the river bank, mid channel bar	Very sparse vegetation cover, multiple mid channel bars present.
18	Aharinagar	5	10	10	25	50	Poor	Bridge, river crossings, minimal presence of riparian vegetation	Linear rural settlement observed on the riparian belt, agricultural activities
19	Hijal	10	10	25	25	70	Fair	Agricultural land	Good riparian vegetation cover with high root depth, maintained sustainable flow, meandering channel
20	Subhasnagar	5	5	10	25	45	Poor	Large agriculture land cover	Moderate riparian coverage on the left bank of the river, good flow condition
21	Lohadaha	10	20	10	25	65	Fair	Jetty service, agricultural activities	Moderate riparian cover, good flow condition
22	Baidyapur	20	20	25	25	90	Good	Bridge	Good vegetation cover with the native species, maintained sustainable flow, meandering channel
23	Dhandanga	10	10	5	25	50	Poor	Adjacent road networks, locate in a vicinity of Hoogly river	New Babla river junction point, sparse riparian vegetation cover

Note: TRC, CS, CQ and CA refers to Total Riparian Cover, Cover Structure, Cover Quality and Channel Alteration components of the QBR Index.

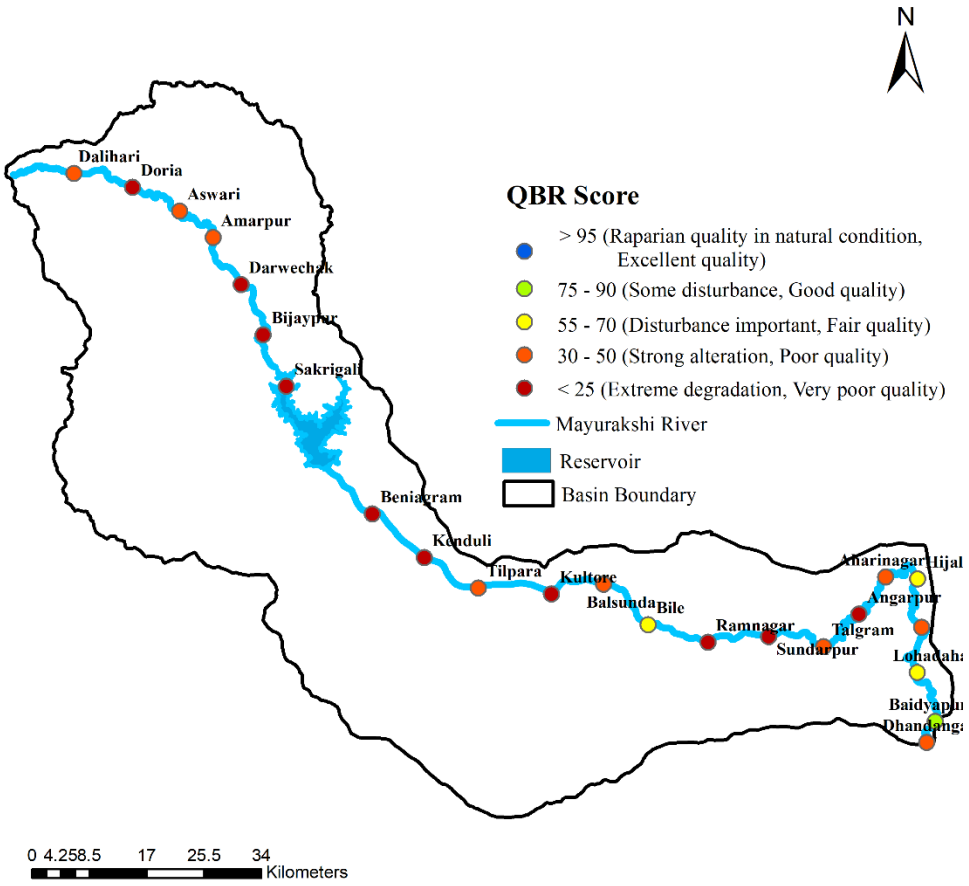

Figure 7.23 *Overall QBR Scores of the studied sites of the Mayurakshi River's Riparian Zone*

Bedrock geology, geomorphological features, soil cover, climatic and hydrological regimes, as well as disturbances by people and other living things, are the main elements influencing the evolution of riparian zones along rivers. These processes take place in various degrees of intensity within and along river reaches, leading to the dominance of a particular geomorphology in the area. Some of the evidences has also observed within the study sites. For example, near Amarpur village, an upper reach portion of the Mayurakshi River (Plate No. 7.1), where river remain almost dry throughout the non-monsoon period, a limited growth of riparian vegetation is found. Similarly the middle reach of the river, mainly near the region of Benigram and Sundarpur village the riparian corridor is severely damaged primarily due to the expansion of settlement and agricultural activity within the riparian area (Plate No. 7.2). Riverine vegetation has a crucial role in reducing nonpoint sources of pollution, managing the temperature of aquatic ecosystems, and maintaining the physico-chemical characteristics of the river. The reduction of riparian forest cover, however, has occurred as a result of the increased demand from human habitation, making it impossible to control pollution from both point and non-point sources (eg. Sainthia village, Plate No. 7.2).

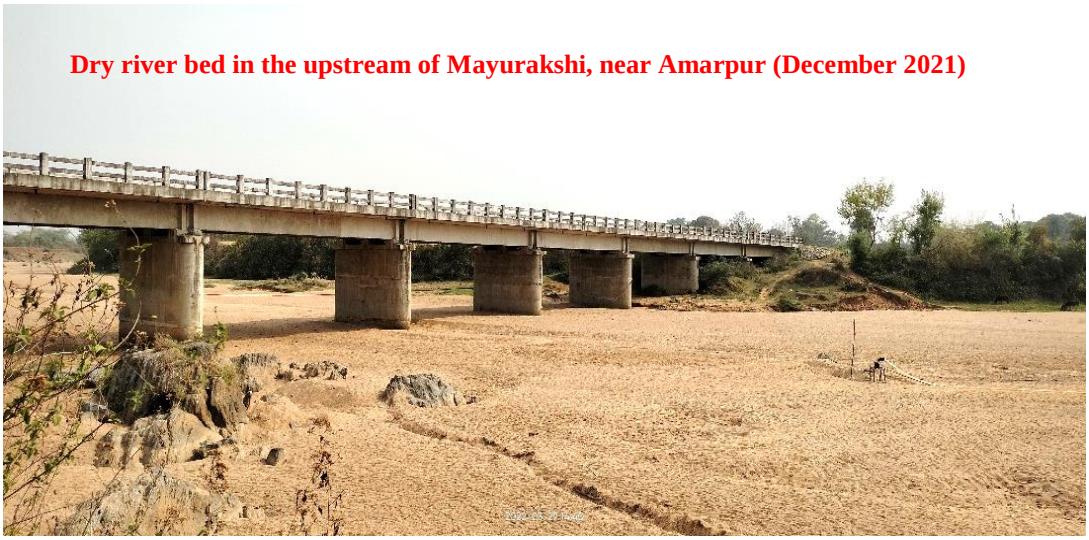

Plate No. 7.1 *Riparian Condition near Upstream of the Mayurakshi River*

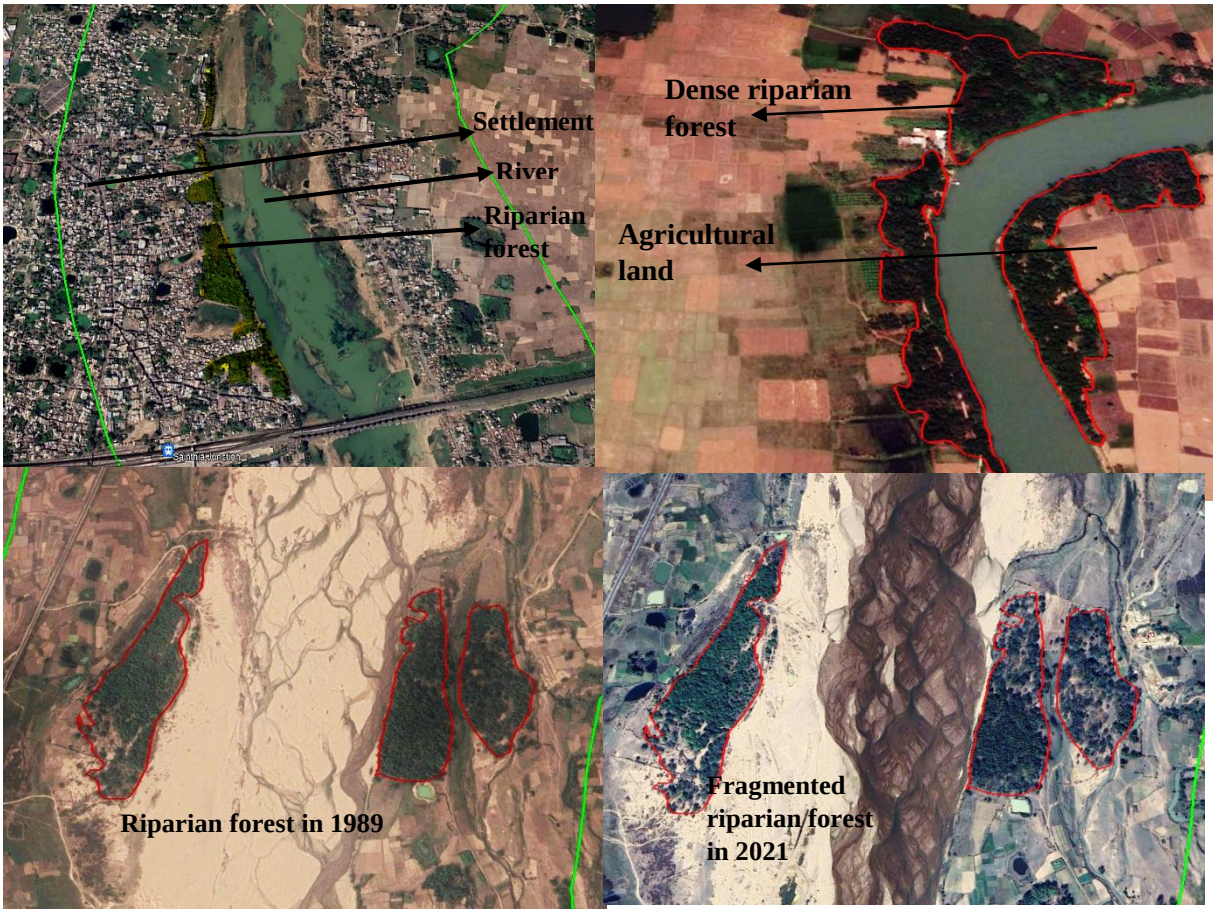

Plate No. 7.2 *Status of Riparian Corridor of the Mayurakshi River*

Nevertheless, a few riparian regions in the Mayurakshi River's lower watershed are still mostly untouched and unspoiled by human activity. For instance, close to the village of Baidyapur,

which is situated close to the point where the Mayurakshi and Bhagirathi rivers converge. The depositional provinces have functioned in this location in a way that the channel produces a meandering course with a constant flow of water, which further promotes the growth of riparian plants in both bank side areas. However, the QBR index of the study area shows that, almost in all cases, the riparian quality has significantly declined since there is little interaction between the river and its surrounding regions. The riparian quality of the Mayurakshi River area has been negatively impacted by riverbed sand mining, agricultural development, and the associated effects of settlement expansion which includes construction of road/bridge building, and residential waste dumps etc. (Plate No. 7.3 and 7.4).

- **Assessment of Normalised Difference Vegetation Index**

A calculation of the NDVI has been done for the years 1989 and 2021 in order to examine the changes in growth and density of the vegetation along the 100 m wide designated riparian zone. In the years 1989 to 2021, the vegetative growth of the riparian zone of the Mayurakshi Rive decreased from 0.74 to 0.41, indicating significant spatial heterogeneity from the upper reach to the lower reach of the study area. This figure 7.24 illustrates the spatiotemporal differences in riparian vegetation robustness. In the year 2021, the lower reach of the basin area is constrained, with the poor value of NDVI denoting low to fragmented vegetative cover along both the bankside of the river. In the year 1989, values higher than 0.15 were taken as indicators of the vegetation vigour, which can be observed throughout the channel.

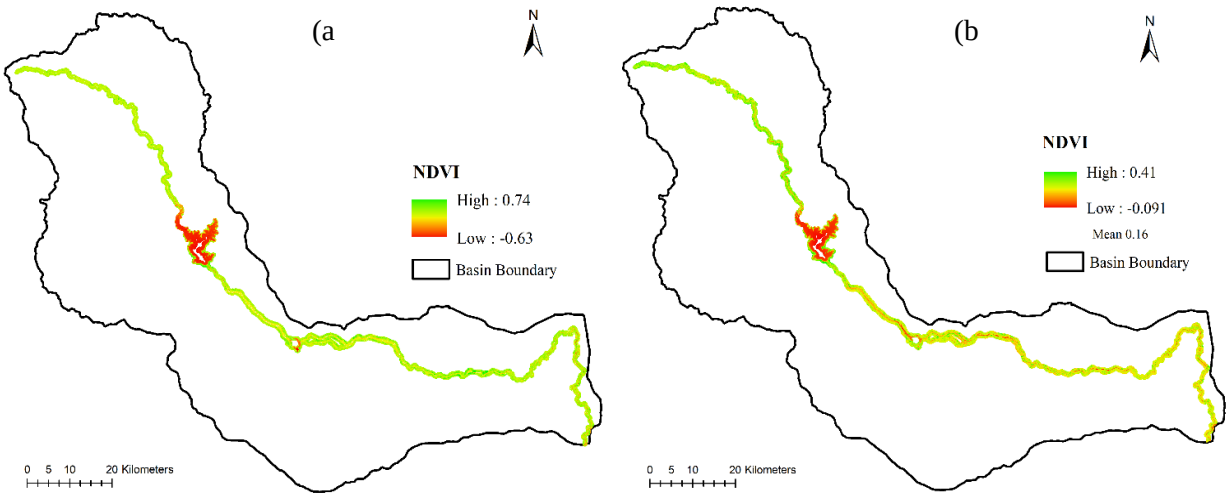

Figure 7.24 *NDVI Scores of the Mayurakshi River's Riparian Zone (a) 1989 (b) 2021*

- **Overall Riparian Health Quality Assessment**

Combining the various ecological criteria (based on field surveys and image analysis) resulted in an overall assessment of the riparian health quality of the riparian tracts along the

Mayurakshi River. This was achieved by separately converting the QBR, RSQI, and NDVI [as measured for the 100 m buffer into a four-point rating system based on their respective site-specific values. The best class for the parameter had a value of 1, while the lowest class had a grade of 4. The five scale classification method of the QBR index (Munne et al. 2003) needs to be slightly modified to generate four scale classes where values >60 are designated as 1, 40-60 are rated as 2, 20-40 are 3, and values less than 20 are denoted as 1. No adjustment is required for the other computed indices (RSQI and NDVI), as they are all already categorised into 4 scale groups of classes. By adding up all of the reclassified classes of each adopted criteria, a final overall riparian health quality score (ORHQS) has been determined. This rating eventually represents the overall condition of the Mayurakshi River's riparian corridor under study. The theoretical range of the ORHQS score for each site is between 4 (the site would be considered to have good quality riparian vegetation) and 16 (which depicts the quality has been mostly degraded in all the parameters). However, the table 7.9 shows that the obtained values of ORHQS has been ranges from 5 observed in Bijaypur (reach 6) to the maximum score of 11 in Kenduli (reach 9) showing that all sites had undergone some disruptions and degradation within their riparian corridor. Additionally, this ORHQS has further been divided into three separate classes, each of which has a different colour code to indicate the degree of overall degradation. These are the groups: Group A is labelled as Fairly Good in green colour (ORHQS < 7), Group B is coded as Partially Degraded in yellow colour (ORHQS 8–10 or higher), and Group C is coded as Mostly Degraded in red colour (ORHQS >10) (Fig. 7.25).

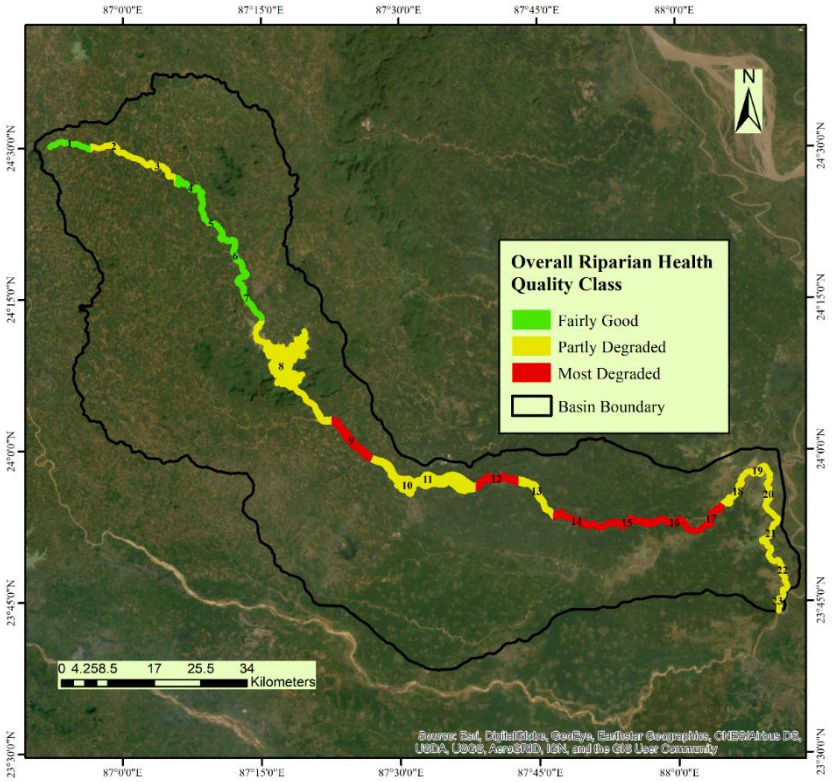

Figure 7.25 *Overall Riparian Health Quality Class of the Mayurakshi River's Riparian Zone*

Table 7.9 *Summary of Site Wise Riparian Quality Assessment of the Mayurakshi River*

Reach No	Site Name	QBR	QBR Rating	RSQI	RSQI Rating	NDVI	NDVI Rating	ORHQS	Riparian Health Quality Class
1	Dalihari	50	2	24.89	4	0.23	1	7	A
2	Doria	15	4	24.36	4	0.21	1	9	B
3	Aswari	45	2	24.99	4	0.20	2	8	B
4	Amarpur	50	2	26.57	3	0.22	1	6	A
5	Darwechak	10	4	31.44	2	0.21	1	7	A
6	Bijaypur	25	3	37.35	1	0.22	1	5	A
7	Sakrigali	10	4	40.53	1	0.22	1	6	A
8	Beniagram	10	4	40.79	1	0.08	4	9	B
9	Kenduli	15	4	24.07	4	0.16	3	11	C
10	Tilpara	30	3	29.94	3	0.16	3	9	B
11	Kultore	20	3	25.83	3	0.16	3	9	B
12	Balsunda	35	3	23.35	4	0.16	3	10	C
13	Bile	70	1	22.46	4	0.15	3	8	B
14	Ramnagar	15	4	22.60	4	0.17	2	10	C
15	Sundarpur	10	4	21.87	4	0.17	2	10	C
16	Talgram	30	3	21.85	4	0.16	3	10	C
17	Angarpur	20	3	22.90	4	0.16	3	10	C
18	Aharinagar	50	2	21.97	4	0.15	3	9	B
19	Hijal	70	1	21.26	4	0.16	3	8	B
20	Subhasnagar	45	2	22.59	4	0.15	3	9	B
21	Lohadaha	65	1	23.49	4	0.16	3	8	B
22	Baidyapur	90	1	24.78	4	0.16	3	8	B
23	Dhandanga	50	2	24.76	4	0.14	3	9	B

Plate No. 7.3 *Degraded Riparian Quality near Mayurakshi River due to Construction of Bridges*

Plate No. 7.4 *(a)Dense riparian cover with a good flow condition (Location: Saraiya, Group A) and (b)Healthy vegetation growth with the presence of annual grasses and helophytes (Location: Sibnagar, Group A) (c) Fragmented vegetation over on the left bank and agricultural activity on the other side of the bank (Location: Bile, Group B) (d) Moderate vegetation cover with an active agricultural activity on the riparian zone (Location: Aharinagar, Group B) (e) Most degraded riparian cover due to huge settlement growth and dumping of wastes directly on the active channel (Location: Sainthia, Group C) (f)Very poor condition of the riparian zone with active human interference, large scale sand mining activity on the river bed (Location: Kultore, Group C)*

The result displays 6 of the river's middle to downstream reaches (Group: C; code: red) show noticeable signs of severe degradation. These reaches are primarily impacted by significant human activities, such as sand mining from the riverbed, clearing forest from the bankside, expanding terrace farming, bank erosion, dumping municipal waste into the main channel, etc. Additionally, the annual flood events have regularly affected the lower sections of the Mayurakshi, which is also a confluence zone of important tributary rivers including the Kushkarini, Kuya, and Dwarka. This has led to the degradation of the river bank and riparian flora. To restore the ecological balance and enhance the amount of green cover in the areas, care must be taken to protect such reaches. The riparian corridor upstream has been found to be in a rather excellent state. Less human influence has been observed in this area as a result of several physiographic and climatic constraints, which has kept the area in quite good stage.

7.2.4. Conclusion

In this study, the riparian vegetation quality for the past (1989) and present scenario (2021) is revealed by the measured ecological indices mentioned above (image-based and field-based), where the present observation has perfectly been paired with each other taking into account the physiography that predominates in the area. The flat floodplain tracts to the gently undulating landscape with relatively fertile soils, which draw more people for expanding settlement and agricultural activities instead of conserving the riparian tract to maintain the ecological sustainability of the area, are where the most degraded reaches are found. The lateritic zone, which encompasses the upper to middle reach reach, is generally less disturbed. Based on the degree of deterioration determined in each analysed part of the river Mayurakshi, such findings can be easily applied for riparian area zonation and the subsequent creation of stream management and restoration plans. Most Degraded (Code C) sites would appear to require the most work in restoring riparian vegetation, whereas Fairly Good (Code A) sites, at the top of the riparian quality scale, would require the least amount and scope of restorative interventions.

The scope of this study can be increased by taking into account how people's aesthetic tastes affect how pleasant and natural a location is (Saha et al. 2020). A larger sample size from a more broad range of backgrounds could lead to more insightful questions on the aesthetics of the riparian zone. The research output has also been improved overall by the study of local geomorphology and more exact morphological and modelling assessments of the channel and floodplain.

7.3. Variations in Ecosystem Service Value in Response to the Changes in Land use Land Cover in Mayurakshi River Basin Area

The ecosystems offer a variety of direct material services, such as the production of food and fresh water, as well as immaterial ones, such as the regulation of the climate, the storage of carbon dioxide, the purification of water, and aesthetic advantages (MEA, 2005). The advantages that individuals receive from natural processes that improve human wellbeing are known as ecosystem services (ESs) (Das and Das 2019a–c; MEA 2003; de Groot et al. 2002). The ESs provide the necessary resources for the organisms while also balancing ecological processes and functions (Sharma et al. 2019a, b). The ecosystems support economic growth by offering a variety of services (Vargas et al. 2019), despite the fact that they have been experiencing unsustainable changes over the past several decades due to the increased demand on natural resources (Steffen et al. 2015; McLaughlin and Mineau 1995). Anthropogenic activities, such as changes in land use and land cover (LU/LC), have caused the ESs to shift. Exploitation of natural resources and its adverse consequences have intensified, posing a risk to the next generation (Xiao et al. 2019; Western 2001). According to the Millennium Ecosystem Assessment (MEA 2005), around 60% of the ESs have already been lost or seriously damaged, which has a negative impact on the ecosystem and its constituent parts. As a result, the dynamics of land use and cover have emerged as the key factors that profoundly affect ecosystem services.

Over time, there have been significant changes in the loss of various environmental resources due to the rising demand for urban land and the concentration of urban people in urban areas. According to He, Zhang, Huang, and Zhao (2016), urban growth is nothing more than the LULC transformation process that changes the natural land cover to built-up urban. The process of urban expansion has a significant impact on several types of ecosystems that exist on the surface of the earth, including forest cover, crop land, and water bodies that offer ecosystem services. In fact, the conversion of natural or semi-natural land covers into impermeable land surface (ILS) alters the biogeochemical cycles and circulation pattern, which in turn impacts ecosystem function and results in the loss of ecosystem services (ESs) (Lawler et al. 2014). Similar circumstances have also been noted in the Indian context. Rahman et al. (2012) claim that the rapid population growth causes the creation of new settlements and urban growth, which causes LU/LC alteration. According to Das and Das (2019), the primary factor

contributing to the loss of ecosystem service value (ESV) in India's Gangetic plain is urbanisation, which accelerated the widespread change of the LU/LC.

The influence of spatiotemporal changes in land use and cover on ecosystem services became the primary objective of this study. However, researchers used a variety of methods, including the cost-based method, the InVEST model, the value/benefit transfer method (VTM), and the energy analysis model, (Zhan et al. 2019; Yang et al. 2018; Plummer 2009), to quantify ecosystem services and their values in response to land use dynamics. The most innovative and successful method for estimating the worldwide ESV in comparison to the average ESV of the USA was created by Costanza et al. (1997) and (2014) which was based on a combination of value transfers and cost-based techniques. In order to estimate total ecosystem service values (ESV_S) and individual ecosystem service functions (ESV_f) change, this work used Remote Sensing data and GIS techniques in accordance with the global Value Coefficient (VC) as given by Costanza et al. (1997 & 2014) for four time periods (1989, 2000, 2010, 2018 and 2021). To estimate the predicted ecosystem service values and ecosystem functions for the study region, the land use data for the projected years (2031, 2041, and 2051) as prepared using the CA-Markov model (described in earlier chapter) have also been included.

7.3.1. Materials

To classify land use and land cover (LULC), this study used cloud-free multi-temporal Landsat 5TM (Thematic Mapper-path/row 139/43 & 139/44; with spatial resolution 30 m) data for 1989 and 2000, Landsat 7ETM+ for 2010 and Landsat 8 OLI data for 2018 & 2021 obtained from the USGS (United Nation Geological Survey) (Table 7.10). The obtained Landsat data are pre-georeferenced using the WGS 84 (World Geodetic System) datum and the UTM (Universal Transverse Mercator) coordinate system. In this work, the supervised maximum likelihood approach is used with ERDAS Imagine 9.2 software for both the categorization of land use and land cover (LULC) and the identification of relevant biomes (Table 7.11).

Table 7.10 *Details of the Satellite Data Used in this Study*

Satellite	Sensor	Path and Row	Date of acquisition	Spatial resolution	Source
Landsat 5	TM	139/43 & 139/44	04/12/1989	30m	USGS Earth Resources Observation Systems
Landsat 5	TM		31/10/2000		
Landsat 7	ETM+		04/11/2010		
Landsat 8	OLI		18/11/2018		
Landsat 8	OLI		02/11/2021		

TM: Thematic Mapper, ETM+: Enhanced Thematic Mapper, OLI: Operational Land Imager, USGS: United States Geological survey

Table 7.11 *Details of the LULC Classes along with Description of Ecosystem Service Coefficient as per Costanza et al. (1997, 2014)*

LULC type	Description	Equivalent biome (Costanza et al. 1997)	Ecosystem service Coefficient (US $ ha−1 yr−1)	
			Costanza et al. 1997	Costanza et al. 2014
River/ water bodies	Area with open water including river, lakes and ponds	Lakes/Rivers	8,498	12,512
Reservoirs	Area with open water including river, lakes and ponds	Lakes/Rivers	8,498	12,512
Bar/ Bare land	Area with total absence of vegetation	Barren land	0	0
Dense forest	Area covered with natural vegetation	Forest	969	3,800
Laterite exposer	Areas with sparse/scanty vegetation with exposed rocks	Rock	0	0
Agricultural land	The area specially used for the production of agricultural crops	Crop land	92	5,597
Cultivable wet/ Wet fallow land	Seasonally flooded area that is a mix of grass/shrub/trees/bare ground	Floodplains	19,580	25,681
Agricultural fallow/ Pasture land	Places covered with small trees and dry bushes combined with grasses	Range land	232	4,166
Waste land	Areas of rock or soil with very sparse to no vegetation for the entire year, not suitable for crop production	Barren land	0	0
Settlement	Land predominantly covered with houses including rural and urban communities	Urban	0	6,661
Homestead with plantation	Rural or urban communities with social forestry	Urban	0	6,661

7.3.2. Methodology

- **Land Use Land Cover Classification and Accuracy Assessment**

In this work, a supervised classification with maximum likelihood method has been executed for the classification of each satellite imageries using ERDAS Imagine 9.2 software. All the images were classified separately and total 11 classes were identified namely dense forest, lateritic exposer, river/water bodies, reservoirs, sand bar, agricultural land, wet fallow land, dry fallow land, waste land, settlement, and homestead with plantation (Table 7.11). After image classification, all the classified imageries are then exported into Arc GIS software for further analysis required for this study. The variations between the two images of the same area have been examined using the change detection approach. It has been used to distinguish between variations in changes that took place in various land-use classes. Furthermore, the authors have used historical land use data to anticipate future land use patterns and create forecasts for the years 2031, 2041, and 2051. In this study, the Land Change Model (LCM) module of TerrSet 18.31, designed by Clark Lab, was employed for the prediction of future LULC of the Mayurakshi River basin area. This model uses multi-layer perceptron neural network approach (MLPNN) which considers the historical alterations in LULC with spatial explanatory variables for the evaluation of future trend of LULC over a region.

Validating the satellite imageries that have been digitally categorised requires accuracy assessment. In this study, a nonparametric Kappa statistical analysis (k) has been done, which calculates the overall classification accuracy (OCA), producer's accuracy (PA), user's accuracy (UA), and generates the kappa coefficient index (k). Here, the overall classification accuracy has been assessed for the all studied land use land cover maps using the following formula (Cohen 1960):

$$k = \frac{P_o - P_e}{1 - P_e} \tag{7.8}$$

where, P_o=relative observed agreement, P_e= hypothetical probability of chance agreement. A classification accuracy rating of greater than 70% can be considered satisfactory, while a kappa value of one (1) indicates perfect agreement and a value of zero (0) indicates no agreement. The majority of applications can tolerate kappa values greater than 0.75 as indicating an

excellent or very good agreement. After accuracy evaluation and correction, the class specific area of each image has been determined within a remotely sensed environment.

- **Estimation of Ecosystem Service Value (ESV)**

In this study, each of the eleven land-use types of Mayurakshi River basin area has been compared to the various biomes as described by Costanza et al. (1997). He calculated the Global VC (value coefficient) for 16 types of ecosystems and 17 types of service function throughout the world to measure the state of ecosystem services. Additionally, Costanza et al. (2014) developed a better method for estimating global ESVs, increasing the ESV of some land use classes while maintaining the ESV of others. For example, ESV of the forest ecosystem, for instance, grew from 969 dollars per hectare per year in 1997 to 3800 dollars per hectare per year in 2014. In this study, the ESV for each land-use class has been estimated using the frameworks developed by Costanza et al. in 1997 and 2014, respectively. The land use categories of the study area have been portrayed by the most representative biomes, as seen in table 7.12. Finally, in order to calculate the overall ecosystem service value (ESV_S) and the specific ecosystem service function (ESV_f), the following equations are used:

$$ESV_t = \sum A_k * VC_k \tag{7.9}$$

$$V_k = \sum_{i=1}^{n} ESV_{ki} \tag{7.10}$$

Where, ESV_t stands for overall ecosystem service value and A_k for the area of LULC type k region, VC_k for the ecosystem service value (US$ ha/year) for LULC type k, and ESV_{ki} for an individual category of ESV for LULC type k.

$$ESV_f = \sum A_k * VC_{kf} \tag{7.11}$$

Here, ESV_f refers to the individual ecosystem service function and VC_{kf} is the value of co-efficient function (US$ ha/year) for k type of LULC category. By comparing the predicted ESV and ESV_f values for the studied land-use type, it was possible to assess how much the value of ecosystem services had changed over time.

7.3.3. Result and Discussions

- **Land Use Land Cover Dynamics**

The classification findings of the land-use changes in the Mayurakshi River basin area of 1989 to 2021 and of 2031 to 2051 are displayed in Table 7.12 and 7.13 (Figures are in the previous chapter 6). Since 1989 to 2021, the LULC shift in the studied terrain demonstrates that the areal coverage of each land use/land cover has changed significantly. Agricultural land, settlement, and homestead with plantation remained the dominating cover categories in the research area over a 32-year period. Settlement and agricultural land areas quickly grew during the whole study period, from 5286 ha to 28396 ha and 91483 ha to 299241 ha, respectively. The decline of dense forest, waste land, and agricultural fallow land—from 97149 ha to 38263 ha (dense forest), 31333 ha to 10914 ha (waste land), and 173618 ha to 26438 ha (agricultural fallow land), respectively—is the main factor contributing to the rapid expansion of agriculture and settlement areas.

Similar kind of assessment have also been made from the CA-Markov model predicted LULC for the respective years of 2031, 2041 and 2051 and is shown in table 7.13. The simulated LULC maps (Figures are in previous chapter 6) show how further settlement growth will reduce the amount of arable land, natural forest cover, and river/water bodies. It shows every classes were equally contributed to the conversion into the settlement that has been increased from 47878 ha to 56138 ha from 2021 to 2051. However, between the time span of 2021 to 2051, land under river or water, agricultural land and natural vegetation is expected to reduce rapidly from 9780 ha to 7090 ha, 422780 ha to 289882 ha and 55421 ha to 26032 ha respectively. These alterations in the future pattern of LULC are maybe the response of ongoing and proposed development of this region in the various sectors like industrial, infrastructure, transportation, etc.

Table 7.12 *Areal Extent and the Rate of Change of the Classified LULC Types in the Study Landscape (1989–2021)*

LULC classes	**Area Coverage (Ha)**					**Rate of Change (%)**				
	1989	**2000**	**2010**	**2018**	**2021**	**(1989-2000)**	**(2000-2010)**	**(2010-2018)**	**(2018-2021)**	**(1989-2021)**
River/ water bodies	8533	8852	8847	8488	8234	3.74	-0.06	-4.06	-2.99	-3.50
Reservoirs	4853	3648	2977	2386	1758	-24.83	-18.39	-19.85	-26.32	-63.77
Bar	2254	4367	1003	405	307	93.74	-77.03	-59.62	-24.20	-86.38
Dense forest	97149	43535	44037	37282	38263	-55.19	1.15	-15.34	2.63	-60.61
Laterite exposer	4268	1699	1372	10721	18441	-60.19	-19.25	681.41	72.01	332.08
Agricultural land	91483	222083	190963	294709	299241	142.76	-14.01	54.33	1.54	227.10
Cultivable wet land	149881	191976	183976	120363	111305	28.09	-4.17	-34.58	-7.53	-25.74
Agricultural fallow land	173618	89234	52498	27433	26438	-48.60	-41.17	-47.74	-3.63	-84.77
Waste land	31333	9604	40851	18612	10914	-69.35	325.35	-54.44	-41.36	-65.17
Settlement	5286	6603	21574	23581	28396	24.91	226.73	9.30	20.42	437.19
Homestead with plantation	14221	1278	34780	48899	49581	-91.01	2621.44	40.60	1.39	248.65
TOTAL	**582878**	**582878**	**582878**	**582878**	**582878**					

Table 7.13 *Areal Extent and the Rate of Change of the Simulated LULC Types in the Study Landscape (2031–2051)*

LULC classes	**Area Coverage (Ha)**				**Rate of Change (%)**		
	2021	**2031**	**2041**	**2051**	**(2021-2031)**	**(2031-2041)**	**(2041-2051)**
River/ water bodies	9780	7290	7090	7090	-25.46	-2.74	0.00
Forest	55421	22327	24925	26032	-59.71	11.64	4.44
Wet fallow land	234	194	169	161	-17.09	-12.89	-4.73
Agricultural land	422780	401200	309381	289882	-5.10	-22.89	-6.30
Settlement	47878	52338	54438	56138	9.32	4.01	3.12
Bare land	211	390	401	432	84.83	2.82	7.73
Pasture land	46506	108501	207722	216115	133.31	91.45	4.04
TOTAL	**582878**	**582878**	**582878**	**582878**			

- **Estimation of Ecosystem Service Value (ESV)**

In this work, the global coefficient values of Costanza et al. 1997 and 2014 were used to estimate the total value of ecosystem services given by the various land use and land cover types for the years 1989, 2000, 2010, 2018, and 2021 (Fig. 7.26 and 7.27). According to Costanza et al. (1997 and 2014) (Table 7.14), the total value of ESV in 1989 was US$ 3191.26 million and US$ 5751 million, with the largest contributions coming from cultivable wet land at US$ 2934.67 million and US$ 3849.10 million (coefficient of 1997 & 2014, respectively). According to the coefficient of 1997 during the period of 1989, agricultural land and dense forests contributed US$ 94.14 million and US$ 8.42 million, respectively, while the coefficient of 2014 assessed these contributions to be US$ 369.17 million and US$ 512.03 million (Table 7.14).The built-up area, fallow land, and sand bar are all regarded as barren land biomes by Costanza et al. (1997) because they don't supply any ecological services. As a result, we decided to value these qualities at zero for our study region. However, in 2014, Costanza and his team modified the coefficient and created a new coefficient value for just the built-up area, leaving the value for the sand bar and fallow land unchanged. As a result, the built-up area in our research region greatly contributed (1989–2021), producing US$ 561.11 million ESV according to the 2014 coefficient.

Table 7.14 *Total Estimated Ecosystem Service Values (ESVs) for Classified LULC Types (1989-2021) Based on Co-efficient of Costanza et al. (1997 & 2014)*

LULC classes		**ESV (US$ million/ha/yr)**					
		1989	**2000**	**2010**	**2018**	**2021**	**TOTAL**
River/ water bodies	1997	72.51	75.23	75.18	72.13	69.97	365.02
	2014	106.76	110.76	110.69	106.20	103.02	537.43
Reservoirs	1997	41.24	31.00	25.30	20.28	14.94	132.76
	2014	60.72	45.64	37.25	29.86	22.00	195.47
Bar	1997	0.00	0.00	0.00	0.00	0.00	0
	2014	0.00	0.00	0.00	0.00	0.00	0
Dense forest	1997	94.14	42.19	42.67	36.13	37.08	252.21
	2014	369.17	165.43	167.34	141.67	145.40	989.01
Laterite exposer	1997	0.00	0.00	0.00	0.00	0.00	0
	2014	0.00	0.00	0.00	0.00	0.00	0
Agricultural land	1997	8.42	20.43	17.57	27.11	27.53	101.06
	2014	512.03	1243.00	1068.82	1649.49	1674.85	6148.19
Cultivable wet land	1997	2934.67	3758.88	3602.25	2356.71	2179.35	14831.86
	2014	3849.10	4930.13	4724.68	3091.04	2858.42	19453.37
Agricultural fallow land	1997	40.28	20.70	12.18	6.36	6.13	85.65
	2014	723.29	371.75	218.71	114.29	110.14	1538.18
Waste land	1997	0.00	0.00	0.00	0.00	0.00	0
	2014	0.00	0.00	0.00	0.00	0.00	0
Settlement	1997	0.00	0.00	0.00	0.00	0.00	0
	2014	35.21	43.98	143.70	157.07	189.15	569.11
Homestead with plantation	1997	0.00	0.00	0.00	0.00	0.00	0
	2014	94.73	8.51	231.67	325.72	330.26	990.89
TOTAL	**1997**	**3191.26**	**3948.43**	**3775.14**	**2518.72**	**2335.00**	
	2014	**5751.00**	**6919.20**	**6702.86**	**5615.33**	**5433.24**	

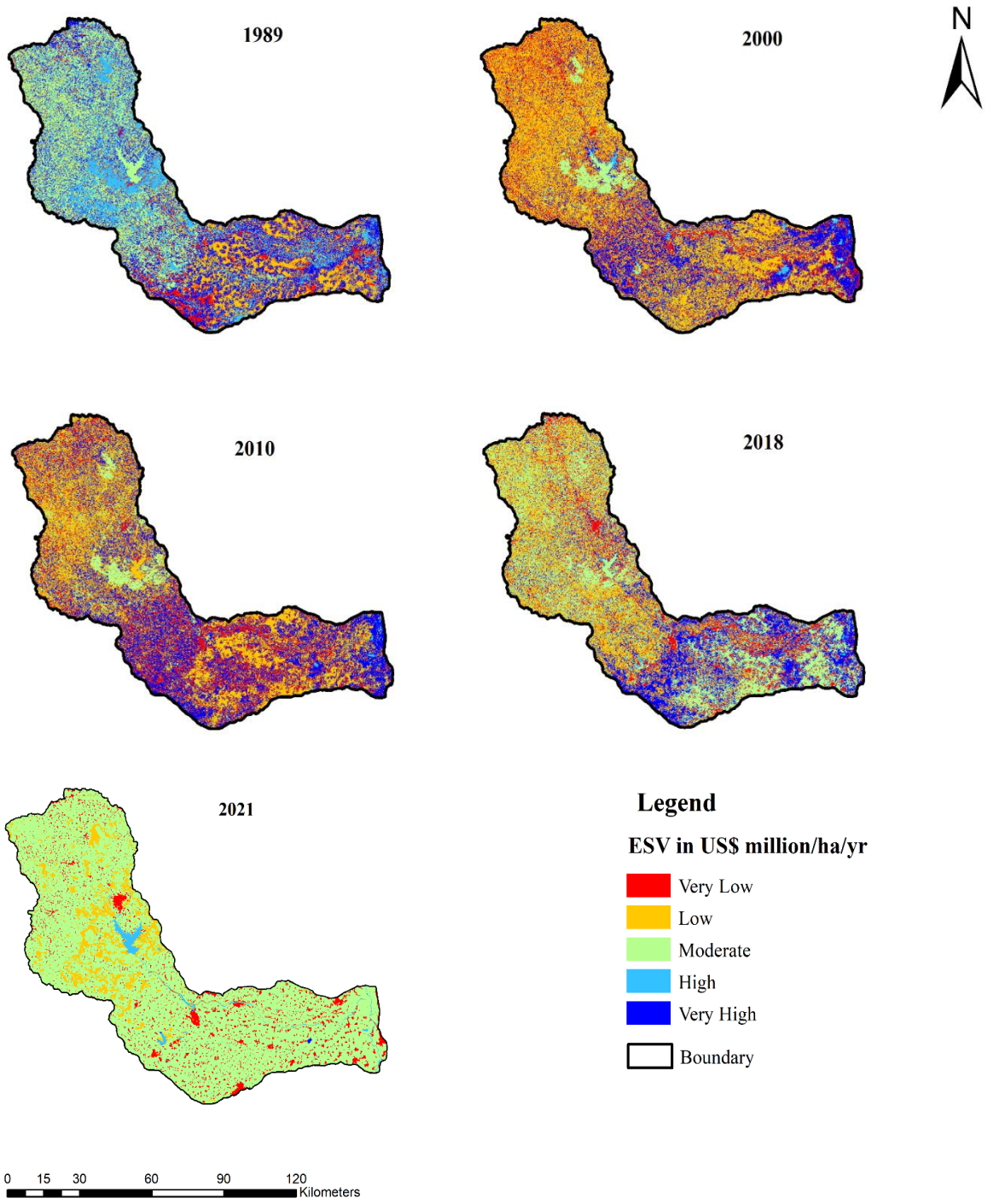

Figure 7.26 *Spatio-temporal Variations of the ESV based on Costanza et al. (1997)*

Based on the 1997 and 2014 co-efficient, the total value of ESs increased somewhat in 2000, reaching US$ 3948.43 million and US$ 6919.20 million, respectively. The area of river/water bodies and agricultural land has increased greatly as a result of the devastating flood in 2000, whereas the area of dense woodland and dry fallow ground has decreased significantly. The increase in the study area's ecosystem service value can be attributed to such beneficial changes

in land use patterns. However, a considerable decrease in the total ecosystem service value has been noticed in the following years from 2010, 2018 and 2021. Based on the co-efficient value of 1997 and 2014, the contribution of cultivable wet fallow land remain high for the year of 2010 (US$ 3602.25 million & US$ 4724.68 million), 2018 (US$ 2356.71 million & US$ 3091.04 million) and 2021 (US$ 2179.35 million & US$ 2858.42 million) (Table 7.14).

Future observations are anticipated to show a continuation of this ESV drop (Table 7.15). The estimated ESV for the predicted years (2031 to 2051) shows that the total ESV has changed from US$ 149.47 million to US$ 165.44 million based on the co-efficient value of 1997, while using the co-efficient value of 2014, a decreasing trend has been seen in the total ESV from US$ 3227.20 million in the 2031 year to US$ 3088.51 million in the 2051 year. Such loss of ecosystem services and deterioration of natural land cover in the study landscape has been brought on by the ongoing expansion of populated areas and agricultural land.

Table 7.15 *Total Estimated Ecosystem Service Values (ESVs) for Simulated LULC Types (2031-2051) Based on Co-efficient of Costanza et al. (1997 & 2014)*

LULC classes		**ESV (US$ million/ha/yr)**				
		2021	**2031**	**2041**	**2051**	**TOTAL**
River/ water bodies	1997	83.11	61.95	60.25	60.25	267.56
	2014	122.37	91.21	88.71	88.71	391
Forest	1997	53.70	21.63	24.15	25.22	124.7
	2014	210.60	84.84	94.72	98.92	489.08
Wet fallow land	1997	4.58	3.80	3.31	3.15	14.84
	2014	6.01	4.99	4.34	4.13	19.47
Agricultural land	1997	38.90	36.91	28.46	26.67	130.94
	2014	2366.30	2245.52	1731.61	1622.47	7965.9
Settlement	1997	0.00	0.00	0.00	0.00	0
	2014	318.92	348.62	362.61	373.94	1404.09
Bare land	1997	0.00	0.00	0.00	0.00	0
	2014	0.00	0.00	0.00	0.00	0
Pasture land	1997	10.79	25.17	48.19	50.14	134.29
	2014	193.74	452.02	865.37	900.34	2411.47
TOTAL	**1997**	**191.08**	**149.47**	**164.37**	**165.44**	
	2014	**3217.94**	**3227.20**	**3147.35**	**3088.51**	

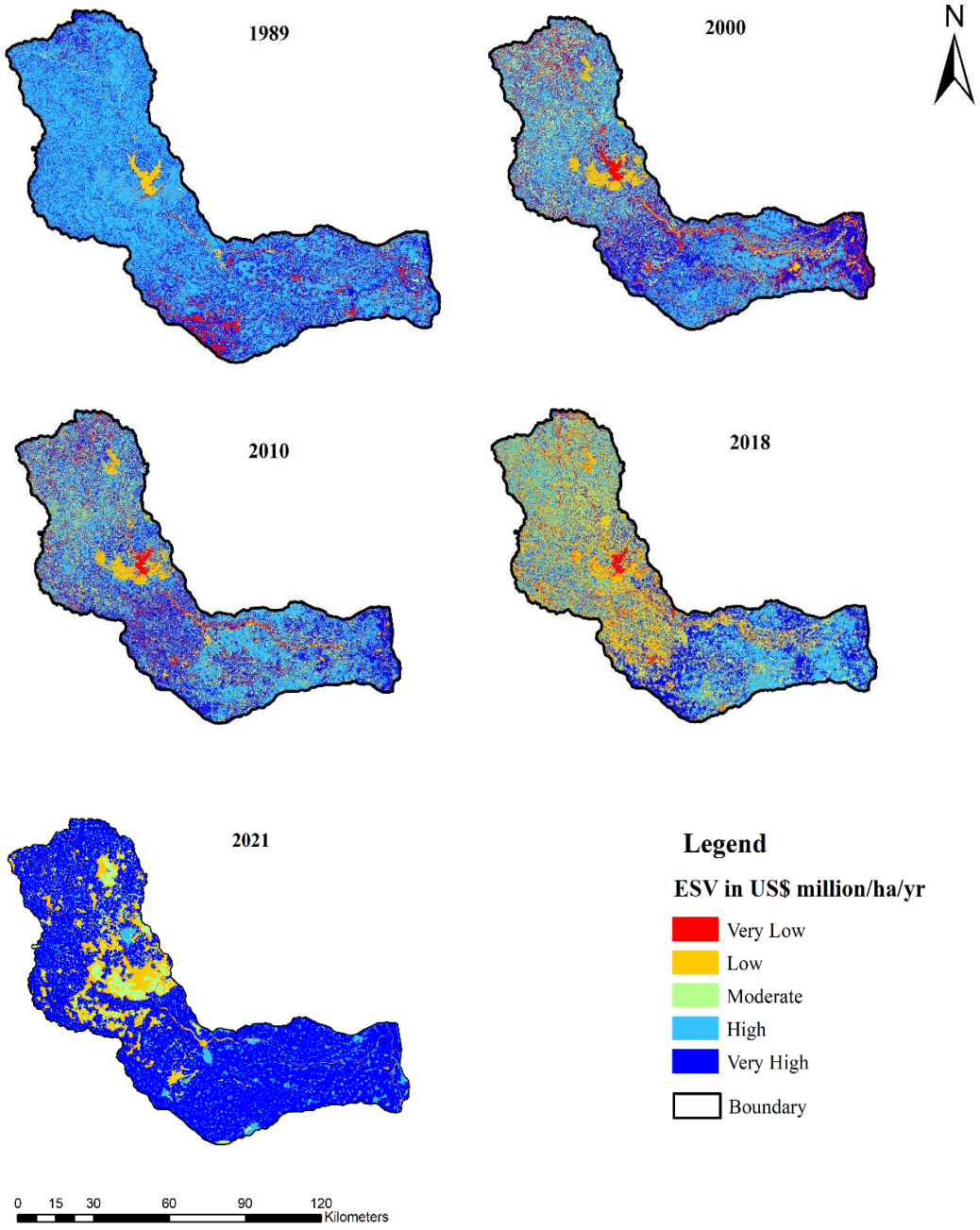

Figure 7.27 *Spatio-temporal Variations of the ESV based on Costanza et al. (2014)*

- **Rate of Change in Total ESV**

Based on Costanza et al. (1997 & 2014), we computed the net change in the ESV (in percentage) from 1989 to 2021 (the observed period) and 2021 to 2051 (the predicted period) (Fig. 7.28a and b). As per the co-efficient value of Costanza et al. (1997), it has been estimated that in the periods 1989-2000, 2000-2010, 2010-2018, 2018-2021, 2021-2031, 2031-2041 and 2041-2051, the net change in the total ESV was/would be 23.73%, -4.39%, -33.28%, -7.29%, -21.78%, 9.97% and 0.65%, respectively (Table 7.16). The net change in the total ESV was/will be 20.31%, -3.13%, -16.22%, -3.24%, 0.29%, -2.47%, and -1.87%, respectively, for the same decadal periods, according to the coefficient values from Costanza et al. (2014).

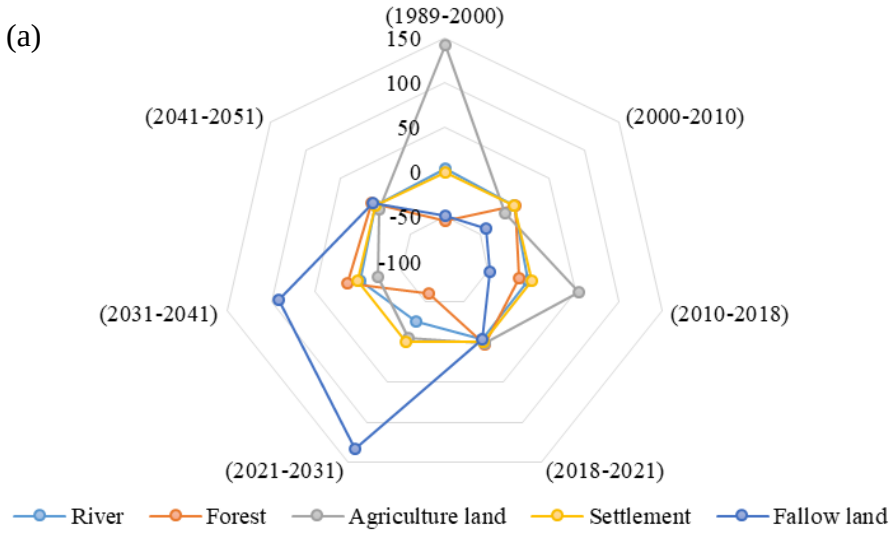

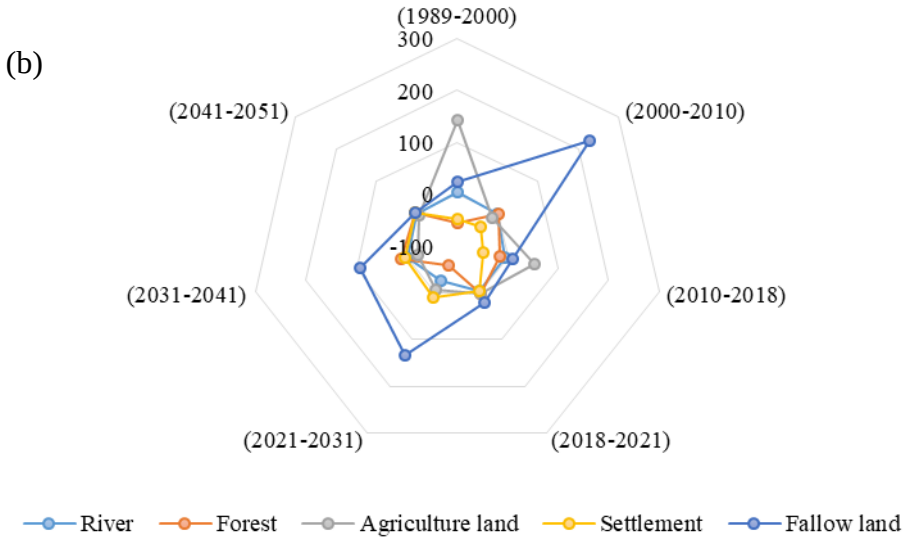

Figure 7.28 *Net change rates of ecosystem services for each LULC classes based on (a) Costanza et al. (1997) and (b) Costanza et al. (2014)*

Table 7.16 *Rate of Change in Total ESV in the Study Landscape*

	Rate of change (%)						
Decadal periods	**(1989-2000)**	**(2000-2010)**	**(2010-2018)**	**(2018-2021)**	**(2021-2031)**	**(2031-2041)**	**(2041-2051)**
Costanza et al. (1997)	23.73	-4.39	-33.28	-7.29	-21.78	9.97	0.65
Costanza et al. (2014)	20.31	-3.13	-16.22	-3.24	0.29	-2.47	-1.87

Table 7.17 *Ecosystem Service Classification (Costanza et al. 1997)*

Ecosystem Services	**Description**
Provisioning	Physical and other resources extracted from ecosystem to support a diversity of human needs, such as food, fibre and natural medicines
Regulating	Regulatory processes within ecosystems maintaining balance, such as pollination, water purification and climate moderation
Supporting	Processes within ecosystems that maintain overall functioning and resilience, such as soil formation, photosynthetic production of oxygen and habitat for wildlife
Cultural	Aspects of ecosystem providing non-material benefits enriching society, such as those supporting tourism, recreation and spiritual interests

- **Estimation of Ecosystem Service Function (ESV_f)**

The contribution of individual ecosystem service functions (ESV_f) have also been estimated for the study period separately (Table 7.17) (Fig. 7.29). The contribution of each ecosystem service value (ESVs) varied during the study period. In the study landscape regulating services contributed highest ecosystem services (more than 80% in almost every year; except 2031) followed by cultural services (11.19% in 2000 and 11.05% in 2021), supporting (4.07% in 1989), provisioning (1.55% in 2021) respectively.

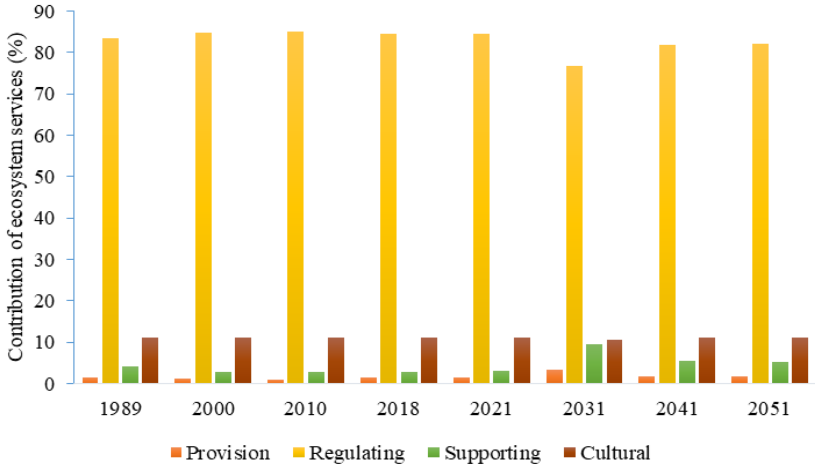

Figure 7.29 *Temporal Variation in the Contribution of Ecosystem Services in the Study Area*

7.3.4. Conclusion

In the study region, rapid and significant LULC changes have occurred over the past 30 years, primarily as a result of planned and unplanned growth of built-up areas to accommodate the high demand for houses, offices, and commercial space. Additionally, the increase of built-up areas has caused changes in the local ESVs, which has led to a decline in the local wetland ecology.

The Millennium Ecosystem Assessment (MEA) report revealed that compared to other periods, human activities had caused more rapid and extensive changes in ecosystems over the previous 50 years. This was primarily because of the rapidly increasing demands of humans for food, fresh water, timer, fibre, and fuel, among other things. The diversity of life on earth has suffered a significant and largely irreversible loss as a result. Changes in socioeconomic traits, land use, biodiversity, atmospheric composition, and climate will affect ecosystems' ability to continue providing these services in the future (Metzger et al. 2006). Land use conversions were found to be the one of these elements that has the biggest impact on ecosystem services, human well-being, and the survival of other species (Geneletti 2013). The provision of ecosystem services, biodiversity conservation, and returns to landowners were all found to be significantly impacted by changes in the size and composition of various land use types (Polasky et al. 2011).

7.4. An Assessment of Surface Water Quality Using a Combination of Water Quality and Pollution Indices in Mayurakshi River Basin area

Water in streams, rivers, springs, ponds, lakes, and reservoirs makes up the majority of surface water. Surface water is created when rain falls on watershed areas. It then travels through streams and rivers before occasionally settling in ponds and lakes (Manahan 2010). The majority of the water utilised for household, agricultural, and industrial uses worldwide comes from this source (Khan et al. 2015). Among the aforementioned water bodies, rivers are the main providers of water for irrigation, industry, and human consumption. A people's way of life is determined by the ecological balance that is maintained by the quantity and quality of water. On the other hand, contaminated water is the main cause of sickness and, in addition to degrading the environment, makes the earth unsuited for sustaining life (Francis 1994). Water supply is currently a problem, but so are environmental quality and ecological balance. Surface waters are becoming progressively more seriously polluted as a result of rising industrialisation, urbanisation, and technical advancement in all industries. Surface water quality deteriorates for a variety of reasons, which includes anthropogenic influences, geochemical factors, chemical composition of river basins (Giridharan et al. 2010), and natural processes like interaction of water with lithogenic structure through which the river flows. This makes the water unfit for drinking, industry, agriculture, and other uses (Simeonov et al. 2003; Sánchez et al. 2007). However, according to Carpenter et al. 1998, Barakat et al. 2016, industrial sewage, household wastewater, and agricultural drainage water are the main causes of river contamination. In addition to endangering aquatic life, the deterioration of surface water quality also has an impact on the quality of underground water, which has an impact on human health (Wats et al. 2019). Thus, it becomes essential to regularly assess the physico-chemical and biological parameters of these natural resources to determine their state of health (Venkatesharaju et al. 2010).

Monitoring of water quality often includes evaluation of the physical, chemical, biological, radiological, and aesthetic qualities of the water (Abdul et al. 2010; Ombaka and Gichumbi 2012).Experts all around the world have proposed and accepted a variety of methods and procedures to evaluate the water's quality, but the most successful method is the use of water quality indices (WQIs). WQIs are regarded as trustworthy tools for assessing and balancing water supply and demand. The indicators are crucial for the management of any project for monitoring the aquatic environment. The WQI approach may reduce a sizable amount of data from a multi-variate and multi-parameter into a single digit score to produce the water quality

index result. However, a variety of indicators enables effective management approaches to reduce river pollution as opposed to using a single indicator to determine the current level of water quality (Ali et al. 2021).

Thus, the primary goals of this study are to: (1) evaluate the physico-chemical characteristics of the river water; (2) establish the water quality through WQI analysis; and (4) assess different water pollution indices, such as the Organic Pollution Index (OPI) (Quan et al. 2005), Eutrophication Index (EI) (Liu et al. 2011), and Comprehensive Pollution Index (CPI) (Zhao et al. 2012).

7.4.1. Location of the Study

The Mayurakshi River is the subject of the current investigation. The river flows 288 km from the Jharkhand region to the West Bengal plains. The principal source of water is the down pouring of heavy monsoonal rain from the higher part of the Jharkhand plateau region, where the water flows from west to east. With a mean annual rainfall of 1400 mm, the months of June to October experience the most rainfall within the basin area (Chaudhury 1966). Massanjore Dam, Tilpara Barrage, Bakreswar Weir, and other dams and gates on the river have led the river system to become fragmented. The discharge locations of the tributaries from which the main river is formed, such as Dhobi, Motihara, Siddheswari, Kushkarini, Kuya, and Kopai, among others, have been selected as sampling sites for this study. A total of 17 sampling sites have been selected from each of the Mayurakshi River's catchments, which are listed in the table 7.18, after dividing the entire river stretch into three sections based on the physiographic condition (Fig. 7.30).

The terrain of the entire river basin is diverse, ranging from a plateau fringe at the top to vast plains of land used for subsistence farming in the lower length. The middle to lower reaches of the river are subject to a variety of pollution sources, from household garbage to agricultural runoff, which contribute to the deterioration of the river's water quality and subsequent ecological damage.

Table 7.18 *Description of the Sampling Locations for Surface Water Quality Analysis in Mayurakshi River Basin Area*

Provinces	Sampling Location	Code	Location		Site description and dominant land use types
			Latitude	Longitude	
Up-Stream	Rerha	S1	24°26'27.09"N	87° 8'18.33"E	Confluence point of Dhobi and Motihara River; Residential and Seasonal fallow land, surface water is used for irrigation purposes
	Gajenda	S2	24°21'50.96"N	87°10'40.40"E	Sandy river bed, minimum flow observed during dry season; Surface water is used for Brick Kiln industries and agriculture
	Maharo	S3	24°19'52.69"N	87°12'0.32"E	Confluence point of Tepra and Mayurakshi River; Presence of rail and road bridge, agricultural wastes are coming into the river
	Dudhani	S4	24°17'7.61"N	87°12'39.98"E	Sandy braided channel, sand mining activity on active river bed; Agricultural wastes are coming into the river
	Poljori	S5	24°14'13.41"N	87°14'5.90"E	Floating algae formed in a stagnant river water; Urban wastes from Dumka city, Huge dependency of river water for irrigational purposes
	Banskuli	S6	24° 3'6.31"N	87°20'5.82"E	Located on Siddheswari river, Braided channel with rocky exposures; Mono crop agricultural field observed on both side of the river bank
	Beniagram	S7	24° 2'35.99"N	87°23'20.55"E	Braided channel; Sand mining activity and other human interference alter the natural depth and flow of the river; presence of Brick Kiln industries
Middle Stream	Diguli	S8	23°59'17.17"N	87°26'52.30"E	Disturbed flow condition, deformated channel by extensive sand mining using JCP, Agricultural wastes coming into the river
	Kultor	S9	23°56'35.09"N	87°37'25.78"E	Diverted channel, River lift irrigation; huge agricultural and residential wastes coming into the river
	Sainthia	S10	23°57'21.62"N	87°40'52.38"E	Good flow condition; Urban waste water are dumped into the river through sewage pipelines, huge population pressure on river, daily bathing of both local people and domestic animals
	Panjona	S11	23°54'4.12"N	87°46'1.37"E	River lift irrigation; Huge pressure of agriculture on both side of the bank
	Gunutia	S12	23°52'37.87"N	87°50'4.76"E	Stable bank side with good vegetation cover; Residential and agricultural wastes coming into the river
Down Stream	Sundarpur	S13	23°52'58.40"N	87°56'31.90"E	Ferry service available; Residential and agricultural wastes coming into the river
	Aharinagar	S14	23°57'7.02"N	88° 6'57.50"E	Good flow condition observed during dry season; Residential and agricultural wastes coming into the river
	Gopalpur	S15	23°55'50.40"N	88° 9'40.60"E	Meandering channel; Residential and agricultural wastes coming into the river
	Lohadaha	S16	23°53'11.20"N	88°10'40.70"E	Ferry service available; animal bathing and huge population pressure on both side of the bank
	Baidyapur	S17	23°49'30.60"N	88° 9'44.60"E	Meandering channel; Residential and agricultural wastes coming into the river

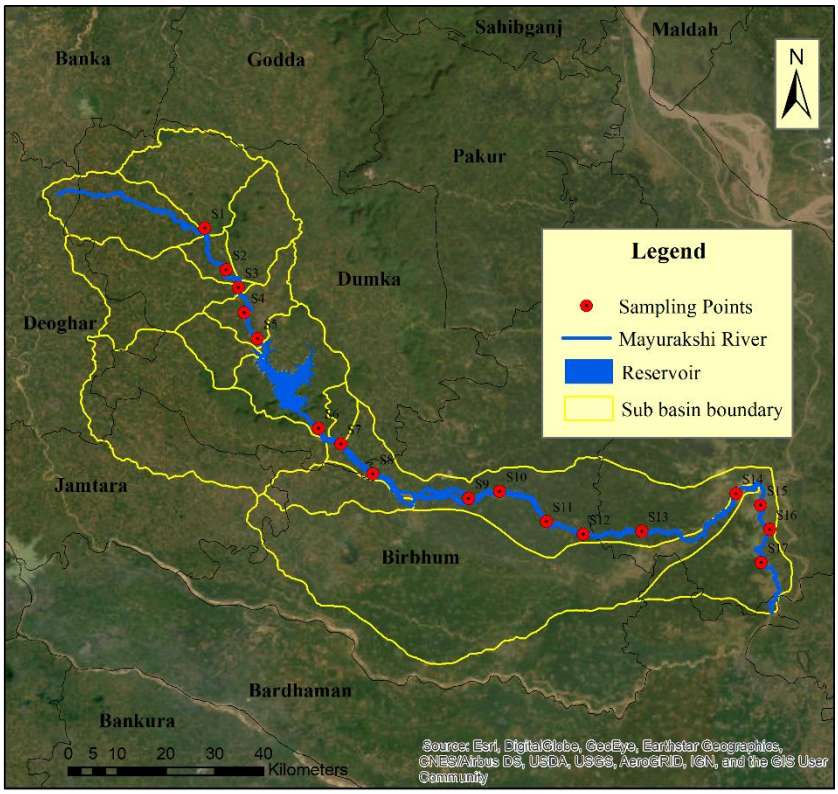

Figure 7.30 *Location of the Sample Sites of Surface water Quality Analysis of Mayurakshi River basin Area*

7.4.2. Materials & Methodology

- **Sample Collection and Analysis**

The water samples were taken in 2022 during the dry season in March (pre-monsoon) and the wet season in June (post-monsoon) from the previously chosen 17 sampling stations (Fig. 7.30), with minor variations depending on the geographic conditions and accessibility (Plate No. 7.5). All the sampling sites were situated along the main stream of the Mayurakshi River. These locations, which were mostly found within straight sections of rivers with a mild flow and a wide channel, were chosen to avoid still water and discharge outfall zones. The Global Positioning System (GPS) captured the coordinates of the sampling stations. Water samples were collected three times from each site. To prevent the mixing of air bubbles, the water sample was collected about 10 cm below the surface using washed polypropylene bottles (1L and 500 ml) and BOD bottles (500 ml) made by Tarson, India. The water sample in the 1 L bottle was utilised for physico-chemical analysis, while the sample in the second bottle (500 ml) was fixed on site with 2 ml of manganous sulphate ($MnSO_4$) and alkali iodide solution kept far from direct sunlight, then used for the determination of dissolved oxygen. For the analysis of the chemical oxygen demand, another bottle (500 ml) had been additionally fixed with 2 ml of concentrated H_2SO_4. For bacteriological examination, a different set of samples were taken

in 50 ml polypropylene bottles and kept in a separate ice box to prevent contamination throughout the laboratory's transit phase.

Plate No. 7.5 *Photographs showing Surface Water Collection from the Sampling Sites near Mayurakshi River*

A laboratory mercury thermometer and a pocket pH metre (both manufactured by HANNA, USA) were used to measure various physicochemical parameters at the sampling locations, including temperature, pH, electrical conductivity, and total dissolved solids. For greater precision, dissolved oxygen and its saturation have also been measured at sample locations using a DO probe, and the results have been calibrated with laboratory findings. Following the steps outlined in APHA (2012), the samples were transferred to the laboratory at a suitable temperature (<4 °C) after being collected and sealed in airtight bottles. The turbidity of the water samples was assessed in the lab using the Systronics EC meter-306 and Digital turbidity metre (EIModel-33E), respectively (Plate No. 7.6b). Total dissolved solids were measured using the conductivity and TDS metre from E-Merck. Ethylenediaminetetraacetic acid (EDTA) was used in the complexometry titrations to evaluate the total hardness and total alkalinity was determined using a titration method using 0.02 N standard sulphuric acid as the titrant and phenolphthalein/methyl orange as the appropriate indicators. The titration method has been executed with potassium chromate as the indicator and 0.014 N silver nitrate as the titrant to measure the amount of chloride present in the water sample. The Hach Spectrophotometer DR 2800 TM (Plate No. 7.6a) was used to analyse additional chemical parameters such as sulphate, phosphate, nitrate, nitrite, and total ammonia using appropriate reagent powder pillows. During the analytical phase, quality control procedures such as procedural blanks, sample duplicates, and repeating experiments were carried out when needed. In the lab, the quantification of DO and BOD has been performed using the iodometric approach (Rice et al. 2017). By titrating with a standard solution of thiosulphate, the amount of DO present in the sample was determined using the modified Winkler's (azide modification) method (APHA, 2017).

(a) (b)

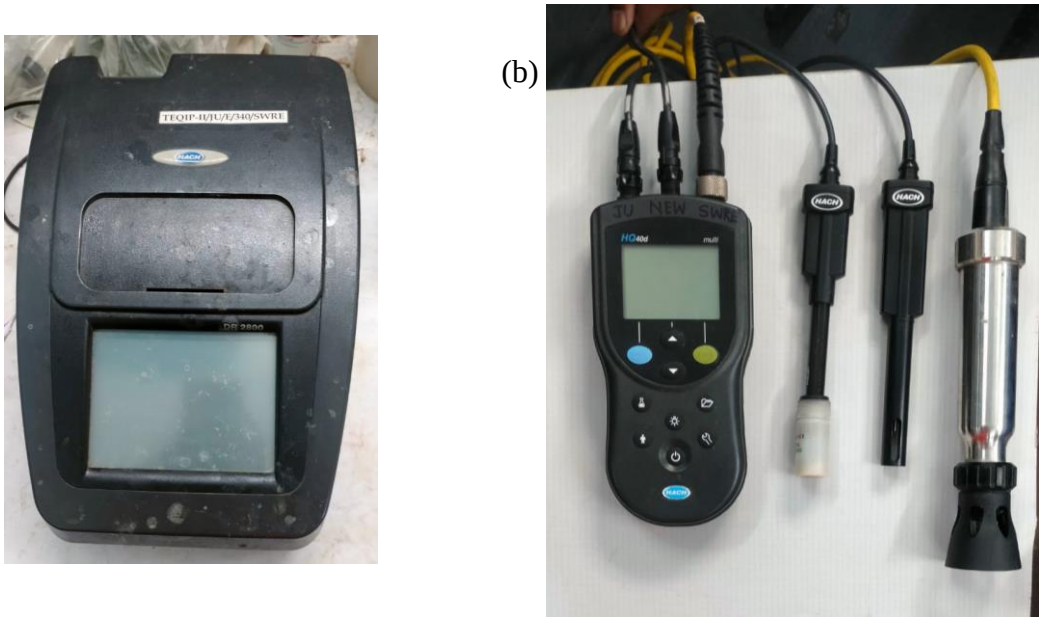

Plate No. 7.6 *(a) Spectrophotometer (b) Hach pH, TDS and DO probe*

The COD value in a 100 ml sample of water was determined using an open refluxed technique (APHA, 2017). A sample is reacted with potassium dichromate in a strongly acidic solution, and the amount of unreduced potassium dichromate that remains after digestion is titrated with ferrous ammonium sulphate. The final oxidizable matter is then calculated in terms of oxygen equivalents, also known as the Chemical Oxygen Demand (COD), or the amount of oxidant that reacts with the sample. BOD determination in the study was accomplished using a three-day BOD (BOD_3) calculation. The test assesses the oxygen required for the biochemical breakdown of organic material during the incubation period (carbonaceous demand) as well as the oxygen required to oxidise inorganic material like sulphide and ferrous ions. The test involves taking the provided sample and diluting it with water to the appropriate quantities in BOD bottles. Three concentrations were used for each sample, and two bottles were taken for each concentration. A single set of bottles was incubated for three days at 27°C in a BOD incubator, and the initial dissolved oxygen concentration (D1) was ascertained instantly. After 3 days, the amount of dissolved oxygen (D2) in the bottles that had been incubated was measured. Finally computing the following equation, final BOD of the sample water has been determined.

$$BOD(mg/L) = D1 - D2 \tag{7.12}$$

Where, $D1$ = DO of the sample (mg/L) immediately after preparation and $D2$ = DO of the sample (mg/L) at 3 days incubation.

The number of coliform bacteria in the sample water has been estimated using the membrane filtration (MF) technique (EPA 2002). This approach uses MI agar to simultaneously identify and count Escherichia coli (E. coli) and total coliforms (TC) in water samples in 24 hours or less, based on their unique enzyme activities. The agar petri dish is incubated at 35°C for the duration of the detection process (24 hrs.). The bacteria contained in the sample were retained after passing through a 0.45-m cellulose ester membrane filter with a volume of 100 ml of sample. The presence of fluorescent blue colour, which is an indicator of the E. coli enzyme, and white fluorescent, which is an indicator of the TC enzyme, is checked in the bacterial colonies that develop on the plate.

Finally the amount of E. coli or TC in 100 millilitres of sample has been done using the general guidelines below:

$$E\ coli/100\ ml\ = \frac{No\ of\ blue\ colonies}{Volume\ of\ sample\ (ml)} * 100 \tag{7.13}$$

$$TC/100\ ml\ = \frac{No\ of\ fluorescent\ \ colonies\ (if\ any)}{Volume\ of\ sample\ (ml)} * 100 \qquad (7.14)$$

If there are too many colonies or TC and E. coli to count on a filter, the output has been noted as too-numerous-to-count (TNTC).

In order to show the spatial fluctuation of parameters along the Mayurakshi River, an inverse distant weighted (IDW) interpolation approach was used in Arc map 10.3 after each physio-chemical water quality parameter had been analysed. The Pearson's correlation analysis, a statistical technique used to determine how closely one variable is related to another linearly, was carried out for all chemical variables using Microsoft Office Excel 2010. The Pearson's correlation analysis, which is regarded as an important statistical tool, was performed to determine the important factors that significantly influenced the features of the water quality in the research location. The connection and strength of associations between the variables are assessed using the correlation coefficient. At a significant level of p 0.05, a correlation coefficient value of + 1 indicates a perfect relationship between the variables, while a value of 1 indicates a perfect relationship, but the variables vary inversely. A value of zero indicates there is no relationship between the variables. In general, r values between 0.5 and 0.7 are regarded as moderate correlation, while r values > 0.7 are seen to indicate significant correlation. The interdependence of variables is readily represented by Pearson's correlation matrix.

- **Water Quality Index (WQI)**

The WQI has been determined to be the most useful water quality indicator. It aids in assessing the status of the water quality and the applicability of aquatic systems for diverse objectives. In the current study, the Weighted Arithmetic Water Quality Index (WAWQI) (Yadav et al. 2010) has been used to calculate WQI using the eleven water quality parameters (mentioned above). The WQI was calculated using the suggested standard limit (Table 7.20) for water for human consumption from various authorities.

The unit weight (Eq. 7.16) of each parameter was then calculated after determining the proportionality constant (Eq. 7.15). The quality grading scale (Eq. 7.17) has been determined by taking into account the ideal values of each parameter. Finally, WQI (Eq. 7.18) is the ratio of the sum of the unit weights of all the parameters that have been determined to the multiplication of the quality rating. The final WQI value has been categorised into six different classes depending on their quality status, mentioned in table 7.19. The weighted arithmetic WQI approach has been used to calculate WQI in a series of steps (Dutta et al. 2018).

1st step: Data on the different water quality parameters should be gathered.

2nd step: Eq. 7.15 can be used to calculate the proportionality constant (K).

$$K = \frac{1}{\sum(1/S_n)} \tag{7.15}$$

Where, S_n refers to the recommended quality value of an n^{th} variable.

3rd step: Using Eq. 7.16, estimate the unit weight (W_i) of each water class variable.

$$W_i = \frac{K}{S_n} \tag{7.16}$$

The 4th step is to use Eq. 7.17 to determine the quality rating scale (Q_n) for each variable.

$$Q_n = \frac{100(V_n - V_{ideal})}{(S_n - V_{ideal})} \tag{7.17}$$

Where, V_{ideal} is the ideal concentration of each individual variable in freshwater, and V_n denotes the measured value of the nth variable.

Finally, in the 5th and final stage, calculation of WQI has been done using Eq. 7.18.

$$WQI = \frac{\sum Q_n W_i}{\sum W_i} \tag{7.18}$$

Table 7.19 *Classification of water quality based on Weighted Arithmetic WQI method (Brown et al. 1972)*

WQI	Status	Possible uses
0-25	Excellent	Drinking, irrigation and industrial uses
26-50	Good	Domestic, irrigation and industrial uses
51-75	Fair	Irrigation and industrial uses
76-100	Poor	Irrigation
101-150	Very Poor	Restricted for irrigational uses
Above 150	Unfit for Drinking	Proper treatment required before irrigation

7.4.3. Methodologies for Pollution Indices

The indices like Comprehensive Pollution Index (CPI), Organic Pollution Index (OPI) and Eutrophication Index (EI) have been evaluated to classify the water quality status in terms of its pollution load within the main channel of Mayurakshi River.

- **Comprehensive Pollution Index (CPI)**

Utilising monitoring statistics, the CPI is used to determine the degree of pollution in a particular watershed (Liu & Zhu 1999).For the purpose of calculating the CPI in this study, a total of 15 parameters were taken into account, including pH, Electrical Conductivity (EC), Total Dissolved Solids (TDS), Dissolved Oxygen (DO), Biochemical Oxygen Demand (BOD), Chemical Oxygen Demand (COD), Turbidity, Chloride (Cl), Total Alkalinity ($CaCO_3$), Total

Hardness ($CaCO_3$), Sulphate (SO_4), Phosphate (PO_4^{3-}), Nitrate (NO_{3-}), Nitrite (NO_{2-}) and Total Ammonia (NH_{4+}).

The following has been followed for the estimation of CPI-

$$CPI = \frac{1}{n}\sum_{i=1}^{n} Pli \tag{7.19}$$

Where, n is the number of parameters and PI is the pollution index for each individual parameter.

According to the following equation, PIi has been determined

$$Pl_i = \frac{Ci}{Si} \tag{7.20}$$

where Si is the parameter number's permissible limit as per environmental standards and Ci is the parameter number's observed concentration in water.

The CPI is divided into five groups:

Category 1: CPI between 0 and 0.20 (clean);

Category 2: CPI between 0.21 and 0.40 (sub-clean);

Category 3: CPI between 0.41 and 1.00 (somewhat polluted);

Category 4: CPI between 1.01-2.00 (medium polluted); and

Category 5: CPI 2.01 (heavily contaminated).

- **Organic Pollution Index (OPI)**

It is a generalised water quality indicator that uses only four physicochemical parameters to categorise the state of the river's water quality: DO, COD, dissolve inorganic phosphate (DIP), and dissolve inorganic nitrogen (DIN) (Quan et al. 2005). The following equation is a representation of the organic pollution index (OPI):

$$OPI = \frac{COD}{COD_s} + \frac{DIN}{DIN_s} + \frac{DIP}{DIP_s} + \frac{DO}{DO_s} \tag{7.21}$$

where CODs, DOs, DINs, and DIPs are the limited concentrations of COD and DO, respectively; DINs is the total limited concentration of nitrate, nitrite, and ammonium; and DIPs is the restricted concentration of phosphate, as per the environmental standard. OPI is divided into four groups: excellent (OPI<0), good (OPI 0-1), contaminated (1-4), and very polluted (4-5).

- **Eutrophication Index (EI)**

Based on the three indicators COD, DIN, and DIP, EI describe the eutrophication of the watershed (Liu et al. 2011). The following is a presentation of the equation to compute EI:

$$EI = \frac{COD*DIP*DIN}{4500} * 10^6 \quad (7.22)$$

The total volumetric content of nitrate, nitrite, and ammonium is used to compute DIN concentration, while the concentration of phosphate in water is used to determine DIP concentration. The EI is divided into two groups:

1. EI 0: Eutrophication is non-existent.
2. Eutrophication (EI> 0)

Table 7.20 *Analysed Surface Water Quality Parameters in 17 Different Locations of Mayurakshi River with Their Permissible Limits*

Parameters	**Unit**	**Measured Technique**	**CPCB Standard**
Surface Water Temperature	°C	Ion Selective Method	-
pH	-	Electrometric Method	6.5-8.5
Electrical Conductivity (EC)	µs/cm	Ion Selective Method	-
Total Dissolved Solids (TDS)	mg/L	Ion Selective Electrode Method	-
Turbidity	NTU	Nephelometric Method	-
Dissolved Oxygen (DO)	mg/L	Electrometric DO meter	6
Dissolved Oxygen Saturation (DO %)	%	Electrometric DO meter	-
Biochemical Oxygen Demand (BOD)	mg/L	3 days incubation, 27°C	3 (3 days,27°C)
Chemical Oxygen Demand (COD)	mg/L	Open reflux	-
Chloride (as Cl)	mg/L	Argentometric Method	1000
Total Alkalinity (as $CaCO_3$)	mg/L	Titration Method	-
Total Hardness (as $CaCO_3$)	mg/L	Titration Method	-
Sulphate (as SO_4)	mg/L	Colorimetric Method using Hach Spectrophotometer DR 2800 TM)	400
Phosphate (PO_4^{3-})	mg/L	Colorimetric Method using Hach Spectrophotometer DR 2800 TM)	-
Nitrate (NO_{3-})	mg/L	Colorimetric Method using Hach Spectrophotometer DR 2800 TM)	-
Nitrite (NO_{2-})	mg/L	Colorimetric Method using Hach Spectrophotometer DR 2800 TM)	-
Total Ammonia (NH_{4+})	mg/L	Colorimetric Method using Hach Spectrophotometer DR 2800 TM)	-
Total Coliform (TC)	cfu/100 ml	Membrane Filtration (MF) technique	-
Faecal Coliform (FC)	cfu/100 ml	Membrane Filtration (MF) technique	-

7.4.4. Results & Discussion

- **Physico-chemical Properties of Surface Water Quality**

Data from 17 sampling locations along the Mayurakahi River have been gathered for overall quality assessment including their range, mean, and standard deviation for both the dry and rainy seasons (Table 7.21). The data shows how several parameters change from upstream to downstream.

Surface water temperature is a significant factor that impacts a variety of other variables that determine the quality of the water, including pH, dissolved oxygen, and alkalinity (Khaiwal et al. 2003).Significant ecological impacts are also caused by water temperature (Whitehead et al. 2009). Increasing water temperature generally leads to more biological activity along with rapid organism growth. Every aquatic organism has a preferred temperature range where it is best for its survival and reproduction (Ezene et al. 2014).The Mayurakshi River's surface water temperature varies from 24.6°C to 33°C during the dry season and from 28.2°C to 32.1°C during the wet season. However, the figure 7.31 depicts the regional variation in temperature values for the dry and wet seasons, respectively.

Any surface water's water quality and pollution levels can be strongly predicted by the **pH** of an aquatic ecosystem. The productivity of the organisms in the water increased as the pH level raised (Ravi Kumar et al. 2013). In the examined area, there has been a small difference in the pH levels of the water between the summer (dry) and monsoon (wet) seasons. According to Fig. 7.31, the monsoon season has the highest pH level of water (8.74) and the dry season has the lowest (7.84). According to the results of the current study, the sampling points that are primarily found in the Chotonagpur plateau region have more alkaline base water than the lower portion of the places that were investigated. Numerous factors, such as the existence of rocks in the area and the surrounding landscape, acid rain, and the discharge of residential garbage into rivers, have been accounted for in this regard.

According to the American Public Health Association (2005), **Electronic Conductivity (EC)** is the capacity of water to conduct an electric current and is influenced by the presence of anions and cations, as well as their relative and total concentrations, mobility, and temperature at the time of measurement. Electrical conductivity, or EC, is used to classify water because lower EC levels are considered to reflect clean water (Sharma and Kumar, 2017; Shah et al.,

2008) and higher EC values are considered to denote greater pollution (Sharma et al., 2014). It further indicates the amount of dissolved compounds, chemicals, and minerals in the water. In the current investigation, the highest EC levels (436 µs/cm) were discovered during the monsoon season with a mean value of 253 µs/cm and the lowest (172 /cm) during the dry season with a mean value of 245 µs/cm, as shown in figure 7.31.

The amount of inorganic salts and trace amounts of organic matter that are dissolved in water are represented by **Total Dissolved Salts (TDS)**. Electrical conductivity readings and total dissolved salts showed a similar seasonal trend. During the dry season, the total dissolved salts in the water of the Mayurakshi River varied between 85-213 mg/l, whereas they slightly increased to 95-220 mg/l during the wet season. The average value of the laboratory result indicating that the river water is only moderately appropriate for everyday applications.

Turbidity is a crucial component that regulates light refraction inside the water and has an effect on aquatic life (Tambekar et al. 2013). The presence of organic and mineral suspended particles, as well as colour-producing substances, causes turbidity, which affects the clarity of the water. During the dry and rainy seasons, respectively, the mean turbidity readings of the samples were in the range from 19.7 to 15.9 NTU respectively. High turbidity values are typically generated by the presence of suspended solid particles and other materials; this is primarily due to the removal of soil particles into the river due to strong downpours of rainfall as well as from the tributary rivers.

The amount of oxygen that has dissolved in water is measured as **Dissolved Oxygen** (DO), which is regarded as a direct indicator of water quality. The volume of dissolved oxygen concentration is one of the most critical aspects of stream health. Its absence has a direct impact on a river's environment because of bioaccumulation and bio-magnification (Appavu et al. 2016). The physical, chemical, and biological properties of the water body determine the concentration of DO. Its presence is essential for preserving the variety of all aquatic life, and it is essentially defined by the oxygen balance of the system in relation to the impact of waste release in a water body (Gupta et al. 2017). The DO of a water body is influenced by a wide range of variables, including the water's temperature, photosynthetic activity, wind speed, life in it, pollution levels, etc. It varies daily, seasonally, and in response to temperature changes (Wavde and Arjun 2010).

Table 7.21 *Surface Water Quality Parameters with Range, Average Values and Standard Deviation in 17 Different Locations of Mayurakshi River during Dry and Wet Season*

Parameters	Unit	Dry Season			Wet Season		
		Range	Average	Standard Deviation	Range	Average	Standard Deviation
Surface Water Temperature	°C	24.6-33	27.92	2.46	28.2-32.1	29.99	1.19
pH	-	7.84-8.69	8.37	0.22	7.91-8.74	8.45	0.21
Electronic Conductivity (EC)	µs/cm	172-428	245.82	77.78	180-436	252.76	81.25
Total Dissolved Solids (TDS)	mg/L	85-213	124.59	39.81	95-220	131.59	41.24
Turbidity	NTU	2.34-78.5	19.71	19.45	2.54-56.2	15.92	14.65
Dissolved Oxygen (DO)	mg/L	6.19-12.49	8.31	1.32	7.59-13.85	8.97	1.37
Dissolved Oxygen Saturation (DO %)	%	77.1-166.8	110.19	21.05	87.5-170.4	116.69	19.66
Biochemical Oxygen Demand (BOD)	mg/L	6.8-32.6	16.7	8.65	3.6-22	10.39	5.88
Chemical Oxygen Demand (COD)	mg/L	12.4-59.45	30.26	15.64	6.61-40.40	19.11	10.79
Chloride (Cl)	mg/L	5.66-101.96	29.46	28.44	4.54-64.82	21.59	17.54
Total Alkalinity	mg/L	60-284	121.88	60.37	52-260	112.47	55.31
Total Hardness	mg/L	64-288	132	64.33	98-592	169.53	118.13
Sulphate (SO_4)	mg/L	4-30	11.06	8.30	3-28	9.88	7.54
Phosphate (PO_4^{3-})	mg/L	0-0.33	0.12	0.14	0.01-0.51	0.18	0.15
Nitrate (NO^-_3)	mg/L	2-21.6	12.59	6.99	2.11-23.3	14.52	7.74
Nitrite (NO^-_2)	mg/L	0.01-0.07	0.03	0.02	0.01-0.12	0.05	0.04
Total Ammonia ($NH4^+$)	mg/L	0.01-0.54	0.11	0.13	0.02-0.58	0.13	0.14
Total Coliform	TNTC						
E-coli	TNTC						

According to CPCB, water classes are divided into A (≥6 mg/l), B (≥5 mg/l), C (≥4 mg/l), and D (≥4 mg/l) according to DO values. In the current study, DO concentrations varied from 6.2 to 12.5 mg/l during the dry season, with an average concentration of 8.31 mg/l, and from 7.6 to 13.9 mg/l with an average value of 8.97 mg/l during the rainy season. The majority of sampling locations reveal good conditions for maintaining the fish population over both seasons.

Biochemical Oxygen Demand (BOD) is used to determine the organic load status in water (Yogendra & Puttaiah 2007). Extreme BOD readings signify severe organic pollution levels (Bora & Goswami 2016). Waters that are naturally clean will have a BOD of 5 mg/l or less. BOD has a direct impact on how much dissolved oxygen is present in rivers and streams. The rate of oxygen loss in the stream increases with BOD. Thus, higher aquatic life forms have less oxygen available to them. As a result, aquatic species experience stress, suffocate, and eventually die. The CPCB divides water into following categories: A (≤ 2 mg/l), B (≤ 3 mg/l), C (≤ 3 mg/l) and D (≤ 4mg/l) based on the BOD concentration. There is a difference in BOD concentration between the monsoon and non-monsoon seasons at the Mayurakshi River sampling site. It fluctuates from 6.8 to 32.6 mg/l with an average concentration of 16.7 mg/l during the dry season (March), and from 3.6 to 22 mg/l with a mean value of 10.39 mg/l during the rainy season (June). As a result, the figure 7.31 suggests that the river water falls within the C or D category. More precisely, both throughout the dry and rainy seasons, the middle section of the examined river, running from the sample sites of Kultor to Goalpur, demonstrates a maximum BOD content. These sites were severely contaminated by numerous human activities, such as the direct disposal of residential and sewage wastes into rivers, animal bathing, etc. Even the disposal of human faeces to the river water raises the BOD level dramatically.

The oxidation of reduced compounds in water is quantified by the **Chemical Oxygen Demand** (COD). The amount of organic matter in water is calculated using the COD value. Because of this, COD can be used as a sign of organic pollution in surface water (King et al. 2003; Faith 2006). According to Sawyer et al. (2003), the COD test, used in conjunction with the BOD test, is useful in identifying hazardous circumstances and the existence of physiologically resistant organic compounds. In the current study, COD levels ranged from 6.6 to 40.4 mg/l during the wet season to 12.4 to 59.4 mg/l during the dry season (Table 7.21). The river's increased microbial activity and the constant breakdown of organic-inorganic material entering into the river are both indicated by the above high class value of COD (Xie et al., 2020). When the

average COD value of the samples were compared to the standard COD value (Table 7.21), it can be seen that the higher deviation indicates that the river water quality is lower. This is because there are more organic compounds in the river water, which raises the COD requirement. As a result, the water is less suitable for fish and other aquatic life during both dry and wet seasons.

Each form of water contains dissolved **Chlorides** (Cl) by nature. High chloride concentrations are considered to be signs of contamination from organic wastes with industrial or animal origins. According to Rajkumar (2004), chlorides can cause problems in irrigation water and are also bad for aquatic life. Aquifers, which are underground geological structures that hold groundwater, are the principal source of chloride ions in water. In this study, the sample sites of the Mayurakshi River had chloride contents that ranged from 5.66 to 101.96 mg/l during the dry period to 4.54-64.82 mg/l during the rainy period (Table 7.21). When there is a dry spell, the river water has a higher chloride concentration, making it less suited for everyday usage and aquatic life (Fig. 7.31).

Water **Hardness** is a crucial factor in deciding whether it is suitable for both residential and industrial purposes. Divalent ions of calcium, magnesium, strontium, ferrous iron, and manganese are the main cations that contribute to hardness. Although some industrial waste and irrigation drainage also contribute, the hardness of the water is primarily caused by the rocks that surround it. The hardness is commonly represented in milligrams of calcium carbonate equivalent per litre. The current study demonstrates that the total hardness of the sample sites varied from 64 to 288 mg/l with a mean value of 132 mg/l in the dry season, and from 98 to 592 mg/l with an average value of 169.53 mg/l during the wet period (Fig. 7.31).

Total Alkalinity demonstrates the water's ability to act as a buffer, aiding in the maintenance of pH (Lodh et al. 2014). The ability of water to neutralise acids is gauged by its alkalinity. Generally speaking, it is not regarded as a contaminant (Sharma and Kumar, 2017). Alkaline waste from industry as well as the addition of lime, calcareous minerals, and fertiliser through leaching of agricultural land can increase water alkalinity. The current study indicates that there has been a minor rise in alkalinity during the non-monsoon period (Dry season), with a mean value of 121.88 mg/l, whereas there has been a decline during the wet season, with a value of 112.47 mg/l (Fig. 7.31). Due to the high rate of decomposition during the summer, which releases CO2 and leads to the addition of carbonate and bicarbonate ions, alkalinity levels reach such high levels (Verma et al. 2012).

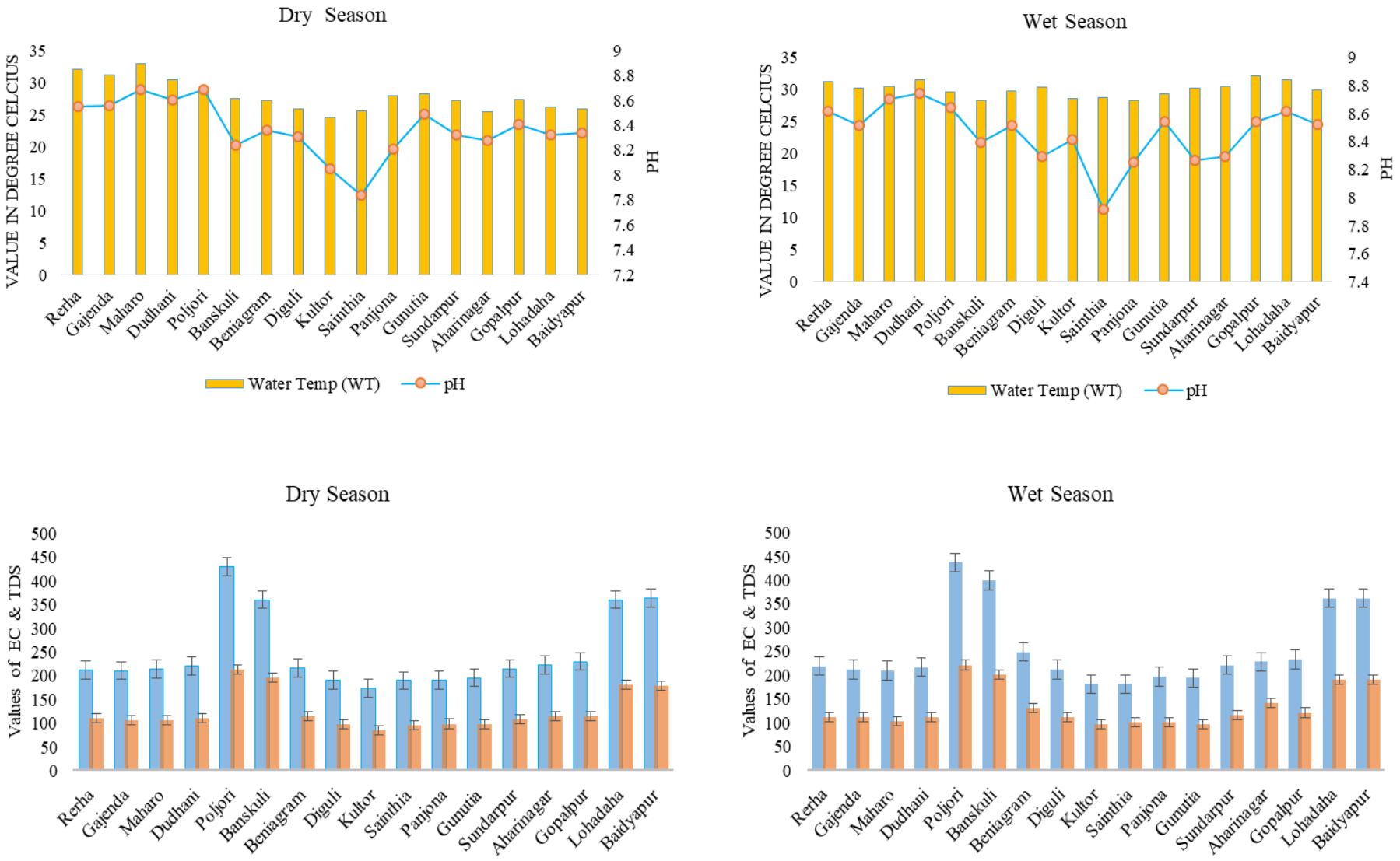

Figure 7.31 *Seasonal Variation in Selected Physico-chemical Properties of Surface Water of the Sample Sites of Mayurakshi River*

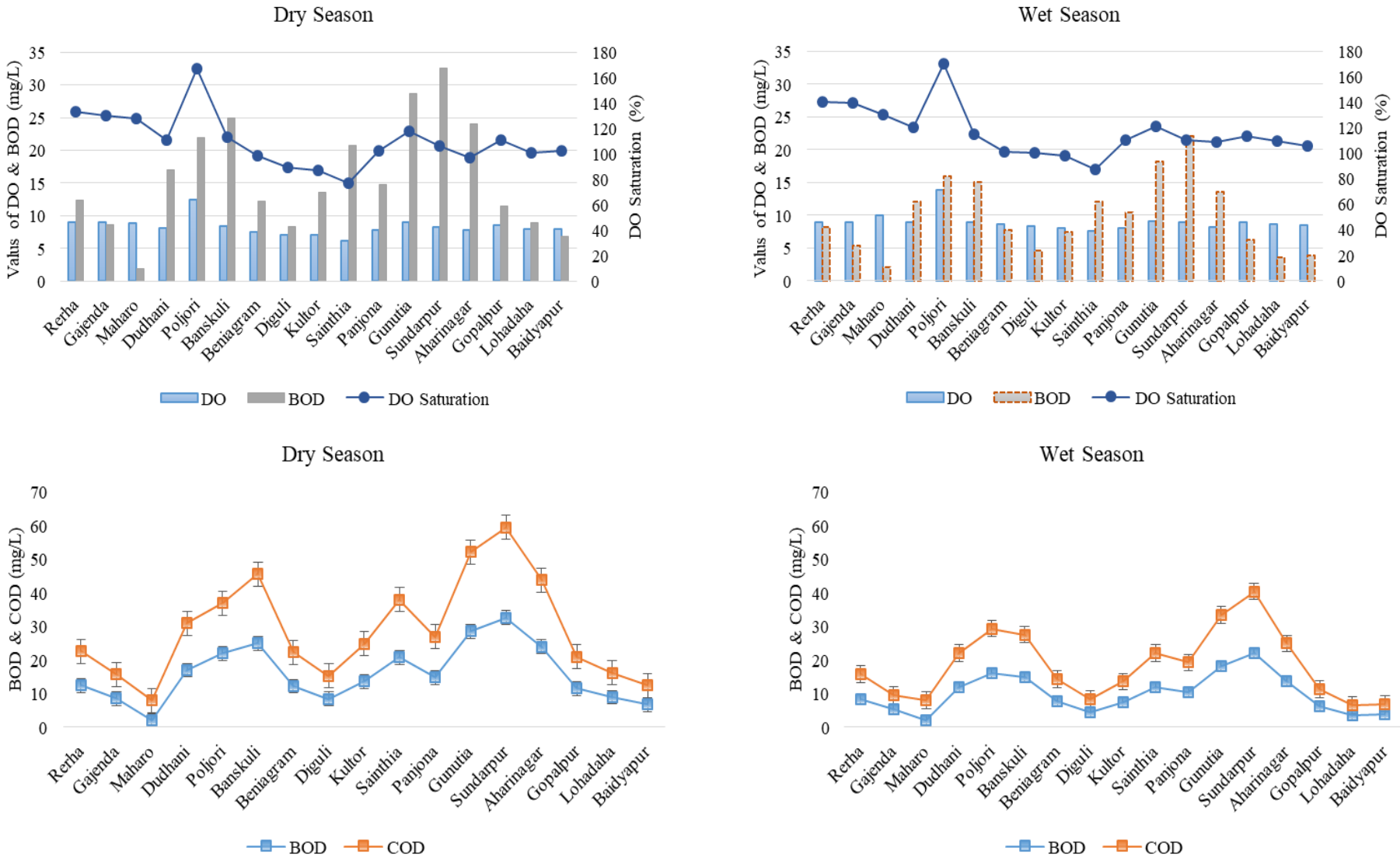

Figure 7.31 *Continued*

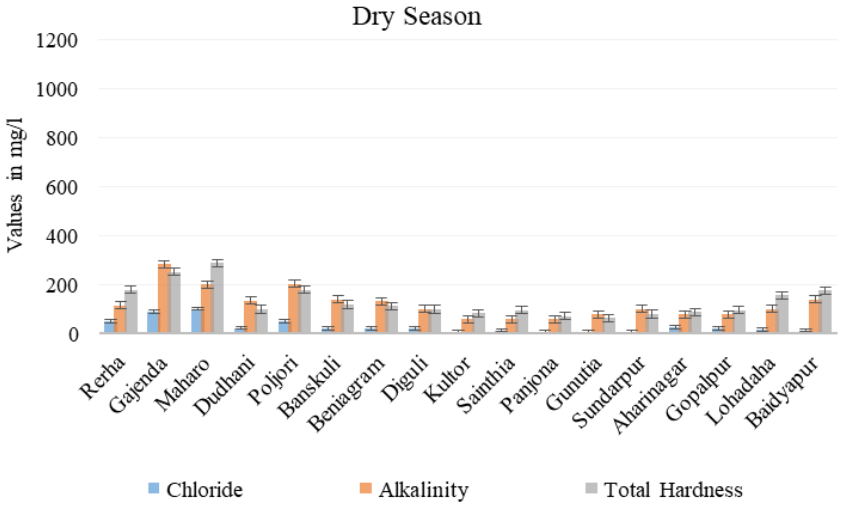

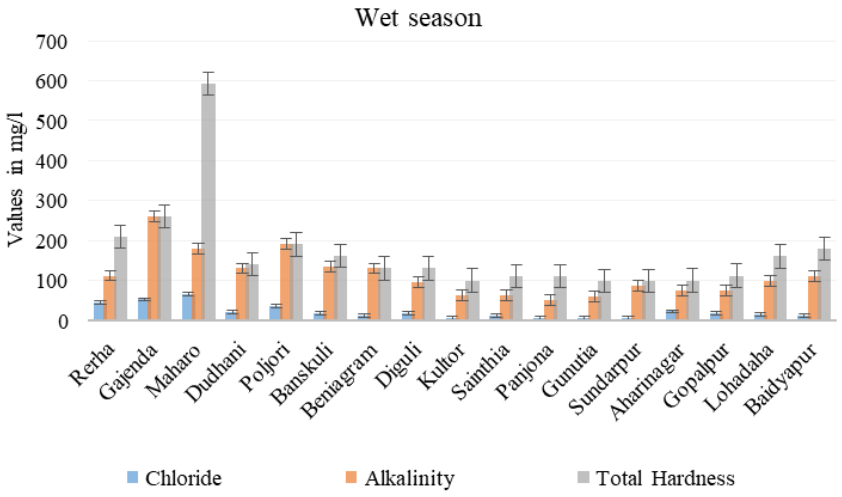

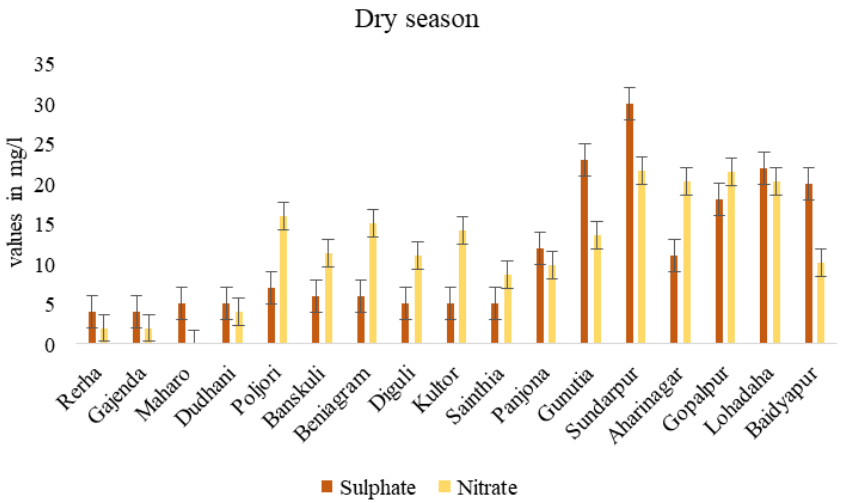

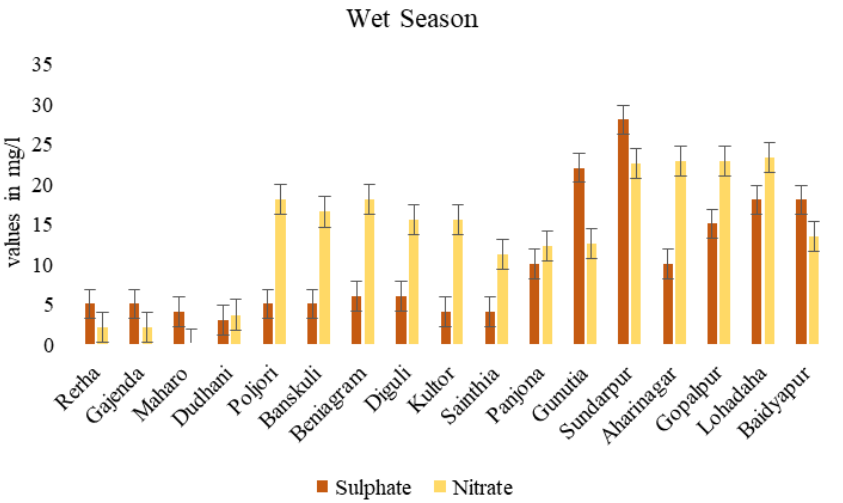

Figure 7.31 *Continued*

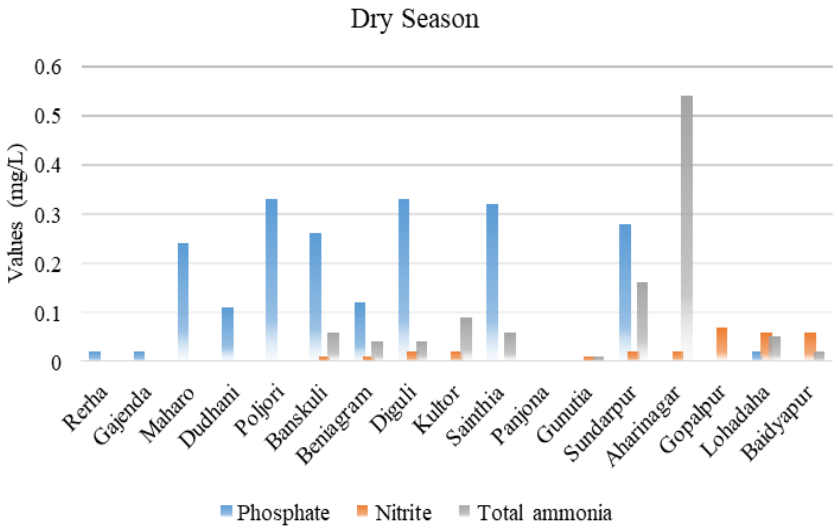

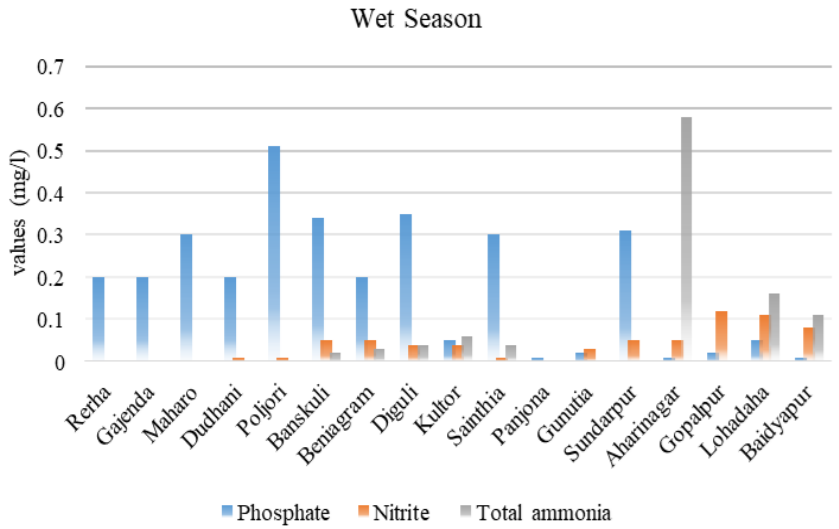

Figure 7.31 *Continued*

An essential factor in establishing a natural water's health for use in industrial and public supplies is its **Sulphate** level. Certain industries' effluents may also be a substantial source of sulphate in receiving waters. Airborne industrial pollutants that contain sulphur oxides and precipitate as acid rain are an important additional source of sulphate in water systems. For irrigation, sulphate levels over 200 mgL-1 are not ideal. In the research region, sulphate concentrations varied from 4 to 30 mg/l during the dry season to 3 to 28 mg/l during the wet season (Table 7.21) denoting its suitability for irrigation use within the study area.

Due to the active uptake by plants, **Phosphate** is rarely found in significant amounts in water. Phosphates are a major contributor to eutrophic conditions and their high quantities can signal the existence of pollution (WHO 1993). The amount of phosphorus added to the river by humans has a big impact on the water's quality. Agricultural runoff and home sewage are the main sources of this phosphate. The phosphate concentration of the examined sample locations ranged from 0 to 0.33 mg/l in dry months to 0.01 to 0.5 mg/l in rainy months respectively (Fig. 7.31).

The most prevalent type of nitrogen in natural waters is inorganic. According to Lodh et al. (2014), it is the primary nutrient that promotes the rapid growth of hydrophytes and aquatic algae. They can be found in surface waters as a result of wastewater discharge, runoff from fertiliser applications made on land, and fertilizer-polluted ground water. Because **nitrite** quickly oxidises to nitrate, **nitrate** concentrations in surface waters are often higher than nitrite concentrations. In this study, the concentrations of nitrate and nitrite vary with a range of 2-21.6 mg/l and 0.01-0.07 mg/l, respectively, while both of these range from 2.11-23.3 mg/l and 0.01-0.12 mg/l, respectively, during the wet season (Fig. 7.31). All of the readings are therefore inside the acceptable range as shown in table 7.20.

The presence of **ammonia** indicates the presence of human waste. In the current study, the sample water's ammonia concentration ranges from 0.01 to 0.54 mg/l in the dry season and 0.02 to 0.58 mg/l in the rainy season, indicates that the river water is of inferior quality and contains some amount of organic materials (Table 7.21). The presence of large amount of coliform bacteria also reflects the same.

- **Pearson's Correlation of Water Quality Parameters**

To comprehend any potential relationships between various water quality metrics for both seasons, a Pearson's correlation analysis was conducted shown in figure 7.32.

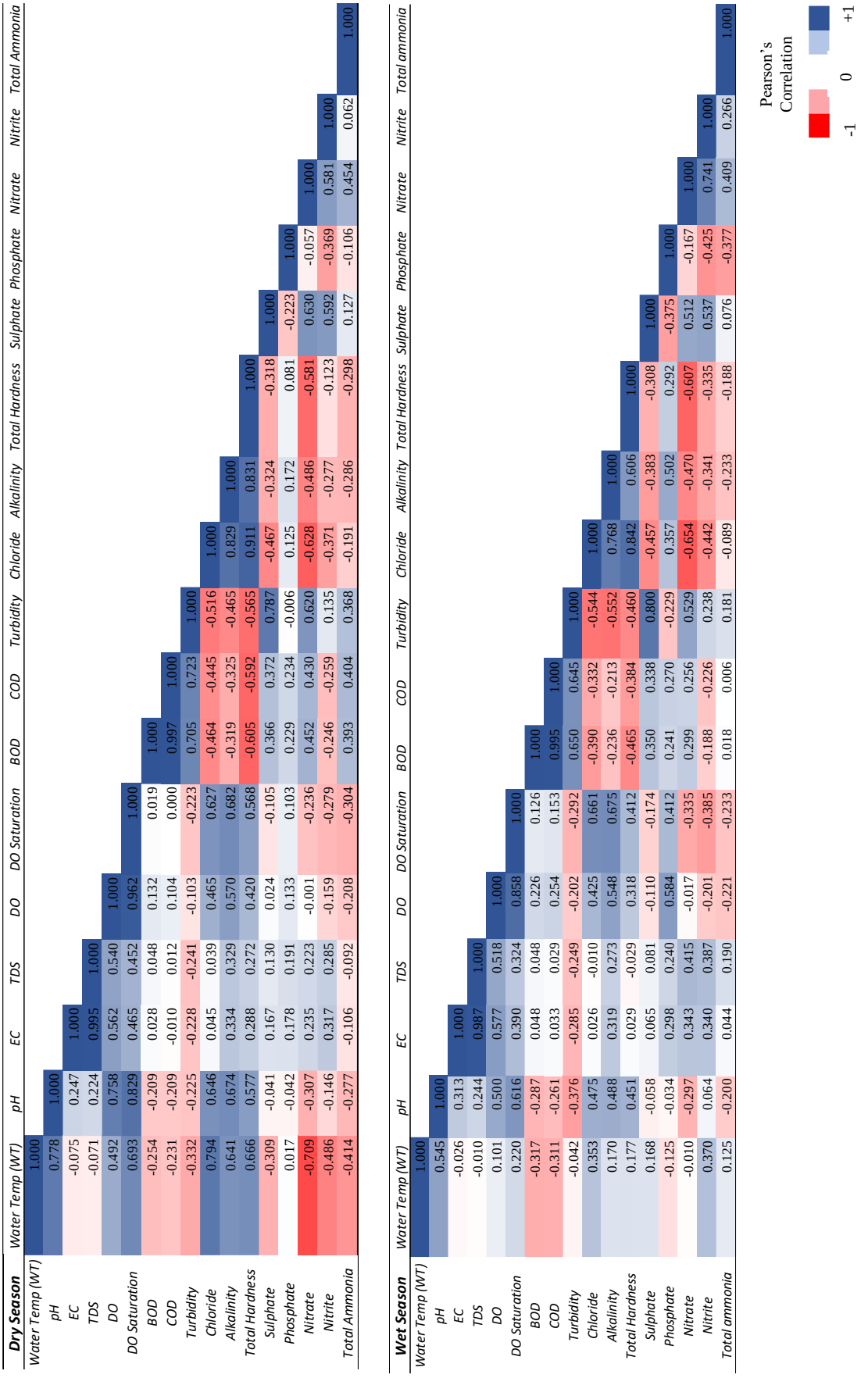

Figure 7.32 *Pearson's Correlation Matrix of Water Quality Parameters for both Dry and Wet season*

According to the study, pH is adversely connected with biochemical oxygen demand (-0.21), chemical oxygen demand (-0.21), and turbidity (-0.23) during the dry month but highly correlated with dissolved oxygen (0.76), chloride (0.65), total alkalinity (0.67), and total hardness (0.58). Total Dissolved Solids has a somewhat positive correlation with total alkalinity (0.33), total hardness (0.27), and dissolved oxygen (0.54). Dissolved oxygen has a substantial link with total alkalinity (0.57) and total hardness (0.42), but turbidity (-0.103), nitrate (-0.001), and total ammonia (-0.21) have a moderately negative correlation. The correlation between biochemical oxygen demand and chemical oxygen demand was similar in that both were positively correlated with turbidity (0.71 and 0.72), nitrate (0.45 and 0.43), and total ammonia (0.39 and 0.40), while they were negatively correlated with chloride (0.46 and 0.45), total alkalinity (0.32 and 0.33), and total hardness (0.61 and 0.59). Total Dissolved Solids has a somewhat positive correlation with total alkalinity (0.33), total hardness (0.27), and dissolved oxygen (0.54). Dissolved oxygen has a substantial link with total alkalinity (0.57) and total hardness (0.42), but turbidity (-0.103), nitrate (-0.001), and total ammonia (-0.21) have a moderately negative correlation. The correlation between biochemical oxygen demand and chemical oxygen demand was similar in that both were positively correlated with turbidity (0.71 and 0.72), nitrate (0.45 and 0.43), and total ammonia (0.39 and 0.40), while they were negatively correlated with chloride (0.46 and 0.45), total alkalinity (0.32 and 0.33), and total hardness (0.61 and 0.59). Total alkalinity has a strong correlation (0.83 with total hardness) but a weak correlation (0.32 with sulphate, 0.49 with nitrate, 0.28 with nitrite, and 0.29 with total ammonia). Nitrate and nitrite were positively correlated with sulphate (0.63) and negatively correlated with phosphate (-0.22).

A similar correlation matrix has also been created for data on water quality during the wet season, which displays a distinct relation matrix from the previously stated dry season variability (Fig. 7.32). In contrast to their previous significant correlation, pH has a modest correlation with dissolved oxygen (0.5), total alkalinity (0.49), chloride (0.48), and total hardness (0.45). Total dissolved solids (0.98) and dissolved oxygen (0.58) have substantial correlations with electrical conductivity, whereas other metrics like biochemical oxygen demand (0.05), chemical oxygen demand (0.03), and total alkalinity (0.32) have weak correlations with electrical conductivity. Additionally, there is a positive correlation between dissolved oxygen and total alkalinity (0.55), chloride (0.43), and total hardness (0.32). Similar to the dry season matrix, the biochemical oxygen demand and chemical oxygen demand maintains a positive relationship with turbidity (0.65), phosphate (0.24), and nitrate

(0.3). On the other hand, it exhibits a negative correlation with total alkalinity (-0.24), total hardness (-0.47), and chloride (-0.39). Total alkalinity (0.77) and total hardness (0.84) have been found to have a strong positive correlation with chloride. All of these correlative values show that the dry season of the research has a stronger relationship than the rainy season.

- **Analysis of Pollution Indices**

Table 7.23 summarises the outcomes of calculating the water pollution indices for both the dry and rainy seasons.

- **Comprehensive Pollution Index (CPI)**

The CPI data demonstrate the value of the entire river with no appreciable variation between the dry and wet seasons. During the dry season, the CPI of the Mayurakshi River ranged from 0.38 to 2.18, falling within the CPI classification of slightly to moderately polluted river water (Fig. 7.33a). The CPI of the Mayurakshi River reached 0.42-1.46 during the wet season, indicating that its quality was at the same level as during the dry season. Despite the fact that overall water quality at each water monitoring location tended to improve throughout the monsoon season.

- **Organic Pollution Index (OPI)**

Similar to the CPI, the OPI was higher in the dry season than in the wet season (5.16 compared to 4.74). Regarding spatial location, the upstream OPI in the dry and rainy seasons was 4.26 and 3.6, respectively, indicating that the region that was under the extreme polluted class in the dry season has been replaced with the polluted group. The OPI in the middle of the river was significantly higher in the dry season (5.16 as opposed to 4.37 in the wet season). In comparison to the OPI during the rainy season (2.80), the average OPI of the downstream during the dry season was 3.19, which is similar to the level of extreme pollution. However, there were a minimal variation in OPI between the two seasons. The OPI of the upstream had the best quality and the OPI of the downstream had the worst quality, which was consistent with the findings of the CIP analysis (Fig.7.33b).

- **Eutrophication Index (EI)**

For both the dry and wet seasons, an EI of roughly 100-900 was obtained for the whole river. This suggests that eutrophication was a serious threat to the river. According to the location, the EI of each monitoring station was greater than zero, indicating extreme eutrophication of the surface water. Algal blooms and other environmental, ecosystem, social, and economic

issues such oxygen depletion, infectious disease, deterioration of aquatic ecosystems, and freshwater unfit for human use are all results of eutrophication (Smith and Schindler, 2008; Vörösmarty et al., 2010). This tendency impedes social and economic advancement. Larger EI is produced during the wet season by significant rainfall and dam opening. However, due to pollution buildup and the destruction of river habitat, the fastest rate of eutrophication has been seen in both seasons close to metropolitan areas (Lei et al. 2012). However, the lesser precipitation during the dry season decreases necessary water recharge and slows water flow. In the Mayurakshi River, the aforementioned variables cause low EI during the dry season (Fig. 7.33c).

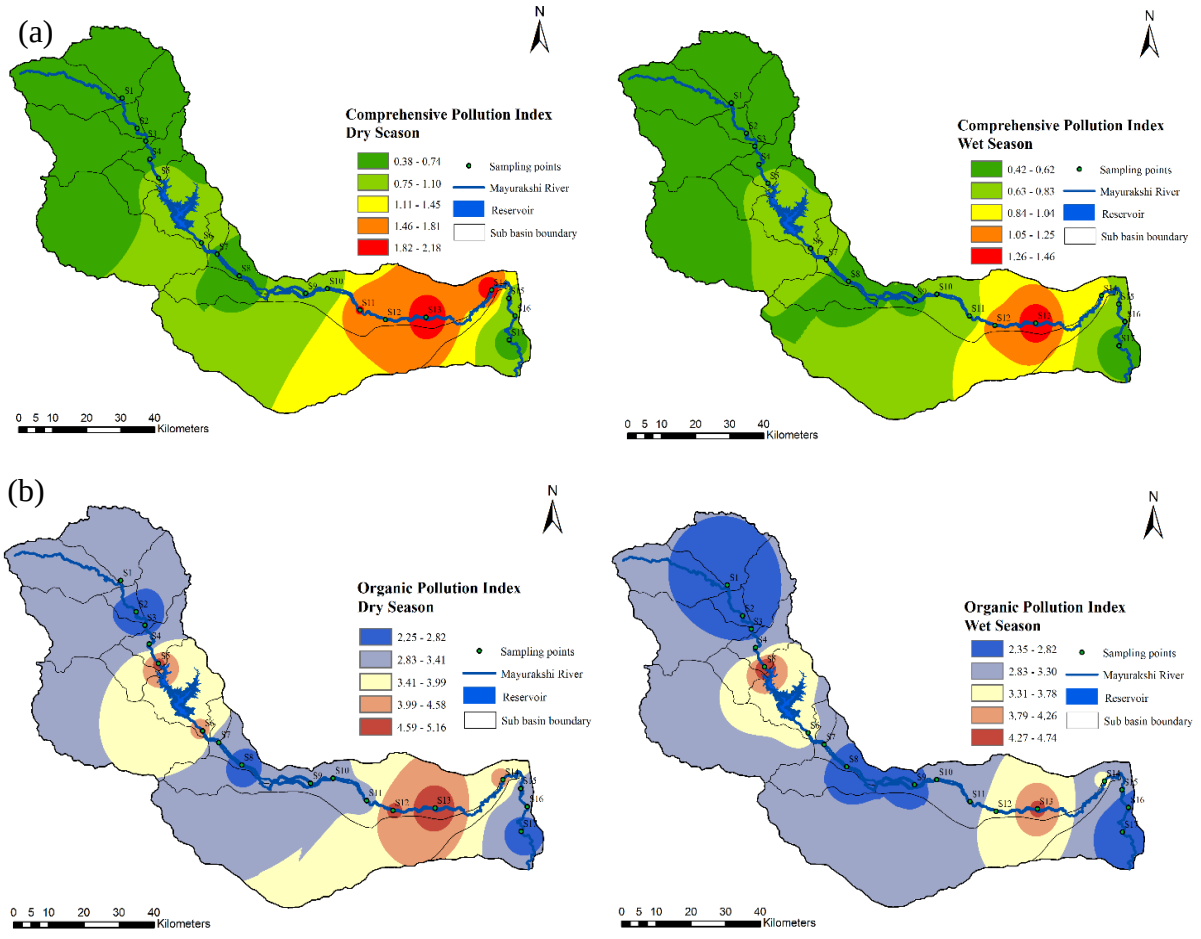

Figure 7.33 *Seasonal Variation in Different Water Pollution Indices in Mayurakshi River Basin Area (a) Comprehensive Pollution Index (b) Organic Pollution Index (c) Eutrophication Index*

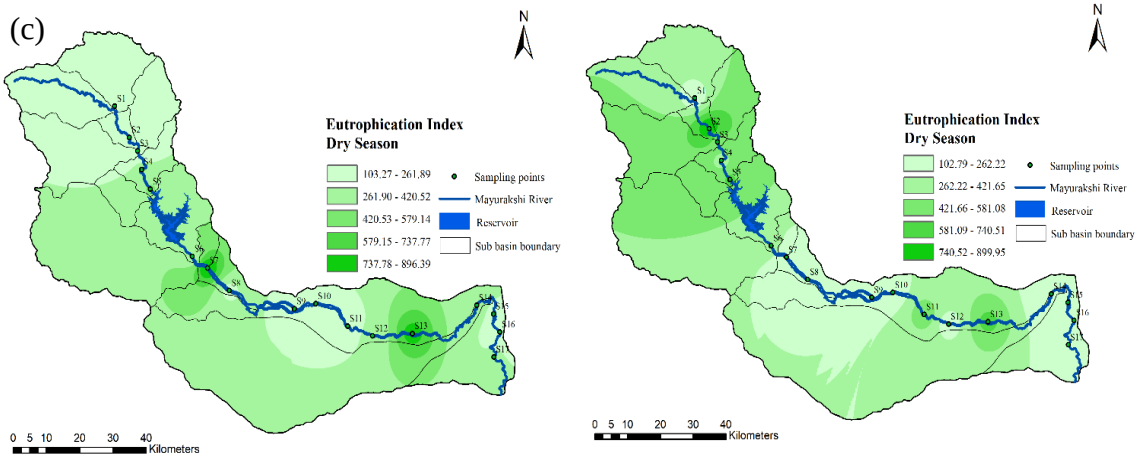

Figure 7.33 *Continued*

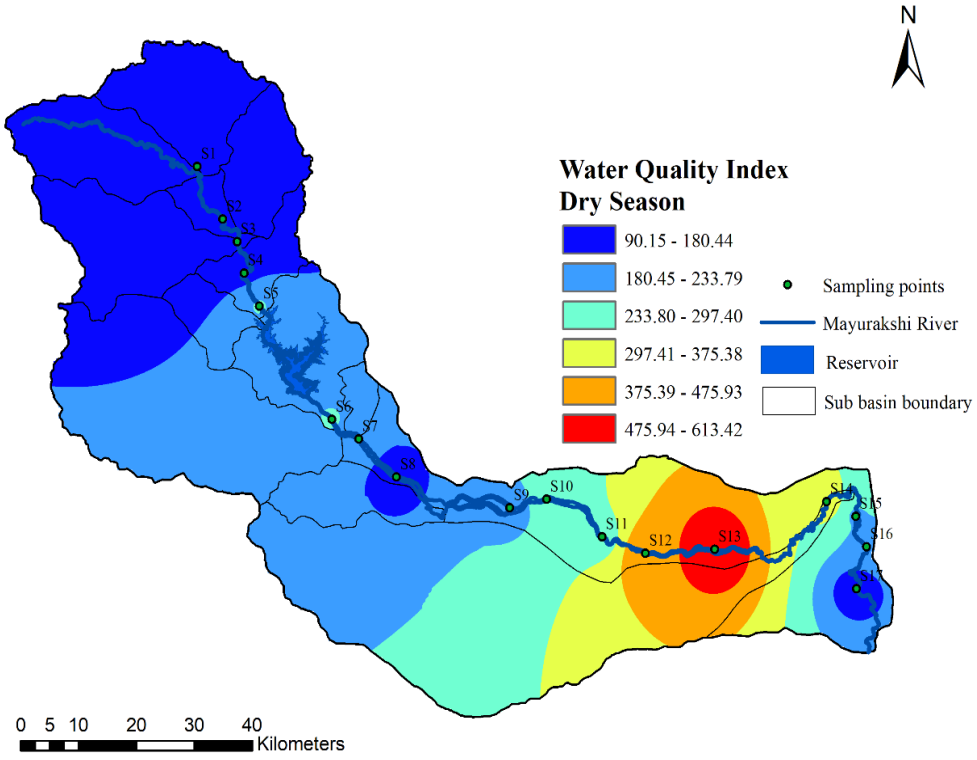

Figure 7.34 *Spatial Variation in Water Quality Index for Dry Season of the Study*

- **Analysis of Water Quality Index**

The WQI is a significant and consistent approach to depict the total water quality levels, which aids in choosing an effective treatment method to address the issue of concern (Mitra & Reddy, 2016). The weighted arithmetic water quality index has been used in this work to measure overall quality of river water utilising seasonal data gathered from 17 sample locations along the Mayurakshi River. For the year 2021, samples were taken in the dry season (March) and

the wet season (June). The station wise computation of weighted arithmetic mean water quality index for both seasons has been summarised in annexure III. In the dry and wet seasons of the research period, the computed WQI value for Mayurakshi River ranges from 89.7-613.5 and 93.87-452.42 respectively (Fig. 7.34 and 7.35). According to the calculated value for various seasons, the general quality of the Mayurakshi River's water has declined from the wet to the dry seasons. According to Jiang et al. (2018) and Wu et al. (2017), physico-chemical characteristics of water may have had an impact on these seasonal changes in WQI. The WQI dropped from upstream to downstream, indicating the accumulation of contaminants from discharge sources. The downstream water quality was adversely impacted by a number of anthropogenic activities, which hampered the overall health of the riverine ecology in the study locations. However, due to geographic factors and the effects of pollution sources, the water quality throughout the dry season varied greatly. The WQI scores in the upper and lower reaches of the river were generally higher than during the dry season (Fig. 7.34). Sampling site 13 (Sundarpur) was designated as a much polluted site because it received the highest quality index for both seasons, indicating the most degraded site of the Mayurakshi River. Increased human interference and agricultural runoff are the primary causes of such water quality declining condition. Additionally, the other sample sites showed similar circumstances that fell under the category of being unfit for ingestion.

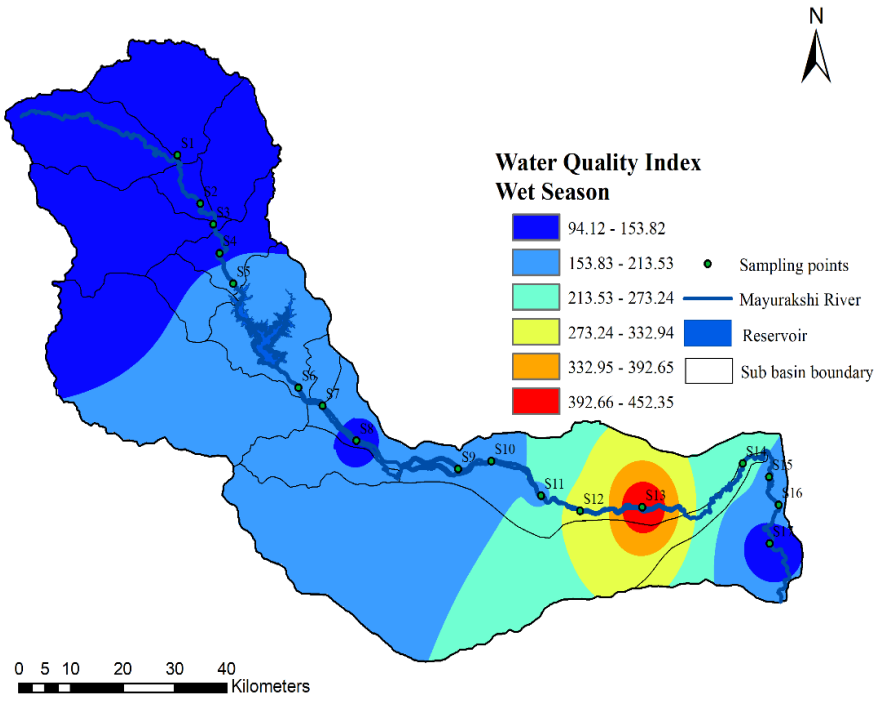

Figure 7.35 *Spatial Variation in Water Quality Index for Wet Season of the Study*

Table 7.22 *Summary of Water Pollution Indices for both Dry and Wet Season*

Sampling Location	EI*		OPI*				CPI*				WAWQI*			
	Dry Season	Wet Season	Dry Season	Status	Wet Season	Status	Dry Season	Status	Wet Season	Status	Dry Season	Status	Wet Season	Status
Rerha	200.89	148.21	2.98	Polluted	2.67	Polluted	0.59	Slightly Polluted	0.51	Slightly Polluted	159.81	Unfit for consumption	137.01	Very Poor
Gajenda	139.56	900.27	2.62	Polluted	2.37	Polluted	0.49	Slightly Polluted	0.43	Slightly Polluted	121.23	Very Poor	104.67	Very Poor
Maharo	102.4	533.33	2.24	Polluted	2.48	Polluted	0.38	Sub clean	0.42	Slightly Polluted	89.7	Poor	93.87	Poor
Dudhani	303.11	357.87	3.27	Polluted	3.01	Polluted	0.65	Slightly Polluted	0.55	Slightly Polluted	175.4	Unfit for consumption	147.71	Very Poor
Poljori	434.13	600.09	4.77	Extremely Polluted	4.74	Extremely Polluted	0.9	Slightly Polluted	0.78	Slightly Polluted	238.04	Unfit for consumption	201.41	Unfit for consumption
Banskuli	299.56	344.28	4.26	Extremely Polluted	3.6	Polluted	0.89	Slightly Polluted	0.68	Slightly Polluted	238.18	Unfit for consumption	171.73	Unfit for consumption
Beniagram	896.81	115.54	2.98	Polluted	2.89	Polluted	0.71	Slightly Polluted	0.66	Slightly Polluted	201.08	Unfit for consumption	164.57	Unfit for consumption
Diguli	224.09	102.78	2.5	Polluted	2.49	Polluted	0.54	Slightly Polluted	0.52	Slightly Polluted	149.59	Very Poor	144.62	Very Poor
Kultor	157.73	235.73	2.96	Polluted	2.63	Polluted	0.73	Slightly Polluted	0.57	Slightly Polluted	210.65	Unfit for consumption	163.03	Unfit for consumption
Sainthia	236.09	165.01	3.39	Polluted	2.93	Polluted	0.86	Slightly Polluted	0.69	Slightly Polluted	247.36	Unfit for consumption	198.56	Unfit for consumption
Panjona	117.61	523.24	3.13	Polluted	2.83	Polluted	1.85	Medium Polluted	0.7	Slightly Polluted	254.75	Unfit for consumption	206.71	Unfit for consumption
Gunutia	315.91	186.09	4.7	Extremely Polluted	3.76	Polluted	1.49	Medium Polluted	1.18	Medium Polluted	461.47	Unfit for consumption	365.19	Unfit for consumption
Sundarpur	804.98	630.37	5.16	Extremely Polluted	4.37	Extremely Polluted	2.16	Heavily Polluted	1.46	Medium Polluted	613.5	Unfit for consumption	452.42	Unfit for consumption
Aharinagar	406.07	130.72	4.22	Extremely Polluted	3.41	Polluted	2.18	Heavily Polluted	0.94	Slightly Polluted	341.88	Unfit for consumption	269.82	Unfit for consumption
Gopalpur	201.32	116.13	3.25	Polluted	2.86	Polluted	0.79	Slightly Polluted	0.65	Slightly Polluted	227.83	Unfit for consumption	186.23	Unfit for consumption
Lohadaha	146.95	172.85	2.84	Polluted	2.57	Polluted	0.76	Slightly Polluted	0.63	Slightly Polluted	211.94	Unfit for consumption	172.1	Unfit for consumption
Baidyapur	280.52	211.41	2.44	Polluted	2.35	Polluted	0.53	Slightly Polluted	0.45	Slightly Polluted	137.56	Very Poor	109.24	Very Poor

*EI= Eutrophication Index; OPI= Organic Pollution Index; CPI= Comprehensive Pollution Index; WAWQI= Weighted Arithmetic Water Quality Index

In order to categorise the monitoring stations with comparable water quality features, cluster analysis has been used together with all the pollution indices and water quality index. The results of the calculation, which are summarised in table 7.23, divided the 17 points into five categories. The results of the cluster analysis are shown in table 7.23, with cluster 1 representing the greatest quality of water and cluster 5 the lowest. The polluted points (belonging to groups 4 and 5) made up approximately 18% (3 of a total of 17 points) of the Mayurakshi River (Fig. 7.36). However, during the wet season, the number of polluted spots in groups 4 and 5 has increased while it has greatly decreased in group 1 (Fig. 7.37). According to the cluster analysis's findings, the Mayurakshi River's water quality was better during the monsoon than it was during the dry season.

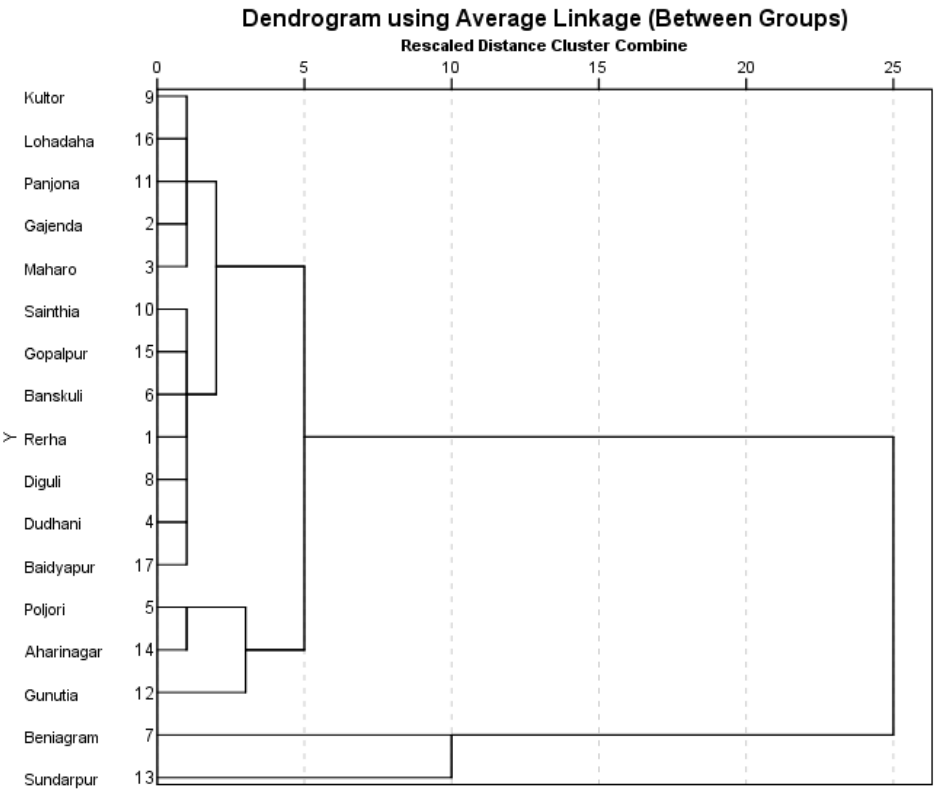

Figure 7.36 *Dendrogram Results of Cluster Analysis in 17 Locations Based On Water Quality and Water Pollution Indices for the Period of Dry Season*

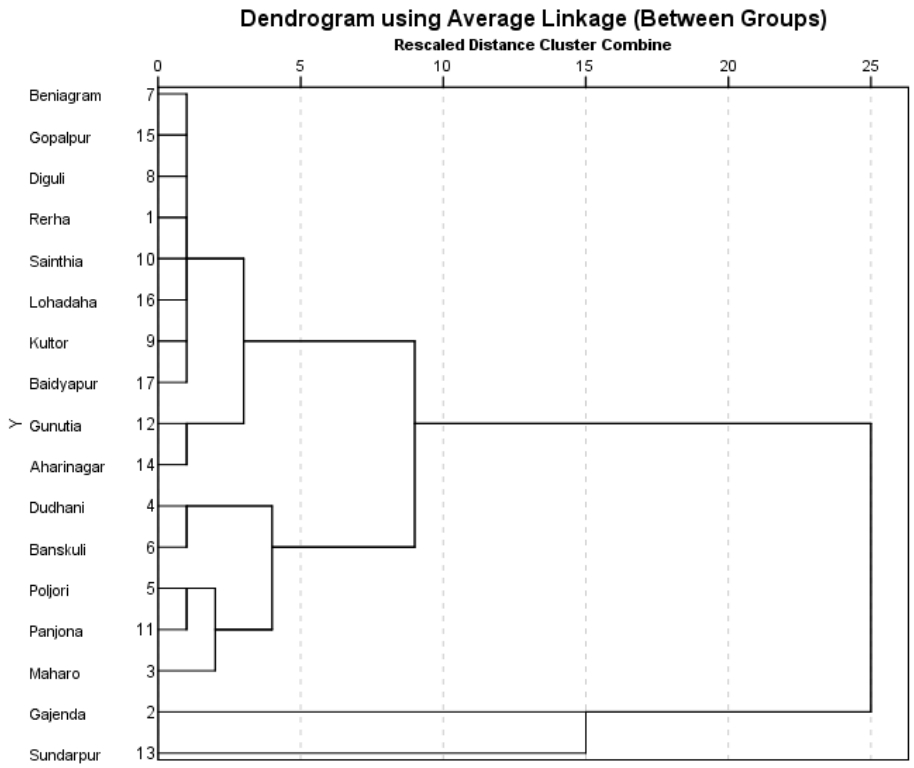

Figure 7.37 *Dendrogram Results of Cluster Analysis in 17 Locations Based On Water Quality and Water Pollution Indices for the Period of Wet Season*

Table 7.23 *Detailed Output of Cluster Analysis for both Dry and Wet Season*

Season	Cluster	CPI	OPI	EI	WQI	Sampling Locations
Dry Season	1	0.75	2.95	197.61	179.69	Rerha, Gajenda, Maharo, Dudhani, Banskuli, Diguli, Kultor, Panjona, Gopalpur, Lohadah, Baidyapur
	2	1.54	4.50	420.10	289.96	Poljori, Aharinagar
	3	0.785	3.185	566.45	224.22	Sainthia, Beniagram
	4	1.49	4.7	315.91	461.47	Gunutia
	5	2.16	5.16	804.98	613.5	Sundarpur
Wet Season	1	0.62	2.76	155.38	171.69	Rerha, Beniagram, Diguli, Kultor, Aharinagar, Gopalpur, Lohadaha, Baidyapur, Sainthia
	2	0.81	3.07	543.18	234.93	Gunutia, Gajenda
	3	0.63	3.35	552.22	167.33	Maharo, Poljori, Panjona
	4	0.62	3.31	351.08	159.72	Banskuli, Dudhani
	5	1.46	4.37	630.37	452.42	Sundarpur

The management of water consumption for various reasons, such as irrigation, residential water supply, aquaculture cultivation, and other uses, may benefit by grouping water monitoring locations with comparable features. The outcomes of water quality clustering also assist managers in creating methods for monitoring water quality, with a focus on paying close attention to major contamination hotspots. These advantages offer significant building blocks for managing sustainable water sources.

7.4.5. Conclusion

Based on monitoring factors affecting the environment, this study has proposed a potential combination of quality and pollution indices for determining the quality of rivers. Depending on the location and the period of monitoring, the water quality indices fluctuated. Upstream of the river, followed by the midstream and downstream, had poor water quality during the dry season than other sections. Calculated pollution levels show that the Mayurakshi River is polluted in several geographic locations. The river is contaminated by organic pollution, or OPI> 1, at many places. EI was over zero, putting the river's water at a high danger of eutrophication.

The Mayurakshi River's pollution indices all tend to rise from upstream to midstream, then decline downstream. The water monitoring stations were divided into five groups using cluster analysis, with the quality gradually declining from the first group to the fifth group. The clustering analysis' classification offered valuable assistance for monitoring water contamination and suitable treatments for water supply.

7.5. Assessment of Groundwater Quality over the Mayurakshi River Basin Area

Groundwater demand in India has risen dramatically due to rapidly population expansion, growing industry, and urban growth (Yisa and Jimoh 2010). According to Panda and Sinha (1991) and Kavitha et al. (2019a, 2019b), inappropriate waste dumping (industrial, domestic, and agricultural) into groundwater reservoirs and overexploitation are seriously affecting groundwater availability and quality at an alarming rate. As a result, the current agricultural practises pose significant risks to human health, especially in regards to the overuse of fertilisers, unhygienic conditions, and sewage discharge into groundwater (Panigrahi et al. 2012). The World Health Organisation (WHO, 2017) estimates that roughly 80% of all human illnesses are water-borne. Once the groundwater is polluted, it is challenging to restore and maintain its proper quality by removing the pollutants at the source. Therefore, it becomes crucial to constantly check the quality of groundwater and devise strategies for keeping it safe from contamination. The evaluation of the water quality is based on a variety of factors, including physical, chemical, and biological properties. It is challenging task to draw conclusions about the water quality from the analysis of such a huge number of parameters. A challenging obligation is having a lot of parameters. It is necessary to combine a variety of characteristics into a single composite value in order to simplify this challenging operation and retain the scientific validity of the water quality summary. It is necessary to create a water quality index (WQI) that can be used globally to measure the suitability of water for human consumption.

In this regard a number of water quality indices are utilised mainly to determine whether water is acceptable for potable use. The most widely used indices around the world include CCME WQI were created by the Canadian Council of Ministers of the Environment to evaluate the water quality for drinking, irrigation, and recreational uses (CCME 2001). The use of WQI in conjunction with GIS to determine whether groundwater is suitable for drinking is a fantastic approach to depict water quality and identify the causes of quality decline (Selvam et al. 2013; Wagh et al. 2016a, 2017a; Vasant et al. 2016; Mukate et al. 2015). However, each indicator has advantages and disadvantages that restrict its usefulness and applicability. Numerous indices have been developed that rely on parameter selection, scaling down to sub-index values, weighting, and aggregation (Horton 1965; Abbasi and Abbasi 2012; Studian et al. 2016). Typically, parameters are equalised or weighted based on their perceived significance to overall water quality (Vasanthavigar et al. 2010). Few indices favour equal weights, but the majority support unequal weights since each characteristic affects water quality differently. It is crucial

to weight the factors according to how much water is used for drinking, residential usage, or irrigation because excessively weighted parameters have the potential to negatively impact the index's sensitivity. As a result, minor changes in weight distribution will have impact on the overall perception of water quality. Therefore, a globally recognised water quality index (WQI) that is adaptable enough to describe the appropriateness of drinking water is needed.

Following the methodology outlined by Mukate et al. 2019, the current work includes an objective water quality index based on the physicochemical and biological parameters connected to the current Bureau of Indian Standard water quality standards for determining the quality of drinking water. Traditional WQI evaluates desired or permissible limits as the standard allowable limit; however, in this study both limits are taken into account to avoid any ambiguity surrounding the adoption of standard values. The Integrated Water Quality Index (IWQI) is the name given to the index since it measures the overall improvement in the index value regardless of whether a parameter's concentration is above or below desired or permissible limits. In accordance with this idea, the IWQI has been divided into five categories: excellent (<1), good (1-2), marginal (2-4), bad (3-5), and unsuitable (> 5); this classification is based on the concentration of physicochemical and biological parameters in the groundwater samples that were collected.

7.5.1. Methodology

In this study, groundwater samples were taken from 228 villages that were randomly chosen from the total number of gram panchayats (423 GP's), which encompass the whole Mayurakshi River Basin area (Fig. 7.38). The wells and tube wells (depths range from 80 to 200 feet) that are mostly used by the nearby communities as drinking water sources are chosen for the sample collection. The study was carried out in 2021 prior to the monsoon season, and sample collection, preservation, and transportation to the lab were completed in accordance with American Public Health Association standards (APHA 2017). With the use of the Garmin eTrex global positioning system, the sample sites were geo-tagged as shown in the plate no 7.7.

After running the tube well for approximately 5 minutes, samples from the production tube wells has been collected in a 1L of washed polypropylene bottles (made by Tarson, India) for the physico-chemical examination. For bacteriological analysis, a different set of samples were gathered in 100 ml High-Density Polythene (HDPE) bottles. A sterilisation of the collection point has been done before collecting the samples. Finally, all samples were placed in a portable

ice box and brought to the laboratory at the Jadavpur University School of Water Resources Engineering.

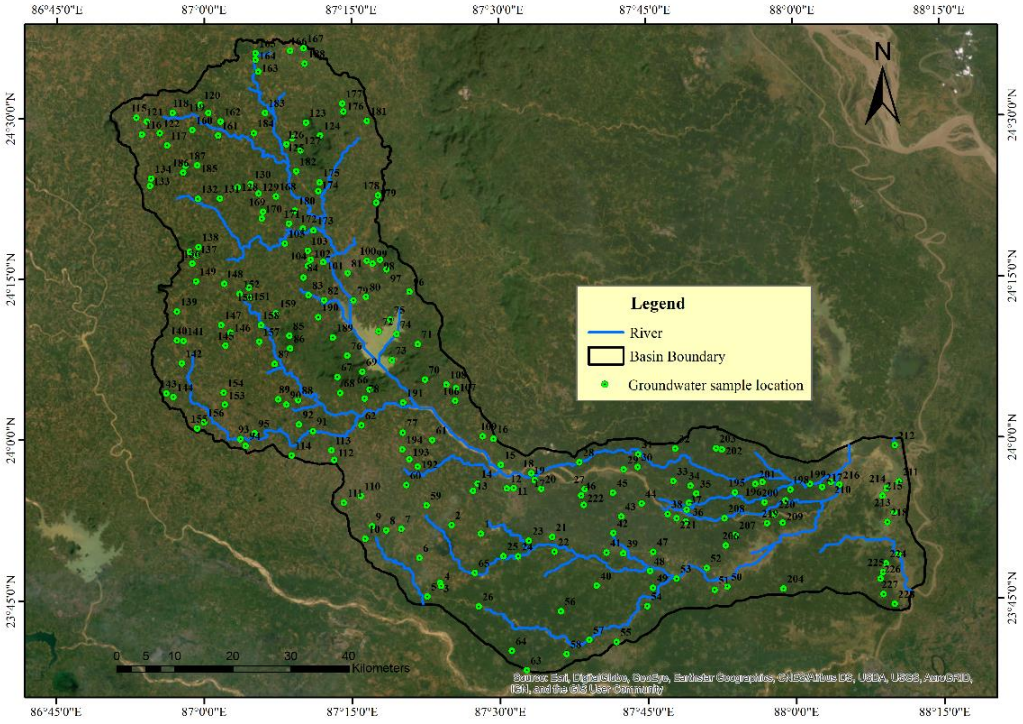

Figure 7.38 *Location of the Sample Sites of Groundwater Quality Analysis within the Mayurakshi River Basin Area*

In the current study, a total of 16 groundwater quality parameters were examined in the laboratory using test standard procedures (APHA 2017). Some parameters, such as pH, electrical conductivity (EC), and total dissolved solids (TDS), are assessed at sample sites using portable devices (pH-meters, EC-meters, and TDS-meters). To measure total suspended solids (TSS), water samples were filtered using Whatman 42 filter paper (pore size 2.5 m). Using the Systronics EC meter-306 and the Digital turbidity metre (EIModel-33E), the turbidity of the water samples was measured in the laboratory. Some chemical parameters, such as iron (Fe), nitrate (NO^{-}_{3}), phosphate (PO_4), manganese (Mn), and sulphate (SO_4), were measured in Atomic Absorption Spectrophotometers (AAS) on flame mode with hollow cathode lamps of metal under analysis. Other parameters, such as alkalinity, total hardness (TH), and chloride (Cl), were assessed using volumetric titrations method. The number of coliform bacteria in the sample water has been estimated using the membrane filtration (MF) technique (EPA 2002). During the analytical phase, quality control procedures such as procedural blanks, sample duplicates, and repeating experiments were carried out when needed.

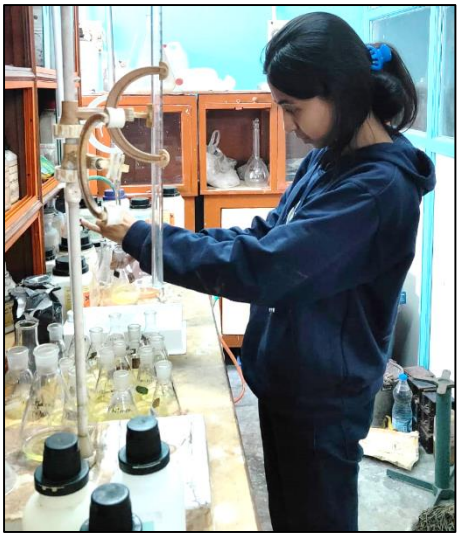

Plate No. 7.7 *Photographs showing Different Phases of Groundwater Quality Analysis*

- **Integrated Water Quality Index (IWQI)**

In view of the IWQI calculation, a total 228 groundwater samples were collected from residential areas of the Mayurakshi River Basin area. A total 12 physicochemical parameters viz., pH, TDS, Turbidity, Alkalinity, Total hardness, Chloride, Iron, Nitrate, Phosphate, Manganese, Sulphate, Fluoride were selected to define the drinking suitability by using IWQI based on their desirable and permissible limits (DL and PL) defined by the Bureau of Indian standards (BIS) 2012 (Table 7.24).

The BIS determines the values of DL and PL for each parameter based on how dangerous they are to human health. Table 7.25 shows the DL, PL, and Range values for the corresponding parameters. The range has been determined using the BIS's permissible and desirable limits (DL and PL). It may be determined mathematically using equation 7.23.

$$Range = Permissible\ limit\ (PL) - Desirable\ limit\ (DL) \qquad (7.23)$$

In the following step the computations of modified permissible limits (MPL) has been calculated by redefining the range of each parameters using the following equation-

$$Modified\ Permissible\ Limits\ (MPL) = Permissible\ limit\ (Pl) - 20\%\ of\ range \quad (7.24)$$

Here, the 20% deficiency of the range of the relevant parameter (Table 7.25) has been chosen to warn of the issue before it reaches the threshold level of pollution because, once the aquifer is contaminated, it is very difficult to restore them to their original state (Table 7.25). This deficiency percentage is quite adaptable and can be modified to suit user needs.

Table 7.24 *Drinking Water Quality Standards and Calculated Range Value (BIS 2012)*

Parameters	Unit	Desirable Limit (DL)	Permissible Limit (PL)	Range	Modified PL (MPL)
pH	-	6.5	8.5	2	8.1
Electronic Conductivity (EC)	µs/cm	750	3000	2250	-
Total Dissolved Solids (TDS)	mg/l	500	2000	1500	1700
Turbidity	NTU	1	5	4	4.2
Alkalinity	mg/l	200	600	400	520
Total Hardness (TH)	mg/l	200	600	400	520
Chloride (Cl)	mg/l	250	1000	750	850
Iron (Fe)	mg/l	0.3	-	0.3	0.24
Nitrate (NO^-_3)	mg/l	-	45	45	36
Phosphate (PO_4)	mg/l	-	0.1	0.1	0.08
Manganese (Mn)	mg/l	0.1	0.3	0.2	0.26
Sulphate (SO_4)	mg/l	200	400	200	360
Fluoride	mg/l	1	1.5	0.5	1.4

In the next step the sub index (SI) were computed for each parameters. Any parameter concentration that is both below the desirable limit (DL) and over the permissible limit (PL) is not acceptable for drinking. The water quality will be impacted by values below the minimal necessary concentration and over the modified permitted limit (MPL), whereas values between DL and MPL can be assumed to be ideal for consumption.

The sub index (SI) will be zero if the observed value of the i^{th} parameter (Pi) is greater than DL but less than MPL. If the value of the i^{th} parameter is smaller than the desired allowed limit, then the following equation has been applied.

$$SI = \frac{(DL-Pi)}{DL} \tag{7.25}$$

On the other hand, the following equation has been used to calculate if Pi is more than the modified permissible limit (MPL), that is, if Pi>MPL.

$$SI = \frac{(Pi-MPL)}{MPL} \tag{7.26}$$

The total of all sub-indices (SI) of each sample derived from the aforementioned equations is used to determine the final IWQI, which is represented by the following equation. IWQI scores are categorised in accordance with Table 7.25's classification.

$$IWQI = \sum_{j=1}^{n} SIij \tag{7.27}$$

SIi j=Sub-index value of the j^{th} water quality parameter for the i^{th} sample.

Table 7.25 *Classification criterion of IWQI.*

WQI Value	Class	Status
<1	Excellent	Excellent for drinking
1-2	Good	Good for drinking
2-3	Marginal	Acceptable for domestic usage
3-5	Poor	Not suitable for drinking
>5	Unsuitable	Unacceptable

7.5.2. Result and Discussion

- **Analysis of Groundwater Quality Parameters**

Utilising the Integrated Water Quality Index (IWQI) and the chosen criteria given below, the groundwater quality of the Mayurakshi River Basin area has been evaluated in this study. The drinking water standards set by the Bureau of Indian Standards (BIS 2012, 2015) have been used as an outline in this investigation. With the aid of ArcGIS software 10.3, the inverse distance weighted (IDW) interpolation approach was employed to represent the geographic variation of each parameter, as shown in figure 7.39a–t.

Considering hydrogen ions (pH) and other chemical components of water are intimately related, is a key indicator for determining the purity and level of pollution in any aquifer system. The pH range in the current study ranges from 6.89 (lowest) to 8.11 (highest), which is within the permissible range (6.5-8.5) and indicates the alkaline character of groundwater (the recommended pH range for human consumption is 6.5-8.5) (Table 7.26). The ability of any substance or solution to conduct electrical energy through water is known as electronic conductivity. EC is inversely correlated with the amount of dissolved matter in a water sample. For drinking purposes, EC should not exceed 750 S/cm. The electrical conductivity in this study ranges from 142 to 1240 S/cm (Table 7.26). Due to their proximity to extensive urbanisation, some sites with high EC indicate that sewage has been diluted in the groundwater. When a water sample is evaporated to a dry condition, the weight of the residue is expressed by the total dissolved solids (TDS) in the water sample. It consists of sulphate, chloride, magnesium, sodium, potassium, carbonate, and bicarbonate. It varies in the current study from 71 to 665 mg/l (500 mg/l TDS for drinkable water according to BIS) (Table 7.26). The main sources of TDS include agricultural practises, household runoff, soil contamination caused by leaching, and point source water pollution discharge from industrial or sewage treatment plants (Boyd 2000).Particles suspended or dissolved in water that scatter light and make the water look foggy or unclear are the source of turbidity. Sediment, particularly clay and silt, fine organic and inorganic materials, soluble coloured organic compounds, algae, and other microscopic organisms are examples of particulate matter. Nephelometric Turbidity Units (NTUs) are used to measure turbidity. In this study, the majority of the sample sites indicated a positive connection between TSS and transparency to turbidity. The spatial variation of all the parameters were represented in figure 7.39a-t.

The amount of carbonate, bicarbonate, and hydroxide ions in water is referred to as total alkalinity in groundwater. Alkalinity in drinking water should not exceed 200 mg/l; else, the flavour will become unpleasant. Alkalinity levels in the study region are between 20 and 422 mg/l, which are within the acceptable range (600 mg/l) (Table 7.26). However, overall hardness refers to the amount of dissolved calcium and magnesium in the water. Water is a strong solvent for calcium and magnesium, so as it moves through soil and rock, it dissolves naturally occurring minerals and transports them into the groundwater. The hardness ranges in this study from 44 to 440 mg/l, which is within the permitted limits (600 mg/l) (Table 7.26). The high levels of TH in groundwater have been linked to kidney stones and heart disease in humans. The concentration of chloride (Cl) in the current study ranges from 11.99 to 211.99 mg/l, which is within the permitted limit (250 mg/l) (Table 7.26). The weathering of iron-bearing minerals and rocks is one of the most frequent sources of iron in groundwater. The iron is present in the aquifer naturally in the reduced Fe^{2+} state, but its dissolution raises the concentration of iron in groundwater. This kind of iron is soluble and normally poses no health risks. If the Fe^{2+} state is converted to the Fe^{3+} state in the presence of oxygen from the atmosphere or by the activity of iron-related bacteria that produce insoluble hydroxides in groundwater. As a result, the levels of iron in groundwater are frequently higher than those found in surface water. The iron levels in the current study vary from 0.01 to 3.7 mg/l, above the permitted limit of 1.0 mg/l (BIS 2015) (Table 7.26). According to Egereonu and Nwachukwu (2005), nitrate ion causes methemoglobinemia in infants younger than 6 months of age, hence it is undesirable to have groundwater containing this ion. In general, if the concentration is higher than the allowed limit of 45 mg/l, it poses health risks (Kumar et al. 2012, 2014). Its content in the studied region ranges from 0 to 41.50 mg/l which proves the entire study region is within the permitted range (Table 7.26). The concentration of phosphate has been found within a range of 0 to 1.48 mg/l which is exceeded from the permissible limit (0.1 mg/l) as per WHO standard (Table 7.26). The chemical composition of the rainfall, the lithology of the aquifer, the geochemical environment, the flow pathways and residence times of the groundwater, etc. all affect the concentrations of Manganese in the groundwater, and these factors can change dramatically over time and place. In addition to from the minerals of the aquifer itself in groundwater, it may also be released through the leaching of minerals from the underlying rocks and soils as well as from the overlying soils. Manganese levels in the current study range from 0.00 to 1.46 mg/l, which is higher than the allowed limit of 0.3 mg/l (Table 7.26). In addition to gypsum, iron sulphides, and other sulfur-bearing compounds, sulphate is a crucial characteristic that is dissolved and leached from rocks. The range in the

current study is 2.25 to 79 mg/l, which is substantially below the 200 mg/l acceptable limit (Table 7.26). Fluoride in groundwater is a geogenic substance. Because of the interaction between groundwater and host rock, fluorides are released from various fluoride-bearing minerals into the groundwater. Fluoride levels in the current study are between 0.05 to 1.06 mg/l, which are within the allowable limit of 1.5 mg/l (Table 7.26).

Table 7.26 *Descriptive Statistics of Groundwater Samples (n=228)*

Parameters	Unit	Minimum	Maximum	Mean	Standard Deviation
pH	-	5.62	7.69	7.10	0.29
Total Dissolved Solids (TDS)	mg/l	71	665	0.0009	0.0096
Turbidity	NTU	0	397	260	134.02
Alkalinity	mg/l	20	420	2.60	8.27
Total Hardness (TH)	mg/l	44	440	169.34	70.12
Chloride (Cl)	mg/l	12	212	198.89	81.03
Iron (Fe)	mg/l	0	4	50.82	47.84
Nitrate (NO^{-}_{3})	mg/l	0	42	0.64	0.85
Phosphate (PO_4)	mg/l	0	1	1.49	4.02
Manganese (Mn)	mg/l	0	1	0.15	0.31
Sulphate (SO_4)	mg/l	3	3	0.17	0.36
Fluoride	mg/l	0	1	2.50	0
IWQI	-	3.21	108.04	0.36	0.23

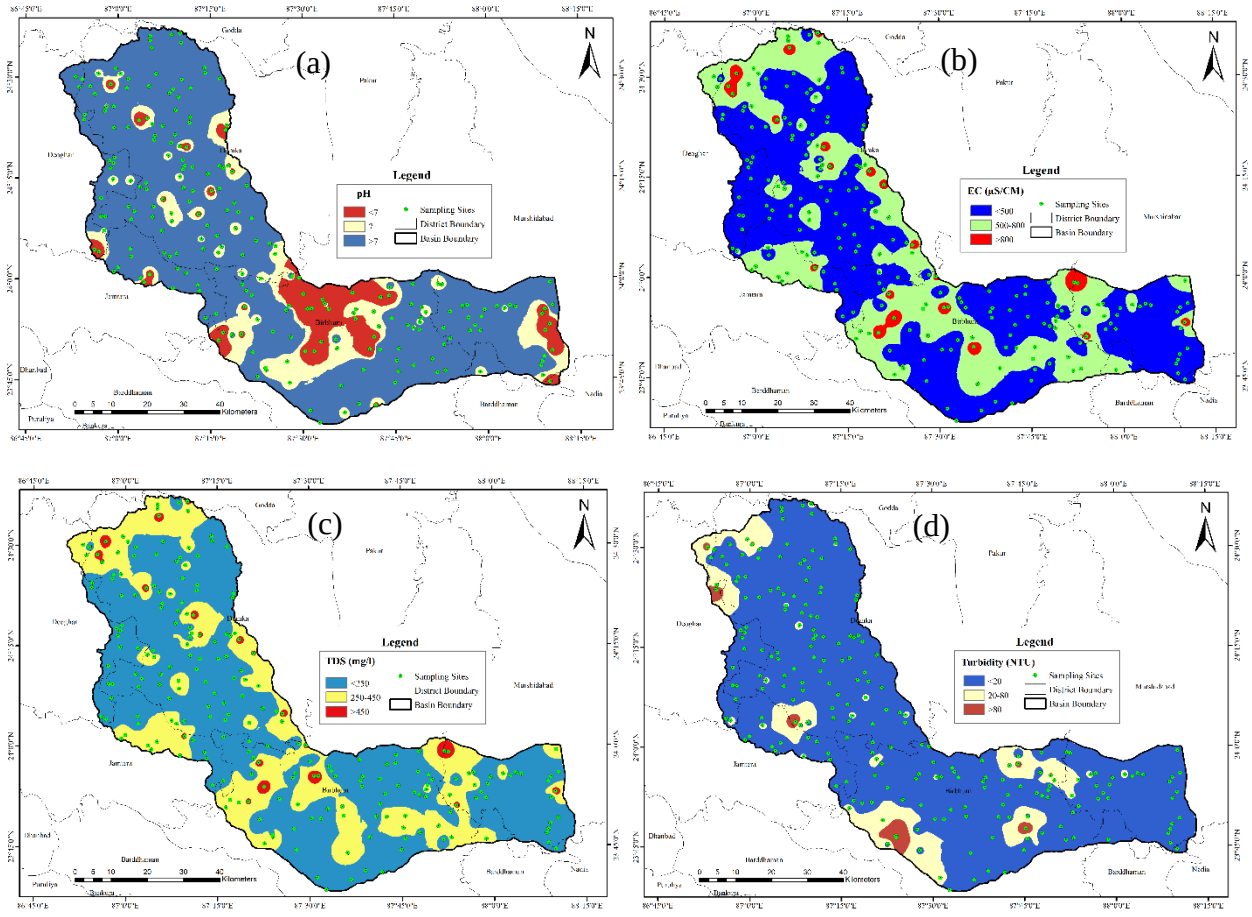

Figure 7.39 *Spatial Distribution of Groundwater Quality Parameters (a) pH (b) EC (c) TDS (d) Turbidity (e) TSS (f) Alkalinity (g) Total Hardness (h) Iron (i) Chloride (j) Nitrate (k) Phosphate (l) Manganese (m) Sulphate (n) Fluoride*

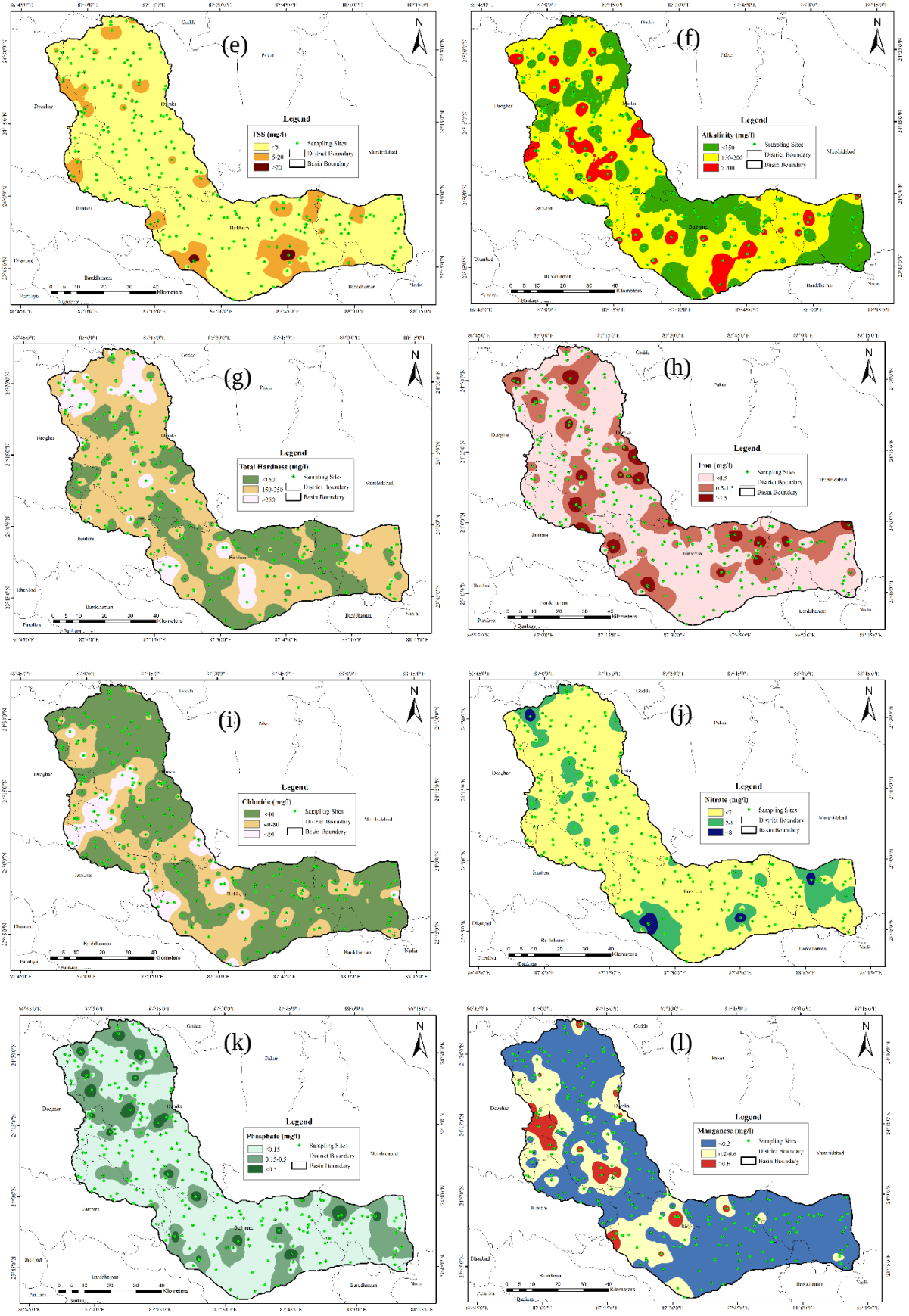

Figure 7.39 *Continued*

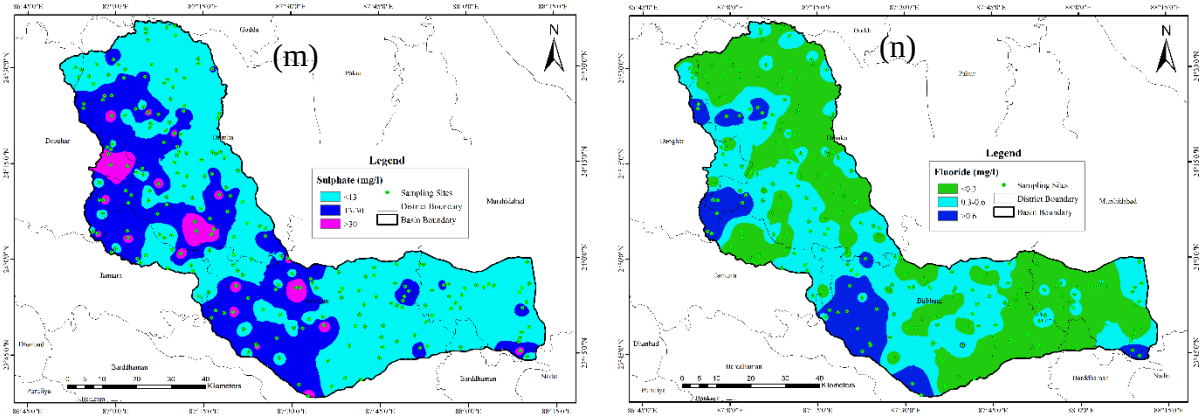

Figure 7.39 *Continued*

Rural parts of the Mayurakshi River Basin struggle with a serious public health issue caused by bacterial contamination of drinking water. Drinking water may contain pathogens that can cause diarrhoea, vomiting, cramps, nausea, and other intestinal diseases if coliform bacteria are present in it. Open defecation, livestock manure, penetration of faecally polluted water from neighbouring latrines, insufficient protection of water sources, and improper management of sources appear to be the main contributors of faecal contamination in drinking water sources. According to the WHO, the health risks associated with E. coli levels in drinking water fall within five categories: conformance (0 cfu/100 ml), low risk (1–10 cfu/100 ml), intermediate risk (10–100 cfu/100 ml), high risk (100–1000 cfu/100 ml) and extremely high risk (>1000 cfu/100 ml). Some of the drinking water sources in this study region have been found to have coliform bacteria, which pose a considerable danger to human health. These bacteria range in number from 10 to 300 cfu per 100 ml. The majority of water sources were down slope of high ground, and settlements and latrine facilities at elevated ground raised concerns that latrine excreta leaching could negatively affect underlying groundwater resources that households rely on for their domestic water supply.

- **Analysis of Integrated Water Quality Index**

The current index is based on the desired and allowed limits of pH, TDS, Turbidity, Alkalinity, Total Hardness, Chloride, Iron, Nitrate, Phosphate, Manganese, Sulphate, and Fluoride established by the BIS. Table 7.26 provides an illustration of the IWQI's descriptive data. The range of the IWQI value is 0.21 to 105.04. Figure 7.40 shows that only 3.95% samples were categorised in an excellent quality of drinking water, 14.47% samples were under good quality of drinking water and 18.86% were marginally suitable for drinking purposes. Majority of the samples were classified under poor (24.56%) and unsuitable (38.16%) for human consumption.

The IWQI value between 3 and 5 indicates that anthropogenic activities have an impact on water quality, limiting their suitability for drinking. This is primarily due to excessive concentrations of Na, Cl and SO4 from domestic activities, which are caused by the lack of concrete sewerage lines, inadequate sanitary seals, and ineffective casing (Mukate et al. 2018).

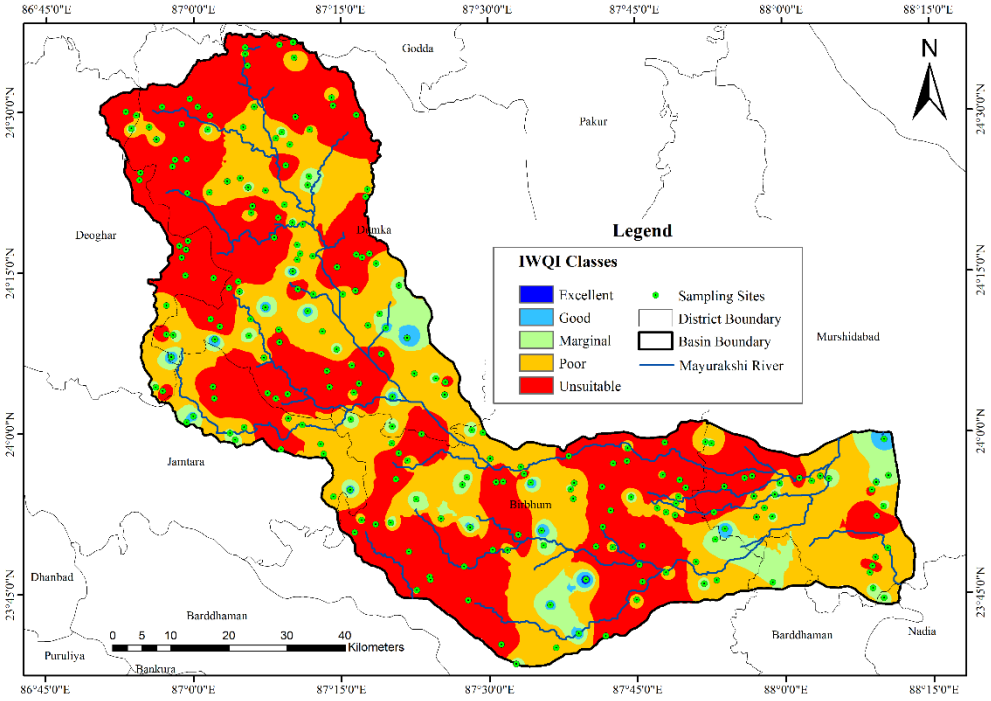

Figure 7.40 *Spatial Distribution of Integrated water Quality Index in Mayurakshi River Basin Area*

Using the IDW approach in the ArcGIS environment, the spatial variation map of IWQI values was created (Fig. 7.40) to show the spatial distribution of water quality across each area. This map was shown to be useful in identifying the research area's locations with good, marginal, and vulnerable water quality in order to improve water resource management. According to figure 7.40, samples of high-quality water are found far from the largest urban centre, indicating that the area is less polluted. The upper and middle portions of the catchment region, which are primarily impacted by agricultural runoff because of the predominance of agriculture, are where the poor drinking water quality is most frequently seen. The poor sealing of bore wells and dug wells results in the mixing of waste materials into the aquifer system, which degrades the quality of groundwater. Additionally, poor sanitation practises, home sewage disposal, and open defecation are to blame for the research area's declining groundwater quality.

7.5.3. Conclusion

Health declines as a result of ion deficiency and excess concentration. As a result, it is critical to evaluate the water quality in terms of the ionic content of several physicochemical parameters. The BIS-established health standards for water quality are represented by the IWQI. This index does not have issues with uncertainty, eclipsing, or grouping that are included in traditional WQI. IWQI only concentrates on the ions that are present in water and how important they are to the human body. It has been noted that in the Mayurakshi River Basin area, agriculture and inappropriate hygienic practises are the main causes of groundwater quality degradation.

The results of the current study also show that anthropogenic and geogenic activities have both contributed to the groundwater's deterioration. Along with agricultural runoff leaching, additional human activities like unlined septic tanks and uncontrolled sewer systems have increased the amount of nitrate in groundwater and reduced the quality of the water for human use.

7.6. An Assessment of Environmental Flows (EFs) Requirements of Mayurakshi River Basin Area

India is confronted with a number of water-related difficulties, including rising water scarcity and conflict for water among various sectors of the economy. Due to periodic rainfall and extended dry spells, India's extensive network of rivers, which serve as the primary source of freshwater, exhibit very substantial seasonal variation in their discharge. The majority of India's rainfall only happens from June to September because of the southwest monsoon's influence. In addition to seasonal variations, the surge in population expansion and the stimulation of industrial development during the past 50 years have resulted in an unprecedented demand for water in both developed and developing nations. Since achieving its independence, India has experienced tremendous urbanization, industrialization, and agricultural intensification, all of which have had various effects on the rivers. The majority of Indian rivers are currently subject to strict regulations (Agrawal and Chak 1991). There have been many barrages built to divert water, as well as hundreds of multipurpose reservoirs for agriculture, hydropower, fisheries, and water supply. The remaining riparian lands are heavily used for intensive agriculture and grazing, and many floodplains have been blocked off from rivers by embankments. All rivers now carry more silt because of human settlements, deforestation, mining, and other activities that have further damaged river catchments. Additionally, over the last few decades, rivers have been receiving progressively larger discharges of industrial effluents, fertilizers, and pesticides from agricultural operations, as well as household garbage (CPCB 1996). Because of these actions, flow regimes have been significantly altered, mostly by decreasing overall flow and changing the unpredictability and seasonality of flows. Environmental deterioration has also been triggered in addition to the altered flow regime of the rivers. The construction of embankments has resulted in the loss of feeding and breeding sites in the floodplain water bodies (Mukherjee 2005), and increased silt load and macrophytic development are key contributors to decreased fish populations (Jhingran 1991).

River preservation and restoration are now essential for the nation's overall sustainable development. Following this, a number of hydrologists and water resource engineers proposed the idea of a single minimum flow requirement after recognizing the behaviour of diverse components of the riverine ecosystem. Although this term is often used to refer to the minimum amount of water required to maintain the biological diversity and ecological atmosphere of riverine regimes, different countries have defined it differently in accordance with the physical, environmental, social, and hydrological requirements of the relevant region. The word

"environment flow" was finally defined in an appropriate way, and it is now understood to refer to the quality, amount, and timing of water flows necessary to maintain freshwater and estuarine ecosystems, as well as the human livelihood and wellbeing that depend on these ecosystems (World Bank, 2007). Different nations have varying degrees of reservations about the flow of the environment. Nevertheless, the 95% reliable flow of the flow duration curve (FDC) is generally accepted as the minimal environmental flow in a global context.

In India, technical challenges and a lack of data have made it difficult for environmental scientists to work more effectively in the field. However, in recent years, the hydrologist has become much more active and has suggested useful and sensible hydrological-based methods that are appropriate for Indian conditions in numerous research studies.

7.6.1. Conventional Methodologies for Environmental Flows Assessment (EFA)

In recent years, a number of EFA techniques have arisen that either directly or indirectly address the preservation of both spatial and temporal patterns of river flow, and the flow variability that affects the structural and functional variety of rivers and their floodplains. EFs should specify not only how much water is required, but also when and how it should flow in the river. According to Knights (2002), every element of the hydrological regime has some sort of ecological value. For the upkeep of riparian vegetation, bird breeding, wetland flooding, and channel maintenance, high flows of various frequencies are essential. While low flows of various magnitudes are crucial for algal control, maintaining water quality, and locals' use of the river, moderate flows may be essential for the cycling of organic materials from river banks and for fish migration. Thus, under an EFs regime, a variety of flow variability components must be maintained.

Different EFA techniques should be employed for various purposes ranging from monitoring dam releases to planning for water resources management. In this context, the following key categories are included: Detailed evaluation primarily utilizing **holistic techniques** or techniques based on habitat modelling and Rapid desktop based assessment using mostly ecologically important **hydrological variables** (indices) or hydrological time series analysis. When evaluating EF, methods from the first group frequently take a whole-ecosystem approach. In these methods, environmentally and/or socially significant flow events are recognized, and a multidisciplinary panel of experts defines an ecologically acceptable flow regime. These methods are, however, extremely sophisticated and necessitate a large amount of input data as well as field labour. The second group of methods, known as desktop EFA, is

far more varied and better suited for initial, reconnaissance- or planning-level analyses of EF. They can be based on a thorough examination of hydrological time series, as in Richter et al. 1997; Hughes and Hannart 2003; or they can take the form of a look-up table (Tennant 1976; Matthews and Bao 1991). Although the assessment of EFs has experienced a significant paradigm shift in recent years, moving from a single hydrologic attribute (i.e. minimum flows) to a full spectrum of flows (floods, average, and low flows) that take into consideration seasonal, inter-, and intra-annual variance in stream flow variability. Due to the fact that EFs are essential for a river's lifetime and have received increased attention over the past 20 years, more than 240 methods have been developed and are documented in the literature. Although Acreman and Dunbar (2004) noted that depending on the goals for calculating EFs and the hydro-geological condition of a watershed, no developed methodology is thought to be the best and all methods have value. As a result, comparative approaches are the best strategy for providing an evaluation of EFs in rivers or streams because all quantitative method categories have value and their use depends on the degree of protection, environmental objectives, and study aims. Jowett (1997) also noted that hydrological and hydraulic methods can be helpful when there is a lack of knowledge about the environment or when a high level of protection is needed for an existing ecosystem. Based on this idea, several comparative hydrological studies have been carried out globally by researchers for a variety of goals (Pandey and Ramasastri, 2003; Caissie et al. 2007; Shokoohi and Hong, 2011). In this work, Tennant and Flow Duration Curve (FDC), two significant hydrological methodologies, are used to assess the environmental flow variability for Massanjore Dam and Tilpara Barrage in the Mayurakshi River Basin area.

7.6.2. Regulative Nature of Flow in Mayurakshi River Basin (MRB)

River Mayurakshi is a fifth order rain fed tributary of Bhagirathi, with catchment area of 5325 sq. kilometres, length of 288 kilometres, extension of 23° 15' N to 24° 34'15' N Lat. and 86° 58' E to 88° 20' 30' E Long. (Fig. 7.41). The Mayurakshi River Basin (MRB), a well-known name in the West Bengal flood scenario, is situated in the transitional zone between the Bengal basin and the Chottanagpur plateau fringe, two significant physiographic provinces (Konar 2008; Saha, 2011; Bhattacharya, 2013). The river produces twisting motions towards the south-east with the tributaries of Motihari, Dhobi, Pusaro, Bhamri, Tepra, Kushkarani, Sidhweswari, etc. at its upper course after emerging from a spring at the foothills of Trikut Pahar, Jharkhand (O'Malley, 1914). In its lower catchment, a number of tributaries, distributaries, anabranching loops, and spill channels, such the Manikornika, Gambhira, Kana Mayurakshi, Mor, Beli, or Tengramari, form an intricate network and flow into the bottom

pocket of the Hizole wetland in the Murshidabad district. The river Babla begins its voyage from the Hizole wetland and eventually drains into the river Bhagirathi (Mukhopadhyay and Pal, 2009).

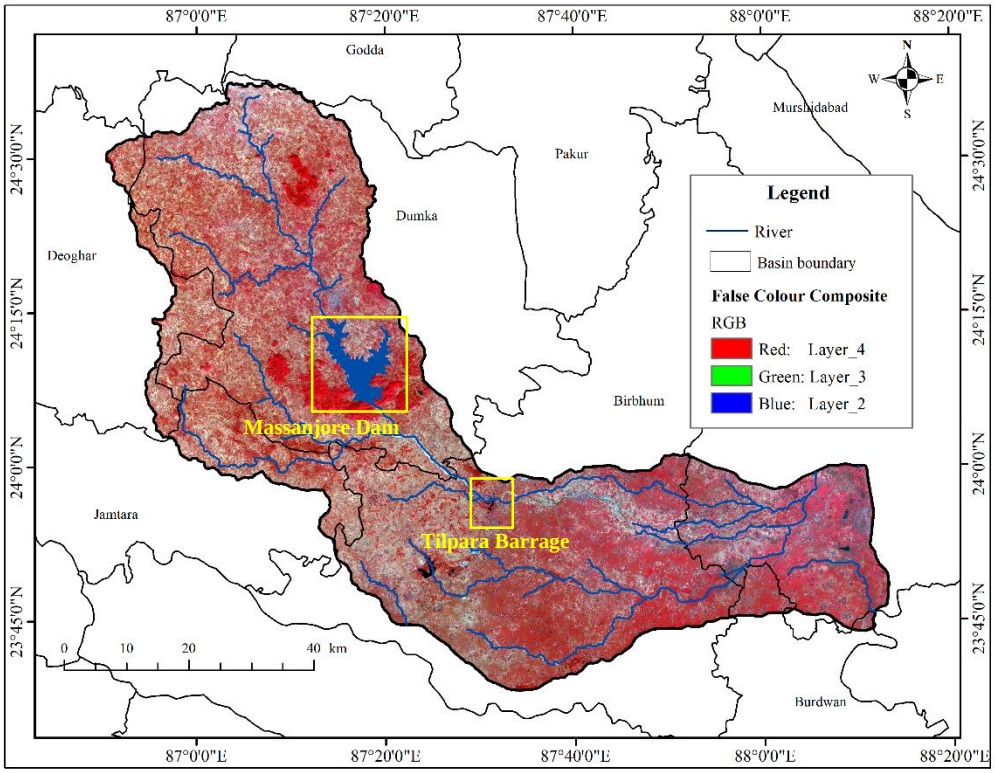

Figure 7.41 *Location of Important Civil Structures of Mayurakshi River*

Plate No. 7.8 *Massanjore/Canada Dam, Build in 1954*

Plate No. 7.9 *Tilpara Barrage, Build in 1976*

Two major river impoundment structures have been constructed on the main channel of the Mayurakshi River, which ultimately regulate the natural flow of the river (Table 7.27). These are Masanjore Dam (661.4 m long and 47.24 m high), built over the Mayurakshi River, and is one of the early post-independence multifunctional river valley projects in Eastern India. It was followed by the construction of Tilpara Barrage to provide irrigation water in the agriculturally promising lower catchment. The Masanjore reservoir has a total area of 67.4 sq. kilometres, a storage capacity of 620,000,000 cubic meters, and an average monsoon release rate of 1.2 lakh cusec. In the extensive areas of this lower section of the current watershed, flooding is a very old occurrence. However, the building of the Masanjore dam in 1954 and the Tilpara Barrage in 1976 (Plate No. 7.8 and 7.9), along with the resulting water storage and diversion projects through the 216.71 km main canal and the 147.07 km branch canal (india-wris.nrsc.gov.in), have resulted in significant changes to river flow and the MRB's dynamic flood character.

Table 7.27 *Structural Details of Massanjore Dam and Tilpara Barrage*

Details	Massanjore Dam	Tilpara Barrage
Location	Near Dumka at Jharkhand	Near Suri, Birbhum district, West Bengal
Distance from source	99.26 km from the source of Mayurakshi River	148 km from the source and 49 km from the Massanjore Dam
Catchment area	1859 sq. km.	3,208 sq. km.
Full reservoir level	398.09 ft. (121.34 m.)	212.04 ft. (64.63 m.)
Design discharge	157,032 Cusec (4,446 Cumec)	300,000 Cusec (8,495 Cumec)
Design flood level	402.09 ft. (122.56 m.)	213.62 ft. (65.11 m.)

Mayurakshi canal irrigational project involves irrigation using the Mayurakshi River and the Massanjore Reservoir known as Massanjore Dam or Canada Dam, with a network of canals that runs along both banks of the Mayurakshi River, starting from a weir at Khatanga. The regions along the river's left bank were watered by the North Bank Canal. The region between the rivers Mayurakshi and Dwarka was initially irrigated. It then used a pickup weir at Dwarka to span the river Dwarka, utilizing the water supply there to begin irrigating the land between the Dwarka and the Brahmani. It then spanned the Brahmani via a pickup weir and used the Brahmani's water supply to irrigate the land between the Brahmani and the Pagla. The South Bank Canal began irrigating the land south of Mayurakshi and later the area between Mayurakshi and the Bakreswar in a manner similar to that of the Tilpara barrage. The canal began irrigating the land between the Bakreswar and the Kopai by utilizing the water from the Bakreswar weir. It then used a pickup weir to cross the Kopai and irrigate the land between the Kopai and the Ajoy. The district of Birbhum, Murshidabad, & Burdwan will gain irrigation potential of 3,211.60 sq.km through the completion of this project. Water is also delivered to the state of Bihar (most recently Jharkhand) from the Massanjore Reservoir for irrigation, covering an area of roughly 60 sq. km., in addition to the above-mentioned irrigated area in West Bengal. Within the overall amount of water resources of the Mayurakshi Reservoir Project that are accessible from the Bakreswar pickup weir, the necessity for providing water to the Bakreswar Thermal Power Project has also been fulfilled.

7.6.3. Hydrological Approaches Applied to Evaluate EFs

Two important hydrological methods- Tennant method and traditional Flow Duration Curve (FDC) were used to assess the environmental flow variability of Massanjore Dam and Tilpara Barrage of Mayurakshi River Basin area.

- **Tennant Method**

The Tennant approach also referred to as the Montana method, was developed by Tennant in 1976 as a means of calculating the environmental flow required for aquatic animals. In this method, the river's mean annual flow is the only variable utilized to calculate the environmental flow. Tennant reviewed 58 cross-sections of 11 rivers in Montana, Nebraska, and Wyoming as part of its reviews, and in light of this and by taking the year's overall time situation (in two 6-month periods), the values of environmental flow were suggested based on various ecological conditions, as shown in table 7.28.

Table 7.28 *Recommended Flow Conditions as per Tennant Method*

Description of General Flow Condition	**Recommended base flow regimes (percentage of mean annual flow)**	
	October- March (Non-Monsoon period)	**April-September (Monsoon period)**
Flushing or Maximum	200	200
Optimum range	60-100	60-100
Outstanding	40	60
Excellent	30	50
Good	20	40
Fair or Degrading	10	30
Poor or Minimum	10	10
Severe degradation	<10	<10

Examining this table 7.28 demonstrates how simple it is to estimate the environmental flow using the Tennant method, which is why this approach is frequently employed to estimate environmental flow (Karimi et al. 2021). Specifically, the application of this method should be viewed as an initial estimation when compared to other methods because it results in the selection of two distinct flow values for two six-month periods per year.

Table 7.29 *36 years Mean Monthly Flow (cumec) of Massanjore Dam and Tilpara Barrage*

Year	Station wise Mean Monthly Flow (MMF)			
	Massanjore Dam		Tilpara Barrage	
	Non-Monsoon	Monsoon	Non-Monsoon	Monsoon
1983	11.00	9.71	-	-
1984	21.53	95.03	-	-
1985	23.10	21.68	-	-
1986	19.36	24.67	-	-
1987	39.13	26.30	-	-
1988	21.50	29.94	-	-
1989	26.57	27.38	-	-
1990	15.27	32.04	-	-
1991	32.10	27.38	-	-
1992	23.99	33.01	14.58	73.71
1993	15.66	15.30	31.42	119.40
1994	33.00	29.09	33.13	88.52
1995	23.05	10.37	23.92	134.07
1996	23.28	41.15	15.23	119.01
1997	15.99	7.49	28.62	146.45
1998	13.70	23.70	52.55	188.74
1999	20.74	17.03	60.52	301.47
2000	35.16	39.25	24.04	362.13
2001	14.14	21.19	53.25	118.89
2002	28.76	30.84	25.98	148.77
2003	20.51	26.49	73.36	103.42
2004	32.64	27.89	82.96	123.36
2005	17.42	34.10	35.05	44.48
2006	17.66	21.70	18.31	229.45
2007	15.44	18.75	24.29	206.36
2008	27.34	28.26	18.42	171.11
2009	33.88	8.96	23.20	92.04
2010	8.93	6.98	19.46	62.86
2011	19.97	15.65	10.72	89.14
2012	11.16	13.26	16.83	57.34
2013	1.15	7.82	56.26	70.99
2014	27.04	39.87	21.97	81.37
2015	12.82	47.61	12.96	136.33
2016	15.44	14.38	24.61	94.68
2017	21.66	17.54	39.22	133.57
2018	-	-	22.68	78.45
2019	-	-	22.98	78.45

According to the Tennant technique, mean monthly flows of the Massanjore Dam (1983–2017) and the Tilpara Barrage (1992–2019) were utilized in this work to estimate the environmental flow in the river (Table 7.29). The Tennant technique proposes a different percentage of mean

annual flow as an environmental flow, which is depend on the ideal ecological conditions for both the time of year (two six-month periods). The recommended percentage of mean annual flow corresponding to different habitat condition of the selected sites are represented in table. For allocating water to flush out sediment deposits and maintain the morphology of the river system and its overall health, water resource managers and planners can utilize this table 7.30. The lower results for each of the stations (taking into account both upstream- Massanjore Dam and downstream- Tilpara barrage) show that the health, water quality, and ecosystem of the river system are being severely or poorly degraded. As recommended by Tennant, flushing, optimal range, and outstanding flows are helpful for removing pollutants and sediments from the river system. However, if sediment deposits cause the flow to be impeded, this could affect the biological balance of the basin. Excellent and good flows are defined as flows that allow the ecosystem to function normally with minimal alteration. The lowest class, or minimum flow, is thought to be below which the basin would suffer catastrophic deterioration, harming the entire ecosystem. The analysis reveals that, according to the long-term mean annual flow of the Massanjore and Tilpara barrages (23.3 and 81.09 cumec), the recommended percentage of mean monthly flow of the best ecological condition is not always achieved. For both the high flow and low flow seasons, the mean monthly flow for the years 1998, 2010, 2012–2013, and 2015 did not meet the requirement of 60–100% of the mean annual flow. For both of the analysed stations in the Mayurakshi River Basin area, a poor to substantially degraded flow condition is present nearly every year (Table 7.31). Such findings offer comprehensive data that may be utilized to calculate the water supply, the water demand for anthropogenic and ecological purposes, and the amount that can be withdrawn in the near future in relation to the intended anthropogenic change and its effects.

Table 7.30 *Comparison of Recommended EFs in cumec for Massanjore Dam and Tilprara Barrage assessed through Tennant Method*

Recommended Flow Regimes	**Sations**	**Massanjore Dam**		**Tilpara Barrage**	
	Period of Record	**1983-2017 (34 yrs.)**		**1992-2019 (27 yrs.)**	
	Mean Annual Flow (MAF) in cumec	23.31		81.09	
Flushing or Maximum	October- March (200% of MAF)	46.62		162.18	
	April-September (200% of MAF)				
Optimum range	October- March (60-100% of MAF)	13.986	23.31	48.654	81.09
	April-September (60-100% of MAF)				
Outstanding	October- March (40% of MAF)	9.324		32.436	
	April-September (60% of MAF)	13.986		48.654	
Excellent	October- March (30% of MAF)	6.993		24.327	
	April-September (50% of MAF)	11.655		40.545	
Good	October- March (20% of MAF)	4.662		16.218	
	April-September (40% of MAF)	9.324		32.436	
Fair or Degrading	October- March (10% of MAF)	2.331		8.109	
	April-September (30% of MAF)	6.993		24.327	
Poor or Minimum	October- March (10% of MAF)	2.331		8.109	
	April-September (10% of MAF)				
Severe degradation	October- March (<10% of MAF)	<2.331		<8.109	
	April-September (<10% of MAF)				

Table 7.31 *Year Satisfying the Different Environmental Flow Conditions for Massanjore Dam and Tilpara Barrage*

Recommended Flow Regimes	Seasons	Massanjore Dam	Tilpara Barrage
		Year satisfied the required flow condition	
Flushing or Maximum	October- March (200% of MAF)	-	-
	April-September (200% of MAF)	1984, 2015	1998-99, 2000, 2006-08
Optimum range	October- March (60-100% of MAF)	1984-1997, 1999-09, 2011, 2014, 2016-17	1998-99, 2001, 2003-04, 2013
	April-September (60-100% of MAF)	1984-96, 1998-08, 2011, 2014-2017	1992-04, 2006-19
Outstanding	October- March (40% of MAF)	1983-09, 2011-12, 2014-17	1994, 1998-99, 2001, 2003-05, 2013, 2017
	April-September (60% of MAF)	1984-94, 1996, 1998-08, 2011, 2014-17	1992-04, 2006-19
Excellent	October- March (30% of MAF)	1983-12, 2014-17	1993-94, 1997-99, 2001-05, 2013, 2016-17
	April-September (50% of MAF)	1984-94, 1996, 1998-08, 2011-12, 2014-17	1992-2019
Good	October- March (20% of MAF)	1983-12, 2014-17	1993-95, 1997-10, 2012-14, 2016-19
	April-September (40% of MAF)	1983-96, 1998-08, 2011-12, 2014-17	1992-2019
Fair or Degrading	October- March (10% of MAF)	1983-12, 2014-17	1992-2019
	April-September (30% of MAF)	1983-12, 2014-17	1992-2019
Poor or Minimum	October- March (10% of MAF)	1983-12, 2014-17	1992-2019
	April-September (10% of MAF)	1983-2017	1992-2019
Severe degradation	October- March (<10% of MAF)	1983-2017	1992-2019
	April-September (<10% of MAF)	1983-2017	1992-2019

- **Flow Duration Curve Method**

An appropriate way for calculating the environmental flow is to use flow duration curves, which can offer useful information on the pattern of river flow fluctuations (Zhang 2017). Researchers frequently take into account the utilization of flow duration curves in environmental flow prediction because of their nature (Verma et al. 2017).

One of the finest ways to show the whole range of river discharges, from low flow events to flood events, is with a flow duration curve. When there is a deficiency in the flow data, the flow Duration Curve technique (FDC) will be applied. This technique aids in determining the environmental flow by graphing the discharge versus the percentile of exceedance. The 34 years of Massanjore Dam inflow data (1983–2017) and the 27 years of Tilpara Barrage inflow data of the Mayurakshi River have been used to assess the environmental flow requirement from FDC in this case. Several indicators were employed for the evaluation of minimal environmental river flow, ranging from Q50 to Q95, in relation to the application of the flow duration curves (McClain and Anderson 2015; Elhatip and Hinis 2015; Ghanbarpour et al. 2013). These indicators are provided for specific purposes; for instance, the Q95 indication of minimal flow is used to safeguard rivers (Shenton et al. 2011; Acreman et al. 2008; Piniewski et al. 2014) and the Q50 indicator is used to maintain aquatic biota (Ghanbarpour 2013). The minimum flow in this study will be determined by the Q95 value in order to protect the river. The following steps were taken to calculate flow duration curves:

The statistical flow data were sorted into descending order to plot the flow duration curves. To put it another way, the greatest number was rated one. The probability value is then displayed against these flows. The Weibull plotting equation (Eq. 7.28) was used to calculate the Percentage of Exceedance (Pp), also known as the exceedance likelihood of the occasion P (Subramanya, K. 2013).

$$P_p = \frac{m}{N+1} * 100\% \tag{7.28}$$

Where, n refers to the number of observations and m is the rank of the corresponding flow events.

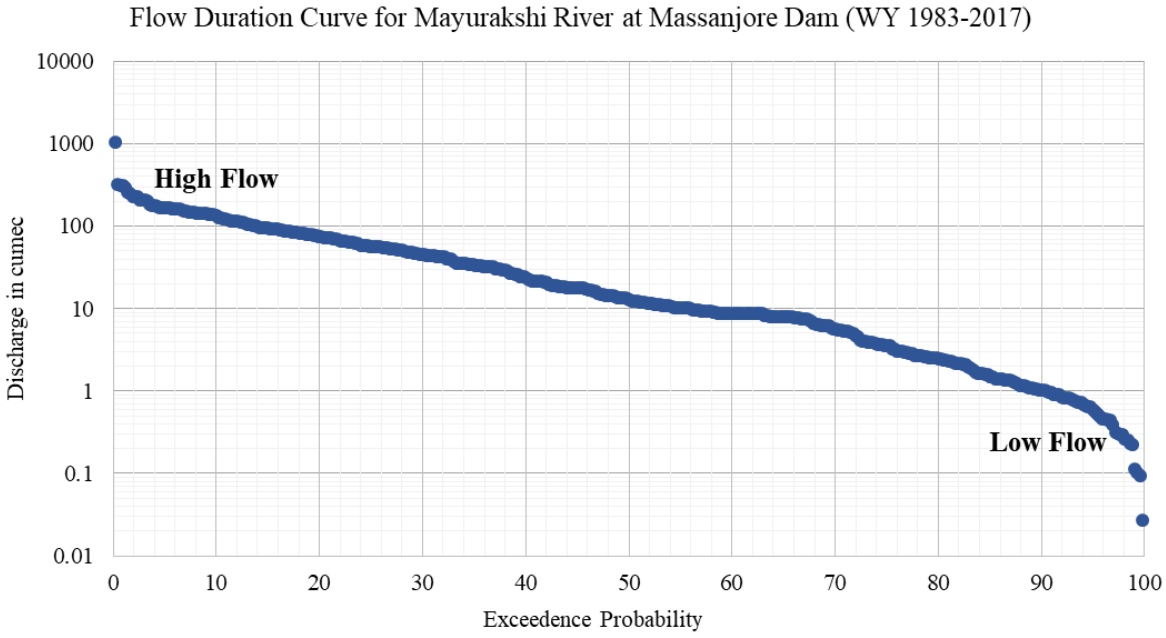

Figure 7.42 *FDC at Massanjore Dam (1983-2017)*

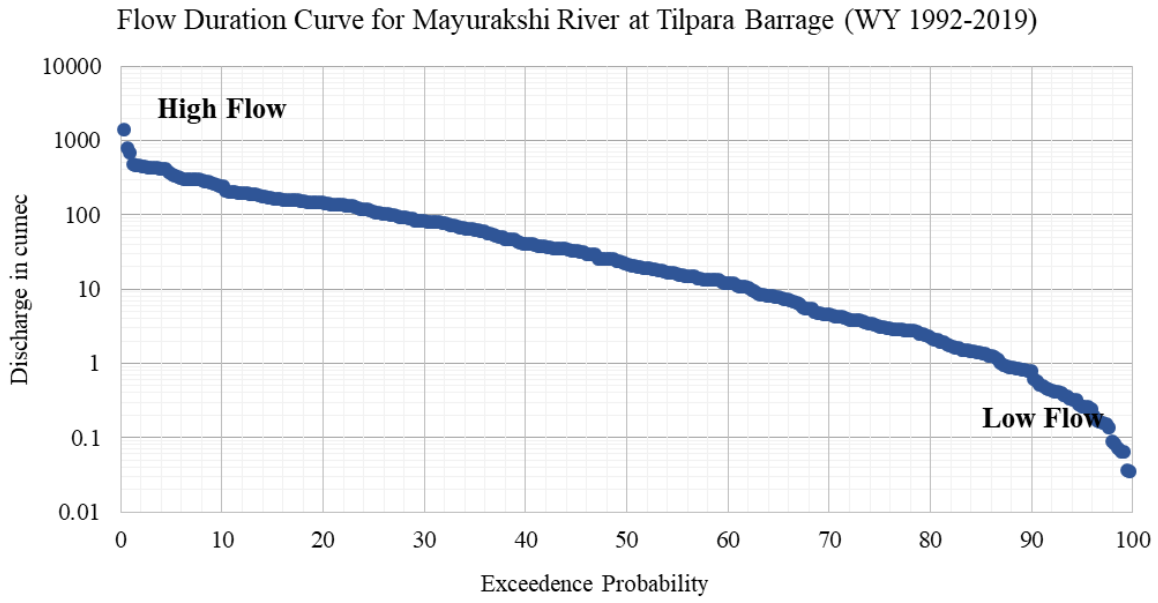

Figure 7.43 *FDC at Tilpara Barrage (1992-2019)*

Monthly FDC at each monitoring site is shown in figure 7.42 and 7.43. It was found that the computed monthly FDCs at each site had varied shapes, which may have been caused by variations in the amount of precipitation, the characteristics of the watershed, meteorological conditions, urbanization, and water demand. The graph shows that, when the lowest flow of

Q95 is taken into account, the Q95 of the FDC value ranges from 0.58 cumec in the Massanjore dam to 0.26 cumec in the Tilpara Barrage.

7.6.4. Conclusion

Two hydrological methods are used in this study to offer the preliminary EFs recommendations: (i) Tennant and (ii) FDC in the MRB. The findings indicate that the rivers' current discharge does not satisfy the ideal flow conditions for preserving the biological and physical environment of the Mayurakshi River Basin area.

These techniques are fundamental ones where there is a lack of ecological and hydraulic data. It is challenging to identify minimum flow thresholds in many freshwater ecosystems around the world due to a lack of eco-hydrological data. Because neither the flow magnitude calculated by Tennant nor the duration calculated by FDC analysis have a consistent link to habitat or productivity across a variety of stream geomorphology, the flow suggestions in this study are frequently taken as direct observations. As a result, it is likely to produce monotonous and uninteresting results, and there is no opportunity for incorporating other related factors, such as ecology, biodiversity, riverine communities, etc. Therefore, a more effective methodology is required that may be used to characterize the correlations between discharge and width, discharge and depth, and discharge and velocity. Therefore, it is determined that not all types of watershed are suitable for using straightforward historical-based methodologies to assess EFs requirements. As a result of the anticipated human alteration and its effects, the data gained offer extensive information that can be used to estimate the water supply, the water demand for both anthropogenic and ecological purposes, and the quantity that can be withdrawn in the near future.

References

- Abbasi, T., & Abbasi, S. A. (2012). *Water quality indices*. Elsevier.
- Abbaspour, K. C. (2015). SWAT calibration and uncertainty programs. *A user manual*, *103*, 17-66.
- Abbaspour, K.C., et al., 2007. Modelling hydrology and water quality in the pre-alpine/ alpine Thur watershed using SWAT. J. Hydrol. 333 (2–4), 413–430.
- Abdul Hameed M Jawad, A., Haider S, A., & Bahram K, M. (2010). Application of water quality index for assessment of Dokan lake ecosystem, Kurdistan region, Iraq. *Journal of Water Resource and protection*, *2010*.
- Acreman, M. C., & Dunbar, M. J. (2004). Defining environmental river flow requirements–a review. *Hydrology and Earth System Sciences*, *8*(5), 861-876.
- Acreman, M., Dunbar, M., Hannaford, J., Mountford, O., Wood, P., Holmes, N., ... & Crookall, D. (2008). Developing environmental standards for abstractions from UK rivers to implement the EU Water Framework Directive/Développement de standards environnementaux sur les prélèvements d'eau en rivière au Royaume Uni pour la mise en œuvre de la directive cadre sur l'eau de l'Union Européenne. *Hydrological Sciences Journal*, *53*(6), 1105-1120.
- Agarwal, A., & Chak, A. (Eds.). (1991). *State of India's environment: a citizen's report: floods, flood plains and environmental myths*. Centre for Science and environment.
- Appavu, A., Thangavelu, S., Muthukannan, S., Jesudoss, J. S., & Pandi, B. (2016). Study of water quality parameters of cauvery river water in Erode region. *Journal of Global Biosciences*, *5*(9), 4556-4567.
- Arnold, J. G., & Allen, P. M. (1996). Estimating hydrologic budgets for three Illinois watersheds. *Journal of hydrology*, *176*(1-4), 57-77.
- Arnold, J. G., Allen, P. M., & Bernhardt, G. (1993). A comprehensive surface-groundwater flow model. *Journal of hydrology*, *142*(1-4), 47-69.
- Arnold, J. G., Srinivasan, R., Muttiah, R. S., & Williams, J. R. (1998). Large area hydrologic modeling and assessment part I: model development 1. *JAWRA Journal of the American Water Resources Association*, *34*(1), 73-89.
- Baird, R., Rice, E., & Eaton, A. (2017). Standard methods for the examination of water and wastewaters. *Water Environment Federation, Chair Eugene W. Rice, American Public Health Association Andrew D. Eaton, American Water Works Association*.
- Barakat, A., El Baghdadi, M., Rais, J., Aghezzaf, B., & Slassi, M. (2016). Assessment of spatial and seasonal water quality variation of Oum Er Rbia River (Morocco) using multivariate statistical techniques. *International soil and water conservation research*, *4*(4), 284-292.
- Barakat, A., Khellouk, R., El Jazouli, A., Touhami, F., & Nadem, S. (2018). Monitoring of forest cover dynamics in eastern area of Béni-Mellal Province using ASTER and Sentinel-2A multispectral data. *Geology, Ecology, and Landscapes*, *2*(3), 203-215.
- Bárdossy, A., & Singh, S. K. (2008). Robust estimation of hydrological model parameters. *Hydrology and earth system sciences*, *12*(6), 1273-1283.
- Belletti, B., Rinaldi, M., Buijse, A. D., Gurnell, A. M., & Mosselman, E. (2015). A review of assessment methods for river hydromorphology. *Environmental Earth Sciences*, *73*, 2079-2100.
- Bhatt, D., Kundu, A., Mall, R. K., & Raju, K. P. (2020). Dynamics of vegetation response to seasonal rainfall in the Gomati river basin (India) using earth observation data sets. *Journal of Scientific Research*, *64*(1), 20-31.

- Bhattacharya, A. (2013) *Evolution of the Hydro-Geonomic Characteristics of Flood in the Mayurakshi River Basin of Eastern India*(pp. 24-82 &100-147). Un-published Ph.D. thesis in Geography, Visva-Bharati University, India.
- BIS, I. (2012). 10500: 2012. *Indian standard drinking water-specification (second revision), Bureau of Indian Standards, New Delhi*.
- Bo, H., Dong, X., Li, Z., Reta, G., & Wei, C. (2020). Analysis of Water Balance Components and Parameter Uncertainties Based on SWAT Model with CMADS Data and SUFI-2 Algorithm in Huangbaihe River Catchment, China. *Nature Environment & Pollution Technology*, *19*(2).
- Boon, P. J., Wilkinson, J., & Martin, J. (1998). The application of SERCON (System for Evaluating Rivers for Conservation) to a selection of rivers in Britain. *Aquatic Conservation: Marine and Freshwater Ecosystems*, *8*(4), 597-616.
- Boyd, C. E., & Claude, E. (2000). Water Quality: An introduction kluwer academic publishers. *Norwell, Massachusetts*, *2061*.
- Caissie, D., & El-Jabi, N. (1995). Comparison and regionalization of hydrologically based instream flow techniques in Atlantic Canada. *Canadian Journal of Civil Engineering*, *22*(2), 235-246.
- Carpenter, S. R., Caraco, N. F., Correll, D. L., Howarth, R. W., Sharpley, A. N., & Smith, V. H. (1998). Nonpoint pollution of surface waters with phosphorus and nitrogen. *Ecological applications*, *8*(3), 559-568.
- Carter, L. W., & Anderson, G. L. (2020). Riparian vegetation on flood control project levees: Constraints and opportunities. *California Riparian Systems*, 548-550.
- Castro-López, D., Guerra-Cobián, V., & Prat, N. (2019). The role of riparian vegetation in the evaluation of ecosystem health: The case of semiarid conditions in Northern Mexico. *River Research and Applications*, *35*(1), 48-59.
- Cohen, J. (1960). A coefficient of agreement for nominal scales. *Educational and psychological measurement*, *20*(1), 37-46.
- Colwell, S. R., & Hix, D. M. (2008, April). Adaptation of the QBR index for use in riparian forests of central Ohio. In *Proceedings 16th Central Hardwood Forest Conference* (Vol. 16, pp. 331-340).
- Costanza, R., d'Arge, R., De Groot, R., Farber, S., Grasso, M., Hannon, B., ... & Van Den Belt, M. (1997). The value of the world's ecosystem services and natural capital. *nature*, *387*(6630), 253-260.
- Costanza, R., De Groot, R., Sutton, P., Van der Ploeg, S., Anderson, S. J., Kubiszewski, I., ... & Turner, R. K. (2014). Changes in the global value of ecosystem services. Global environmental change, 26, 152-158.
- CPCB (Central Pollution Control Board). 1996. Water Quality Status and Statistics (1993 & 1994). Monitoring of Current State and Trends. Island Press, Washington, DC.
- Daggupati, P., Yen, H., White, M. J., Srinicasan, R., Arnold, J. G., Keitzer, C. S. and Sowa, S. P. 2015. Impact of model development, calibration and validation decisions on hydrological simulations in West Lake Erie Basin. Hydrological Processes, 29: 5307-5320
- Das, M., & Das, A. (2019). Estimation of ecosystem services (EESs) loss due to transformation of local climatic zones (LCZs) in Sriniketan-Santiniketan planning area (SSPA) West Bengal, India. *Sustainable cities and society*, *47*, 101474.
- Das, M., & Das, A. (2019b). Estimation of ecosystem services (EESs) loss due to transformation of local climatic zones (LCZs) in Sriniketan-Santiniketan planning area (SSPA) West Bengal, India. *Sustainable cities and society*, *47*, 101474.

- Das, M., & Das, A. (2019c). Dynamics of Urbanization and its impact on Urban Ecosystem Services (UESs): A study of a medium size town of West Bengal, Eastern India. *Journal of Urban Management*, *8*(3), 420-434.
- De Groot, R. S., Wilson, M. A., & Boumans, R. M. (2002). A typology for the classification, description and valuation of ecosystem functions, goods and services. *Ecological economics*, *41*(3), 393-408.
- Dhami, Bir & Himanshu, Sushil & Pandey, Ashish & Gautam, Amar Kant. (2018). Evaluation of the SWAT model for water balance study of a mountainous snowfed river basin of Nepal. Environmental Earth Sciences. 77. 10.1007/s12665-017-7210-8.
- Directorate, Govt. of West Bengal, Kolkata, pp. 30-43.
- Dufour, S., Rodríguez-González, P. M., & Laslier, M. (2019). Tracing the scientific trajectory of riparian vegetation studies: Main topics, approaches and needs in a globally changing world. *Science of the total environment*, *653*, 1168-1185.
- Dutta, I., & Das, A. (2019a). Exploring the dynamics of urban sprawl using geo-spatial indices: a study of English Bazar Urban Agglomeration, West Bengal. *Applied Geomatics*, *11*, 259-276.
- Egereonu, U. U., & Nwachukwu, U. L. (2005). Evaluation of the surface and groundwater resources of Efuru River Catchment, Mbano, South Eastern, Nigeria. *J. Assoc. Adv. Model. Simulat. Tech. Enterpr*, *66*, 53-71.
- Elhatip, H., & Ali Hinis, M. (2015). Statistical approaches for estimating the environmental flows in a river basin: case study from the Euphrates River catchment, Eastern Anatolian part of Turkey. *Environmental Earth Sciences*, *73*, 4633-4646.
- EPA, U. (2002). Method 1603: Escherichia coli (E. coli) in water by membrane filtration using modified membrane-thermotolerant Escherichia coli agar (modified mTEC). *United States Environmental Protection Agency Office of Water, Washington, DC*.
- Erskine, W. D., & Webb, A. A. (2003). Desnagging to resnagging: new directions in river rehabilitation in southeastern Australia. *River Research and Applications*, *19*(3), 233-249.
- Ezenne, G. I., Ndulue, E. L., & Yakubu, O. L. (2014). WATER TEMPERATURE SIMULATION OF OWENA RIVER AT OWENA DAM SITE USING HEC-RAS MODEL. *JOURNAL OF AGRICULTURAL ENGINEERING AND TECHNOLOGY*, *22*(2), 131-139.
- Faramarzi, M., Abbaspour, K. C., Schulin, R., & Yang, H. (2009). Modelling blue and green water resources availability in Iran. *Hydrological Processes: An International Journal*, *23*(3), 486-501.
- Fatih Ali, S., Hamud Hays, H., & Abdul-Jabar, R. A. (2021). Application of CCME water quality index for drinking purpose in Tigris River within Wasit Province, Iraq. *Caspian Journal of Environmental Sciences*, *19*(5), 781-787.
- Fierro, P., Bertrán, C., Tapia, J., Hauenstein, E., Peña-Cortés, F., Vergara, C., ... & Vargas-Chacoff, L. (2017). Effects of local land-use on riparian vegetation, water quality, and the functional organization of macroinvertebrate assemblages. *Science of the total environment*, *609*, 724-734.
- Fujita, T., de Morais, M. V. B., Dos Santos, V. C., Rudke, A. P., de Eiras, M. M., Xavier, A. C. F., ... & Martins, J. A. (2022). Simulating Discharge in a Non-Dammed River of Southeastern South America Using SWAT Model. *Water*, *14*(3), 488.
- Geneletti, D. (2013). Assessing the impact of alternative land-use zoning policies on future ecosystem services. *Environmental Impact Assessment Review*, *40*, 25-35.

- Ghanbarpour, M. R., Zolfaghari, S., Geiss, C., & Darvari, Z. (2013). Investigation of river flow alterations using environmental flow assessment and hydrologic indices: Tajan River Watershed, Iran. *International journal of river basin management*, *11*(3), 311-321.
- Giridharan, L., Venugopal, T., & Jayaprakash, M. (2010). Identification and evaluation of hydrogeochemical processes on river Cooum, South India. *Environmental monitoring and assessment*, *162*, 277-289.
- Gupta, H. V., Sorooshian, S., & Yapo, P. O. (1998). Toward improved calibration of hydrologic models: Multiple and noncommensurable measures of information. *Water Resources Research*, *34*(4), 751-763.
- Gupta, H. V., Sorooshian, S., & Yapo, P. O. (1999). Status of automatic calibration for hydrologic models: Comparison with multilevel expert calibration. *Journal of hydrologic engineering*, *4*(2), 135-143.
- Gupta, N., Pandey, P., & Hussain, J. (2017). Effect of physicochemical and biological parameters on the quality of river water of Narmada, Madhya Pradesh, India. *Water Science*, *31*(1), 11-23.
- Gupta, V. D., Areendran, G., Raj, K., Ghosh, S., Dutta, S., & Sahana, M. (2021). Assessing habitat suitability of leopards (Panthera pardus) in unprotected scrublands of Bera, Rajasthan, India. In *Forest Resources Resilience and Conflicts* (pp. 329-342). Elsevier.
- He, C., Zhang, D., Huang, Q., & Zhao, Y. (2016). Assessing the potential impacts of urban expansion on regional carbon storage by linking the LUSD-urban and InVEST models. *Environmental Modelling & Software*, *75*, 44-58.
- Hughes, D. A., & Hannart, P. (2003). A desktop model used to provide an initial estimate of the ecological instream flow requirements of rivers in South Africa. *Journal of hydrology*, *270*(3-4), 167-181.
- Hunter, H., Fellows, C., Rassam, D., DeHayr, R., Pagendam, D., Conway, C., ... & Beard, N. (2006). Managing riparian lands to improve water quality: optimising nitrate removal via denitrification. *Indooroopilly, Qld., Australia, Cooperative Research Centre for Coastal Zone, Estuary and Waterway Management (Coastal CRC)*.
- Indian Aquatic Resources (MINARS/10/1995-96). New Delhi: Central Pollution Control Board. 459 pp.
- Islam, A., Barman, S. D., Islam, M., & Ghosh, S. (2020). Role of human interventions in the evolution of forms and processes in the Mayurakshi River Basin. *Anthropogeomorphology of Bhagirathi-Hooghly river system in India*, 135-187.
- Jacobs, H. L., Gabrielson, I. N., Horton, R. K., Lyon, W. A., Hubbard, E. C., & McCallum, G. E. (1965). Water quality criteria-stream vs. effluent standards. *Journal (Water Pollution Control Federation)*, 292-315.
- Jansen, A. (2005). Rapid appraisal of riparian condition: scaling up from on-ground measurement to remote sensing. In *Australian Stream Management Conference* (pp. 313-319). Department of primary Industries, Water and Environment.
- Jhingran, V. G. (1991). Fish and Fisheries of India, Hindustan Pub. *Co., New Delhi*, *727*.
- Jowett, I. G. (1997). Instream flow methods: a comparison of approaches. *Regulated Rivers: Research & Management: An International Journal Devoted to River Research and Management*, *13*(2), 115-127.
- Karimi, S., Salarijazi, M., Ghorbani, K., & Heydari, M. (2021). Comparative assessment of environmental flow using hydrological methods of low flow indexes, Smakhtin, Tennant and flow duration curve. *Acta Geophysica*, *69*(1), 285-293.

- Kazoglou, Y., Fotiadis, G., Koutseri, I., & Vrahnakis, M. (2010). Assessment of structural components of riparian forest vegetation of the Prespa Basin with the means of the QBR index. *BALWOIS, Ohrid, Republic of Macedonia*.
- Khatun, S., Sahana, M., Jain, S. K., & Jain, N. (2018). Simulation of surface runoff using semi distributed hydrological model for a part of Satluj Basin: parameterization and global sensitivity analysis using SWAT CUP. *Modeling Earth Systems and Environment*, *4*, 1111-1124.
- Knights, P. (2002, October). Environmental flows: lessons from an Australian experience. In *Proceedings of International Conference: Dialog on Water, Food and Environment*.
- Konar, S. (2008) *Mayurakshi Nadi Babostha, Puno Puno Bonya, Karon Nirnoi O Protibidhan* (Mayurakshi River System: Recurrent Flood, Causes And Remedies). In: Mukherjee, D.K. (Ed.), *Sechpatra 13* (January), Journal of the Irrigation and Waterways
- Krishna Kumar, S., Chandrasekar, N., Seralathan, P., Godson, P. S., & Magesh, N. S. (2012). Hydrogeochemical study of shallow carbonate aquifers, Rameswaram Island, India. *Environmental monitoring and assessment*, *184*, 4127-4138.
- Krishna Kumar, S., Logeshkumaran, A., Magesh, N. S., Godson, P. S., & Chandrasekar, N. (2015). Hydro-geochemistry and application of water quality index (WQI) for groundwater quality assessment, Anna Nagar, part of Chennai City, Tamil Nadu, India. *Applied Water Science*, *5*, 335-343.
- Krysanova, V., White, M., 2015. Advances in water resources assessment with SWAT—an overview. Hydrol. Sci. J. 60 (5), 771–783.
- Ladson, A. R., White, L. J., Doolan, J. A., Finlayson, B. L., Hart, B. T., Lake, P. S., & Tilleard, J. W. (1999). Development and testing of an Index of Stream Condition for waterway management in Australia. *Freshwater biology*, *41*(2), 453-468.
- Lawler, J. J., Lewis, D. J., Nelson, E., Plantinga, A. J., Polasky, S., Withey, J. C., ... & Radeloff, V. C. (2014). Projected land-use change impacts on ecosystem services in the United States. *Proceedings of the National Academy of Sciences*, *111*(20), 7492-7497.
- Liu, S., Lou, S., Kuang, C., Huang, W., Chen, W., Zhang, J., & Zhong, G. (2011). Water quality assessment by pollution-index method in the coastal waters of Hebei Province in western Bohai Sea, China. *Marine pollution bulletin*, *62*(10), 2220-2229.
- Matthews, R. C., & Bao, Y. (1991). The Texas method of preliminary instream flow determination. *Rivers*, *2*(4), 295-310.
- McClain, M. E., & Anderson, E. P. (2015). The gap between best practice and actual practice in the allocation of environmental flows in integrated water resources management. *Sustainability of Integrated Water Resources Management: Water Governance, Climate and Ecohydrology*, 103-120.
- McLaughlin, A., & Mineau, P. (1995). The impact of agricultural practices on biodiversity. *Agriculture, Ecosystems & Environment*, *55*(3), 201-212.
- Metzger, M. J., Rounsevell, M. D., Acosta-Michlik, L., Leemans, R., & Schröter, D. (2006). The vulnerability of ecosystem services to land use change. *Agriculture, ecosystems & environment*, *114*(1), 69-85.
- Millennium Ecosystem Assessment (MEA), 2003. Ecosystems and Human Well-being:
- Millennium ecosystem assessment, M. E. A. (2005). *Ecosystems and human well-being* (Vol. 5, p. 563). Washington, DC: Island press.
- Miller, S. J., Wardrop, D. H., Mahaney, W. M., & Brooks, R. P. (2006). A plant-based index of biological integrity (IBI) for headwater wetlands in central Pennsylvania. *Ecological Indicators*, *6*(2), 290-312.

- Mohamed, A. E. A. (2017). Mapping tree canopy cover in the semi-arid Sahel using satellite remote sensing and Google Earth imagery. *Student thesis series INES*.
- Mohanakavitha, T., Divahar, R., Meenambal, T., Shankar, K., Rawat, V. S., Haile, T. D., & Gadafa, C. (2019a). Dataset on the assessment of water quality of surface water in Kalingarayan Canal for heavy metal pollution, Tamil Nadu. *Data in brief*, *22*, 878-884.
- Mohanakavitha, T., Shankar, K., Divahar, R., Meenambal, T., & Saravanan, R. (2019b). Impact of industrial wastewater disposal on surface water bodies in Kalingarayan canal, Erode district, Tamil Nadu, India. *Archives of Agriculture and Environmental Science*, *4*(4), 379-387.
- Mondal, S., & Patel, P. P. (2018). Examining the utility of river restoration approaches for flood mitigation and channel stability enhancement: a recent review. *Environmental Earth Sciences*, *77*, 1-25.
- Moriasi, D. N., Arnold, J. G., Van Liew, M. W., Bingner, R. L., Harmel, R. D., & Veith, T. L. (2007). Model evaluation guidelines for systematic quantification of accuracy in watershed simulations. *Transactions of the ASABE*, *50*(3), 885-900.
- Mukate, S., Panaskar, D., Wagh, V., Muley, A., Jangam, C., & Pawar, R. (2018). Impact of anthropogenic inputs on water quality in Chincholi industrial area of Solapur, Maharashtra, India. *Groundwater for Sustainable Development*, *7*, 359-371.
- Mukate, S., Wagh, V., Panaskar, D., Jacobs, J. A., & Sawant, A. (2019). Development of new integrated water quality index (IWQI) model to evaluate the drinking suitability of water. *Ecological indicators*, *101*, 348-354.
- Mukhopadhyay, S. and Pal, S. (2009) Impact of Tilpara barrage on the environment of Mayurakshi confluence domain-a
- Munné, A., Prat, N., Solà, C., Bonada, N., & Rieradevall, M. J. A. C. M. (2003). A simple field method for assessing the ecological quality of riparian habitat in rivers and streams: QBR index. *Aquatic conservation: marine and freshwater ecosystems*, *13*(2), 147-163.
- Munné, A., Solá, C., & Prat, N. (1998). QBR: An index to evaluate the quality of riparian ecosystems; QBR: Un indice rapido para la evaluacion de la calidad de los ecosistemas de ribera. *Tecnología del agua*, *175*.
- Naiman, R. J., Decamps, H., & McClain, M. E. (2010). *Riparia: ecology, conservation, and management of streamside communities*. Elsevier.
- Nash, J. E., & Sutcliffe, J. V. (1970). River flow forecasting through conceptual models part I—A discussion of principles. *Journal of hydrology*, *10*(3), 282-290.
- Neitsch, S.L., Arnold, J.G., Kiniry, J.R., Williams, J.R., 2011. Soil and Water Assessment Tool Theoretical Documentation Version 2009 (Texas Water Resources Institute).
- Newson, M. D., & Large, A. R. (2006). 'Natural'rivers,'hydromorphological quality'and river restoration: a challenging new agenda for applied fluvial geomorphology. *Earth Surface Processes and Landforms: The Journal of the British Geomorphological Research Group*, *31*(13), 1606-1624.
- Nyeko, M. 2015. Hydrologic Modelling of Data Scarce Basin with SWAT Model: Capabilities and Limitations. Water Resources Management, 29: 81-94.
- O'Malley, L.S.S. (1914) Reprint, (1996) *Rivers of Bengal*. Bengal District Gazetteers. pp. 1-25, 97-154 &177-204.
- Ollero, A., Ibisate, A., Gonzalo, L. E., Acín, V., Ballarín Ferrer, D., Díaz Bea, E., ... & Sánchez, M. (2011). The IHG index for hydromorphological quality assessment of rivers and streams: updated version. *Limnetica*, *30*(2), 0255-262.

- Ombaka, O., & Gichumbi, J. M. (2012). Investigation of Physicochemical and Bacteriological Characteristics of Water Samples from Irigu River Meru South, Kenya.
- Pal, S. (2010). Changing inundation character in Mayurakshi River basin: a spatio temporal review. PractisingGeographer, 14(1), 58–71
- Pandey, R. P., & Ramasastri, K. S. (2003). Estimation of lean season water availability in streams with limited data. *Journal of the Institution of Engineers. India. Civil Engineering Division*, *84*(nov), 149-152.
- Panigrahi, T., Das, K. K., Dey, B. S., & Panda, R. B. (2012). Assessment of Water Quality of river Sono, Balasore. *International Journal Environmental Science*, *3*(1), 49-56.
- Petersen Jr, R. C. (1992). The RCE: a riparian, channel, and environmental inventory for small streams in the agricultural landscape. *Freshwater biology*, *27*(2), 295-306.
- Piniewski, M., Laizé, C. L., Acreman, M. C., Okruszko, T., & Schneider, C. (2014). Effect of climate change on environmental flow indicators in the Narew Basin, Poland. *Journal of Environmental Quality*, *43*(1), 155-167.
- Plummer, M. L. (2009). Assessing benefit transfer for the valuation of ecosystem services. *Frontiers in Ecology and the Environment*, *7*(1), 38-45.
- Polasky, S., Nelson, E., Pennington, D., & Johnson, K. A. (2011). The impact of land-use change on ecosystem services, biodiversity and returns to landowners: a case study in the state of Minnesota. *Environmental and Resource Economics*, *48*, 219-242.
- Pratiksha, T., Morey, P. P., Batra, R. J., & Weginwar, R. G. (2013). Physico-chemical parameter evaluation of water quality around Chandrapur District Maharastra, India. *Journal of Chemical and Pharmaceutical Research*, *5*(5), 27-36.
- Pusey, B. J., & Arthington, A. H. (2003). Importance of the riparian zone to the conservation and management of freshwater fish: a review. *Marine and freshwater Research*, *54*(1), 1-16.
- Rahman, A., Kumar, S., Fazal, S., & Siddiqui, M. A. (2012). Assessment of land use/land cover change in the North-West District of Delhi using remote sensing and GIS techniques. *Journal of the Indian Society of Remote Sensing*, *40*, 689-697.
- Ramey, T. L., & Richardson, J. S. (2017). Terrestrial invertebrates in the riparian zone: mechanisms underlying their unique diversity. *BioScience*, *67*(9), 808-819.
- Raven, P. J., Holmes, N. T. H., Dawson, F. H., & Everard, M. (1998). Quality assessment using river habitat survey data. *Aquatic conservation: marine and freshwater ecosystems*, *8*(4), 477-499.
- Rice, E. W., Bridgewater, L., & American Public Health Association (Eds.). (2012). *Standard methods for the examination of water and wastewater* (Vol. 10). Washington, DC: American public health association.
- Richter, B., Baumgartner, J., Wigington, R., & Braun, D. (1997). How much water does a river need?. *Freshwater biology*, *37*(1), 231-249.
- Ridoutt, B. G., Eady, S. J., Sellahewa, J., Simons, L., & Bektash, R. (2009). Water footprinting at the product brand level: case study and future challenges. *Journal of Cleaner Production*, *17*(13), 1228-1235.
- Rinaldi, M., Surian, N., Comiti, F., & Bussettini, M. (2013). A method for the assessment and analysis of the hydromorphological condition of Italian streams: The Morphological Quality Index (MQI). *Geomorphology*, *180*, 96-108.
- Rodrigues, C., Alves, P., Bio, A., Vieira, C., Guimarães, L., Pinheiro, C., & Vieira, N. (2019). Assessing the ecological status of small Mediterranean rivers using benthic macroinvertebrates and macrophytes as indicators. *Environmental monitoring and assessment*, *191*, 1-23.

- Rykken, J. J., Moldenke, A. R., & Olson, D. H. (2007). Headwater riparian forest-floor invertebrate communities associated with alternative forest management practices. *Ecological Applications*, *17*(4), 1168-1183.
- Saha, D., Das, D., Dasgupta, R., & Patel, P. P. (2020). Application of ecological and aesthetic parameters for riparian quality assessment of a small tropical river in eastern India. *Ecological Indicators*, *117*, 106627.
- Saha, M.K. (2011) *Bengali: Rarh Banglar Dui Duranta Nadi Mayurakshi Abong Ajoy* (Mayurakshi and Aajy: two Roguish River of the Rarh Bengal). Alser Art, Shriumpur, Hoogli, West Bengal, India, pp. 82-193.
- Saint-Jacques N. and Richard Y. Development of a riparian strip quality index: application to the Chaudière River and relationship to the biotic integrity of the aquatic environment, 1998, p 6.1 at 6.41; in the ministry of the environment and wildlife (ed), direction of aquatic ecosystems, Quebec, envirodop n° EN980022.
- Sánchez, E., Colmenarejo, M. F., Vicente, J., Rubio, A., García, M. G., Travieso, L., & Borja, R. (2007). Use of the water quality index and dissolved oxygen deficit as simple indicators of watersheds pollution. *Ecological indicators*, *7*(2), 315-328.
- Schuol, J., Abbaspour, K. C., Srinivasan, R., & Yang, H. (2008). Estimation of freshwater availability in the West African sub-continent using the SWAT hydrologic model. *Journal of hydrology*, *352*(1-2), 30-49.
- Selvam, S., Manimaran, G., & Sivasubramanian, P. (2013). Hydrochemical characteristics and GIS-based assessment of groundwater quality in the coastal aquifers of Tuticorin corporation, Tamilnadu, India. *Applied Water Science*, *3*, 145-159.
- Sharma, R., Rimal, B., Baral, H., Nehren, U., Paudyal, K., Sharma, S., ... & Kandel, P. (2019). Impact of land cover change on ecosystem services in a tropical forested landscape. *Resources*, *8*(1), 18.
- Shenton, W., Hart, B. T., & Chan, T. (2011). Bayesian network models for environmental flow decision-making: 1. Latrobe River Australia. *River Research and Applications*, *27*(3), 283-296.
- Shokoohi, A., & Hong, Y. (2011). Using hydrologic and hydraulically derived geometric parameters of perennial rivers to determine minimum water requirements of ecological habitats (case study: Mazandaran Sea Basin—Iran). *Hydrological Processes*, *25*(22), 3490-3498.
- Simeonov, V., Stratis, J. A., Samara, C., Zachariadis, G., Voutsa, D., Anthemidis, A., ... & Kouimtzis, T. (2003). Assessment of the surface water quality in Northern Greece. *Water research*, *37*(17), 4119-4124.
- Singh, L., & Saravanan, S. (2020). Simulation of monthly streamflow using the SWAT model of the Ib River watershed, India. *HydroResearch*, *3*, 95-105.
- Sirombra, M. G., & Mesa, L. M. (2012). A method for assessing the ecological quality of riparian forests in subtropical Andean streams: QBRy index. *Ecological indicators*, *20*, 324-331.
- Somura, H., Hoffman, D., Arnold, J. G., Takeda, I., & Mori, Y. (2009). Application of the SWAT Model to the Hii River Basin, Shimane Prefecture, Japan. *Soil and Water Assessment Tool (SWAT) Global Applications. World Association of Soil and Water Conservation. Special Pub*, *4*.
- Srinivasan, R., Ramanarayanan, T. S., Arnold, J. G., & Bednarz, S. T. (1998). Large area hydrologic modeling and assessment part II: model application 1. *JAWRA Journal of the American Water Resources Association*, *34*(1), 91-101.
- Standard, D. I. (2022). Bureau of Indian Standards.

- Steffen, W., Richardson, K., Rockström, J., Cornell, S. E., Fetzer, I., Bennett, E. M., ... & Sörlin, S. (2015). Planetary boundaries: Guiding human development on a changing planet. *Science*, *347*(6223), 1259855.
- Subramanya, K. (2008). *Engineering hydrology*. McGraw-Hill.
- Sutadian, A. D., Muttil, N., Yilmaz, A. G., & Perera, B. J. C. (2016). Development of river water quality indices—a review. *Environmental monitoring and assessment*, *188*, 1-29.
- SV, M., Panaskar, D. B., Wagh, V. M., & Pawar, R. S. Assessment of Groundwater Quality for Drinking and Irrigation Purpose: A Case Study of Chincholikati MIDC Area, Solapur (MS), India.
- Tennant, D. L. (1976). Instream flow regimens for fish, wildlife, recreation and related environmental resources. *Fisheries*, *1*(4), 6-10.
- Tockner, K., & Stanford, J. A. (2002). Riverine flood plains: present state and future trends. *Environmental conservation*, *29*(3), 308-330.
- Vairavamoorthy, K., Gorantiwar, S. D., & Pathirana, A. (2008). Managing urban water supplies in developing countries–Climate change and water scarcity scenarios. *Physics and Chemistry of the Earth, Parts A/B/C*, *33*(5), 330-339.
- Van Oel, P. R., Mekonnen, M. M., & Hoekstra, A. Y. (2009). The external water footprint of the Netherlands: Geographically-explicit quantification and impact assessment. *Ecological Economics*, *69*(1), 82-92.
- Vargas, L., Willemen, L., & Hein, L. (2019). Assessing the capacity of ecosystems to supply ecosystem services using remote sensing and an ecosystem accounting approach. *Environmental management*, *63*, 1-15.
- Vasant, W., Dipak, P., Aniket, M., Ranjitsinh, P., Shrikant, M., Nitin, D., ... & Abhay, V. (2016). GIS and statistical approach to assess the groundwater quality of Nanded Tehsil,(MS) India. In *Proceedings of First International Conference on Information and Communication Technology for Intelligent Systems: Volume 1* (pp. 409-417). Springer International Publishing.
- Vasanthavigar, M., Srinivasamoorthy, K., Vijayaragavan, K., Rajiv Ganthi, R., Chidambaram, S., Anandhan, P., ... & Vasudevan, S. (2010). Application of water quality index for groundwater quality assessment: Thirumanimuttar sub-basin, Tamilnadu, India. *Environmental monitoring and assessment*, *171*, 595-609.
- Venkatesharaju, K., Somashekar, R. K., & Prakash, K. L. (2010). Study of seasonal and spatial variation in surface water quality of Cauvery river stretch in Karnataka. *Journal of ecology and the natural environment*, *2*(1), 001-009.
- Verma, R. K., Murthy, S., Verma, S., & Mishra, S. K. (2017). Design flow duration curves for environmental flows estimation in Damodar River Basin, India. *Applied Water Science*, *7*, 1283-1293.
- Vidal-Abarca, M. R., Santos-Martín, F., Martín-López, B., Sánchez-Montoya, M. M., & Suárez Alonso, M. L. (2016). Exploring the capacity of water framework directive indices to assess ecosystem services in fluvial and riparian systems: towards a second implementation phase. *Environmental Management*, *57*, 1139-1152.
- Wada, Y., Van Beek, L. P. H., & Bierkens, M. F. (2011). Modelling global water stress of the recent past: on the relative importance of trends in water demand and climate variability. *Hydrology and Earth System Sciences*, *15*(12), 3785-3808.
- Wagh, V. M., Panaskar, D. B., & Muley, A. A. (2017). Estimation of nitrate concentration in groundwater of Kadava river basin-Nashik district, Maharashtra, India by using artificial neural network model. *Modeling earth systems and environment*, *3*, 1-10.

- Wagh, V. M., Panaskar, D. B., Muley, A. A., Mukate, S. V., Lolage, Y. P., & Aamalawar, M. L. (2016). Prediction of groundwater suitability for irrigation using artificial neural network model: a case study of Nanded tehsil, Maharashtra, India. *Modeling Earth Systems and Environment*, *2*, 1-10.
- Wats, R. K., Grover, A. S., Kumar, R., & Wats, M. (2019). Status of surface water quality in river Markanda and its correlation with ground water quality and health of the residents of Shahabad, Kurukshetra, Haryana, India-A case study. *International Journal of Health and Economic Development*, *5*(1), 1-11.
- Western, D. (2001). Human-modified ecosystems and future evolution. *Proceedings of the National Academy of Sciences*, *98*(10), 5458-5465.
- Whitehead, P. G., Wilby, R. L., Battarbee, R. W., Kernan, M., & Wade, A. J. (2009). A review of the potential impacts of climate change on surface water quality. *Hydrological sciences journal*, *54*(1), 101-123.
- Woodward, B. D., Evangelista, P. H., Young, N. E., Vorster, A. G., West, A. M., Carroll, S. L., ... & Jarnevich, C. (2018). Co-Rip: A riparian vegetation and corridor extent dataset for Colorado river basin streams and rivers. *ISPRS International Journal of Geo-Information*, *7*(10), 397.
- World Health Organization. (2017). Guidelines for drinking-water quality: first addendum to the fourth edition.
- Xiao, R., Liu, Y., Fei, X., Yu, W., Zhang, Z., & Meng, Q. (2019). Ecosystem health assessment: A comprehensive and detailed analysis of the case study in coastal metropolitan region, eastern China. *Ecological indicators*, *98*, 363-376.
- Xu, C. Y., & Singh, V. P. (2004). Review on regional water resources assessment models under stationary and changing climate. *Water resources management*, *18*, 591-612.
- Yadav, A. K., Khan, P., & Sharma, S. K. (2010). Water Quality Index Assessment ofGroundwater in Todaraisingh Tehsil of Rajasthan State, India-A Greener Approach. *E-journal of Chemistry*, *7*(S1), S428-S432.
- Yang, S., Zhao, W., Liu, Y., Wang, S., Wang, J., & Zhai, R. (2018). Influence of land use change on the ecosystem service trade-offs in the ecological restoration area: Dynamics and scenarios in the Yanhe watershed, China. *Science of the total environment*, *644*, 556-566.
- Yisa, J., & Tijani, J. O. (2010). Analytical studies on water quality index of river Landzu.
- Zalewski, M., Santiago-Fandino, V., & Neate, J. (2003). Energy, water, plant interactions:'Green feedback'as a mechanism for environmental management and control through the application of phytotechnology and ecohydrology. *Hydrological Processes*, *17*(14), 2753-2767.
- Zhan, J., Zhang, F., Chu, X., Liu, W., & Zhang, Y. (2019). Ecosystem services assessment based on emergy accounting in Chongming Island, Eastern China. *Ecological Indicators*, *105*, 464-473.
- Zhang, Z. (2017). The index gage method to develop a flow duration curve from short-term streamflow records. J Hydrol 553:119–129
- Zhao, J., Wang, R., Luo, P., Xing, L., & Sun, T. (2017). Visual ecology: exploring the relationships between ecological quality and aesthetic preference. *Landscape and Ecological Engineering*, *13*, 107-118.

CHAPTER 8

ASSESSMENT OF THE SOCIAL INDICATORS OF THE STUDY AREA

8. People's Perception on Mayurakshi River and its Surroundings

Hydrological processes, variations in river flows, and water management measures are all becoming more and more important to society in the context of climate change. People's attention has been diverted towards managing hydrological processes due to the rapidly increasing need for water, hydropower, and water security. According to Postel et al. (1996), the global increase in safe water supply due to dam construction is 28%, with a projected increase to 34% by 2025. The popularity of reservoir development has grown significantly as a result of certain optimistic thoughts to benefit society. Around 70% of the world's rivers are currently blocked by sizable reservoirs as a result of increased dam construction in recent decades, particularly in regions with extreme warm climate, high precipitation rates, and intense soil erosion (Vorosmarty et al. 2003). In India, there are still diversified outlooks in favor or against the construction of dam. Man-made obstacles, such as dams and storage reservoirs, cause excessive upstream deposition and downstream erosion, which raise flood levels and their extent (Kale 1998). Ghosh and Guchhait (2014), and others have issued warnings against building a dam across a river due to the potential long-term hydro-ecological consequences. In addition to destroying common public properties, the construction of such massive civil constructions on the river has caused a significant loss in riparian flora. Thus it is crucial to concentrate on the benefits and drawbacks of dams on the environment in the short- and long-term monitoring of reservoirs, fluvial systems, and ecological conditions as well.

The current research area is part of a perception study on the Mayurakshi River and its surroundings. The Mayurakshi River is a well-known name in the Indian River system that runs through the states of Jharkhand and west Bengal. It is situated between 23°40'N and 24°34'N latitude and 86°58'E and 88°10'E longitude. It is a significant western tributary of the Bhagirathi River, which originates in Jharkhand and empties into the Bengal plain. It plays a crucial function in supplying water to the principal river Ganga after Bangladesh's Padma drains the majority of the Ganga's flow. The primary source of flowing water for this river is the massive monsoonal rainfall that comes from the top half of the plateau region because it is located in a tropical environment (Roy, 2013). With a mean annual rainfall of 1400 mm, the months of June to October get the most rain (Chaudhury 1966). River water rises at this season (June-September) and becomes practically lean (there is only some base flow in the lower reach) during non-monsoon times as a result of a tropical monsoon's alternately dry and wet spells. This river's seasonal hydrological regime is therefore a very clear reality, and it

undoubtedly regulates sedimentological and geomorphic characteristics in a consistent manner (Pal 2016). In addition to such hydrological uncertainty, a number of unscientific human activities such as the construction of large anthropogenic structures like dams and barrages, the removal of riparian forest due to the expansion of agriculture and settlement along the riverbank, excessive sand mining activities, and waste dumping can seriously degrade the Mayurakshi River and its surroundings.

The quality of the riparian forest in the Mayurakshi River basin area was assessed in the preceding chapter. A riparian region is defined as the area that is between a river or stream and the neighbouring terrestrial highland environment by Corbacho et al. (2003) and Goebel et al. (2003). It encompasses both the actual stream channel and the vicinity that is impacted by shifting water levels. In addition to providing considerable wildlife habitat, these forested areas also preserve water quality, naturally control floods, stabilise stream banks, and provide immediate human advantages including aesthetics and enjoyment (Carver et al. 2004).

Although riverine biological study is crucial for developing frameworks for channel rehabilitation, some stream restoration initiatives have failed due to a lack of public support (Junker and Buchecker 2008). Thus, determining the quality of the landscape and how it is perceived is critical to any restoration project like landscape management for ecological benefits and restoration (Kienast et al. 2015). Therefore the evaluation of human perceptions, opinions, and attitudes is therefore essential for landscape management for ecological benefits and restoration (Kienast et al. 2015), as these encourage choices that ultimately affect a location's ecological functions and its aesthetic qualities (Lopez- Rodriguez et al., 2018). Planning landscape alterations with consideration for both public aesthetic perception and ecological aims would increase the likelihood that such projects would meet societal needs and enjoy long-term acceptability and support (Nassauer et al. 2001).

This chapter deals with findings of people's perceptions of the current state of the riparian vegetation as well as the current situation of the Mayurakshi River and its water supply. This section offers a thorough examination of the Qualitat del Bosc de Ribera (QBR) Index (Munne et al. 2003).

8.1. Data Collection and Procedure

In order to investigate social perspectives on the overall quality of the riparian vegetation in the Mayurakshi River basin area, this study performed a questionnaire survey with 386 local

residents. This study employed an indirect survey methodology and incorporated qualitative research as part of the surveying procedure by asking the locals. First, a questionnaire survey form was created to collect data. Later, other researchers visited the study area with some people to interview them directly. There were both closed- and open-ended questions on the survey form. In the first section of the survey, participants were asked to self-report their socio-demographic information. The second phase of the survey was separated into four sections to correspond with the main aspects of QBR index. Therefore, each component was evaluated independently before being integrated at the end for the QBR index's final scoring as given by Munne et al. 2003 (Adopted score sheet attached in Appendix IV). The entire fieldwork was done in January 2021.

The total vegetation cover was the first part of the QBR index to be completed. Several steps were taken to complete this section, starting with an approximate observation of the amount of riparian cover present including a combined percentage of the cover from trees, shrubs, and perennial herbaceous plants but not that of annual plants. If the percent cover was above 80%, the portion received the highest score; if it was below 80%, the score varied based on how low the percent cover was. If the cover was less than 10%, the score was zero. Depending on the level of connectedness, disconnected vegetation patches also result in a reduction in the initial score. The amount of trees, bushes, and other types of vegetation present is indicated by the cover structure, which also counts the complexity of the riparian zone's vegetation structure. In contrast, the presence of helophytes or undergrowth in the riparian forest raises the initial score. The presence of linear vegetation layouts that indicate plantations or the prevalence of any foreign species lowers scores. The geomorphological type of the stream reach (as established by the QBR scheme) is first calculated, and this information recommends the number of species that should ideally be present inside the stream reach's riparian zone. This information is then used to determine the cover quality. Three stream categories (such as Type-1, Type-2, and Type-3) were determined by Munne et al. (2003) based on the riverbank slope and riparian habitat characteristics. According to Munne et al. (2003), Type-1 streams are closed headwater riparian habitats, Type-2 streams are headwater or midland riparian habitats, and Type-3 streams are substantial riparian zones in the lower course. The fourth factor, which assesses the extent to which anthropogenic activities have altered the initial natural stream state, lowers scores proportionately as permanent structures become more prevalent. Once all four components had been completed, the scores from all four were added together to get a final QBR site score has been computed (as discussed in chapter 7).

- **Sample Size and Technique**

With the QBR index, riparian quality can be quickly and easily assessed. Each survey, as well as subsequent surveys of the same site, can be conducted by several observers. On succeeding occasions, however, various observers might assign various index scores for the same sampling site. The effect of disturbances is dismissed because there were no significant environmental changes in the riparian area during the study, and as a result, variations in the score at each site may be interpreted as errors resulting from observer subjectivity or a misapplication of the methodology.

Total 23 study sites (Table 8.1) has been chosen by dividing the whole river stretch equally at an interval of 10 km which are located near the vicinity of river bank. Ten observers participated in the survey work, and all of them had undergone prior training from individuals in charge of designing the index (Munne et al. 2003) then each site's mean score was determined by taking the mean value of the observed data. Therefore, simple random sampling was used in this work to obtain the best results that could be seen in the study area.

8.2. People's Perceptions about the Mayurakshi River and its Surroundings

This study includes a thorough questionnaire survey of over 230 respondents, most of whom live close to riverbank areas and have knowledge of the surroundings and local dynamics. However, the study cannot completely eliminate bias in the self-selection of the respondents. Participants in the study came from a variety of age groups and occupations, which is why the results for each topic were varied. The gender distribution of respondents and their occupation were also taken into account in the study. Along with the fundamental category, the study also paid attention to the participants' families and how long they had been connected to the study location. Each of the 45 respondents was invited to complete a survey that included more than 10 questions, and the study received enough responses to satisfy each question.

Table 8.2 summarises the general information about the survey respondents. It shows that almost 40% of them have completed higher secondary education, while 22% have completed primary and undergraduate education. This shows that the survey respondents are competent enough to comprehend the survey's goals. Additionally, it was noted that just roughly 31% of respondents were female, with men making up the majority of respondents. The poll also revealed that the majority of respondents have resided in the river region for at least ten years (Table 8.2).

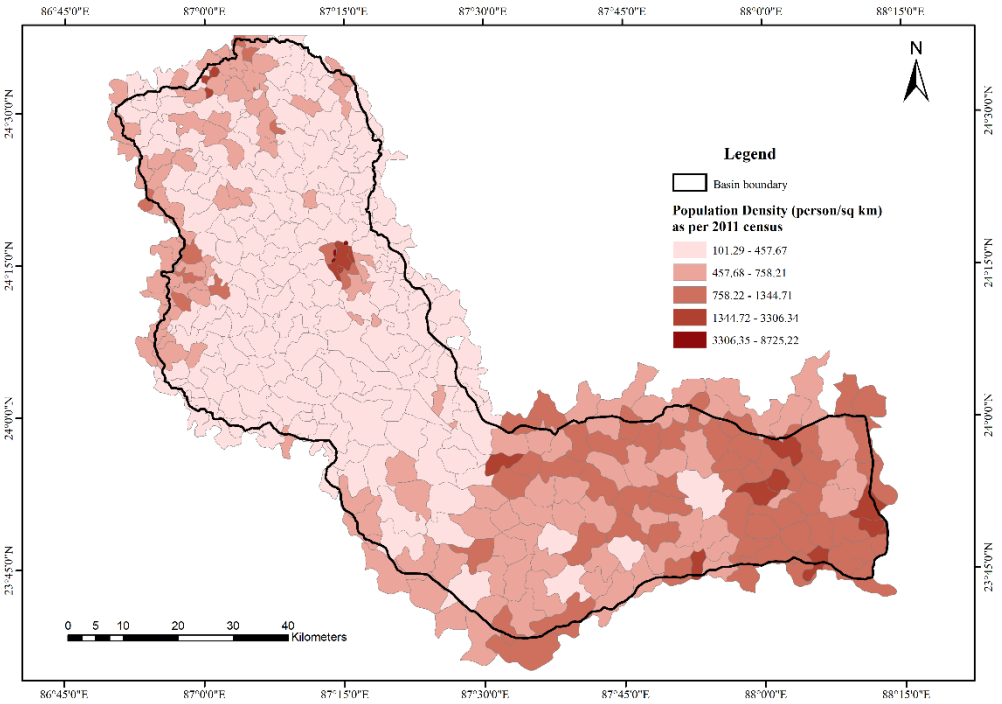

Figure 8.1 *Population Density of the Mayurakshi River Basin Area as per Census 2011*

Table 8.1 *Site Description for the Study of People's Perception*

Reach No	Site Name	Distance from the source (km)	Bank side	Catchment	Final QBR Score	QBR Category
1	Dalihari	9.5	Right	Upper	50	Poor
2	Doria	19	Left	Upper	15	Very poor
3	Aswari	28.2	Left	Upper	45	Poor
4	Amarpur	39.1	Left	Upper	50	Poor
5	Darwechak	51.3	Left	Upper	10	Very poor
6	Bijaypur	57.6	Left	Upper	25	Very poor
7	Sakrigali	70.5	Right	Upper	10	Very poor
8	Beniagram	80	Right	Middle	10	Very poor
9	Kenduli	91.5	Right	Middle	15	Very poor
10	Tilpara	100.2	Right	Middle	30	Poor
11	Kultore	110.1	Middle of shoal	Middle	20	Very poor
12	Balsunda	123.2	Right	Middle	35	Poor
13	Bile	130.2	Right	Lower	70	Fair
14	Ramnagar	141.2	Right	Lower	15	Very poor
15	Sundarpur	150.3	Right	Lower	10	Very poor
16	Talgram	160.4	Right	Lower	30	Poor
17	Angarpur	171	Right	Lower	20	Very poor
18	Aharinagar	182.1	Right	Lower	50	Poor
19	Hijal	190	Right	Lower	70	Fair
20	Subhasnagar	200.3	Right	Lower	45	Poor
21	Lohadaha	210.5	Right	Lower	65	Fair
22	Baidyapur	220.6	Left	Lower	90	Good
23	Dhandanga	226.5	Left	Lower	50	Poor

Table 8.2 *General Information of the Surveyed Respondents*

1	**Age distribution**	A total of 45 people participated in this study project; of them, 144 (62.7%) were over 30 years old and 86 (38%) were between the ages of 15 and 30. This tells us that the majority of the respondents were older than 30.
2	**Gender distribution**	The majority of persons living and working in the Mayurakshi River area are men, with 149 out of the 230 respondents (64.9%) being men and 81 (35.22%) being women.
3	**Family structure**	66.7% (153 people) of the 230 responses are family members of 0 to 5, 31.1% (72 people) are family members of 5 to 10, and 2.2% (5 people) are family members of 10 or more.
4	**Educational level**	230 respondents who resided in the Mayurakshi River area participated in this study. The respondents' levels of education varied from person to person; 22.2% (51 people) had completed their primary education, 40% (92 people) had completed their higher secondary education, 32% (74 people) had finished their undergraduate studies, and 5.8% (13 people) had never attended school. The results of this study indicated that participants with a higher secondary education made up the majority.
5	**Occupational structure**	Among 230 people, 63.4% (146 people) of the respondents are farmers, 21.2% (49 people) are businessmen, 10.4% (24 people) are employees, and 4.8% (11 people) are students. It is therefore understandable that the greater proportion of respondents who are employees do not have as great of an interest in the environment or water pollution.
6	**Duration of living**	According to this study, 42.2% (97 people) of respondents had lived in the Mayurakshi River region for more than five years, while 46.7% (107 people) had lived there for the year between 10 and 5. Only 26 respondents, or 11.2%, had a life expectancy of less than five years.

The main drivers of any area's development and expansion are its location and sociocultural significance. According to census statistics from 2011, the lower portion of the river basin has the highest concentration of inhabitants (Fig. 8.1), since this area has exceptionally fertile alluvial soil that encourages greater food production and draws more people to live there. However, the upper portion of the basin is physiographically restricted, and as a result, agricultural operations are only visible during the monsoon season. Therefore, it is abundantly obvious from the data that those living close to the lower catchment area have made the best use of river water for their daily needs. A questionnaire survey was conducted as part of this

study to learn how concerned people are with the environment and the long-term viability of the Mayurakshi River. Table 8.3 summarised all the important information that has been gathered from survey sheet.

According to the study, the majority of respondents (62.5%) believe that the river has been extremely contaminated, whereas out of 230 respondents, 11.9% (27 individuals) and 2.4% (6 people), respectively, believed that the river is moderately polluted to clean and safe for daily use. This study also reveals that more than half of the respondents (84.6%) agree that the volume of water present in the channel is steadily decreasing day by day, while only 15% of the population chosen for the study claimed that there has been no change in the volume of water present in the channel, primarily in the downstream section. This statement is further supported by an additional finding, which shows that while 71.3% (164 people) of respondents claimed that no recent flooding had occurred, only 29% (66 people) reported experiencing flood-like conditions, mostly in the middle to lower reaches of the Mayurakshi River, where major tributaries (Kushkarini, Kuya, and Dwarka) join the main Mayurakshi channel. Along with the decrease in water levels in the channel, 36.8% (85 respondents) have argued that the unpredictable nature of rainfall is the primary cause of the Mayurakshi River's degradation. In contrast, 22% (50 respondents) and 19% (43 respondents) of respondents said that the effects of rapid urbanisation and indiscriminate sand mining from the river bed are the main contributors to the degradation of the channel.

The Mayurakshi River basin is well recognised for its fertile terrain for which enormous number of people were engaged in agriculture related activities for their daily subsistence (Halder and Sarkar 2016). Because of this, there is a constant need for water in this area. However, the presence of Mayurakshi River and its canal irrigation facilities help to attenuate this demand for water, which is primarily used for irrigation. Despite the fact that some regions were too far from the canal provinces to be able to use the canal water, local farmers in those areas were reliant on river water to meet their irrigation needs. The other usage that are satisfied using river water and have an impact on its ecological significance were also evaluated in table 7.35.In addition to using rivers for irrigation (40.5% of respondents), 22% (51 respondents) were dependent on rivers for bathing, and 35% of respondents used rivers for washing and cleaning. A minimum percentage of respondents (2.5%) indicated that they used rivers primarily as disposal sites for their everyday household waste. Such practises by the locals exacerbate the lack of awareness that is creating water contamination in the Mayurakshi River. However, same study also reveals that 36.8% (85 respondents) and 20% (46 respondents) are only moderately to mildly concern about the current state of health of the Mayurakshi River, while 43.2% (99 respondents) are extremely concerned about the river's current scenario.

Table 8.3 *People's Perceptions about the Mayurakshi River and its Surroundings Environment*

Q1.	**What is your opinion regarding the current status of the Mayurakshi River?**	**Frequency**	**Percentage**
	Safe and clean	6	2.4
	Polluted	27	11.9
	Very polluted	144	62.5
	Totally degraded	53	23.2
Q2.	**In recent time, does the river flood its nearby area?**	**Frequency**	**Percentage**
	Yes	66	28.7
	No	164	71.3
Q3.	**Does the river water decreasing in the recent days?**	**Frequency**	**Percentage**
	Yes	195	84.6
	No	35	15.4
Q4.	**What are the major causes regarding the degradation of river water?**	**Frequency**	**Percentage**
	Irregular rainfall	85	36.8
	Rapid urbanisation	50	21.6
	Waste dumping	34	14.6
	Extraction of river water during dry season	18	7.8
	Sand mining activity	43	19.2
Q5.	**In recent time, does any sand mining activity occur in the nearby areas?**	**Frequency**	**Percentage**
	Yes	207	89.9
	No	23	10.1
Q6.	**How much have you dependent on river water?**	**Frequency**	**Percentage**
	Not really	14	6.2
	Dependent	94	41.1
	Very much dependent	122	52.7
Q7.	**On what purpose have you used the river water most?**	**Frequency**	**Percentage**
	Washing and cleaning	80	34.9
	Bathing	51	22.1
	Irrigation	93	40.5
	Waste dump	6	2.5
Q8.	**How much are you concerned about the present condition of river?**	**Frequency**	**Percentage**
	Slighty concerned	46	20
	Moderately concerned	85	36.8
	Extremely concerned	99	43.2

8.3. People's Perceptions on Riparian Health Quality of Mayurakshi River

For the purpose of evaluating the biological quality of the riparian habitat using the QBR index, the opinions of the villagers in the Mayurakshi River basin area have also been thoroughly surveyed. According to Munne et al. 2003, a table 8.4 summarising public opinion included the four main elements of riparian habitat: total riparian vegetation cover, cover structure, cover quality, and channel changes. The study gathered enough data to draw conclusions on the current situation of the riparian plant cover along the banks of the Mayurakshi River basin today. About 11.6% of respondents (26 out of 230) claimed that there was very little riparian cover along the river's edge, whereas 36.4% to 32.5% of respondents reported low to moderate amounts of forest cover are present within the river corridor. Only 19.5% (45 persons) of the upstream sections, where lush green highlands are predominant, are noted to have dense riparian forest cover along the river bank. Within this thick canopy of vegetation along the flood plain, 41.5% of respondents noted different annual plants and grass covering, and 58.5% are said to have just shrubs and grass coverage in the riparian zone. A significant decrease in the riparian forest cover and the loss of many annual species were brought about by the construction of the Massanjore Dam, the Tilpara barrage, and the Bakreswar weir (Plate No. 8.1).

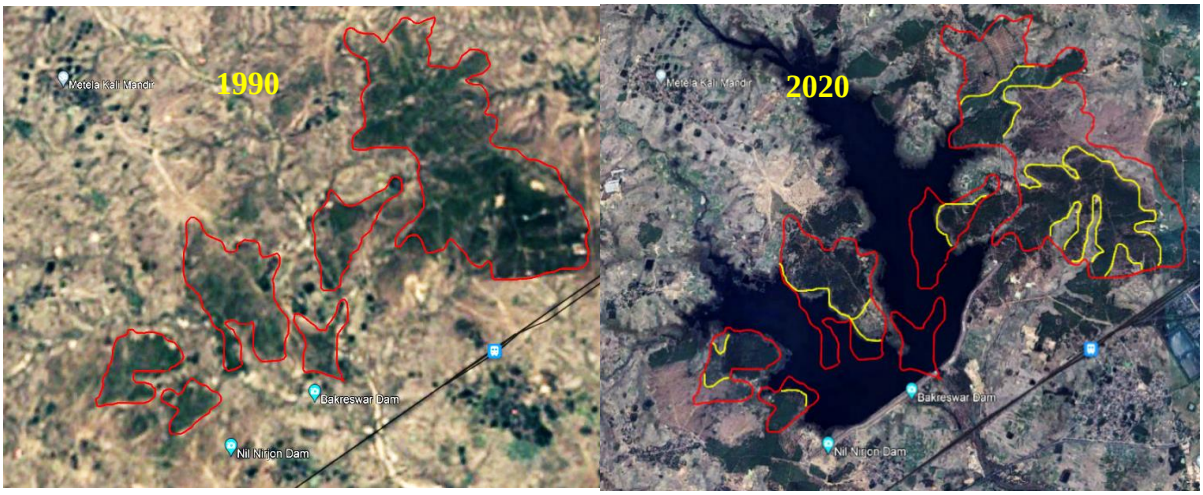

Plate No. 8.1 *Loss of Riparian Cover after the Construction of Bakreswar Dam*

According to the locals, urbanisation is the primary factor causing the declining riparian forest cover from the study area, which is then followed by agricultural activity close to the floodplain, various construction projects like roads and bridges, as well as the growth of brick kiln industries. However, 6.4% (15 persons) of the respondents also noted that the annual flood or water logging scenario could potentially be the reason for the decline in flora along the

riverbank. In addition to identifying the primary factors that contribute to the loss of forest cover, it is more important to raise public knowledge of the value of riparian habitat in protecting the environment. This will motivate residents to considerably green the area. According to the questionnaire survey, roughly half of all respondents (49.9%) believe that the presence or expansion of riparian forest can prevent the land from severe bank erosion, while 36.5% (84 people) believe that this green cover along the bank side can control the situation when it comes to runoff and flooding, and 2.5% (5 people) only support this because the area continues to be beautiful in nature. In terms of aesthetics and naturalness, 73.6% of respondents gave this area a good rating, 12.9% gave it a poor rating, and 31 respondents (or 13.5%) gave it an average rating.

Table 8.4 *Public Opinion on Riparian Health Quality of Mayurakshi River*

Q1	**How much forest cover did you observed within the riparian corridor of this area?**	**Frequency**	**Percentage**
	Very low	26	11.6
	Low	84	36.4
	Moderate	75	32.5
	Dense cover	45	19.5
Q2	**What kind of vegetation structure are more prominent within river corridor?**	**Frequency**	**Percentage**
	Annual plants with shrubs	95	41.5
	Only shrubs and grasses	135	58.5
Q3	**Have you experiencing any kind of reduction in riparian forest cover within your locality?**	**Frequency**	**Percentage**
	Yes	195	84.6
	No	35	15.4
Q4	**Is this area is only covered with native plants?**	**Frequency**	**Percentage**
	Yes	177	76.8
	No	53	23.2
Q5	**What are the major reasons behind the reduction in riparian areas?**	**Frequency**	**Percentage**
	Growing settlements	84	36.5
	Agricultural activities	53	22.9
	Brick kiln industry	28	12.3
	Annual floods	15	6.4
	Constructional activities	50	21.9

Q6	**What do you feel is it necessary for our environment?**	**Frequency**	**Percentage**
	Yes	153	66.5
	No	60	26.2
	Don't know	17	7.3
Q7	**For what reason this forest cover is important to you?**	**Frequency**	**Percentage**
	Bank protection	115	49.9
	Green and clean environment	26	11.1
	Runoff and flood control	84	36.5
	Beautification	5	2.5
Q8	**In terms of naturalness and beauty, how much do you rank this place?**	**Frequency**	**Percentage**
	5 (good)	169	73.6
	1 (bad)	31	13.5
	3 (moderate)	30	12.9

*n=230

Plate No. 8.2 *Photographs during Field Study*

8.4. Conclusion

There are many and widespread consequences of human civilization on rivers around the world, and worldwide calls for rivers to be returned to their pre-impacted conditions have gathered momentum (Wohl et al. 2005). The first stage in restoration is to evaluate the health

of streams on a reach-by-reach basis. Such evaluations are also highly popular since they represent society's concerns about deteriorating ecosystems and are simple for the general public to grasp and relate to (Boulton 1999). Among other things, riparian vegetation is commonly regarded as a reliable indication of river health and is employed as a stand-in for riparian ecology in many river restoration programmes. The computation of the QBR index for evaluating the riparian quality of the area has been done in this study through a perception study regarding the current situation in the Mayurakshi River basin area. The results of the survey will demonstrate how well the general population comprehends the effects of the physical, ecological, and perceptual characteristics of the study region and can help to identify and prioritise the reaches that need restoration.

References

- Boulton, A. J. (1999). An overview of river health assessment: philosophies, practice, problems and prognosis. *Freshwater biology*, *41*(2), 469-479.
- Carver, A. D., Danskin, S. D., Zaczek, J. J., Mangun, J. C., & Williard, K. W. (2004). A GIS methodology for generating riparian tree planting recommendations. *Northern Journal of Applied Forestry*, *21*(2), 100-106.
- Chaudhury, A. K. (1966). On the meteorological conditions responsible for heavy rainfall in Ajay catchment Area. *Indian J Meteorol Geophys*, *17*, 127-132.
- Corbacho, C., Sánchez, J. M., & Costillo, E. (2003). Patterns of structural complexity and human disturbance of riparian vegetation in agricultural landscapes of a Mediterranean area. *Agriculture, Ecosystems & Environment*, *95*(2-3), 495-507.
- Ghosh, S., & Guchhait, S. K. (2014). Hydrogeomorphic variability due to dam constructions and emerging problems: a case study of Damodar River, West Bengal, India. *Environment, Development and Sustainability*, *16*, 769-796.
- Goebel, P. C., Palik, B. J., & Pregitzer, K. S. (2003). Plant diversity contributions of riparian areas in watersheds of the northern Lake States, USA. *Ecological Applications*, *13*(6), 1595-1609.
- Halder, S., & Sarkar, S. (2014). A critical analysis on block wise status of agricultural productivity and efficiency: A case study on birbhum district, west bengal. *International Journal of Multidisciplinary Research and Development*, *3*(1), 341–345.
- Junker, B., & Buchecker, M. (2008). Aesthetic preferences versus ecological objectives in river restorations. *Landscape and urban planning*, *85*(3-4), 141-154.
- Kale, V. S. (1998). Monsoon floods in India: A hydro-geomorphic perspective. *Memoirs-Geological Society of India*, 229-259.
- Kienast, F., Frick, J., van Strien, M. J., & Hunziker, M. (2015). The Swiss Landscape Monitoring Program–A comprehensive indicator set to measure landscape change. *Ecological modelling*, *295*, 136-150.
- López-Rodríguez, A., Escribano-Bombín, R., Hernández-Jiménez, V., & Bell, S. (2019). Perceptions of ecological and aesthetic quality by natural resource professionals and local people. A qualitative exploration in a mountainous landscape (La Rioja, Spain). *Landscape research*, *44*(2), 241-255.
- Munné, A., Prat, N., Solà, C., Bonada, N., & Rieradevall, M. J. A. C. M. (2003). A simple field method for assessing the ecological quality of riparian habitat in rivers and streams: QBR index. *Aquatic conservation: marine and freshwater ecosystems*, *13*(2), 147-163.
- Nassauer, J. I., Kosek, S. E., & Corry, R. C. (2001). MEETING PUBLIC EXPECTATIONS WITH ECOLOGICAL INNOVATION IN RIPARIAN LANDSCAPES 1. *JAWRA Journal of the American Water Resources Association*, *37*(6), 1439-1443.
- Pal, S. (2016). Impact of Massanjore dam on hydro-geomorphological modification of Mayurakshi river, Eastern India. *Environment, development and sustainability*, *18*, 921-944.
- Postel, S. L., Daily, G. C., & Ehrlich, P. R. (1996). Human appropriation of renewable fresh water. *Science*, *271*(5250), 785-788.
- Roy, S., & Mistri, B. (2013). Estimation of peak flood discharge for an ungauged river: a case study of the Kunur River, West Bengal. *Geography journal*, *2013*.
- Vörösmarty, C. J., Meybeck, M., Fekete, B., Sharma, K., Green, P., & Syvitski, J. P. (2003). Anthropogenic sediment retention: major global impact from registered river impoundments. *Global and planetary change*, *39*(1-2), 169-190.
- Wohl, E., Angermeier, P. L., Bledsoe, B., Kondolf, G. M., MacDonnell, L., Merritt, D. M., ... & Tarboton, D. (2005). River restoration. *Water Resources Research*, *41*(10).

CHAPTER 9
FINAL CONCLUSION

9. Overall Conclusion

The Mayurakshi river basin's overall fluvial ecology has become promptly deteriorating as a result of overbearing human intrusion and poor river basin management program regulations. The combination of intense natural events and human endeavours today has resulted in the destruction of the riverine ecology. Both of these together have a multiplicative impact on the worsening of river health, which makes the Mayurakshi River's pattern unpredictable. Even though rainfall concentration in a short period of time is one of the important factors, it is not solely responsible for sustaining the minimum flow necessary to support the ecosystem.

The current study investigates the Mayurakshi River Basin area's overall ecological and environmental significance, by analysing the form, amount, and quality of the river flow as well as the factors that contribute to water resources' vulnerability, which not only impede the river's natural flow but also affect the surrounding ecosystem and livelihoods that depend on it. After examining the ecological relevance of the area, it is apparent that the considerable human encroachment over the major river's floodplain is severely harming the riparian vegetation cover. Population expansion can lead to an increase in the requirement for land resources to meet people basic needs including farming, which causes riparian ecosystems to be severely lost along with river banks. The values and functions of these ecosystem services continued to diminish as a result of the degradation of this floodplain area. The natural environment will suffer as a result of a significant decline in the value of all ecosystem services, and future generations will also be put in danger. There are no such management strategies or community awareness to restore the region's environmental equilibrium. Along with the decrease in flow, the quality of the existing water resources has been worse for both surface water and groundwater. The degradation of groundwater has been caused by both anthropogenic and geogenic processes. The amount of nitrate in groundwater has increased due to agricultural runoff leaching as well as extra human activities including unlined septic tanks, poor sanitation practices, and unmanaged sewer systems. This has decreased the quality of the water suitable for human consumption. The author has drawn some potential findings that could help in restoring the ecological and environmental balance of the river basin area in light of all the factors degrading the overall health of the Mayurakshi River and its surroundings.

- In the Mayurakshi River Basin area, a 40-year span of time with a 95% confidence level showed a general decreasing tendency in the geographical and temporal aspects of mean

annual temperature and precipitation. Additionally, it has been seen from the estimated IDF curves that the projected volume of rainfall rises with increasing return periods while the intensity of the rainfall tends to fall as the length of the rainfall remains constant over all return times.

- Prioritizing Mayurakshi River sub-watersheds based on different morphometric characteristics has been shown to be a helpful predictor of erosion vulnerability throughout the study area. When the results of a multi-criteria decision-making process (TOPSIS model) are combined with the Shannon entropy method, they reflect the erosional characteristics of each sub-watershed. After the results are validated with the rainfall erosivity index, it is revealed that the SW 6 region is more susceptible to erosion due to the higher kinetic energy of raindrops in the area.
- In order to demonstrate the hydrological and ecological activities carried out within the study region, the dynamic nature of surface water and ground water resources has also been studied. The analysis shows that although the density of ponds has decreased throughout the study area, the dispersion of water bodies has increased during the past 18 years. Due to the increasing need for irrigational water caused by this situation, farmers and other local stakeholders are building temporary recharge pools and nalas (Patra 2008) to supply the farmers' daily demands, especially during the hot summer months.
- However, the availability of such artificial water bodies is insufficient to meet the irrigational needs of the studied region. Farmers in the lower watershed of the river basin primarily use groundwater resources to irrigate their vast farmlands. Due to excessive groundwater usage from wells and submersible pumps, the present aquifer system is under a great deal of stress, which lowers the future potential of groundwater resources. This study also came to the conclusion that the dominant landscape above the ground has a significant impact on the movement of groundwater and the capacity for recharging. Among all the other contributing factors, LULC has a significant impact on establishing the study area's groundwater recharge potential zone.
- The Mayurakshi River has also experienced substantial channel geometry abnormalities from upstream to downstream. According to research on river channel geometry and hydro-geomorphological behaviour, increased human interference is degrading channel geomorphology and obstructing natural river flow. Because of the Massanjore Dam and Tilpara Barrage, the upper portion of the river has a broader width than typical. Furthermore, the successive addition of water by the tributaries increases the flow

momentum and depth of the flow in the main river's lower sections. The post-monsoon flow velocity and discharge volume of the Mayurakshi River have also been determined by the authors, which reflects the amount of flows in the river have not been sufficient during the lean season to meet irrigation as well as daily human needs in that region, subsequently causing the hydrological system to collapse.

- The classified land use land cover map demonstrates that during a time period of 32 years, a dramatic change has been observed in every chosen LULC class over the research area. This change was detected using advanced remote sensing and GIS technologies as well as high spatial resolution Landsat images. Such changes in land use and cover have the potential to impact the overall physical and economic health of the river basin. The majority of the land area in the Mayurakshi River basin (37%) has been quantified as having undergone a negative transformation (non-productive change), as opposed to 27% of the area has undergone beneficial transformation (productive change), which reflects the degradation of natural resources as a result of population growth and the expansion of cultivable land areas.
- In order to accurately forecast water availability and distribution systems under various demand loading and operational circumstances, hydraulic models have recently made substantial improvements. Here, the agricultural, climatological, and hydrological processes of the research area have been incorporated into a semi-distributed SWAT hydrological model. The estimated stream flow characteristics of the investigated catchments suggest that a rapid rise in stream flow discharge (1053.25 cumec at Massanjore Dam and 1380 cumec at Tilpara Barrage) occurred during the month of September 2000. This was due to the arrival of an extensive rainfall storm near to the upstream portion of the basin, resulting in a considerable water release from the upstream of Massanjore Dam to the downstream of Tilpara Barrage, causing a serious flood disaster (Islam et al. 2020).
- In the present research, characteristics of an important water balance component and indicators of the availability of water resources are further discussed. According to the study, the watershed received 1432.4 mm of precipitation annually on average over the previous 38 years. Evapotranspiration is the most significant water balance component, accounting for roughly 580.1 mm (34%) of water loss from the watershed. However, this study also investigates the future trajectory of the water budget throughout the area. A much lower mean annual precipitation (1404.7 mm) has been forecast for the ten-year simulated time span (2021–2031). A large decrease in the mean annual

evapotranspiration, which was estimated to be 542.1 mm or 38% of the mean precipitation in the future scenario. A reduction in vegetation cover can be blamed for such a big drop in evapotranspiration. The groundwater table will continue to fall in the near future as a result of the soil's lower capacity to hold water, which was indicated by the decline in canopy interception, percolation, and evapotranspiration as well as the increase in runoff.

Using the calibrated SWAT model, this work has also quantified the essential components of the water cycle at the sub-basin level of the Mayurakshi River basin. These include green water flow (actual and projected evapotranspiration), blue water flow (water yield plus deep aquifer recharging), and green water storage (soil moisture). For the long-term planning of a region's food and water supply, among other things, this study can offer strategic information regarding internal, renewable water resources that are easily accessible.

- One of the main goals of this project is to determine how spatiotemporal changes in land use and cover affect ecosystem services. Over the past 30 years, there have been considerable and swift LULC changes in the study region, primarily as a result of the planned and unplanned expansion of built-up areas to meet the strong demand for residential and commercial space. The local wetland ecology has declined as a result of changes in the local ESVs brought on by the expansion of built-up regions.
- The channel's floodplain structure and connectivity must be preserved in order to maintain stream health and safeguard its biological functions. As a result, between 1989 and 2021, researchers evaluated and looked at how the riparian ecosystems in the Mayurakshi River Basin were evolving. Here, certain significant field-based and image-based indicators have been used including the Riparian Strip Quality Index (RSQI), the Qualitat del Bosc de Ribera (QBR) Index, and the Normalised Difference Vegetation Index (NDVI) and the Overall Riparian Health Quality Score (ORHQS) to assess the research area's overall riparian health quality. The final outcome shows that the middle and downstream parts of the river have suffered substantial damage. These reaches are predominantly affected by significant human activity, such as sand mining from the riverbed, cutting forest from the bankside, expanding terrace farming, bank erosion, dumping municipal rubbish into the main channel, etc. The lower portions of the Mayurakshi, which is also a confluence zone for significant tributary rivers including the Kushkarini, Kuya, and Dwarka, have furthermore frequently been impacted by the

annual flood occurrences. This has further caused the riparian flora and riverbank to deteriorate.

- Finally, the environmental flow variability of Massanjore Dam and Tilpara Barrage in the Mayurakshi River Basin area was assessed using two significant hydrological methods: the Tennant method (Tennant 1976) and the classic Flow Duration Curve (FDC) (Verma et al. 2017). The analysis shows that the recommended percentage of mean monthly flow of the optimal ecological condition is not always obtained based on the long-term mean annual flow of the Massanjore and Tilpara barrages (23.3 and 81.09 cumec). A poor to significantly impaired flow condition is evident for both of the stations in the Mayurakshi River Basin area almost every year. These results provide thorough information that may be used to estimate water availability, demand for anthropogenic and ecological purposes, and the amount that can be removed in the near term in connection to the projected anthropogenic change and its repercussions.
- Another significant contribution to this study is the quantification of the physical, chemical, and biological properties of the surface (rivers) and ground (tube well) water supplies over the Mayurakshi River Basin area. For both low and high rainfall seasons, river sample water has been collected from 17 sample sites, ranging from the plateau of the upstream to the plain land of the lower basin. The calculated water quality index demonstrates that numerous pollution sources, such as domestic waste and agricultural runoff, are largely affecting the middle to lower reach of the research region. This degradation of the river's water quality leads to subsequent ecological damage. The Mayurakshi River is polluted in multiple different places, according to calculated pollution levels. Many locations along the river are affected by organic pollution, or OPI> 1. The river's water was under high danger of eutrophication since EI was greater than zero. However, due to an increase in water during the monsoon season, the amount of pollution in the river has been slightly reduced.
- An Integrated Water Quality Index (IWQI) (Mukate et al. 2019) has been employed among 228 tube well water samples taken from the randomly selected gram panchayats of the Mayurakshi River Basin area to assess the appropriateness of groundwater quality for human consumption. By extrapolating the IWQI values and adhering to the BIS-established health guidelines, it is shown that samples of high-quality water are discovered outside of the main metropolitan centre, indicating that the area is less contaminated. Poor drinking water quality is most frequently observed in the top and intermediate reaches of the catchment area, which are predominantly affected

by agricultural runoff due to the prevalence of agriculture. Poorly sealed bore wells and excavated wells mix waste elements into the aquifer system, lowering the quality of the groundwater. Furthermore, inadequate sanitation practices, residential sewage disposal, and open defecation are also responsible for the diminishing groundwater quality over the study area.

- To assess the social aspects of the deterioration of the watershed's environment, perception research has also been done. This study used an indirect survey methodology and asked the locals as part of the surveying process to add qualitative research. The results indicate that a higher majority of the sample population approved of the quantity and quality of the Mayurakshi River continuing to deteriorate. However, a serious lack of understanding on the part of people encourages the river to become a dumping ground and weakens its ecological and environmental stability.

This study also includes a perception assessment on the Mayurakshi River's riparian health state. The opinions of the villagers in the Mayurakshi River basin area have also been in-depth surveyed using the same approach used for the QBR index (Munne et al., 1998). According to the study's findings, in addition to recognizing the main factors (urbanization and agricultural development) responsible for the destruction of riparian vegetation, public awareness raising is also important in order to preserve and boost the amount of greenery close to the floodplain of the study area.

CHAPTER 10
RECOMMENDATIONS

10. Recommendations

The Mayurakshi River is a significant resource that supports numerous ecological, socio-cultural, and economic activities in its catchment area. However, the focus of the current study is on the elements that undermine the river's ecological and environmental significance. The results demonstrate that the river is dealing with a number of issues (Plate No. 8.3), both in terms of quality and quantity. This chapter discusses several potential actions that ought to be taken right away at the administrative and community levels.

- Afforestation is the primary and most important strategy to controlling excessive erosion of the top soil and reducing sediment load to the river. An increase in the amount of greenery in an area can also hold the fertile soil, which is good for agricultural production and also allows more water to seep into the ground by lowering surface runoff from the land surface.
- A portion of the riparian floodplain should be reserved for useful regulatory operations. The ideal land use and permitted activities in the river floodplains would be regulated in some way by the city's development plan or master plan. However, these regions have been occupied by unauthorized colonies or used for prohibited business entities like agriculture, sand mining, etc. The river's health depends on only allowing authorized construction and activities in the floodplains, which can be achieved by strictly enforcing the law, adopting river-sensitive planning guidelines, increasing farmer awareness and capacity, and developing strategies for relocating unauthorized colonies.
- Another focus has been on establishing and maintaining native trees alongside the rivers and lakes, which aids in preventing pollutants and silt from entering the river and traps millions of tons of carbon that harm the ecosystem.

Plate No. 10.1 *Photographs Showing Field Observations within the Study Area*

- To maintain the river's natural flow of water, unchecked and excessive water lifting needs to be prevented. The improper lifting of surface water, mainly for irrigation purposes should be absolutely restricted. Additionally to preserve the natural grading of the river course, unauthorized actions such as the construction of bridges and crossways, as well as the unscientific gathering of silt from the riverbed, must stop immediately. The government can implement some measures for scientifically dredging the river.
- Unsustainable land use has a serious consequences for the prevailing ecology and society, which will continue to get more serious. In order to solve unsustainable land-use practices, transformational change is necessary as the demands on land-use systems increase.
- In general, ecosystems supply a variety of goods and services that benefit human well-being, including food supplying, recycling nutrients, water quality, habitat providing, and carbon sequestration. Unscientific land-use decisions disrupt the flow of these services by altering ecosystems, ranging from slight and reversible modifications to complete and irreversible transformation of natural and human-dominated landscapes. In this situation, coordinated land use strategies are crucial to achieving the sustainable development of land resources. In order to minimize land degradation, restoration of degraded land, ensuring its sustainable use and increase resilience, it is crucial to choose the appropriate land uses for the given biophysical and socioeconomic conditions of the study area.
- By introducing several varieties of less water-intensive crops, the government should support sustainable farming techniques. Additionally, by improving the current irrigation methods and changing the cropping pattern, it is possible to increase both the productivity and sustainability of the land over the study area.
- The government's agricultural department and non-governmental organizations should properly train the farmers and encourage them to switch from chemical fertilizers and pesticides to more natural alternatives, such as substitutes made from cow dung and plant extracts, or by sowing cover crops. These methods can also improve the soil's capacity to hold moisture so as increases crop productivity over the area.
- Solid trash dumping and the release of harmful compounds into rivers need to be stop since these materials change the river's flow dynamics. Government should take the initiative to establish disposal sites where waste would be sorted out according to type

and disposed of appropriately. Some structural and non-structural measures are necessary to prevent pollution load from the river water. Constructing the necessary sewage infrastructure (such as sewer networks, interceptor drains, sewage treatment facilities, etc.) are examples of structural measures. Non-structural solutions include community workshops to urge residents to link their homes to the sewer network, awareness raising, encouraging businesses and sizable residential societies to establish in-house treatment facilities, etc.

- It should be encouraged to revive depleted water bodies, clean up dirty water bodies, and beautify water bodies for commercial and recreational uses, which will help reduce the stress on the Mayurakshi River. Water bodies and wetlands typically have an innate connection to rivers, either through groundwater movement or drainage patterns. They enhance groundwater recharge, which in turn serves to increase the study area's water supply and lowers the burden on rivers. Rejuvenated wetlands work similarly to "wastewater treatment plants" and can drastically reduce the number of pollutants that enters into the river. An additional incentive for the research location is the recreational advantages that these two interventions can deliver.
- Reusing wastewater is a fantastic way to reduce the pressure on river. As a result, less freshwater would be removed from the river, leaving more water available to sustain the river's natural flow. However, in most of the rural areas, the direct reuse of treated wastewater is limited. There are several potential uses for treated wastewater, including agriculture, horticulture, road cleaning, vehicle cleaning, reviving aquatic bodies, groundwater replenishment, and many more.
- In the research area, groundwater sources predominantly used for human consumption are frequently contaminated by harmful microorganisms as a result of insufficient sanitation facilities. To avoid microbiological contamination and water-borne diseases, groundwater sources (tube wells) should be kept at a safe distance from human waste disposal sites.
- The long-term viability of healthy river basins and the accomplishments of any undertaking by urban local bodies largely depend on public support. This support is significantly easier to obtain when residents are aware of the challenges at present as well as how they may assist in addressing them. Cities must create a focused plan to raise awareness about the environmental advantages of healthy rivers using new communication techniques. This will serve as the foundation for the necessary

behavioural transformation of the local inhabitants. This also conveys a suggestion that water resource management cannot be solely the responsibility of the government. Residents must take the initiative and bear the burden of duty.

- Another component of the effort aimed at raising public awareness and involving hundreds of organizations and communities in ecosystem protection and water quality restoration. This includes women villagers who rely heavily on the river for their everyday household duties.

10.1 Limitations of the Work

- Data scarcity- both in climatological and hydrological data.
- Discontinuous survey due to Covid-19 pandemic situation.
- Some of the downstream location has not been able to survey due to its locational inaccessibility.

10.2 Future Scope of Research

The current study discovered that the Mayurakshi River's environmental significance does not support the survival of aquatic organisms or the growth of society and the economy. Though environmental consciousness and protection measures are becoming more important around the world, the situation in West Bengal, particularly for the Mayurakshi River, is not encouraging. Therefore, more focused research is needed in several dimensions.

- More research is needed to determine the properties of river sedimentation in relation to the reservoir storage capacity, life span, and river flow. Future research should also emphasize how sediment build up in river beds can change the river's normal flow pattern and lead to extreme hydrological occurrences.
- It has become necessary to conduct a more thorough examination of the environmental flow demand utilizing more sophisticated procedures, such as the hydraulic rating method, habitat modeling, and other all-encompassing approaches. Even though the application flow duration curve has been included in the current research, a sub basin level interpretation will be more useful for developing its seasonal fluctuation of minimum flow requirements.
- To investigate the relationships between the ecological quality and aesthetic appeal of the researched sites, it is important to consider the visual tastes of the local stakeholders. The evaluation of human perceptions, beliefs, and attitudes is crucial for landscape

management for ecological benefits and restoration since these factors affect the ecological functions and aesthetic qualities of a particular place. Thus, planning landscape alterations with both public aesthetic perception and ecological objectives would increase the probability that such designs would satisfy societal ambitions and win long-term acceptance and support.

- The composition and structures of the vegetation, which have a significant impact on the nearby uplands and aquatic ecology, must be taken into account while evaluating the characteristics of riparian vegetation. As a result, a complete analysis must require based on the number, richness, and variety of native species of both flora and fauna.
- Finding long-term solutions to water-related issues involving both the quantity and quality of the water resources requires a thorough evaluation of the water resources that are accessible in a region or a river basin. In this regard, there is a significant need for an overall review of the security of water resources from the perspectives of water consumption balance, water availability, and demand and supply balance.

ANNEXURE I

Table for Computed Frequency Precipitation Values and Intensities for Different Durations and Return Periods Using Gumbel Method for ***Maharo Rain Gauge Station*** *(Rainfall in mm)*

Tr (Year)	10 min			20 min			30 min		
	P_{ave}=20.53	S = 12.35		P_{ave}=25.86	S = 15.56		P_{ave}=29.61	S = 17.81	
	K	P_T	I_T	K	P_T	I_T	K	P_T	I_T
2	-0.156	18.608	111.644	-0.156	23.444	70.333	-0.156	26.837	53.674
10	1.489	38.907	233.440	1.489	49.020	147.061	1.489	56.114	112.229
25	2.316	49.125	294.742	2.316	61.893	185.679	2.316	70.850	141.700
50	2.930	56.704	340.219	2.930	71.443	214.329	2.930	81.782	163.563
100	3.539	64.228	385.360	3.539	80.922	242.766	3.539	92.633	185.266
	60 min			120 min			180 min		
	P_{ave}=37.30	S = 22.44		P_{ave}=46.99	S = 28.27		P_{ave}=53.80	S = 32.36	
	K	P_T	I_T	K	P_T	I_T	K	P_T	I_T
2	-0.156	33.812	33.812	-0.156	42.601	21.300	-0.156	48.766	16.255
10	1.489	70.700	70.700	1.489	89.076	44.538	1.489	101.966	33.989
25	2.316	89.265	89.265	2.316	112.467	56.234	2.316	128.743	42.914
50	2.930	103.038	103.038	2.930	129.820	64.910	2.930	148.607	49.536
100	3.539	116.710	116.710	3.539	147.045	73.523	3.539	168.325	56.108
	360 min			720 min			1440 min		
	P_{ave}=67.78	S = 40.77		P_{ave}=85.40	S = 40.77		P_{ave}=107.60	S = 64.71	
	K	P_T	I_T	K	P_T	I_T	K	P_T	I_T
2	-0.156	61.441	10.240	-0.156	77.411	6.451	-0.156	97.532	4.064
10	1.489	128.470	21.412	1.489	161.862	13.488	1.489	203.933	8.497
25	2.316	162.206	27.034	2.316	204.367	17.031	2.316	257.486	10.729
50	2.930	187.233	31.206	2.930	235.899	19.658	2.930	297.214	12.384
100	3.539	212.076	35.346	3.539	267.199	22.267	3.539	336.650	14.027

Table for Computed Frequency Precipitation Values and Intensities for Different Durations and Return Periods Using Gumbel Method for ***Dumka Rain Gauge Station*** *(Rainfall in mm)*

Tr (Year)	10 min			20 min			30 min		
	P_{ave}=20.53	S = 12.35		P_{ave}=25.86	S = 15.56		P_{ave}=29.61	S = 17.81	
	K	P_T	I_T	K	P_T	I_T	K	P_T	I_T
2	-0.156	18.608	111.644	-0.156	23.444	70.333	-0.156	26.837	53.674
10	1.489	38.907	233.440	1.489	49.020	147.061	1.489	56.114	112.229
25	2.316	49.125	294.742	2.316	61.893	185.679	2.316	70.850	141.700
50	2.930	56.704	340.219	2.930	71.443	214.329	2.930	81.782	163.563
100	3.539	64.228	385.360	3.539	80.922	242.766	3.539	92.633	185.266
	60 min			120 min			180 min		
	P_{ave}=37.30	S = 22.43		P_{ave}=46.99	S = 28.27		P_{ave}=53.80	S = 32.36	
	K	P_T	I_T	K	P_T	I_T	K	P_T	I_T
2	-0.156	33.812	33.812	-0.156	42.601	21.300	-0.156	48.766	16.255
10	1.489	70.700	70.700	1.489	89.076	44.538	1.489	101.966	33.989
25	2.316	89.265	89.265	2.316	112.467	56.234	2.316	128.743	42.914
50	2.930	103.038	103.038	2.930	129.820	64.910	2.930	148.607	49.536
100	3.539	116.710	116.710	3.539	147.045	73.523	3.539	168.325	56.108
	360 min			720 min			1440 min		
	P_{ave}=67.78	S = 40.77		P_{ave}=85.40	S = 51.36		P_{ave}=107.60	S = 64.72	
	K	P_T	I_T	K	P_T	I_T	K	P_T	I_T
2	-0.156	61.441	10.240	-0.156	77.411	6.451	-0.156	97.532	4.064
10	1.489	128.470	21.412	1.489	161.862	13.488	1.489	203.933	8.497
25	2.316	162.206	27.034	2.316	204.367	17.031	2.316	257.486	10.729
50	2.930	187.233	31.206	2.930	235.899	19.658	2.930	297.214	12.384
100	3.539	212.076	35.346	3.539	267.199	22.267	3.539	336.650	14.027

Table for Computed Frequency Precipitation Values and Intensities for Different Durations and Return Periods Using Gumbel Method for ***Massanjore Rain Gauge Station*** *(Rainfall in mm)*

Tr (Year)	10 min			20 min			30 min		
	P_{ave}=21.45	S = 16.08		P_{ave}=27.04	S = 20.26		P_{ave}=30.95	S = 23.19	
	K	P_T	I_T	K	P_T	I_T	K	P_T	I_T
2	-0.156	18.957	113.739	-0.156	23.884	71.653	-0.156	27.341	54.681
10	1.489	45.389	272.330	1.489	57.187	171.560	1.489	65.463	130.925
25	2.316	58.693	352.150	2.316	73.948	221.845	2.316	84.650	169.300
50	2.930	68.562	411.366	2.930	86.383	259.149	2.930	98.884	197.768
100	3.539	78.359	470.144	3.539	98.726	296.178	3.539	113.013	226.026
	60 min			120 min			180 min		
	P_{ave}=38.99	S = 29.21		P_{ave}=49.13	S = 36.81		P_{ave}=56.24	S = 42.13	
	K	P_T	I_T	K	P_T	I_T	K	P_T	I_T
2	-0.156	34.447	34.447	-0.156	43.400	21.700	-0.156	49.681	16.560
10	1.489	82.478	82.478	1.489	103.915	51.958	1.489	118.953	39.651
25	2.316	106.652	106.652	2.316	134.373	67.187	2.316	153.819	51.273
50	2.930	124.586	124.586	2.930	156.969	78.484	2.930	179.684	59.895
100	3.539	142.388	142.388	3.539	179.397	89.699	3.539	205.358	68.453
	360 min			720 min			1440 min		
	P_{ave}=70.85	S = 53.08		P_{ave}=89.27	S = 66.88		P_{ave}=112.47	S = 84.27	
	K	P_T	I_T	K	P_T	I_T	K	P_T	I_T
2	-0.156	62.594	10.432	-0.156	78.864	6.572	-0.156	99.362	4.140
10	1.489	149.872	24.979	1.489	188.827	15.736	1.489	237.907	9.913
25	2.316	193.800	32.300	2.316	244.172	20.348	2.316	307.638	12.818
50	2.930	226.388	37.731	2.930	285.231	23.769	2.930	359.368	14.974
100	3.539	258.735	43.123	3.539	325.986	27.166	3.539	410.717	17.113

Table for Computed Frequency Precipitation Values and Intensities for Different Durations and Return Periods Using Gumbel Method for ***Kundahit Rain Gauge Station*** *(Rainfall in mm)*

Tr (Year)	10 min			20 min			30 min		
	P_{ave}=21.45	S = 16.09		P_{ave}=27.03	S = 20.26		P_{ave}=30.94	S = 23.19	
	K	P_T	I_T	K	P_T	I_T	K	P_T	I_T
2	-0.156	18.952	113.710	-0.156	23.878	71.634	-0.156	27.334	54.667
10	1.489	45.389	272.326	1.489	57.186	171.558	1.489	65.462	130.923
25	2.316	58.694	352.159	2.316	73.950	221.851	2.316	84.652	169.304
50	2.930	68.565	411.384	2.930	86.387	259.161	2.930	98.888	197.777
100	3.539	78.364	470.172	3.539	98.732	296.196	3.539	113.020	226.040
	60 min			120 min			180 min		
	P_{ave}=38.98	S = 29.22		P_{ave}=49.12	S = 36.81		P_{ave}=56.23	S = 42.14	
	K	P_T	I_T	K	P_T	I_T	K	P_T	I_T
2	-0.156	34.438	34.438	-0.156	43.389	21.695	-0.156	49.668	16.556
10	1.489	82.476	82.476	1.489	103.914	51.957	1.489	118.952	39.651
25	2.316	106.655	106.655	2.316	134.377	67.188	2.316	153.823	51.274
50	2.930	124.592	124.592	2.930	156.976	78.488	2.930	179.692	59.897
100	3.539	142.396	142.396	3.539	179.408	89.704	3.539	205.371	68.457
	360 min			720 min			1440 min		
	P_{ave}=70.84	S = 53.09		P_{ave}=89.25	S = 66.89		P_{ave}=112.45	S = 84.28	
	K	P_T	I_T	K	P_T	I_T	K	P_T	I_T
2	-0.156	62.578	10.430	-0.156	78.844	6.570	-0.156	99.337	4.139
10	1.489	149.870	24.978	1.489	188.824	15.735	1.489	237.903	9.913
25	2.316	193.805	32.301	2.316	244.178	20.348	2.316	307.646	12.819
50	2.930	226.398	37.733	2.930	285.244	23.770	2.930	359.384	14.974
100	3.539	258.751	43.125	3.539	326.005	27.167	3.539	410.741	17.114

Table for Computed Frequency Precipitation Values and Intensities for Different Durations and Return Periods Using Gumbel Method for ***Tilpara Rain Gauge Station*** *(Rainfall in mm)*

Tr (Year)	10 min			20 min			30 min		
	P_{ave}=18.24	S = 10.77		P_{ave}=22.98	S = 13.56		P_{ave}=26.31	S = 15.53	
	K	P_T	I_T	K	P_T	I_T	K	P_T	I_T
2	-0.156	16.568	99.405	-0.156	20.874	62.622	-0.156	23.895	47.790
10	1.489	34.269	205.612	1.489	43.177	129.530	1.489	49.425	98.850
25	2.316	43.179	259.068	2.316	54.402	163.206	2.316	62.275	124.549
50	2.930	49.788	298.724	2.930	62.729	188.188	2.930	71.807	143.614
100	3.539	56.349	338.087	3.539	70.995	212.986	3.539	81.269	162.539
	60 min			120 min			180 min		
	P_{ave}=33.15	S = 19.56		P_{ave}=41.77	S = 24.65		P_{ave}=47.81	S = 28.22	
	K	P_T	I_T	K	P_T	I_T	K	P_T	I_T
2	-0.156	30.106	30.106	-0.156	37.931	18.965	-0.156	43.420	14.473
10	1.489	62.272	62.272	1.489	78.457	39.229	1.489	89.811	29.937
25	2.316	78.461	78.461	2.316	98.855	49.427	2.316	113.160	37.720
50	2.930	90.471	90.471	2.930	113.987	56.993	2.930	130.482	43.494
100	3.539	102.393	102.393	3.539	129.007	64.504	3.539	147.676	49.225
	360 min			720 min			1440 min		
	P_{ave}=60.24	S = 35.55		P_{ave}=75.89	S = 44.79		P_{ave}=95.62	S = 56.43	
	K	P_T	I_T	K	P_T	I_T	K	P_T	I_T
2	-0.156	54.706	9.118	-0.156	68.925	5.744	-0.156	86.840	3.618
10	1.489	113.155	18.859	1.489	142.566	11.881	1.489	179.622	7.484
25	2.316	142.573	23.762	2.316	179.631	14.969	2.316	226.321	9.430
50	2.930	164.397	27.400	2.930	207.128	17.261	2.930	260.964	10.874
100	3.539	186.060	31.010	3.539	234.421	19.535	3.539	295.352	12.306

Table for Computed Frequency Precipitation Values and Intensities for Different Durations and Return Periods Using Gumbel Method for ***Kultore Rain Gauge Station*** *(Rainfall in mm)*

Tr (Year)	10 min			20 min			30 min		
	P_{ave}=18.24	S = 10.76		P_{ave}=22.99	S = 13.56		P_{ave}=26.32	S = 15.52	
	K	P_T	I_T	K	P_T	I_T	K	P_T	I_T
2	-0.156	16.573	99.434	-0.156	20.880	62.640	-0.156	23.902	47.804
10	1.489	34.270	205.614	1.489	43.177	129.531	1.489	49.425	98.851
25	2.316	43.177	259.056	2.316	54.399	163.198	2.316	62.272	124.543
50	2.930	49.785	298.702	2.930	62.725	188.174	2.930	71.802	143.604
100	3.539	56.344	338.055	3.539	70.989	212.966	3.539	81.262	162.523
	60 min			120 min			180 min		
	P_{ave}=33.16	S = 19.56		P_{ave}=41.78	S = 24.64		P_{ave}=47.82	S = 28.21	
	K	P_T	I_T	K	P_T	I_T	K	P_T	I_T
2	-0.156	30.114	30.114	-0.156	37.942	18.971	-0.156	43.432	14.477
10	1.489	62.272	62.272	1.489	78.458	39.229	1.489	89.812	29.937
25	2.316	78.457	78.457	2.316	98.850	49.425	2.316	113.155	37.718
50	2.930	90.465	90.465	2.930	113.978	56.989	2.930	130.473	43.491
100	3.539	102.383	102.383	3.539	128.995	64.497	3.539	147.662	49.221
	360 min			720 min			1440 min		
	P_{ave}=60.25	S = 35.54		P_{ave}=75.91	S = 44.77		P_{ave}=95.64	S = 56.42	
	K	P_T	I_T	K	P_T	I_T	K	P_T	I_T
2	-0.156	54.721	9.120	-0.156	68.945	5.745	-0.156	86.865	3.619
10	1.489	113.156	18.859	1.489	142.567	11.881	1.489	179.624	7.484
25	2.316	142.567	23.761	2.316	179.623	14.969	2.316	226.310	9.430
50	2.930	164.385	27.398	2.930	207.112	17.259	2.930	260.945	10.873
100	3.539	186.043	31.007	3.539	234.399	19.533	3.539	295.324	12.305

Table for Computed Frequency Precipitation Values and Intensities for Different Durations and Return Periods Using Gumbel Method for ***Sainthia Rain Gauge Station*** *(Rainfall in mm)*

Tr (Year)	10 min			20 min			30 min		
	P_{ave}=20.48	S = 12.14		P_{ave}=25.80	S = 15.29		P_{ave}=29.54	S = 17.51	
	K	P_T	I_T	K	P_T	I_T	K	P_T	I_T
2	-0.156	18.591	111.546	-0.156	23.424	70.271	-0.156	26.813	53.627
10	1.489	38.550	231.295	1.489	48.570	145.709	1.489	55.599	111.197
25	2.316	48.595	291.566	2.316	61.226	183.679	2.316	70.086	140.173
50	2.930	56.047	336.278	2.930	70.615	211.846	2.930	80.834	161.669
100	3.539	63.445	380.660	3.539	79.935	239.806	3.539	91.503	183.006
	60 min			120 min			180 min		
	P_{ave}=37.22	S = 22.06		P_{ave}=46.88	S = 27.79		P_{ave}=53.67	S = 31.81	
	K	P_T	I_T	K	P_T	I_T	K	P_T	I_T
2	-0.156	33.783	33.7828	-0.156	42.564	21.282	-0.156	48.723	16.241
10	1.489	70.050	70.04981	1.489	88.257	44.129	1.489	101.029	33.676
25	2.316	88.303	88.30344	2.316	111.255	55.628	2.316	127.356	42.452
50	2.930	101.845	101.845	2.930	128.317	64.158	2.930	146.886	48.962
100	3.539	115.287	115.2866	3.539	145.252	72.626	3.539	166.272	55.424
	360 min			720 min			1440 min		
	P_{ave}=67.62	S = 40.08		P_{ave}=85.20	S = 50.50		P_{ave}=107.34	S = 63.63	
	K	P_T	I_T	K	P_T	I_T	K	P_T	I_T
2	-0.156	61.387	10.231	-0.156	77.343	6.445	-0.156	97.446	4.060
10	1.489	127.289	21.215	1.489	160.374	13.365	1.489	202.059	8.419
25	2.316	160.458	26.743	2.316	202.164	16.847	2.316	254.711	10.613
50	2.930	185.065	30.844	2.930	233.167	19.431	2.930	293.772	12.240
100	3.539	209.490	34.915	3.539	263.940	21.995	3.539	332.544	13.856

Table for Computed Frequency Precipitation Values and Intensities for Different Durations and Return Periods Using Gumbel Method for ***Shekhampore Rain Gauge Station*** *(Rainfall in mm)*

Tr (Year)	10 min			20 min			30 min		
	P_{ave}=18.63	S = 9.33		P_{ave}=23.48	S = 11.75		P_{ave}=26.87	S = 13.45	
	K	P_T	I_T	K	P_T	I_T	K	P_T	I_T
2	-0.156	17.181	103.084	-0.156	21.647	64.940	-0.156	24.779	49.559
10	1.489	32.517	195.095	1.489	40.968	122.905	1.489	46.897	93.794
25	2.316	40.235	241.406	2.316	50.693	152.079	2.316	58.029	116.058
50	2.930	45.961	275.762	2.930	57.907	173.722	2.930	66.288	132.575
100	3.539	51.645	309.864	3.539	65.069	195.206	3.539	74.485	148.970
	60 min			120 min			180 min		
	P_{ave}=33.86	S = 16.95		P_{ave}=42.66	S = 21.35		P_{ave}=48.83	S = 24.44	
	K	P_T	I_T	K	P_T	I_T	K	P_T	I_T
2	-0.156	31.220	31.220	-0.156	39.335	19.667	-0.156	45.027	15.009
10	1.489	59.087	59.087	1.489	74.444	37.222	1.489	85.218	28.406
25	2.316	73.112	73.112	2.316	92.115	46.058	2.316	105.446	35.149
50	2.930	83.517	83.517	2.930	105.225	52.612	2.930	120.452	40.151
100	3.539	93.845	93.845	3.539	118.238	59.119	3.539	135.348	45.116
	360 min			720 min			1440 min		
	P_{ave}=61.52	S = 30.79		P_{ave}=77.51	S = 38.80		P_{ave}=97.66	S = 48.89	
	K	P_T	I_T	K	P_T	I_T	K	P_T	I_T
2	-0.156	56.730	9.455	-0.156	71.476	5.956	-0.156	90.054	3.752
10	1.489	107.367	17.895	1.489	135.274	11.273	1.489	170.435	7.101
25	2.316	132.853	22.142	2.316	167.385	13.949	2.316	210.892	8.787
50	2.930	151.761	25.293	2.930	191.206	15.934	2.930	240.905	10.038
100	3.539	170.528	28.421	3.539	214.852	17.904	3.539	270.696	11.279

Table for Computed Frequency Precipitation Values and Intensities for Different Durations and Return Periods Using Gumbel Method for ***Kandi Rain Gauge Station*** *(Rainfall in mm)*

Tr (Year)	10 min			20 min			30 min		
	P_{ave}=18.83	S = 8.64		P_{ave}=21.55	S = 9.89		P_{ave}=27.15	S = 12.46	
	K	P_T	I_T	K	P_T	I_T	K	P_T	I_T
2	-0.156	17.482	104.888	-0.156	20.011	60.034	-0.156	25.213	50.426
10	1.489	31.688	190.123	1.489	36.273	108.820	1.489	45.702	91.403
25	2.316	38.838	233.023	2.316	44.458	133.375	2.316	56.014	112.028
50	2.930	44.142	264.848	2.930	50.530	151.591	2.930	63.664	127.328
100	3.539	49.407	296.439	3.539	56.557	169.672	3.539	71.258	142.516
	60 min			120 min			180 min		
	P_{ave}=34.21	S = 15.70		P_{ave}=43.10	S = 19.78		P_{ave}=49.33	S = 22.64	
	K	P_T	I_T	K	P_T	I_T	K	P_T	I_T
2	-0.156	31.766	31.766	-0.156	40.023	20.011	-0.156	45.815	15.272
10	1.489	57.581	57.581	1.489	72.547	36.273	1.489	83.045	27.682
25	2.316	70.573	70.573	2.316	88.917	44.458	2.316	101.784	33.928
50	2.930	80.212	80.212	2.930	101.061	50.530	2.930	115.686	38.562
100	3.539	89.779	89.779	3.539	113.115	56.557	3.539	129.484	43.161
	360 min			720 min			1440 min		
	P_{ave}=62.16	S = 28.53		P_{ave}=78.32	S = 35.95		P_{ave}=98.68	S = 45.29	
	K	P_T	I_T	K	P_T	I_T	K	P_T	I_T
2	-0.156	57.723	9.621	-0.156	72.727	6.061	-0.156	91.630	3.818
10	1.489	104.631	17.438	1.489	131.826	10.986	1.489	166.091	6.920
25	2.316	128.240	21.373	2.316	161.572	13.464	2.316	203.568	8.482
50	2.930	145.755	24.292	2.930	183.639	15.303	2.930	231.371	9.640
100	3.539	163.140	27.190	3.539	205.543	17.129	3.539	258.969	10.790

Table for Computed Frequency Precipitation Values and Intensities for Different Durations and Return Periods Using Gumbel Method for ***Bharatpur Rain Gauge Station*** *(Rainfall in mm)*

Tr (Year)	10 min			20 min			30 min		
	P_{ave}=18.83	S = 8.64		P_{ave}=23.72	S = 10.89		P_{ave}=27.15	S = 12.46	
	K	P_T	I_T	K	P_T	I_T	K	P_T	I_T
2	-0.156	17.483	104.894	-0.156	22.027	66.080	-0.156	25.214	50.429
10	1.489	31.688	190.123	1.489	39.924	119.772	1.489	45.702	91.403
25	2.316	38.837	233.019	2.316	48.932	146.796	2.316	56.013	112.026
50	2.930	44.141	264.842	2.930	55.615	166.844	2.930	63.663	127.325
100	3.539	49.406	296.431	3.539	62.248	186.743	3.539	71.256	142.512
	60 min			120 min			180 min		
	P_{ave}=34.21	S = 15.70		P_{ave}=43.10	S = 19.78		P_{ave}=49.34	S = 22.64	
	K	P_T	I_T	K	P_T	I_T	K	P_T	I_T
2	-0.156	31.768	31.768	-0.156	40.025	20.013	-0.156	45.817	15.272
10	1.489	57.580	57.580	1.489	72.547	36.273	1.489	83.045	27.682
25	2.316	70.572	70.572	2.316	88.915	44.458	2.316	101.783	33.928
50	2.930	80.210	80.210	2.930	101.058	50.529	2.930	115.683	38.561
100	3.539	89.777	89.777	3.539	113.112	56.556	3.539	129.481	43.160
	360 min			720 min			1440 min		
	P_{ave}=62.17	S = 28.53		P_{ave}=78.32	S = 28.53		P_{ave}=98.68	S = 45.29	
	K	P_T	I_T	K	P_T	I_T	K	P_T	I_T
2	-0.156	57.726	9.621	-0.156	72.731	6.061	-0.156	91.635	3.818
10	1.489	104.631	17.438	1.489	131.826	10.986	1.489	166.091	6.920
25	2.316	128.238	21.373	2.316	161.570	13.464	2.316	203.565	8.482
50	2.930	145.751	24.292	2.930	183.635	15.303	2.930	231.366	9.640
100	3.539	163.135	27.189	3.539	205.538	17.128	3.539	258.961	10.790

Table for Computed Frequency Precipitation Values and Intensities for Different Durations and Return Periods Using Gumbel Method for ***Narayanpur Rain Gauge Station*** *(Rainfall in mm)*

Tr (Year)	10 min			20 min			30 min		
	P_{ave}=17.56	S = 7.92		P_{ave}=20.11	S = 9.07		P_{ave}=25.34	S = 11.42	
	K	P_T	I_T	K	P_T	I_T	K	P_T	I_T
2	-0.156	16.335	98.009	-0.156	18.699	56.097	-0.156	23.559	47.119
10	1.489	29.358	176.142	1.489	33.606	100.818	1.489	42.341	84.682
25	2.316	35.912	215.468	2.316	41.109	123.327	2.316	51.794	103.588
50	2.930	40.774	244.641	2.930	46.675	140.025	2.930	58.807	117.614
100	3.539	45.601	273.600	3.539	52.200	156.600	3.539	65.768	131.536
	60 min			120 min			180 min		
	P_{ave}=31.92	S = 14.39		P_{ave}=40.22	S = 18.13		P_{ave}=46.04	S = 20.76	
	K	P_T	I_T	K	P_T	I_T	K	P_T	I_T
2	-0.156	29.683	29.683	-0.156	37.398	18.699	-0.156	42.810	14.270
10	1.489	53.346	53.346	1.489	67.212	33.606	1.489	76.939	25.646
25	2.316	65.256	65.256	2.316	82.218	41.109	2.316	94.116	31.372
50	2.930	74.092	74.092	2.930	93.350	46.675	2.930	106.859	35.620
100	3.539	82.862	82.862	3.539	104.400	52.200	3.539	119.508	39.836
	360 min			720 min			1440 min		
	P_{ave}=58.00	S = 26.15		P_{ave}=73.08	S = 32.95		P_{ave}=92.08	S = 41.52	
	K	P_T	I_T	K	P_T	I_T	K	P_T	I_T
2	-0.156	53.938	8.990	-0.156	67.957	5.663	-0.156	85.621	3.568
10	1.489	96.937	16.156	1.489	122.133	10.178	1.489	153.878	6.412
25	2.316	118.579	19.763	2.316	149.400	12.450	2.316	188.232	7.843
50	2.930	134.634	22.439	2.930	169.628	14.136	2.930	213.718	8.905
100	3.539	150.571	25.095	3.539	189.707	15.809	3.539	239.016	9.959

Table for Computed Frequency Precipitation Values and Intensities for Different Durations and Return Periods Using Gumbel Method for ***Salar Rain Gauge Station*** *(Rainfall in mm)*

Tr (Year)	10 min			20 min			30 min		
	P_{ave}=18.35	S = 8.97		P_{ave}=23.12	S = 11.30		P_{ave}=26.47	S = 12.93	
	K	P_T	I_T	K	P_T	I_T	K	P_T	I_T
2	-0.156	16.959	101.750	-0.156	21.366	64.099	-0.156	24.459	48.917
10	1.489	31.702	190.205	1.489	39.941	119.824	1.489	45.722	91.443
25	2.316	39.122	234.726	2.316	49.290	147.871	2.316	56.423	112.847
50	2.930	44.627	267.755	2.930	56.226	168.678	2.930	64.363	128.726
100	3.539	50.091	300.539	3.539	63.110	189.331	3.539	72.243	144.487
	60 min			120 min			180 min		
	P_{ave}=33.35	S = 16.29		P_{ave}=42.02	S = 20.53		P_{ave}=48.10	S = 23.50	
	K	P_T	I_T	K	P_T	I_T	K	P_T	I_T
2	-0.156	30.816	30.816	-0.156	38.825	19.413	-0.156	44.444	14.815
10	1.489	57.606	57.606	1.489	72.578	36.289	1.489	83.082	27.694
25	2.316	71.089	71.089	2.316	89.567	44.783	2.316	102.528	34.176
50	2.930	81.092	81.092	2.930	102.170	51.085	2.930	116.955	38.985
100	3.539	91.021	91.021	3.539	114.679	57.340	3.539	131.275	43.758
	360 min			720 min			1440 min		
	P_{ave}=60.60	S = 29.61		P_{ave}=76.36	S = 37.30		P_{ave}=96.20	S = 47.00	
	K	P_T	I_T	K	P_T	I_T	K	P_T	I_T
2	-0.156	55.996	9.333	-0.156	70.551	5.879	-0.156	88.888	3.704
10	1.489	104.676	17.446	1.489	131.884	10.990	1.489	166.163	6.923
25	2.316	129.177	21.530	2.316	162.753	13.563	2.316	205.056	8.544
50	2.930	147.354	24.559	2.930	185.654	15.471	2.930	233.910	9.746
100	3.539	165.396	27.566	3.539	208.386	17.366	3.539	262.550	10.940

Table for Computed Frequency Precipitation Values and Intensities for Different Durations and Return Periods Using Log Pearson Type III Method for ***Maharo Rain Gauge Station*** *(Rainfall in mm)*

Computed precipitation (P_T) and intensity (I_T) (Log Pearson III method)												
Tr (Year)	10 min				20 min				30 min			
	K_T	P^*_T	P_T	I_T	K_T	P^*_T	P_T	I_T	K_T	P^*_T	P_T	I_T
2	-0.116	1.228	16.908	101.447	-0.116	1.328	21.303	63.908	-0.116	1.387	24.385	48.771
10	1.333	1.545	35.051	210.306	1.333	1.645	44.161	132.484	1.333	1.704	50.552	101.104
25	1.967	1.683	48.220	289.322	1.967	1.784	60.754	182.262	1.967	1.842	69.546	139.092
50	2.407	1.779	60.169	361.013	2.407	1.880	75.808	227.424	2.407	1.938	86.779	173.557
100	2.824	1.870	74.214	445.286	2.824	1.971	93.504	280.512	2.824	2.030	107.036	214.071
	60 min				120 min				180 min			
	K_T	P^*_T	P_T	I_T	K_T	P^*_T	P_T	I_T	K_T	P^*_T	P_T	I_T
2	-0.116	1.487	30.724	30.724	-0.116	1.588	38.709	19.355	-0.116	1.647	44.311	14.770
10	1.333	1.804	63.692	63.692	1.333	1.904	80.247	40.123	1.333	1.963	91.860	30.620
25	1.967	1.943	87.622	87.622	1.967	2.043	110.397	55.199	1.967	2.102	126.373	42.124
50	2.407	2.039	109.334	109.334	2.407	2.139	137.752	68.876	2.407	2.198	157.687	52.562
100	2.824	2.130	134.856	134.856	2.824	2.230	169.908	84.954	2.824	2.289	194.496	64.832
	360 min				720 min				1440 min			
	K_T	P^*_T	P_T	I_T	K_T	P^*_T	P_T	I_T	K_T	P^*_T	P_T	I_T
2	-0.116	1.747	55.829	9.305	-0.116	1.847	70.340	5.862	-0.116	1.948	88.622	3.693
10	1.333	2.063	115.736	19.289	1.333	2.164	145.818	12.151	1.333	2.264	183.719	7.655
25	1.967	2.202	159.220	26.537	1.967	2.302	200.605	16.717	1.967	2.403	252.746	10.531
50	2.407	2.298	198.673	33.112	2.407	2.398	250.313	20.859	2.407	2.499	315.374	13.141
100	2.824	2.389	245.050	40.842	2.824	2.490	308.744	25.729	2.824	2.590	388.993	16.208

Table for Computed Frequency Precipitation Values and Intensities for Different Durations and Return Periods Using Log Pearson Type III Method for ***Dumka Rain Gauge Station*** *(Rainfall in mm)*

Computed precipitation (P_T) and intensity (I_T) (Log Pearson III method)												
Tr (Year)	10 min				20 min				30 min			
	K_T	P^*_T	P_T	I_T	K_T	P^*_T	P_T	I_T	K_T	P^*_T	P_T	I_T
2	-0.116	1.228	16.908	101.447	-0.116	1.328	21.303	63.908	-0.116	1.387	24.385	48.771
10	1.333	1.545	35.051	210.306	1.333	1.645	44.161	132.484	1.333	1.704	50.552	101.104
25	1.967	1.683	48.220	289.322	1.967	1.784	60.754	182.262	1.967	1.842	69.546	139.092
50	2.407	1.779	60.169	361.013	2.407	1.880	75.808	227.424	2.407	1.938	86.779	173.557
100	2.824	1.870	74.214	445.286	2.824	1.971	93.504	280.512	2.824	2.030	107.036	214.071
	60 min				120 min				180 min			
	K_T	P^*_T	P_T	I_T	K_T	P^*_T	P_T	I_T	K_T	P^*_T	P_T	I_T
2	-0.116	1.487	63.692	30.724	-0.116	1.588	38.709	19.355	-0.116	1.647	44.311	14.770
10	1.333	1.804	87.622	63.692	1.333	1.904	80.247	40.123	1.333	1.963	91.860	30.620
25	1.967	1.943	109.334	87.622	1.967	2.043	110.397	55.199	1.967	2.102	126.373	42.124
50	2.407	2.039	134.856	109.334	2.407	2.139	137.752	68.876	2.407	2.198	157.687	52.562
100	2.824	2.130	63.692	134.856	2.824	2.230	169.908	84.954	2.824	2.289	194.496	64.832
	360 min				720 min				1440 min			
	K_T	P^*_T	P_T	I_T	K_T	P^*_T	P_T	I_T	K_T	P^*_T	P_T	I_T
2	-0.116	1.747	55.829	9.305	-0.116	1.847	70.340	5.862	-0.116	1.948	88.622	3.693
10	1.333	2.063	115.736	19.289	1.333	2.164	145.818	12.151	1.333	2.264	183.72	7.655
25	1.967	2.202	159.220	26.537	1.967	2.302	200.605	16.717	1.967	2.403	252.75	10.531
50	2.407	2.298	198.673	33.112	2.407	2.398	250.313	20.859	2.407	2.499	315.37	13.141
100	2.824	2.389	245.050	40.842	2.824	2.490	308.744	25.729	2.824	2.590	388.99	16.208

Table for Computed Frequency Precipitation Values and Intensities for Different Durations and Return Periods Using Log Pearson Type III Method for ***Massanjore Rain Gauge Station*** *(Rainfall in mm)*

Computed precipitation (P_T) and intensity (I_T) (Log Pearson III method)												
Tr (Year)	10 min				20 min				30 min			
	K_T	P^*_T	P_T	I_T	K_T	P^*_T	P_T	I_T	K_T	P^*_T	P_T	I_T
2	-0.148	1.234	17.148	102.886	-0.148	1.335	21.605	64.814	-0.148	1.393	24.731	49.463
10	1.339	1.562	36.440	218.641	1.339	1.662	45.912	137.735	1.339	1.721	52.556	105.111
25	2.018	1.711	51.412	308.473	2.018	1.811	64.775	194.326	2.018	1.870	74.149	148.298
50	2.498	1.817	65.575	393.452	2.498	1.917	82.620	247.859	2.498	1.976	94.576	189.152
100	2.957	1.918	82.755	496.528	2.957	2.018	104.264	312.793	2.957	2.077	119.353	238.706
	60 min				120 min				180 min			
	K_T	P^*_T	P_T	I_T	K_T	P^*_T	P_T	I_T	K_T	P^*_T	P_T	I_T
2	-0.148	1.494	31.160	31.160	-0.148	1.594	39.259	19.629	-0.148	1.653	44.940	14.980
10	1.339	1.821	66.216	66.216	1.339	1.921	83.427	41.714	1.339	1.980	95.500	31.833
25	2.018	1.970	93.422	93.422	2.018	2.071	117.704	58.852	2.018	2.129	134.738	44.913
50	2.498	2.076	119.158	119.158	2.498	2.176	150.130	75.065	2.498	2.235	171.856	57.285
100	2.957	2.177	150.375	150.375	2.957	2.278	189.461	94.730	2.957	2.336	216.879	72.293
	360 min				720 min				1440 min			
	K_T	P^*_T	P_T	I_T	K_T	P^*_T	P_T	I_T	K_T	P^*_T	P_T	I_T
2	-0.148	1.753	56.621	9.437	-0.148	1.853	71.338	5.945	-0.148	1.954	89.880	3.745
10	1.339	2.080	120.323	20.054	1.339	2.181	151.597	12.633	1.339	2.281	191.000	7.958
25	2.018	2.230	169.759	28.293	2.018	2.330	213.883	17.824	2.018	2.431	269.476	11.228
50	2.498	2.336	216.525	36.088	2.498	2.436	272.805	22.734	2.498	2.536	343.712	14.321
100	2.957	2.437	273.250	45.542	2.957	2.537	344.273	28.689	2.957	2.637	433.757	18.073

Table for Computed Frequency Precipitation Values and Intensities for Different Durations and Return Periods Using Log Pearson Type III Method for ***Kundahit Rain Gauge Station*** *(Rainfall in mm)*

Computed precipitation (P_T) and intensity (I_T) (Log Pearson III method)												
Tr (Year)	10 min				20 min				30 min			
	K_T	P^*_T	P_T	I_T	K_T	P^*_T	P_T	I_T	K_T	P^*_T	P_T	I_T
2	-0.148	1.234	17.141	102.845	-0.148	1.334	21.596	64.788	-0.148	1.393	24.721	49.443
10	1.339	1.562	36.441	218.646	1.339	1.662	45.913	137.739	1.339	1.721	52.557	105.114
25	2.018	1.711	51.424	308.542	2.018	1.812	64.790	194.369	2.018	1.870	74.166	148.331
50	2.498	1.817	65.599	393.595	2.498	1.917	82.650	247.949	2.498	1.976	94.610	189.221
100	2.957	1.918	82.796	496.774	2.957	2.018	104.316	312.948	2.957	2.077	119.412	238.824
	60 min				120 min				180 min			
	K_T	P^*_T	P_T	I_T	K_T	P^*_T	P_T	I_T	K_T	P^*_T	P_T	I_T
2	-0.148	1.493	31.147	31.147	-0.148	1.594	39.243	19.621	-0.148	1.652	44.922	14.974
10	1.339	1.821	66.218	66.218	1.339	1.921	83.429	41.715	1.339	1.980	95.503	31.834
25	2.018	1.971	93.443	93.443	2.018	2.071	117.731	58.865	2.018	2.130	134.768	44.923
50	2.498	2.076	119.202	119.202	2.498	2.177	150.185	75.092	2.498	2.235	171.918	57.306
100	2.957	2.177	150.450	150.450	2.957	2.278	189.555	94.777	2.957	2.336	216.986	72.329
	360 min				720 min				1440 min			
	K_T	P^*_T	P_T	I_T	K_T	P^*_T	P_T	I_T	K_T	P^*_T	P_T	I_T
2	-0.148	1.753	56.598	9.433	-0.148	1.853	71.309	5.942	-0.148	1.953	89.843	3.743
10	1.339	2.080	120.326	20.054	1.339	2.181	151.601	12.633	1.339	2.281	191.005	7.959
25	2.018	2.230	169.797	28.300	2.018	2.330	213.931	17.828	2.018	2.431	269.536	11.231
50	2.498	2.336	216.604	36.101	2.498	2.436	272.904	22.742	2.498	2.536	343.837	14.327
100	2.957	2.437	273.385	45.564	2.957	2.537	344.444	28.704	2.957	2.637	433.972	18.082

Table for Computed Frequency Precipitation Values and Intensities for Different Durations and Return Periods Using Log Pearson Type III Method for ***Tilpara Rain Gauge Station*** *(Rainfall in mm)*

Computed precipitation (P_T) and intensity (I_T) (Log Pearson III method)												
Tr (Year)	10 min				20 min				30 min			
	K_T	P^*_T	P_T	I_T	K_T	P^*_T	P_T	I_T	K_T	P^*_T	P_T	I_T
2	-0.116	1.187	15.372	92.234	-0.116	1.245	17.597	52.791	-0.116	1.346	22.171	44.341
10	1.333	1.478	30.090	180.537	1.333	1.537	34.444	103.332	1.333	1.637	43.397	86.793
25	1.967	1.606	40.368	242.208	1.967	1.665	46.210	138.629	1.967	1.765	58.221	116.441
50	2.407	1.695	49.500	297.001	2.407	1.753	56.664	169.991	2.407	1.854	71.392	142.783
100	2.824	1.779	60.055	360.328	2.824	1.837	68.746	206.237	2.824	1.938	86.614	173.228
	60 min				120 min				180 min			
	K_T	P^*_T	P_T	I_T	K_T	P^*_T	P_T	I_T	K_T	P^*_T	P_T	I_T
2	-0.116	1.446	27.933	27.933	-0.116	1.546	35.194	17.597	-0.116	1.605	40.287	13.429
10	1.333	1.738	54.676	54.676	1.333	1.838	68.888	34.444	1.333	1.897	78.857	26.286
25	1.967	1.865	73.353	73.353	1.967	1.966	92.420	46.210	1.967	2.024	105.794	35.265
50	2.407	1.954	89.948	89.948	2.407	2.054	113.327	56.664	2.407	2.113	129.727	43.242
100	2.824	2.038	109.127	109.127	2.824	2.138	137.491	68.746	2.824	2.197	157.388	52.463
	360 min				720 min				1440 min			
	K_T	P^*_T	P_T	I_T	K_T	P^*_T	P_T	I_T	K_T	P^*_T	P_T	I_T
2	-0.116	1.706	50.758	8.460	-0.116	1.806	63.951	5.329	-0.116	1.906	80.574	3.357
10	1.333	1.997	99.354	16.559	1.333	2.098	125.178	10.431	1.333	2.198	157.714	6.571
25	1.967	2.125	133.292	22.215	1.967	2.225	167.938	13.995	1.967	2.325	211.588	8.816
50	2.407	2.213	163.446	27.241	2.407	2.314	205.929	17.161	2.407	2.414	259.454	10.811
100	2.824	2.297	198.296	33.049	2.824	2.398	249.838	20.820	2.824	2.498	314.776	13.116

Table for Computed Frequency Precipitation Values and Intensities for Different Durations and Return Periods Using Log Pearson Type III Method for ***Kultore Rain Gauge Station*** *(Rainfall in mm)*

Computed precipitation (P_T) and intensity (I_T) (Log Pearson III method)												
Tr (Year)	10 min				20 min				30 min			
	K_T	P^*_T	P_T	I_T	K_T	P^*_T	P_T	I_T	K_T	P^*_T	P_T	I_T
2	-0.116	1.187	15.378	92.271	-0.116	1.287	19.376	58.127	-0.116	1.346	22.180	44.359
10	1.333	1.478	30.090	180.541	1.333	1.579	37.911	113.733	1.333	1.637	43.397	86.795
25	1.967	1.606	40.362	242.172	1.967	1.706	50.853	152.559	1.967	1.765	58.212	116.424
50	2.407	1.694	49.487	296.922	2.407	1.795	62.350	187.049	2.407	1.854	71.373	142.745
100	2.824	1.778	60.032	360.192	2.824	1.879	75.636	226.907	2.824	1.937	86.581	173.162
	60 min				120 min				180 min			
	K_T	P^*_T	P_T	I_T	K_T	P^*_T	P_T	I_T	K_T	P^*_T	P_T	I_T
2	-0.116	1.446	27.945	27.945	-0.116	1.547	35.208	17.604	-0.116	1.605	40.303	13.434
10	1.333	1.738	54.677	54.677	1.333	1.838	68.889	34.445	1.333	1.897	78.858	26.286
25	1.967	1.865	73.342	73.342	1.967	1.966	92.406	46.203	1.967	2.024	105.778	35.259
50	2.407	1.954	89.924	89.924	2.407	2.054	113.297	56.648	2.407	2.113	129.693	43.231
100	2.824	2.038	109.086	109.086	2.824	2.138	137.439	68.720	2.824	2.197	157.329	52.443
	360 min				720 min				1440 min			
	K_T	P^*_T	P_T	I_T	K_T	P^*_T	P_T	I_T	K_T	P^*_T	P_T	I_T
2	-0.116	1.706	50.779	8.463	-0.116	2.098	63.977	5.331	-0.116	1.906	80.606	3.359
10	1.333	1.997	99.355	16.559	1.333	2.225	125.180	10.432	1.333	2.198	157.717	6.572
25	1.967	2.125	133.272	22.212	1.967	2.314	167.912	13.993	1.967	2.325	211.556	8.815
50	2.407	2.213	163.403	27.234	2.407	2.397	205.874	17.156	2.407	2.414	259.385	10.808
100	2.824	2.297	198.222	33.037	2.824	2.098	249.744	20.812	2.824	2.498	314.657	13.111

Table for Computed Frequency Precipitation Values and Intensities for Different Durations and Return Periods Using Log Pearson Type III Method for ***Sainthia Rain Gauge Station*** *(Rainfall in mm)*

Computed precipitation (P_T) and intensity (I_T) (Log Pearson III method)												
Tr (Year)	10 min				20 min				30 min			
	K_T	P^*_T	P_T	I_T	K_T	P^*_T	P_T	I_T	K_T	P^*_T	P_T	I_T
2	-0.033	1.249	17.724	106.342	-0.033	1.349	22.330	66.991	-0.033	1.408	25.562	51.124
10	1.301	1.536	34.393	206.356	1.301	1.637	43.332	129.996	1.301	1.696	49.603	99.205
25	1.818	1.648	44.468	266.808	1.818	1.748	56.026	168.078	1.818	1.807	64.134	128.268
50	2.159	1.722	52.680	316.078	2.159	1.822	66.372	199.117	2.159	1.881	75.977	151.955
100	2.472	1.789	61.546	369.274	2.472	1.890	77.543	232.628	2.472	1.948	88.764	177.528
	60 min				120 min				180 min			
	K_T	P^*_T	P_T	I_T	K_T	P^*_T	P_T	I_T	K_T	P^*_T	P_T	I_T
2	-0.033	1.508	32.206	32.206	-0.033	1.608	40.577	20.289	-0.033	1.667	46.449	15.483
10	1.301	1.796	62.495	62.495	1.301	1.896	78.739	39.370	1.301	1.955	90.134	30.045
25	1.818	1.907	80.804	80.804	1.818	2.008	101.806	50.903	1.818	2.066	116.539	38.846
50	2.159	1.981	95.725	95.725	2.159	2.081	120.606	60.303	2.159	2.140	138.060	46.020
100	2.472	2.049	111.836	111.836	2.472	2.149	140.904	70.452	2.472	2.208	161.295	53.765
	360 min				720 min				1440 min			
	K_T	P^*_T	P_T	I_T	K_T	P^*_T	P_T	I_T	K_T	P^*_T	P_T	I_T
2	-0.033	1.767	58.522	9.754	-0.033	1.868	73.733	6.144	-0.033	1.968	92.898	3.871
10	1.301	2.055	113.562	18.927	1.301	2.156	143.079	11.923	1.301	2.256	180.268	7.511
25	1.818	2.167	146.830	24.472	1.818	2.267	184.994	15.416	1.818	2.368	233.078	9.712
50	2.159	2.240	173.945	28.991	2.159	2.341	219.156	18.263	2.159	2.441	276.120	11.505
100	2.472	2.308	203.219	33.870	2.472	2.408	256.040	21.337	2.472	2.509	322.590	13.825

Table for Computed Frequency Precipitation Values and Intensities for Different Durations and Return Periods Using Log Pearson Type III Method for ***Shekhampore Rain Gauge*** *Station (Rainfall in mm)*

Computed precipitation (P_T) and intensity (I_T) (Log Pearson III method)												
Tr (Year)	10 min				20 min				30 min			
	K_T	P^*_T	P_T	I_T	K_T	P^*_T	P_T	I_T	K_T	P^*_T	P_T	I_T
2	0.033	1.228	16.923	101.538	0.033	1.329	21.322	63.965	0.033	1.388	24.407	48.814
10	1.258	1.487	30.696	184.177	1.258	1.587	38.675	116.024	1.258	1.646	44.271	88.543
25	1.680	1.576	37.685	226.111	1.680	1.677	47.480	142.441	1.680	1.735	54.351	108.703
50	1.945	1.632	42.866	257.196	1.945	1.732	54.008	162.023	1.945	1.791	61.823	123.647
100	2.178	1.681	48.007	288.039	2.178	1.782	60.484	181.453	2.178	1.840	69.237	138.475
	60 min				120 min				180 min			
	K_T	P^*_T	P_T	I_T	K_T	P^*_T	P_T	I_T	K_T	P^*_T	P_T	I_T
2	0.033	1.488	30.751	30.751	0.033	1.588	38.744	19.372	0.033	1.647	44.351	14.784
10	1.258	1.746	55.778	55.778	1.258	1.847	70.277	35.138	1.258	1.906	80.447	26.816
25	1.680	1.836	68.478	68.478	1.680	1.936	86.277	43.139	1.680	1.995	98.763	32.921
50	1.945	1.891	77.893	77.893	1.945	1.992	98.139	49.069	1.945	2.051	112.341	37.447
100	2.178	1.941	87.234	87.234	2.178	2.041	109.908	54.954	2.178	2.100	125.813	41.938
	360 min				720 min				1440 min			
	K_T	P^*_T	P_T	I_T	K_T	P^*_T	P_T	I_T	K_T	P^*_T	P_T	I_T
2	0.033	1.747	55.879	9.313	0.033	1.848	70.403	5.867	0.033	1.948	88.702	3.696
10	1.258	2.006	101.356	16.893	1.258	2.106	127.701	10.642	1.258	2.207	160.893	6.704
25	1.680	2.095	124.433	20.739	1.680	2.195	156.776	13.065	1.680	2.296	197.526	8.230
50	1.945	2.151	141.540	23.590	1.945	2.251	178.330	14.861	1.945	2.352	224.681	9.362
100	2.178	2.200	158.514	26.419	2.178	2.300	199.715	16.643	2.178	2.401	251.625	10.484

Table for Computed Frequency Precipitation Values and Intensities for Different Durations and Return Periods Using Log Pearson Type III Method for ***Kandi Rain Gauge Station*** *(Rainfall in mm)*

Computed precipitation (P_T) and intensity (I_T) (Log Pearson III method)												
Tr (Year)	10 min				20 min				30 min			
	K_T	P^*_T	P_T	I_T	K_T	P^*_T	P_T	I_T	K_T	P^*_T	P_T	I_T
2	0.116	1.253	17.920	107.518	0.116	1.354	22.577	67.732	0.116	1.412	25.845	51.689
10	1.183	1.480	30.167	181.001	1.183	1.580	38.008	114.024	1.183	1.639	43.508	87.016
25	1.488	1.544	35.010	210.059	1.488	1.645	44.110	132.329	1.488	1.703	50.493	100.986
50	1.663	1.581	38.132	228.792	1.663	1.682	48.043	144.130	1.663	1.740	54.996	109.992
100	1.806	1.612	40.889	245.333	1.806	1.712	51.517	154.550	1.806	1.771	58.972	117.944
	60 min				120 min				180 min			
	K_T	P^*_T	P_T	I_T	K_T	P^*_T	P_T	I_T	K_T	P^*_T	P_T	I_T
2	0.116	1.513	32.562	32.562	0.116	1.613	41.026	20.513	0.116	1.672	46.963	15.654
10	1.183	1.739	54.817	54.817	1.183	1.839	69.065	34.532	1.183	1.898	79.060	26.353
25	1.488	1.804	63.617	63.617	1.488	1.904	80.152	40.076	1.488	1.963	91.752	30.584
50	1.663	1.841	69.290	69.290	1.663	1.941	87.300	43.650	1.663	2.000	99.934	33.311
100	1.806	1.871	74.300	74.300	1.806	1.971	93.612	46.806	1.806	2.030	107.159	46.806
	360 min				720 min				1440 min			
	K_T	P^*_T	P_T	I_T	K_T	P^*_T	P_T	I_T	K_T	P^*_T	P_T	I_T
2	0.116	1.772	59.169	9.862	0.116	1.872	74.549	6.212	0.116	1.973	93.925	3.914
10	1.183	1.998	99.609	16.601	1.183	2.099	125.499	10.458	1.183	2.199	158.119	6.588
25	1.488	2.063	115.600	19.267	1.488	2.163	145.647	12.137	1.488	2.264	183.503	7.646
50	1.663	2.100	125.909	20.985	1.663	2.200	158.635	13.220	1.663	2.301	199.868	8.328
100	1.806	2.130	135.012	22.502	1.806	2.231	170.105	14.175	1.806	2.331	214.318	8.930

Table for Computed Frequency Precipitation Values and Intensities for Different Durations and Return Periods Using Log Pearson Type III Method for ***Bharatpur Rain Gauge Station*** *(Rainfall in mm)*

Computed precipitation (P_T) and intensity (I_T) (Log Pearson III method)												
Tr (Year)	10 min				20 min				30 min			
	K_T	P^*_T	P_T	I_T	K_T	P^*_T	P_T	I_T	K_T	P^*_T	P_T	I_T
2	0.116	1.253	17.921	107.525	0.116	1.354	22.579	67.736	0.116	1.412	25.846	51.693
10	1.183	1.480	30.168	181.005	1.183	1.580	38.009	114.026	1.183	1.639	43.509	87.018
25	1.488	1.544	35.010	210.061	1.488	1.645	44.110	132.330	1.488	1.703	50.493	100.987
50	1.663	1.581	38.132	228.792	1.663	1.682	48.043	144.130	1.663	1.740	54.996	109.992
100	1.806	1.612	40.889	245.332	1.806	1.712	51.516	154.549	1.806	1.771	58.972	117.943
	60 min				120 min				180 min			
	K_T	P^*_T	P_T	I_T	K_T	P^*_T	P_T	I_T	K_T	P^*_T	P_T	I_T
2	0.116	1.513	32.564	32.564	0.116	1.613	41.028	20.514	0.116	1.672	46.966	15.655
10	1.183	1.739	54.818	54.818	1.183	1.839	69.066	34.533	1.183	1.898	79.061	26.354
25	1.488	1.804	63.618	63.618	1.488	1.904	80.153	40.077	1.488	1.963	91.752	30.584
50	1.663	1.841	69.290	69.290	1.663	1.941	87.301	43.650	1.663	2.000	99.934	33.311
100	1.806	1.871	74.300	74.300	1.806	1.971	93.612	46.806	1.806	2.030	107.159	35.720
	360 min				720 min				1440 min			
	K_T	P^*_T	P_T	I_T	K_T	P^*_T	P_T	I_T	K_T	P^*_T	P_T	I_T
2	0.116	1.772	59.173	9.862	0.116	1.872	74.554	6.213	0.116	1.973	93.932	3.914
10	1.183	1.998	99.611	16.602	1.183	2.099	125.502	10.458	1.183	2.199	158.123	6.588
25	1.488	2.063	115.601	19.267	1.488	2.163	145.648	12.137	1.488	2.264	183.505	7.646
50	1.663	2.100	125.909	20.985	1.663	2.200	158.636	13.220	1.663	2.301	199.868	8.328
100	1.806	2.130	135.011	22.502	1.806	2.231	170.104	14.175	1.806	2.331	214.317	8.930

Table for Computed Frequency Precipitation Values and Intensities for Different Durations and Return Periods Using Log Pearson Type III Method for ***Narayanpur Rain Gauge*** *Station (Rainfall in mm)*

Computed precipitation (P_T) and intensity (I_T) (Log Pearson III method)												
Tr (Year)	10 min				20 min				30 min			
	K_T	P^*_T	P_T	I_T	K_T	P^*_T	P_T	I_T	K_T	P^*_T	P_T	I_T
2	0.083	1.219	16.552	99.315	0.083	1.319	20.855	62.564	0.083	1.378	23.873	47.745
10	1.216	1.446	27.912	167.470	1.216	1.546	35.167	105.500	1.216	1.605	40.256	80.511
25	1.567	1.516	32.816	196.897	1.567	1.616	41.346	124.037	1.567	1.675	47.329	94.658
50	1.777	1.558	36.153	216.919	1.777	1.658	45.550	136.651	1.777	1.717	52.142	104.284
100	1.955	1.594	39.246	235.477	1.955	1.694	49.447	148.342	1.955	1.753	56.603	113.206
	60 min				120 min				180 min			
	K_T	P^*_T	P_T	I_T	K_T	P^*_T	P_T	I_T	K_T	P^*_T	P_T	I_T
2	0.083	1.478	30.078	30.078	0.083	1.579	37.896	18.948	0.083	1.637	43.380	14.460
10	1.216	1.705	50.719	50.719	1.216	1.806	50.719	31.951	1.216	1.864	73.149	24.383
25	1.567	1.775	59.631	59.631	1.567	1.876	59.631	37.565	1.567	1.935	86.003	28.668
50	1.777	1.818	65.695	65.695	1.777	1.918	65.695	41.385	1.777	1.977	94.748	31.583
100	1.955	1.853	71.315	71.315	1.955	1.954	71.315	44.926	1.955	2.012	102.854	34.285
	360 min				720 min				1440 min			
	K_T	P^*_T	P_T	I_T	K_T	P^*_T	P_T	I_T	K_T	P^*_T	P_T	I_T
2	0.083	1.738	54.655	9.109	0.083	1.838	68.861	5.738	0.083	1.938	86.759	3.615
10	1.216	1.965	92.162	15.360	1.216	2.065	116.117	9.676	1.216	2.165	146.299	6.096
25	1.567	2.035	108.356	18.059	1.567	2.135	136.520	11.377	1.567	2.236	172.005	7.167
50	1.777	2.077	119.375	19.896	1.777	2.177	150.404	12.534	1.777	2.278	189.497	7.896
100	1.955	2.113	129.588	21.598	1.955	2.213	163.271	13.606	1.955	2.313	205.709	8.571

Table for Computed Frequency Precipitation Values and Intensities for Different Durations and Return Periods Using Log Pearson Type III Method for ***Salar Rain Gauge Station*** *(Rainfall in mm)*

Computed precipitation (P_T) and intensity (I_T) (Log Pearson III method)												
Tr (Year)	10 min				20 min				30 min			
	K_T	P^*_T	P_T	I_T	K_T	P^*_T	P_T	I_T	K_T	P^*_T	P_T	I_T
2	0.148	1.245	17.562	105.371	0.148	1.345	22.127	66.380	0.148	1.404	25.329	50.657
10	1.147	1.477	30.012	180.071	1.147	1.578	37.813	113.438	1.147	1.636	43.285	86.569
25	1.407	1.538	34.503	207.020	1.407	1.638	43.471	130.414	1.407	1.697	49.762	99.525
50	1.549	1.571	37.234	223.404	1.549	1.671	46.912	140.736	1.549	1.730	53.701	107.402
100	1.806	1.631	42.738	256.425	1.806	1.731	53.846	161.538	1.806	1.790	61.638	123.277
	60 min				120 min				180 min			
	K_T	P^*_T	P_T	I_T	K_T	P^*_T	P_T	I_T	K_T	P^*_T	P_T	I_T
2	0.148	1.504	31.912	31.912	0.148	1.604	40.207	20.103	0.148	1.663	46.025	15.342
10	1.147	1.737	54.535	54.535	1.147	1.837	68.710	34.355	1.147	1.896	78.653	26.218
25	1.407	1.797	62.697	62.697	1.407	1.898	78.993	39.496	1.407	1.956	90.424	30.141
50	1.549	1.830	67.659	67.659	1.549	1.931	85.245	42.622	1.549	1.989	97.581	32.527
100	1.806	1.890	77.659	77.659	1.806	1.957	90.474	45.237	1.806	2.015	103.567	34.522
	360 min				720 min				1440 min			
	K_T	P^*_T	P_T	I_T	K_T	P^*_T	P_T	I_T	K_T	P^*_T	P_T	I_T
2	0.148	1.763	57.988	9.665	0.148	1.864	73.060	6.088	0.148	1.964	92.050	3.835
10	1.147	1.996	99.097	16.516	1.147	2.096	124.854	10.405	1.147	2.197	157.306	6.554
25	1.407	2.057	113.927	18.988	1.407	2.157	143.540	11.962	1.407	2.257	180.849	7.535
50	1.549	2.090	122.944	20.491	1.549	2.190	154.900	12.908	1.549	2.290	195.162	8.132
100	1.806	2.116	130.487	21.748	1.806	2.216	164.403	13.700	1.806	2.316	207.135	8.631

ANNEXURE II

Table for Accuracies and Kappa Co-efficient of Land Use Land Cover Classification Map for the year 1989

Classified Data	Dense Forest	Lateritic exposer	Agricultural land	Reservoir	River/ water	Sand bar	Settlement	HSP	Dry fallow	Wet fallow	Waste land	Row Total
Dense Forest	8544	0	30	0	0	0	0	0	3	0	0	8577
Lateritic exposer	76	218	0	71	26	0	0	0	0	0	0	391
Agricultural land	1	0	17012	0	0	0	0	0	0	1	67	17081
Reservoir	0	0	0	5561	104	0	0	0	0	0	0	5665
River/water	1	0	0	277	3531	0	0	0	0	4	2	3815
Sand bar	0	0	0	0	0	885	0	0	0	0	1	886
Settlement	0	10	0	0	0	0	517	5	0	58	0	590
HSP	14	1	1	0	0	0	73	46	0	53	0	188
Dry fallow	0	0	37	0	0	0	0	0	5678	3	141	5859
Wet fallow	0	0	15	0	27	0	13	1	127	3418	1	3602
Waste land	0	0	328	0	0	0	0	0	21	0	5934	6283
Column Total	8636	229	17423	5909	3688	885	603	52	5829	3537	6146	52937
Overall Accuracy (%)						**97**						
Overall Kappa Accuracy (%)						**96**						

Table for Accuracies and Kappa Co-efficient of Land Use Land Cover Classification Map for the year 2000

Classified Data	Agricultural land	Wet fallow land	Waste land	Dry fallow land	Reservoir	River/ water	Settlement	Dense forest	Sand bar	Lateritic exposer	Homestead with plantation	Row Total
Agricultural land	29268	117	0	0	0	0	0	211	0	0	1	29597
Wet fallow land	432	6433	0	0	0	3	0	7	0	1	2	6878
Waste land	39	0	106	0	0	0	0	0	0	0	0	145
Dry fallow land	130	0	1	199	0	3	0	0	0	0	0	333
Reservoir	0	0	0	0	4874	879	0	0	0	0	0	5753
River/water	0	0	0	0	126	9563	0	0	0	0	0	9689
Settlement	0	18	0	0	0	0	43	0	0	0	2	63
Dense forest	2417	123	0	0	0	0	0	2235	0	1	0	4776
Sand bar	0	0	0	0	0	0	0	0	46	0	0	46
Lateritic exposer	3	13	0	0	0	4	0	0	0	179	0	199
Homestead with plantation	3	218	0	0	0	1	1	2	0	0	52	277
Column Total	32292	6922	107	199	5000	10453	44	2455	46	181	57	57756
Overall Accuracy (%)						**92**						
Overall Kappa Accuracy (%)						**87**						

Table for Accuracies and Kappa Co-efficient of Land Use Land Cover Classification Map for the year 2010

Classified Data	Agricultural land	Settlement	Reservoir	River/water	Lateritic expo	Sand Bar	Waste land	Wet fallow	HSP	Dry fallow	Dense forest	Row Total
Agricultural land	24477	0	0	0	0	0	0	0	0	54	47	24578
Settlement	0	88	0	0	0	0	0	3	0	0	0	91
Reservoir	0	0	5742	0	0	0	0	0	0	0	0	5742
River/water	0	0	25	196	2	0	0	11	0	0	1	235
Lateritic exposer	0	0	0	0	232	0	0	3	0	0	0	235
Sand Bar	0	0	0	0	0	97	0	0	0	0	0	97
Waste land	57	0	0	0	0	0	194	0	0	10	0	261
Wet fallow	77	0	0	2	0	0	0	1681	3	692	1	2456
HSP	288	0	0	0	0	0	0	82	26	1	24	421
Dry fallow	31	0	0	3	0	0	0	18	0	15471	0	15523
Dense forest	444	0	0	0	0	0	0	5	0	15	3273	3737
Column Total	25374	88	5767	201	234	97	194	1803	29	16243	3346	53376
Overall Accuracy (%)						**96**						
Overall Kappa Accuracy (%)						**95**						

Table for Accuracies and Kappa Co-efficient of Land Use Land Cover Classification Map for the year 2018

Classified Data	Agricultural land	Dense forest	Settlement	HSP	Dry fallow	Wet fallow	Waste land	Reservoir	River/ Water	Exposer	Sand Bar	Row Total
Agricultural land	21411	2946	0	5	0	1260	0	0	0	1	0	25623
Dense forest	426	19941	0	1	0	74	0	0	0	28	0	20470
Settlement	2	1	2126	81	0	160	0	0	0	0	0	2370
HSP	192	152	362	553	0	356	0	0	0	41	0	1656
Dry fallow	1629	0	0	0	2045	1	107	0	2	0	0	3784
Wet fallow	770	170	9	25	0	21688	0	0	2	6	0	22670
Waste land	2	0	0	0	30	0	2280	0	2	0	0	2314
Reservoir	0	0	0	0	0	0	0	5598	25	0	0	5623
River/Water	0	0	1	0	0	0	0	402	2167	0	0	2570
Exposer	18	4235	0	22	0	21	0	0	0	1031	0	5327
Sand Bar	0	0	0	0	0	0	0	0	52	0	295	347
Column Total	24450	27445	2498	687	2075	23560	2387	6000	2250	1107	295	92754

Overall Accuracy (%)	**85**
Overall Kappa Accuracy (%)	**81**

Table for Accuracies and Kappa Co-efficient of Land Use Land Cover Classification Map for the year 2021

Classified Data	Agricultural land	Wet fallow	Settlement	Reservoir	River/ water	Sand Bar	Dense forest	Exposer	HSP	Waste land	Dry fallow	Row Total
Agricultural land	11909	143	3	0	6	0	7	0	0	11	0	12079
Wet fallow	3668	6805	103	0	6	0	34	0	0	3	0	10619
Settlement	42	232	2300	0	0	0	13	0	1	0	0	2588
Reservoir	0	0	0	3785	0	0	0	0	0	0	0	3785
River/water	0	2	0	215	1204	0	0	0	0	0	0	1421
Sand Bar	0	0	0	0	0	182	0	0	0	0	0	182
Dense forest	3050	174	4	0	0	0	678	0	0	0	0	3906
Exposer	0	1	4	0	0	0	0	477	0	0	0	482
HSP	34	13	288	0	0	0	1	0	11	0	0	347
Waste land	22	38	0	0	0	0	0	0	0	3614	0	3674
Dry fallow	0	0	0	0	0	1	0	0	0	0	838	839
Column Total	18725	7408	2702	4000	1216	183	733	477	12	3628	838	39922

Overall Accuracy (%)	**82**
Overall Kappa Accuracy (%)	**81**

ANNEXURE III

Table for Computation of the Dry Season Weighted Arithmetic Water Quality Index for the Site Rerha

Parameters	BIS standard (Sn)	1/Sn	Sum of 1/Sn	K= 1/sum of 1/Sn	Wi=k/Sn	Mean conc value (Vn)	Vn/Sn	Qn= Vn/Sn*100	Wi*Qn
pH	7.5	0.133333	0.82988889	1.204980586	0.160664	8.55	1.14	114	18.3157
EC	300	0.003333	0.82988889	1.204980586	0.004017	211	0.703	70.33	0.282501
TDS	500	0.002	0.82988889	1.204980586	0.00241	110	0.22	22	0.053019
DO	5	0.2	0.82988889	1.204980586	0.240996	8.99	1.798	179.8	43.3311
BOD	5	0.2	0.82988889	1.204980586	0.240996	12.4	2.48	248	59.76704
COD	20	0.05	0.82988889	1.204980586	0.060249	22.61	1.1305	113.06	6.811684
Turbidity	5	0.2	0.82988889	1.204980586	0.240996	6.25	1.25	125	30.12451
Chloride	250	0.004	0.82988889	1.204980586	0.00482	51.98	0.20	20.792	0.100216
Alkalinity	200	0.005	0.82988889	1.204980586	0.006025	116	0.58	58	0.349444
Total Hardness	200	0.005	0.82988889	1.204980586	0.006025	180	0.9	90	0.542241
Sulphate	200	0.005	0.82988889	1.204980586	0.006025	4	0.02	2	0.01205
Nitrate	45	0.022222	0.82988889	1.204980586	0.026777	2	0.04	4.44	0.11901
		0.829889			**1**				**159.8085**

Table for Computation of the Dry Season Weighted Arithmetic Water Quality Index for the Site Gajenda

Parameters	BIS standard (Sn)	1/Sn	Sum of 1/Sn	K= 1/sum of 1/Sn	Wi=k/Sn	Mean conc value (Vn)	Vn/Sn	Qn= Vn/Sn*100	Wi*Qn
pH	7.5	0.133333	0.82988889	1.204980586	0.160664	8.56	1.141	114.13	18.33713
EC	300	0.003333	0.82988889	1.204980586	0.004017	210	0.7	70	0.281162
TDS	500	0.002	0.82988889	1.204980586	0.00241	106	0.212	21.2	0.051091
DO	5	0.2	0.82988889	1.204980586	0.240996	8.96	1.792	179.2	43.1865
BOD	5	0.2	0.82988889	1.204980586	0.240996	8.6	1.72	172	41.45133
COD	20	0.05	0.82988889	1.204980586	0.060249	15.68	0.78	78.41	4.724233
Turbidity	5	0.2	0.82988889	1.204980586	0.240996	2.34	0.468	46.8	11.27862
Chloride	250	0.004	0.82988889	1.204980586	0.00482	89.97	0.35988	35.988	0.173459
Alkalinity	200	0.005	0.82988889	1.204980586	0.006025	284	1.42	142	0.855536
Total Hardness	200	0.005	0.82988889	1.204980586	0.006025	252	1.26	126	0.759138
Sulphate	200	0.005	0.82988889	1.204980586	0.006025	4	0.02	2	0.01205
Nitrate	45	0.022222	0.82988889	1.204980586	0.026777	2	0.044	4.44	0.11901
		0.829889			**1**				**121.2293**

Table for Computation of the Dry Season Weighted Arithmetic Water Quality Index for the Site Maharo

Parameters	BIS standard (Sn)	1/Sn	Sum of 1/Sn	K= 1/sum of 1/Sn	Wi=k/Sn	Mean conc value (Vn)	Vn/Sn	Qn= Vn/Sn*100	Wi*Qn
pH	7.5	0.133333	0.82988889	1.204980586	0.160664	8.69	1.159	115.87	18.61561
EC	300	0.003333	0.82988889	1.204980586	0.004017	213	0.71	71	0.285179
TDS	500	0.002	0.82988889	1.204980586	0.00241	106	0.212	21.2	0.051091
DO	5	0.2	0.82988889	1.204980586	0.240996	8.94	1.788	178.8	43.09011
BOD	5	0.2	0.82988889	1.204980586	0.240996	2	0.4	40	9.639845
COD	20	0.05	0.82988889	1.204980586	0.060249	8	0.4	40	2.409961
Turbidity	5	0.2	0.82988889	1.204980586	0.240996	2.89	0.578	57.8	13.92958
Chloride	250	0.004	0.82988889	1.204980586	0.00482	101.96	0.407	40.784	0.196576
Alkalinity	200	0.005	0.82988889	1.204980586	0.006025	200	1	100	0.60249
Total Hardness	200	0.005	0.82988889	1.204980586	0.006025	288	1.44	144	0.867586
Sulphate	200	0.005	0.82988889	1.204980586	0.006025	5	0.025	2.5	0.015062
Nitrate	45	0.022222	0.82988889	1.204980586	0.026777	0	0	0	0
		0.829889			**1**				**89.70308**

Table for Computation of the Dry Season Weighted Arithmetic Water Quality Index for the Site Dudhani

Parameters	BIS standard (Sn)	1/Sn	Sum of 1/Sn	K= 1/sum of 1/Sn	Wi=k/Sn	Mean conc value (Vn)	Vn/Sn	Qn= Vn/Sn*100	Wi*Qn
pH	7.5	0.133333	0.82988889	1.204980586	0.160664	8.6	1.146	114.66	18.42281
EC	300	0.003333	0.82988889	1.204980586	0.004017	220	0.733	73.33	0.294551
TDS	500	0.002	0.82988889	1.204980586	0.00241	110	0.22	22	0.053019
DO	5	0.2	0.82988889	1.204980586	0.240996	8.06	1.612	161.2	38.84857
BOD	5	0.2	0.82988889	1.204980586	0.240996	17	3.4	340	81.93868
COD	20	0.05	0.82988889	1.204980586	0.060249	31	1.55	155	9.3386
Turbidity	5	0.2	0.82988889	1.204980586	0.240996	5.29	1.058	105.8	25.49739
Chloride	250	0.004	0.82988889	1.204980586	0.00482	23.99	0.09596	9.596	0.046252
Alkalinity	200	0.005	0.82988889	1.204980586	0.006025	136	0.68	68	0.409693
Total Hardness	200	0.005	0.82988889	1.204980586	0.006025	100	0.5	50	0.301245
Sulphate	200	0.005	0.82988889	1.204980586	0.006025	5	0.025	2.5	0.015062
Nitrate	45	0.022222	0.82988889	1.204980586	0.026777	4	0.088	8.888	0.238021
		0.829889			**1**				**175.4039**

Table for Computation of the Dry Season Weighted Arithmetic Water Quality Index for the Site Poljori

Parameters	BIS standard (Sn)	1/Sn	Sum of 1/Sn	K= 1/sum of 1/Sn	Wi=k/Sn	Mean conc value (Vn)	Vn/Sn	Qn= Vn/Sn*100	Wi*Qn
pH	7.5	0.133333	0.82988889	1.204980586	0.160664	8.69	1.158	115.866	18.61561
EC	300	0.003333	0.82988889	1.204980586	0.004017	428	1.4266	142.666	0.573035
TDS	500	0.002	0.82988889	1.204980586	0.00241	213	0.426	42.6	0.102664
DO	5	0.2	0.82988889	1.204980586	0.240996	12.49	2.498	249.8	60.20083
BOD	5	0.2	0.82988889	1.204980586	0.240996	22	4.4	440	106.0383
COD	20	0.05	0.82988889	1.204980586	0.060249	37	1.85	185	11.14607
Turbidity	5	0.2	0.82988889	1.204980586	0.240996	8.12	1.624	162.4	39.13777
Chloride	250	0.004	0.82988889	1.204980586	0.00482	51.98	0.207	20.792	0.100216
Alkalinity	200	0.005	0.82988889	1.204980586	0.006025	204	1.02	102	0.61454
Total Hardness	200	0.005	0.82988889	1.204980586	0.006025	180	0.9	90	0.542241
Sulphate	200	0.005	0.82988889	1.204980586	0.006025	7	0.035	3.5	0.021087
Nitrate	45	0.022222	0.82988889	1.204980586	0.026777	16	0.355556	35.55	0.952083
		0.829889			**1**				**238.0444**

Table for Computation of the Dry Season Weighted Arithmetic Water Quality Index for the Site Banskuli

Parameters	BIS standard (Sn)	1/Sn	Sum of 1/Sn	K= 1/sum of 1/Sn	Wi=k/Sn	Mean conc value (Vn)	Vn/Sn	Qn= Vn/Sn*100	Wi*Qn
pH	7.5	0.133333	0.82988889	1.204980586	0.160664	8.24	1.09	109.866	17.65163
EC	300	0.003333	0.82988889	1.204980586	0.004017	359	1.196	119.66	0.480653
TDS	500	0.002	0.82988889	1.204980586	0.00241	195	0.39	39	0.093988
DO	5	0.2	0.82988889	1.204980586	0.240996	8.41	1.682	168.2	40.53555
BOD	5	0.2	0.82988889	1.204980586	0.240996	25	5	500	120.4981
COD	20	0.05	0.82988889	1.204980586	0.060249	45.58823529	2.27	227.941	13.73323
Turbidity	5	0.2	0.82988889	1.204980586	0.240996	9.06	1.812	181.2	43.6685
Chloride	250	0.004	0.82988889	1.204980586	0.00482	22.06	0.088	8.824	0.042531
Alkalinity	200	0.005	0.82988889	1.204980586	0.006025	140	0.7	70	0.421743
Total Hardness	200	0.005	0.82988889	1.204980586	0.006025	120	0.6	60	0.361494
Sulphate	200	0.005	0.82988889	1.204980586	0.006025	6	0.03	3	0.018075
Nitrate	45	0.022222	0.82988889	1.204980586	0.026777	11.3	0.251	25.11	0.672409
		0.829889			**1**				**238.1779**

Table for Computation of the Dry Season Weighted Arithmetic Water Quality Index for the Site Beniagram

Parameters	BIS standard (Sn)	1/Sn	Sum of 1/Sn	K= 1/sum of 1/Sn	Wi=k/Sn	Mean conc value (Vn)	Vn/Sn	Qn= Vn/Sn*100	Wi*Qn
pH	7.5	0.133333	0.82988889	1.204980586	0.160664	8.36	1.114667	111.46	17.90869
EC	300	0.003333	0.82988889	1.204980586	0.004017	216	0.72	72	0.289195
TDS	500	0.002	0.82988889	1.204980586	0.00241	114	0.228	22.8	0.054947
DO	5	0.2	0.82988889	1.204980586	0.240996	7.59	1.518	151.8	36.58321
BOD	5	0.2	0.82988889	1.204980586	0.240996	12.2	2.44	244	58.80305
COD	20	0.05	0.82988889	1.204980586	0.060249	22.247	1.112	111.235	6.701818
Turbidity	5	0.2	0.82988889	1.204980586	0.240996	16.4	3.28	328	79.04673
Chloride	250	0.004	0.82988889	1.204980586	0.00482	19.99	0.0799	7.996	0.03854
Alkalinity	200	0.005	0.82988889	1.204980586	0.006025	132	0.66	66	0.397644
Total Hardness	200	0.005	0.82988889	1.204980586	0.006025	112	0.56	56	0.337395
Sulphate	200	0.005	0.82988889	1.204980586	0.006025	6	0.03	3	0.018075
Nitrate	45	0.022222	0.82988889	1.204980586	0.026777	15.1	0.335	33.55	0.898529
		0.829889			**1**				**201.0778**

Table for Computation of the Dry Season Weighted Arithmetic Water Quality Index for the Site Diguli

Parameters	BIS standard (Sn)	1/Sn	Sum of 1/Sn	K= 1/sum of 1/Sn	Wi=k/Sn	Mean conc value (Vn)	Vn/Sn	Qn= Vn/Sn*100	Wi*Qn
pH	7.5	0.133333	0.82988889	1.204980586	0.160664	8.31	1.108	110.8	17.80158
EC	300	0.003333	0.82988889	1.204980586	0.004017	190	0.633	63.333	0.254385
TDS	500	0.002	0.82988889	1.204980586	0.00241	96	0.192	19.2	0.046271
DO	5	0.2	0.82988889	1.204980586	0.240996	7.15	1.43	143	34.46244
BOD	5	0.2	0.82988889	1.204980586	0.240996	8.4	1.68	168	40.48735
COD	20	0.05	0.82988889	1.204980586	0.060249	15.317	0.765	76.588	4.614367
Turbidity	5	0.2	0.82988889	1.204980586	0.240996	10.5	2.1	210	50.60918
Chloride	250	0.004	0.82988889	1.204980586	0.00482	19.85	0.0794	7.94	0.03827
Alkalinity	200	0.005	0.82988889	1.204980586	0.006025	100	0.5	50	0.301245
Total Hardness	200	0.005	0.82988889	1.204980586	0.006025	100	0.5	50	0.301245
Sulphate	200	0.005	0.82988889	1.204980586	0.006025	5	0.025	2.5	0.015062
Nitrate	45	0.022222	0.82988889	1.204980586	0.026777	11	0.244	24.44	0.654557
		0.829889			**1**				**149.586**

Table for Computation of the Dry Season Weighted Arithmetic Water Quality Index for the Site Kultore

Parameters	BIS standard (Sn)	1/Sn	Sum of 1/Sn	K= 1/sum of 1/Sn	Wi=k/Sn	Mean conc value (Vn)	Vn/Sn	Qn= Vn/Sn*100	Wi*Qn
pH	7.5	0.133333	0.82988889	1.204980586	0.160664	8.05	1.073	107.333	17.24461
EC	300	0.003333	0.82988889	1.204980586	0.004017	172	0.573	57.333	0.230285
TDS	500	0.002	0.82988889	1.204980586	0.00241	85	0.17	17	0.040969
DO	5	0.2	0.82988889	1.204980586	0.240996	7.05	1.41	141	33.98045
BOD	5	0.2	0.82988889	1.204980586	0.240996	13.6	2.72	272	65.55094
COD	20	0.05	0.82988889	1.204980586	0.060249	24.8	1.24	124	7.47088
Turbidity	5	0.2	0.82988889	1.204980586	0.240996	17.6	3.52	352	84.83063
Chloride	250	0.004	0.82988889	1.204980586	0.00482	5.67	0.022	2.268	0.010932
Alkalinity	200	0.005	0.82988889	1.204980586	0.006025	60	0.3	30	0.180747
Total Hardness	200	0.005	0.82988889	1.204980586	0.006025	84	0.42	42	0.253046
Sulphate	200	0.005	0.82988889	1.204980586	0.006025	5	0.025	2.5	0.015062
Nitrate	45	0.022222	0.82988889	1.204980586	0.026777	14.2	0.3155	31.555	0.844974
		0.829889			**1**				**210.6535**

Table for Computation of the Dry Season Weighted Arithmetic Water Quality Index for the Site Sainthia

Parameters	BIS standard (Sn)	1/Sn	Sum of 1/Sn	K= 1/sum of 1/Sn	Wi=k/Sn	Mean conc value (Vn)	Vn/Sn	Qn= Vn/Sn*100	Wi*Qn
pH	7.5	0.133333	0.82988889	1.204980586	0.160664	7.84	1.04	104.533	16.79475
EC	300	0.003333	0.82988889	1.204980586	0.004017	189	0.63	63	0.253046
TDS	500	0.002	0.82988889	1.204980586	0.00241	95	0.19	19	0.045789
DO	5	0.2	0.82988889	1.204980586	0.240996	6.19	1.238	123.8	29.83532
BOD	5	0.2	0.82988889	1.204980586	0.240996	20.8	4.16	416	100.2544
COD	20	0.05	0.82988889	1.204980586	0.060249	37.929	1.89	189.647	11.42605
Turbidity	5	0.2	0.82988889	1.204980586	0.240996	18.2	3.64	364	87.72259
Chloride	250	0.004	0.82988889	1.204980586	0.00482	14.18	0.0567	5.672	0.027339
Alkalinity	200	0.005	0.82988889	1.204980586	0.006025	60	0.3	30	0.180747
Total Hardness	200	0.005	0.82988889	1.204980586	0.006025	96	0.48	48	0.289195
Sulphate	200	0.005	0.82988889	1.204980586	0.006025	5	0.025	2.5	0.015062
Nitrate	45	0.022222	0.82988889	1.204980586	0.026777	8.7	0.193	19.33	0.517695
		0.829889			**1**				**247.362**

Table for Computation of the Dry Season Weighted Arithmetic Water Quality Index for the Site Panjona

Parameters	BIS standard (Sn)	1/Sn	Sum of 1/Sn	K= 1/sum of 1/Sn	Wi=k/Sn	Mean conc value (Vn)	Vn/Sn	Qn= Vn/Sn*100	Wi*Qn
pH	7.5	0.133333	0.82988889	1.204980586	0.160664	8.21	1.094	109.466	17.58736
EC	300	0.003333	0.82988889	1.204980586	0.004017	190	0.633	63.333	0.254385
TDS	500	0.002	0.82988889	1.204980586	0.00241	98	0.196	19.6	0.047235
DO	5	0.2	0.82988889	1.204980586	0.240996	7.84	1.568	156.8	37.78819
BOD	5	0.2	0.82988889	1.204980586	0.240996	14.8	2.96	296	71.33485
COD	20	0.05	0.82988889	1.204980586	0.060249	26.988	1.349	134.941	8.130075
Turbidity	5	0.2	0.82988889	1.204980586	0.240996	24.6	4.92	492	118.5701
Chloride	250	0.004	0.82988889	1.204980586	0.00482	8.51	0.034	3.404	0.016407
Alkalinity	200	0.005	0.82988889	1.204980586	0.006025	60	0.3	30	0.180747
Total Hardness	200	0.005	0.82988889	1.204980586	0.006025	72	0.36	36	0.216897
Sulphate	200	0.005	0.82988889	1.204980586	0.006025	12	0.06	6	0.036149
Nitrate	45	0.022222	0.82988889	1.204980586	0.026777	9.8	0.2177	21.777	0.583151
		0.829889			**1**				**254.7455**

Table for Computation of the Dry Season Weighted Arithmetic Water Quality Index for the Site Gunutia

Parameters	BIS standard (Sn)	1/Sn	Sum of 1/Sn	K= 1/sum of 1/Sn	Wi=k/Sn	Mean conc value (Vn)	Vn/Sn	Qn= Vn/Sn*100	Wi*Qn
pH	7.5	0.133333	0.82988889	1.204980586	0.160664	8.49	1.132	113.2	18.18717
EC	300	0.003333	0.82988889	1.204980586	0.004017	195	0.65	65	0.261079
TDS	500	0.002	0.82988889	1.204980586	0.00241	96	0.192	19.2	0.046271
DO	5	0.2	0.82988889	1.204980586	0.240996	8.97	1.794	179.4	43.2347
BOD	5	0.2	0.82988889	1.204980586	0.240996	28.6	5.72	572	137.8498
COD	20	0.05	0.82988889	1.204980586	0.060249	52.152	2.607	260.764	15.71082
Turbidity	5	0.2	0.82988889	1.204980586	0.240996	50.8	10.16	1016	244.8521
Chloride	250	0.004	0.82988889	1.204980586	0.00482	8.51	0.03404	3.404	0.016407
Alkalinity	200	0.005	0.82988889	1.204980586	0.006025	80	0.4	40	0.240996
Total Hardness	200	0.005	0.82988889	1.204980586	0.006025	64	0.32	32	0.192797
Sulphate	200	0.005	0.82988889	1.204980586	0.006025	23	0.115	11.5	0.069286
Nitrate	45	0.022222	0.82988889	1.204980586	0.026777	13.6	0.302222	30.22	0.809271
		0.829889			**1**				**461.4706**

Table for Computation of the Dry Season Weighted Arithmetic Water Quality Index for the Site Sundarpur

Parameters	BIS standard (Sn)	1/Sn	Sum of 1/Sn	K= 1/sum of 1/Sn	Wi=k/Sn	Mean conc value (Vn)	Vn/Sn	Qn= Vn/Sn*100	Wi*Qn
pH	7.5	0.133333	0.82988889	1.204980586	0.160664	8.32	1.109	110.933	17.823
EC	300	0.003333	0.82988889	1.204980586	0.004017	214	0.713	71.333	0.286518
TDS	500	0.002	0.82988889	1.204980586	0.00241	107	0.214	21.4	0.051573
DO	5	0.2	0.82988889	1.204980586	0.240996	8.3	1.66	166	40.00536
BOD	5	0.2	0.82988889	1.204980586	0.240996	32.6	6.52	652	157.1295
COD	20	0.05	0.82988889	1.204980586	0.060249	59.447	2.9723	297.235	17.90814
Turbidity	5	0.2	0.82988889	1.204980586	0.240996	78.5	15.7	1570	378.3639
Chloride	250	0.004	0.82988889	1.204980586	0.00482	5.66	0.02264	2.264	0.010912
Alkalinity	200	0.005	0.82988889	1.204980586	0.006025	100	0.5	50	0.301245
Total Hardness	200	0.005	0.82988889	1.204980586	0.006025	80	0.4	40	0.240996
Sulphate	200	0.005	0.82988889	1.204980586	0.006025	30	0.15	15	0.090374
Nitrate	45	0.022222	0.82988889	1.204980586	0.026777	21.6	0.48	48	1.285313
		0.829889			**1**				**613.4968**

Table for Computation of the Dry Season Weighted Arithmetic Water Quality Index for the Site Aharinagar

Parameters	BIS standard (Sn)	1/Sn	Sum of 1/Sn	K= 1/sum of 1/Sn	Wi=k/Sn	Mean conc value (Vn)	Vn/Sn	Qn= Vn/Sn*100	Wi*Qn
pH	7.5	0.133333	0.82988889	1.204980586	0.160664	8.28	1.104	110.4	17.73731
EC	300	0.003333	0.82988889	1.204980586	0.004017	222	0.74	74	0.297229
TDS	500	0.002	0.82988889	1.204980586	0.00241	114	0.228	22.8	0.054947
DO	5	0.2	0.82988889	1.204980586	0.240996	7.87	1.574	157.4	37.93279
BOD	5	0.2	0.82988889	1.204980586	0.240996	24	4.8	480	115.6781
COD	20	0.05	0.82988889	1.204980586	0.060249	43.764	2.188	218.823	13.18391
Turbidity	5	0.2	0.82988889	1.204980586	0.240996	32.2	6.44	644	155.2015
Chloride	250	0.004	0.82988889	1.204980586	0.00482	25.52	0.1020	10.208	0.049202
Alkalinity	200	0.005	0.82988889	1.204980586	0.006025	80	0.4	40	0.240996
Total Hardness	200	0.005	0.82988889	1.204980586	0.006025	88	0.44	44	0.265096
Sulphate	200	0.005	0.82988889	1.204980586	0.006025	11	0.055	5.5	0.033137
Nitrate	45	0.022222	0.82988889	1.204980586	0.026777	20.3	0.451	45.11	1.207956
		0.829889			**1**				**341.8822**

Table for Computation of the Dry Season Weighted Arithmetic Water Quality Index for the Site Gopalpur

Parameters	BIS standard (Sn)	1/Sn	Sum of 1/Sn	K= 1/sum of 1/Sn	Wi=k/Sn	Mean conc value (Vn)	Vn/Sn	Qn= Vn/Sn*100	Wi*Qn
pH	7.5	0.133333	0.82988889	1.204980586	0.160664	8.41	1.1213	112.13	18.0158
EC	300	0.003333	0.82988889	1.204980586	0.004017	229	0.763	76.33	0.306601
TDS	500	0.002	0.82988889	1.204980586	0.00241	114	0.228	22.8	0.054947
DO	5	0.2	0.82988889	1.204980586	0.240996	8.65	1.73	173	41.69233
BOD	5	0.2	0.82988889	1.204980586	0.240996	11.5	2.3	230	55.42911
COD	20	0.05	0.82988889	1.204980586	0.060249	20.970	1.04	104.852	6.317288
Turbidity	5	0.2	0.82988889	1.204980586	0.240996	21.6	4.32	432	104.1103
Chloride	250	0.004	0.82988889	1.204980586	0.00482	19.85	0.0794	7.94	0.03827
Alkalinity	200	0.005	0.82988889	1.204980586	0.006025	80	0.4	40	0.240996
Total Hardness	200	0.005	0.82988889	1.204980586	0.006025	96	0.48	48	0.289195
Sulphate	200	0.005	0.82988889	1.204980586	0.006025	18	0.09	9	0.054224
Nitrate	45	0.022222	0.82988889	1.204980586	0.026777	21.5	0.4777	47.77	1.279362
		0.829889			**1**				**227.8284**

Table for Computation of the Dry Season Weighted Arithmetic Water Quality Index for the Site Lohadaha

Parameters	**BIS standard (Sn)**	**1/Sn**	**Sum of 1/Sn**	**K= 1/sum of 1/Sn**	**Wi=k/Sn**	**Mean conc value (Vn)**	**Vn/Sn**	**Qn= Vn/Sn*100**	**Wi*Qn**
pH	7.5	0.133333	0.82988889	1.204980586	0.160664	8.32	1.109	110.933	17.823
EC	300	0.003333	0.82988889	1.204980586	0.004017	359	1.196	119.666	0.480653
TDS	500	0.002	0.82988889	1.204980586	0.00241	180	0.36	36	0.086759
DO	5	0.2	0.82988889	1.204980586	0.240996	7.91	1.582	158.2	38.12559
BOD	5	0.2	0.82988889	1.204980586	0.240996	8.9	1.78	178	42.89731
COD	20	0.05	0.82988889	1.204980586	0.060249	16.2	0.8114	81.1470	4.889032
Turbidity	5	0.2	0.82988889	1.204980586	0.240996	21.9	4.38	438	105.5563
Chloride	250	0.004	0.82988889	1.204980586	0.00482	17.02	0.06808	6.808	0.032814
Alkalinity	200	0.005	0.82988889	1.204980586	0.006025	100	0.5	50	0.301245
Total Hardness	200	0.005	0.82988889	1.204980586	0.006025	156	0.78	78	0.469942
Sulphate	200	0.005	0.82988889	1.204980586	0.006025	22	0.11	11	0.066274
Nitrate	45	0.022222	0.82988889	1.204980586	0.026777	20.3	0.451	45.111	1.207956
		0.829889			**1**				**211.9369**

Table for Computation of the Dry Season Weighted Arithmetic Water Quality Index for the Site Baidyapur

Parameters	BIS standard (Sn)	1/Sn	Sum of 1/Sn	K= 1/sum of 1/Sn	Wi=k/Sn	Mean conc value (Vn)	Vn/Sn	Qn= Vn/Sn*100	Wi*Qn
pH	7.5	0.133333	0.82988889	1.204980586	0.160664	8.34	1.112	111.2	17.86585
EC	300	0.003333	0.82988889	1.204980586	0.004017	362	1.2066	120.666	0.48467
TDS	500	0.002	0.82988889	1.204980586	0.00241	179	0.358	35.8	0.086277
DO	5	0.2	0.82988889	1.204980586	0.240996	7.98	1.596	159.6	38.46298
BOD	5	0.2	0.82988889	1.204980586	0.240996	6.8	1.36	136	32.77547
COD	20	0.05	0.82988889	1.204980586	0.060249	12.4	0.62	62	3.73544
Turbidity	5	0.2	0.82988889	1.204980586	0.240996	8.82	1.764	176.4	42.51172
Chloride	250	0.004	0.82988889	1.204980586	0.00482	14.18	0.05672	5.672	0.027339
Alkalinity	200	0.005	0.82988889	1.204980586	0.006025	140	0.7	70	0.421743
Total Hardness	200	0.005	0.82988889	1.204980586	0.006025	176	0.88	88	0.530191
Sulphate	200	0.005	0.82988889	1.204980586	0.006025	20	0.1	10	0.060249
Nitrate	45	0.022222	0.82988889	1.204980586	0.026777	10.1	0.2244	22.444	0.601003
		0.829889			**1**				**137.5629**

Table for Computation of the Wet Season Weighted Arithmetic Water Quality Index for the Site Rerha

Parameters	BIS standard (Sn)	1/Sn	Sum of 1/Sn	K= 1/sum of 1/Sn	Wi=k/Sn	Mean conc value (Vn)	Vn/Sn	Qn= Vn/Sn*100	Wi*Qn
pH	7.5	0.133333	0.829888889	1.204980586	0.160664078	8.61	1.148	114.8	18.44423618
EC	300	0.003333	0.829888889	1.204980586	0.004016602	218	0.7266	72.666	0.291873075
TDS	500	0.002	0.829888889	1.204980586	0.002409961	110	0.22	22	0.053019146
DO	5	0.2	0.829888889	1.204980586	0.240996117	8.98	1.796	179.6	43.28290266
BOD	5	0.2	0.829888889	1.204980586	0.240996117	8.2	1.64	164	39.52336323
COD	20	0.05	0.829888889	1.204980586	0.060249029	15.8	0.79	79	4.759673316
Turbidity	5	0.2	0.829888889	1.204980586	0.240996117	6.11	1.222	122.2	29.44972553
Chloride	250	0.004	0.829888889	1.204980586	0.004819922	45.68	0.18272	18.272	0.088069621
Alkalinity	200	0.005	0.829888889	1.204980586	0.006024903	112	0.56	56	0.337394564
Total Hardness	200	0.005	0.829888889	1.204980586	0.006024903	210	1.05	105	0.632614808
Sulphate	200	0.005	0.829888889	1.204980586	0.006024903	5	0.025	2.5	0.015062257
Nitrate	45	0.022222	0.829888889	1.204980586	0.026777346	2.11	0.0468	4.688	0.125556002
		0.829889			**1**				**137.0034904**

Table for Computation of the Wet Season Weighted Arithmetic Water Quality Index for the Site Gajenda

Parameters	BIS standard (Sn)	1/Sn	Sum of 1/Sn	K= 1/sum of 1/Sn	Wi=k/Sn	Mean conc value (Vn)	Vn/Sn	Qn= Vn/Sn*100	Wi*Qn
pH	7.5	0.133333	0.829888889	1.204980586	0.160664078	8.51	1.134	113.467	18.23001741
EC	300	0.003333	0.829888889	1.204980586	0.004016602	211	0.703	70.333	0.282501004
TDS	500	0.002	0.829888889	1.204980586	0.002409961	110	0.22	22	0.053019146
DO	5	0.2	0.829888889	1.204980586	0.240996117	8.99	1.798	179.8	43.33110189
BOD	5	0.2	0.829888889	1.204980586	0.240996117	5.3	1.06	106	25.54558843
COD	20	0.05	0.829888889	1.204980586	0.060249029	9.6	0.48	48	2.891953407
Turbidity	5	0.2	0.829888889	1.204980586	0.240996117	2.6	0.52	52	12.5317981
Chloride	250	0.004	0.829888889	1.204980586	0.004819922	52.3	0.2092	20.92	0.100832775
Alkalinity	200	0.005	0.829888889	1.204980586	0.006024903	260	1.3	130	0.783237381
Total Hardness	200	0.005	0.829888889	1.204980586	0.006024903	260	1.3	130	0.783237381
Sulphate	200	0.005	0.829888889	1.204980586	0.006024903	5	0.025	2.5	0.015062257
Nitrate	45	0.022222	0.829888889	1.204980586	0.026777346	2.11	0.046	4.688	0.125556002
		0.829889			**1**				**104.6739052**

Table for Computation of the Wet Season Weighted Arithmetic Water Quality Index for the Site Maharo

Parameters	BIS standard (Sn)	1/Sn	Sum of 1/Sn	K= 1/sum of 1/Sn	Wi=k/Sn	Mean conc value (Vn)	Vn/Sn	Qn= Vn/Sn*100	Wi*Qn
pH	7.5	0.133333	0.829888889	1.204980586	0.160664078	8.7	1.16	116	18.63703307
EC	300	0.003333	0.829888889	1.204980586	0.004016602	209	0.696	69.666	0.27982327
TDS	500	0.002	0.829888889	1.204980586	0.002409961	102	0.204	20.4	0.049163208
DO	5	0.2	0.829888889	1.204980586	0.240996117	9.99	1.998	199.8	48.15102423
BOD	5	0.2	0.829888889	1.204980586	0.240996117	2	0.4	40	9.639844691
COD	20	0.05	0.829888889	1.204980586	0.060249029	8	0.4	40	2.409961173
Turbidity	5	0.2	0.829888889	1.204980586	0.240996117	2.54	0.508	50.8	12.24260276
Chloride	250	0.004	0.829888889	1.204980586	0.004819922	64.82	0.25928	25.928	0.124970947
Alkalinity	200	0.005	0.829888889	1.204980586	0.006024903	180	0.9	90	0.542241264
Total Hardness	200	0.005	0.829888889	1.204980586	0.006024903	592	2.96	296	1.783371268
Sulphate	200	0.005	0.829888889	1.204980586	0.006024903	4	0.02	2	0.012049806
Nitrate	45	0.022222	0.829888889	1.204980586	0.026777346	0	0	0	0
		0.829889			**1**				**93.87208569**

Table for Computation of the Wet Season Weighted Arithmetic Water Quality Index for the Site Dudhani

Parameters	BIS standard (Sn)	1/Sn	Sum of 1/Sn	K= 1/sum of 1/Sn	Wi=k/Sn	Mean conc value (Vn)	Vn/Sn	Qn= Vn/Sn*100	Wi*Qn
pH	7.5	0.133333	0.829888889	1.204980586	0.160664078	8.74	1.1653	116.533	18.72272058
EC	300	0.003333	0.829888889	1.204980586	0.004016602	216	0.72	72	0.289195341
TDS	500	0.002	0.829888889	1.204980586	0.002409961	110	0.22	22	0.053019146
DO	5	0.2	0.829888889	1.204980586	0.240996117	8.94	1.788	178.8	43.09010577
BOD	5	0.2	0.829888889	1.204980586	0.240996117	12	2.4	240	57.83906815
COD	20	0.05	0.829888889	1.204980586	0.060249029	22.0	1.101	110.19	6.638916455
Turbidity	5	0.2	0.829888889	1.204980586	0.240996117	4.15	0.83	83	20.00267773
Chloride	250	0.004	0.829888889	1.204980586	0.004819922	20.5	0.082	8.2	0.039523363
Alkalinity	200	0.005	0.829888889	1.204980586	0.006024903	130	0.65	65	0.391618691
Total Hardness	200	0.005	0.829888889	1.204980586	0.006024903	140	0.7	70	0.421743205
Sulphate	200	0.005	0.829888889	1.204980586	0.006024903	3	0.015	1.5	0.009037354
Nitrate	45	0.022222	0.829888889	1.204980586	0.026777346	3.65	0.0811	8.111	0.217194032
		0.829889			**1**				**147.7148198**

Table for Computation of the Wet Season Weighted Arithmetic Water Quality Index for the Site Poljori

Parameters	BIS standard (Sn)	1/Sn	Sum of 1/Sn	K= 1/sum of 1/Sn	Wi=k/Sn	Mean conc value (Vn)	Vn/Sn	Qn= Vn/Sn*100	Wi*Qn
pH	7.5	0.133333	0.829888889	1.204980586	0.160664078	8.64	1.152	115.2	18.50850181
EC	300	0.003333	0.829888889	1.204980586	0.004016602	436	1.453	145.33	0.583746151
TDS	500	0.002	0.829888889	1.204980586	0.002409961	220	0.44	44	0.106038292
DO	5	0.2	0.829888889	1.204980586	0.240996117	13.85	2.77	277	66.75592449
BOD	5	0.2	0.829888889	1.204980586	0.240996117	16	3.2	320	77.11875753
COD	20	0.05	0.829888889	1.204980586	0.060249029	29.4	1.469	146.92	8.851888606
Turbidity	5	0.2	0.829888889	1.204980586	0.240996117	5.64	1.128	112.8	27.18436203
Chloride	250	0.004	0.829888889	1.204980586	0.004819922	34.6	0.1384	13.84	0.066707725
Alkalinity	200	0.005	0.829888889	1.204980586	0.006024903	190	0.95	95	0.572365779
Total Hardness	200	0.005	0.829888889	1.204980586	0.006024903	190	0.95	95	0.572365779
Sulphate	200	0.005	0.829888889	1.204980586	0.006024903	5	0.025	2.5	0.015062257
Nitrate	45	0.022222	0.829888889	1.204980586	0.026777346	18	0.4	40	1.071093855
		0.829889			**1**				**201.4068143**

Table for Computation of the Wet Season Weighted Arithmetic Water Quality Index for the Site Banskuli

Parameters	BIS standard (Sn)	1/Sn	Sum of 1/Sn	K= 1/sum of 1/Sn	Wi=k/Sn	Mean conc value (Vn)	Vn/Sn	Qn= Vn/Sn*100	Wi*Qn
pH	7.5	0.133333	0.829888889	1.204980586	0.160664078	8.39	1.1186	111.866	17.97295488
EC	300	0.003333	0.829888889	1.204980586	0.004016602	398	1.3266	132.666	0.532869193
TDS	500	0.002	0.829888889	1.204980586	0.002409961	200	0.4	40	0.096398447
DO	5	0.2	0.829888889	1.204980586	0.240996117	8.97	1.794	179.4	43.23470344
BOD	5	0.2	0.829888889	1.204980586	0.240996117	15	3	300	72.29883519
COD	20	0.05	0.829888889	1.204980586	0.060249029	27.5	1.377	137.73	8.298645568
Turbidity	5	0.2	0.829888889	1.204980586	0.240996117	5.68	1.136	113.6	27.37715892
Chloride	250	0.004	0.829888889	1.204980586	0.004819922	16.8	0.0672	6.72	0.032389878
Alkalinity	200	0.005	0.829888889	1.204980586	0.006024903	134	0.67	67	0.403668496
Total Hardness	200	0.005	0.829888889	1.204980586	0.006024903	162	0.81	81	0.488017138
Sulphate	200	0.005	0.829888889	1.204980586	0.006024903	5	0.025	2.5	0.015062257
Nitrate	45	0.022222	0.829888889	1.204980586	0.026777346	16.5	0.3666	36.666	0.981836033
		0.829889			**1**				**171.7325394**

Table for Computation of the Wet Season Weighted Arithmetic Water Quality Index for the Site Beniagram

Parameters	BIS standard (Sn)	1/Sn	Sum of 1/Sn	K= 1/sum of 1/Sn	Wi=k/Sn	Mean conc value (Vn)	Vn/Sn	Qn= Vn/Sn*100	Wi*Qn
pH	7.5	0.133333	0.829888889	1.204980586	0.160664078	8.51	1.1346	113.466	18.23001741
EC	300	0.003333	0.829888889	1.204980586	0.004016602	248	0.8266	82.666	0.332039095
TDS	500	0.002	0.829888889	1.204980586	0.002409961	130	0.26	26	0.06265899
DO	5	0.2	0.829888889	1.204980586	0.240996117	8.69	1.738	173.8	41.88512518
BOD	5	0.2	0.829888889	1.204980586	0.240996117	7.8	1.56	156	37.5953943
COD	20	0.05	0.829888889	1.204980586	0.060249029	14.3	0.71624	71.624	4.315295696
Turbidity	5	0.2	0.829888889	1.204980586	0.240996117	12.5	2.5	250	60.24902932
Chloride	250	0.004	0.829888889	1.204980586	0.004819922	12.5	0.05	5	0.024099612
Alkalinity	200	0.005	0.829888889	1.204980586	0.006024903	130	0.65	65	0.391618691
Total Hardness	200	0.005	0.829888889	1.204980586	0.006024903	130	0.65	65	0.391618691
Sulphate	200	0.005	0.829888889	1.204980586	0.006024903	6	0.03	3	0.018074709
Nitrate	45	0.022222	0.829888889	1.204980586	0.026777346	18.1	0.40222	40.22	1.077044376
		0.829889			**1**				**164.5720161**

Table for Computation of the Wet Season Weighted Arithmetic Water Quality Index for the Site Diguli

Parameters	BIS standard (Sn)	1/Sn	Sum of 1/Sn	K= 1/sum of 1/Sn	Wi=k/Sn	Mean conc value (Vn)	Vn/Sn	Qn= Vn/Sn*100	Wi*Qn
pH	7.5	0.133333	0.829888889	1.204980586	0.160664078	8.29	1.1053	110.53	17.75873611
EC	300	0.003333	0.829888889	1.204980586	0.004016602	211	0.703	70.333	0.282501004
TDS	500	0.002	0.829888889	1.204980586	0.002409961	110	0.22	22	0.053019146
DO	5	0.2	0.829888889	1.204980586	0.240996117	8.28	1.656	165.6	39.90895702
BOD	5	0.2	0.829888889	1.204980586	0.240996117	4.6	0.92	92	22.17164279
COD	20	0.05	0.829888889	1.204980586	0.060249029	8.4	0.422	42.23	2.544917974
Turbidity	5	0.2	0.829888889	1.204980586	0.240996117	12.5	2.5	250	60.24902932
Chloride	250	0.004	0.829888889	1.204980586	0.004819922	16.5	0.066	6.6	0.031811487
Alkalinity	200	0.005	0.829888889	1.204980586	0.006024903	95	0.475	47.5	0.286182889
Total Hardness	200	0.005	0.829888889	1.204980586	0.006024903	130	0.65	65	0.391618691
Sulphate	200	0.005	0.829888889	1.204980586	0.006024903	6	0.03	3	0.018074709
Nitrate	45	0.022222	0.829888889	1.204980586	0.026777346	15.5	0.3444	34.44	0.922330819
		0.829889			**1**				**144.618822**

Table for Computation of the Wet Season Weighted Arithmetic Water Quality Index for the Site Kultore

Parameters	BIS standard (Sn)	1/Sn	Sum of 1/Sn	K= 1/sum of 1/Sn	Wi=k/Sn	Mean conc value (Vn)	Vn/Sn	Qn= Vn/Sn*100	Wi*Qn
pH	7.5	0.133333	0.829888889	1.204980586	0.160664078	8.41	1.1213	112.133	18.01579863
EC	300	0.003333	0.829888889	1.204980586	0.004016602	180	0.6	60	0.240996117
TDS	500	0.002	0.829888889	1.204980586	0.002409961	95	0.19	19	0.045789262
DO	5	0.2	0.829888889	1.204980586	0.240996117	7.98	1.596	159.6	38.46298032
BOD	5	0.2	0.829888889	1.204980586	0.240996117	7.4	1.48	148	35.66742536
COD	20	0.05	0.829888889	1.204980586	0.060249029	13.6	0.679	67.951	4.09399848
Turbidity	5	0.2	0.829888889	1.204980586	0.240996117	13.5	2.7	270	65.06895167
Chloride	250	0.004	0.829888889	1.204980586	0.004819922	4.54	0.01816	1.816	0.008752979
Alkalinity	200	0.005	0.829888889	1.204980586	0.006024903	62	0.31	31	0.186771991
Total Hardness	200	0.005	0.829888889	1.204980586	0.006024903	100	0.5	50	0.301245147
Sulphate	200	0.005	0.829888889	1.204980586	0.006024903	4	0.02	2	0.012049806
Nitrate	45	0.022222	0.829888889	1.204980586	0.026777346	15.5	0.3444	34.444	0.922330819
		0.829889			**1**				**163.0270906**

Table for Computation of the Wet Season Weighted Arithmetic Water Quality Index for the Site Sainthia

Parameters	BIS standard (Sn)	1/Sn	Sum of 1/Sn	K= 1/sum of 1/Sn	Wi=k/Sn	Mean conc value (Vn)	Vn/Sn	Qn= Vn/Sn*100	Wi*Qn
pH	7.5	0.133333	0.829888889	1.204980586	0.160664078	7.91	1.0546	105.46	16.94470478
EC	300	0.003333	0.829888889	1.204980586	0.004016602	180	0.6	60	0.240996117
TDS	500	0.002	0.829888889	1.204980586	0.002409961	100	0.2	20	0.048199223
DO	5	0.2	0.829888889	1.204980586	0.240996117	7.59	1.518	151.8	36.5832106
BOD	5	0.2	0.829888889	1.204980586	0.240996117	12	2.4	240	57.83906815
COD	20	0.05	0.829888889	1.204980586	0.060249029	22.0	1.1019	110.191	6.638916455
Turbidity	5	0.2	0.829888889	1.204980586	0.240996117	16.4	3.28	328	79.04672647
Chloride	250	0.004	0.829888889	1.204980586	0.004819922	12.26	0.04904	4.904	0.023636899
Alkalinity	200	0.005	0.829888889	1.204980586	0.006024903	62	0.31	31	0.186771991
Total Hardness	200	0.005	0.829888889	1.204980586	0.006024903	110	0.55	55	0.331369661
Sulphate	200	0.005	0.829888889	1.204980586	0.006024903	4	0.02	2	0.012049806
Nitrate	45	0.022222	0.829888889	1.204980586	0.026777346	11.2	0.2488	24.88	0.666458398
		0.829889			**1**				**198.5621086**

Table for Computation of the Wet Season Weighted Arithmetic Water Quality Index for the Site Panjona

Parameters	BIS standard (Sn)	1/Sn	Sum of 1/Sn	K= 1/sum of 1/Sn	Wi=k/Sn	Mean conc value (Vn)	Vn/Sn	Qn= Vn/Sn*100	Wi*Qn
pH	7.5	0.133333	0.829888889	1.204980586	0.160664078	8.25	1.1	110	17.6730486
EC	300	0.003333	0.829888889	1.204980586	0.004016602	196	0.653	65.333	0.262417994
TDS	500	0.002	0.829888889	1.204980586	0.002409961	100	0.2	20	0.048199223
DO	5	0.2	0.829888889	1.204980586	0.240996117	7.99	1.598	159.8	38.51117954
BOD	5	0.2	0.829888889	1.204980586	0.240996117	10.5	2.1	210	50.60918463
COD	20	0.05	0.829888889	1.204980586	0.060249029	19.3	0.9641	96.417	5.809051898
Turbidity	5	0.2	0.829888889	1.204980586	0.240996117	19.2	3.84	384	92.54250904
Chloride	250	0.004	0.829888889	1.204980586	0.004819922	6.74	0.02696	2.696	0.012994511
Alkalinity	200	0.005	0.829888889	1.204980586	0.006024903	52	0.26	26	0.156647476
Total Hardness	200	0.005	0.829888889	1.204980586	0.006024903	110	0.55	55	0.331369661
Sulphate	200	0.005	0.829888889	1.204980586	0.006024903	10	0.05	5	0.030124515
Nitrate	45	0.022222	0.829888889	1.204980586	0.026777346	12.2	0.2711	27.111	0.725963613
		0.829889			**1**				**206.7126907**

Table for Computation of the Wet Season Weighted Arithmetic Water Quality Index for the Site Gunutia

Parameters	BIS standard (Sn)	1/Sn	Sum of 1/Sn	K= 1/sum of 1/Sn	Wi=k/Sn	Mean conc value (Vn)	Vn/Sn	Qn= Vn/Sn*100	Wi*Qn
pH	7.5	0.133333	0.829888889	1.204980586	0.160664078	8.54	1.1386	113.866	18.29428304
EC	300	0.003333	0.829888889	1.204980586	0.004016602	193	0.643	64.33	0.258401392
TDS	500	0.002	0.829888889	1.204980586	0.002409961	95	0.19	19	0.045789262
DO	5	0.2	0.829888889	1.204980586	0.240996117	9.05	1.81	181	43.62029723
BOD	5	0.2	0.829888889	1.204980586	0.240996117	18.2	3.64	364	87.72258669
COD	20	0.05	0.829888889	1.204980586	0.060249029	33.4	1.6712	167.123	10.06902329
Turbidity	5	0.2	0.829888889	1.204980586	0.240996117	42.3	8.46	846	203.8827152
Chloride	250	0.004	0.829888889	1.204980586	0.004819922	6.58	0.02632	2.632	0.012686036
Alkalinity	200	0.005	0.829888889	1.204980586	0.006024903	59	0.295	29.5	0.177734636
Total Hardness	200	0.005	0.829888889	1.204980586	0.006024903	98	0.49	49	0.295220244
Sulphate	200	0.005	0.829888889	1.204980586	0.006024903	22	0.11	11	0.066273932
Nitrate	45	0.022222	0.829888889	1.204980586	0.026777346	12.5	0.277	27.77	0.743815177
		0.829889			**1**				**365.1888261**

Table for Computation of the Wet Season Weighted Arithmetic Water Quality Index for the Site Sundarpur

Parameters	BIS standard (Sn)	1/Sn	Sum of 1/Sn	K= 1/sum of 1/Sn	Wi=k/Sn	Mean conc value (Vn)	Vn/Sn	Qn= Vn/Sn*100	Wi*Qn
pH	7.5	0.133333	0.829888889	1.204980586	0.160664078	8.26	1.10133	110.133	17.69447048
EC	300	0.003333	0.829888889	1.204980586	0.004016602	220	0.7333	73.33	0.29455081
TDS	500	0.002	0.829888889	1.204980586	0.002409961	115	0.23	23	0.055429107
DO	5	0.2	0.829888889	1.204980586	0.240996117	8.98	1.796	179.6	43.28290266
BOD	5	0.2	0.829888889	1.204980586	0.240996117	22	4.4	440	106.0382916
COD	20	0.05	0.829888889	1.204980586	0.060249029	40.4	2.02017	202.0171	12.17134683
Turbidity	5	0.2	0.829888889	1.204980586	0.240996117	56.2	11.24	1124	270.8796358
Chloride	250	0.004	0.829888889	1.204980586	0.004819922	5.21	0.02084	2.084	0.010044718
Alkalinity	200	0.005	0.829888889	1.204980586	0.006024903	88	0.44	44	0.265095729
Total Hardness	200	0.005	0.829888889	1.204980586	0.006024903	98	0.49	49	0.295220244
Sulphate	200	0.005	0.829888889	1.204980586	0.006024903	28	0.14	14	0.084348641
Nitrate	45	0.022222	0.829888889	1.204980586	0.026777346	22.6	0.502	50.22	1.34481784
		0.829889			**1**				**452.4161545**

Table for Computation of the Wet Season Weighted Arithmetic Water Quality Index for the Site Aharinagar

Parameters	BIS standard (Sn)	1/Sn	Sum of 1/Sn	K= 1/sum of 1/Sn	Wi=k/Sn	Mean conc value (Vn)	Vn/Sn	Qn= Vn/Sn*100	Wi*Qn
pH	7.5	0.133333	0.829888889	1.204980586	0.160664078	8.29	1.105	110.53	17.75873611
EC	300	0.003333	0.829888889	1.204980586	0.004016602	227	0.7566	75.666	0.303922881
TDS	500	0.002	0.829888889	1.204980586	0.002409961	140	0.28	28	0.067478913
DO	5	0.2	0.829888889	1.204980586	0.240996117	8.25	1.65	165	39.76435935
BOD	5	0.2	0.829888889	1.204980586	0.240996117	13.6	2.72	272	65.5509439
COD	20	0.05	0.829888889	1.204980586	0.060249029	25.0	1.248	124.88	7.524105315
Turbidity	5	0.2	0.829888889	1.204980586	0.240996117	28.4	5.68	568	136.8857946
Chloride	250	0.004	0.829888889	1.204980586	0.004819922	22.31	0.08924	8.924	0.043012987
Alkalinity	200	0.005	0.829888889	1.204980586	0.006024903	75	0.375	37.5	0.22593386
Total Hardness	200	0.005	0.829888889	1.204980586	0.006024903	100	0.5	50	0.301245147
Sulphate	200	0.005	0.829888889	1.204980586	0.006024903	10	0.05	5	0.030124515
Nitrate	45	0.022222	0.829888889	1.204980586	0.026777346	22.9	0.5088	50.88	1.362669404
		0.829889			**1**				**269.818327**

Table for Computation of the Wet Season Weighted Arithmetic Water Quality Index for the Site Gopalpur

Parameters	BIS standard (Sn)	1/Sn	Sum of 1/Sn	K= 1/sum of 1/Sn	Wi=k/Sn	Mean conc value (Vn)	Vn/Sn	Qn= Vn/Sn*100	Wi*Qn
pH	7.5	0.133333	0.829888889	1.204980586	0.160664078	8.54	1.1386	113.866	18.29428304
EC	300	0.003333	0.829888889	1.204980586	0.004016602	232	0.7733	77.333	0.310617218
TDS	500	0.002	0.829888889	1.204980586	0.002409961	120	0.24	24	0.057839068
DO	5	0.2	0.829888889	1.204980586	0.240996117	8.94	1.788	178.8	43.09010577
BOD	5	0.2	0.829888889	1.204980586	0.240996117	6.2	1.24	124	29.88351854
COD	20	0.05	0.829888889	1.204980586	0.060249029	11.4	0.569	56.93	3.430106835
Turbidity	5	0.2	0.829888889	1.204980586	0.240996117	18.5	3.7	370	89.1685634
Chloride	250	0.004	0.829888889	1.204980586	0.004819922	17.7	0.0708	7.08	0.03412505
Alkalinity	200	0.005	0.829888889	1.204980586	0.006024903	75	0.375	37.5	0.22593386
Total Hardness	200	0.005	0.829888889	1.204980586	0.006024903	112	0.56	56	0.337394564
Sulphate	200	0.005	0.829888889	1.204980586	0.006024903	15	0.075	7.5	0.045186772
Nitrate	45	0.022222	0.829888889	1.204980586	0.026777346	22.8	0.5067	50.667	1.356718882
		0.829889			**1**				**186.234393**

Table for Computation of the Wet Season Weighted Arithmetic Water Quality Index for the Site Lohadaha

Parameters	BIS standard (Sn)	1/Sn	Sum of 1/Sn	K= 1/sum of 1/Sn	Wi=k/Sn	Mean conc value (Vn)	Vn/Sn	Qn= Vn/Sn*100	Wi*Qn
pH	7.5	0.133333	0.829888889	1.204980586	0.160664078	8.61	1.148	114.8	18.44423618
EC	300	0.003333	0.829888889	1.204980586	0.004016602	361	1.203	120.333	0.483331102
TDS	500	0.002	0.829888889	1.204980586	0.002409961	190	0.38	38	0.091578525
DO	5	0.2	0.829888889	1.204980586	0.240996117	8.58	1.716	171.6	41.35493373
BOD	5	0.2	0.829888889	1.204980586	0.240996117	3.6	0.72	72	17.35172044
COD	20	0.05	0.829888889	1.204980586	0.060249029	6.6	0.3305	33.057	1.991674936
Turbidity	5	0.2	0.829888889	1.204980586	0.240996117	18.7	3.74	374	90.13254786
Chloride	250	0.004	0.829888889	1.204980586	0.004819922	15.6	0.0624	6.24	0.030076315
Alkalinity	200	0.005	0.829888889	1.204980586	0.006024903	98	0.49	49	0.295220244
Total Hardness	200	0.005	0.829888889	1.204980586	0.006024903	160	0.8	80	0.481992235
Sulphate	200	0.005	0.829888889	1.204980586	0.006024903	18	0.09	9	0.054224126
Nitrate	45	0.022222	0.829888889	1.204980586	0.026777346	23.3	0.5177	51.777	1.38647149
		0.829889			**1**				**172.0980072**

Table for Computation of the Wet Season Weighted Arithmetic Water Quality Index for the Site Baidyapur

Parameters	BIS standard (Sn)	1/Sn	Sum of 1/Sn	K= 1/sum of 1/Sn	Wi=k/Sn	Mean conc value (Vn)	Vn/Sn	Qn= Vn/Sn*100	Wi*Qn
pH	7.5	0.133333	0.829888889	1.204980586	0.160664078	8.52	1.136	113.6	18.25143928
EC	300	0.003333	0.829888889	1.204980586	0.004016602	361	1.2033	120.33	0.483331102
TDS	500	0.002	0.829888889	1.204980586	0.002409961	190	0.38	38	0.091578525
DO	5	0.2	0.829888889	1.204980586	0.240996117	8.51	1.702	170.2	41.01753916
BOD	5	0.2	0.829888889	1.204980586	0.240996117	3.8	0.76	76	18.31570491
COD	20	0.05	0.829888889	1.204980586	0.060249029	7.0	0.3489	34.89	2.102323544
Turbidity	5	0.2	0.829888889	1.204980586	0.240996117	5.65	1.13	113	27.23256125
Chloride	250	0.004	0.829888889	1.204980586	0.004819922	12.4	0.0496	4.96	0.023906815
Alkalinity	200	0.005	0.829888889	1.204980586	0.006024903	110	0.55	55	0.331369661
Total Hardness	200	0.005	0.829888889	1.204980586	0.006024903	180	0.9	90	0.542241264
Sulphate	200	0.005	0.829888889	1.204980586	0.006024903	18	0.09	9	0.054224126
Nitrate	45	0.022222	0.829888889	1.204980586	0.026777346	13.4	0.297	29.7	0.79736987
		0.829889			1				109.2435895

ANNEXURE IV

SCORE SHEET OF QBR INDEX (*Munne et al. 2003*)

Section 1: Total Riparian Cover

Score	
25	>80% of riparian cover (excluding annual plants)
10	50-80% of riparian cover 5 10-50% of riparian cover
5	10-50% of riparian cover
0	<10% of riparian cover
+10 +5	If connectivity between the riparian forest and the woodland is total If the connectivity is higher than 50%
-5 -10	Connectivity between 25% and 50% Connectivity lower than 25%

Section 2: Cover Structure

Score	
25	>75% of tree cover
10	50-75% of tree cover or 25-50% tree cover but 25% covered by shrubs
5	Tree cover lower than 50% but shrub cover at least between 10% and 25%
0	<10% of either tree or shrub cover
+10 +5 +5	At least 50% of the channel has helophytes or shrubs If 25-50% of the channel has helophytes or shrubs If trees and shrubs are in the same patches
-5 -5 -10	If trees are regularly distributed and shrubland is >50% If trees and shrubs are distributed in separate patches, without continuity Trees distributed regularly, and shrubland <50%

Section 3: Cover Quality (The Geomorphological Type Should Be First Determined)

Score		Type 1	Type 2	Type 3
25	Number of native tree species	>1	>2	>3
10	Number of native tree species	1	2	3
5	Number of native tree species	0	1	1-2
0	Absence of native trees	-		
+10 +5 +5 +5	If the tree community is continuous along the river and covers at least 75% of the edge riparian area The tree community is nearly continuous and covers at least 50% of the riparian area If the riparian community is structured in gallery When the number of shrub species is	>2	>3	>4
-5 -5 -10 -10	If there are some man-made buildings in the riparian area If there are some isolated species of non-native[b] trees Presence of communities of non-native[b] trees Presence of garbage			

Section 4: Channel Alteration

Score	
25	Unmodified river channel
10	Fluvial terraces modified and constraining the river channel
5	Channel modified by rigid structures along the margins
0	Channelized river
-10 -10	River bed with rigid structures (e.g., wells) Transverse structures into the channel (e.g., weirs)

Final score (sum of four section scores)

Interview schedule for environmental and sociological scenario for the Mayurakshi River bank dwellars

Block: **Date of Interview:**

Gram panchayet:

Village name:

Personal Information

1. Name of the Interview person:
2. Family type: Joint/ Nuclear
3. Caste: General/ SC/SCT/ OBC/others
4. Religion: Hindu/ Muslim/ Marwari/ Others
5. Number of family member:

Details

Name	Sex	Relation	Age	Qualification	Profession

6. Residing Duration:

7. Source of income: 8. Annual Income:

9. Economic status: BPL …… APL…….. Red card……

10. Type of House: 1 Stored……..2 Stored…….More than 2 stored……Bunglow…….

11. House structure type

Type		Pucca		Kacha		Semi kacha		Others	
Roof material		RCC		Title		Tin		Others	
Floor		Cement		Mosaic		Mud		Others	
Wall		Brick		Mud		Others			

12. **Domestic waste disposal (non-sanitation)**

Pond	River	Barren land	Dumping ground	Canal	Others	Taken by panchayet

13. Is there is any presence of drainage (manmade) line in your village? Yes……No……..

14. **If yes type of drainage**

Open drainage		Close drainage	

Facility (Sanitation)

15. **Latrine**

Type	Individual		Open		Common		Others	
Structure type	Kacha		Pacca		Semi Pacca		Others	
Liquid and Solid Waste disposal	Soak pit		Barren land		Septic tank			

16. If soak pit/septic tank, How often it is being cleared……

17. Cleaning of own surrounding environment……Daily/ weekly/Monthly/ Yearly

18. Does any smell come /pollution occurs from waste disposal in barren land… Yes/ No

19. **Nearest Facility**

Name	Distance	Name	Distance	Name	Distance	Name	Distance
Market		P.O		College/Univ		Parks	
Hospital		P.S		Bus stop		Cinema Hall	
Bank		School		Rail Station		Others	

20. **Perception of living (Last 5 years)**

	Excellent	Good	Satisfactory	Poor
Transport				
Water supply				
Waste Disposal				
Power supply				
Medical				
Education				
Recreation				
Banking				

Water Resources Status

21. Mode of water usages

Type	Drinking	Cooking	Washing	Cleaning	Bathing	Gardening	Others
River water							
Pond water							
Tube well/ Dugwell							
Tap Water							
Spring water							

22. **If Tube well/ Dug well**

Distance in km	Individual		>1km		1-2km		2-3km	
Depth								
Month of Lowered depth								
How many in your village								
Status of water	Fresh		Cloudy		Suspended particles		Bad smell	
Presence of elements	Fluoride		Arsenic		Iron		Salinity	
Overall quality of drinking water	Excellent		Good		Medium		Poor	

23. **If Tap water**

Type	In Own house		In Village by government		Others			
Days of availability	All Day		2 times		More than two times		Monthly/ weekly	
How many in your village								
Presence of elements	Fluoride		Arsenic		Iron		Salinity	
Status of water	Fresh		Cloudy		Cloudy with particles		Bad smell	

24. Interruption of Tap Water: Yes……../ No…….

25. How many days it remains interrupted: …….. Season……..

26. Where your Store water? Drums……..Buckets……...Bottles……Pot……..

27. How many family/ Houses take water if community tube well is there? ….....

28. How many times you go to take water per day (Domestic purpose)? ….....

29. Family water consumption for cooking per day…….

30. Family water consumption for drinking per day…….

31. Family water consumption for sanitation per day……..

32. From the last 10 years, demand for water is increasing or decreasing? .....

33. Do you have tank in your house for water holding? Yes/ No

34. If Yes, Does it is connected with the household water distribution system? Yes/ No

35. If tank

Type of Tank	Underground		Elevated		Others	
Capacity						
Days of cleaning	At gap of 1 months		1-3 months		<3months	

36. Do you filter your drinking water**?** Yes……. No……

37. If yes,

Boiling		Filter		Aquagaurd		Solar disinfection		Chlorination/ Zeoline		Keeping water for hours	

38. Is the groundwater extraction increased in recent days? Yes……..No…….

39. If yes, what is the reason? ….....

40. Do you harvest rain water? Yes/ No……. if Yes how? ….....

41. Do you reuse water? Yes/ No ……if yes how? ….....

42. Do you have any river nearby? Yes/ No…….If yes name ……

43. How far it is (km)……

44. Types of activity performed in river

Activities	Regular	Seasonal
Bathing		
Fishing		
Direct uptake		
Cleaning cloths		
Cleaning livestock		
Recreational		
Religious		
Irrigational		
Waste Disposal		
Defecation		

45. Epidemiology (last 5 years)

46. Does any sand mining activity occur in the nearby rivers? Yes/ No……..

Diseases	Seasons	Frequency	Death occurred
Typhoid			
Cholera			
Diarrhoea			
Malaria			
Dengue			
Hepatitis			
Arsenicosis			
Dental Fluorosis			
Gastro related problems			
Jaundice			

47. Does the river flood its nearby area? Yes/ No……

48. Does the river water decreasing in the recent days? Yes/ No…..

49. If, Yes, reason……

Agricultural and Irrigational status

50. Do you have Farm land/ Agricultural land? Yes/ No

51. If Yes…….Personal……Work for other's farm…….

52. What is the area of the agricultural farm? ….....

53. Do you have nearby river/ canal? Yes/No……

54. If yes please specify……..

55. Sources of water for crop production

Source	Rain		River lift		Shallow/ Submersible		Pond		canal		Storage tank	
Months of availability												

56. Water requirement for agricultural purpose: (Average)

Crop Type	Rabi (Winter)	Kharif (Rainy Season)	Zaid (Onset of summer)
Recent			
5/ 10 years before			

57. **Status of canal water (if present)**

Kharif	Sufficient		To some extent		To large extent		Very poor	
Rabi	Sufficient		To some extent		To large extent		Very poor	
Zaid	Sufficient		To some extent		To large extent		Very poor	

58. Who approves water distribution in canal? Government……Farmer organization…….Others……

59. **Canal water discharge time**

Months	Amount	Frequency

60. Do you have domestic animals? Yes/ No……

61. If yes.

Domestic animals	Cow		Goat		Chickens		Others	
Water requirement of livestock								

62. Crop Type

Rabi (Winter)	Kharif (Rainy Season)	Zaid (Onset of summer)

63. Production time

64. Water requirement

	Rabi crop	Kharif crop	Zaid crop
Planation			
Harvesting time			

Crop type	Amount of water used
Rabi	
Kharif	
Zaid	

65. **Pumping hours (if submersible/River lift)……..**

Season	Amount of extract	Pumping hours	Cost (If applicable)

66. Do you have agricultural machinery? Yes/ No…..

67. Specify……

68. **Fertilizer use pattern**

Nitrogen	Phosphorus	Potash	Organic	Inorganic	Urea

69. Did you pay any amount to government for irrigational water? Yes/ No

70. If Yes, How much?

71. **Agricultural production (Last 5 years)**

Increasing		Decreasing	

72. Reasons behind the decrease in production?

……

73. Do you have compost yard?.....Yes/ No

74. Do you have backyard garden? Yes/No

75. If yes…..what you grows? .....

76. Any deadly pest attacks to your crop?

77. If yes …please specify…….....

76. Is government support organic farming? …….. Yes/ No.

77. Do you have nearby forest? .....If yes name it? .....……...

78. Are you belong to any forest committee/ group? Yes/No

79. Did you observed any deforestation in your surroundings?....Yes/No

80. Did you observed any kind of pollution in your surroundings?

81. If Yes……

Pollution type	
Water pollution	
Air pollution	
Soil Sound pollution	

Date:

Signature of the interviewer:

IJEP 38 (8) : 659-670 (2018)

Study of Ganga River Health Condition Based on Water Quality Indicators with Environmental Aspects and Adaptation Strategies Thereof

Pankaj Kumar Roy[1], Sudipa Halder[1], Swetasree Nag[1], Malabika Biswas Roy[2] and Arunabha Majumder[1]

1. Jadavpur University, School of Water Resources Engineering, Kolkata-700 032

2. Women's College, Calcutta, Kshirode Vidyavinode Avenue, Kolkata-700 003

The challenge on environmental sustainability before India is taking a frightful shape when it comes to the pollution of water. The long stretch of Ganga which is regarded as the holy flow is being messed up by the different anthropogenic activities. Ganga has now become contaminated in its many arms giving rise to a question to our water availability. There has been a long tradition of idol immersion and is too popular in the Ghats of Kolkata whose harmful effects are creating alteration on various components of a river of which water and soil are the most prominent. In this study in order to curb such situation and to establish a rapid assessment the physico-chemical parameters of water samples were collected from different hotspot areas at before and after idol immersion activity and were analyzed as prescribed by APHA guideline. Soil samples were also collected from the same position and tested accordingly in the laboratory of School of Water Resources Engineering, Jadavpur University. Water quality index (WQI) was calculated using the result indicated an increase in pollution load after immersion and quality deterioration characteristics change as well. The water quality index values reflected that an overall water quality is getting deteriorated at a greater extent immediately when the idol immersion process is going on. The results also highlighted that higher amount of lead was used as a raw material received in the river Ganga which may come from idol immersion. Thus it can be concluded that the overall health condition of river Ganga is getting hampered which may reduce the saturation value of dissolved oxygen and disturb the ecological flow at higher rate near by the bank.

KEYWORDS

Water quality index (WQI), Ganga river, Idol immersion, Rapid assessment.

INTRODUCTION

Besides being effected from the various sources of disposal from the inhabiting bank of Ganges, idol immersion is a major seasonal anthropogenic activity which years after years hampering the normal ecological flow of the channels leading to the degradation of water quality and loss of aquatic species. In India, mainly the Hindu religious group celebrate Durga Puja during September to October in every year. Idol immersion is a part of that festival. The materials which are being used to prepare such idols are changing from day to day with the growing economic price. The old clay models are now replaced with plaster of Paris, harmful paints, iron rods, plastics, decorative, etc. The plaster of Paris doesn't dissolve quickly into the water which consist of gypsum, sulphur, magnesium, etc., reduces the dissolved oxygen level in the water and kills fish and other organisms and increases the eutrophication and concentration of pollutant in both water and the soil. Moreover, the chemical paints used to polish these idols contain various heavy metals which are potent carcinogenic and highly toxic are responsible for adding further pollution load

© 2018 - Kalpana Corporation

Proceedings of International Conference on Energy and Sustainable Develeopment
Jointly organized by Jadavpur University and The Institution of Engineers, India
February 14-15, 2020

Surface water source estimation for sustainable management using remote sensing and GIS

Shuvoshri Bhattacharya[1], Sudipa Halder [2], Swetasree Nag [3], Malabika Biswas Roy [4], Pankaj kumar Roy [5]

[1]*Project Assistant, School of Water Resources Engineering, Jadavpur University 700032*
[2, 3] *Junior Research Fellow, School of Water Resources Engineering, Jadavpur University 700032*
[4]*Assistant Professor, Women's College Calcutta 7000003*
[5]*Professor and Joint Director of School of Water Resources Engineering, Jadavpur University 700032*
[5] *Dean of FISLM, Jadavpur University 700032*

{shuvoshri.bhattacharya@gmail.com}

Abstract- **Surface based water resources are becoming vulnerable day by day because of climate change and extensive anthropogenic activities. Surface water bodies include river, pond, wetlands etc. embanked through natural as well as manmade process. A sustainable management for the lentic water is necessary in present days. In this study particularly closed surface water bodies has been delineated using satellite images in ArcGIS software for the year 2009 and 2018. A comprehensive analysis of volume and area of the water bodies has been made for an eastern river basin of India. Parameters like Normalized Difference Water Index (NDWI), Normalized Difference Vegetation Index (NDVI), and Land Surface Temperature (LST) has been calculated to analyses the environmental variability over the region. Field survey revealed the anthropogenic pressure over the water bodies. This study will help the stake holders and policy makers to manage water resources sustainability technique like check dam, slit trap construction, clay barrier, and rain water harvesting.**

Keywords- Water Resource; Normalized Difference Water Index; Normalized Difference Vegetation Index; Land Surface Temperature.

INTRODUCTION

Surface water bodies play a major role in ecosystem. It also has a great hydrological, economical value in our environment. It also recognized as a great sinker of carbon di oxide. For domestics purposes people depend on ground water as well as surface water resources. Surface water bodies support directly and indirectly of people in every region in the world. In this era due to the effect of climate change and global warming fresh water bodies are depleting day by day [1]. So surface based water management need to be focused. To conserve and manage the water bodies it is important to notice an overall view of its catchment's water bodies, vegetation cover, and surface temperature also [2]. Digital maps are very useful to get an overall view of it. Through the remote sensing we get an [1]observation of the total scenario over a period of that particular region [3].

OBJECTIVES

The main objectives of this study are i) to find out the changing trends of surface water bodies with time, ii) to observe the change in vegetation growth over the time. iii) To analyse spatial and temporal changes of land surface temperature.

STUDY AREA

Shilabati river basin is located at the south eastern part of west Bengal. It rise from Barogram in Puncha block, Puruliya and drains into Rupnarayan River near Ghatal, West Medina pore.

The total area of the drainage basin is 3881.07.km^2. The longitudinal and latitudinal extent is 22º32'N to 23º14'N and 86º40'E to 87º46'E [Fig.1]. Total length of the stream is approximately. 250 km. and it covers the parts of Purulia, Bankura and West Mednapur dist. The average monthly rainfall is 120-130mm. and average temperature is 40-44ºc in this total study area. In the upper part of the basin area it has been observe some isolated hillocks which is a part of chotonagpur plateau and metamorphic rock is mainly observed here. The soil type of the upper part is laterite and lower part is alluvial in origin. General slope of the basin is from North West to south east. Vegetation can also be seen scattered throughout the basin.

MATERIALS AND METHODS

The basin map has been delineated with the help of Survey of India Topographical maps numbers 731/12, 731/16, 73J/13, 73M/4, 73M/8, 73M/12, 73N/1, 73N/2, 73N/5,

Author would like to acknowledge RUSA 2.0 Jadavpur University for funding the project.

Author's personal copy

Modeling Earth Systems and Environment (2020) 6:1529–1544
https://doi.org/10.1007/s40808-020-00768-z

ORIGINAL ARTICLE

Optimum prioritisation of sub-watersheds based on erosion-susceptible zones through modeling and GIS techniques

Swetasree Nag[1] · Malabika Biswas Roy[2] · Pankaj Kumar Roy[1]

Received: 21 February 2020 / Accepted: 2 April 2020 / Published online: 16 April 2020
© Springer Nature Switzerland AG 2020

Abstract

The priority assessment of erosion-susceptible zone in a drainage basin is an important approach to diminish various environmental threats related to soil erosion. In a large drainage basin, management and conservation of the entire area at an optimum level are sometimes inefficient due to lack of human resources and financial strength. Therefore, it is prerequisite to establish a viable technique for prioritisation of sub-watersheds in such way that ensures sustainability and high productivity of the region. The objective of this study is to identify erosion-susceptible areas within the sub-watersheds of Mayurakshi river basin located in a transitional zone between Chotanagpur Plateau and Bengal Basin where the risk of soil erosion is very much noticeable. The whole basin has been divided into number of sub-watersheds (SW), and a set of drainage morphometric parameters have been used to identify the potentiality of erosion. Finally, Technique for Order Preference by Similarity to Ideal Solution (TOPSIS) model has been implemented to prioritise the critical areas for better management strategy. This method specifically considered the interdependencies of all criteria for which it has been very much applicable for the assessment of erosion risk zones. The output of TOPSIS model reveals SW6 and SW11 have been fall under high- and low-erosion-susceptible zones, respectively. To validate the output of the model, rainfall erodibility index (*R* factor) has been calculated which shows that the same watershed (SW6) has been fall under high rainfall erosivity zone depicting the need of prioritisation at an earliest convenience.

Keywords Drainage basin · Morphometric parameters · Sub-watershed prioritisation · Erosion susceptibility · GIS

Introduction

Priority-wise management of natural resources plays a crucial role for the development of a sustainable environment which has been disturbed by various natural and anthropogenic factors. Among them, climate change, deforestation, population explosion and other unscientific human activities are the prime cause which leads to various environmental hazards related to land degradation, soil erosion, water pollution, etc. (Arami et al. 2017). Soil erosion is regarded as one of the frequently occurring hazards that causes various negative consequences in our environment like degradation of the reservoir capacity, increases flood risk, disturbs the natural flow of river and hampers the overall land productivity of a region. Soil and water are considered as two most essential natural resources not only to sustain livelihood but also for the development of social and economic aspects of a region (Debelo et al. 2017). But unfortunately, within last 150 years, half of the topsoil on the earth surface has been removed by various wind- and water-related erosional activities. On a global scale, about 20–30 Gt (gigaton) soil has been eroded by water-related action in every year (FAO 2015). The worldwide effects of such environmental degradation are also noticeable in India, where about 57% of the total area has been degraded by water-related action (Jhariya et al. 2018). A large number population in India is dependent on agriculture-related activities that invoke exploitation and unscientific use of land and water resources. It can be regarded as one of the major obstacles towards achieving more success in agricultural production and other sectors of economy (Arabameri et al. 2018; Molla and Sisheber 2017). In this context, the need of decision making for priority-wise conservation plan has created an interest in the field

✉ Malabika Biswas Roy
malabikabiswasroy@gmail.com

[1] School of Water Resources Engineering, Jadavpur University, Kolkata, West Bengal, India

[2] Department of Geography, Women's College, Calcutta, Kolkata, West Bengal, India

CHAPTER

25

Land reclamation and reuse of waste water on the backdrop of urban sprawl of Kolkata metropolitan: a case study of East Kolkata, Wetland, India

Pankaj Kumar Roy[1,*], Malabika Biswas Roy[2], Sritama Chatterjee[1], Sudipa Halder[1], Swetasree Nag[1], Arunabha Majumder[1]

[1]*School of Water Resources Engineering, Jadavpur University, Kolkata, West Bengal, India;* [2]*Department of Geography, Women's College, Kolkata, West Bengal, India*

[*]*Corresponding author: pk1roy2014@gmail.com*

Chapter outline head

25.1 Introduction 557
25.2 Land reclamation 560
25.3 Importance of study area—EKW 561
25.4 Land use pattern due to urban planning 565
25.5 Materials and methods 569
25.6 Results and discussions 569
25.6.1 Land use and land cover change detection 569
25.6.2 Wastewater reuse efficiency 572
25.6.3 Impact of change in land use and land cover pattern on groundwater quality 572
25.7 Discussion 573
25.8 Conclusion 578
References 578
Further reading 579

25.1 Introduction

The land reclamation has an age-old history all over the world. Land reclamation of study area which dates back to the era of British Rule in India when this area was known to be Salt Water Lakes brings forth contemporary development of planned sewerage and drainage system of the Calcutta city passing

Land Reclamation and Restoration Strategies for Sustainable Development. https://doi.org/10.1016/B978-0-12-823895-0.00027-0
Copyright © 2021 Elsevier Inc. All rights reserved.

Chapter 4
Tri-Decadal Visualization Analysis on River Health Studies: A Global Perspective

Malabika Biswas Roy, Swetasree Nag, Arnab Ghosh, and Pankaj Kumar Roy

Introduction

The impact of global climate change poses a serious threat to the water resources of the world. Both the ground and surface water hydrology alteration has turned to be an immediate challenge to humankind. Such kinds of alterations in water resources may result in environmental degradation in terms of quality, quantity, flow pattern, water availability, and other environmental aspects. Furthermore, overexploitation and unscientific use of water resources may lead to almost no-flow condition in a river during the dry season period [28, 31, 32]. Keeping this detrimental issue in mind, the survival of rivers has turned to be an immediate challenge to humankind [16]. To sustain a river basin for the long run, priority-wise assessment of the critical areas has been regarded as an important approach to maintain the physical environment and overall health status of the area [25].

Rivers are the lifeline of human society. From the period of human civilization, river water plays a vital role in controlling its ecological, social, and economic value for the environment. But excessive human interruptions are deteriorating the fitness of rivers in terms of their physical, chemical, and biological health. At such juncture, the concept of river health has arrived which focused on the maintenance of the inherent character of the river system and also the management and restoration into an undisturbed environment (Clean Water Act, 1972). To protect the dynamic nature of the river system Nandi et al. [26] proposed a comprehensive model on River Health Assessment (RHA) which encompasses numerous influential aspects of river system management like Catchment Health (CH), Floodplain Health (FPH), River Channel Health (RCH), Flow Health (FH), River

M. B. Roy (✉)
Department of Geography, Women's College, Calcutta, Kolkata, West Bengal, India
e-mail: malabikabiswasroy@gmail.com

S. Nag · A. Ghosh · P. K. Roy
School of Water Resources Engineering, Jadavpur University, Kolkata, West Bengal, India

© The Author(s), under exclusive license to Springer Nature Singapore Pte Ltd. 2021

P. K. Roy et al. (eds.), *Advances in Water Resources Management for Sustainable Use*,
Lecture Notes in Civil Engineering 131,
https://doi.org/10.1007/978-981-33-6412-7_4

Chapter 18
Assessment of Drought Using Multi-parameter Indices

Shuvoshri Bhattacharya, Sudipa Halder, Swetasree Nag, Pankaj Kumar Roy, and Malabika Biswas Roy

Introduction

Drought is one of the slow calamities that can put danger to the environment, hydrology, agriculture, economy and society worldwide. The basic concept of drought in our community is shortage of rainfall, lack of surface water, scarcity of water in society [1]. Drought is a complicated phenomenon and is difficult to study. It is often tough to find out the exact initiation of drought. Drought is roughly classified into four segments, i.e. Meteorological drought (deficit of precipitation), Hydrological Drought (shortage of total water), Agriculture Drought (scarcity of soil moisture and production decrease due to water) and Socio-economic Drought (inadequate water supply and demand) [2]. The reason for drought can be occurred by natural or anthropogenic activities. It is a clumping physical process and its effects vary spatially so it can be called a 'crawling disaster' [3]. Generally, meteorological drought rises when an area receives less than 75% rainfall over a season. But a rapid cutting of forests, global warming is also the cause of drought in recent days.

S. Bhattacharya (✉) · S. Halder · S. Nag
School of Water Resources Engineering, Jadavpur University, Kolkata 700032, India
e-mail: shuvoshri.bhattacharya@gmail.com

S. Halder
e-mail: sudipa.halder92@gmail.com

S. Nag
e-mail: nag.swetasree@gmail.com

P. K. Roy
Jadavpur University, Kolkata 700032, India
e-mail: pk1roy2014@gmail.com

M. B. Roy
Women's College, Calcutta, Kolkata 7000003, India
e-mail: malabikabiswasroy@gmail.com

© The Author(s), under exclusive license to Springer Nature Singapore Pte Ltd. 2021

P. K. Roy et al. (eds.), *Advances in Water Resources Management for Sustainable Use*,
Lecture Notes in Civil Engineering 131,
https://doi.org/10.1007/978-981-33-6412-7_18

Chapter 32
Assessment of Topographic Complexity Zone of a Drainage Basin Using Geographic Information System

Swetasree Nag, Malabika Biswas Roy, Shuvoshri Bhattacharya, Souvik Mondal, and Pankaj Kumar Roy

Introduction

Evolution of the earth's surface and its topography has been operated by various chemical, biological, and geomorphic processes. Various endogenetic and exogenetic forces like tectonic activities, folding of the rock structure, different erosional as well as depositional agents are operated within the earth's surface and are equally responsible for the modification of the land surface. Among all such geomorphic processes, fluvial processes are the most dominant ones to alter the earth's topography. The behavior of the fluvial processes is very much dependent on the prevailing geology, rock structure, and geomorphology of that region. Therefore drainage basin characterization plays an important role to assess the hydrogeological behavior of a region. So, evaluation of the drainage network in terms of its morphometric analysis to assess its hydrogeological behavior with respect to the physiographic character of the basin area. The nature of the basin topography plays an important role in terms of basin developmental work and resource utilization of that region. Depending on the character of the basin topography, utilization of land, as well as water resources, varies at a different spatial extent. Several important correlations have been observed between various hydrological phenomena with the physiographic characteristics of drainage basin such as size, shape, slope, etc. In this regard, the study of the watershed dynamicity concerning the nature of basin topography pays high attention to sustain the watershed for a long run.

S. Nag · S. Bhattacharya · S. Mondal · P. K. Roy
School of Water Resources Engineering, Jadavpur University, Kolkata, West Bengal, India
e-mail: shuvoshri.bhattacharya@gmail.com

S. Mondal
e-mail: souvik134@gmail.com

M. B. Roy (✉)
Department of Geography, Women's College, Calcutta, Kolkata, West Bengal, India
e-mail: malabikabiswasroy@gmail.com

© The Author(s), under exclusive license to Springer Nature Singapore Pte Ltd. 2021

P. K. Roy et al. (eds.), *Advances in Water Resources Management for Sustainable Use*,
Lecture Notes in Civil Engineering 131,
https://doi.org/10.1007/978-981-33-6412-7_32

Chapter 16
An Analytical Study on Interplay Between Physiographic Condition and Land Use Land Cover Dynamicity

Swetasree Nag, Malabika Biswas Roy, and Pankaj Kumar Roy

Abstract Land use land cover dynamicity over a region primarily depends on numerous physiographical factors like relief, slope, drainage, etc. A rhythmic correlation between these factors will promote sustainable land use land cover practices within a region. Likewise in a low relief area having a good drainage cover permits the development of settlement and agricultural activity. But sometimes an unnatural behaviour between these parameters may hamper the land utilisation activities. In this work, authors have tried to draw attention to such kind of behaviour among the topographical elements of the Kuya River Basin which makes the topography more erosive and complex in nature. This paper also enumerates how the land use land cover practices of the study area can be influenced by the topographical complexity. To explore such a topographic complex zone, a weighted overlay analysis has been carried out using six major morphometric parameters. A multiple correspondence analysis (MCA) has also been executed which proves that human beings cannot overcome the adverseness of nature as they were well accustomed with the physiographical complexity by utilising the land in a sustainable way.

Keywords Topographic complexity · Multiple correspondence analyses · Land use land cover dynamicity · Sustainable management

16.1 Introduction

Physiographic conditions play a major role determining the land utilisation pattern of the region. Depending upon the nature of relief and slope the drainage network develops. As 75% of the Indian population has been depending on the agricultural activity, areas having high water resource potentiality are occupied first. Under such circumstances settlement and communication network starts to develop from the

S. Nag · P. Kumar Roy
School of Water Resources Engineering, Jadavpur University, Kolkata, West Bengal, India

M. Biswas Roy (✉)
Department of Geography, Women's College, Kolkata, West Bengal, India

© The Author(s), under exclusive license to Springer Nature Singapore Pte Ltd. 2022

N. C. Jana and R. B. Singh (eds.), *Climate, Environment and Disaster in Developing Countries*, Advances in Geographical and Environmental Sciences, https://doi.org/10.1007/978-981-16-6966-8_16

Biswas Roy *et al.*
Bulletin of the National Research Centre (2022) 46:59
https://doi.org/10.1186/s42269-022-00740-0

Bulletin of the National Research Centre

REVIEW

Open Access

Assessment of wetland potential and bibliometric review: a critical analysis of the Ramsar sites of India

Malabika Biswas Roy[1*], Swetasree Nag[2], Sudipa Halder[2] and Pankaj Kumar Roy[2]

Abstract

Background: This study focussed on effective bibliometric analysis of research on Ramsar sites in India within the last 30 years using VOS viewer software. The study focused on the estimation of the current areal extent and meteorological impact on wetland together with bibliometric analysis. The online data source of Web of Science has been used to extract all the relevant documents on Indian Ramsar sites published within a period of 1989 to 2020.

Main body: The main objective is to analyze the trend of research on the Indian Ramsar site both qualitatively and quantitatively. The peak of research growth has been lifted after the twentieth century as most of the Indian water bodies have been designated or put into the land from this period. A geographical location-based mapping was prepared based on the number of publications during the study period to observe the growing research interest in wetland studies in India. The highest publications have been documented on East Calcutta Wetland located in West Bengal followed by Loktak Lake in Manipur, Deepor Beel in Assam and others. The most frequently used keywords were "Ramsar site", "India", "wetland", "wetlands", "remote sensing" etc. India published most of the documents on wetland studies in the Indian context. England, Australia, Canada also had various international collaborative works with Indian researchers.

Conclusions: The research output shows an upward research trend on Indian Ramsar sites both quantitative and qualitatively. Such kind of research can provide a panoramic view towards the worldwide research trend and help to generate further effective approaches for the betterment of our environment.

Keywords: Ramsar sites, Bibliometric analysis, Web of Science, VOSviewer, Research trend

Background

Wetlands are considered as a unique ecological unit, which contributes enormous goods and services to human society (Prasad et al. 2002). It also consists of rich biodiversity and states, as the most valuable natural resource on the earth (Whitehouse et al. 2008). They are the invaluable resources of the environment, resource potential ecology and biodiversity in India (Biswas Roy et al. 2016). Globally the areal extent of wetlands accounts for about 12.1 million km^2 showing diverse characteristics in its geographical locations, dominant species, soil–water chemistry etc. Such productive natural resources can also be well utilised by several landless people of rural India, where pisciculture activity is very dominant (Biswas Roy et al. 2016). Not only that, several other environmental benefits like flood management, groundwater recharge, water supply, irrigational activities are also well practiced in wetland areas. In this regard to gain international importance Ramsar Convention on wetlands has been signed in the year of 1971 to conserve and augment the ecological functions of wetlands. In India, only 37 wetlands are designated as Ramsar sites (MoEFCC 2020). Environmental education and awareness is required to

*Correspondence: malabikabiswasroy@gmail.com
[1] Department of Geography, Women's College, Calcutta, Kolkata, West Bengal, India
Full list of author information is available at the end of the article

© The Author(s) 2022. **Open Access** This article is licensed under a Creative Commons Attribution 4.0 International License, which permits use, sharing, adaptation, distribution and reproduction in any medium or format, as long as you give appropriate credit to the original author(s) and the source, provide a link to the Creative Commons licence, and indicate if changes were made. The images or other third party material in this article are included in the article's Creative Commons licence, unless indicated otherwise in a credit line to the material. If material is not included in the article's Creative Commons licence and your intended use is not permitted by statutory regulation or exceeds the permitted use, you will need to obtain permission directly from the copyright holder. To view a copy of this licence, visit http://creativecommons.org/licenses/by/4.0/.

J. Earth Syst. Sci. (2022)131 146
https://doi.org/10.1007/s12040-022-01872-7

© Indian Academy of Sciences

Study on the functionality of land use land cover over the evaluation of groundwater potential zone: A fuzzy AHP based approach

Swetasree Nag[1], Malabika Biswas Roy[2,*] and Pankaj Kumar Roy[1]

[1]*School of Water Resources Engineering, Jadavpur University, Kolkata, West Bengal, India.*
[2]*Department of Geography, Women's College, Calcutta, Kolkata, West Bengal, India.*
**Corresponding author. e-mail: malabikabiswasroy@gmail.com*

MS received 17 February 2021; revised 10 November 2021; accepted 18 January 2022

Identification of groundwater potential zone has become a prime concern for the developing countries, where the dependency of groundwater is more, because of the increasing demand for water for irrigational uses. Furthermore, the rapid population growth is hindering the aquifer recharge process by altering the land use land cover (LULC) of any region. The present work aims to assess how the modification of land use land cover can affect the groundwater recharge potential zones over a river basin area in West Bengal, India. Enumerating 13 influential parameters and employing the fuzzy analytical hierarchical process (FAHP), delineation of groundwater potential zones have been done for 2000 and 2018. The outputs produced by such a predictive decision-making model have been validated by water level data acquired from the Central Ground Water Board (CGWB) and field survey for respective years. The effect of LULC over groundwater potentiality has been investigated through a change analysis of land use land cover and recharge potential areas from the year 2000 to 2018. This study witnessed an augmented groundwater resource scenario due to maximum positive changes in land utilization patterns by the community, which ensures the effectiveness of anthropogenic control on any kind of resource management system.

Keywords. Groundwater potential zones; fuzzy analytical hierarchical process (FAHP); land use land cover (LULC); sustainable management.

1. Introduction

Deciphering the groundwater potential zones has become a global concern for hydrogeologists, hydraulic engineers, and environmental scientists around the world. Groundwater can be regarded as an important freshwater resource for both rural and urban areas (Hossein 2004). The occurrence of groundwater in any region may be influenced greatly by various hydrogeomorphic/hydrogeological formations, presence of drainage network, soil properties, lineament density, temperature, precipitation, etc. (Singh *et al.* 2011; Şener *et al.* 2018). It also plays a significant role by fulfilling the daily need of human beings, maintaining the ecosystem, and also in various activities of economic development (IPCC 2013). Despite these natural factors, some of the human-induced factors like rapid population growth, urbanization, and improved standard of living may lead to overutilization of groundwater resources resulting substantial decline in groundwater level (Qadir and Singh 2019). In India, 60% of wells are facing a major water table lowering issue, which accelerates

Published online: 11 June 2022

Research Square

Preprints are preliminary reports that have not undergone peer review.
They should not be considered conclusive, used to inform clinical practice,
or referenced by the media as validated information.

A Combined use of Hydraulic and Hydrological Model to Characterise Channel Hydro-Geomorphology of a Tropical River Basin of West Bengal, India

Swetasree Nag
Jadavpur University
Sayak Karmakar
Jadavpur University
Malabika Biswas Roy
Women's College
Pankaj Kumar Roy (pankaj.kroy@jadavpuruniversity.in)
Jadavpur University

Research Article

Keywords: Channel geometry, Flow pattern, Manning's equation, Kinematic wave parameter (KWP), Differential Global Positioning System (DGPS) survey

Posted Date: January 4th, 2023

DOI: https://doi.org/10.21203/rs.3.rs-2409387/v1

License: This work is licensed under a Creative Commons Attribution 4.0 International License. Read Full License

Abstract

The present research work is intended to portray the changing nature of channel hydro-geomorphological properties from upstream to downstream of the Mayurakshi River located in a plateau fringe region of Jharkhand and West Bengal. An intensive field investigation has been done on 14 different cross-sectional sites to measure some important geomorphic parameters like channel depth, width, bank height, hydraulic radius, wetted perimeter, etc. during the post monsoon season of 2021. For more accurate locational information, a Post Processed Kinematic Survey (PPK) using Differential Global Positioning System (DGPS) survey and a Current Meter instrument have been done to measure the river bed profile and channel velocity respectively. The objective of this paper is to compare the field observed discharge data with selected hydraulic and hydrological models and to determine the scientifically accepted and cost-effective way of estimating lean period flow amount within a section of a tropical river like the Mayurakshi River. Here, Manning's equation and Kinematic Wave Parameter (KWP) - two important geomorphic-based methods have been executed for computing the discharge amount, where the study reveals Hydraulic method of Manning's equation provide better result in discharge estimation compared to the hydrological method. Moreover, the role fragmented nature of the flow pattern, human intervention in active river bed areas by continuous sand mining activity and installation of dams and barrages restrict the free flow of the river causing inadequate discharge and higher channel in-efficiency throughout the studied reach.

1 Introduction

A series of cross profiles reveals the fundamental hydro-geomorphological behaviour of a channel. The cross-section of a channel is function of its shape, size, flow, sediments that are moved through the section and deposited around the river bank (Leopold et al. 1964). The cross-section of a natural channel is characterised by irregularly outlined water surface width, mean flow depth and a volume of discharge (Swamee 2000), which are assumed to get balanced with the underlying topography to form a stable reach irrespective of the scour and fill of river bed (Richards 1982). The study of channel geometry and the hydro-geomorphological behaviour may be monitored as a key concern for the scientific management of a river health (Lord et al. 2009; Singh 2003). In river hydraulics, the geometry of a cross section changes more frequently than a longitudinal profile. Any alteration in water discharge or sediment flow induces a noticeable change in channel geometry. Such changes are mainly instigated by the human intervention on river bed. Construction of various civil structures like dam, barrages, rail or road bridges, creation of temporary nala's for irrigation purposes and excessive sand extraction from the active channel are the major catalyst behind the degradation of channel geometric properties resulting channel in-efficiency to carry enough water for a long run. Channel efficiency is largely dependent on the channel adjustment. In recent time, controlled or human regulated flow pattern is very much observed across the world. Most of rivers are being impounded with dam and barrages, which are not able met the sustainable development strategies (Hoque et al. 2022). Unfortunately, the main flow of river is now maintained within a narrow active channel area. River loses its natural flow due to the construction of water holding structures and also disturbed the movement of sediment, nutrient to the downstream on which the fluvial community depends (Mitra and Singh 2018; Mc Manamay and Bevelhimer 2013). Not only the controlled flow, scouring activity near the dam area generate a huge aggradation of sediment which may chock the downstream channel width significantly (Petts 1979; Williams and Wolman 1984).

In Ganga Bramhaputra Delta, the alteration in channel geometry due to anthropogenic intervention is well documented. Pal (2016) discussed the changes in channel morphology due to construction of Massanjore Dam and Tilpara Barrages in the Mayurakshi River. Ghosh and Guchhait (2016) noted the gradual shifting in flood duration during the post dam period of Damodar River. Moreover, the effect of post Farakka Barrage Project on the Bhagirathi Hugli River is worth mentioning. Mistry (1972) documented the problems of ship navigation due to the growth of mid-channel bar near the port area. Besides this, Basu et al. (2005) studied the changing nature of channel shape from meander to straight so as to maintain its perennial nature of flow throughout the year.

All the studies stated above indicates the channel hydro-geomorphological changes due to various constructional activities on the river bed. Estimation of river discharge is a major component of river hydraulics mainly when the understanding of its spatio-temporal dynamism is unacquainted to ourselves. The measurement of available surface water resources and the temporal heterogeneity of flow magnitude, frequency both during peak and lean flow period is crucial for the assessment of flood or drought like situation under changed climate scenarios (Xu et al. 2018). Rivers with such civil structures like dam or barrages, have their own gauge stations to monitor and document the daily records. But in West Bengal, most of the rivers are ungauged due to some environmental or financial limitations or rivers having monitoring station does not maintain the data properly. However, the direct measurement of river discharge using traditional gauging system or to via installing instrument are some points not suitable in remote or inaccessible areas along the river reach and thereby various indirect methodologies are becoming useful and feasible. Numerous studies have already done for estimating the discharge amount in relation the channel geometric properties using various indirect methodologies like application of Unmanned Aerial Vehicles (UAVs) (Yang et al. 2019), remote sensing-based methods (Bjerklie et al. 2003; Getirana et al. 2009) etc. Tabata and Hickin (2003) used the 'inter-channel hydraulic geometry' model on Columbia River (Canada) and observed the changes in channel discharge capacity due to alteration in channel flow pattern. Pandey and Ramasastri (2003) applied various set of flow duration curve method from daily/weekly/monthly discharge data for lean period to assess the potentiality of dependable lean season flows in San and Barah watersheds of Orissa. Above all, an accurate measurement of river hydraulics (width, depth, slope etc) from filed survey and compare the result with various multi-variate open channel flow equation gives the better output in discharge estimation (Sichangi et al. 2016).

The present study is focussed on the changing nature of channel hydro-geomorphological properties of the Mayurakshi River. Massanjore Dam and Tilpara Barrage are the only river gauge sites which measures the daily amount of inflow and discharge of the water from the dam. Here the study is tries to fill the gap of insufficient streamflow databases in a sparsely gauged river basin (e.g., Mayurakshi River), 14 cross-sectional sites have been chosen to portray the channel geometry and the nature of lean period flow velocity and discharge scenario. Therefore, the objective of the study includes a) estimation of lean period discharge using two classical hydraulic and hydrological algorithm and b) validation of the calculated values with the field observed discharge data using RMSE. Nevertheless, this study will ensure the benefit of field work besides the usage of such established numerical methodologies for estimating the hydraulic properties of a channel.

2 Materials And Methods